Differentiation and growth of the mammalian pancreas

Seymour, Philip Allan

Award date:
2003

Awarding institution:
University of Bath

Differentiation and Growth of the Mammalian Pancreas

submitted by Philip Allan Seymour BSc. Hons. (Dunelm)
for the degree of PhD
of the University of Bath
2003

ProQuest LLC
789 East Eisenhower Parkway
P.O. Box 1346
Ann Arbor, MI 48106-1346

Acknowledgements

First and foremost, I would like to express my gratitude to my supervisor, Prof. Jonathan Slack for his excellent support and constant patience and encouragement over the last three and a half years. I should like to thank him and Dr. David Tosh for reading draft thesis chapters. I am also very grateful to both of my assessors, Dr. Andrew Ward and Prof. Chris Graham for their time and effort spent preparing for and conducting my viva voce.

I would like to express my appreciation to the people who have contributed directly to the work reported here. Many thanks to Dr. Bill Bennett for maintaining and providing the X-inactivation mosaic mice and for his friendly advice and encouragement throughout my time in Bath and beyond. The help given by Dr. Richard Adams in the computer-generated 3D reconstructions was invaluable and much appreciated. I would like to thank Dr. Andrew Ward for the opportunity to work on the characterisation of the Elijah and Ripley lines and also Dr. Marika Charalambous for advice regarding statistical analysis. I am indebted to Dr. David Tosh for all of his help regarding tissue culture and general immunocytochemistry and also for the chance to work on the dexamethasone-induced pancreatic hepatocytes.

I have been fortunate to receive help, advice and general encouragement from everyone in Lab. 0.62, past and present all of whom have made working in the lab a very pleasant experience. A sincere thanks to Dr. Chia-Ning (Kenny) Shen in particular for all of his advice regarding antibodies and immunostaining. Thank you to Mrs. Lori Horb for her advice and coaching in establishing cultures on my arrival in Bath. I am particularly indebted to Dr. Caroline Beck, Dr. Marko Horb, Dr. Bea Christen and Dr. Aurora Lombardo for their technical advice and warm support. I would like to express my gratitude to Mr. Chris Apark for providing reagents and solutions and to Mrs. Catherine Skuse for her assistance with counterstaining. Thank you to Dr. Cesare Gargioli and Wei-Yuan (John) Yu for discussion and support and to Cesare, John and Gloria Yu and Diya Lahiri for providing me with accommodation and wonderful food on my frequent visits to Bath from Yorkshire.

Finally, thank you to all of the staff at 5 West for their hard work and their friendship over the three years and to the MRC for funding this work. I am also indebted to my parents for their support and encouragement - thank you.

Abbreviations

ABC	(Strept)avidin-biotin complex
AMCA	7-Amino-4-methylcoumarin-3-acetic acid
ANOVA	Analysis of variance
AP	Alkaline phosphatase
APTES	3-Aminopropyltriethoxysilane
BB	Blocking buffer
BDC	Blue dot cell
BrdU	5'-Bromo-2'-deoxyuridine
C/EBPβ	CCAAT enhancer binding protein β
CPS I	Carbamoylphosphate synthetase I
CTL	Control
DAB	3,3'-Diaminobenzidine
DAPI	4',6-Diamidino-2-phenylindole
Dex	Dexamethasone
DNA	Deoxyribonucleic acid
cDNA	Complementary deoxyribonucleic acid
E	Embryonic day
EGF	Epidermal growth factor
FBS	Fetal bovine serum
FGF	Fibroblast growth factor
FITC	Fluorescein isothiocyanate
β-Gal	β-Galactosidase
GS	Glutamine synthetase
H & E	(Ehrlich's) haematoxylin and eosin
HGF	Hepatocyte growth factor
HMG CoA reductase	3-Hydroxy-3-methylglutaryl coenzyme A reductase
HNF	Hepatocyte nuclear factor
HRP	Horseradish peroxidase
IAPP	Islet amyloid polypeptide (amylin)
IGF	Insulin-like growth factor
IGF1R	Insulin-like growth factor 1 receptor
IGFBP	Insulin-like growth factor binding protein

INGAP	Islet neogenesis-associated protein
INSR	Insulin receptor
Ipf1	Insulin promoter factor 1
IRS	Insulin receptor substrate
KGF	Keratinocyte growth factor (FGF7)
LDL	Low density lipoprotein
MODY	Maturity onset diabetes of the young
N-CAM	Neural cell adhesion molecule
NGF	Nerve growth factor
Ngn	Neurogenin
NPY	Neuropeptide Y
PBSA	Phosphate-buffered saline A
PCNA	Proliferating cell nuclear antigen
Pdx1	Pancreatic duodenal homeobox 1
PFA	Paraformaldehyde
PN	Postnatal day
PC	Prohormone convertase
PP	Pancreatic polypeptide
PYY	Peptide YY
Reg	Regenerating protein
RIP	Rat insulin I promoter
RNA	Ribonucleic acid
mRNA	Messenger ribonucleic acid
RT-PCR	Reverse transcriptase-polymerase chain reaction
S.E.	Standard error
TFN	Transferrin
TG	Transgenic
TGF-β	Transforming growth factor β
TRITC	Tetramethylrhodamine isothiocyanate
TTR	Transthyretin (prealbumin)
TUNEL	Terminal deoxynucleotidyl transferase-mediated biotin dUTP nick-end labelling
USC	Uniformly stained cell
VEGF	Vascular endothelial growth factor
X-Gal	4-chloro-5-bromo-3-indolyl-β-D-galactopyranoside

Summary

Despite its medical significance relatively little is known about pancreatic growth, particularly in postnatal life. The existence of a pancreatic stem cell population and the limitation on the division potential of the differentiated cells, are matters of contention. In this work, a number of studies were conducted to investigate the growth and differentiation of the mammalian (mouse) pancreas.

A characterisation was made of a sub-population of migratory epithelial cells in cultures of recombinant pancreatic buds combining the epithelium from a β-gal-expressing ROSA-26 embryo and an intact bud from a wild-type embryo. The migratory characteristics of these cells were studied and a proportion was found to express insulin or glucagon.

Extending a previous study (Shen *et al.*, 2000), showing that the synthetic glucocorticoid dexamethasone (Dex) induces hepatocytes in intact pancreatic cultures, an investigation was made into the relationship between two Dex-induced pancreatic hepatocyte populations expressing either of two hepatic enzymes. By depriving the pancreatic epithelium of mesenchyme it was demonstrated that induction of the two populations occurs independently of the other.

The postnatal clonal development of the pancreatic islets and ducts was followed in β-gal-expressing X-inactivation mosaic mice. The consistent heterogeneous ductal β-gal$^+$/β-gal$^-$ cell composition showed that pancreatic ducts arise from multiple progenitor cells and retain this polyclonal state postnatally. Although at birth islets were mixed, confirming their formation from multiple progenitor cells, by three weeks after birth almost 95 % of islets were homogeneous indicating a shift towards monoclonality. This "clonal purification" might be assisted by an unreported process of islet fission for which morphological and cell composition evidence is presented.

A morphometric analysis was made of histological sections from transgenic mice specifically overexpressing IGF-II either in the pancreatic acini or islet β-cells. Both lines demonstrated a similar phenotype of islet hyperplasia with disorganised islet architecture suggesting that the effects of IGF-II are not cell-autonomous.

Contents

1. Introduction

1.1. Medical Significance

The pancreas (*pl.* pancreata) is an especially important organ from a medical perspective because it is affected by two significant diseases: diabetes mellitus and pancreatic cancer. A total of 150 million people worldwide currently suffer from type 1 or type 2 diabetes mellitus and this figure is predicted to rise to 300 million over the course of the next 20 years (Zimmet *et al.*, 2001). Despite the availability of insulin, diabetes mellitus is still problematic, causing premature death and prolonged ill health. Approximately 6700 people are diagnosed with pancreatic cancer each year in the UK, accounting for about 3 % of all cases of cancer in this country (Cancer Research UK, 2002). Despite being the 11th most common cancer in the UK, it is the fifth most common cause of cancer mortality owing to the disease being virtually incurable. The five-year survival rate for patients suffering from cancer of the pancreas is only about 2 % (Cancer Research UK, 2002). It follows that a better understanding of the development of the organ as a whole is likely to lead to the development of novel therapies for the treatment of these diseases, diabetes in particular. However, despite the obvious significance of this organ, the pancreas was largely overlooked in the field of developmental biology until relatively recently.

1.2. Anatomy and Histology of the Pancreas

1.2.1. Gross Morphology and Function

The pancreas is a flattened and elongated compound *racemose gland*, that is a gland bearing branching ducts that terminate in sacs of secreting cells. The human pancreas comprises an organ of 70-150 grams in weight and 15-25 cm in length, lying laterally to the upper right hand side of the abdominal cavity. It is connected to the duodenum by the ampulla of Vater, where the main pancreatic duct joins with the common bile duct from the liver and gallbladder (**Figs. 1.1.** and **1.2.**). Regions of the human pancreas are usually designated as the head, body and tail, from proximal to distal and some textbooks also include a neck and an *uncinate* (or "hook-like") process, which is the posterior part of the head. The form of the pancreas in rodents however, is less well defined although the terms head and tail are also typically applied.

Figure 1.1. Anatomy of the Adult Human Pancreas. (Reproduced from *Gray's Anatomy*, 38th Edition, Williams, P. L., Copyright [1995], with Permission from Elsevier)

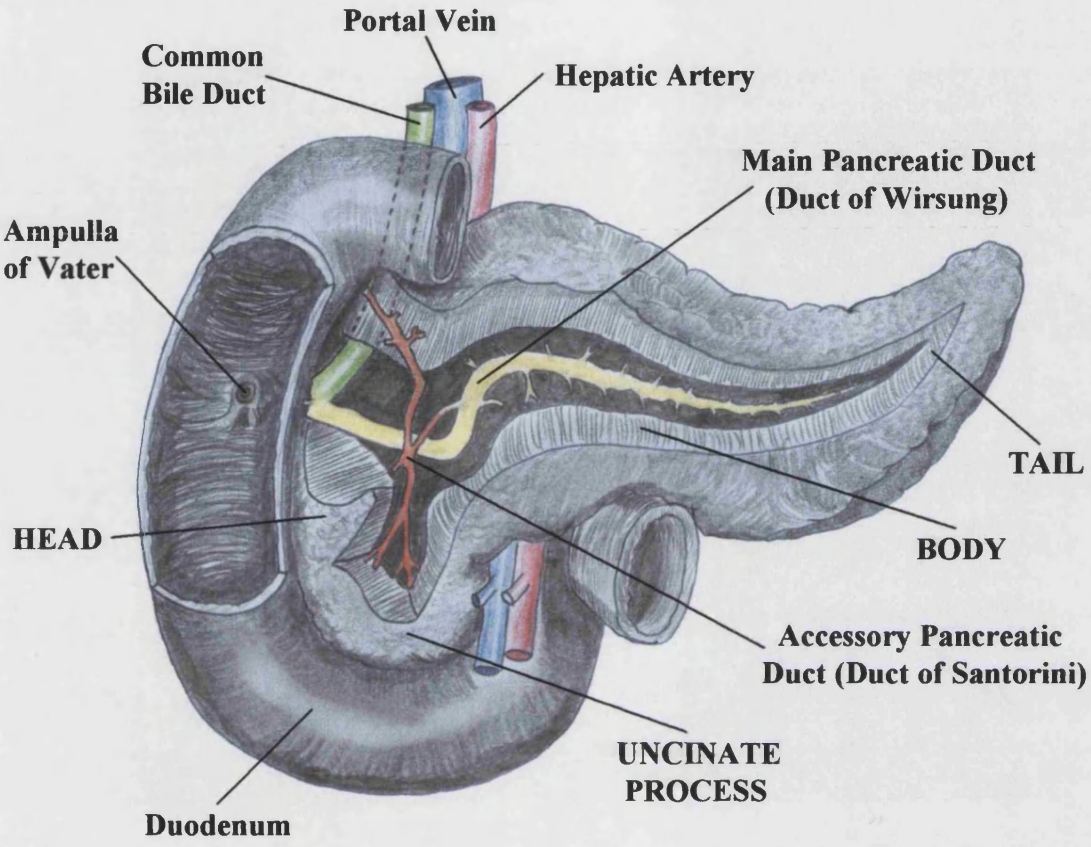

Figure 1.2. Location of the Dorsal and Ventral Pancreatic Buds in a Human Embryo of About 36 Days (After Slack, 1995)

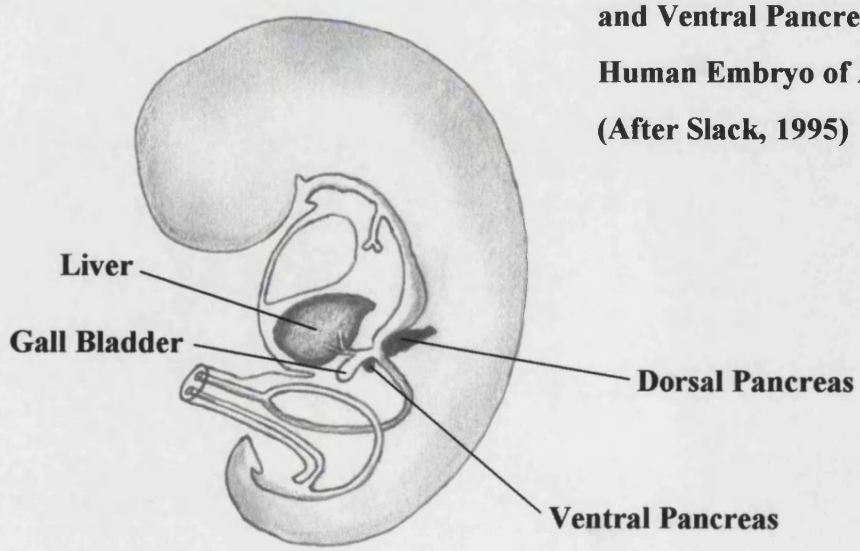

The pancreas is an organ with two distinct functions: the secretion of enzymes and salts into the digestive tract and secretion of hormones into the bloodstream which regulate blood glucose levels. These functions are performed by two quite distinct types of glandular tissue: the exocrine and endocrine tissue respectively. However, the pancreas is a single integrated organ from a biological perspective, despite the frequent segregation of its endocrine and exocrine functions in many medical texts.

1.2.2. The Exocrine Pancreas

The exocrine pancreas is a lobulated, branched, acinar gland. The secretory exocrine cells form a system of terminal or intercalary acini of small lumens, connected by ducts (**Fig. 1.3.**). The acinar cells are pyramidal in shape and are specialised for protein synthesis, characterised especially by a prominent Golgi complex and numerous secretory (zymogen) granules containing digestive enzymes including proteases, amylases, lipases and nucleases. The majority of these enzymes are secreted as inactive precursors, only becoming activated upon entering the duodenum. Low cuboidal centroacinar cells, located at the junction of acini and ducts secrete non-enzymic components of the pancreatic juice, including bicarbonate. The ducts themselves are lined with columnar epithelial cells, and small numbers of goblet and brush cells are present in the larger ducts, much like those of the intestine. Secretion of the pancreatic juice is modulated by hormonal stimulation, principally by secretin, cholecystokinin and gastrin, and also by neural stimuli. The acini and smaller ducts are encapsulated by a delicate, loose connective tissue or septa, which becomes more extensive around the larger ducts.

1.2.3. The Endocrine Pancreas

The endocrine cells are predominantly aggregated into the islets of Langerhans. The islets are compact spheroidal clusters embedded in the exocrine tissue and form the functional endocrine units of the pancreas (**Figs. 1.3.** and **1.4.**). The human pancreas contains approximately one million of these structures and although distributed throughout the organ, they are more abundant in the tail. The islets vary considerably in size, ranging from tens of cells to several thousand though all are richly vascularised by a network of fenestrated capillaries.

Figure 1.3. Schematic of Histological Architecture in the Mammalian Pancreas (Reproduced from *Color Textbook of Histology*, Gartner, L. P. and Hiatt, J. L., p. 342, Copyright [1997], with Permission from Elsevier)

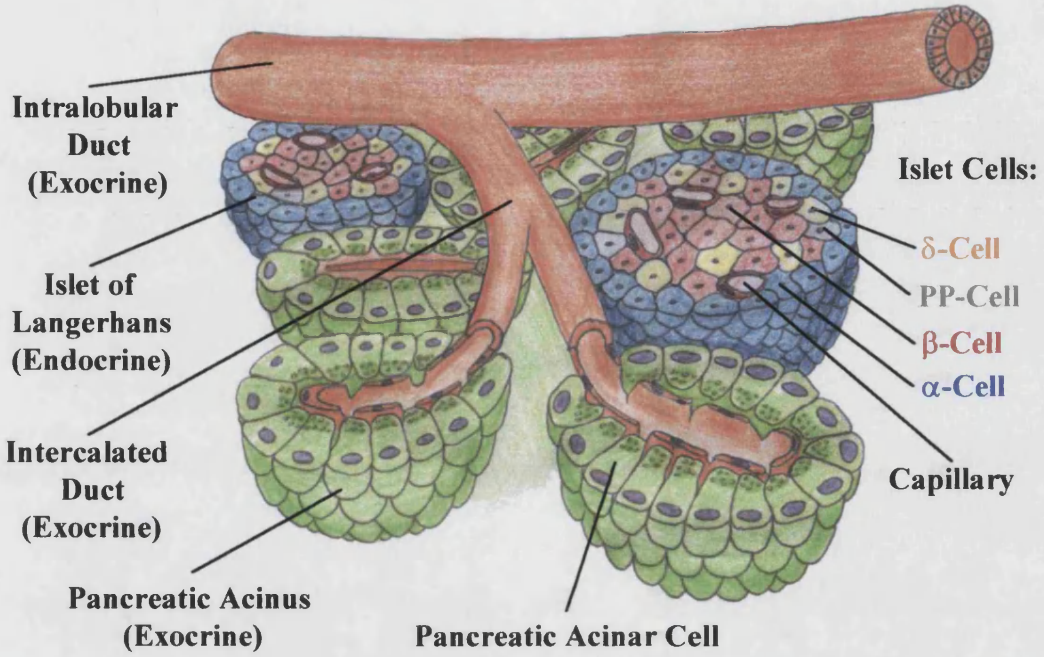

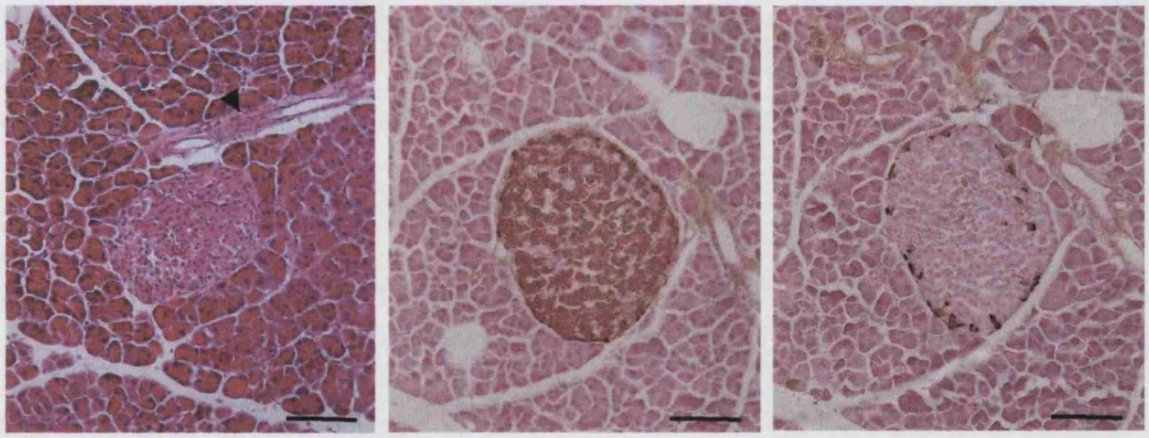

Figure 1.4. Histology of the Adult Mouse Pancreas

(a) An islet adjacent to a duct (arrowhead), surrounded by secretory acini (H & E stain). (b) Immunostaining for insulin showing β-cells in centre (core) of islet. (c) Immunostaining for glucagon, revealing less numerous α-cells in the periphery (mantle) of the islet. Bar = 100 μm

There are four principal endocrine cell types within the islet. The β (or B) cells secrete the hormone insulin and the insulin antagonist amylin or islet amyloid polypeptide (IAPP). They constitute the majority (approximately 60-80 %) of the islet cells and form the core of the islet, around which cells of the other three endocrine cell types are arranged. The α (or A or A2) cells represent approximately 20 % of the islet cells and are generally located around the periphery or mantle of the islet. They synthesise and secrete the hormone glucagon. They respond to gastrointestinal hormones, neural inputs and paracrine agents such as the insulin secretion inhibitor somatostatin (SS), secreted by the δ (or D or A1) cells which form about 5 % of the islet cells. Finally, the PP (or F or γ) cells can constitute up to 1 % of the islet cells. They release pancreatic polypeptide (PP), a paracrine inhibitor of acinar cell secretion. A fraction of the adult islet cells synthesise peptide YY in addition to their principal product (Ali-Rachedi *et al.*, 1984). Activin A, a member of the TGF-β superfamily, is abundant in the A and D cells (Yasuda *et al.*, 1993). In rodents, there is a marked delineation within the islets between the central β-cells and the peripheral cells of other types. Although present, such segregation in humans is less pronounced. Despite their obvious functional significance, the proportion of endocrine cells is a small fraction of the total, accounting for only about 4 % of total cells in the adult rat (Githens, 1988). Small numbers of endocrine cells also occur outside the islets: so-called extra-insular β-cell clusters or single cells, some of them duct-associated, represent less than 1 % of all beta cells in the rat pancreas (Wang *et al.*, 1994, 1995). Endocrine cells which synthesise glucagon, somatostatin, amylin and peptide YY are present elsewhere in the gut in addition to the pancreas. All islet cell types, further to their specific hormones, also express a number of gene products characteristic of neuroendocrine cells, such as neuron-specific enolase, tetanus toxin receptor, A2B5 antigen (Le Douarin, 1988) and the homeodomain-LIM protein Islet-1 or Isl1 (Thor *et al.*, 1991). The whole of the early pancreatic rudiment also expresses the enzyme L-amino acid decarboxylase (AADC), which becomes confined to islet cells postnatally (Teitelman *et al.*, 1987). The enzyme tyrosine hydroxylase is also expressed by some cells in the early pancreas, although this is not an invariable characteristic (Teitelman and Lee, 1987).

1.2.3.1. Insulin and Diabetes

Insulin is a dimeric disulphide-linked protein. It is synthesised as a single chain precursor which initially loses its signal peptide, before losing its so-called "C-peptide"

segment during conversion to the mature hormone molecule. Mature insulin is stored in secretory granules and its release is modulated by the level of glucose in the perfusing blood. The effects of insulin on the target tissues are both metabolic, especially in promoting glucose uptake, and mitogenic. The hormone acts via a tyrosine kinase type receptor, the major intracellular target of which is insulin receptor substrate 1 (IRS-1; Siddle, 1992).

β-Cell function and insulin synthesis is of great consequence to the well-being of the animal. Decreased insulin secretion or impaired insulin action leads to diabetes mellitus, of which there are two principal forms. Type 1 or insulin-dependent diabetes, found most often in children and young people, manifests itself as β-cell destruction as a result of an autoimmune reaction. Severe permanent insulin deficiency consequently ensues. Type 2 or non-insulin-dependent diabetes is the most common form of diabetes, accounting for more than 90 % of diagnosed cases and affecting about 4 % of the population worldwide. It is more frequently an affliction of mature individuals and is a more complex and heterogeneous range of conditions. Type 2 diabetes usually involves a degree of insulin non-responsiveness in the target tissues, β-cell dysfunction, or a combination of both. It may involve a contribution from pancreatic pathology since the islets of patients are frequently invested with a deposit of amyloid, the major component of which is a precipitated form of the amylin produced by the β-cells. The manifestations of the illness are widespread. Diabetes mellitus causes premature death and prolonged ill health from severe complications including kidney, cardiovascular, and eye disease (reviewed by Sander and German, 1997). A more comprehensive understanding of β-cell biology and islet and pancreas development in general would be beneficial to the development of improved therapy for type 1 diabetes, either by stimulating β-cell regeneration or by being able to culture and graft β-cells between individuals.

1.2.4. Blood and Nervous Supply

In addition to its glandular components, the pancreas possesses an extensive blood supply; arterial blood passes in each lobule first to the islets and then to the surrounding acini. There is also an extensive lymphatic drainage, and a rich sympathetic and parasympathetic nerve supply. Smooth muscle occurs around the larger ducts and in the sphincter muscles of the two ampullae. The fibroblastic, lymphatic and smooth

muscle components of the pancreas are presumed to arise from the abundant mesenchyme enveloping the embryonic pancreatic buds.

1.3. Pancreatic Morphogenesis

1.3.1. Origin from Two Buds

Much of today's knowledge of the morphological development of the early mammalian pancreas stems from the detailed descriptions of Wessels and Cohen (1967), Pictet *et al.* (1972) and Pictet and Rutter (1972). Relatively little has been contributed to the understanding of the morphological basis of pancreas development in the intervening years. Many aspects of pancreatic development are homologous between species, especially during the early phases. A distinctive feature of pancreatic development in mammals, birds and amphibians is that the pancreas originates embryologically as separate dorsal and ventral rudiments which initially develop independently before meeting and fusing to form a single organ (Slack, 1995) (**Figs. 1.2.** and **1.5.**). In the mouse at around embryonic day 9.5 (E9.5), the dorsal pancreatic bud first appears as an evagination in the primitive gut endoderm, near the junction of the foregut and midgut in the area that is destined to give rise to the duodenum (Wessells and Cohen, 1967). Approximately one day later, the ventral pancreatic bud arises on the opposite side of the gut tube, immediately adjacent to the hepatic diverticulum, its developmental progression mirroring that of the dorsal bud albeit with a small time delay (Spooner *et al.*, 1970). It remains unclear how the initially separate programs of dorsal and ventral pancreatic bud development are coordinated to produce a convergent developmental program.

Owing to differential growth of the foregut wall, the stomach and duodenum rotate to the left. The ventral pancreatic rudiment and hepatopancreatic orifice (hepatic duct) migrate round the foregut until they come into apposition with the dorsal bud and at around E16-17 fusion of the two buds occurs (Pictet and Rutter, 1972). The dorsal bud gives rise to the majority of the pancreas whilst the ventral bud forms only the posterior portion of the head, or uncinate process which remains visible postnatally in humans. Although the dorsal pancreatic rudiment is the larger of the two, it is the ventral duct which persists as the main pancreatic duct (duct of Wirsung) by fusing with the distal part of the dorsal duct. The remnant, proximal part of the dorsal duct regresses, though it is not uncommon for the dorsal duct to persist into adulthood as a

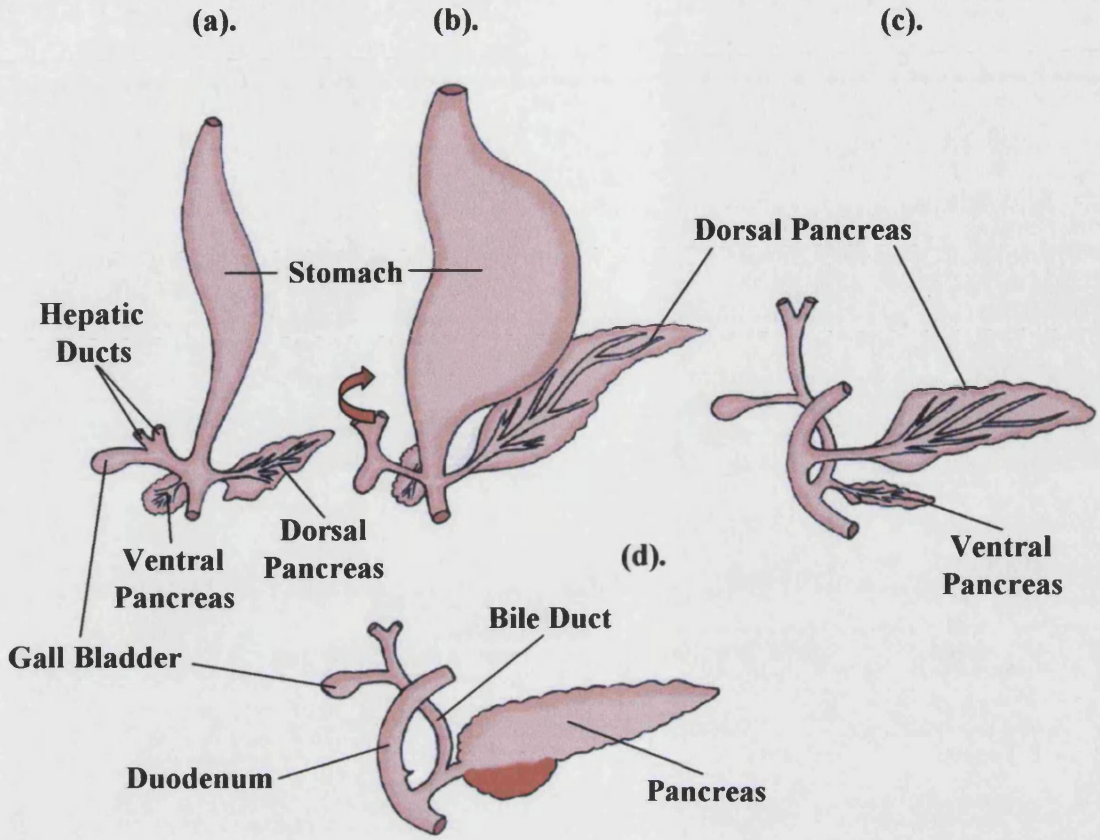

Figure 1.5. Schematic Diagram Showing the Development and Fusion of the Pancreatic Buds to Form the Pancreas in the Mouse. (After Dubois, 1989)

The two pancreatic primordia are shown in ventral view, prior to fusion in (a)-(c). Owing to differential growth of the foregut wall, the stomach and duodenum rotate to the left (b). The ventral bud and hepatopancreatic orifice (hepatic duct) migrate round the foregut until they come into apposition with the dorsal bud and fusion of the two buds occurs at around E16-17 (Pictet and Rutter, 1972).
The dorsal pancreatic bud gives rise to the main mass of the adult pancreas whilst the ventral bud forms the uncinate process, the posterior part of the head of the organ, highlighted in (d)

small accessory pancreatic duct (duct of Santorini), typically with its own opening into the duodenum.

1.3.2. Appearance of Endocrine Cells

The pancreatic buds grow into their surrounding mesoderm and rapidly form new protrusions, leading to a highly branched structure. *In vitro* studies suggest that this budding of the epithelium may be driven by a local increase in cell division (Horb and Slack, 2000). The tubules subsequently terminate in distinct aggregates of cells, the presumptive acini. Murine acini and ducts become clearly visible as histologically differentiated structures by E14.5. Low levels of the various terminal differentiation products can be detected throughout pancreatic development (the "protodifferentiated state"; Pictet and Rutter, 1972, further extended to the reverse transcriptase-polymerase chain reaction [RT-PCR] level in Gittes and Rutter, 1992). Somatostatin mRNA can be detected prior to formation of the pancreatic anlage as early as E8.5; insulin and glucagon mRNA expression can be observed from E9.5, PP from E10.5, and amylase mRNA from E12.5 (Gittes and Rutter, 1992; Herrera *et al.*, 1991). Amylase becomes detectable by immunostaining from about E14.5. Endocrine cells can be detected in the forming pancreas from the earliest stages. As a consequence of the temporal divergence in development between the two pancreatic buds, the first endocrine cells appear in the dorsal bud at least 36 h prior to the overt differentiation of endocrine cells in the ventral bud (Pictet and Rutter, 1972; Spooner *et al.*, 1970). Three immunostaining studies on the formation of the endocrine cells (Herrera *et al.*, 1991; Teitelman *et al.*, 1993; Upchurch *et al.*, 1994) have generated conflicting results. Certain common conclusions can, however, be extrapolated: the first cells containing insulin or glucagon appear at about E9.5 in the dorsal pancreatic bud. These early endocrine cells frequently reside in the region lining the ductules (Wessells and Evans, 1968). As insulin-containing cells have been reported to be much less prevalent at E9.5 than glucagon-containing cells, many of which lack insulin reactivity, this has prompted the idea that glucagon-expressing cells appear initially in endocrine development (Herrera *et al.*, 1991; Pictet and Rutter, 1972; Teitelman and Lee, 1987; Upchurch *et al.*, 1994). It has recently been shown that blocking the early expression and function of glucagon prevents insulin-positive differentiation in E11 mouse pancreas, leading to speculation that glucagon plays a key role in the paracrine induction of differentiation of other pancreatic components in the early embryonic pancreas (Prasadan *et al.*, 2002). At E10.5-11.5,

cells are frequently observed expressing insulin and glucagon simultaneously. Somatostatin- or PP-expressing cells only arise later in development; somatostatin appears in the primordial pancreas at around E15 and then PP is first detected perinatally (Teitelman and Lee, 1987; Teitelman *et al.*, 1993; Upchurch *et al.*, 1994). During development, the majority if not all of the immature endocrine cells coexpress PYY, but only a fraction of the mature islet cells continue to coexpress PYY in addition to their principal product (Upchurch *et al.*, 1994). As mentioned, it has been frequently observed that between E10.5 and E14.5, many of the early endocrine cells stain simultaneously with antibodies to multiple hormones (both insulin and glucagon for example). This is in contrast to the "*one cell, one hormone*" rule which applies to the postnatal pancreas, so there is a distinction to be made between such early multihormone-expressing cells and the later mature endocrine cells (Slack, 1999). Indeed it has been proposed that the multihormone-expressing population represent endocrine cell precursors (Alpert *et al.*, 1988). Also expressed in early endocrine cells are the enzyme tyrosine hydroxylase (Teitelman, 1990), and the signalling molecule activin (Yasuda *et al.*, 1993), implicated in a wide variety of developmental processes.

1.3.2.1. PP-Fold Peptides

There has been much debate over expression of the "PP-fold" peptides in the developing pancreas. The three peptides, pancreatic polypeptide (PP), neuropeptide Y (NPY) and peptide YY (PYY), exhibit very similar primary sequences. Antibodies specific to one frequently cross-react with the others. PP is one of the products of a subset of the mature endocrine cells and is postulated to play a physiological role in the antagonism of insulin secretion. Some evidence suggests the expression of PP in the early multihormone cell population (Herrera *et al.*, 1991), although this has also been claimed to be NPY (Teitelman *et al.*, 1993). The most widely supported view however is that it is PYY which is expressed in many or all of the early endocrine cells (Upchurch *et al.*, 1994). It has not been resolved whether such cells are actually the precursors of the mature endocrine cells.

1.3.3. Islet Development

The pancreas grows very rapidly during the midgestation period with vascularisation occurring from about E14 in mouse. By E15.5, endocrine cells

constitute about 10 % of the total cells although they are still predominantly individual and associated with the ducts. Islets, with the characteristic distribution of insulin-expressing cells in the centre and non-insulin-producing cells in the periphery, do not form until the end of gestation, at about E18.5 in the mouse (Herrera *et al.*, 1991). The presumptive islets form as aggregates or "clumps" of cells, distinct from those of the terminal structures, which bud off from the walls of the smaller branches. These early endocrine cells separate from the cell layer of the developing exocrine gland, probably by a change in the axis of cell division allowing the escape from the ductule lumen of one of the daughter cells (Pictet and Rutter, 1972). Expression of the cell adhesion molecule R-cadherin in the intraductal primitive endocrine cells disappears prior to islet formation; this downregulation is associated with and presumably facilitates, migration out of the duct epithelium to form islets (Hutton *et al.*, 1993; Sjödin *et al.*, 1995). Migration of endocrine cells into the extracellular matrix and islet morphogenesis are probably dependent on matrix degradation by activated matrix metalloproteinases (MMPs). MMP overactivation *in vitro* has been shown to result in a perturbation of normal islet architecture (Miralles *et al.*, 1998a). As the presumptive islet cell groups migrate away from the tubules into the stroma of the developing gland, new aggregates continue to form and bud off. It is not yet known to what extent islet formation occurs by aggregation of pre-existing cells or by monoclonal growth from individual precursors. The islets may expand by merging or recruiting cell clusters in close proximity or through proliferation of the islet cell precursors or through a combination of the two. In an aggregation chimera study using human C-peptide/proinsulin product as a cell marker, islets were seen that contained cells from both aggregated embryos, suggesting that at least some islets are formed by cell aggregation (Deltour *et al.*, 1991). Conclusions were, however, drawn from only two informative cases. In a more recent study (Percival and Slack, 1999), it was demonstrated that when pancreatic epithelium from transgenic ROSA-26 mouse embryos which ubiquitously express *Escherichia coli* β-galactosidase is recombined with mesenchyme from unlabelled embryos, both individual acini and individual islets in the resulting culture are frequently of mixed cellular composition. This study also suggests that the islets are initially formed by cell aggregation although it must be assumed that events *in vitro* accurately reflect those *in situ*. The rate of increase of endocrine cell numbers could be accounted for by multiplication of the precursors present early in development, but a cell kinetic study in the rat by Kaung (1994) suggested recruitment into the endocrine population both preceding and following birth. The integrity of the islets is apparently reliant on cell

adhesion. Transgenic mice in which a dominant negative E-cadherin gene is driven by the insulin promoter exhibit a failure of β-cells to aggregate, though α-cells are unaffected and selectively aggregate into clusters lacking β-cells (Dahl *et al.*, 1996). Neural cell adhesion molecule (N-CAM) has been shown to play a role in the segregation of islet cells *in vitro* and it is presumed that owing to its expression being mostly confined to peripheral non-β-cells, it is principally responsible for maintaining this peripheral arrangement *in vivo* (Cirruli *et al.*, 1994; Rouiller *et al.*, 1990).

1.4. Pancreatic Determination and Transcription Factor Expression

1.4.1. Timing of Pancreatic Determination

It is not known precisely when the pancreatic anlage is specified in relation to the surrounding endoderm. However, Wessells and Cohen (1967) showed that by E8.5 in the mouse the region of the embryonic foregut from which the pancreas develops has acquired the ability to give rise to a differentiated pancreas when explanted and cultured *in vitro*. Dorsal gut endodermal cells are committed towards a pancreatic fate prior to the appearance of the first terminal differentiation products. Using RT-PCR, Gittes and Rutter (1992) were able to detect somatostatin mRNA at E8.5, preceding the first morphological evidence of pancreas development by one day. It cannot be excluded that the future pancreatic endodermal cells are subdivided into an endocrine and an exocrine compartment prior to bud formation (Sander and German, 1997). It is presumed that the fate of the individual endodermal cells is determined by an intrinsic "epigenetic code" established by the expression of a distinct set of transcription factors in the cells of the future pancreatic anlage (Sander and German, 1997). Transcription factor expression permits cells in this region to respond to the signals from the pancreatic mesenchyme or other surrounding tissues that induce pancreatic growth and cell differentiation.

1.4.2. Endoderm Formation and Extrinsic Signals Initiating Pancreatic Bud Outgrowth

1.4.2.1. Signals from the Notochord

In the mouse, the three germ layers, endoderm, ectoderm and mesoderm, are established by the close of gastrulation at E7.5. Little is known regarding the nature of

signals instructing the pluripotent embryonic cells to form endoderm. However, numerous soluble growth factors are produced in the adjacent germ layers and are presumed to influence endoderm patterning. Recently, the mesodermal Fibroblast Growth Factor (FGF)4 has been implicated in early endoderm specification (Wells and Melton, 2000). FGF4 is able to induce the expression of specific pancreatic genes in the endoderm *in vitro*. Further data from Wells and coworkers also suggests that these soluble factors render the endoderm competent to respond to subsequent inductive signals from the adjacent notochord. Two members of the hedgehog family of signalling molecules, Sonic hedgehog (Shh) and Indian hedgehog (Ihh), are together expressed uniformly, although in a partially overlapping manner, in regions of the gut endoderm anterior and posterior to the position at which the pancreas develops (Apelqvist *et al.*, 1997; Bitgood and McMahon, 1995). In the pancreatic endoderm, the expression of both Shh and Ihh is restricted to the lateral prospective intestinal part of the epithelium and is excluded from both the dorsal and ventral pancreatic epithelium (Apelqvist *et al.*, 1997; Bitgood and McMahon, 1995). Repression of Shh in the pancreatic endoderm has been shown to be critical for proper pancreas development since ectopic expression of Shh in the prospective pancreatic epithelium of the posterior foregut results in disrupted pancreatic morphogenesis (Apelqvist *et al.*, 1997) and a compensatory enhancement of intestinal development with inhibition of spleen development.

The region of the gut epithelium fated to form the dorsal pancreatic bud is initially in direct contact with the notochord (Slack, 1995; Wessells and Cohen, 1967) (**Fig. 1.6.**). It has been demonstrated that activin-βB, a member of the transforming growth factor β (TGF-β) family, and FGF2 which are both expressed by the notochord, are able to repress *Shh* and *Ihh* expression in the presumptive dorsal pancreatic endoderm (Hebrok *et al.*, 1998; Kim *et al.*, 1997; Kim and Melton, 1998). Abrogation of Shh function invokes a relative increase in endocrine cell number and pancreas size (Hebrok *et al.*, 2000) and mutations of activin receptor ActRIIA and ActRBII lead to a disruption in pancreas development (Kim *et al.*, 2000). Under such conditions, islets are formed, but insulin expression is markedly reduced, showing that type II activin receptors are required for endocrine differentiation in pancreas. In contrast, the ventral gut epithelium fated to form the ventral pancreatic bud is never contacted by the notochord, implying that the exclusion of *Shh* and *Ihh* gene expression from the ventral pancreatic epithelium is achieved by a distinct notochord-independent mechanism.

Figure 1.6. Signals Initiating Outgrowth of the Dorsal and Ventral Pancreatic Buds

(a). Before the formation of the pancreatic buds, a pre-patterning of the gut endoderm renders the dorsal endoderm competent to respond to specific signals from the notochord (dark blue arrows) and cardiac mesoderm (red arrows):

- Notochord factors such as activin-βB, FGF2 and probably other unidentified factors repress endodermal *Shh* and *Ihh* expression (dark blue arrows), permitting the expression of *Pdx1* and other pancreatic developmental genes (blue region) - outgrowth of the dorsal pancreatic bud (DB) is initiated

- FGF signalling from the cardiac mesoderm is sufficient (uniformly red arrow) to direct proximal endoderm from the default pancreatic fate to a hepatic fate (green region). Endoderm that is *not* proximal to the cardiac mesoderm, for example at the lip that extends the foregut to the midgut, does *not* receive sufficient FGF from the cardiac mesoderm (red fading arrow) to activate the hepatic developmental program. Therefore, the intrinsic developmental program for pancreas is followed without perturbation (blue region), allowing the ventral pancreatic bud (VB) to form. While the cardiac mesoderm has a net positive effect on hepatic induction, mechanistically it appears to block the intrinsic program for pancreas and thereby promote liver development within the ventral foregut endoderm

(b). As the pancreatic buds form and proliferate, factors produced by the mesenchyme surrounding the pancreatic epithelium promote the development of the exocrine tissue while inhibiting endocrine differentiation (pale blue arrows). Follistatin and additional unknown factors probably participate in this process. Proximal endoderm meanwhile, continues to follow a program of hepatic development (green arrows), giving rise to the liver

(After Deutsch *et al.*, 2001 and St.-Onge *et al.*, 1999)

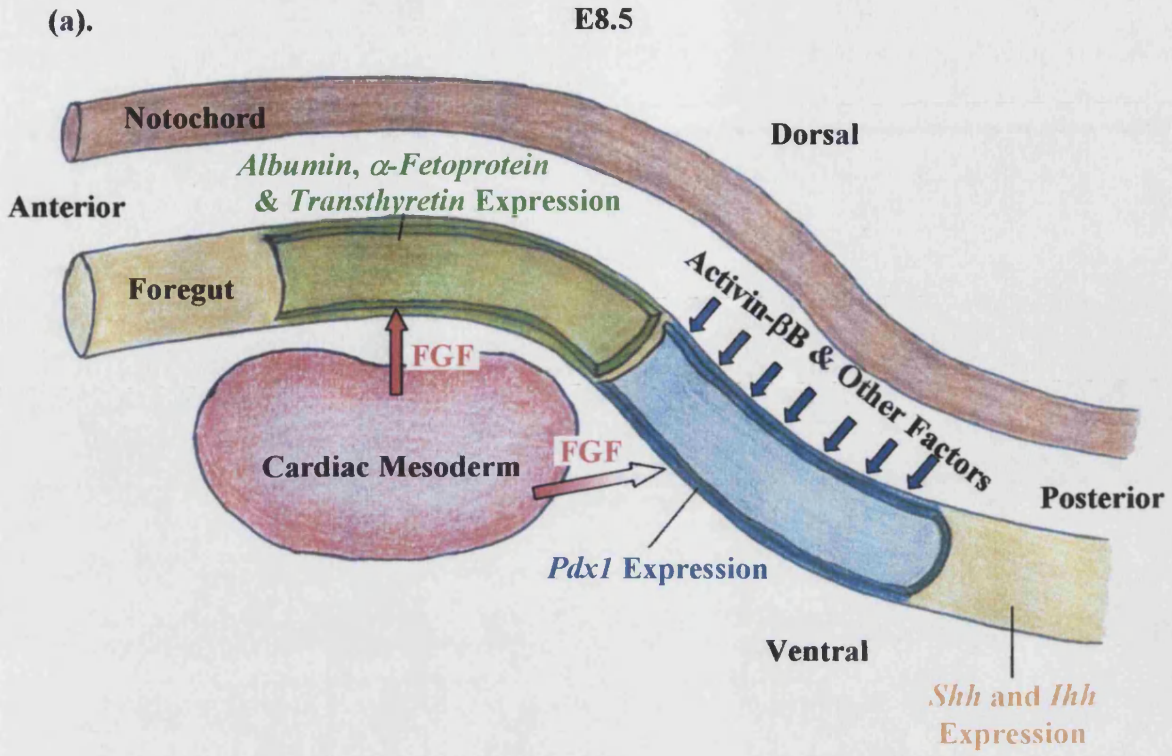
(a).
E8.5
Notochord
Dorsal
Albumin, α-Fetoprotein
& Transthyretin Expression
Anterior
Foregut
Activin-βB & Other Factors
FGF
Cardiac Mesoderm
FGF
Posterior
Pdx1 Expression
Ventral
Shh and Ihh
Expression

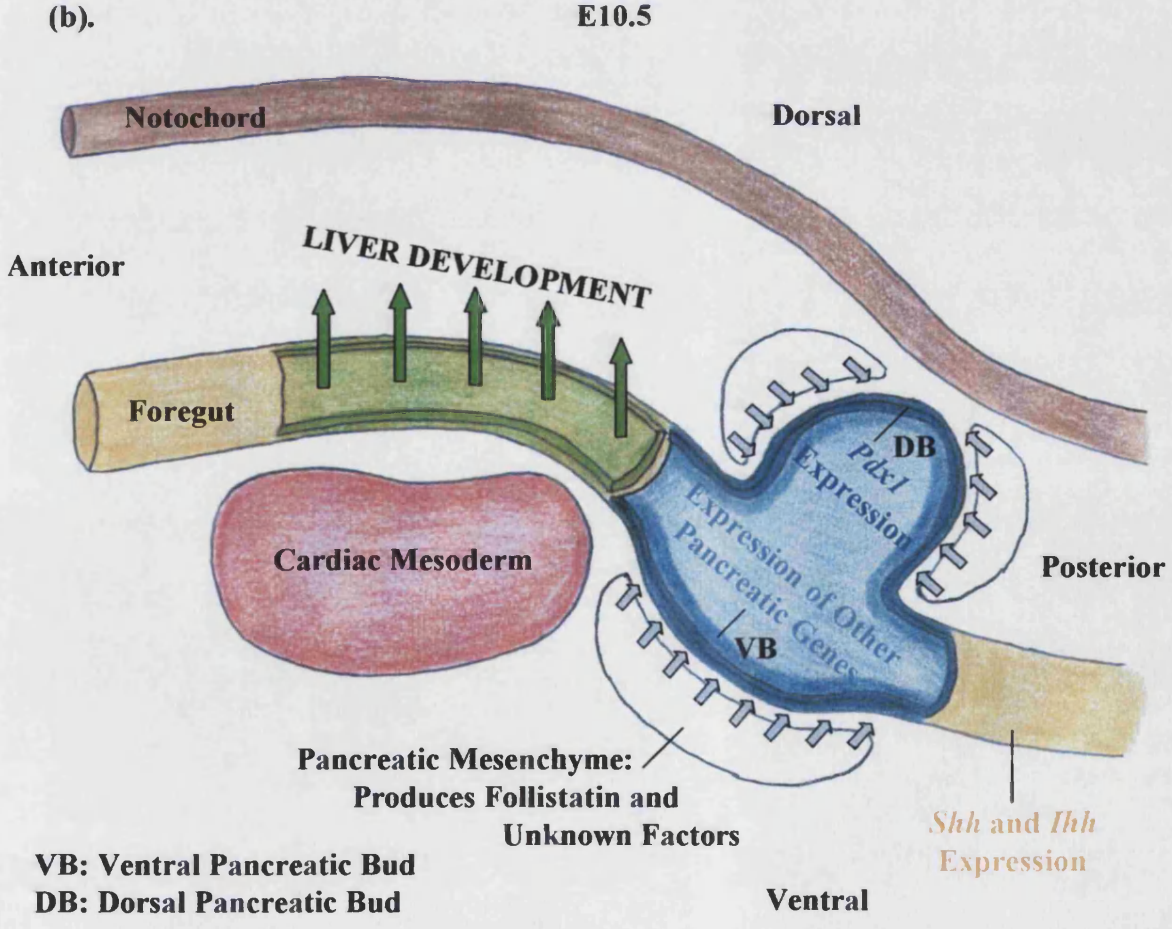
(b).
E10.5
Notochord
Dorsal
LIVER DEVELOPMENT
Anterior
Foregut
DB
Pdx1
Expression
Expression of Other
Pancreatic Genes
Cardiac Mesoderm
Posterior
VB
Pancreatic Mesenchyme:
Produces Follistatin and
Unknown Factors
Shh and Ihh
Expression
VB: Ventral Pancreatic Bud
DB: Dorsal Pancreatic Bud
Ventral

1.4.2.2. Signals from the Cardiac Mesoderm

A more recent study has offered insight into the mechanisms responsible for patterning of the ventral endoderm and so generation of the ventral pancreas. The ventral endoderm from which the ventral pancreatic bud derives, lies in close proximity to the developing heart and can also give rise to liver cells or hepatocytes (Gualdi *et al.*, 1996), suggesting that development of the pancreas and liver is related. Deutsch and colleagues (Deutsch *et al.*, 2001) showed that E8.5 ventral endoderm lying adjacent to the cardiac mesoderm gives rise to cells expressing the liver marker albumin whilst cells expressing the pancreatic marker, Pdx1, originate from a region of endoderm extending beyond the cardiac anlage. This indicates that both tissues derive from non-overlapping domains of ventral endoderm. Hepatic development has been shown to be induced by FGFs secreted from the cardiac mesoderm which act on the underlying ventral endoderm (Jung *et al.*, 1999); ventral endoderm cultured in the absence of FGF or cardiac tissue fails to activate an hepatic developmental program. Deutsch and coworkers (Deutsch *et al.*, 2001) demonstrated that if isolated endoderm from 2-6 somite-stage embryos prior to its interaction with the cardiac mesoderm, is cultured in isolation, all ventral endoderm cells initiate expression of both exocrine and endocrine pancreatic markers. If cultured with cardiac mesoderm or FGF2 however, pancreatic development is inhibited and the endoderm cells progress towards a hepatic fate. These findings can be explained by a model in which ventral endoderm cells are bipotential, competent to follow either a pancreatic or hepatic developmental program and are actively driven towards a hepatic fate by the action of cardiac-secreted FGFs (**Fig. 1.6.**). Therefore, ventral endoderm lying beyond the immediate vicinity of the cardiac mesoderm gives rise to the ventral pancreas by a default program of pancreatic differentiation followed in the absence of cardiac-secreted FGFs. So, in the development of the ventral pancreas, FGFs inhibit the pancreatic program, whereas they function to promote development of the dorsal bud.

1.4.2.3. Signals from the Mesenchyme

In addition to the cardiac mesoderm, the pancreatic mesenchyme may provide an extrinsic signal for induction of pancreatic anlage formation. At the same stage that the notochord is in apposition to the dorsal gut endoderm the lateral sides of the gut are enclosed by mesenchyme (**Fig. 1.7.**). When the notochord separates from the dorsal gut

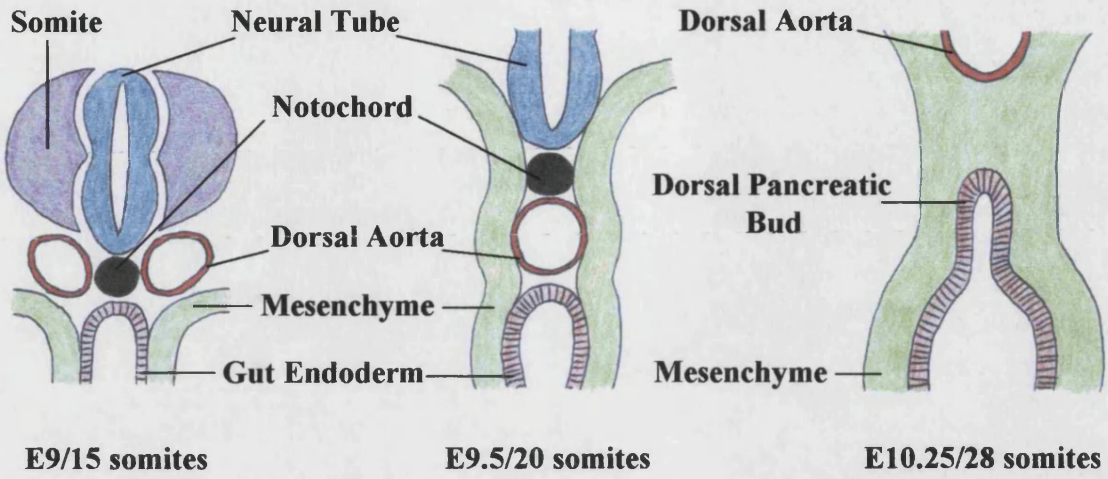

Figure 1.7. Orientation of the Mesenchyme and Notochord with Respect to the Gut Endoderm in the Early Development of the Mouse Pancreas. Views are from the Dorsal Aspect. (After Slack, 1995 and Yamaoka and Itakura, 1999)

At the 15-somite stage the notochord lies in apposition to the neural tube and gut; by the 20-somite stage the dorsal aorta separates the gut and notochord. By the 28-somite stage mesenchyme surrounds the entire gut and the dorsal pancreatic bud has formed

at E9 the mesenchyme begins to accumulate on the dorsal side of the gut. The exact timing of mesenchyme accumulation in the region of the dorsal pancreatic bud is contentious: either prior to or simultaneous with bud formation (Gittes and Rutter, 1992; Pictet and Rutter, 1972; Wessells and Cohen, 1967) or immediately subsequent to bud formation (Ahlgren *et al.*, 1996). Resolving the exact timing is significant. Mesenchyme induces pancreatic growth and differentiation in culture and so could be the inducer of bud formation if it is present at the appropriate time.

It has been known for some time that the Hox gene cluster specifies anterior-posterior positional value in the central nervous system and axial mesoderm (McGinnis and Krumlauf, 1992; Slack *et al.*, 1993). Although not expressed in the endodermal epithelium, these genes are expressed in the early developing gut mesenchyme (Roberts *et al.*, 1995; Yokouchi *et al.*, 1995). It has been suggested that the mesenchyme dictates the positional character of the epithelium through mesenchymal-epithelial inductive interactions (Wessells, 1977). Hence, the Hox gene state might be transmitted via extracellular factors that induce regionally-specific non-Hox factors in the epithelium (Roberts *et al.*, 1998).

So in summary, activin-βB and FGF2 from the notochord repress *Shh* and *Ihh* expression in the adjacent presumptive dorsal pancreatic endoderm, allowing formation of the dorsal pancreas. The ventral pancreas is formed by a default developmental program from bipotential ventral endoderm cells lying beyond the "sphere of influence" of FGFs secreted from the cardiac mesoderm which otherwise actively drive the same cells towards a hepatic fate. Therefore FGFs function to promote development of the dorsal pancreas, whereas in the development of the ventral pancreas they act to inhibit the pancreatic program.

1.5. Role of Transcription Factors in Pancreas Development

Following gut closure, transcription factors are expressed in a nested manner in the definitive endoderm. Those involved in pancreas development belong to three distinct families: the homeodomain family, the basic helix-loop-helix (bHLH) family and the winged helix family of proteins. Within the last decade, a large number of gene disruption studies in mice have contributed massively to our understanding of the function and hierarchy of transcription factors in pancreas development.

Hepatocyte Nuclear Factor (HNF)-3β/Forkhead Box (Fox) a2

HNF-3β or Foxa2 is a winged helix transcription factor. It is a member of the HNF3 family of forkhead-related genes, expressed in the gut epithelium and initially identified as transcriptional regulators of hepatocyte-specific genes (Lai *et al.*, 1991; Liu *et al.*, 1991). HNF-3β is first expressed at E5.5-6.5 in the anterior part of the early primitive streak and then later in the definitive endoderm (Ang *et al.*, 1993; Monaghan *et al.*, 1993; Ruiz i Altaba *et al.*, 1993; Sasaki and Hogan, 1993). Homozygous inactivation of HNF-3β in mice results in defects in foregut morphogenesis. The null mutants die around E11 however (Ang and Rossant, 1994; Weinstein *et al.*, 1994), precluding detailed analysis of the role of HNF-3β in pancreas formation. It is envisaged that tissue-specific inactivation of the gene will overcome this limitation. HNF-3β has been reported to upregulate the expression of another pancreatic transcription factor, Pdx1 (Wu *et al.*, 1997; see below), indicating a role in maintaining β-cell function. Most recently it has been shown that a β-cell-specific deletion of HNF-3β results in downregulation of *Pdx1* mRNA and a subsequent reduction of Pdx1 protein levels in islets, providing the first *in vivo* demonstration that HNF-3β acts upstream of *Pdx1* in the differentiated β-cell (Lee *et al.*, 2002).

Hepatocyte Nuclear Factor (HNF)-3α/Forkhead Box (Fox) a1

HNF-3α, recently reassigned as Foxa1, is a member of the same family of transcription factors as HNF-3β. Like HNF-3β, it exhibits a wide expression pattern and is expressed in the endoderm from E7.5. Targeted disruption of HNF-3α results in a 70 % reduction of glucagon mRNA levels whilst the number of pancreatic α-cells remains undiminished (Kaestner *et al.*, 1999). The decreased glucagon level was therefore attributed to reduced transcriptional activity of the glucagon gene (Kaestner *et al.*, 1999).

Hlxb9

The protein Hb9 encoded by the homeobox gene *Hlxb9* (Harrison *et al.*, 1994) is expressed earliest at E8 in the epithelium of the foregut-midgut junction (Li *et al.*, 1999). It is transiently expressed in the developing pancreatic anlagen: by E12.5, its

expression level decreases but one day later expression increases again in the dorsal and ventral region of the pancreas (Harrison *et al.*, 1999). By E17.5, Hb9 is restricted to islet cells and in the adult pancreas it becomes further restricted to only the β-cells. Targeted disruption of Hlxb9 leads to absence of the dorsal pancreas and a lack of dorsal expression of the transcription factors Pdx1 and Isl1. The ventral portion of the pancreas develops normally, expresses Pdx1 and subsequently generates exocrine cells and all four types of endocrine cell. This would imply that early development of the ventral pancreas is independent of Hb9. However, at E18.5, islets are reduced in size due to a specific 65 % decrease in the number of insulin-immunopositive cells. Hb9 is therefore required dorsally for specifying gut epithelium to a pancreatic fate and ventrally for ensuring the terminal differentiation and maturation of β-cells. The requirement for Hlxb9 in pancreatic development also reveals a molecular distinction in the dorsal and ventral bud differentiation programs.

Pancreatic Duodenal Homeobox 1 (Pdx1)/Insulin Promoter Factor 1 (Ipf1)

The most prominent of those genes expressed specifically in the early pancreatic buds is *Pdx1* (also known as *Ipf1, Idx1, Stf1, Iuf1* or *XlHbox8*) (Miller *et al.*, 1994; Offield *et al.*, 1996; Ohlsson *et al.*, 1993; Wright *et al.*, 1988). It was initially characterised in mammals as a homeobox-containing transcription factor and transactivator of the somatostatin (Leonard *et al.*, 1993; Miller *et al.*, 1994) and insulin genes (Ohlsson *et al.*, 1993; Peers *et al.*, 1995; Peshavaria *et al.*, 1994; Petersen *et al.*, 1994). More recently, it has been found to also transactivate the gene promoters of the glucose transporter GLUT2 (Waeber *et al.*, 1996), glucokinase (Watada *et al.*, 1996c), and amylin (Carty *et al.*, 1997; Watada *et al.*, 1996a). It has been proposed that *Pdx1* activation is dependent to some degree on HNF-3β (Sharma *et al.*, 1996, 1997; Wu *et al.*, 1997). *Pdx1* is homologous to a gene family expressed in the leech gut (Lox 3A, B, C; Wysocka-Diller *et al.*, 1995). As invertebrates lack a recognisable pancreas, this would suggest that *Pdx1* has been associated with gut development for a long evolutionary period and specifically with the pancreas from vertebrate origins (Slack, 1999). Pdx1 is uniformly expressed in the pancreatic bud at the foregut-midgut junction at E8.5 and marks the territory of the future pancreas (Ahlgren *et al.*, 1996). In later development expression becomes restricted to fully differentiated β-cells and the duodenal mucosa, with infrequent expression in δ-cells (Guz *et al.*, 1995; Leonard *et al.*, 1993; Miller *et al.*, 1994; Offield *et al.*, 1996; Ohlsson *et al.*, 1993; Wright *et al.*, 1988).

Pdx1 has been shown to be integral to pancreas development since its inactivation by targeted mutagenesis results in a suppression of pancreas formation (pancreatic agenesis), although there is some early bud development (Jonsson *et al.*, 1994; Offield *et al.*, 1996). Epithelium-mesenchyme recombinations have shown the defect to be associated with the epithelium, since the pancreatic mesenchyme grows and develops both morphologically and functionally, independent of the epithelium (Ahlgren *et al.*, 1996). Pdx1 is therefore required for growth and complete differentiation of the pancreatic buds. β-Cell-specific inactivation of Pdx1 later in development results in a 3.5-fold increase in the number of glucagon$^+$ cells but a 60 % decrease in the number of insulin-expressing cells and a loss of the β-cell phenotype and diabetes (Ahlgren *et al.*, 1998). In later development, Pdx1 positively regulates insulin and amylin expression and represses glucagon expression. Therefore, Pdx1 also plays an additional role in maintaining the insulin production and glucose-sensing system in β-cells.

Hepatocyte Nuclear Factor (HNF)6

HNF6 is a member of the one-cut class of homeodomain transcription factors, which share a common single cut domain and a divergent homeodomain (Lannoy *et al.*, 1998; Lemaigre *et al.*, 1996). During early embryonic development, HNF6 is expressed at E9.5 in epithelial cells of the pancreas, in pancreatic ducts, developing acinar cells and differentiating endocrine cells (Landry *et al.*, 1997; Rausa *et al.*, 1997). Expression is then downregulated in endocrine cells at late gestation, coincident with initiation of islet morphogenesis and separation from the ductal epithelium, suggesting that persistent *HNF6* expression is incompatible with islet maturation. Subsequent studies have confirmed that such *HNF6* downregulation is essential for the proper formation and function of islets (Gannon *et al.*, 2000). Targeted disruption of HNF6 leads to a normal exocrine pancreas although endocrine development is severely inhibited (Jacquemin *et al.*, 2000). At E9.5, glucagon expression is normal but at E12.5 no insulin-immunopositive cells are detected and the number of glucagon-expressing cells is reduced by 85 %. Neonatally, null mutants show a markedly reduced number of all four endocrine cell types. Furthermore, islet architecture is perturbed; α-cells are seen throughout the islet core instead of being restricted to the islet periphery. Expression of Pdx1 and a second transcription factor, Nkx6.1, is normal in nullizygous mice.

In the absence of HNF6, the epithelial cells are specified but fail to give rise to an expected pool of endocrine precursor cells. This hypothesis is supported by the

greatly diminished expression of neurogenin (ngn)3, a putative marker of endocrine precursor cells (Jensen *et al.*, 2000a; Schwitzgebel *et al.*, 2000). HNF6 and ngn3 are coexpressed in wild-type embryos in epithelial cells and transfection experiments have shown that HNF6 can stimulate the ngn3 promoter (Jacquemin *et al.*, 2000). This suggests that HNF6 regulates differentiation of endocrine precursors and identifies it as the first positive regulator of the pro-endocrine gene *ngn3* in the pancreas. Recent studies of the HNF transcriptional network indicate that HNF6 transactivates HNF-3β, which in turn transactivates HNF-4α, and then the latter transactivates HNF-1α (Duncan *et al.*, 1998; Kuo *et al.*, 1992; Rausa *et al.*, 1997). These HNFs are all expressed in the fetal and adult pancreas, and HNF-3β, as mentioned, is reported to upregulate Pdx1 gene expression (Rausa *et al.*, 1997; Wu *et al.*, 1997).

Neurogenin (Ngn)3

Discovered recently, ngn3 is a member of the basic helix-loop-helix (bHLH) family of transcription factors and is transiently but abundantly expressed in the developing pancreas (Schwitzgebel *et al.*, 2000; Sommer *et al.*, 1996). Ngn3 immunoreactivity is detected from E9.0-9.5 in the pancreatic anlage; expression increases to a peak at E15.5 then decreases thereafter with only a few ngn3-positive cells being detected at E18.5 (Apelqvist *et al.*, 1999; Jensen *et al.*, 2000a; Schwitzgebel *et al.*, 2000). Ngn3 is not detected in the adult pancreas. Ngn3 was found to be expressed in ductal and scattered periductal cells, which aroused interest as ductal cells are widely presumed to represent an islet cell precursor population. Studies demonstrating induction of precocious islet cell differentiation by early (E8.5) expression of ngn3 and a lack of expression in mature islet cells have lead to the supposition that ngn3 is expressed in islet cell progenitors and functions as a pro-endocrine gene driving islet cell differentiation (Apelqvist *et al.*, 1999). Coexpression with markers of differentiating endocrine cells, including Pdx1 and the β-cell differentiation factors Nkx6.1 and Nkx2.2 supports the idea that ngn3 marks islet cell precursors (Jensen *et al.*, 2000a; Schwitzgebel *et al.*, 2000). Absence of all islet cells in homozygous null mice bearing an otherwise grossly normal pancreas, shows that ngn3 is required for the formation of a common precursor for all four islet cell types (Gradwohl *et al.*, 2000).

NeuroD1/BETA2

The bHLH protein NeuroD1 or BETA2 (beta cell E-box transactivator-2) was cloned from a hamster insulinoma tumour cell cDNA library and initially identified as a differentiation factor for neurogenesis because it can convert *Xenopus laevis* ectoderm into neurons (Lee *et al.*, 1995). Expression commences from E9.5 in the pancreatic bud and can be induced by ngn3 (Huang *et al.*, 2000; Naya *et al.*, 1995; Schwitzgebel *et al.*, 2000). The majority of E9.5 pancreatic epithelial cells expressing NeuroD1 also express glucagon, indicating that NeuroD1 is present in the earliest islet precursors. In neonates, NeuroD1 is expressed in α-, β-, and δ-cells, but not in exocrine cells. In the adult, NeuroD1 expression becomes restricted to brain and islet α- and β-cells (Naya *et al.*, 1995). Loss of *NeuroD1* function results in a reduced number of differentiated β- (75 %), α- (40 %) and δ- (20 %) cells in neonates as well as disorganised islet architecture (Naya *et al.*, 1995, 1997). The depletion in cell number was shown to be largely due to apoptosis of endocrine cells. Despite the role of NeuroD1 as an activator of the insulin gene (Dumonteil *et al.*, 1998), the remaining β-cells in the homozygous null mice continued to produce insulin. The neonatal mice became diabetic however, dying 3-6 days after birth. In addition to activating the insulin gene, NeuroD1 also transactivates glucagon (Dumonteil *et al.*, 1998) and secretin genes (Mutoh *et al.*, 1998) and regulates selective expression of rat *Pdx1* (Sharma *et al.*, 1997).

Pax4

Pax4 is a paired domain homeobox (paired-box) gene. *Pax4* is expressed in the early pancreas from E9.5 but becomes restricted to the β-cells in adulthood (Sosa-Pineda *et al.*, 1997; Turque *et al.*, 1994). Mice nullizygous for Pax4 appear normal at birth, but are growth-retarded by 48 h and die 3-5 days following birth. The pancreas of neonatal null mutants is of normal size, but lack of expression of Pdx1 and somatostatin indicated an absence of mature β- and δ-cells respectively (Sosa-Pineda *et al.*, 1997). The *Pax4* knockout pancreas bears an unusually large number of α-cells however. During development at E10.5, glucagon- and insulin-producing cells are detected in *Pax4*-null mice at the same level as in wild-type animals at which time Pdx1 is also expressed. By E13.5 however, insulin is no longer detected and differentiated β-cell markers like Pdx1 and a second transcription factor, Nkx6.1 are also absent.

These studies demonstrate a requirement for Pax4 in β- and δ-cell differentiation. Although Pax4 is not critical for the development of early insulin-expressing cells, it is required for their maturation and maintenance. Two hypotheses have been proposed to account for the expansion in α-cell numbers in null mutant mice. Firstly, a significant proportion of early endocrine precursors could have lost their initial commitment to become β-cells and instead become α-cells. Secondly, the absence of the β-cell-specific gene *Pax4* could lead the progenitor cells towards a program of α-cell differentiation, so α-cells would be formed by default.

Nkx2.2

Nkx2.2 is a member of the NK class of homeodomain proteins. It is expressed from E9.5 at the onset of pancreatic bud evagination but becomes progressively restricted to the α-, β- and PP-cells of the mature islet; expression is absent from the δ-cells (Sussel *et al.*, 1998). Disruption of the *Nkx2.2* gene not only leads to a reduction in α- and PP-cell numbers, but also effects a specific block in late steps of β-cell differentiation, leading to an accumulation of incompletely differentiated β-cells (Sussel *et al.*, 1998). Such cells express some β-cell markers, like amylin and prohormone convertase (PC) 1/3, but not insulin. Amylin is a peptide hormone, normally co-secreted with insulin and PC 1/3 is a proinsulin processing enzyme that is restricted to the β-cells. In the Nkx2.2-null mutants, the early expression of the transcription factors Pdx1 and Nkx6.1 is not affected, but their later β-cell-restricted expression is disturbed. These mice develop diabetes neonatally and die as a consequence of hyperglycaemia (high blood glucose levels). These findings suggest the involvement of Nkx2.2 in the differentiation of all endocrine cell types. It would also appear to be required for the maintenance of Nkx6.1 expression and the upregulation of Pdx1 expression in β-cells, which are necessary for terminal β-cell differentiation.

Nkx6.1

Like Nkx2.2, Nkx6.1 is a member of the NK class of the homeodomain family of transcription factors (Jensen *et al.*, 1996; Oster *et al.*, 1998; Rudnick *et al.*, 1994). Nkx6.1 was cloned from a hamster β-tumour cell (HIT-T15 insulinoma) cDNA library (Rudnick *et al.*, 1994). The Nkx6.1 protein is expressed broadly in the pancreatic bud

from E10.5 then becomes restricted to insulin-positive cells and some scattered ductal and periductal cells by E15.5. In the adult pancreas, Nkx6.1 expression is restricted to the β-cells (Jensen *et al.*, 1996; Sander *et al.*, 2000). Targeted disruption of the *Nkx6.1* gene severely inhibits β-cell formation, but this defect is only manifested after E12.5 (Sander *et al.*, 2000). Until this stage of development, insulin-producing cells are detected at the same level as in wild-type siblings. At birth, β-cells are reduced by approximately 95 % in comparison to wild-type animals. Ngn3-expressing progenitor cells are present at the same level as in wild-type littermates. Hence, two distinct pathways may exist in the developing pancreas for generating insulin-positive cells: an early pathway independent of Nkx6.1 and a later pathway dependent on its expression. Near the time of birth, a third pathway is invoked comprising the replication of existing β-cells.

The presence of Nkx2.2 in the Nkx6.1-null mutant pancreas suggests a function upstream of Nkx6.1. Double nullizygous embryos are phenotypically indistinguishable from Nkx2.2 single null mutants. Nkx6.1 is therefore required for the expansion and terminal differentiation of β-cell progenitors.

Pax6

Pax6, like Pax4, is a paired domain homeobox gene; its protein is expressed in discrete cells of the pancreatic epithelium from E9.0 (St.-Onge *et al.*, 1997; Sander *et al.*, 1997; Turque e*t al.*, 1994). At E10.5, cells coexpressing Pax6 and glucagon are seen; at E15.5, Pax6-positive cells express either glucagon or insulin. In neonates, Pax6-positive cells synthesise insulin, glucagon, PP or somatostatin, indicating that *Pax6* is expressed in all mature endocrine cells in the islet (St.-Onge *et al.*, 1997). A recent cell lineage study (Zhang *et al.*, 2003) further suggests that Pax6-expressing progenitors contribute not only to the adult islets but also to the pancreatic ducts. Pax6-null mutants possess no or few α-cells and a depleted number of β-, δ- and PP-cells; the islets themselves display disrupted architecture (St.-Onge *et al.*, 1997; Sander *et al.*, 1997). Mice doubly nullizygous for both Pax4 and Pax6 display an entire lack of mature endocrine cells (St.-Onge *et al.*, 1997). These studies demonstrate that Pax6 is required for the regulation of the number of islet cells, and particularly for the generation of α-cells, acting like Pax4, downstream of Pdx1 in the islet cell differentiation pathway. Pax6 is further involved in organising the endocrine cells into islets and in modulating the level of islet hormone synthesis. Pax6 binds to a common element in the glucagon,

insulin, and somatostatin promoters, and transactivates the glucagon and insulin promoters (Sander *et al.*, 1997).

Islet1 (Isl1)

Islet1 (*Isl1*) encodes a LIM-homeodomain transcription factor (Ahlgren *et al.*, 1997; Karlsson *et al.*, 1990) which has been shown to activate transcription of the somatostatin, glucagon, and amylin genes (Leonard *et al.*, 1992; Wang and Drucker, 1995, 1996). Perhaps more importantly, it is also involved in early pancreatic determination (Ahlgren *et al.*, 1997). Isl1 expression commences at E9.5 in the dorsal pancreatic epithelium and in the mesenchyme surrounding the dorsal pancreatic bud. At E9.5, all glucagon-expressing cells also express Isl1. Subsequently, Isl1 is detectable in all islet cells.

Inactivation of *Isl1* results in arrested development soon after E9.5 and subsequent death during embryogenesis, principally due to an absence of motor neuron development in which it is usually expressed (Dong *et al.*, 1991; Pfaff *et al.*, 1996; Thor *et al.*, 1991). At this stage, no glucagon-positive cells are detected (Ahlgren *et al.*, 1997). Formation of the dorsal but not the ventral pancreatic bud is suppressed in *Isl1* knockout embryos due to a virtually complete depletion of mesenchyme flanking the dorsal pancreatic epithelium (Ahlgren *et al.*, 1997). The early embryonic lethality of Isl1 homozygous null embryos dictated that *in vitro* studies with pancreatic explants were necessary to elucidate the role of Isl1 in pancreas development. Explants from the dorsal bud region of Isl1 nullizygous embryos will not develop in culture unless supplied with wild-type mesenchyme, in which case the dorsal bud will form exocrine but not endocrine tissue. These experiments show that *Isl1* is initially required in the mesenchyme to produce a signal required for pancreatic epithelial development and subsequently in the epithelium to permit islet cell differentiation.

Hes1

Hes1 encodes a transcriptional repressor of bHLH genes capable of counteracting bHLH activators (Sasai *et al.*, 1992) and its expression in the pancreas commences at around E9.5. Hes1 is normally expressed at E12 in Pdx1-positive cells in the pancreatic bud and probably inhibits ngn3-mediated activation of NeuroD1. Hes1 expression is absent from α-cells. Hes1 mutant mice exhibit reduced pancreas growth

(pancreatic hypoplasia) and consequently reduced pancreas size, and an increased number of glucagon-expressing cells at E9 at the expense of Pdx1-positive cells (Jensen *et al.*, 2000b). Jensen and coworkers attribute pancreatic hypoplasia to premature endocrine differentiation with a consequent depletion of pancreatic precursor cells. Absence of Hes1 therefore results in premature differentiation of endocrine cells due to the absence of the negative regulation by Hes1.

PTF1/p48 (PTF1a)

PTF1 is a hetero-oligomeric protein complex composed of three distinct subunits, all of which are bHLH proteins. The PTF1 complex binds to transcriptional enhancers of genes specifying the products of the exocrine pancreas but for transcriptional activation of target genes, PTF1 must cooperatively interact with other transcription factors (Cockell *et al.*, 1989). The p75 subunit does not contact the DNA directly but is required for import of the factor into the cell nucleus (Sommer *et al.*, 1991). The two DNA-binding subunits, p64 and p48 or PTF1a, recognise as a heterodimer a bipartite cognate site that contains two distinct sequence motifs. The p48 subunit is the only cell-specific constituent of the PTF1 complex (Krapp *et al.*, 1996). An antisense RNA-mediated reduction of p48 synthesis in exocrine pancreatic cells in culture inhibits the exocrine transcription program, showing that the protein is essential for maintaining the terminally differentiated state (Krapp *et al.*, 1996). In the mouse embryo, p48 synthesis precedes the appearance of PTF1 at E15 by several days (Krapp *et al.*, 1996; Petrucco *et al.*, 1990), suggesting that p48 on its own plays an alternate role during early embryogenesis. Mice homozygous for a null mutation of the *p48* allele exhibit a complete absence of exocrine tissue and its specific products including α-amylase and carboxypeptidase A whilst development of the endocrine pancreas is unaffected (Krapp *et al.*, 1998). Null mutants exhibit all four endocrine cell types in the mesentery that normally surrounds the pancreas until E16 after which, they are found to colonise the spleen. The endocrine cells remain in a functional state within the spleen until the animal dies shortly after birth. These findings show that p48 is required for differentiation and/or proliferation of the exocrine cell lineage and is so far the only developmental regulator known to be required exclusively for committing cells to an exocrine cell fate. Furthermore, the presence of the exocrine pancreas is required for the correct spatial assembly of the endocrine pancreas and in its absence, endocrine cells are directed by default to the spleen. A recent study (Kawaguchi *et al.*, 2002) combining

inactivation of p48/PTF1a with β-galactosidase cell lineage labelling has confirmed the absence of the exocrine pancreas in null mutants and verified these conclusions. It was further shown that *Ptf1a* is expressed in progenitors of all pancreatic cell types and is silenced in endocrine and duct cells concomitant with or shortly after the partitioning of progenitors into acinar cells. Results from this study suggested that in the absence of PTF1a, cells normally fated to form ventral pancreas will assume an alternative endodermal fate for intestinal epithelium, differentiating into enteroendocrine cells, goblet cells, and other gut cell types. Therefore, PTF1a plays a further role in governing the initial cell-type decision to form the pancreas.

1.5.1. Lateral Specification of Endocrine Cells

Recent studies (Apelqvist *et al.*, 1999; Beatus *et al.*, 1999) have begun to establish signalling events upstream of *ngn3* and *Hes1* that determine whether or not undifferentiated progenitor cells are driven towards an endocrine fate. Pancreatic endocrine cells have been shown to be specified by the process of lateral specification via Notch signalling (Apelqvist *et al.*, 1999). This process generates scattered differentiated cells from an initially homogenous field of cells as in neuronal differentiation and is mediated by the Notch signalling pathway (Beatus and Lendahl, 1998; Lewis, 1996). Differentiating cells express high levels of the ligands (Delta or Serrate) and signal to activate Notch receptors on neighbouring cells to suppress the same ("primary") fate in these cells (**Fig. 1.8.**). The activated intracellular domain of Notch (NIC) interacts with the DNA-binding protein RBP-Jκ to activate expression of bHLH repressor genes, i.e. the *Hes* genes, which in turn repress expression of downstream target genes (Beatus and Lendahl, 1998; Lewis, 1996), including the *ngn* genes (Fode *et al.*, 1998; Ma *et al.*, 1998) which if expressed would promote the primary cell fate. By analysing mice genetically altered at several steps in the Notch signalling pathway, lateral specification was found to occur in the pancreas. Mice deficient in *delta-like gene 1* (*Dll1*) or the intracellular mediator *RBP-Jκ* exhibited accelerated differentiation of pancreatic endocrine cells and so, a depleted pool of pancreatic precursor cells (Apelqvist *et al.*, 1999). Overexpression of either *ngn3* or the intracellular form of *Notch3*, both of which act as repressors of Notch signalling (i.e. repressors of Delta signalling to Notch on neighbouring cells), produced a similar phenotype (Apelqvist *et al.*, 1999; Beatus *et al.*, 1999). These findings were later confirmed by the gene inactivation studies (Gradwohl *et al.*, 2000; Jensen *et al.*, 2000b)

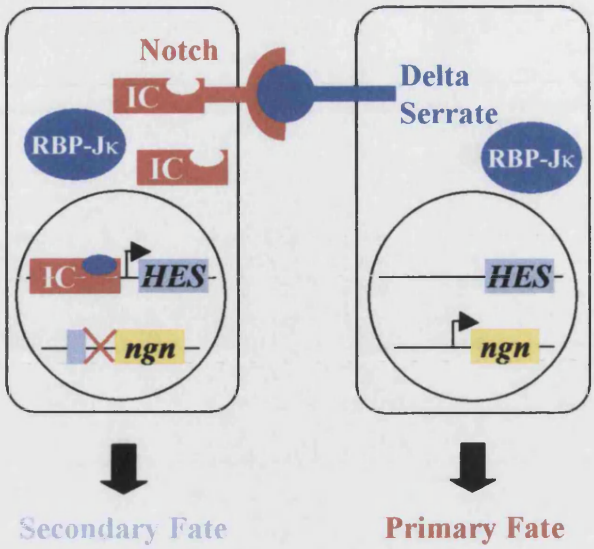

Figure 1.8. Notch signalling involves cell-to-cell signalling between neighbouring cells via membrane-bound receptors, encoded by the *Notch* genes, and membrane-bound ligands, encoded by the *Delta* and *Serrate* genes. (After Edlund, 2001)

IC, intracellular region of the Notch receptor

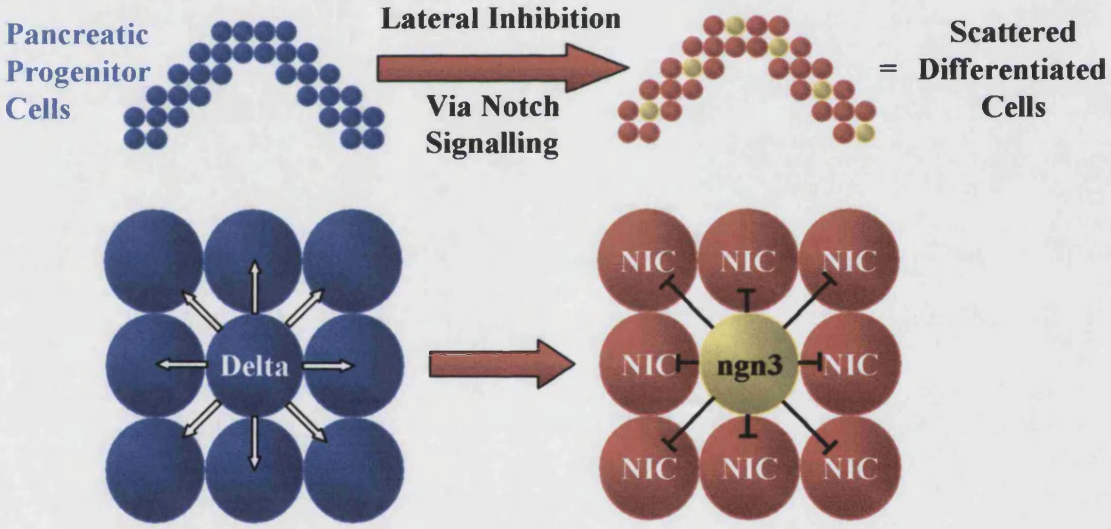

Figure 1.9. Differentiated endocrine cells appear amongst the pool of early pancreatic stem cells in a scattered manner. The specification of pancreatic endocrine cells within the pool of equivalent progenitor cells is mediated by lateral inhibition through the Notch signalling pathway where *ngn3* acts as the proendocrine gene. (After Edlund, 2001)

mentioned above in which mice lacking a functional copy of *ngn3* lack differentiated endocrine cells whilst embryos deficient for Hes1 exhibit accelerated endocrine cell differentiation and a depleted pool of pancreatic progenitor cells. These studies demonstrate that by altering the Notch signalling pathway at the ligand, receptor, and intracellular mediator level, the pancreatic cell differentiation fate is affected. These experiments thereby provide evidence that in the developing pancreas, Notch signalling controls the choice between differentiated endocrine and progenitor cell fates so that the lack of Notch pathway signalling, resulting in high *ngn3* levels, promotes the endocrine fate (**Fig. 1.9.**). However, cells with active Notch signalling, and a consequent upregulation of Hes1 expression, remain as undifferentiated progenitor cells, permitting the subsequent proliferation, morphogenesis, and differentiation of the pancreatic epithelial precursor cells analogous to the function of Notch signalling during early mammalian neurogenesis (Beatus and Lendahl, 1998; Lewis, 1996).

As differentiated endocrine cells appear, they separate from the epithelium and migrate into the adjacent mesenchyme where they aggregate. This migration is therefore likely to result in a decrease in Notch signalling (so, lateral inhibition) among progenitor cells and permit islet formation. This would allow a continued appearance of cells with a primary, endocrine fate that can respond to later inductive signals, generating distinct endocrine cells throughout pancreatic development depending on the combination of inductive signals. Progenitor cells that are not driven towards an endocrine fate will subsequently differentiate into acinar cells or ductal cells (Edlund, 2001).

1.5.1.1. Transcription Factors in Pancreas Development: Summary

Gene targeting studies in mice have helped to begin to elucidate the roles of the different transcription factors in pancreas development. Most of the gene-disrupted mice mentioned above exhibit defective islet morphogenesis and depleted numbers of different types of islet cells. Few genes, when inactivated, can result in a total ablation or one or more endocrine cell types throughout pancreas development. These studies have contributed to the notion that there exists a common precursor cell, which is subject to a cascade of precisely timed gene activation events under the control of an increasing number of transcription factors. Some of these factors appear to determine the cell fate of the cell lineage whilst others may govern the terminal differentiation. For example, *ngn3* plays a key role by promoting endocrine differentiation at an early stage.

Ngn3 also appears to occupy a higher rank in the transcription factor hierarchy than most of the genes described above. *NeuroD1*, *Pax6* and *Isl1* appear to be more closely related than the other factors, since they are expressed in all types of islet cells. However, the genetic relationship among them and the other genes largely remains to be determined. The number of transcription factors found to be involved in pancreas development seems to be still expanding. Future identification and characterisation of these genes will lead to an improved understanding of the cascade of transcription factors involved in pancreatic cell differentiation. This work will need to take into account different expression levels of a combination of the array of transcription factors that have been found to play a role in pancreas development to date.

1.5.2. Involvement of Transcription Factors in Diabetes Mellitus

1.5.2.1. Maturity Onset Diabetes of the Young (MODY)

Several of the above transcription factors are implicated in diabetes mellitus in humans. The best understood example to date is Pdx1, where a loss of function may cause diabetes as a consequence of abnormal development and/or insufficient maintenance of mature β-cell function. In particular, mutations of transcription factor genes have been associated with a number of genetic forms of type 2 diabetes mellitus, clinical symptoms of which usually manifest during early adulthood and are therefore referred to as maturity onset diabetes of the young (MODY). To date, five different forms are known. MODY1 and 3-5 are associated with transcription factors while MODY2 is caused by an inactivating mutation of glucokinase, a key enzyme of the glycolytic pathway. All forms are monogenic diseases and are characterised by an onset usually before 25 years of age, by an autosomal dominant inheritance and a genetic defect in β-cell function. They are of epidemiological significance, as it has been estimated that 2-5 % of patients diagnosed with type 2 diabetes mellitus actually suffer from MODY. MODY1 is associated with mutations in HNF-4α (Fajans, 1990; Yamagata *et al.*, 1996a) whilst heterozygous mutations in the gene encoding HNF-1α cause MODY3 (Winter *et al.*, 1999; Yamagata *et al.*, 1996b), accounting for the majority of MODY cases. Gene inactivation experiments have provided insight into the effects of HNF-4α and HNF-1α mutation responsible for the diabetic phenotypes of MODY 1 and 3 respectively. HNF-4α is an upstream regulator of the HNF-1α gene which is a weak transactivator of the insulin gene (Emens *et al.*, 1992; Kuo *et al.*, 1992).

HNF-4α-null embryonic stem cells show a decreased expression of several genes encoding components of the glucose-dependent insulin secretion pathway, including GLUT2 (Stoffel and Duncan, 1997). It has been shown that the islets of HNF-1α-null mice are hypoplastic due to β-cell depletion. Consequently, the serum insulin level, pancreatic insulin content, and response of insulin secretion to glucose and arginine are reduced compared to wild-type animals, leading to diabetes (Lee *et al.*, 1998; Pontoglio *et al.*, 1998). As diabetes does not develop in heterozygous HNF-1α-null mice, heterozygous HNF-1α mutations in MODY3 patients are considered to function in a dominant negative fashion (Yamagata *et al.*, 1998).

A homozygous point deletion in Pdx1 has been found to be responsible for pancreatic agenesis and neonatal diabetes mellitus in a human patient (Stoffers *et al.*, 1997b). The single nucleotide change and consequent frameshift in the Pdx1 gene results in the production of a truncated protein with a dominant negative effect and replicates complete loss of Pdx1 function (Stoffers *et al.*, 1998). MODY linked to Pdx1 mutation is called MODY4. HNF-1β mutations cause MODY5 which account for only a very small number of total MODY cases. Only a few families carrying HNF-1β mutations have been described to date (Horikawa *et al.*, 1997; Iwasaki *et al.*, 1998; Lindner *et al.*, 1999; Nishigori *et al.*, 1998; Weng *et al.*, 2000). This form of diabetes mellitus has also been found to be associated with acute kidney disease.

1.5.2.2. Maturity Onset Type 2 Diabetes Mellitus

Very recently, several of these transcription factors have been found to be associated with the development of the late onset form of type 2 diabetes mellitus. However, to date all reports appear to represent one contributing factor in a polygenic disease among others. For example, a single mutation in HNF-4α, several mutations in Pdx1 and in HNF-3β have been described (Hani *et al.*, 1998, 1999; Zhu *et al.*, 2000). Type 2 diabetes mellitus is also associated with mutations in NeuroD1 (Malecki *et al.*, 1999).

1.5.2.3. Pancreas Development and Diabetes Therapies

The finding that mutations in transcription factors involved in pancreas development in the mouse underlie several forms of human diabetes, provides evidence

that the late function of genes such as Pdx1 is conserved from mice to humans. These recent discoveries justify the study of pancreas development in the mouse as being of application to the treatment of human pancreatic disease. The ultimate goal of understanding pancreas development must be the cure of pancreatic cancer and diabetes mellitus. The different treatment strategies currently in use for the management of diabetes, such as intensified insulin therapy, are accompanied by negative side effects and the micro- and macrovascular complications cannot be fully overcome. One of the most physiologic approaches would be to activate endogenous pancreatic stem cells to form β-cells and even intact islets to substitute for the defective ones. In the case of type 1 diabetes, an additional major task will be to protect the newly grafted cells from autoimmune destruction.

1.6. Tissue Transformations Involving Pancreas Tissue

The pancreatic state can also be investigated by studying the conversion of pancreas tissue into other tissue types or vice versa since such transformations are likely to result from the change of activity of one or a few genes and would therefore indicate which other tissues had similar epigenetic codes. Although it is generally accepted that the differentiated state is permanent and irreversible, in some cases, terminally differentiated cells can interconvert (Slack, 1986, 1992), undergoing phenotypic alterations after a proper stimulus and under a permissive environment. Such alterations are associated with distinct morphological changes and are accompanied by the elaboration of new gene products, indicating activation of genes that are normally repressed in that cell type (DiBerardino *et al.*, 1984; Okada, 1986). The phenotypic interconversion of one differentiated cell to another usually arises in situations of chronic tissue damage and associated regeneration. Some changes may be indirect, occurring via an intervening stem cell, whereas others may be direct transformations, sometimes called *transdifferentiations* (Eguchi and Kodama, 1993; Okada, 1991). Many examples have been reported, some of which are known to predispose to cancer (Slack, 1986, 1992). However, the molecular and cellular mechanisms involved remain largely uncharacterised.

Pancreatic heterotopia occurs during human embryonic development in about 2 % of post-mortem examinations and is most frequently seen in the stomach, the duodenum, the jejunum, the ileum, the vitellointestinal duct and the gall bladder (Branch and Gross, 1935; de Castro Barbosa *et al.*, 1946). These heterotopic patches

usually bear ducts opening into the gut lumen and the presence of a duct strongly suggests *in situ* differentiation as opposed to migration from elsewhere. It would therefore appear that the stomach, intestine and bile duct have very similar epigenetic codes to pancreas.

A similar phenomenon is the appearance of pancreatic cells in the liver of a human cancer patient (Wolf *et al.*, 1990). Transdifferentiation of liver to pancreas has also been found to occur in the livers of rats treated with polychlorinated biphenyls (Rao *et al.*, 1986a) and in fish liver tumours induced by chemical carcinogens (Lee *et al.*, 1989). Endocrine tissue was not present in any of these examples. Most recently however, Horb *et al.* (2003) demonstrated a conversion of liver tissue to both exocrine *and* endocrine pancreatic tissue in transgenic *Xenopus laevis* tadpoles overexpressing an activated form of the *Xenopus* homolog of *Pdx1*, *Xlhbox8-VP16*, in the liver. Furthermore, transfection of the same construct into the human hepatoma cell line, HepG2, also converts the liver cells into amylase- or insulin-expressing pancreatic cells, confirming that the result is not limited to *Xenopus*, or to larval stages of development (Horb *et al.*, 2003).

In the reverse of the tissue transformation in the cases mentioned above, liver cells or hepatocytes have been observed in the pancreas of another primate, the vervet monkey (Wolfe-Coote *et al.*, 1996). It has proved possible to induce the metaplasia of pancreas to liver experimentally. Hepatic foci have been reported to occur in the pancreas of rats or hamsters in response to various experimental treatments, including treatment with the protein synthesis inhibitor ethionine (Scarpelli and Rao, 1981) and copper depletion of the diet (Rao *et al.*, 1986b; Rao and Reddy, 1995). This causes substantial ablation of acinar tissue whilst leaving ducts and islets unaffected. Restoration of copper provokes regeneration leading to substantial hepatic differentiation which commences in both periductal and interstitial cells (Rao *et al.*, 1989, 1990). Similar foci of pancreatic hepatocytes have been reported following transplantation (Dabeva *et al.*, 1997), or in transgenic mice overexpressing keratinocyte growth factor (KGF, also known as FGF7) in the pancreas (Krakowski *et al.*, 1999). Most recently, hepatocyte-like cells expressing the liver marker albumin have been reported in the islets of mice in which the rat glucagon promoter has been used to drive specific FGF8 overexpression in the pancreatic α-cells (Yamaoka *et al.*, 2002). Although such whole-organism observations suggest a relatively high-frequency conversion between pancreatic cells and hepatocytes, they cannot prove that the hepatocytes derive from pancreatic cells. In a recent study, foci of hepatocytes were

induced *in vitro* in the pancreatic cell line AR42J-B13 and in cultures of isolated mouse embryonic pancreatic buds with the synthetic glucocorticoid dexamethasone (Shen *et al.*, 2000). It was demonstrated that a proportion of the hepatocytes arose directly from differentiated exocrine-like cells, with no intervening cell division. In all of the above cases, the foci of hepatocytes are most probably clones. The fact that liver is the predominant phenotype of the transdifferentiated foci suggests that fewer changes are required to convert pancreas to liver than to invoke any other transformation (Slack, 1999). This indicates an intimacy in the determined states of liver and pancreas in terms of their expression of transcription factors; indeed, pancreatic and hepatic developmental programs might be distinguished by a single "master switch gene". This is most probably a reflection of the close anatomical and developmental relationship shared by the pancreatic buds and liver which originate from adjacent regions of the foregut endoderm (Slack, 1995; Zaret, 2000). As mentioned above, it has recently been shown that the ventral foregut region is autonomously programmed to develop into the ventral pancreas unless it is exposed to FGF which diverts the differentiation program to an hepatic fate (Deutsch *et al.*, 2001). Indeed, the common embryological origin of the pancreas and liver may be reflected in certain evolutionary and pathological states. Primitive invertebrates such as molluscs possess only a single organ, the hepatopancreas, that performs functions of both organs (Hoar, 1975) and the caudal pancreas in the sea lamprey is believed to develop by the transdifferentiation of cells in the hepatic duct (Elliot and Youson, 1993).

1.7. Cell Lineage Studies

1.7.1. Evidence for a Neural Crest Origin of Pancreatic Endocrine Cells

Until relatively recently, it had frequently been assumed that the pancreatic endocrine cells have a distinct embryological origin from the exocrine cells and are neural crest-derived, an hypothesis stemming from the "APUD" (Amine Precursor Uptake and Decarboxylation) theory of Pearse, identifying common properties of the neuroendocrine cells in different tissues and organs (Pearse, 1984; reviewed by Le Douarin, 1988). It has been known for many years that the pancreatic endocrine cells share numerous morphological and molecular characteristics with neurons, such as electrical excitability and their expression of enzymes and hormones including neuron-specific enolase, tyrosine hydroxylase, dopa decarboxylase, somastostatin, insulin, glucagon, tetanus toxin receptor and A2B5 antigen (reviewed by Le Douarin, 1988) and

also nerve growth factor (NGF) (Miralles *et al.*, 1998c; Rosenbaum *et al.*, 1998) and the high- and low-affinity NGF receptors, Trk-A and p75NGF-R respectively (Kanaka-Gantenbein *et al.*, 1995; Miralles *et al.*, 1998c; Rosenbaum *et al.*, 1998; Scharfmann *et al.*, 1993; Teitelman *et al.*, 1998). Furthermore, the transcription factors Isl1 (Ahlgren *et al.*, 1997; Pfaff *et al.*, 1996), NeuroD1 (Lee *et al.*, 1995; Miyata *et al.*, 1999; Naya *et al.*, 1997), Pax4 (Sosa-Pineda *et al.*, 1997), Pax6 (Ericson *et al.*, 1997; St.-Onge *et al.*, 1997; Sander *et al.*, 1997), and Nkx2.2 (Briscoe *et al.*, 1999; Sussel *et al.*, 1998) which are vital for proper pancreatic endocrine differentiation, are also expressed during, and in some cases are critical for, neuronal differentiation. Also, during pancreatic development, the endocrine cells initially appear in a scattered manner (Ahlgren *et al.*, 1997; Pictet and Rutter, 1972) that resembles the process of neurogenesis (Beatus and Lendahl, 1998; Lewis, 1996). This implies that cell differentiation in the pancreas and in the nervous system may be, at least in part, under similar control (Edlund, 2001).

The APUD theory is corroborated by the association of pancreatic endocrine cells with neuroendocrine cells in lower animals, suggesting that such cells in mammals are of neural crest origin. If the sequence of pancreatic endocrine cell organisation in a range of invertebrates and vertebrates of differing complexity, from protostome-type invertebrates, invertebrate chordate tunicates and cartilaginous fish, is considered one of evolutionary descent, then it can be argued that the pancreatic endocrine cells "migrated" from the brain to the gut, then aggregated in the exocrine pancreas. However, all of the animals that can be examined today are contemporary species and it has proved very difficult to order the divergence times of the major groups of animal in evolution using molecular sequence trees. It cannot be assumed that the state found in invertebrates today was also that present in the ancestor of all vertebrates 600 million years ago.

Initially, all mammalian neuroendocrine cells were proposed by Pearse (1984) to have a neural crest origin and although found true in such cases as the C cells of the thyroid, the theory was not corroborated in others. Using quail to chick embryo grafts, Andrew (1976) tested the theory experimentally with regard to the gut endocrine cells. In quail cells, a large mass of DNA is associated with the nucleolus which can easily be detected by Feulgen staining (Le Douarin, 1982), rendering the grafted cells distinguishable from those of the chick host. Quail neural tube was grafted into chick embryos and after differentiation of the pancreas it was examined for the presence of quail cells. The sympathetic (enteric) ganglia of the gut were found to exhibit the quail

nucleolar marker and so were irrefutably shown to be of neural crest origin whereas such an origin was *not* demonstrated for the endocrine cells of the gut and pancreas.

1.7.2. Endocrine and Exocrine Cells are Endoderm-Derived

Although not proving that the endocrine cells derive from the endodermal epithelium, descriptive studies make this the most probable origin. Differentiation of endocrine cells from isolated pancreatic buds cultured *in vitro* indicates that they must arise from a cell type present in the pancreatic endoderm or in the adjacent mesenchyme (Wessells and Cohen, 1967). Unpublished results quoted by Pictet and Rutter (1972) suggest that both exocrine and endocrine cells can originate *in vitro* from isolated epithelium. Both tissues could be formed from rudiments isolated prior to the appearance of blood vessels or nerves, showing that interactions with these later emerging tissues are not necessary for differentiation. These results support an endodermal origin for the endocrine cells, but endorse the possibility that there may be discrete rudiments for exocrine and endocrine tissue within the epithelium. However, in a recent study, it was shown that when pancreatic epithelium from transgenic ROSA-26 mouse embryos which ubiquitously express *Escherichia coli* β-galactosidase is recombined with mesenchyme from unlabelled embryos, both the resulting exocrine and endocrine cells in the cultured recombinants are entirely β-gal-positive (Percival and Slack, 1999). This provides robust evidence for an endodermal origin of both the exocrine and endocrine cells.

1.7.3. Multihormone Endocrine Progenitors?

Many authors have developed models about islet cell lineage, mostly based on studies of coexpression of the different hormones during development as described above. The common expression of molecular markers in two cells has for some time been taken as evidence that the cells possess a common origin (Le Douarin, 1988; Teitelman and Lee, 1987; Teitelman *et al.*, 1993). This has in turn led to the widely-held assumption that progenitors that transiently expressed two or more hormones (the early "multihormone-expressing population") gave rise to mature hormone-secreting cells (Alpert *et al.*, 1988; Teitelman *et al.*, 1993; Upchurch *et al.*, 1994, 1996). Coexpression does not, however, prove a lineage relationship, since cells within one lineage may switch given genes on and off at distinct times during development. Furthermore, cells

are motile, so their place of residence at the time of detection may not be the position of origin. The MSL cell line, isolated from a transplantable insulinoma (Madsen *et al.*, 1996) lends supports to the hypothesis of endocrine cell formation from early multihormone-expressing precursors. MSL differentiates *in vitro* heterogeneously to form a diverse range of endocrine cells secreting numerous gut or pancreatic hormones but *in vivo* it can become an insulinoma or glucagonoma. Pdx1 expression in the parent cell is maintained in the insulinomas but Pdx1 is not expressed in the glucagonomas. In this way, the MSL cell resembles the embryonic multihormone cells. However, it does not constitute evidence of any particular pathway of endocrine cell formation in normal development, as it derives from an X-ray-induced tumour and has been passaged for many years, most probably undergoing mutations and abnormalities over this duration.

1.7.4. Evidence from Transgenic Mice

1.7.4.1. Early Toxigenic and Cell Ablation Studies

To obtain more definite results regarding cell lineage of the different islet cells, several groups have generated transgenic mice, either stable lines or transient transgenics, in which a promoter for one of the endocrine islet cell hormones is employed to drive a modifying reporter gene or a toxin. In both cases it is necessary to assume that the short promoter drives the transgene with the same tissue-specificity as its own endogenous gene. This is not necessarily the case as correct expression of a particular gene often requires elements that are located far up- or downstream of the actual coding region. Non-specific expression is known to occur when the transgene does not include a silencer element sufficient to repress the expression in non-targeted cells. In addition, integration of the transgene at random positions in the genome may result in an altered expression pattern. This applies to transient transgenics in which each embryo is likely to bear a different number of transgene copies that are inserted at a different position in the genome. Therefore, the transgenic studies on islet cell lineage must be interpreted with caution. In 1988, Alpert *et al.* conducted a pancreatic cell lineage study using transgenic RIP-Tag mice, in which the rat insulin promoter is employed to drive expression of the SV40 T antigen. This approach can be considered to approximate to a reporter study since the biological effects of the T-antigen are subtle in embryonic life (Slack, 1995). In the embryo, most of the endocrine cells express T-antigen while postnatally only the adult β-cells do so, supporting the existence of an early endocrine progenitor in which several or all the hormones are expressed. A similar

study (Upchurch *et al.*, 1994) utilised the peptide YY-promoter. T-antigen was expressed from E12 in peptide YY-positive cells. Coexpression of T-antigen with three of the four islet hormones (insulin, PP and somatostatin) was found during development but very few islet cells expressed T-antigen in adult mice. This is consistent with the proposition that all endocrine precursors express peptide YY at an early stage. Promoter function does not become fully restricted to one islet cell type until mature islets have formed.

Diphtheria toxin A chain causes ablation of cells expressing the toxin by curtailing protein synthesis and inducing cell death. As the toxin lacks the B chain normally required for entry into intact cells, the ablation effect should be cell-autonomous and therefore specific, leading it to being widely-used for studying cell lineage relationships in conjunction with a suitable promoter to drive toxin expression in target cells (Evans, 1989). Using the elastase promoter, mice deficient in almost all exocrine pancreas and with a reduced complement of ductal tissue and islets were generated (Palmiter *et al.*, 1987). In a transient transgenic study, Herrera *et al.* (1994) used promoters for insulin, glucagon and pancreatic polypeptide to drive the toxin. Toxin expression driven by the insulin or glucagon promoter led only to ablation of the targeted cell type, suggesting that a hormone coexpressing cell is not required for α- or β-cell development. In contrast, the PP promoter-driven transgene led to a loss not only of PP-expressing cells but also of insulin- and somatostatin-producing cells although α-cells developed without abnormality. This is unexpected, as PP itself is supposed to be expressed only in the late embryo. It was presumed by the authors (Herrera *et al.*, 1994) that the PP gene promoter is used either in β-cell progenitors or in cells that are necessary (through a paracrine effect on unidentified progenitors) for β-cells to differentiate. An associated study using human growth hormone as a reporter demonstrated that the putative PP promoter drove expression in 12 % of embryonic PP-fold peptide-expressing cells, but it is not clear whether these are a subset of the peptide YY cells or precocious PP-cells. One possibility not excluded by the findings of these studies is that the PP promoter may display less specificity than the native endogenous gene and function in any islet cell. Common to all of these early studies was the fact that they were beset by uncertainties such as the specificity of transgene expression, the cell autonomy of the ablation effects and the neutrality of the lineage marker employed.

1.7.4.2. Cre-LoxP Tagging

More recently, studies on pancreatic cell lineage in transgenic animals have exploited powerful cell marking techniques, most notably the Cre-LoxP system (Sauer, 1994, 1998). This cell labelling technique can be used to indelibly mark or "tag" all the progeny of cells arising from cells in which Cre is transiently expressed. Herrera (Herrera, 2000) used the Cre-LoxP system to irreversibly tag cells that transcribed the insulin, glucagon or PP genes, or cells that express Pdx1, as a marker of pancreatic progenitor cells (Jonsson *et al.*, 1994; Offield *et al.*, 1996). Mice were generated bearing two transgenes (**Fig. 1.10.**). The first "reporter" transgene, placed under the control of either the insulin2 (β-cell-specific), or the glucagon (α-cell-specific) gene promoter, contains a human growth hormone- (hGH-) coding region placed downstream of a loxP-flanked transcription termination site (STOP sequence) (Sauer, 1993). It is assumed in such experiments that hGH is not active in promoting cell growth or differentiation. The native reporter transgene cannot be expressed in β- or α-cells because of the STOP sequence. To be expressed, the Cre recombinase must excise the DNA (comprising the STOP sequence) between the two loxP recognition sequences. A second "tagger" transgene consists of the Cre recombinase gene placed under the control of a promoter active in putative progenitor cells; its expression results in the deletion of the STOP site of the reporter transgenes, allowing hGH synthesis. Provided that the promoter of the tagger transgene has been activated and Cre recombinase expressed in the progenitor of the same target cell(s) in which the reporter transgene is expressed, then crossing of two strains carrying a tagger and a reporter transgene respectively will lead to reporter expression in the target cell(s) of the doubly transgenic offspring. Mice carrying the following tagger transgenes were prepared: insulin2 gene promoter-Cre, glucagon gene promoter-Cre, PP gene promoter-Cre and Pdx1 gene promoter-Cre. Mouse families were selected bearing only stable and complete expression of one of each of the reporter or tagger transgenes. Adult doubly transgenic mice with complete and stable transgene expression (Cre activity) were analysed for reporter gene expression (hGH) in islet cells by immunofluorescence on pancreas sections. As expected, no hGH expression was observed in single transgenic mice bearing only either a reporter or a tagger transgene. Also as expected, hGH *was* expressed by β-cells in doubly transgenic animals bearing the β-cell-specific reporter gene and β-cell-expressed tagger genes (either driven by the insulin2 or Pdx1 promoters since Pdx1 is expressed in adult β-cells). Similarly, almost all α-cells from mice bearing both the α-cell-expressed reporter gene and α-cell-

Figure 1.10. General Cre/LoxP-Based Strategy to Genetically Label Islet Endocrine Cell Precursors

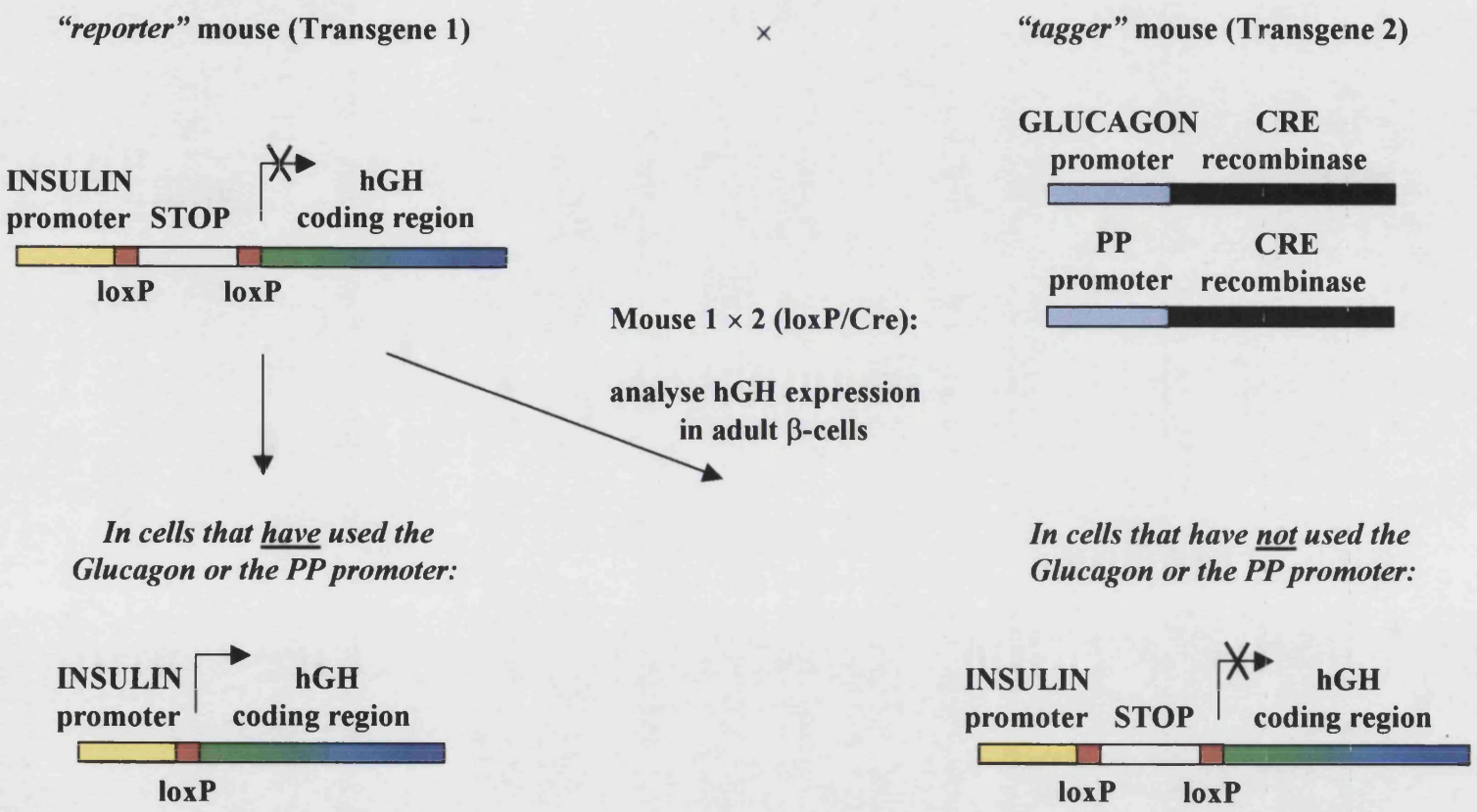

For simplicity, only one example is illustrated: the experiment is designed to assess whether adult β-cells descend from glucagon- and/or PP-producing progenitors. The reverse experiment, planned to determine whether insulin, PP or Pdx1 are expressed in the α-cell lineage, was also conducted. (After Herrera, 2000)

specific tagger gene were hGH^+. However, in no case was hGH detected in adult β-cells of doubly transgenic animals bearing both the α-cell-specific tagger gene and β-cell-specific reporter gene, demonstrating irrefutably that the glucagon gene is *not* expressed in the precursors of β-cells. Similarly, in the reverse experiment, hGH was never detected in mature α-cells of doubly transgenic animals bearing both the β-cell-specific tagger gene and α-cell-specific reporter gene, showing that the insulin gene is *not* expressed in α-cell progenitors. Therefore, the glucagon- and insulin-coexpressing cells reported in early pancreatic buds (Larsson, 1998) are unlikely to be the progenitors of either mature α- or β-cells. This finding corroborated the aforementioned results of the earlier transient transgenic study by Herrera's group (Herrera *et al.*, 1994) in which diphtheria toxin A chain expression driven by the insulin or glucagon promoter led only to ablation of the targeted cell type, which also suggested that a hormone coexpressing cell is not required for α- or β-cell development. In this earlier study (Herrera *et al.*, 1994), PP promoter-driven expression of the toxin transgene was shown to result in a loss of insulin- and somatostatin-producing cells as well as PP^+ cells. Using the Cre-LoxP system, Herrera (Herrera, 2000) found that in adult mice bearing only an hGH reporter gene (lacking a STOP sequence) driven by the PP promoter, hGH is detected only in PP-cells and not in β-cells. This confirmed the widespread assumption that adult β-cells do not produce PP and excluded the possibility that the PP promoter is active in the mature β-cell. Furthermore, in doubly transgenic mice bearing both a PP promoter-driven tagger gene and the β-cell-specific reporter gene, all islet β-cells were found to be hGH^+. On the contrary, double transgenics bearing the same PP promoter-driven tagger gene and the α-cell-specific reporter gene, showed no hGH expression in their α-cells (Herrera, 2000). Therefore, these results appear to be consistent with those of the earlier toxigenic study (Herrera *et al.*, 1994). Combined, these results imply that adult α- and β-cells belong to distinct cell lineages and that mature β-, PP- and δ-cells are descended from a PP-expressing progenitor which does not give rise to mature α-cells.

As has been mentioned in some detail, gene inactivation studies affecting transcription factors involved in pancreas development have generated a wealth of information concerning their role in endocrine cell differentiation. Such experiments do not however, prove a lineage relationship. Gene inactivation has particularly focused attention on *Pdx1* and *ngn3*. The finding that *Pdx1* inactivation by targeted mutagenesis results in pancreatic agenesis has promoted the idea that $Pdx1^+$ cells are general pancreatic progenitors (Jonsson *et al.*, 1994; Offield *et al.*, 1996). However, *Pdx1*

mutants do generate some glucagon- and insulin-expressing cells in early embryogenesis and a pancreatic bud forms and later regresses. This raises the question of whether a *Pdx1*-independent pathway exists for pancreas generation. Studies demonstrating induction of precocious islet cell differentiation by early (E8.5) expression of ngn3 and a lack of expression in mature islet cells have lead to the supposition that ngn3 is expressed in islet cell progenitors and functions as a pro-endocrine gene driving islet cell differentiation (Apelqvist *et al.*, 1999). The absence of all islet cells in *ngn3* homozygous null mice bearing an otherwise grossly normal pancreas and *ngn3* coexpression with *Pax6*, *Nkx6.1* and *NeuroD1*, three putative endocrine progenitor markers, have confirmed this hypothesis (Gradwohl *et al.*, 2000; Jensen *et al.*, 2000a; Schwitzgebel *et al.*, 2000).

A very recent study, again using the Cre-LoxP system has examined the origins of all of the main pancreatic cell types - the endocrine, acinar and ductal cells (Gu *et al.*, 2002). This study sought to determine whether cells expressing the putative pancreatic progenitor marker Pdx1, do indeed give rise to all pancreatic tissue and whether cells expressing the putative endocrine progenitor marker ngn3, produce all endocrine cell types. The *Pdx1* or *ngn3* promoters were used to drive expression of CRE or an inducible form, CRE-ER™ (Danielian *et al.*, 1998; Metzger *et al.*, 1995; Nagy and Mar, 2001; Rossant and McMahon, 1999; Sauer, 1998). The progeny of $Pdx1^+$ or $ngn3^+$ cells were irreversibly tagged with human placental alkaline phosphatase (HPAP). The advantage of using the CRE-ER™ version for lineage analysis is that this protein remains in the cytoplasm and is inactive until a ligand, tamoxifen, is provided (Danielian *et al.*, 1998; Metzger *et al.*, 1995). When tamoxifen is introduced, tamoxifen-bound CRE-ER™ is transported to the nucleus and catalyses recombination, allowing expression of the HPAP reporter gene (Lobe *et al.*, 1999). Cells can therefore be marked at any time during development, not just at the point when *Pdx1* or *ngn3* is first expressed so that by controlling the time at which tamoxifen is administered, it is possible to characterise the progeny of specific sets of $Pdx1^+$ or $ngn3^+$ cells born at different stages of development. This avoids the problems of labelled cell accumulation accompanying CRE; cells are marked from the time when the promoter driving *Cre* expression is initially switched on. Consequently, marked progeny accumulate as development proceeds and new cells activate CRE so that it is not possible to follow the progeny of cells born at defined developmental stages. Using the *Pdx1* promoter to drive expression of *Cre* recombinase, acini, islets and ducts were all demonstrated to express HPAP, showing that all pancreatic cells are derived from *Pdx1*-expressing

progenitors. HPAP was not detected in the mesenchyme-derived endothelial and smooth muscle cells showing, as expected, that $Pdx1^+$ cells do not give rise to mesodermal tissues (blood vessels and mesenchyme). Furthermore, when using the *Pdx1* promoter to drive expression of CRE-ER™, the HPAP label was only observed in ductal cells if the tamoxifen was administered between E9.5-11.5. Based on the frequency with which $Pdx1^+$ cells adopt islet, acinar, or duct fates for different time-points of tamoxifen injection, $Pdx1^+$ cells at E10.5 were estimated to be 35 times more likely to adopt an adult duct fate than those *Pdx1*-expressing cells at E8.5. As tamoxifen remains active for 24-48 h, it was inferred that in excess of 95 % of the duct progenitors express a high level of *Pdx1* between E9.5-12.5. Acinar and endocrine $Pdx1^+$ precursors are found at all stages of embryonic development however. This would suggest that the vast majority of progenitors for duct and acinar/islet cells are separated prior to E12.5. Using the *ngn3* promoter to drive expression of CRE-ER™, and administering tamoxifen at various time-points between E8.5-14.5, HPAP expression was detected in endocrine cells of all four types, showing that $ngn3^+$ cells from different stages of embryogenesis give rise to all four islet cell types. Less than 1/1000 acini or duct cells were seen to be $HPAP^+$ in double transgenic animals in which the *ngn3* promoter was used to drive CRE expression, demonstrating that mature pancreatic ductal cells derive from progenitors that do not express *ngn3*.

However, even these highly informative experiments using Cre-LoxP to mark cell progeny indelibly lack the ability to trace the fate of individual cells over time. For example, with the experimental designs of the cell labelling experiments mentioned, it is not practical to label a single endocrine progenitor during embryogenesis and search for its progeny in the adult. Therefore, it cannot be ascertained whether a single $ngn3^+$ cell gives rise to all four islet cell types. Until this can be achieved, the exact islet cell lineage remains to be determined. It is a point of note that no study has yet provided robust evidence supporting the existence of a multihormone-expressing endocrine progenitor cell. Common conclusions can, however, be extrapolated from the experiments mentioned (**Fig. 1.11.**). Firstly, it is apparent that the cells of the islets, acini and ducts are all descended from a common *Pdx1*-expressing general pancreatic progenitor cell. Secondly, a common $ngn3^+$ endocrine progenitor cell gives rise to all four endocrine cell types; ductal cells are instead descended from progenitors that do not express *ngn3*. Thirdly, adult α- and β-cells belong to distinct cell lineages and mature β-, PP- and δ-cells are descended from a PP-expressing progenitor which does not give rise to mature α-cells.

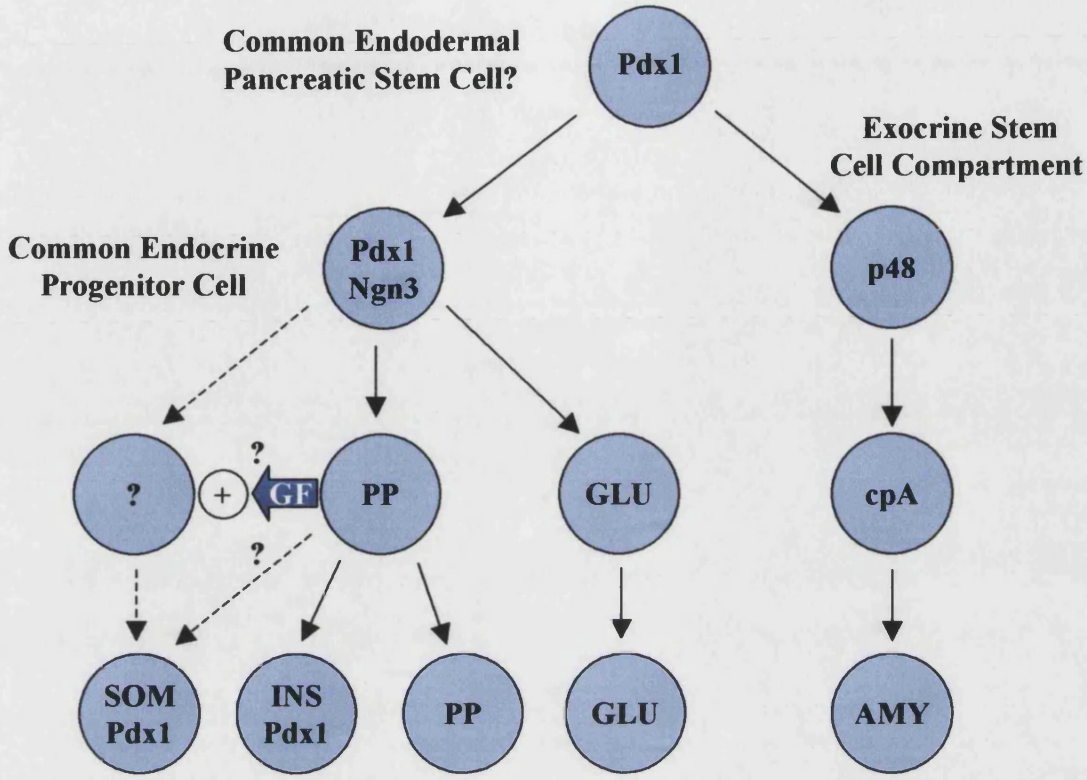

Figure 1.11. Proposed Pancreatic Cell Lineages as Deduced from Results of Cre-LoxP Studies by Gu *et al.* (2002) and Herrera (2000) and Literature Data (Gradwohl *et al.*, 2000; Krapp *et al.*, 1998; Larsson, 1998). (After Herrera, 2000)

The p48 subunit of the exocrine pancreas-specific transcription factor PTF1 is the earliest exocrine marker known to date (Krapp *et al.*, 1998). That somatostatin-expressing cells could descend from PP-expressing precursors is deduced from the cell ablation experiments in transgenic mice (Herrera *et al.*, 1994). cpA, carboxy-peptidase A; AMY, amylase; GLU, glucagon; SOM, somatostatin; INS, insulin; GF, unknown growth or differentiation factor

1.7.5. Endocrine Progenitor Cells

In the light of the above studies, it would appear that the final cell division of a pancreatic epithelial cell does not give rise to both endocrine and exocrine daughters and so the hypothesis of a common "endocrine progenitor cell" can be justified. The ability to identify an endocrine precursor cell population offers many therapeutic applications in the management of type 1 and type 2 diabetes. It provides the possibility of expanding such cells *in vitro* and selectively inducing β-cells before amplifying them and then grafting them into the patient. Cell lineage and gene inactivation studies have contributed to an increasing number of transcription factors being employed as molecular markers of putative endocrine progenitor cells. Such endocrine precursor cells have variously been characterised by their expression of *ngn3*, *Isl1*, *Nkx2.2*, *Nkx6.1*, *NeuroD1* and *Pax6* (Apelqvist *et al.*, 1999; Jensen *et al.*, 2000a; Naya *et al.*, 1997; St.-Onge *et al.*, 1997; Schwitzgebel *et al.*, 2000).

1.8. Growth Control of the Embryonic and Postnatal Pancreas

1.8.1. Mesenchyme Influences Differentiation of the Fetal Pancreatic Epithelium

For 40 years it has been known that inductive signals originating in the mesenchyme play an essential role in the development of the pancreatic epithelium. Classic studies by Golosow and Grobstein (1962), Rutter *et al.* (1964) and Wessels and Cohen (1967) used recombined embryonic tissues to show that pancreatic buds could develop *in vitro*, but that isolated epithelium would not undergo any growth or morphogenesis in the absence of mesenchyme. Pancreatic growth and cytodifferentiation is now a classic example of a mesenchymal-epithelial interaction. In the study by Golosow and Grobstein (1962), salivary mesenchyme was shown to be even more effective than pancreatic mesenchyme in promoting growth and differentiation of the mouse pancreatic epithelium *in vitro*. As the effects of mesenchyme could be exerted across a Millipore filter, it was suggested that the mesenchyme secreted a soluble growth factor required by the epithelium (Golosow and Grobstein, 1962). In some circumstances, the mesenchyme could be substituted by a chick embryo extract, the necessary factor being trypsin-sensitive (Rutter *et al.*, 1964). Although the mitogen from chick embryos was partially purified (Ronzio and Rutter,

1973), the identity of the "mesenchymal factor" remains elusive, partly because it may in fact comprise multiple substances.

A number of experiments in which isolated pancreatic epithelium was cultured in a range of environments have shown that the default state of the pancreatic epithelium is to form islets, and mesenchyme provides an instructive signal for differentiation of exocrine cells (Gittes *et al.*, 1996; Miralles *et al.*, 1998b). Gittes and coworkers (Gittes *et al.*, 1996) isolated pancreatic epithelium of E11 mouse embryos from its surrounding mesenchyme and cultured it under various conditions. When cultured under the renal capsule, the rudiments gave rise to mature islets only, whilst acinar structures developed only in the presence of mesenchyme. Mesenchyme acts quantitatively as a repressor of endocrine tissue development; the insulin-expressing cells that develop in the absence of pancreatic mesenchyme appear to be four-fold greater and also more mature than those that develop in its presence (Miralles *et al.*, 1998b). It had been hypothesised that the pancreatic epithelium produces factors such as activins or bone morphogenetic proteins (BMPs) which act on epithelial cells in an autocrine manner to promote endocrine differentiation (Furukawa *et al.*, 1995; Lyons *et al.*, 1995; Ritvos *et al.*, 1995). The activin inhibitor follistatin (Nakamura *et al.*, 1990) has been shown to be expressed in E12.5 pancreatic mesenchyme. It has been demonstrated that exogenous application of this inhibitor promotes amylase expression whilst repressing insulin expression and thus mimics the effects of the mesenchyme (Miralles *et al.*, 1998b). Furthermore, transforming growth factor β1 (TGF-β1) has been shown to promote endocrine development whilst epidermal growth factor (EGF) stimulates development of ducts (Sanvito *et al.*, 1994). It is, however, unknown whether these proteins are expressed in the mesenchyme surrounding the developing pancreas; therefore their function for pancreatic growth *in vivo* is yet to be determined.

1.8.1.1. Requirement for Activin Signalling in Later Endocrine Development

In addition to activin being integral for endocrine development in the early pancreatic anlage (Miralles *et al.*, 1998b), it also appears necessary for the normal development of islets in later development (Yamaoka *et al.*, 1998). Both transgenic mice expressing dominant negative and constitutively active forms of activin receptor under the control of the insulin promoter exhibit lower survival rates, islet hypoplasia and lower pancreatic insulin content with impaired glucose tolerance when compared with control transgenic mice expressing an intact activin receptor (Yamaoka *et al.*,

1998). The similar phenotypes in the activin receptor mutant animals indicates that a precisely regulated intensity of activin signalling is necessary for normal islet development. Furthermore, in the transgenic animals expressing the dominant negative receptor, the insulin response to glucose was severely impaired. Activin is expressed with follistatin in normal adult islets (Ogawa *et al.*, 1993; Wada *et al.*, 1996; Yasuda *et al.*, 1993) and greatly enhances the insulin response of rat islets to glucose (Totsuka *et al.*, 1988; Yasuda *et al.*, 1993). Activin and betacellulin (a factor purified from the conditioned medium of mouse β-tumour cells; Shing *et al.*, 1993; Watanabe *et al.*, 1994a), or activin and hepatocyte growth factor (HGF) are able to co-ordinately convert pancreatic AR42J cells into endocrine cells expressing insulin, GLUT2, glucokinase, and PP (Mashima *et al.*, 1996a, 1996b; Shibata *et al.*, 1993). Activin may therefore play an important role in the maturation and function of β-cells, in addition to the development of endocrine cells.

1.8.2. Effects of Growth Factors on Fetal and Postnatal Pancreatic Growth

The soluble factors that have been shown to exert an influence on both cell proliferation and cell differentiation are usually referred to as growth factors (Rosenberg, 1995). They act as mitogens, initiating cell growth, cell division and cell differentiation and promote cell survival. Growth factors also influence cell function. They act in a paracrine or an autocrine manner.

Fibroblast Growth Factors (FGFs)

One candidate for the "mesenchymal factor" mentioned above is FGF. FGF1, FGF7 and FGF10 are all expressed in the pancreas during development and have been shown to be capable of activating epithelial cell proliferation in isolated pancreatic epithelium *in vitro* (Bhushan *et al.*, 2001; Mason *et al.*, 1994; Miralles *et al.*, 1999). These three FGFs bind to a specific FGF receptor (FGFR), FGFR2IIIb known to be expressed in the fetal pancreatic epithelium (Finch *et al.*, 1995; Orr-Urtreger *et al.*, 1993). FGF has also been shown to influence differentiation in such isolated pancreatic epithelial cultures; FGF can promote exocrine differentiation from isolated pancreatic epithelium (Horb and Slack, 2000; Miralles *et al.*, 1999). Also, culturing intact pancreatic buds in the presence of a dominant negative form of the FGFR2b receptor

has the effect of reducing cell proliferation (Miralles *et al.*, 1999). These experiments collectively implicate FGFs in pancreatic epithelial cell proliferation.

Experiments in adult animals have shown that FGF7 stimulates cell proliferation of pancreatic cells postnatally. Exogenous FGF7 has been shown to be five-fold more potent than FGF1 or FGF2 in stimulating DNA synthesis (as measured by tritiated thymidine incorporation) within endocrine cells of isolated rat islets (Arany and Hill, 2000). FGF7 also provokes the proliferation of pancreatic ductal cells in adult rats following one-two weeks of exposure (Yi *et al.*, 1994) and transgenic mice overexpressing FGF7 under the control of the liver-specific apolipoprotein E promoter show ductal hyperplasia (Nguyen *et al.*, 1996).

A role for FGFs has also been implicated in the maintenance of the Pdx1-expressing pancreatic progenitor cell population during early pancreatic organogenesis. Inactivation of FGF10 results in a reduced number of $Pdx1^+$ pancreatic cells compared to wild-type littermates (Bhushan *et al.*, 2001). Although the specification of $Pdx1^+$ cells occurs in the absence of *Fgf10*, the maintenance and expansion of the $Pdx1^+$ progenitor cell population is dependent upon FGF10 signalling from the mesenchyme. More recently, it has been shown that when the pancreatic epithelium is cultured for seven days in the presence of FGF7 or EGF, endocrine differentiation is repressed whilst an undifferentiated endocrine progenitor cell population is expanded (Cras-Méneur *et al.*, 2001; Elghazi *et al.*, 2002). Furthermore, FGFR1-IIIb transcripts have been shown to be enriched in pancreatic epithelia cultured with FGF7 or EGF when compared with untreated epithelia, suggesting that FGFR1-IIIb represents a marker for pancreatic progenitor cells (Cras-Méneur and Scharfmann, 2002).

Experiments using dominant negative (dn) forms of the variantly spliced FGF receptors have recently provided evidence for a role of FGF signalling in the control of the neogenesis and glucose-sensing/insulin processing functions of β-cells. Gene inactivation approaches to elucidate the role of FGF signalling in the mouse have been hampered by early embryonic lethality or functional redundancy (Kato and Sekine, 1999; Szebenyi and Fallon, 1999). Hence, dn forms of FGFRs have been used to attenuate FGF signalling by binding to and blocking the interaction of FGFs with the normal receptor. It is known that FGFR1 and FGFR2, along with the ligands FGF1, FGF2, FGF4, FGF5, FGF7 and FGF10 are all selectively expressed in β-cells (Hart *et al.*, 2000). Two transgenic mouse lines which express a dn version of *FGFR1c* (Cheon *et al.*, 1994), denoted FRID1, or *FGFR2b* (Celli *et al.*, 1998; Cheon *et al.*, 1994), denoted FRIND2, in the developing pancreas under the control of the *Pdx1* promoter

have been generated (Hart *et al.*, 2000). FGFR c splice forms such as FGFR1c have been shown to recognise FGF2, FGF4, FGF5, FGF6, FGF8 and FGF9, whilst FGFR2b is activated by FGF3, FGF7 and FGF10 (Igarashi *et al.*, 1998; Ornitz *et al.*, 1996). Although FRIND2 mice remain healthy, FRID1 mice develop diabetes at around 15 weeks of age. This is most probably due to impaired β-cell expression of GLUT2 and PC 1/3 in FRID1 mice, resulting in impaired glucose sensing and insulin processing respectively. This hypothesis is supported by the observed accumulation of proinsulin in the β-cells of FRID1 animals which is strikingly similar to the increased proinsulin content of β-cells in type 2 diabetic patients (Guiot *et al.*, 2001). These findings indicate that FGFR1c signalling in the β-cell is required to ensure normal expression of key components in glucose sensing and insulin processing machinery and thus to maintain normoglycaemia. Moreover, FRID1 mice also display a reduced number of β-cells compared with non-transgenic littermates, implying a role for FGFR1c signalling in the expansion of β-cell number. Hyperplasia of β-cells has been observed in both humans and rodents under conditions such as pregnancy and non-diabetic obesity when there is an increased insulin demand, demonstrating the compensatory capacity of the β-cell (Hellerström *et al.*, 1988; Marynissen *et al.*, 1983; Parsons *et al.*, 1992). Therefore, the reduced β-cell number in FRID1 mice also indicates that FGFR1c signalling is required for maintaining the competence of β-cells to proliferate in response to hyperglycaemia. It is plausible that analogous to the mouse, FGF signalling will prove to be important for human β-cell function and that perturbation of this signalling pathway in adult human β-cells could be linked to type 2 diabetes.

Hepatocyte Growth Factor (HGF)

The HGF mRNA level in fetal pancreas-derived fibroblasts is more than 10-fold that in adult pancreatic fibroblasts. HGF receptor is preferentially expressed in developing β-cells, and their proliferation is stimulated by conditioned medium from fetal pancreatic fibroblasts (Otonkoski *et al.*, 1996) or HGF (Otonkoski *et al.*, 1994a). HGF has even been shown to stimulate proliferation of adult β-cells (Hayek *et al.*, 1995). When amylase-producing AR42J cells are incubated with HGF and activin, the amylase content decreases, and insulin, PP, GLUT2, and glucokinase are expressed (Mashima *et al.*, 1996b). HGF may therefore be a fetal mesenchyme-derived factor regulating β-cell growth and differentiation (Beattie *et al.*, 1996).

Epidermal Growth Factor (EGF) Family and TGF-α

EGF receptors are expressed in the endocrine and exocrine cells of fetal pancreas (Ebert *et al.*, 1995; Miettinen and Heikinheimo, 1992), but EGF is not (Kasselberg *et al.*, 1985), so other factors that can bind to EGF receptors such as betacellulin, TGF-α, and heparin-binding EGF-like growth factor (HB-EGF) may be more important for islet development than EGF itself. As mentioned, betacellulin and activin co-ordinately convert cells of the pancreatic acinar cell line AR42J into insulin-secreting cells (Mashima *et al.*, 1996a; Shibata *et al.*, 1993). Betacellulin has been shown to induce insulin and glucokinase expression in glucagonoma cells stably transfected with Pdx1 (Watada *et al.*, 1996b). TGF-α shares a 50 % sequence similarity with that of betacellulin (Shing *et al.*, 1993), and is expressed in the fetal pancreas (Miettinen and Heikinheimo, 1992). Overexpression of TGF-α in transgenic mice by the elastase or metallothionein promoter induces ductular metaplasia containing numerous insulin-expressing cells resembling pancreatic ductal precursors (Jhappan *et al.*, 1990; Sandgren *et al.*, 1990). This also has the effect of increasing the size of the pancreas, though principally by fibrosis. HB-EGF is expressed in fetal endocrine cells and primitive ducts, and its expression pattern is similar to that of Pdx1 (Kaneto *et al.*, 1997). Pdx1 is able to transactivate the HB-EGF gene promoter. Collectively, these findings suggest that signalling via EGF receptors plays an important role in islet development.

Growth Hormone (GH) Family

GH, prolactin (PRL), and placental lactogen (PL) all stimulate β-cell proliferation as well as insulin production and secretion (Brelje *et al.*, 1993; Hill and Hogg, 1991; Nielsen, 1982). Increased β-cell mass and islet hyperplasia are known to occur during pregnancy in the mother. Although this has been attributed to high levels of glucose in the fetal circulation (Hellerström and Swenne, 1985), it is now thought to represent intrinsic growth under the control of PL (Sorenson and Brelje, 1997); nevertheless, glucose *has* been shown to be a stimulus for expansion of β-cell mass both *in vivo* and *in vitro* (Bonner-Weir *et al.*, 1989; Hellerström *et al.*, 1988; Schuppin *et al.*, 1992; Swenne, 1992). GH receptor (Delehaye-Zervas *et al.*, 1994; Lobie *et al.*, 1990; Miettinen *et al.*, 1993) and PRL receptor (Freemark *et al.*, 1997; Garcia-Caballero *et al.*, 1996; Royster *et al.*, 1995) are expressed in pancreatic islets. In rats bearing GH- and

PRL-producing tumours (Parsons *et al.*, 1983; Sorenson and Parsons, 1985), GH-expressing transgenic mice (Parsons *et al.*, 1995), and in pregnant animals (Sorenson and Parsons, 1985), β-cell mass increases and insulin secretion is enhanced. In pituitary GH- and PRL-deficient dwarf mice, islet volume decreases between two- and five-fold (Parsons *et al.*, 1995). PRL increases GLUT2 expression (De Mazancourt *et al.*, 1994; Weinhaus *et al.*, 1996) and islet sensitivity to glucose (Boschero *et al.*, 1993; Sorenson and Parsons, 1985), and may therefore play a role in β-cell maturation. GH induces IGF-I production from islets, resulting in islet DNA replication via IGF-I receptor (Swenne *et al.*, 1987).

Parathyroid Hormone-related Protein (PTHrP)

Pancreatic islets are known both to produce PTHrP and to possess PTHrP receptors (Gaich *et al.*, 1993; Porter *et al.*, 1998; Vasavada *et al.*, 1996). Transgenic mice expressing PTHrP driven by the rat insulin II promoter display hypoglycaemia, inappropriate hyperinsulinaemia, and increased total islet number and total islet mass (Porter *et al.*, 1998; Vasavada *et al.*, 1996). As these phenotypes are exhibited postnatally, PTHrP may regulate the postnatal endocrine tissue mass.

Thyrotropin-Releasing Hormone (TRH)

TRH is expressed in adult (Martino *et al.*, 1978) and fetal islets (Kawano *et al.*, 1983), and colocalised with insulin in the secretory granules of β-cells (Kawano *et al.*, 1983; Leduque *et al.*, 1986; Ouafik *et al.*, 1987), resulting in glucose-stimulated secretion of TRH from β-cells (Dolva *et al.*, 1983). The roles of TRH in islet development and pancreatic hormone secretion are currently controversial. It is known however, that TRH-null mutants exhibit hyperglycaemia accompanied by impaired insulin secretion in response to glucose (Yamada *et al.*, 1997).

Insulin and Insulin-Like Growth Factor (IGF)

Gene targeting studies have demonstrated that peptides in the extended insulin family, insulin, and IGF-I and IGF-II are important trophic hormones during embryonic and fetal development whose absence results in profound fetal growth retardation (DeChiara *et al.*, 1990; Duvillié *et al.*, 1997; Liu *et al.*, 1993).

Insulin

The amount of insulin made available to the fetus during development is obviously dependent on the volume of the β-cell mass. It has been demonstrated that in rats subjected to hyperglycaemia ("hyperglycaemic clamping") for five days, the islet area is more than twice the size of controls, and the number of islets is almost double and the level of proinsulin mRNA is increased (Chen *et al.*, 1989), suggesting that insulin stimulates β-cell growth in an autocrine manner. β-Cells are equipped to respond to secreted insulin: insulin receptors have been shown to be expressed in rat islets and on β-cells (Harbeck *et al.*, 1996; Verspohl and Ammon, 1980). In transgenic mice expressing mutant forms of human insulin displaying an increased affinity for the insulin receptor, the rate of fetal β-cell growth is three-fold higher compared with that in non-transgenic littermates (Vincent *et al.*, 1995). Glucose and insulin induce phosphorylation of the insulin receptor (INSR) and the insulin receptor substrate (IRS)-1 and IRS-2 in rat islets (Velloso *et al.*, 1995). Genetic inactivation of these signalling components has revealed the mechanism by which insulin promotes β-cell growth. IRS-2 inactivation has been found to result in a decrease in β-cell mass despite insulin resistance in the liver and skeletal muscle, leading to diabetes (Withers *et al.*, 1998). In contrast, IRS-1-null mice exhibit both increased β-cell mass and insulin secretion which compensate for mild insulin resistance (Araki *et al.*, 1994; Tamemoto *et al.*, 1994). Also, the expression level of IRS-2 in rat insulinoma cells is 60-70 times greater than that in rat primary β-cells, whereas IRS-1 mRNA levels are equivalent (Schuppin *et al.*, 1998). These findings suggest that insulin stimulates β-cell growth, especially during embryogenesis (Vincent *et al.*, 1995), via the phosphorylation of IRS-2. Insulin signalling in β-cells influences insulin secretion in addition to their growth. β-Cells overexpressing wild-type insulin receptors display a three-fold increase in cellular insulin content and a five-fold elevation in the rate of both basal and glucose-stimulated insulin secretion (Xu and Rothenberg, 1998). Conversely, the β-cell-specific disruption of insulin receptors results in defective insulin secretion with impaired glucose tolerance (Kulkarni *et al.*, 1998). IRS-2 also mediates the effects of insulin on the production of this hormone: transcription of the insulin gene by insulin itself is activated via IRS-2 phosphorylation (Leibiger *et al.*, 1998). These mechanisms can therefore explain both hyperinsulinaemia and the hyperplasia (overgrowth) of islets in prediabetic patients displaying insulin resistance.

IGFs

Pancreatic Expression

There is substantial evidence to suggest that continuous β-cell proliferation in early life is dependent on IGF-I and II which both exhibit a complex pattern of pancreatic expression. IGF-II is expressed most abundantly in fetal rat pancreas and then declines neonatally (Hogg *et al.*, 1994; Petrik *et al.*, 1998) as in most other tissues (LeRoith, 1991, 1997; Schofield, 1992). Some IGF-II immunoreactivity can be detected in the β-cells of healthy rats and humans (Hoog *et al.*, 1996; Maake and Reinecke, 1993). IGF-II mRNA is expressed throughout the islets and in ductal epithelium (Hill *et al.*, 1999; Petrik *et al.*, 1998). Conversely, IGF-I expression is low during fetal life and does not attain adult levels until after weaning. IGF-I mRNA is barely detectable in the islets but its expression in the pancreatic acini increases with age (Hogg *et al.*, 1994). IGF-I and IGF-II immunoreactivity are associated with islet cells throughout development, suggesting that IGF peptide distribution may be dependent on the pancreatic expression of locally-produced IGF-binding proteins or IGFBPs expressed within the pancreas (Hogg *et al.*, 1994). At least six IGFBPs modulate the stability, biological availability to tissues, and mitogenic effects of IGFs in a wide range of human and rat fetal tissues (Hogg *et al.*, 1993; McCusker and Clemmons, 1992). IGFBP3, IGFBP4 and IGFBP5 are predominant in the fetal and neonatal periods, while increased expression of IGFBP1 and IGFBP2 occurs two-three weeks after birth, suggesting a circulatory source during early pancreatic development (Hill *et al.*, 1999). The ontogeny of *IGFBP* gene expression in the pancreas may be related to changes in the nutritional input.

Mitogenic Effects In Vitro

Experiments with isolated islets from the rat or human fetus, or using established β-cell lines, have shown that exogenous IGF-I and IGF-II will promote DNA synthesis in β-cells through the type 1 IGF receptor (Asfari *et al.*, 1995; Hogg *et al.*, 1993; Sieradzki *et al.*, 1988; Swenne *et al.*, 1987; Van Schravendijk *et al.*, 1987). Upregulation of IGF-II has been shown to be associated with β-cell tumorigenesis (Christofori *et al.*, 1994, 1995). A study (Hogg *et al.*, 1993) using fetal rat islets has suggested that although IGF-I is a more potent mitogen than IGF-II, IGF-II is released in much greater abundance. Some evidence also suggests that IGFs are capable of

stimulating growth of the exocrine pancreas; IGF signalling has been shown to promote growth of cultured acinar cells and enhance amylase gene expression (Ludwig *et al.*, 1999; O'Brien and Granner, 1996; Williams *et al.*, 1984) and it has been hypothesised that acinar tissue growth is mediated by the IGF-II ligand (Louvi *et al.*, 1997). It is presumed that both IGF-I and IGF-II operate through the IGF1 receptor (IGF1R; De Meyts *et al.*, 1994; LeRoith *et al.*, 1995) which is primarily responsible for initiating intracellular mitogenic signalling pathways such as the MAP kinase (ERK) and PI3-kinase pathways. The former is usually associated with cell division, but it is probably the latter that is more important for overall growth. The IGF1 receptor is abundantly expressed on α-, β-, and δ-cells (Fehmann *et al.*, 1996; Van Schravendijk *et al.*, 1987; Withers *et al.*, 1999). Studies in fibroblasts from mouse embryos homozygous for null alleles of *Igfr1* have shown that IGF-II can also stimulate cell proliferation through the insulin receptor (INSR; Morrione *et al.*, 1997) which is known to be expressed on β-cells. IGF-II is known to bind to both the IGF1R and INSR receptors with a high affinity (Frasca *et al.*, 1999). It has also been suggested that IGF-I-induced β-cell growth is also mediated by IRS-2 phosphorylation (Hugl *et al.*, 1998; Zhang *et al.*, 1998). In addition to a trophic action on β-cells, IGF can also influence β-cell function at least in the adult. Both IGF-I and IGF-II have been shown to alter glucose-stimulated insulin release by adult β-cells, with a biphasic action which can be modulated by endogenous IGFBPs (Hill *et al.*, 1997; Van Schravendijk *et al.*, 1990).

Mitogenic Effects In Vivo - Transgenic Models

Until recently, evidence for a trophic action of IGF-I or IGF-II on islets *in vivo* has been scarce. Although a general increase in birth size and organ weights of mice expressing either IGF-I or IGF-II transgenes was demonstrated (Quaife *et al.*, 1989; Wolf *et al.*, 1994), only one study reported substantially increased pancreatic weight at birth following IGF-II overexpression (Blackburn *et al.*, 1997). However, the endocrine component represents only 1-2 % of the pancreatic volume (Bonner-Weir and Smith, 1994) so significant changes in islet mass may occur without a noticeable change in pancreatic weight. So, Petrik and coworkers (Petrik *et al.*, 1999) examined islet morphology in IGF-II transgenic animals for possible changes resulting from altered pancreatic expression of IGF-II or from increased circulating levels. In these animals, the endogenous mouse IGF-II gene becomes widely overexpressed during the second half of gestation (Sun *et al.*, 1997) and they exhibit increased fetal weight from E13,

often attaining a birth weight 60 % greater than controls. The transgenic IGF-II mice also show selective organ overgrowth (organomegaly) of the heart, kidney, liver and tongue, all of which demonstrate increased IGF-II mRNA. The model of IGF-II transgenesis used was unusual in that the mouse IGF-II transgene driven by fetal promoters, is repressed during embryonic development but is associated with an increased expression of the endogenous IGF-II gene (Sun *et al.*, 1997). Expression of the IGF-II gene is regulated by parental imprinting, leading to expression of only a paternal copy in most fetal tissues, excepting the choroid plexus and meninges of the brain (DeChiara *et al.*, 1991). The IGF-II gene contains regions that are methylated on the paternal allele and could act as silencer sequences (Feil *et al.*, 1994). In the model of IGF-II gene transgenesis used, the changes in DNA methylation may suppress the transgene but relax imprinting of the endogenous IGF-II gene, leading to its increased expression and selective tissue overgrowth (Sun *et al.*, 1997). As the IGF-II-overexpressing animals die shortly after birth, fetuses were examined on E19.5-20. Transgenic fetuses exhibited elevated circulating levels of IGF-II and islet abnormalities although islet number was no different from control animals. Islets from transgenic animals were of irregular shape and mean individual islet area was five-fold greater than in controls. Cell size was unchanged however from which increased islet size was attributed to hyperplasia (an increase in cell number). Transgenic islets contained proportionately fewer β-cells but a greater proportion of α-cells than control islets. Overall however, increases were observed in the populations of β-, α-, and δ-cells. Many of the α-cells in the islets of IGF-II-overexpressing animals were present in the islet core, illustrating a disruption of normal islet architecture. Immunostaining for the proliferating cell nuclear antigen (PCNA) showed twice as many islet cells to be in a state of active replication in transgenic animals than in controls, whereas the number of cells undergoing apoptosis was reduced. Despite islet hyperplasia, circulating insulin and serum glucose levels were not significantly increased in transgenic animals. These findings show that IGF-II overexpression in fetal life results in islet hyperplasia by increasing the populations of all three major endocrine cell types but does not affect the number of mature islets. It is unclear however, whether islet hyperplasia was primarily caused by increased local pancreatic expression of IGF-II or resulted from exposure to the increased circulating levels. Interestingly, the IGF-II-induced islet overgrowth did not result in hyperinsulinaemia, possibly because of a downregulation of insulin release by IGF-II. A subsequent study by the same group (Hill *et al.*, 2000) on a second transgenic mouse model of IGF-II overexpression confirmed these findings. In the

transgenic Blast line, mouse IGF-II is selectively overexpressed in skin, gut, and uterus driven by a keratin 10 promoter, so that circulating IGF-II is retained postnatally until at least six months after birth, instead of declining after birth to disappear by weaning as usual (Brown *et al.*, 1986; Da Costa *et al.*, 1994). The increased circulating IGF-II is available to target tissues and produces a local overgrowth of tissues at sites of targeted overexpression (Da Costa *et al.*, 1994; Ward *et al.*, 1994). Islets in IGF-II-overexpressing Blast mice exhibited a significantly greater mean area from postnatal day (PN)11 to PN16 relative to controls although proportions of β- and α-cells and circulating insulin levels were unaltered. Again, IGF-II overexpression was found not to influence the total number of islets. The authors concluded that the persistent presence of circulating IGF-II postnatally results in an increased mean islet size and increased populations of both α- and β-cells. This is due to IGF-II suppression of a wave of islet cell apoptosis that occurs in the neonatal pancreas around two weeks after birth (see below).

Most recently, it was demonstrated that targeted overexpression of IGF-II in the pancreatic β-cells driven by the rat insulin I (RIP) promoter produces a similar phenotype to that resulting from elevated levels of IGF-II in the circulation (Devedjian *et al.*, 2000). Islets from transgenic animals were shown to display high levels of IGF-II mRNA and protein whilst their pancreata exhibited a three-fold increase in β-cell mass and a consequent increase in insulin mRNA levels relative to controls. The islets in animals bearing the IGF-II transgene were found to be larger than those in controls and displayed a more elongated, irregular shape. As in the previous two mouse models of IGF-II overexpression (Hill *et al.*, 2000; Petrik *et al.*, 1999), transgenic islets exhibited altered architecture with α-cells randomly distributed throughout the islet core. As a result of β-cell-targeted IGF-II-overexpression, the transgenic animals exhibited hyperinsulinaemia and mild hyperglycaemia and about 30 % of these animals subsequently developed overt diabetes when fed a high-fat diet.

Little is known in general about growth factors that mediate exocrine pancreatic proliferation (Kim and Hebrok, 2001) and as such, few studies have examined the effect of the IGFs on acinar growth. The fact that development of the exocrine pancreas is critically dependent upon mesenchymal-epithelial interactions would, however, suggest that locally produced growth factors play a significant role in this process (Ahlgren *et al.*, 1996; Gittes *et al.*, 1996; Rose *et al.*, 1999; Sanvito *et al.*, 1994). A very recent gene inactivation study has provided evidence that IGF-II has a mitogenic effect on the exocrine pancreas. Kido and coworkers (Kido *et al.*, 2002) demonstrated that combined

inactivation of *Insr* and *Igf1r* decreases mean acinar diameter by approximately 40 % due to reduced cellular proliferation whilst islet development is unaffected. Inactivation of either receptor alone however, produced no effect. Furthermore, combined ablation of the two ligands *Igf1* and *Igf2* results in an identical phenotype. Some studies suggest that there is functional overlap between the growth-promoting functions of the two receptors. IGF-II has been shown to promote embryonic growth in mice not only through its cognate receptor IGF1R, but also through INSR (Efstratiadis, 1998; Louvi *et al.*, 1997; Ludwig *et al.*, 1996) and furthermore, IGF-II is known to bind to both the IGF1R and INSR receptors with a high affinity (Frasca *et al.*, 1999). Since exocrine tissue reduction is not observed in single $Insr^{-/-}$ or $Igf1r^{-/-}$ mutant embryos, it is unlikely to be a consequence of impaired insulin or IGF-I signalling, which activate only the cognate receptor. On the basis of the known interactions of IGF-II with both IGF1R and INSR, the decrease of exocrine tissue in double $Insr^{-/-}Igf1r^{-/-}$ mutants is consistent with the hypothesis that acinar tissue growth is mediated by the IGF-II ligand (Louvi *et al.*, 1997).

1.8.3. Growth and Regeneration of the Postnatal Pancreas

1.8.3.1. Remodelling of Neonatal Islets

During fetal and early neonatal life, β-cell mass continues to increase in the rodent pancreas. However, there is a transient plateau between one and three weeks after birth during which β-cell mass does not increase despite the continued growth of the animal (Finegood *et al.*, 1995). This has been attributed to a remodelling of the neonatal endocrine tissue compartment in the second week of postnatal life. In 1995, Finegood *et al.* described a postnatal wave of β-cell death in the developing rat pancreas using a mathematical model of β-cell mass dynamics. The peak rate of this wave was predicted to be 9 % of β-cells/day at PN12. The predicted apoptotic wave was subsequently validated by direct histochemical detection of apoptotic cells. Studies in rats using the fluorescent dye propidium iodide or terminal deoxynucleotidyl transferase- (TdT)-mediated biotin dUTP nick-end labelling (TUNEL) to morphologically identify apoptotic cells have identified peaks of β-cell apoptosis occurring between PN13 and PN14 (Petrik *et al.*, 1998; Scaglia *et al.*, 1997). More recently, this phenomenon has also been shown to occur in the mouse pancreas, with the wave of β-cell apoptosis peaking at PN12 (Trudeau *et al.*, 2000). TUNEL staining

translates into a very high rate of cell removal per day when it is realised that cells can only be observed as TUNEL-positive for a short period of a few hours (Petrik *et al.*, 1998). Estimates of apoptotic rate derived from TUNEL staining are therefore very conservative.

Further evidence also implicates an involvement of IGF-II in this wave of endocrine cell death. It has been demonstrated that the neonatal wave of islet cell apoptosis in the rat pancreas is temporally associated with a fall in the islet cell expression of IGF-II (Hill *et al.*, 1999; Hogg *et al.*, 1994; Petrik *et al.*, 1998). It has been known for some time that the IGFs are able to prevent apoptosis in a variety of cell types (Geier *et al.*, 1992; Stewart and Rotwein, 1996) by mechanisms that include an inhibition of caspases (Jung *et al.*, 1996). Moreover, both IGF-I and II have been shown to function as islet survival factors *in vitro* by suppressing cytokine-mediated islet cell death in isolated neonatal rat islets (Petrik *et al.*, 1998). In a subsequent study by the same group (Hill *et al.*, 2000) mentioned above, it was demonstrated that in transgenic mice in which IGF-II is overexpressed, the wave of islet cell apoptosis is substantially decreased in comparison to wild-type littermates due to the persistent presence of circulating IGF-II postnatally. Islets from these IGF-II transgenic mice consequently exhibited a significantly greater mean area from PN11-16 than islets from non-transgenic siblings (Hill *et al.*, 2000).

The functional significance of this neonatal remodelling of the islet cell mass is unknown. However, in other systems such as in male germ cells (Wang *et al.*, 1998) and cardiac myocytes (Kajstura *et al.*, 1995), similar waves of neonatal apoptosis contribute to tissue remodelling coincident with changing function or cellular demand. It is possible that this remodelling is associated with the maturation of the glucose response by β-cells. The glucose sensitivity of β-cells has been reported to be acquired neonatally, and the response to glucose matures only after weaning, around three weeks after birth (Asplund, 1973; Hole *et al.*, 1988; Otonkoski *et al.*, 1988a; Weinhaus *et al.*, 1995). The signals that initiate maturation of glucose sensing in islet cells remain unknown (Sander and German, 1997).

1.8.3.2. Postnatal Turnover of the Endocrine Compartment

Until quite recently it was widely believed that there is a fixed population of pancreatic β-cells that are incapable of recovery following ablation. Islet cells were presumed to exhibit no appreciable growth during adult life (Hellerström *et al.*, 1989).

This belief was based on the sustained lack of function in severe cases of type 1 diabetes mellitus and secondly, on the failure of recovery of experimental animals from diabetes induced with the β-cell toxin streptozotocin. These effects do not, however, exclude the possibility of there being a normal turnover of β-cells in the pancreas. By extrapolating the available cell kinetic data (Kaung, 1994; Montana *et al.*, 1994; Swenne and Eriksson, 1982), Finegood and colleagues (Finegood *et al.*, 1995) determined that approximately 20 % of β-cells in the PN1 neonatal rat pancreas are in a state of active proliferation and this figure declines progressively in the weeks following birth. However, the replication rate stabilises at an adult level of 3 % β-cell turnover per day at approximately PN40. Later studies have confirmed that the β-cell mass does continue to grow well into adulthood. Morphometric data from wild-type mice aged from four weeks to six months and of the same mixed background (C57Bl/6J/129J) (Bruning *et al.*, 1997; Kopin *et al.*, 1999; Westphal *et al.*, 1999; Withers *et al.*, 1998) shows that β-cell mass increases at least 10-fold over the five-month period examined and is linearly correlated with body weight. The β-cell mass also increases throughout the life of the male Lewis rat: initially by an increase in cell number and then, from 15 months onwards, by an increase in cell size (hypertrophy) of the β-cell (Montanya *et al.*, 2000). It was a widespread belief that because β-cell replication after the neonatal period is relatively low (3 %), the β-cell mass does not turn over significantly during adult life and that the number of β-cells remains virtually static from birth. However, even the "low" level of β-cell replication in the adult rodent pancreas is sufficient to bring about dramatic changes in β-cell mass. Hellerström *et al.* (1988) pointed out that with a β-cell birthrate of just under the adult level of 3 % new cells per day, the β-cell mass would double in one month if there were negligible cell death or apoptosis. The β-cell mass does not continue to double each month in postnatal life so the β-cell like the majority of other cell types, must have a finite life span. The mathematical model of Finegood and coworkers (Finegood *et al.*, 1995) suggests a mean turnover time of 20 days for β-cells in the adult rat and a life span of approximately 58 days. Indeed, if the rate of β-cell death approaches the replication rate of 3 %, then complete replacement of the β-cell population could occur in a one-month period. So, the endocrine pancreas of the adult should be considered to be a slowly renewed tissue (Finegood *et al.*, 1995). This β-cell production can be achieved through the replication of pre-existing β-cells (Hellerström *et al.*, 1988) or via neogenesis, the budding of endocrine cells from the ducts (Bonner-Weir, 2000).

1.8.3.3. Postnatal Neogenesis and Regeneration

Evidence for neogenesis or novel tissue formation is found in pancreata from obese humans and a number of animal models. Conditions that provoke chronic trauma or inflammation of pancreas tissue (pancreatitis) appear to induce novel islet formation by budding from ductules (Gu and Sarvetnick, 1993; Gu *et al.*, 1994; Rosenberg *et al.*, 1983). Such conditions can occur spontaneously during pathological processes or more commonly, are induced experimentally in animal models. The rare human condition of nesidioblastosis is one example of a pathological condition causing neogenesis in which novel islets appear to be formed continuously (Goossens *et al.*, 1989). An experimental example is that of wrapping the head of the hamster pancreas with cellophane tape such that there is a stasis of secretions in the smaller ducts (Rosenberg *et al.*, 1983). This leads to a local inflammation and fibrosis. The ducts exhibit hyperplasia and metaplasia to goblet-like cells as in the intestine. Moreover, some budding of islets from the hyperplastic ductules is observed. A similar phenomenon is replicated in transgenic mice in which expression of interferon γ is driven by an insulin promoter (Gu and Sarvetnick, 1993; Gu *et al.*, 1994). This provokes an autoimmune attack on the β-cells leading to chronic inflammation and tissue destruction with consequent goblet cell and hepatic metaplasia. Cell kinetic studies with 5'-bromo-2'-deoxyuridine (BrdU) support the origination of β-cells from the ducts.

Ligation of the main pancreatic duct has traditionally been employed to cause pancreatic destruction. The effect of this is to prevent the outflow of the pancreatic secretions; although most of the enzymes are in the form of inactive precursors, sufficient activity is presumably released to lead to a rapid destruction of the acinar tissue, and a slower destruction of ducts and islets (Goss, 1978; Hughes, 1956). Whilst prolonged ligation leads to a permanent and irreversible fibrosis, temporary ligation ablates the majority of the acinar tissue with little detrimental effect on the ducts and islets. A similar effect can be obtained by administration of the protein synthesis inhibitor ethionine in conjunction with a protein-free diet (Fitzgerald *et al.*, 1966). Following termination of any of these damaging treatments, a rapid regeneration of the acinar tissue ensues, with complete restoration after a few weeks. These results demonstrate that the adult acinar tissue retains a capacity for rapid regenerative growth. This capacity is also exhibited following the surgical removal of parts of the pancreas or "partial pancreatectomy" although the extent of regeneration is not as dramatic. It is possible to remove up to 90 % of the rat pancreas without serious effect on the animal's

rate of growth. Studies have shown some regeneration, defined as growth of the remnant in excess of that shown by the same region of pancreas in sham-operated animals, but total organ size is never completely restored to that of the controls (Friedmann and Marble, 1941; Lehv and Fitzgerald, 1968; Sidorova, 1978). Reinforcing earlier studies, it has recently been shown that within four weeks of 90 % pancreas removal, the β-cell mass was 45 % and pancreatic weight (reflecting exocrine mass) was 27 % that of sham-treated animals (Bonner-Weir *et al.*, 1993, 1997; Sharma *et al.*, 1999), showing that regeneration occurred in a discordant fashion. Although mitotic index is elevated both in the acinar and islet cells (Brockenbrough *et al.*, 1988), this rapidly declines over the first two weeks post-surgery whereas the slight growth advantage of the remnant is maintained for about six months. Although some regeneration is due to enhanced replication of pre-existing differentiated cells, it has been reported that there is some sprouting of ducts at the cut surface and subsequently some differentiation of new acinar and islet cells. Duct cells have been claimed to transiently re-express Pdx1 before differentiating into islet, acinar or ductal phenotypes (Sharma *et al.*, 1999). The numbers of $Pdx1^+$ ductal epithelial cells have been shown to increase in the main pancreatic duct of the rat pancreas following the induction of necrotising pancreatitis by the intraductal infusion of sodium taurocholate (Taguchi *et al.*, 2002). Islet cell hyperplasia can be stimulated by administering nicotinamide or 3-aminobenzamide, both inhibitors of poly ADPR synthetase (Yonemura *et al.*, 1984). A differential cDNA screen on regenerating pancreata following 90 % pancreatectomy led to the cloning of the genes encoding regenerating proteins (Reg) I, II, and III (Narushima *et al.*, 1997; Suzuki *et al.*, 1994; Terazono *et al.*, 1988; Unno *et al.*, 1993). Reg I has also been shown to be induced by nicotinamide (Watanabe *et al.*, 1990). Although usually secreted from pancreatic acinar cells, Reg I is expressed in β-cells of hyperplastic islets during regeneration; expression has also been shown to increase following cellophane wrapping, and pancreatitis (Rafaeloff *et al.*, 1995; Satomura *et al.*, 1993; Terazono *et al.*, 1988, 1990). The level of islet Reg I expression has been shown to be positively and negatively correlated with islet cell replication and islet cell differentiation respectively (Francis *et al.*, 1992; Otonkoski *et al.*, 1994b). Reg I is able to stimulate proliferation in the rat pancreatic duct-derived ARIP cell line, but not in AR42J (acinar) or RIN (β-) cell lines (Zenilman *et al.*, 1996). Moreover, intraperitoneal administration of recombinant rat Reg I protein is able to ameliorate the diabetic symptoms resulting from 90 % pancreatectomy by increasing β-cell mass (Watanabe *et al.*, 1994b). Reg I knockout mice recently produced by homologous recombination have

been found to develop normally although display a reduced rate of islet cell proliferation in comparison to control mice (Unno *et al.*, 2002). The related islet neogenesis-associated protein (INGAP) is expressed in regenerating hamster pancreas (Rafaeloff *et al.*, 1997). It has been shown to stimulate the incorporation of tritiated thymidine into hamster duct epithelia in primary culture and a rat pancreatic duct cell line, but is without effect on a hamster insulinoma tumour cell line. INGAP may therefore invoke ductal cell proliferation, a requirement for islet neogenesis (Rafaeloff *et al.*, 1997). Reg I and INGAP therefore appear to be involved in the maintenance of β-cell mass, especially in islet neogenesis in adult pancreas. Some evidence (Gorden *et al.*, 1997; Oberg-Welsh *et al.*, 1997; Rooman *et al.*, 1997) also suggests that vascular endothelial growth factor (VEGF) might act as a mitogen for ductal epithelial cells like INGAP since it increases the insulin content in fetal islets and stimulates ductal proliferation, a prerequisite for β-cell formation. NGF secretion from islet cells has been demonstrated to increase in response to streptozotocin-induced β-cell injury (Teitelman *et al.*, 1998), which has lead some to suggest that it might also play an important role in islet neogenesis following injury in the adult.

Alloxan and streptozotocin have been widely used to specifically destroy pancreatic β-cells and produce animal models of diabetes (Chang and Diani, 1985). Both produce rapid β-cell necrosis although streptozotocin has fewer side effects and is therefore preferentially used. It is a glucose-conjugated nitrosourea which is presumed to gain access to the β-cells via the glucose-sensing machinery. If administered in a sufficiently large amount, a single dose will destroy the majority of the β-cells, inducing a permanent severe diabetes from which there is no significant recovery in β-cell numbers (Brosky and Logothetpoulos, 1969; Hamming and Reynolds, 1977). A lower dose will destroy fewer β-cells and provoke a less acute diabetes, although this too is permanent (Bonner-Weir *et al.*, 1981; Steiner *et al.*, 1970).

Collectively, these studies of experimentally-induced pancreatic regeneration demonstrate that acinar cell destruction is followed by rapid regeneration whereas β-cell ablation results in an almost total absence of regeneration. The different tissue compartments therefore exhibit very disparate behaviour. However, it would appear that all the cell types exhibit some potential for division. It is also apparent that there is no systemic means of sensing the total size of the organ as there is in the liver, which results in the rapid regeneration of a remnant until its original size is restored, usually within a matter of days. The relative health of animals suffering the loss of a significant

portion of pancreas tissue indicates that the normal pancreas size represents a considerable functional excess capacity for both exocrine and endocrine functions. These studies also demonstrate the existence of pathological stimuli that can stimulate growth of pancreatic tissues, so local signals must exist that possess the capacity for promoting growth postnatally. The weight of descriptive evidence supporting the budding of acini and islets from hyperplastic ducts, although not conclusive in relation to the cell lineage, suggests that the ductal tissue comprises, or contains, a stem cell population (Githens, 1988). Indeed, incubation of postnatal ductal tissue with embryonic mesenchyme appears able to induce islet formation (Dudek *et al.*, 1991). Furthermore, some cells of the normally amylase-secreting AR42J pancreatic cell line, if treated with activin A and betacellulin, become neuron-like and secrete insulin or PP (Mashima *et al.*, 1996a; Shibata *et al.*, 1993). If this cell line corresponds in behaviour with cells *in vivo*, then it would support long-term competence to generate endocrine cells from non-endocrine precursors. A ductal origin for the other pancreatic cell types is also consistent with the descriptive reports of endocrine cell production in the embryo. The failure of regeneration following treatment with streptozotocin or alloxan may suggest that these agents target these putative stem or precursor cells in addition to the differentiated β-cells (Slack, 1995). The possibility also cannot be excluded that such stem cells reside within the islets themselves. In support of this hypothesis, it has been shown both by *in situ* hybridisation and immunohistochemistry that a subset of endocrine cells in the islets of four-week old mice expresses the intermediary filament protein nestin, considered to be a marker for stem cells (Hunziker and Stein, 2000; Lendahl *et al.*, 1990). These cells were found to express neither insulin, glucose, nor somatostatin although expression of PP was not examined. It has also been claimed that isolated nestin$^+$ islet cells can differentiate into endocrine and exocrine cells *in vitro* (Zulewski *et al.*, 2001). Most recently however, it was reported that nestin is expressed only in mesenchymal cells surrounding the pancreatic epithelium and is not expressed in pancreatic epithelial cells at any stage of development, refuting a stem cell role in the pancreas (Selander and Edlund, 2002).

It cannot be ascertained whether the continuous, slow turnover of cells in the postnatal pancreas is fed from a stem cell population. Certainly, studies on other tissue renewal systems show that there is no requirement for a stem cell population to divide more rapidly than the other, differentiated cells within that tissue. The existence or otherwise of a pancreatic stem cell population and the extent of the limitation on the division potential of the differentiated cells, are matters of contention. Very little is

known about growth control in the pancreas despite the significant period over which the organ has been studied.

1.9. Current Studies

The results of the studies reported hereafter on various aspects of differentiation and growth of the mammalian (mouse) pancreas, have been segregated into five chapters. The results of the studies are described more or less in the order in which the work was conducted. Since a specific introduction to each study has been included at the beginning of each chapter, only a very brief overview is given here. **Chapter 3** describes the characterisation of a sub-population of motile epithelial cells in recombination cultures of β-gal-labelled pancreatic epithelium from E11.5 β-gal-expressing transgenic ROSA-26 strain mouse embryos and unlabelled intact dorsal pancreatic buds from E11.5 MF1 albino strain embryos. **Chapter 4** outlines an immunocytochemical analysis of cell lineage and clonal development of the major pancreatic cell types in the postnatal pancreas using β-gal-expressing H253 X-inactivation mosaic mice. **Chapter 5** describes an investigation into the three-dimensional structure and clonal composition of irregularly-shaped islets observed in the H253 mice during the analysis of pancreatic cell lineage. These islets appeared to resemble two or more conjoined islets and were hypothesised to represent islet(s) undergoing either division (fission) or fusion. **Chapter 6** reports the findings of a statistical morphometry-based investigation into the effects of specifically targeted and hence, local overexpression of the growth factor IGF-II within the exocrine and endocrine tissue compartments of the pancreas. Finally, **Chapter 7** describes an immunocytochemistry-based investigation into the relationship between two sub-populations of hepatocytes induced in cultures of E11.5 mouse pancreatic buds by exposure to the synthetic glucocorticoid dexamethasone.

2. Materials and Methods

2.1. Pancreatic Bud Cultures

The protocol employed for establishing pancreatic bud cultures and their subsequent immuno- and X-gal staining was essentially that developed by Percival and Slack (1999) with some minor procedural modifications.

2.1.1. Dorsal Pancreatic Bud Dissection

Pregnant mice were sacrificed by cervical dislocation and uteri explanted by severing their connection with the oviducts. The uteri were then dissected in ice-cold sterile phosphate-buffered saline (PBSA, Oxoid). Under a dissecting microscope in a laminar flow hood, embryos were removed from the decidua and transferred to ice-cold BME medium with Hank's salts supplemented with 10 % fetal bovine serum (FBS), 1 × L-glutamine and 50 μg/ml gentamicin (all Gibco-BRL, Life Technologies) and the gut was dissected out. Using a microscalpel and fine forceps the dorsal pancreatic bud was excised from its position just posterior to the stomach (**Fig. 2.1.**). Pancreata were collected in ice-cold BME/Hank's medium.

2.1.2. In Vitro Cultures

Glass coverslips (No. 1, 22 × 22 mm, Chance Propper) were immersed in 2 % 3-aminopropyltriethoxysilane (APTES, Sigma) in acetone overnight, rinsed twice in acetone and twice in sterile, MilliRO water, and dried at 37°C. They were subsequently sterilised by baking for 2 hours (h) at 180°C then placed in 30 mm Petri plates (Nunc). In a flow hood, a 40 μl drop of bovine plasma fibronectin (lyophilized, Gibco-BRL, Life Technologies) at 50 μg/ml in sterile water was placed on the centre of each coverslip and was left to evaporate for 3 h. Plates were stored at 4°C prior to use.

To establish intact dorsal pancreatic bud cultures, 3 ml of BME medium with Earle's salts (Gibco-BRL), 20 % FBS, 1 × glutamine and 50 μg/ml gentamicin was added to each dish. The FBS content of the culture medium was doubled from 10 % to permit more infrequent replenishment of the medium and so impose less of a

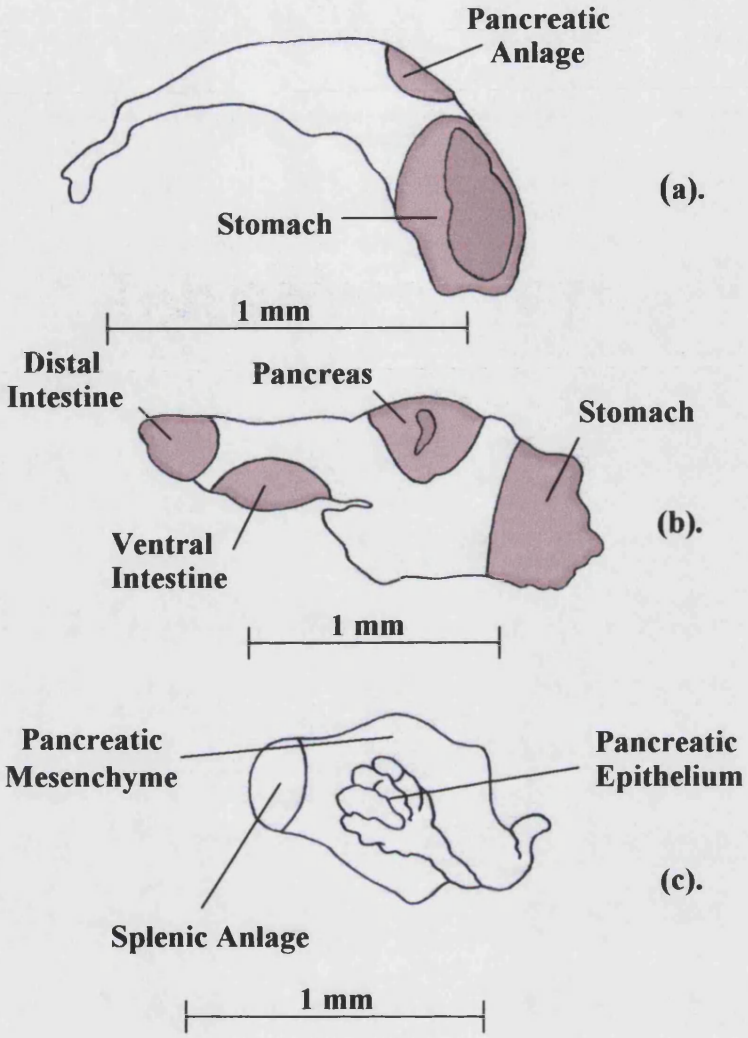

Figure 2.1. Schematic Depiction of Microdissection of the Developing Mouse Foregut and Pancreas. (After Gittes and Rutter, 1992)

(a) 20-somite stage (E9.5) foregut. The area of the incipient stomach and the duodenal anlage are shown. (b) 26-somite stage (E10) when the pancreas is first beginning to evaginate from the dorsal surface of the foregut. (c) 48-somite stage (E11.5) pancreas. The pancreatic epithelium within the surrounding pancreatic mesenchyme is beginning to branch in the formation of early acini

disturbance. A stainless steel ring ("cloning ring") of 4 mm internal diameter was placed over the fibronectin-coated region, and the pancreatic bud was placed into the centre. This cloning ring immobilised the bud during the initial culture period whilst it adhered to the substrate. To ensure spreading during culture, the buds were turned if necessary with a fine needle so that they were orientated cut-surface downwards. Cultures of isolated pancreatic epithelium were established similarly; the epithelium was manually segregated from the surrounding mesenchyme by teasing the latter away with fine forceps before the epithelial bud was "plated" on to the fibronectin substrate. In a third type of culture, isolated epithelium and mesenchyme derived from the same dorsal pancreatic bud were explanted on the centre of the same fibronectin-coated coverslip whereupon each tissue fragment was immobilised by a separate cloning ring.

All cultures were maintained at 37°C, in 5 % CO_2 for up to 9 days. The medium was replenished either each day or every other day of the culture period dependent upon the experiment, and the stainless steel ring was removed on day 2 *in vitro*.

2.2. Specimen Fixation and Storage

2.2.1. Cultures

After the desired duration of growth *in vitro*, cultures were fixed either in mammalian MEMFA (10 % formalin, 0.15 M Mops, pH 7.4, 2 mM EGTA, 1 mM $MgSO_4$) for 40 minutes (min) at room temperature, 4 % paraformaldehyde (PFA) for 20 min or 40 min at room temperature, or in a 1:1 acetone:methanol fixative for 5 min at -20°C. They were then washed in PBSA and stored in PBSA with the addition of 0.02 % NaN_3 at 4°C for a few days though occasionally for up to several months.

2.2.2. Embryos

Freshly dissected E11.5-15.5 wholemount mouse embryos or their dissected organs (such as brains and guts) were fixed for 1-2 h and 35 min-2 h respectively depending on size in 4 % PFA in PBSA (including 0.1 % H_2O_2 if subsequent immunocytochemistry employed immunoperoxidase detection) at room temperature with gentle agitation. Prior to fixation of larger embryos, the fourth ventricle was opened to minimise precipitation of reagents within body compartments. Specimens were subsequently rinsed and stored in PBSA at 4°C for up to a few days if necessary.

2.2.3. Pancreata

Animals were sacrificed by cervical dislocation and their pancreata rapidly excised. They were then typically divided into two equal-sized portions, one of which was subjected to paraffin histology and the other destined for the preparation of frozen sections. Pieces of pancreata were either fixed in ice-cold 4 % paraformaldehyde in PBSA, pH 7.4 at 4°C for 48 h (paraffin embedding) or 1.5 h (cryoembedding) after which they were washed at 4°C in PBSA.

2.3. Staining for β-Galactosidase Activity

2.3.1. Cultures and Frozen Sections

Histochemical X-gal staining of cultures or frozen pancreas sections (refer below) for β-galactosidase activity was performed in freshly-constructed Tissue Stain Base: 2 mM $MgCl_2$, 0.01 % (weight/volume or w/v) sodium deoxycholate, 0.02 % (w/v) Nonidet P-40, 5 mM $K_3Fe(CN)_6$, 5 mM $K_4Fe(CN)_6.6H_2O$ in 100 mM Sorensen's PO_4 buffer, pH 7.4 (comprising 1 M Na_2HPO_4 and 1 M NaH_2PO_4) with 1 mg/ml of X-gal (4-chloro-5-bromo-3-indolyl-β-D-galactopyranoside; Boehringer Mannheim or Melford Laboratories). X-Gal was prepared as an 80 mg/ml stock solution in dimethylsulphoxide (DMSO) and was diluted immediately prior to use into Tissue Stain Base pre-warmed to 37°C to prevent precipitation of the substrate. Incubation was at 37°C in the dark; cultures were incubated within the 30 mm Petri plates for 2 h whilst frozen sections were subjected to overnight incubation. Cultures and frozen sections were then washed in PBSA after which they were mounted in Gelvatol medium. The pH of this mountant is optimal for fluorescein fluorescence; the *n*-propyl gallate contained reduces fluorescein quenching. Gelvatol medium was constructed by dissolving 20 g of polyvinyl alcohol in 80 ml of 10 mM Tris, pH 8.6, including 0.2 % NaN_3. This was mixed with 50 ml glycerol containing 3 g of *n*-propyl gallate.

2.3.2. Pancreata and Earclips

Whole pancreata or earclips were fixed by immersion in Tissue Fixative (4 % PFA, 2 mM $MgSO_4$, 5 mM EGTA in 100 mM Sorensen's phosphate buffer, pH 7.4) for 45 min-1.5 h on ice. They were subsequently washed in Tissue Rinse Solution A (2 mM

$MgCl_2$, 5 mM EGTA in 100 mM PO_4 buffer, pH 7.4) for 30 min at room temperature, then rinsed in Tissue Rinse Solution B (2 mM $MgCl_2$, 0.01 % sodium deoxycholate, 0.02 % Nonidet P-40 in 100 mM PO_4 buffer, pH 7.4) for 5 min at room temperature. After draining, the tissue was incubated in freshly constructed, pre-warmed Tissue Stain Base with 1 mg/ml of X-gal. For pancreata, incubation was at 37°C or 30°C overnight in the dark. Earclips from different animals were incubated separately in distinct wells of a 96-well MicroWell™ microplate (Nunc) at 37°C for 2 h in the dark, during which the intensity of earclip X-gal staining was periodically monitored. Following reaction, pancreata were rinsed in three changes of PBSA in which they were stored at 4°C prior to embedding.

2.4. Histology

2.4.1. Preparation of Paraffin Sections

Fixed (and X-gal-stained if performed) pancreata were dehydrated from 70 % vol/vol through to 100 % ethanol overnight in a Leica TP 1020 Tissue Processor, and were then embedded in paraffin-wax and sectioned at 7 μm on a Leica RM 2155 rotary microtome before mounting on glass microscope slides. Slides were either obtained pre-coated (Polysine™, BDH) or untreated (Single Frost Blue Star, Chance Propper Ltd.) and then coated with APTES; slides were initially washed in hot soapy water, rinsed in MilliRO water, treated with 95 % ethanol/1 % acetic acid, then dried before immersion in 2 % APTES in acetone for 8 min, acetone for 2 × 10 seconds (sec) and MilliRO water for 10 sec; prepared slides were dried overnight. The paraffin sections were dewaxed in Histoclear (National Diagnostics) and rehydrated through a graded ethanol series prior to immunocytochemical processing. If necessary (for examination of pancreata from Elijah and Ripley animals), selected slides were counterstained in Ehrlich's haematoxylin and eosin (H & E) then, after dehydration and clearing, were mounted in DPX (BDH).

2.4.2. Preparation of Frozen Sections

Fixed pancreata were cryoprotected in 5 %, then 15 % sucrose in 0.1 M potassium phosphate buffer (0.1 M KH_2PO_4 and 0.1 M K_2HPO_4), pH 7.6 at 4°C over successive nights then embedded in O.C.T. compound (BDH). Sealed cryoblocks were

stored at -20°C for up to several weeks. Frozen sections or *cryosections* (10 μm or 15 μm) were cut on a Shandon AS620 cryotome at -17°C and mounted on gelatin-coated glass microscope slides (Single Frost Blue Star, Chance Propper Ltd.). To prepare the slides, they were first submerged in 1:1 hydrochloric acid and 100 % vol/vol ethanol for 2 h minimum and washed under running water. Following draining, slides were submerged for 10 min in freshly prepared ice-cold gelatin chrome alum solution (0.6 % gelatin w/v; 0.03 % w/v chromium potassium sulphate) and allowed to air-dry. Following air-drying for 1 h, mounted cryosections were stored in sealed containers at -20°C in the presence of silica desiccant.

2.5. Immunostaining

2.5.1. Antisera

The primary antibodies used for all immunostaining applications, with source and working concentration in 2 % blocking buffer (BB, Boehringer Mannheim) containing 0.1 % Triton X-100 were as follows (**Table 2.1.**):

Table 2.1. Source and Working Dilution of All Primary Antibodies Used

ANTIBODY	SPECIES	SOURCE	DILUTION
Bovine Insulin	Polyclonal Guinea Pig	Sigma I-6136	1/300
Glucagon	Monoclonal Mouse	Sigma G-2654	1/100 or 1/300 *
Glucagon	Polyclonal Rabbit	DAKO A0565	1/100 or 1/300 †
Glucagon	Polyclonal Rabbit	Abcam ab9379	1/100 or 1/300 †
Human Amylase	Polyclonal Rabbit	Sigma A-0273	1/200
β-Galactosidase	Polyclonal Rabbit	Molecular Probes A-11132	1/300
Neurogenin3	Monoclonal Mouse	Transduction Labs. N63520	1/100 or 1/300 †‡
Neurogenin3	Polyclonal Rabbit	Abcam ab7560	1/100 or 1/300 †‡
Ipf1-c Serum	Polyclonal Rabbit	Made In-house	1/100
Pan-Cytokeratin	Monoclonal Mouse	Sigma C-2931	1/300
Carbamoylphosphate Synthetase I (CPS I)	Polyclonal Rabbit	Professor Wouter Lamers (Gift)	1/500
Glutamine Synthetase (GS)	Monoclonal Mouse	Transduction Labs.	1/500
Transferrin	Polyclonal Rabbit	DAKO A0061	1/200
Transthyretin (TTR) (Prealbumin)	Polyclonal Rabbit	DAKO A0002	1/100
Albumin	Goat	Sigma A-1151	1/300

* This antibody was used at a working concentration of 1/100 for triple-immunofluorescence cytochemistry on cultures for the simultaneous demonstration of insulin, glucagon and amylase.

† These antibodies were employed at a working concentration of 1/100 in an attempt to obtain successful staining of cultures.

‡ The two anti-neurogenin3 antibodies were employed in conjunction with antigen retrieval.

Various secondary, species-specific antibodies were employed in the various immunostaining applications. Again, these are given with source and working concentration (**Table 2.2.**):

Table 2.2. Source and Working Dilution of All Secondary Antibodies Used

ANTIBODY	SPECIES	SOURCE	DILUTION
Fluorescein-Conjugated Anti-Rabbit IgG	Goat	Vector FI-1000	1/150 or 1/300 *
Fluorescein-Conjugated Anti-Mouse IgG	Horse	Vector FI-2000	1/100
Fluorescein-Conjugated Anti-Goat IgG	Rabbit	Vector FI-5000	1/100
FITC-Conjugated Anti-Rabbit IgG	Goat	Sigma F-0382	1/300
Fluorescein Streptavidin	N/A	Vector SA-5001	1/100
Texas Red-Conjugated Anti-Rabbit IgG	Goat	Vector TI-1000	1/300
Texas Red-Conjugated Anti-Mouse IgG	Horse	Vector TI-2000	1/300
TRITC-Conjugated Anti-Rabbit IgG	Swine	DAKO R0156	1/100 or 1/200 †
TRITC-Conjugated Anti-Guinea Pig IgG	Rabbit	Sigma T-7153	1/300
AMCA-Conjugated Anti-Mouse IgG	Horse	Vector CI-2000	1/100
Biotin-Conjugated Anti-Mouse IgG	Horse	Vector BA-2000	1/300
Biotin-Conjugated Anti-Guinea Pig IgG	Goat	Sigma B-5518	1/300
Biotin-Conjugated Anti-Rabbit IgG	Goat	Sigma B-9642	1/200

* This antibody was used at a working concentration of 1/150 for staining of cultures but at 1/300 for detection of β-galactosidase on frozen sections.

† This antibody was used at a working concentration of either 1/100 or 1/200 for staining of cultures, depending upon the experiment.

2.5.2. Immunofluorescence Cytochemistry

2.5.2.1. General Protocol for Cultures and Frozen Sections

Specimens were successively; (1) permeabilised in 1 % (cultures) or 0.15 % (sections) Triton X-100 in PBSA for 30 min (cultures) or 1 h (sections) at room temperature; (2) blocked to avoid non-specific staining with 2 % blocking buffer (BB) containing 0.1 % Triton X-100 for 2-3 h at room temperature; (3) incubated with primary antiserum diluted in 2 % BB/0.1 % Triton X-100 overnight at 4°C; (4)

incubated with the relevant fluorescence-conjugated secondary antibody diluted in 2 % BB/0.1 % Triton X-100 for 2 h at room temperature in the dark and (5) mounted in Gelvatol in the dark in the absence of further rounds of antibody incubations. In some experiments, specimens were counterstained in 0.5 μg/ml 4',6-diamidino-2-phenylindole (DAPI; Sigma D-9542) in PBSA for 5 min before mounting. Following each incubation, specimens were washed in PBSA for 3 × 10 min (cultures) or 3 × 15 min (sections). Where more than one primary antibody was used, the first staining cycle was completed before the second was commenced. Incubations with primary antisera were performed overnight at 4°C or occasionally, for 3 h at room temperature; secondary antibody incubations were conducted for 2 h at room temperature.

2.5.2.2. Modifications for Cultures

Staining was performed within the 30 mm Petri plates. Although the first staining cycle was usually completed before the second was commenced, as an exception to this, when double-staining for CPS I and GS only one incubation was conducted with both primary antibodies: polyclonal rabbit anti-CPS I (gift from Professor Wouter Lamers [University of Amsterdam, Amsterdam, The Netherlands], 1/500) and monoclonal mouse anti-GS (Transduction Laboratories, 1/500), and one 2.5 h incubation (at room temperature) for the two secondary antisera: TRITC-conjugated swine anti-rabbit (DAKO, Denmark R0156, 1/100) and fluorescein-conjugated horse anti-mouse (Vector FI-2000, 1/100).

In some experiments, cultures stained with either of the two anti-neurogenin3 primary antibodies (mouse monoclonal; Transduction Laboratories N63520 or rabbit polyclonal; Abcam ab7560) were subjected to antigen retrieval. This was performed by incubation with pH 6.0 citrate buffer (9.5 mM citric acid and 41.5 mM sodium citrate) for 1 h at 37°C or with 50 mM ammonium chloride in PBSA for 30 min at room temperature (as recommended by accompanying literature) following permeabilisation in 1 % Triton X-100. (In some experiments, 1:1 acetone:methanol-fixed cultures were not subjected to the subsequent permeabilisation step). Cultures were subsequently rinsed in PBSA prior to blocking. Also, some cultures stained for neurogenin3 were subjected to avidin-biotin signal amplification. Following primary antibody incubation and washing, cultures were incubated with biotinylated horse anti-mouse antibody (Vector BA-2000) diluted 1/300 in 2 % BB/0.1 % Triton X-100 for 2 h at room temperature. After washing, cultures were incubated with fluorescein streptavidin

(Vector SA-5001) diluted 1/100 in 2 % BB/0.1 % Triton X-100 for 1 h at room temperature in the dark. Following washing, cultures were either mounted or the second cycle of staining was commenced.

2.5.2.3. Modifications for Frozen Sections

The frozen sections were processed at 4°C in a humid chamber. Adjacent serial sections on the same slide were isolated using a hydrophobic barrier pen (ImmEdge™ Pen, Vector) to permit them to be differentially immunostained (for distinct antigens such as insulin or glucagon, or their absence as control) and to conserve antisera. Prior to permeabilisation, frozen sections were washed for 3 × 5 min to solubilise the O.C.T.

2.5.3. Immunoperoxidase Cytochemistry

2.5.3.1. Paraffin Sections

Sections were processed at 4°C in a humid chamber according to the streptavidin-biotin peroxidase complex (ABC) method in which horseradish peroxidase (HRP) was visualised using 3,3'-diaminobenzidine (DAB) as substrate, yielding a brown reaction product. The deparaffinized and rehydrated sections were successively; (1) treated with 0.6 % H_2O_2 in PBSA for 30 min at room temperature; (2) washed in running water; (3) permeabilised in 0.1 % Triton X-100 in PBSA for 1 h at room temperature; (4) blocked to avoid non-specific staining with 2 % BB containing 0.1 % Triton X-100 for 1 h at 4°C; (5) incubated with primary antiserum diluted in 2 % BB/0.1 % Triton X-100 overnight at 4°C; (6) incubated with the relevant biotin-conjugated secondary antiserum diluted in 2 % BB/0.1 % Triton X-100 for 1 h at 4°C; (7) treated with the HRP-labelled streptavidin-biotin complex kit (StreptABComplex; DAKO, Denmark) for 1 h at 4°C according to the manufacturers' instructions (45 µl streptavidin and 45 µl biotinylated peroxidase in 5 ml of 0.1 M Tris, pH 7.4) and (8) treated with 0.1 M Tris buffer, pH 7.4, containing 0.67 mg/ml DAB (Sigma) and 0.03 % H_2O_2 until appearance of reaction product (approximately 3-15 min) at room temperature. When colour development had reached the desired stage, the reaction was halted with tap water, intensifying the reaction product. Between each incubation, sections were washed in PBSA for 3 × 15 min. Sections were counterstained in nuclear

Fast Red (Vector), dehydrated in graded ethanol, cleared in Histoclear and mounted in DPX (BDH).

Either the primary antibody or secondary biotinylated antiserum was omitted from the immunocytochemical procedure as one type of control procedure to substantiate specific immunocytochemical staining. Lack of staining demonstrates the absence of electrostatic and hydrophobic binding of immunocytochemical reagents to tissues (Leduque *et al.*, 1987) as well as the absence of endogenous peroxidase.

2.5.3.2. Wholemounts (Embryos)

Following post-fixation in 4 % PFA in PBSA, larger (> E13.5) embryos and brains were halved dorsolaterally on dry ice to facilitate penetration. Specimens were then successively; (1) blocked overnight in blocking buffer (PBST - 1 % Triton X-100 in PBSA - containing 1 % BSA, 10 % heat-inactivated FBS and 2 % Boehringer Mannheim blocking buffer); (2) incubated in primary antibody in blocking buffer for 4 days and (3) incubated overnight in alkaline phosphatase- (AP-) or biotin-conjugated secondary antibody in blocking buffer. Between incubations, specimens were washed at room temperature for 3 × 10 min then 3 × 45 min in PBST. All washing and incubation steps were conducted with gentle agitation and all incubations were performed at 4°C. For AP detection, embryos were washed for 3 × 10 min in alkaline phosphatase buffer (APB; 0.1 M Tris-HCl, pH 9.5, 50 mM $MgCl_2$, 100 mM NaCl, 0.1 % Tween 20 and 1 mM levamisole). They were then incubated in the dark at room temperature in a change of APB containing 337.5 μg/ml Nitro Blue Tetrazolium (NBT) and 175 μg/ml 5-bromo-4-chloro-3-indolylphosphate (BCIP) until colour reaction developed then washed twice in PBSA. Immunoperoxidase detection was conducted according to the ABC method. Following washes in PBST, embryos were incubated overnight at 4°C in HRP-labelled streptavidin biotin complex (StreptABComplex; DAKO, Denmark) then washed again in PBST then in 0.1 M Tris, pH 7.4 for 2 × 20 min and were then pre-incubated in 0.5 mg/ml DAB (Sigma) in 0.1 M Tris, pH 7.4 for 1 h at 4°C in the dark with gentle agitation. H_2O_2 was added to a final concentration of 0.003 % and embryos were incubated for 5-20 min at room temperature. When colour development had reached the desired stage, the reaction was halted with tap water.

3. Migratory Cells in the Embryonic Pancreas In Vitro

3.1. Introduction

3.1.1. A Novel In Vitro Culture System for Pancreatic Rudiments

Percival and Slack (1999) recently devised a novel system for the *in vitro* culture of pancreatic buds from the mouse embryo. This culture system enables the developing organ to grow as a flat, branched structure, which is sufficiently thin to be amenable to wholemount immunostaining methods. Differentiation of each of the principal cell types in culture, as monitored by immunostaining, was shown to closely resemble the situation *in vivo* with a slight one-day delay over a four-day culture period. The obvious advantage afforded by this system is that it permits the visualisation of complete acini or islets as opposed to the partial view provided by histological sections. Using their novel *in vitro* system, Percival and Slack (1999) investigated cell lineage in the pancreatic islets and acini and aimed to ascertain whether there is an identifiable endocrine precursor cell population at an early stage of pancreas development. The ROSA-26 mouse was employed as a source of lineage-labelled tissue. This is a gene trap strain engineered by Zambrowicz *et al.* (1997), in which the *lacZ* reporter transgene, is expressed constitutively, at all stages of development in all tissues. The *lacZ* gene encodes the enzyme β-galactosidase (β-gal), which is readily detectable by X-gal histochemistry in individual cells. β-Gal cleaves the colourless substrate 4-chloro-5-bromo-3-indolyl-β-D-galactopyranoside (X-gal) to a robust, blue-coloured indole derivative. The level of β-gal expression was found to vary between tissues: expression in the epithelium of the developing intestine and pancreas was shown to be greater than that in the mesenchyme. However, it was demonstrated that all parts of the pancreas expressed the transgene at all time-points examined (**Fig. 3.1.**) and furthermore, that this expression was retained *in vitro* (Percival and Slack, 1999). In combinations of pancreatic epithelium from β-gal-expressing ROSA-26 embryos with mesenchyme from strain MF1 albino embryos, X-gal staining was found to coincide exactly with the boundary of the epithelium. These experiments demonstrated the eminent suitability of β-gal expressed by ROSA-26 tissue as a lineage label in embryological experiments. Similar combination cultures of pancreatic epithelium from E11.5 ROSA-26 embryos

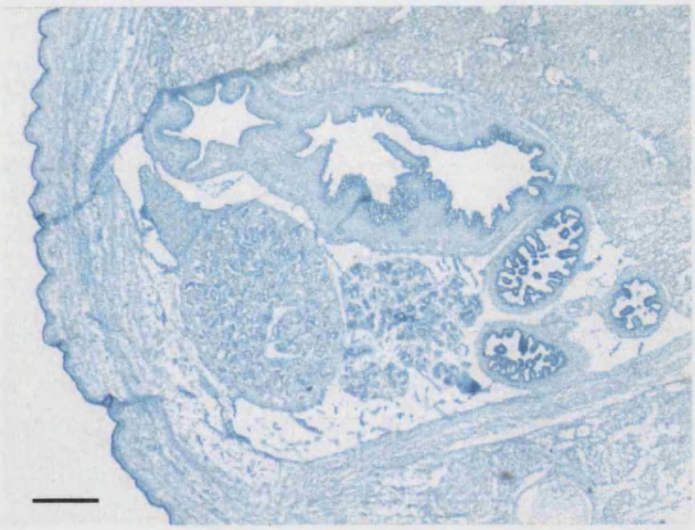

Figure 3.1. Ubiquitous *LacZ* Expression in the ROSA-26 Pancreas (Professor J. M. W. Slack)

Section of an X-gal-stained E16.5 ROSA-26 embryo. Part of the pancreas lies in the centre. All tissues are stained although the epithelia show higher levels of staining than the mesenchymal tissues. Bar = 200 μm

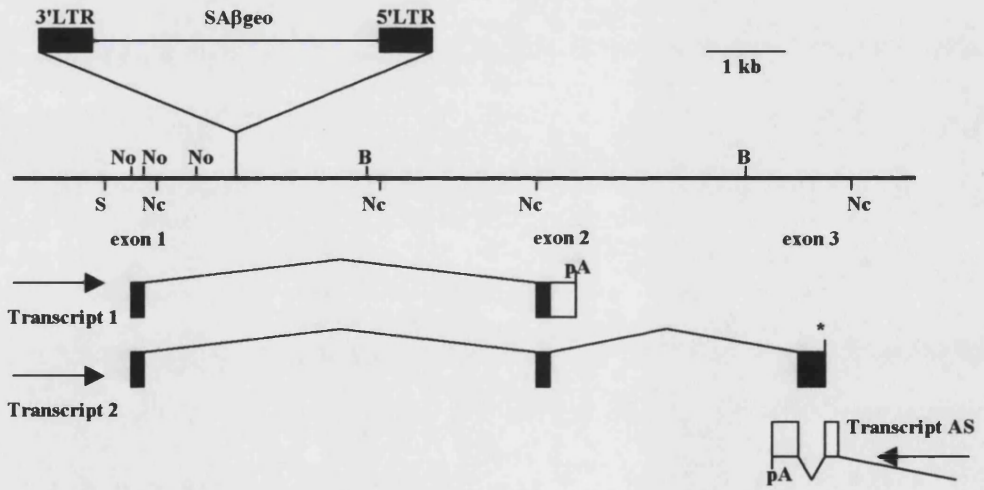

Figure 3.2. Map of the ROSA-26 Genomic Region

Line indicates genomic DNA drawn with the scale and restriction enzyme sites as indicated. The position and orientation of the ROSAβgeo retroviral integration is indicated. LTR, long terminal repeat. B, *Bgl*II; Nc, *Nco*I; No, *Not*I; S, *Sal*I; pA, poly(A) addition signal. (Zambrowicz *et al.*, 1997)

with mesenchyme from E11.5 unlabelled MF1 embryos revealed that both the acinar cells and the β-cells arise from the endoderm while the smooth muscle cells arise from the mesenchyme (Percival and Slack, 1999). This constituted the first formal proof of the endodermal origin of both the exocrine and endocrine cells.

3.1.2. Blue Dot Cells

In these recombinant cultures of ROSA-26-derived, β-gal-expressing pancreatic epithelium and unlabelled MF1 pancreatic mesenchyme, β-cells could be clearly visualized by immunostaining for insulin (Percival and Slack, 1999). As in intact pancreatic bud cultures, they were present both as single cells and as islet-like aggregates and were seen both in the β-gal-expressing epithelium and at some distance away, in the unlabelled mesenchyme. Unexpectedly, following X-gal histochemistry, the β-cells did not stain blue with the same intensity and uniformity as the exocrine cells. Rather, the β-cells were found to contain prominent blue spots indicative of β-gal expression (Percival and Slack, 1999). PYY-expressing cells in such recombinant cultures similarly exhibited this pronounced blue dot-type expression of β-gal, implying that they too originate from the epithelial bud. Although a minority of these blue dot cells produced recognised endocrine products such as insulin or PYY, the majority did not. The blue spot-type β-gal expression by early endocrine cells could not be explained though was presumed to be a consequence of cell processing of the bacterial β-gal protein (Percival and Slack, 1999). The possibility that the expression pattern represents phagocytosis of labelled debris by unlabelled cells was dismissed since blue dot cells could occur at some distance from uniformly stained cells and second, the mesenchymal cells immediately adjacent to the X-gal-stained epithelial tissue did not contain the blue dots. Blue dots were therefore perceived to be representative of endogenous β-gal synthesis and the cells themselves were assumed to be genuinely of epithelial origin.

3.1.3. Current Study

Blue dot expression in cells expressing PYY, known to characterise immature endocrine cells, and their high degree of motility (as demonstrated by their frequent occurrence in the unlabelled mesenchyme at some distance from the β-gal$^+$ epithelium) led to the proposal that such blue dot cells (BDCs) represented a population of

committed endocrine precursor cells. Therefore, the first aim of the current study was to further characterise these blue dot cells in combinations of β-gal-labelled pancreatic epithelium from E11.5 ROSA-26 strain mouse embryos and unlabelled intact dorsal pancreatic buds from E11.5 MF1 albino strain embryos. Physical parameters relating to the occurrence of blue dot cells were investigated, including the frequency of isolated and grouped BDCs and the size of BDC clusters as well as their distance from the labelled epithelium. In the combination cultures of β-gal-labelled epithelium and unlabelled intact bud used here, it could also be investigated whether blue dot cells preferentially migrated away from the epithelium on a stratum of epithelial or mesenchymal cells. A further aim of the study was to determine whether migration of β-gal-labelled cells from the epithelium is restricted to the BDCs. In the event of other, uniformly expressing migratory epithelial cells being detected, these too were to be characterised in the same way as the BDCs.

3.2. Materials and Methods

The protocol employed for establishing pancreatic bud cultures and their subsequent immuno- and X-gal staining was essentially that developed by Percival and Slack (1999) with some minor procedural modifications.

3.2.1. ROSA-26 and MF1 Mouse Embryos

Mouse embryos were generated by timed matings. The day of appearance of the vaginal plug was designated day 0.5 (E0.5). The ROSAβgeo26 (ROSA-26) mouse strain was originally generated by random retroviral gene trapping in embryonic stem cells (Zambrowicz *et al.*, 1997) and demonstrates ubiquitous expression of the proviral βgeo/*lacZ* reporter gene (**Fig. 3.2.**). The *lacZ* gene encodes the enzyme β-galactosidase (β-gal) which is readily detectable by X-gal histochemistry in individual cells.

3.2.1.1. Outbreeding of the ROSA-26 Colony

The ROSA-26 mice were originally of strain 129, but owing to low homozygous survival, they were outcrossed to the Pathology Oxford albino strain at the University of Oxford. Homozygotes of this background proved completely viable during two years of breeding within the colony at the University of Bath. However, following a decline in embryo viability when small litters (< 7), *in utero* resorption and cranial deformities were prevalent, further ROSA-26 outbreeding was necessary.

ROSA-26 animals were initially crossed with the MF1 albino strain, generating pups that were heterozygous for the ROSA-26 transgene. Upon attaining sexual maturity, crosses were performed between these heterozygous animals. Conforming to Mendelian rules, 50 % of the offspring were expected to be heterozygous for the ROSA-26 transgene, 25 % to be homozygous for the transgene and 25 % were expected to be non-transgenic. Genotyping was performed via an assay of comparative rates of X-gal reaction catalysed by the β-gal in earclips from the litters. Earclips from pups lacking the transgene fail to stain with X-gal. Although tissues from offspring heterozygous *or* homozygous for the ROSA-26 transgene both stain ubiquitously with X-gal, the staining reaction proceeds at a visibly greater rate in homozygotes due to their tissues harbouring twice as much β-gal as heterozygous pups. Earclips from each

animal were fixed and X-gal-stained in a 96-well MicroWell™ microplate (Nunc) as in **Chapter 2, Section 2.3.2.** During incubation in the reaction mixture, the intensity of X-gal staining was monitored. Subsequent X-gal staining assays of offspring from crosses between 61 putative homozygotes and MF1 animals revealed only eight of the 61 to be heterozygous, giving a 53/61 = 86.9 % success level for distinguishing between pups heterozygous *vs.* homozygous for the ROSA-26 transgene by the staining assay used.

Following outbreeding, mean ROSA-26 litter size increased from 7.4 (n = 19 litters) to 9.3 (n = 39 litters) and the viability of the embryos increased substantially.

3.2.2. Pancreatic Bud Dissection and Establishing Cultures

Dorsal pancreatic buds were dissected and intact pancreatic bud cultures were established as in **Section 2.1.** Recombinations of pancreatic epithelium from a ROSA-26 strain embryo and an intact dorsal pancreatic bud from an MF1 strain embryo were established by preparing 30 mm Petri plates coated with 2 ml of 1 % molecular biology grade agarose dissolved in L-15 medium (Gibco-BRL, Life Technologies) with 25 μg/ml gentamicin. The agarose was covered with 2 ml of the normal culture medium, BME with Earle's salts, 20 % FBS, 1 × glutamine, and 50 μg/ml gentamicin. Using fine forceps, a well was made in the agarose and the ROSA-26 pancreatic epithelium and MF1 intact bud were placed in the well in close apposition with each other. As adhesion of the two tissue fragments takes several hours, they were incubated overnight and then plated the following morning on a fibronectin-coated coverslip as for intact buds.

3.2.3. X-Gal Staining and Immunofluorescence Cytochemistry

Cultures were fixed after 4, 5 or 6 days *in vitro* as described in **Section 2.2.1.** Then, immediately thereafter or following storage, cultures were subjected to X-gal staining or immunofluorescence cytochemistry as in **Sections 2.3.1.** and **2.5.2.** respectively. In the latter case, β-galactosidase was demonstrated with fluorescein and TRITC or Texas Red was employed to localise the endocrine marker being stained for (insulin, glucagon, Ipf1/Pdx1 or neurogenin3). The first staining cycle was completed before the second was commenced. Immunostaining for β-galactosidase was performed as the first cycle to avoid cross-reactivity between antisera. In some experiments when

staining for neurogenin3, antigen retrieval was performed and occasionally, staining intensity was enhanced by avidin-biotin signal amplification as in **Section 2.5.2.2.**

3.2.4. Wholemount Immunocytochemistry

Freshly dissected E11.5-15.5 MF1 strain whole embryos, intact guts and brains were fixed in 4 % PFA in PBSA then subjected to wholemount immunocytochemistry as described in **Sections 2.2.2.** and **2.5.3.2.** respectively. The antigen was demonstrated either with the alkaline phosphatase substrates NBT and BCIP or by immunoperoxidase detection using DAB as a substrate to visualise horseradish peroxidase (HRP).

3.2.5. Scoring Migratory Epithelial Cells and Image Capture

X-Gal- and immunostained pancreatic bud cultures were examined using a Leica DMRB fluorescent microscope. Numbers of single and aggregated β-gal-labelled migratory epithelial cells (including blue dot cells) were recorded in 18 X-gal-stained recombinant cultures as were the locations of such cells and their distance from the labelled epithelium. The 18 cultures comprised 11 cultures fixed after four days *in vitro*, two cultures fixed after five days and five cultures fixed after a six-day period *in vitro*. Measurements were generally made directly from the observed culture but where very large numbers of migratory cells were evident, data was collected from hard copies of images at up to 230 × magnification following spatial calibration of the printed images. An image was collected of the calibration slide at the same magnification employed for collecting images of the cultures. All images were then printed at the same, suitable scale for measuring from and spatial calibration was performed by determining the factor of magnification between the 1 mm calibration slide scale and its printed length on paper. Distance was measured from the periphery of the nearest branch of β-gal$^+$ epithelium to the centre of the cell or cell cluster. Images of stained specimens were taken with a Spot RT Color digital camera (National Diagnostics Inc.) driven by the Spot 3.3 software and stored as uncompressed 24-bit TIFF images. Colocalisation of β-gal-labelled migratory epithelial cells with immunofluorescence staining for insulin or glucagon was scored from merged images of eight four-day cultures and six five-day cultures following adjustment of the two colour channels using the Adobe Photoshop 6.0 package.

3.3. Results

3.3.1. Growth of Pancreatic Bud In Vitro

The two components of each recombinant pancreatic bud - the ROSA-26-derived epithelium and the unlabelled intact MF1 dorsal pancreatic bud - had usually adhered to one another by six hours following their being brought into contact with each other. Once placed on to the fibronectin substrate, the recombinant or intact buds adhered within a few hours and gradually flattened out over the first one-two days as described by Percival and Slack (1999). Mesenchymal cells spread rapidly out of the explant to form a monolayer of cells both above and below the mass in the centre and on the second or third day of culture, branches began to appear in the epithelia. The epithelia developed a number of buds at their periphery which then spread out and produced further buds. In the recombinant cultures, two populations of pancreatic epithelium developed - one β-gal-labelled and one unlabelled - both of which were surrounded by unlabelled mesenchyme (**Fig. 3.3.**). Over the subsequent three days *in vitro*, the epithelium became an extended branched structure radiating from the original centre (**Fig. 3.4.**). The mesenchyme resolved into a periphery mainly composed of smooth muscle cells and an inner region dominated by fibroblastic cells with occasional patches of lymphoid tissue, consistent with the work by Percival and Slack (1999).

3.3.2. Incidence of Blue Dot Cells

No X-gal staining for β-galactosidase activity was ever observed in any of the negative control unlabelled MF1-derived intact pancreatic bud cultures. Staining was obtained as expected in both intact ROSA-26-derived intact bud cultures and recombinant pancreatic bud cultures. Blue dot cells (BDCs) were observed in a number of these recombinant cultures. As described (Percival and Slack, 1999), these cells did not stain blue following X-gal incubation with the same intensity and uniformity as the exocrine cells, but instead contained prominent blue spots indicative of β-gal expression. They must therefore be derived from the epithelium. BDCs occurred with differing frequency between individual recombinant cultures. Certain cultures examined were completely devoid of such cells whereas in others, BDCs were seen to be present in abundance throughout the unlabelled pancreatic mesenchyme (**Fig. 3.5.**). BDCs where present were evident both as isolated cells and in closely associated groups

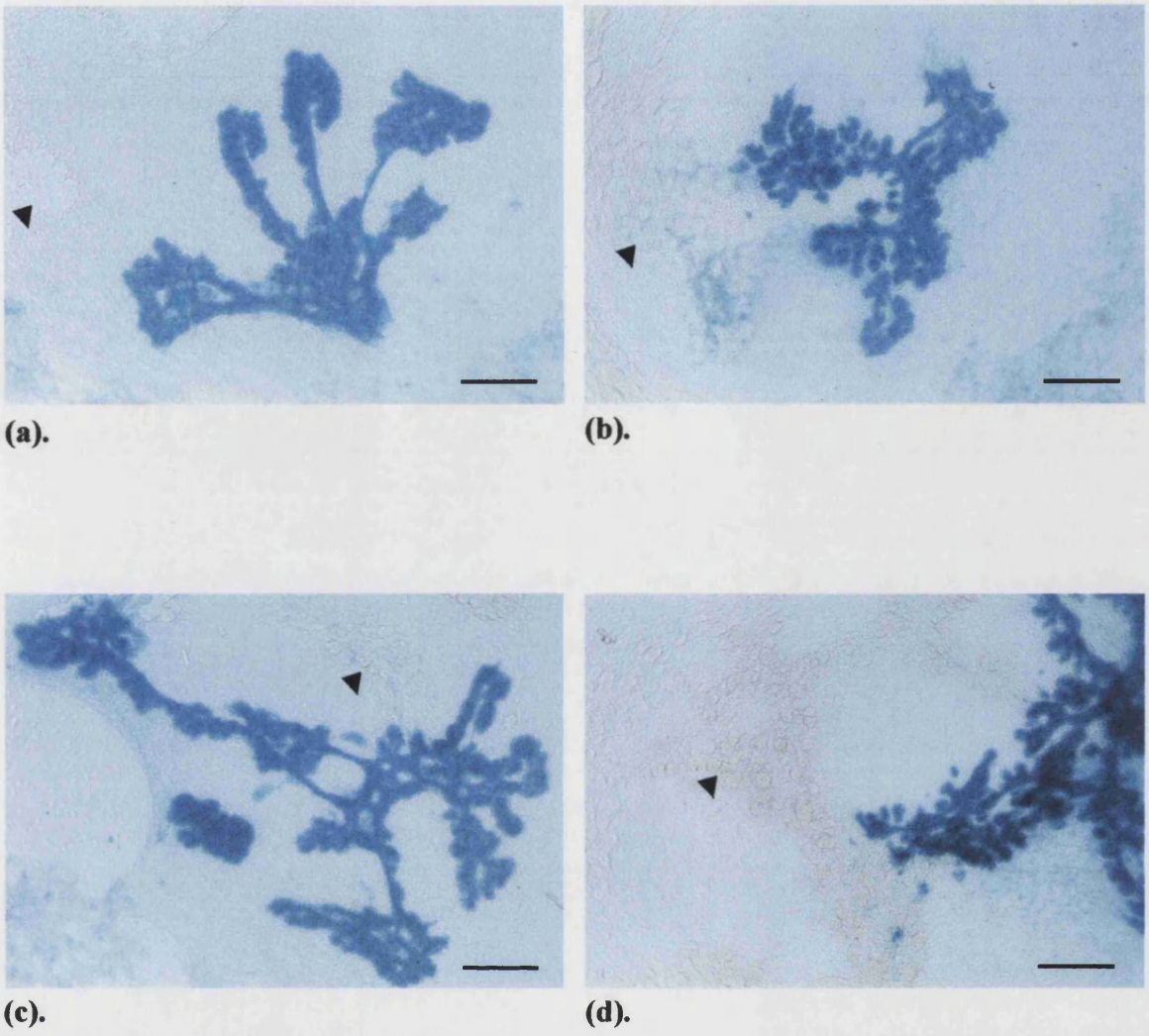

Figure 3.3. Recombinant Pancreatic Bud Cultures Showing X-Gal Staining of β-Gal$^+$ ROSA-26-Derived Pancreatic Epithelium

The two populations of epithelium are evident: the more obvious β-gal-labelled epithelium and the unlabelled MF1-derived epithelium (arrowheads). Both populations are surrounded by unlabelled mesenchyme

(a) 5 day (5d) culture. (b) and (c) 6d cultures. (d) 7d culture. Bar = 200 μm

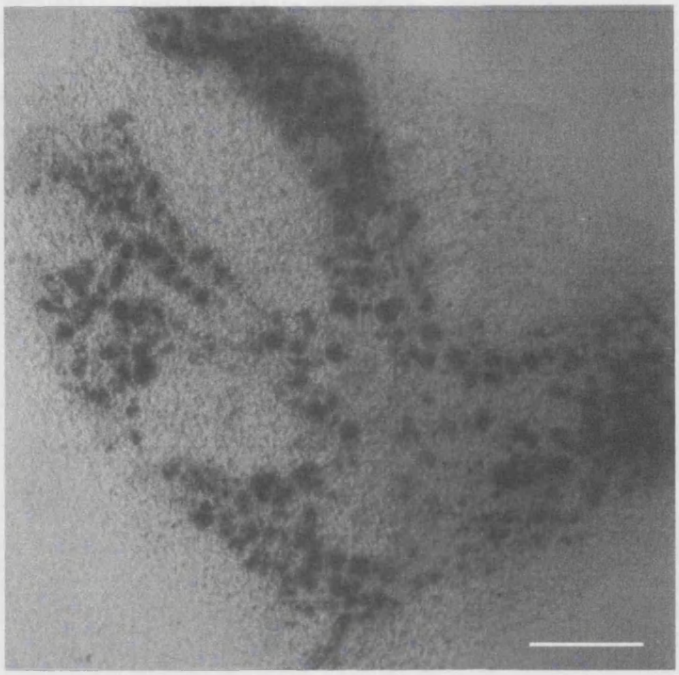

Figure 3.4. An 8d Intact Pancreatic Bud Culture Showing the Extended Branched Epithelial Structure and Peripheral Mesenchyme. Bar = 200 μm

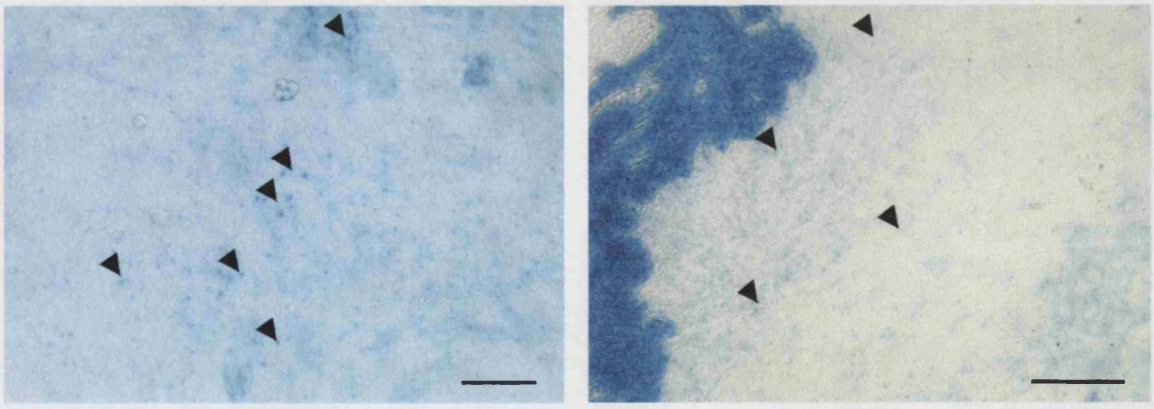

(a). **(b).**

Figure 3.5. Recombinant Pancreatic Bud Cultures Showing Abundant BDCs (Arrowheads) Throughout the Unlabelled Mesenchyme

(a) 4d culture; (b) 6d culture. (a) Bar = 50 μm; (b) Bar =100 μm

or "clusters" (**Fig. 3.6.**), consistent with the previous report (Percival and Slack, 1999). BDCs were infrequently observed within labelled epithelium, probably because the surrounding β-gal-labelled epithelial cells hindered their identification. BDCs were most evident against the unlabelled background epithelium or mesenchyme (**Fig. 3.6.**). Their epithelial origin and incidence at some distance from the labelled epithelium indicated that they must have migrated from the β-gal$^+$ epithelium. Hence the size of BDC clusters and their localisation within the pancreatic bud culture were quantitatively examined in order to further characterise such cells and test the hypothesis that they might represent a population of endocrine precursor cells. These parameters were measured in 18 recombinant cultures maintained for either four days (11 cultures), five days (two cultures) or six days (five cultures) *in vitro*. Any increase in size of clusters or increased distance from the β-gal$^+$ epithelium could be followed with culture duration.

3.3.3. Occurrence of "Uniformly Stained Cells"

In a number of cultures, uniformly stained cells (USCs) were observed within the unlabelled epithelium and mesenchyme following X-gal incubation (**Fig. 3.7.**). These large, rounded cells displayed homogeneous blue X-gal staining throughout as did the exocrine cells within the labelled epithelium. The USCs could be clearly distinguished from the BDCs by focusing the microscope on the cell(s) concerned. In a BDC, a definite blue dot of X-gal staining could be resolved within the otherwise unstained cytoplasm at the correct focal plane whilst a USC never demonstrated such a blue dot at any focal plane and always appeared to exhibit uniform X-gal staining throughout the entire cell. As for the BDCs, the presence of β-gal expression in the USCs indicated an epithelial origin and their localisation within the MF1-derived pancreatic tissue was consistent with such USCs being a second class of migratory epithelial cell. USCs occurred in the majority of cultures examined. Their presence was not dependent on that of BDCs as USCs were on occasion absent from cultures containing abundant BDCs (one of 18 BDC-containing cultures lacked USCs). Conversely, cultures could be devoid of BDCs yet contain abundant USCs (one of 18 cultures), disputing the obligatory dependence of one on the other. Like BDCs, USCs could occur either in isolation (**Fig. 3.7.**) or in aggregates. USCs were also found in association with BDCs on occasion. As for the BDCs, the size of USC clusters and their separation from the labelled epithelium were quantified in the same sample of four-, five- or six-day recombinant cultures to further characterise these cells.

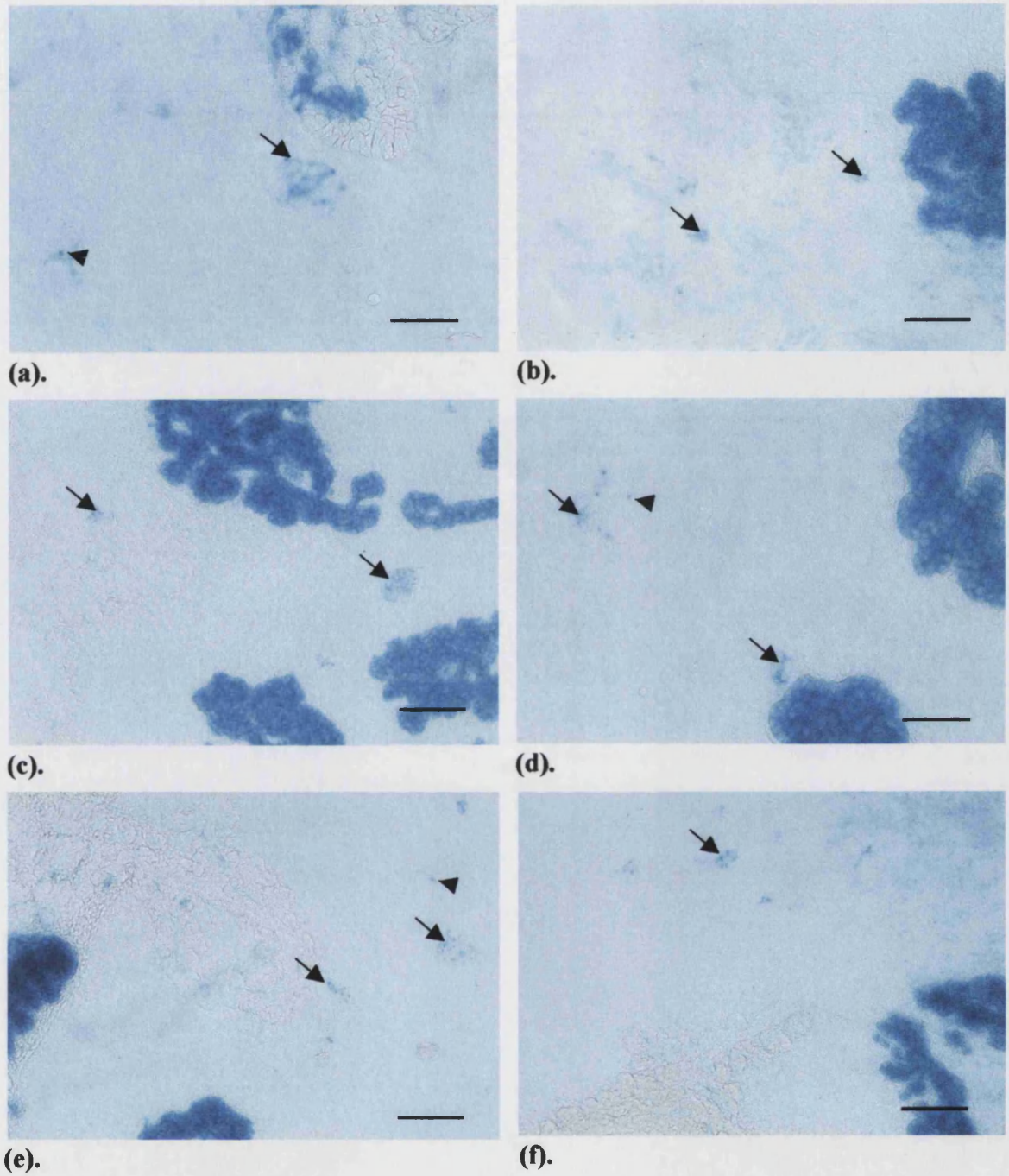

Figure 3.6. BDCs Occur Either as Isolated Cells or as Clusters

Isolated BDCs (arrowheads) and BDC clusters (arrows) are evident in the unlabelled mesenchyme

(a) 4d culture. (b) and (c) 5d cultures. (d) and (e) 6d cultures. (f) 7d culture. (a) and (d) Bar = 50 μm; (b), (c), (e) and (f) Bar = 100 μm

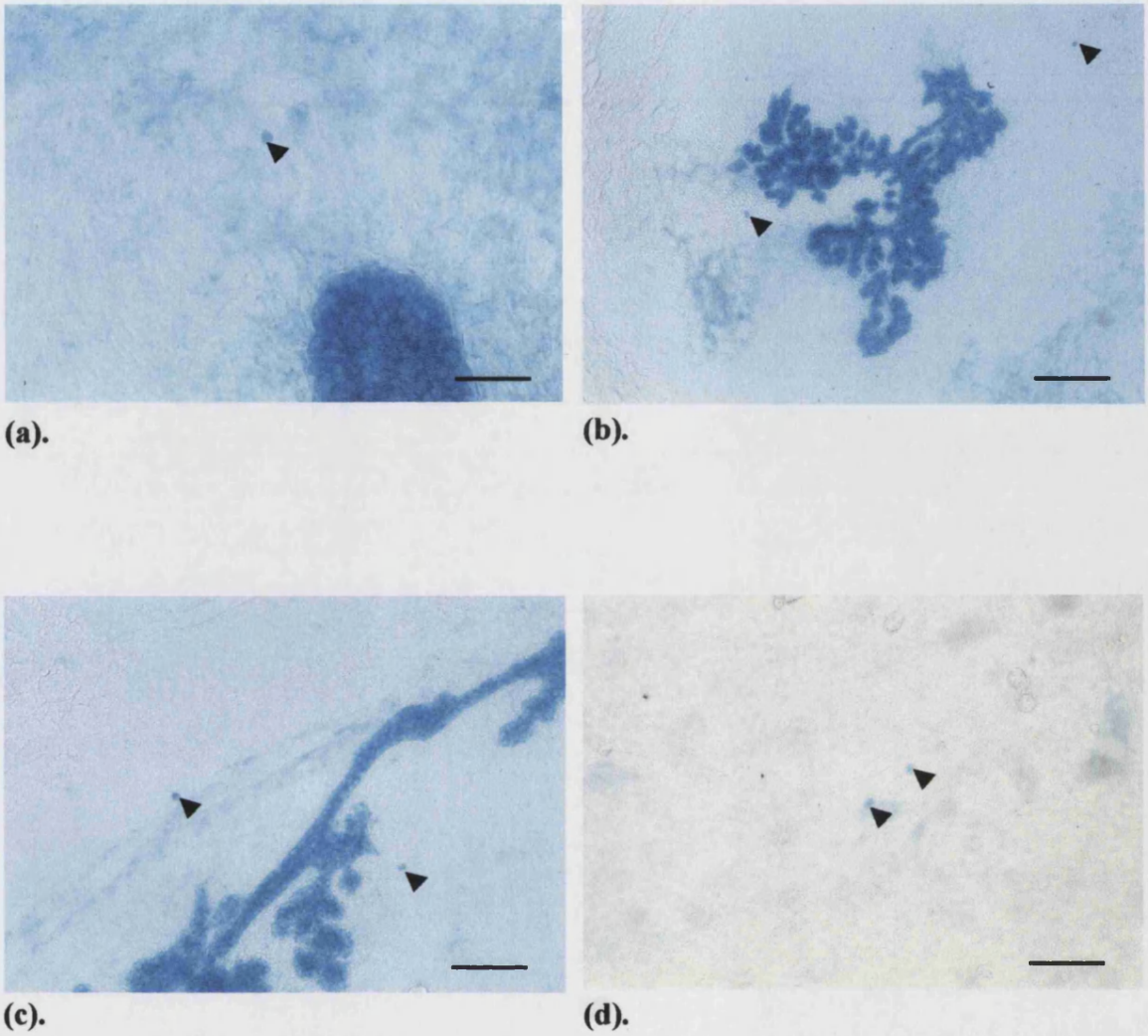

Figure 3.7. Isolated Uniformly Stained Cells (USCs) in the Unlabelled Mesenchyme (Arrowheads)

(a) 4d culture. (b)-(d) 6d cultures. (a) and (d) Bar = 50 μm; (b) Bar = 200 μm; (c) Bar = 100 μm

3.3.4. Spatial Distribution

3.3.4.1. Increase in Number of BDC and USC Clusters Per Culture Over Culture Period

The mean number of both BDC and USC clusters identified in each culture increased over the 48 h culture period. The mean (± standard error [S.E.] of the mean) number of BDC clusters per culture after four days of culture (4d) was found to be 14.5 ± 5.14, increasing to 168.5 ± 34.3 at 5d and attaining 172.6 ± 85.1 by 6d (**Table 3.1.** and **Graph 3.1.**). This resulted in the mean total number of BDCs per culture after 4d, 5d and 6d maintenance *in vitro* being 119.7 ± 25.3 cells, 602 ± 169.7 cells and 667.2 ± 234.4 cells respectively (**Table 3.1.**). Similarly, the mean number of USC clusters per culture increased from 53.1 ± 10.8 at 4d to 68 ± 38.2 at 5d and by 6d, each culture contained on average 102 ± 34.2 USC clusters (**Table 3.1.** and **Graph 3.1.**). The mean total number of USCs per culture over the 48 h culture duration was found to be 139.2 ± 31.0 cells, 90 ± 50.2 cells and 175 ± 62.5 cells respectively (**Table 3.1.**).

3.3.4.2. No Increase in Mean Cluster Size with Duration of Culture

To investigate whether clusters of BDCs or USCs grow in size with duration of culture, the mean cluster size was determined for each class of migratory epithelial cell after either four, five or six days *in vitro*. Since the inclusion of isolated cells (a cluster size of one cell) reduces the mean cluster size, values were calculated to reflect either the inclusion or exclusion of single cells (**Table 3.1.** and **Graphs 3.2.** and **3.3.**). No increase was seen in mean cluster size for either the BDC or USC aggregates over the 48 h *in vitro* that was examined. Mean (± S.E.) BDC cluster size, including isolated cells decreased from 8.23 ± 1.02 cells at 4d to 3.57 ± 0.229 cells at 5d and by 6d was 3.87 ± 0.191 cells. Mean size excluding BDCs occurring in isolation was greater at each time-point as expected, but reflected the same trend: 12.5 ± 1.47 cells at 4d, 5.07 ± 0.320 cells at 5d and 6.05 ± 0.302 cells by 6d. At all time-points during culture, the mean size of clusters of USCs was markedly reduced compared with sizes of BDC aggregates. Mean USC cluster size (single USCs inclusive) decreased from 2.62 ± 0.247 cells at 4d to 1.32 ± 0.0605 cells at 5d and attained 1.72 ± 0.112 cells by 6d. Again, the mean USC cluster size excluding single cells was greater for each of the three days but

Table 3.1. Summary of Total and Mean (± S.E.) Number of Blue Dot Cell and Uniformly Stained Cell Clusters and Total Cells Per Culture and Cluster Size and Distance from β-Gal$^+$ Epithelium Over Days 4-6 in Culture

	BLUE DOT CELLS			UNIFORMLY STAINED CELLS		
	Day 4	Day 5	Day 6	Day 4	Day 5	Day 6
No. of Cultures Examined Per Day of Culture *	11	2	5	11	2	5
Total No. of Clusters in *All* Cultures: Isolated Cells INCLUDED	160	337	863	584	136	510
Mean (± S.E.) Cluster No. Per Culture	14.5 ± 5.14	168.5 ± 34.3	172.6 ± 85.1	53.1 ± 10.8	68.0 ± 38.2	102.0 ± 34.2
Mean (± S.E.) Total Cell No. Per Culture	119.7 ± 25.3	602.0 ± 169.7	667.2 ± 234.4	139.2 ± 31.0	90.0 ± 50.2	175.0 ± 62.5
Mean (± S.E.) Cluster Size: Isolated Cells INCLUDED	8.23 ± 1.02	3.57 ± 0.229	3.87 ± 0.191	2.62 ± 0.247	1.32 ± 0.0605	1.72 ± 0.112
Mean (± S.E.) Cluster Size: Isolated Cells EXCLUDED	12.5 ± 1.47 $n = 101$ †	5.07 ± 0.320 $n = 213$ †	6.05 ± 0.302 $n = 490$ †	5.57 ± 0.649 $n = 207$ †	2.42 ± 0.143 $n = 31$ †	3.59 ± 0.361 $n = 141$ †
Mean (± S.E.) Distance from β-Gal$^+$ Epithelium (μm)	154.3 ± 13.58	450.3 ± 16.97	486.9 ± 11.50	525.5 ± 14.16	717.0 ± 33.32	657.4 ± 14.27

* The spatial distribution and migratory properties of both the BDC and USC clusters were recorded from the same 18 recombinant cultures

† Sample size, *n*, refers to the total number of cell clusters in excess of one cell (isolated cells excluded) counted after either 4, 5 or 6 days *in vitro*

Graph 3.1. Mean Number of Blue Dot Cell or Uniformly Stained Cell Clusters Per Culture Over Days 4-6 *In Vitro*

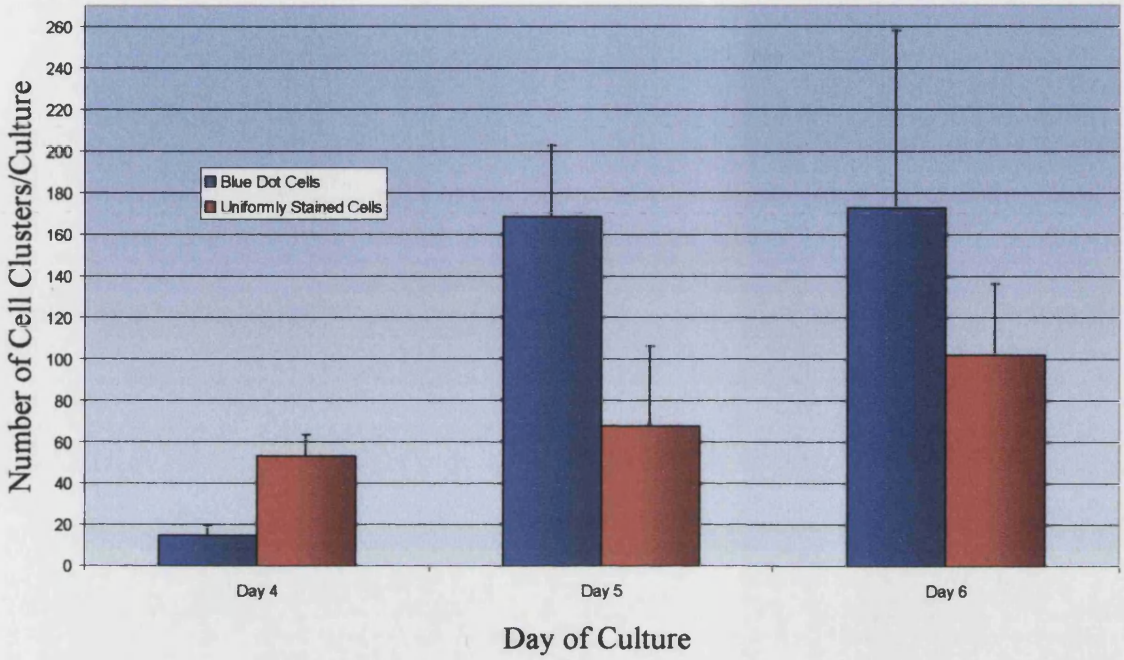

Graph 3.2. Mean Blue Dot Cell Cluster Size Over Days 4-6 of *In Vitro* Culture

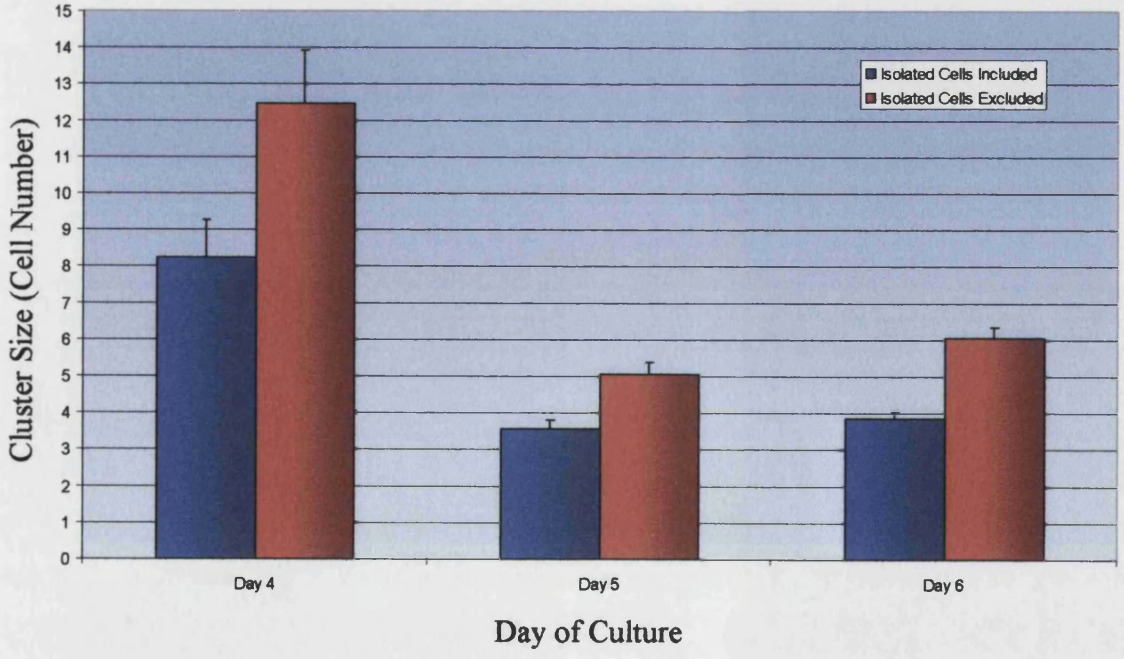

Graph 3.3. Mean Uniformly Stained Cell Cluster Size Over Days 4-6 of *In Vitro* Culture

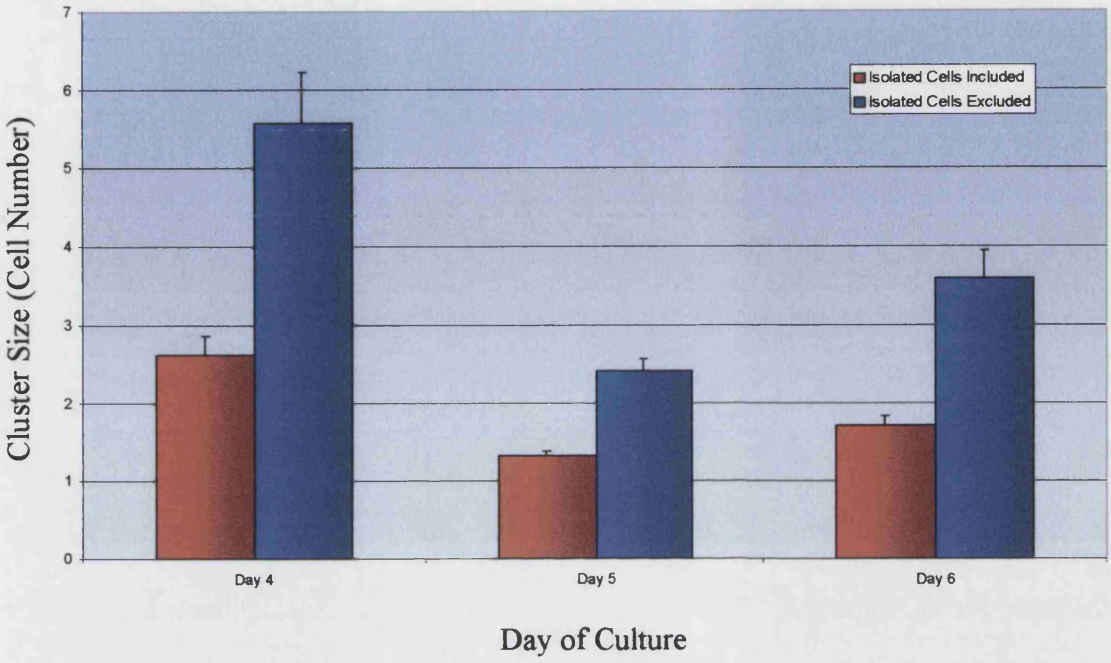

Graph 3.4. Mean Distance of Blue Dot Cell Clusters and Uniformly Stained Cell Clusters from Periphery of β-Gal$^+$ Epithelium Over Days 4-6 of *In Vitro* Culture

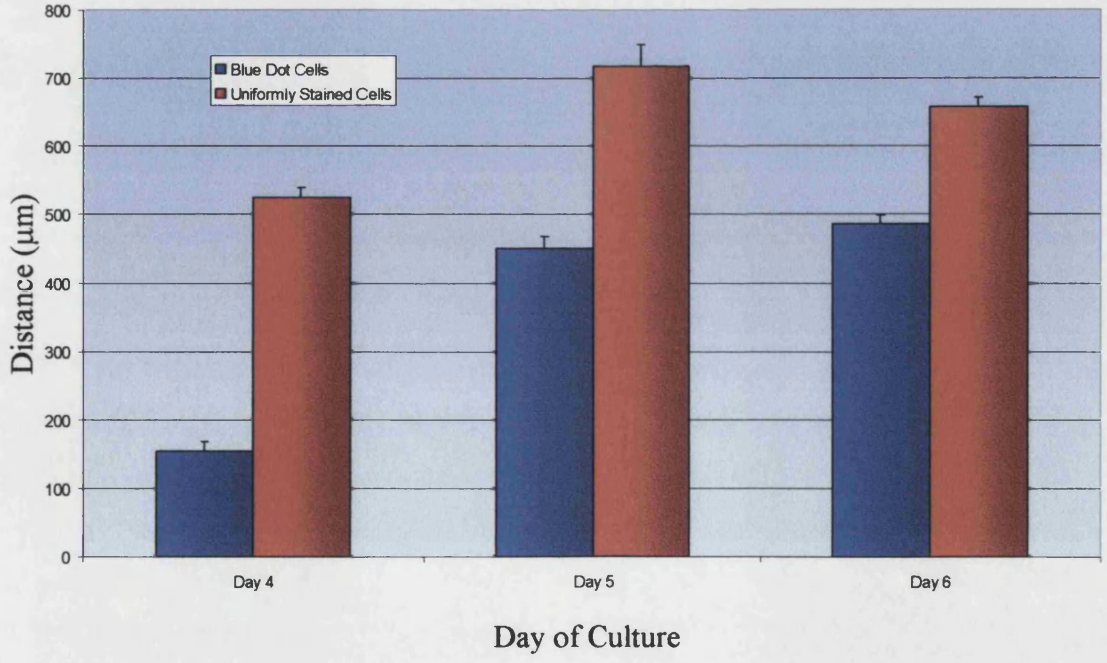

followed the same trend: 5.57 ± 0.649 cells at 4d, 2.42 ± 0.143 cells at 5d and 3.59 ± 0.361 cells by 6d.

3.3.4.3. Increasing Distance of BDCs from β-Gal$^+$ Epithelium with Culture Duration

To investigate whether BDCs and USCs migrate away from the labelled epithelium from which they originate, the mean distance of BDCs and USCs from the β-gal$^+$ epithelium was determined after 4d, 5d and 6d *in vitro*. There was an obvious increase in the mean distance of separation of BDCs from the epithelium over the 48 h in culture: 154.3 ± 13.58 μm, 450.3 ± 16.97 μm and 486.9 ± 11.50 μm at 4d, 5d and 6d respectively (**Table 3.1.** and **Graph 3.4.**). The BDCs found to be furthest from their point of origin were measured to be at distances of 665 μm, 1722 μm and 1744 μm from the β-gal$^+$ epithelium at 4d, 5d and 6d respectively. Using the mean distance values, a BDC migration speed of 166.3 μm/day was calculated: (486.9-154.3)/2. This could not be presented as a migration *velocity* however, as the directional component was not known and could not be assumed to take a linear path. The pattern of increase in distance from the labelled epithelium was less obvious for the USCs however. At 4d, mean distance was found to be 525.5 ± 14.16 μm, increasing to 717.0 ± 33.32 μm at 5d and then dropping to 657.4 ± 14.27 μm by 6d (**Table 3.1.** and **Graph 3.4.**). The maximum distances of USCs at 4d, 5d and 6d were ascertained to be 2340 μm, 2157 μm and 2326 μm respectively.

3.3.4.4. BDCs and USCs Predominantly Mesenchyme-Localised

To investigate whether BDCs and USCs prefer to migrate on a substratum of epithelium or mesenchyme, epithelial or mesenchymal localisation of migratory epithelial BDCs and USCs was determined. It was found that only 57/1360 or 4.19 % of BDC clusters were identified on (unlabelled) pancreatic epithelium with the remainder being localised within the mesenchyme. This corresponded to 616/5857 or 10.5 % of the total number of BDCs being resident in the epithelium. Similarly, just 38/1230 or 3.09 % of USC clusters were found within the epithelium, representing 79/2586 or 3.05 % of total counted USCs. This indicates that both the blue dot and uniformly stained epithelial cells prefer to migrate on a mesenchymal substratum as opposed to the pancreatic epithelium.

3.3.4.5. BDC and USC Cluster Sizes Inconsistent with Clonal Groups

To investigate whether clusters of BDCs and USCs are clonal in size (two cells, four cells, eight cells, 16 cells, 32 cells etc.) as might be expected if the clusters contained symmetrically-dividing stem cells, the frequency of clusters of each size was determined. Peaks in the frequency of cell clusters of such sizes were not observed for either the BDCs (**Table 3.2.** and **Graph 3.5.**) or USCs (**Table 3.2.** and **Graph 3.6.**). The frequency of both BDC and USC cluster sizes declined sharply from one-two cells. Whereas 556 isolated BDCs were found, the frequencies of BDC clusters of two, three, four and five cells were found to be 215, 139, 89 and 73 respectively. For any clusters of 15 cells or more, no more than 10 clusters were observed of any given size. The maximum size of BDC cluster observed was a sole 74-cell aggregate in a 4d culture. Similarly, 851 isolated USCs were observed although the frequencies of USC clusters of two, three, four and five cells were found to be only 165, 84, 33 and 29 respectively. No more than 10 clusters were observed of any given size for clusters of nine cells or greater. The largest USC cluster identified was a 77-cell aggregate in a 4d culture.

3.3.4.6. Greater Tendency of USCs to Exist as Isolated Cells

Comparing the frequency distribution for cluster size between BDC clusters and USC aggregates, it was found that the USCs exhibited a greater tendency to occur as either isolated cells or in small (< 5 cells) clusters than did the BDCs (**Table 3.2.** and **Graph 3.7.**). The decline in frequency was markedly greater over cluster sizes of one to 20 cells for the USCs than the BDCs (**Table 3.2.** and **Graph 3.7.**). Of the 1230 USC clusters scored, 851 or 69.2 % were found to occur as isolated cells compared with just 40.9 % (556 of 1360 clusters) of BDC aggregates. Of the USC sample, 94.5 % of cell aggregates were composed of five cells or less, compared with 78.8 % of BDC clusters.

To verify the divergence in the frequency distribution of the sizes of BDC and USC clusters in each population sample, a chi-square (χ^2) test was conducted to compare the observed BDC cluster size distribution with the "expected" distribution based on the USC cluster size frequency data (**Table 3.3.** and **Graph 3.8.**). The proportion of the total sample of USC cluster sizes within each size category was multiplied by the total sample number of BDC clusters to give the "expected" number of BDC cell clusters of that size from the USC data. In this way, the BDC and USC cluster size frequency distributions could be compared directly. There was found to be a

Table 3.2. Frequency Distribution of Sizes of Blue Dot Cell Clusters and Uniformly Stained Cell Clusters Over Days 4-6 of *In Vitro* Culture

CLUSTER SIZE (CELL NO.)	FREQUENCY							
	BLUE DOT CELLS				UNIFORMLY STAINED CELLS			
	Day 4	Day 5	Day 6	Total	Day 4	Day 5	Day 6	Total
1	59	124	373	**556**	377	105	369	**851**
2	14	62	139	**215**	82	23	60	**165**
3	12	46	81	**139**	35	4	45	**84**
4	6	28	55	**89**	18	3	12	**33**
5	11	16	46	**73**	20	1	8	**29**
6	4	15	36	**55**	11	0	4	**15**
7	9	11	20	**40**	8	0	3	**11**
8	3	4	19	**26**	5	0	6	**11**
9	4	9	12	**25**	5	0	0	**5**
10	2	3	14	**19**	5	0	2	**7**
11	3	6	12	**21**	3	0	0	**3**
12	4	2	10	**16**	3	0	0	**3**
13	2	2	7	**11**	3	0	0	**3**
14	4	1	6	**11**	1	0	0	**1**
15	2	0	6	**8**	1	0	0	**1**
16	0	2	3	**5**	1	0	0	**1**
17	1	0	3	**4**	0	0	0	**0**
18	4	0	4	**8**	0	0	0	**0**
19	0	1	2	**3**	0	0	0	**0**
20	0	1	0	**1**	1	0	0	**1**
21	0	0	1	**1**	0	0	0	**0**
22	0	0	2	**2**	1	0	0	**1**
23	1	1	2	**4**	0	0	0	**0**
24	0	1	0	**1**	0	0	0	**0**
25	0	0	0	**0**	0	0	0	**0**
26	1	0	0	**1**	0	0	0	**0**
27	1	0	0	**1**	0	0	0	**0**
28	1	0	1	**2**	0	0	0	**0**
29	0	0	1	**1**	0	0	0	**0**
30	2	0	1	**3**	0	0	0	**0**
31	1	0	0	**1**	0	0	0	**0**
32	0	0	0	**0**	0	0	0	**0**
33	0	0	1	**1**	0	0	0	**0**
34	1	2	0	**3**	0	0	0	**0**
35	0	0	2	**2**	0	0	0	**0**
36	1	0	1	**2**	1	0	0	**1**
37	0	0	0	**0**	0	0	0	**0**
38	0	0	0	**0**	0	0	0	**0**
39	0	0	0	**0**	0	0	0	**0**
40	0	0	1	**1**	0	0	0	**0**
41	0	0	0	**0**	0	0	0	**0**

42	0	0	0	**0**	0	0	0	**0**
43	1	0	0	**1**	0	0	0	**0**
44	0	0	0	**0**	0	0	0	**0**
45	0	0	0	**0**	0	0	0	**0**
46	0	0	0	**0**	0	0	0	**0**
47	0	0	0	**0**	0	0	0	**0**
48	0	0	0	**0**	0	0	0	**0**
49	0	0	0	**0**	0	0	0	**0**
50	0	0	0	**0**	0	0	1	**1**
51	1	0	0	**1**	0	0	0	**0**
52	2	0	0	**2**	0	0	0	**0**
53	0	0	0	**0**	0	0	0	**0**
54	0	0	0	**0**	0	0	0	**0**
55	0	0	0	**0**	0	0	0	**0**
56	1	0	0	**1**	0	0	0	**0**
57	0	0	0	**0**	0	0	0	**0**
58	0	0	0	**0**	0	0	0	**0**
59	0	0	0	**0**	0	0	0	**0**
60	0	0	0	**0**	0	0	0	**0**
61	0	0	0	**0**	0	0	0	**0**
62	0	0	1	**1**	0	0	0	**0**
63	0	0	0	**0**	0	0	0	**0**
64	0	0	0	**0**	0	0	0	**0**
65	0	0	0	**0**	0	0	0	**0**
66	0	0	0	**0**	0	0	0	**0**
67	0	0	0	**0**	0	0	0	**0**
68	0	0	0	**0**	0	0	0	**0**
69	0	0	0	**0**	0	0	0	**0**
70	0	0	0	**0**	0	0	0	**0**
71	0	0	1	**1**	0	0	0	**0**
72	0	0	0	**0**	0	0	0	**0**
73	1	0	0	**1**	0	0	0	**0**
74	1	0	0	**1**	2	0	0	**2**
75	0	0	0	**0**	0	0	0	**0**
76	0	0	0	**0**	0	0	0	**0**
77	0	0	0	**0**	1	0	0	**1**
TOTAL	**160**	**337**	**863**	**1360**	**584**	**136**	**510**	**1230**

Graph 3.5. Frequency Histogram Showing Size Distribution of Blue Dot Cell Clusters (and Isolated Cells)

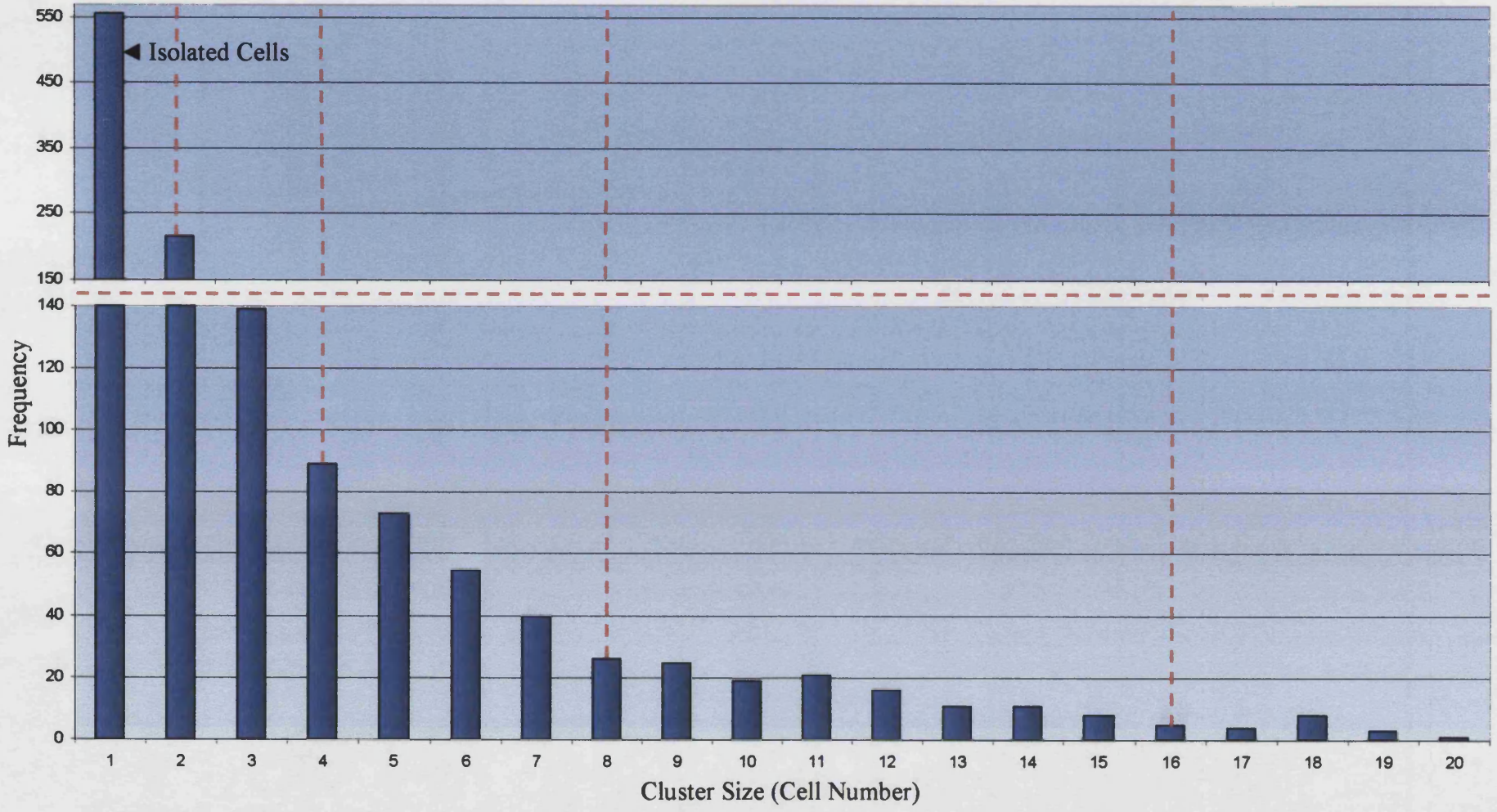

Graph 3.6. Frequency Histogram Showing Size Distribution of Uniformly Stained Cell Clusters (and Isolated Cells)

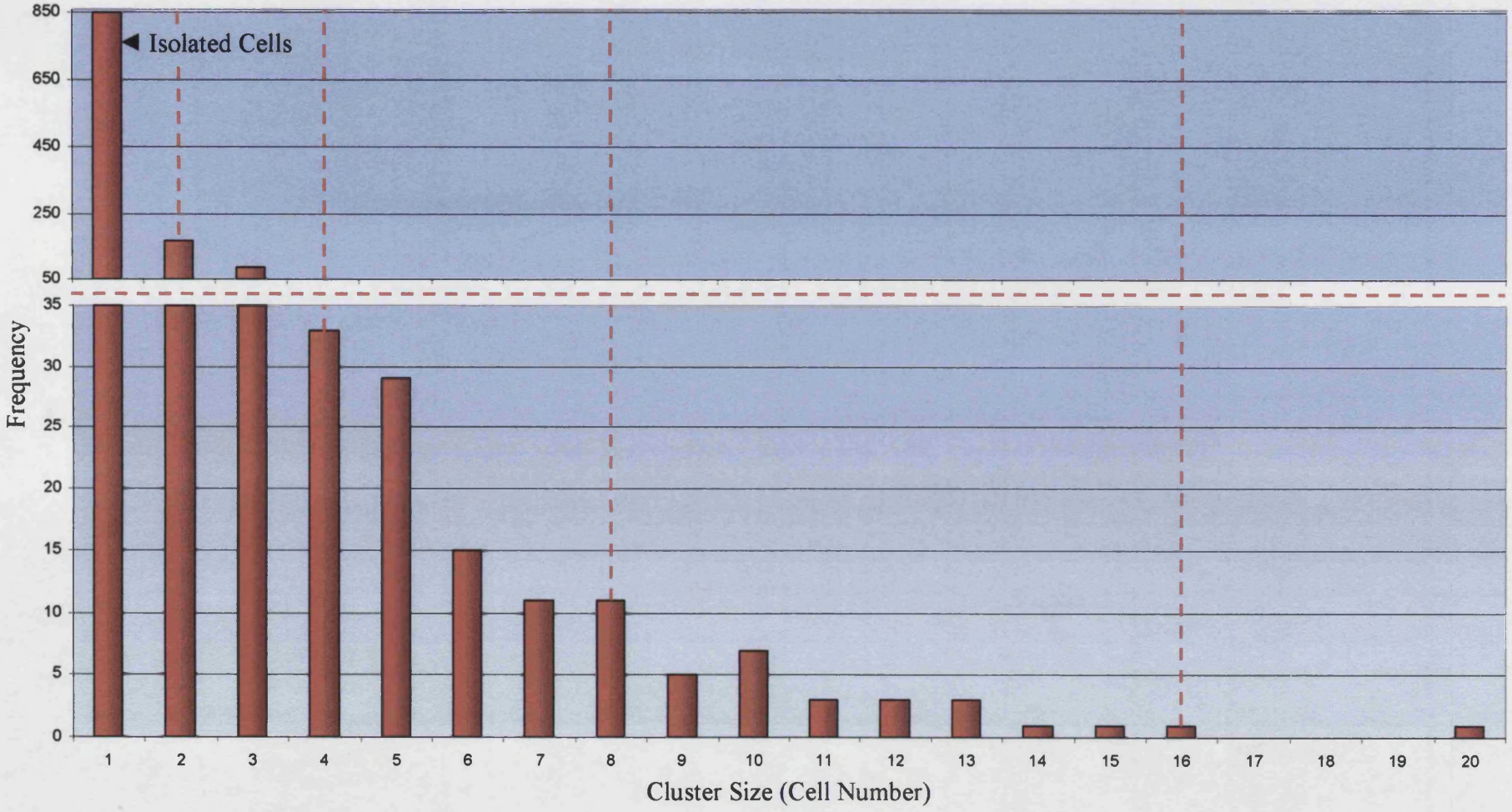

Graph 3.7. Frequency Histogram Comparing Sizes of Blue Dot Cell and Uniformly Stained Cell Clusters

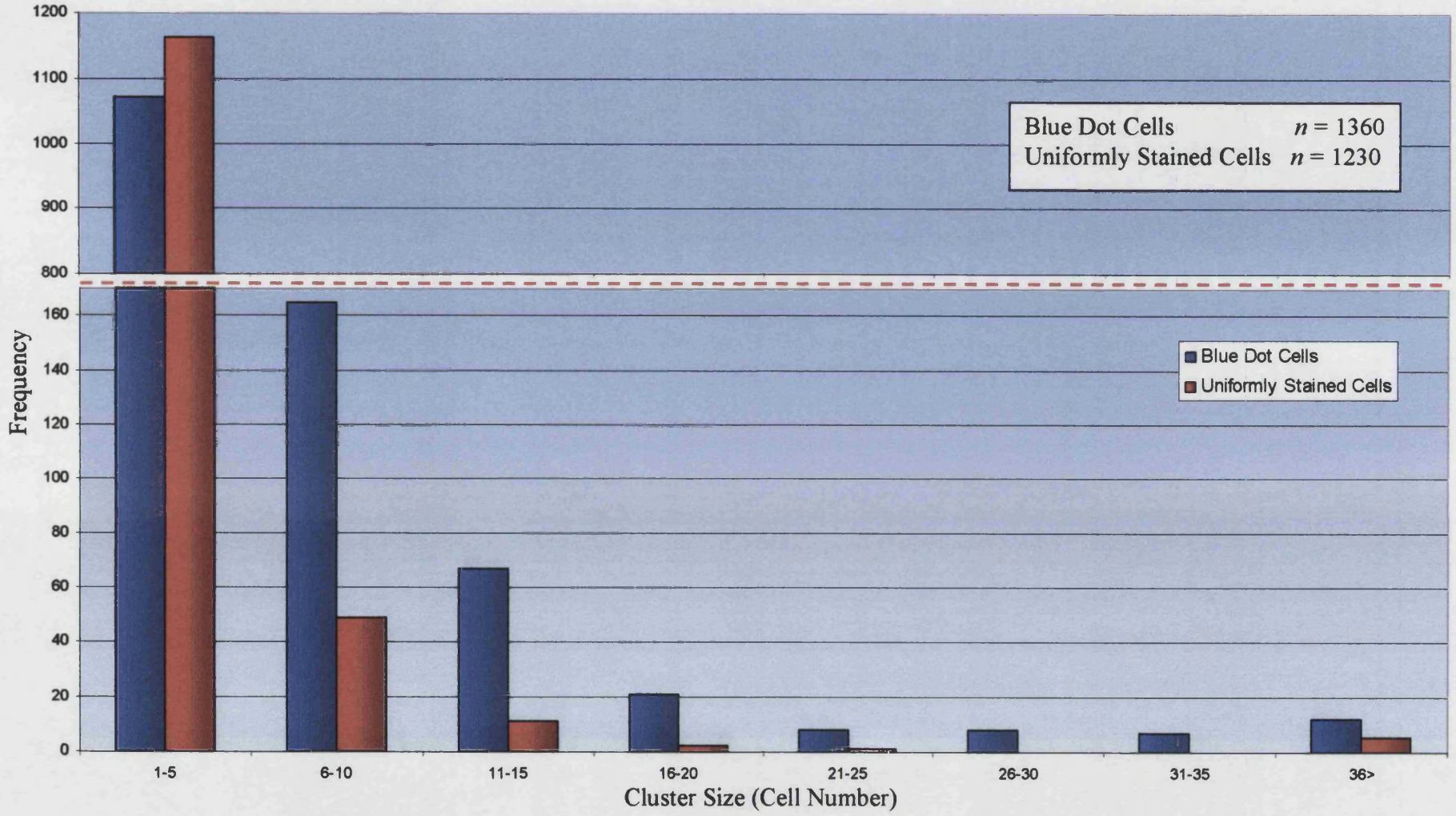

Graph 3.8. Frequency Histogram Comparing the Observed Sizes of Blue Dot Cell Clusters with the "Expected" Frequency Distribution Calculated from the Uniformly Stained Cell Cluster Size Distribution

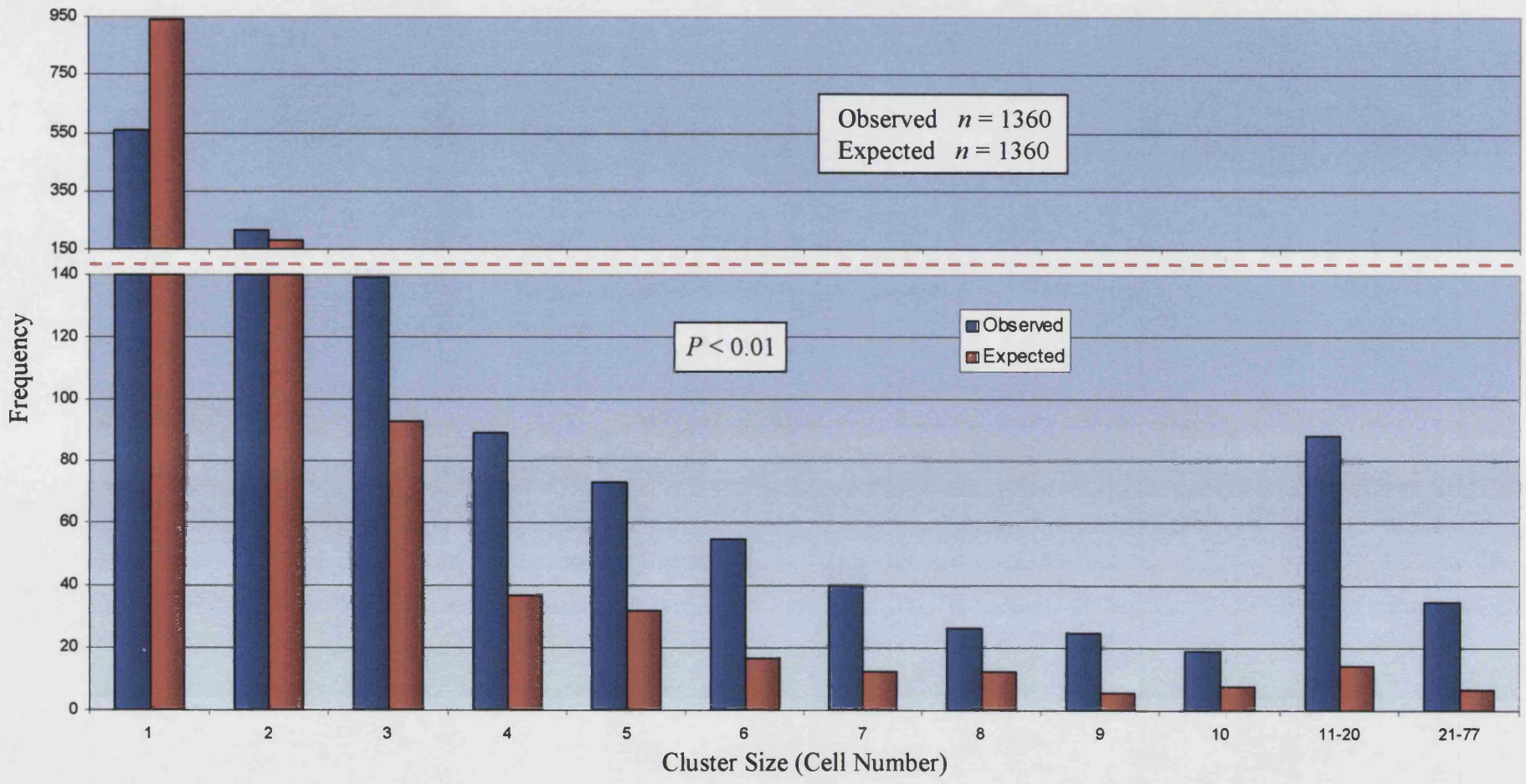

highly significant difference ($P < 0.01$) between the frequency distributions of BDC and USC cluster sizes.

$$\chi^2 = \Sigma \frac{(\text{Observed} - \text{Expected})^2}{\text{Expected}} \qquad \text{with } df = c \text{ (number of categories)} - 1$$

Table 3.3. Calculating χ^2 to Test Whether the Observed BDC Cluster Size Distribution Differs from that of the USC Clusters

Cluster Size (Cell No.)	FREQUENCY			Observed - Expected	$O - E^2$	$\frac{O - E^2}{E}$
	Uniformly Stained Cells	Blue Dot Cells: Observed	Expected from USCs			
1	851	556	940.9	-384.9	148181.2	157.5
2	165	215	182.4	32.6	1060.2	5.81
3	84	139	92.9	46.1	2127.2	22.9
4	33	89	36.5	52.5	2757.5	75.6
5	29	73	32.1	40.9	1675.7	52.3
6	15	55	16.6	38.4	1475.7	89.0
7	11	40	12.2	27.8	774.9	63.7
8	11	26	12.2	13.8	191.5	15.7
9	5	25	5.53	19.5	379.1	68.6
10	7	19	7.74	11.3	126.8	16.4
11-20	13	88	14.4	73.6	5420.8	377.1
21-77	6	35	6.63	28.4	804.6	121.3
Σ	**1230**	**1360**	**1360**	**0**	**164975.3**	**1065.8 (χ^2)**

NB: Data was segregated into the above categories of cluster size by considering that:-
(1). in the χ^2 test, the expected frequency of each category under the null hypothesis must be at least *five*,
(2). the higher the number of categories, the greater the sensitivity of the test.

$\chi^2 = 24.72$, $df = 11$, $p = 0.01$. As the calculated value of χ^2 is greater, the null hypothesis can be rejected.

The frequency distribution of USC cluster sizes was therefore determined to be significantly different to that for the BDC aggregates. The USC cluster size distribution was shifted towards the lower end of the size spectrum compared with the BDCs and USCs exhibited a much greater tendency to occur as isolated cells.

3.3.5. Immunofluorescence Cytochemistry

3.3.5.1. A Proportion of BDCs and USCs are Glucagon- or Insulin-Immunopositive

In order to test the hypothesis that BDCs represent a population of committed endocrine precursor cells, immunofluorescence cytochemistry was performed on eight 4d and six 5d recombinant cultures for either β-gal and glucagon *or* β-gal and insulin. Intact MF1 and ROSA-26 pancreatic bud cultures were employed as negative and positive controls for detection of β-galactosidase activity respectively (**Fig. 3.8.**). Immunofluorescence analysis was conducted in preference to immunohistochemical approaches because of its high resolution and to avoid problems afflicting the latter approach caused by the superposition of one chromogen by a more dense stain resulting in masking. Of the 83 BDCs identified by immunofluorescence signal for β-gal, 13 cells or 15.7 % were glucagon-immunopositive whilst 12 of 67 BDCs (17.9 %) were found to be immunopositive for insulin (**Fig. 3.9.** and **Graph 3.9.**). Of 351 USCs localised by immunofluorescence staining for β-gal, 57 cells or 16.2 % displayed staining for glucagon whilst 24.7 % (21 cells) of 85 USCs were ascertained to be insulin-immunopositive (**Fig. 3.9.** and **Graph 3.9.**).

3.3.5.2. Unsuccessful Immunocytochemistry for Neurogenin3

With the aim of further characterising the BDCs, efforts were made to conduct immunofluorescence analysis for the bHLH protein neurogenin3 (ngn3) which has been used as a marker of endocrine cell progenitors (Apelqvist *et al.*, 1999; Jensen *et al.*, 2000a; Schwitzgebel *et al.*, 2000). Despite repeated attempts, immunofluorescence cytochemistry using either of the two anti-ngn3 antibodies (mouse monoclonal, Transduction Laboratories N63520 and rabbit polyclonal, Abcam ab7560) proved to be unsuccessful. Pancreatic bud cultures maintained *in vitro* for either 4d, 5d or 6d consistently failed to display any ngn3-immunopositive cells irrespective of whether fixation had been achieved using MEMFA, 4 % PFA or 1:1 acetone:methanol. Since the latter fixative exerts a permeabilisation effect on cells, subsequent permeabilisation in 1 % Triton X-100 for 30 min was omitted in some experiments to ensure that cells were not being excessively permeabilised. However, this course of action had no effect on the unsuccessful outcome. Incorporation of citrate buffer or ammonium chloride (recommended by Abcam) antigen retrieval and/or avidin-biotin signal amplification steps into the staining protocol also failed to yield a satisfactory result.

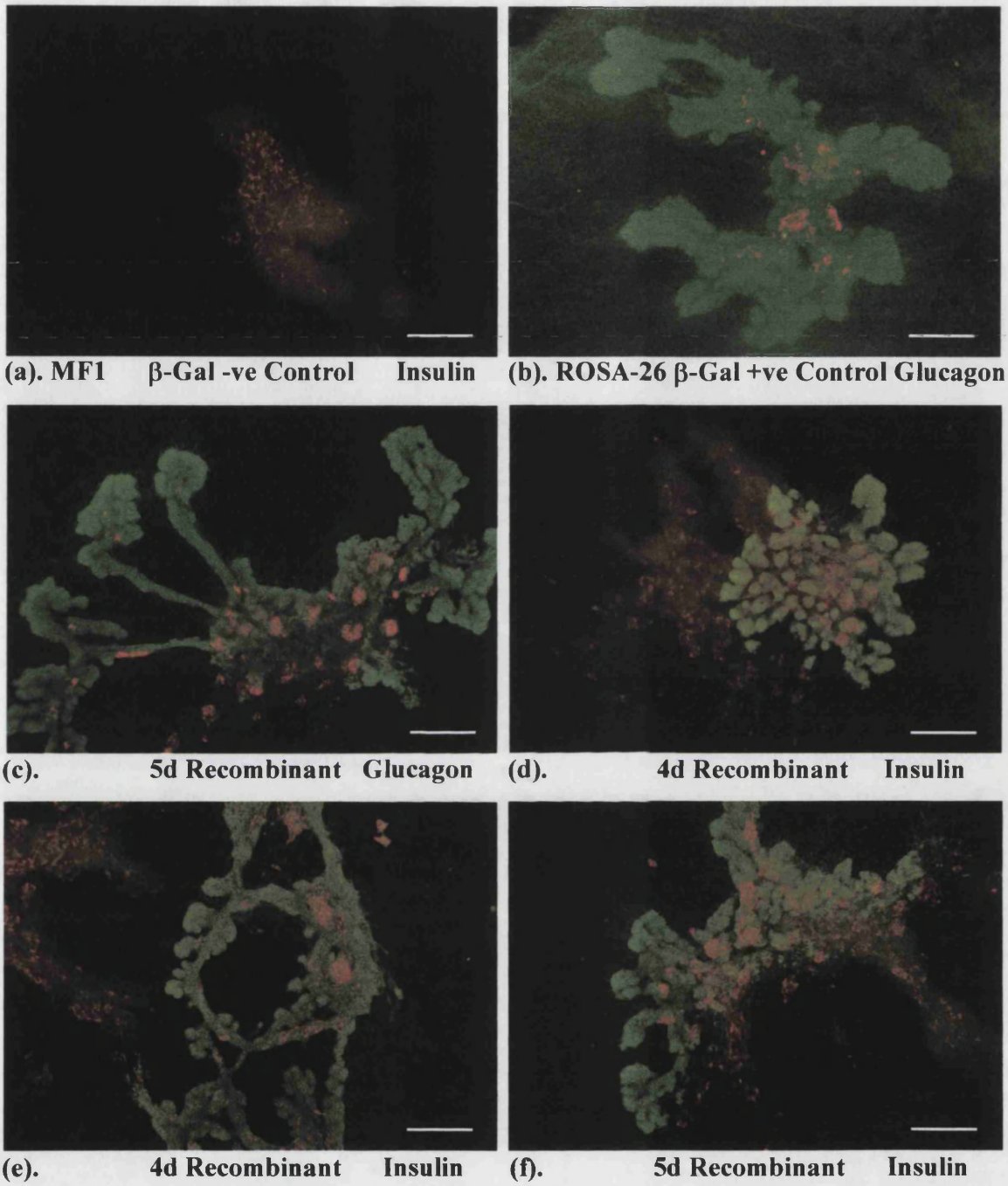

Figure 3.8. Immunofluorescence Staining for β-Gal and Glucagon *or* β-Gal and Insulin in Recombinant Pancreatic Bud Cultures

(a) 4d intact MF1 culture devoid of β-gal staining (but showing staining for insulin). (b) 4d intact ROSA-26 culture shows β-gal staining in epithelium *and* mesenchyme (staining for glucagon also visible). (c)-(f) 4d or 5d recombinant cultures stained for β-gal and glucagon *or* β-gal and insulin. Bar = 200 μm

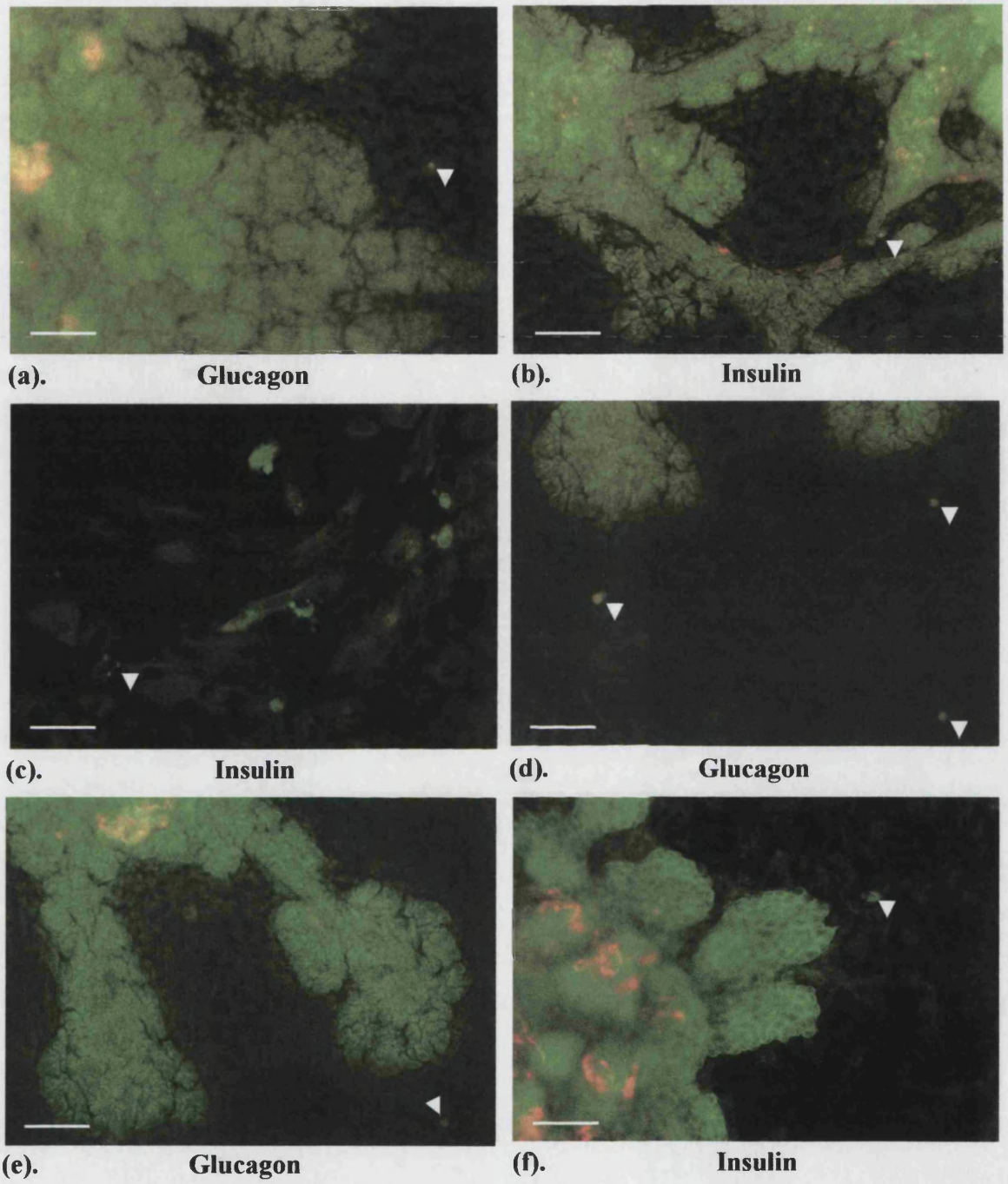

Figure 3.9. A Small Proportion of BDCs and USCs are Immunopositive for Glucagon or Insulin

Arrowheads denote:

(a) glucagon$^+$ BDC; (b) insulin$^+$ BDC; (c) insulin$^-$ BDC; (d) three glucagon$^+$ USCs; (e) glucagon$^-$ USC; (f) insulin$^-$ USC. Bar = 50 μm

Graph 3.9. Percentage of Blue Dot Cells and Uniformly Stained Cells that are Immunopositive for Glucagon or Insulin

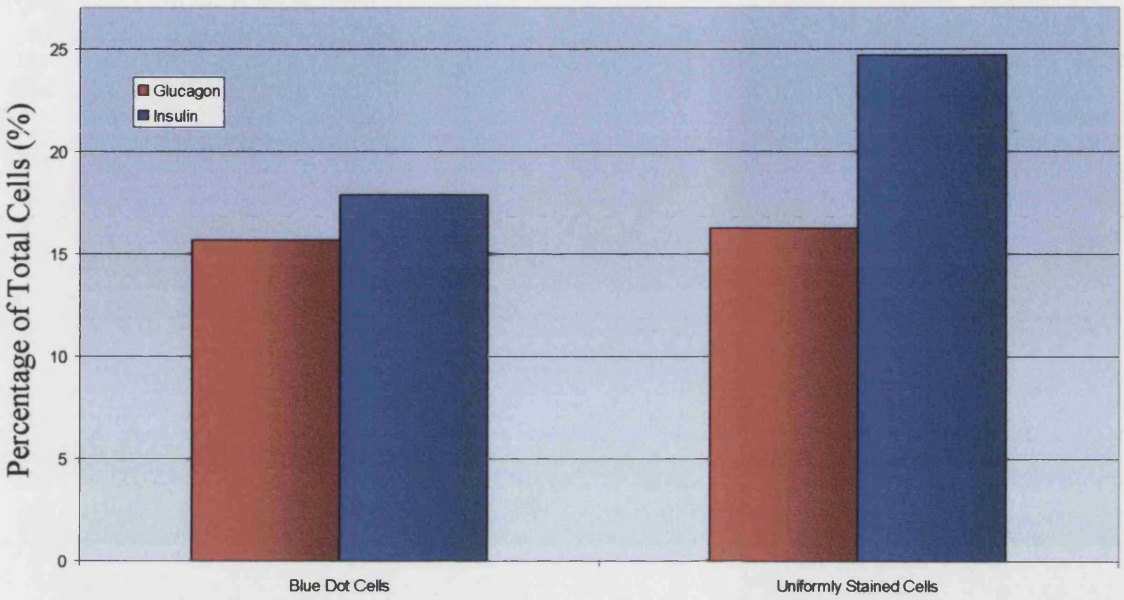

Wholemount immunostaining for ngn3 was performed on E11.5, E12.5, E13.5, E14.5 and E15.5 whole MF1 strain embryos, intact guts and brains as a positive control for specific immunostaining with the same two antibodies as above. Maximal pancreatic expression of ngn3 protein is reported to occur at E15.5 (Schwitzgebel *et al.*, 2000). Widespread non-specific immunostaining was observed throughout the tissues using either alkaline phosphatase or immunoperoxidase detection, despite precautions to suppress endogenous enzyme activity (1 mM levamisole or 0.1 % H_2O_2 respectively).

3.4. Discussion

3.4.1. Incidence of Migratory Epithelial Cells

Blue dot cells or BDCs were observed in a number of recombinant pancreatic bud cultures as previously reported (Percival and Slack, 1999). Their prominent X-gal staining indicated that they must be of an epithelial origin. The total number of both BDC and USC clusters and total cells in each culture was found to increase over the 48 h culture period. However, the frequency of BDC occurrence varied greatly between individual recombinant cultures: some were completely devoid of such cells whereas in others, BDCs were present in abundance, distributed throughout the unlabelled mesenchyme. Although the surrounding β-gal-labelled epithelial cells hindered their identification, blue dot cells were observed within labelled epithelium in recombinant cultures and so should be present within intact ROSA-26 pancreatic bud cultures. However, BDCs were most evident against an unlabelled background and so were most obviously identified against unlabelled MF1 epithelium or mesenchyme in recombinant cultures. Their epithelial origin and incidence at some distance from the labelled epithelium indicated that they must have migrated from the β-gal$^+$ epithelium.

3.4.1.1. Uniformly Stained Cells: A Second Class of Migratory Epithelial Cell?

In the great majority (17 of 18) of recombinant cultures, a second class of large, rounded X-gal staining cell was observed. These cells exhibited uniform blue staining throughout each cell following incubation with X-gal and so were termed uniformly stained cells or USCs. Unlike the BDCs, no blue dot of X-gal stain could be resolved at any focal plane within any of the USCs, rendering the two cell types clearly distinguishable. Like the BDCs, the β-gal expression in the USCs was indicative of an epithelial origin and their segregation from the β-gal$^+$ epithelium further suggested them to be migratory like the BDCs. As a consequence of their uniform staining, USCs within the labelled epithelium would not have been distinguishable from neighbouring, homogeneously staining exocrine cells and so their incidence or otherwise in the β-gal$^+$ epithelium could not be ascertained. The presence of either class of migratory epithelial cell was found not to be dependent on the presence of the other since either class of cell could occur in the absence of the other.

3.4.1.2. Preferential Migration on the Mesenchyme

Confirming the migratory nature of the BDCs, their mean distance from the labelled epithelium where they originate was found to increase from 154.3 ± 13.58 μm to 486.9 ± 11.50 μm over 48 h of culture, implying a migration speed of at least 166.3 μm/day. Similarly, the mean distance of USCs from the labelled epithelium showed an increase over the 2d culture period examined, from 525.5 ± 14.16 μm to 717.0 ± 33.32 μm after 24 h. Only 4.19 % of BDC clusters and 3.09 % of USC clusters were found within the pancreatic epithelium of the recombinant cultures, indicating that both the blue dot and uniformly stained epithelial cells prefer to migrate on a mesenchymal substratum as opposed to the pancreatic epithelium. This conclusion holds true even when it is considered that the area of unlabelled epithelium in each recombinant culture is less than the area of *lacZ* mesenchyme, such is the predominance of mesenchymal BDC and USC localisation. Reasons for this substratum preference might include the provision of trophic factors from the monolayer of mesenchymal cells or the lower resistance to cell movement afforded by the less densely packed mesenchyme as opposed to the pavement-like arrangement of epithelial cells.

3.4.2. BDCs: A Population of Committed Endocrine Precursor Cells?

3.4.2.1. Expression of Endocrine Markers

To test the hypothesis that BDCs represent a population of committed endocrine precursor cells, immunofluorescence cytochemistry was performed for β-gal and for one of the endocrine markers glucagon or insulin. Consistent with previous findings, although a minority of BDCs produced recognised endocrine products, the majority did not. 15.7 % of BDCs and 16.2 % of USCs were found to be glucagon-immunopositive whilst 17.9 % of BDCs and 24.7 % of USCs were shown to be immunopositive for insulin. More conclusive identification of the BDC and USC populations was hindered by lack of success in performing immunofluorescence analysis for the endocrine progenitor marker ngn3 (Apelqvist *et al.*, 1999; Jensen *et al.*, 2000a; Schwitzgebel *et al.*, 2000). Ngn3 expression within the mouse embryonic pancreas is maximal at E15.5 when scattered immunopositive cells can be seen throughout the pancreatic bud (Schwitzgebel *et al.*, 2000). Hence, a high level of immunofluorescence staining for ngn3 would have been expected especially in the 4d pancreatic bud cultures, even

considering the one-day delay of differentiation *in vitro* compared with developmental events *in vivo* (Percival and Slack, 1999).

3.4.2.2. Sensitivity Differences in β-Gal Detection Methods

It was obvious from the data that the number of BDCs and USCs identified in each culture by immunofluorescence detection was markedly less than the number of such migratory cells identified per culture by histochemical X-gal staining. The mean total number of BDCs per culture detected by X-gal staining after 4d and 5d was 119.7 ± 25.3 cells and 602 ± 169.7 cells respectively whereas only 10.5 ± 3.51 and 11.0 ± 2.96 BDCs/culture were detected by immunofluorescence analysis after 4d and 5d respectively. Similarly, the mean total number of X-gal-stained USCs per culture after 4d and 5d was 139.2 ± 31.0 cells and 90 ± 50.2 cells respectively whilst only 13.9 ± 6.62 and 54.2 ± 17.8 USCs were identified per culture by immunofluorescence detection after 4d and 5d of culture respectively. This was attributed to there being a marked distinction between the thresholds of β-gal detection between histochemical X-gal staining and immunofluorescence analysis in conjunction with an anti-β-gal antibody. The former method which relies on the catalysis of a chemical reaction by the β-galactosidase enzyme, is more sensitive than is localisation of the protein using an antibody. The extent of this difference in practical terms was quantified as described in **Chapter 4, Sections 4.3.3.1.** and **4.3.3.2.**

3.4.2.3. Technical Difficulties

The evidence obtained in this work is clearly insufficient to determine whether or not the blue dot cells are representative of a population of committed endocrine precursor cells. This was in large part a consequence of protracted technical difficulties. These included the long period of time (23 months) to obtain sufficient numbers of high-quality E11.5 ROSA-26 embryos after a decline in embryo viability made outbreeding with MF1 animals a necessity. During the first 12 months of the project prior to outbreeding, 60 % of ROSA-26 plugs were found not to bear embryos. Furthermore, the successful construction of recombinant cultures proved initially to be very challenging, especially concerning the satisfactory adherence of the components to one another and the minimisation of "contamination" by β-gal$^+$ mesenchyme inclusion.

3.4.2.4. Markers of Endocrine Precursors

The second area of complications concerned the immunofluorescence characterisation of BDCs (and USCs) on the basis of their expression of endocrine markers. A small proportion, approaching a quarter of both the BDC and USC population identified by immunofluorescence staining for β-gal, expressed either insulin or glucagon. This shows that a proportion of the migratory BDCs and USCs are endocrine cells. It could not be determined from these experiments what proportion of the BDC population expressed *both* insulin *and* glucagon which might have afforded greater characterisation of these cells. It is a widely held belief that cells transiently expressing two or more hormones such as insulin and glucagon give rise to mature hormone-secreting cells and represent a population of endocrine precursor cells (Alpert *et al.*, 1988; Teitelman *et al.*, 1993; Upchurch *et al.*, 1994, 1996). Technical difficulties ensured that neither the BDCs nor USCs could be subjected to immunofluorescence analysis for Pdx1 or ngn3 which could have yielded the most informative evidence on their endocrine precursor role or otherwise. Other proposed markers of endocrine precursors which might be stained for in future work include Isl1, Nkx2.2, Nkx6.1, NeuroD1, and Pax6. A proportion of the migratory cells are, however, endocrine cells.

3.4.2.5. Cell Clusters Disaggregate and are Not Clonal

It was found that the mean cluster size of both USC and BDC clusters decreased over the 48 h culture period. Mean BDC cluster size, including isolated cells decreased from 8.23 ± 1.02 cells to 3.87 ± 0.191 cells over the two days whilst the mean USC cluster size (single USCs inclusive) decreased from 2.62 ± 0.247 cells to 1.72 ± 0.112 cells over the same period. This would suggest that the cell clusters disintegrate over the culture period. This progressive decrease in cluster size might be due to migration of cells away from the cluster or by the death of cells within the group. This latter hypothesis might be tested by subjecting cultures to TUNEL analysis for the detection of cells undergoing apoptosis.

Although many migratory BDCs and USCs occurred in groups, clusters of neither migratory cell type were found to be clonal in size (two cells, four cells, eight cells, 16 cells, 32 cells etc.) as might be expected if such clusters contained symmetrically-dividing stem cells able to give rise to further stem cells as consistent with an endocrine precursor role. In order to examine whether the BDCs and USCs are

actively proliferating, staining for the proliferating cell nuclear antigen PCNA, might be conducted in one avenue of future work. Alternatively, an index of cell proliferation could be derived by the incorporation of BrdU and its subsequent immunodetection in pancreatic bud cultures.

One source of BDC and USC scoring error was determining what constituted a "cluster". When large numbers of β-gal$^+$ migratory epithelial cells were distributed throughout the mesenchyme (especially after 5d or 6d *in vitro*), on occasion it proved difficult to establish the boundaries of given cell clusters. It was speculated that the decrease in mean BDC and USC cluster sizes over the 48 h culture period might partially be a consequence of the greater difficulty in determining boundaries of clusters in 4d cultures when the migratory cells are less well distributed from the labelled epithelium. However, this factor was not deemed to be problematic in terms of the integrity of the overall data.

3.4.2.6. A Distinction Between BDCs and USCs?

At all time-points during culture, the mean size of clusters of USCs was markedly reduced compared with sizes of BDC aggregates. Indeed, USCs exhibited a greater tendency to occur as either isolated cells or in small (< 5 cells) clusters than did the BDCs. As a result of this, the frequency distribution of USC cluster sizes was determined to be significantly different to that for the BDC aggregates ($\chi^2 = 1065.8$; $P < 0.01$). USCs also tended to occur at greater distances from the β-gal-labelled epithelium than did the BDCs. It therefore appears that despite their superficial similarities, the BDCs and USCs represent distinct classes of migratory cells since their patterns of distribution are so significantly different from one another.

3.4.3. Explaining Blue Spot β-Gal Expression

3.4.3.1. Endogenous β-Gal Synthesis

In the study by Percival and Slack (1999), the blue spot-type β-gal expression of BDCs could not be explained though was presumed to be a consequence of cell processing of the bacterial β-gal protein. The possibility that the expression pattern represents phagocytosis of labelled debris by unlabelled cells was dismissed since blue dot cells could occur at some distance from uniformly stained cells and second, the

mesenchymal cells immediately adjacent to the X-gal-stained epithelial tissue did not contain the blue dots. Both observations were confirmed in the current study. It was therefore considered that the blue dots were representative of endogenous β-gal synthesis and the cells were genuinely of epithelial origin.

3.4.3.2. Blue Spots a Product of Culture Stress?

Similar blue spot-type β-gal expression in a second study provides further explanations for the observations of BDCs. Beddington and coworkers (Beddington *et al.*, 1989) studied the deployment of cells during gastrulation and early organogenesis using the *lacZ* gene as a cell marker to follow cell fate. Using pronuclear DNA injection, they created a transgenic mouse strain expressing six copies of the *E. coli lacZ* gene under the control of the rat β-actin promoter. X-Gal staining of postimplantation hemizygous mouse embryos during gastrulation and early organogenesis demonstrated β-gal expression to be ubiquitous and constitutive in all epiblast derivatives of the E10 embryo. No β-galactosidase activity was seen in trophectoderm and primitive endoderm derivatives. In late primitive streak stage (E8.5) embryos, whilst mesoderm and presumptive definitive endoderm cells demonstrated uniform, generalised cytoplasmic X-gal staining, staining in the epiblast was punctate as if the β-galactosidase was localised to intracellular vesicles. In excess of 80 % of epiblast cells demonstrated a blue spot following incubation in X-gal. In early somite stage (E9.5) embryos, neurectoderm and somatic and lateral mesoderm were also found to exhibit this punctate pattern of X-gal staining. By E10.5, the entire cytoplasm of cells stained with X-gal (Beddington *et al.*, 1989). As mentioned, in the current study, it could not be determined whether the BDCs lose their blue spot expression pattern to become USCs. In the study of Beddington *et al.* (1989), punctate staining was speculated to be a feature of cells expressing β-galactosidase at low levels. Cleavage-stage blastomeres, with low bacterial β-galactosidase activity, show a similar punctate staining pattern (Ueno *et al.*, 1987), but there was no evidence for segregation of enzyme activity with particular subcellular fractions. Therefore, the blue spots were considered to represent cytoplasmic oxidation centres which facilitate the deposition of insoluble pigment (Ueno *et al.*, 1987). So, the blue spot X-gal staining pattern might be indeed representative of endocrine precursors which specifically express low levels of β-galactosidase enzyme relative to other cells in the cultures for some unknown reason. Alternatively, blue spots might simply occur

in any cell (exocrine or endocrine) in the cultures if that cell expresses low levels of the enzyme, perhaps as a response to stress. This hypothesis is not supported by the observation that a markedly greater proportion of BDCs and USCs express the endocrine hormones insulin or glucagon than might be expected amongst the general epithelial cell population in the pancreatic bud culture. As the endocrine component represents only 1-2 % of the pancreatic volume (Bonner-Weir and Smith, 1994), then it might reasonably be expected that only 1-2 % of BDC or USC cells express insulin or glucagon, not the 15.7-24.7 % observed. However, this hypothesis is consistent with the great variation observed in the incidence of BDCs between individual cultures. In some cultures, no BDCs were observed whilst in others, BDCs were abundantly distributed throughout the entire mesenchyme. It might be speculated that the latter cultures might have been exposed to a higher level of stress whilst being cultured *in vitro* than other cultures, inducing a high amount of BDC formation.

3.4.4. Summary

3.4.4.1. Future Work

It remains to be seen which, if either of these hypotheses is correct and whether the BDCs (and USCs) represent a committed endocrine precursor population. Although this study has quite comprehensively determined the properties of the BDCs in terms of their physical distribution, it has raised more questions than it set out to address regarding their identity. Further work is needed to characterise the BDCs and USCs more fully by their expression of the aforementioned endocrine and exocrine markers, including insulin, glucagon, amylase, peptide YY, ngn3 and Pdx1. Thus, double- or triple-immunofluorescence analysis for β-galactosidase and a second cellular marker must be perfected localising amylase, peptide YY, ngn3 and Pdx1 (Ipf1) before this work can be undertaken. If the BDCs or USCs can be identified as being endocrine precursors, then their proliferative behaviour should first be investigated as mentioned. Future avenues of work would involve studying their differentiation in various environments (for example, in combination with normal epithelium or with mesenchyme) with the long-term objective being the isolation of BDCs into pure culture. This might be achieved through exploiting the neomycin resistance of ROSA-26 tissues.

3.4.4.2. Motile Cells

Irrespective of whether the BDCs represent an endocrine precursor population, this work has conclusively demonstrated the existence of epithelial migratory cells within the mouse embryonic pancreas. Many of these migratory cells occur in clusters and at least a proportion of them are endocrine cells. Exploiting the *lacZ* cell lineage label has allowed us to identify such motile pancreatic cells *in vitro* and investigate their spatial distribution as they migrate on the mesenchyme.

4. Cell Lineage Analysis

4.1. Introduction

4.1.1. Origin of the Pancreatic Structural Units

Little is known regarding the origin of the main structural units in the pancreas: the islets, acini and pancreatic ducts. Do they arise from individual cells or from groups of cells? The origin of islets has been examined in only a very limited number of studies. Using the human C-peptide/proinsulin product as a cell marker in aggregation mouse chimaeras, Deltour *et al.* (1991) tested three hypotheses of islet growth: (1) a single progenitor cell gives rise to all the precursors of the islets, (2) each of a few progenitor cells is the founder of a different islet, or (3) each islet is a mixture of cells originating from a pool of progenitor cells. If all the β-cells of a given pancreatic islet are derived from a single progenitor cell, each islet in mouse chimaeras will be entirely of one parental genotype or the other. However, if an islet is derived from multiple progenitor cells, it will be composed of a mixture of cells from both genotypes. In two of the four aggregation chimaeras, islets containing cells from both aggregated embryos were demonstrated. This finding was taken to support the third hypothesis above, suggesting that islets originate by cell aggregation. This conclusion was later supported by the mixed cellular composition of individual islets in combination cultures of a *lacZ*-expressing and an unlabelled pancreatic epithelium with an unlabelled mesenchyme (Percival and Slack, 1999). However, both studies were affected by limitations. In the aggregation chimaera study, only a very small number of animals and so, islets were examined. The second is restricted by it being *in vitro*.

4.1.2. Stem Cells in the Small Intestine

Clonal development of structural units from stem cells has been extensively studied in the intestinal crypts of Lieberkühn of the mouse small intestine (Li *et al.*, 1994; Ponder *et al.*, 1985; Schmidt *et al.*, 1988; Winton *et al.*, 1988; Winton and Ponder, 1990) and more recently, in the gastric glands of the stomach (Canfield *et al.*, 1996; Nomura *et al.*, 1998). Stem cells are the cells which establish the cell lineages which form tissues and organs in the embryo. They are also responsible for the sustained production of cells in tissues characterised by constant renewal. The small

intestinal murine crypt provides an elegant system for studying the control of stem cell proliferation and differentiation.

The adult mouse small intestine is lined with an epithelial monolayer which is morphologically highly organised into the villi and crypts which function as the source of intestinal proliferation. The 1.1 million or so crypts (Hagemann *et al.*, 1970) each contain approximately 250 cells (Kellett *et al.*, 1992). Cell proliferation is confined to the crypt base, from where cells migrate to the villi, whereupon they are shed (Potten and Hendry, 1983). These basal crypt cells are candidate stem cells owing to the frequent localisation of stem cells at the origin of cell flux (Wright, 2000). Evidence from experiments with mutagens which induce phenotypic crypt changes, suggests the number of active actual stem cells in each crypt to range from four to 16 (most probably about four). The proliferating basal crypt stem cells divide asymmetrically (at least on a statistical basis) to produce daughter cells which migrate up towards the crypt mouth and are known as transit amplifying (TA) cells. Whilst migrating, they undergo a further series of divisions, proliferating rapidly and then differentiating, appearing at the mouth of the crypt as postmitotic, terminally differentiated cells which line the upper parts of the crypts and villi (Potten and Loeffler, 1990). Hence, the concept of a few basally sited crypt stem cells which supply progeny to the proliferative compartment of dividing transit cells has emerged. A stem cell hierarchy is established in which stem cells with maximum pluripotency and proliferative potential reside in the stem cell zone near the crypt base with cells lying above this zone displaying reduced pluripotency and proliferative potential, which reduces further as the distance from the stem cell zone increases (Potten and Loeffler, 1990).

4.1.3. Clonal Purification of Intestinal Crypts

Ponder and coworkers (Ponder *et al.*, 1985) examined clonality of the intestinal crypts using mouse aggregation chimaeras constructed from inbred mouse strains exhibiting differences in binding of the *Dolichos biflorus* agglutinin (DBA) lectin. These differences resulted from a carbohydrate polymorphism which was exploited as a cell marker. The epithelium of individual crypts in small and large intestine of adult animals was always seen to be composed of cells of a single parental type. It was inferred that the epithelium of each adult intestinal crypt forms a clonal population, with each adult crypt being derived from a single progenitor or stem cell. Although polyclonal intestinal crypts have been observed in neonatal mice up to two weeks of age

they rapidly disappear (Schmidt *et al.*, 1988) to give way to the monoclonal units of the adult. This progression of polyclonal embryonic crypts to a state of monoclonality is an obscure process that has been called "crypt cleansing".

Mechanisms proposed to account for this clonal purification process always involve the overgrowth of one stem cell lineage in the crypt and the loss of others so the progeny of one stem cell eventually displace all others (**Fig. 4.1. (a)**). This model assumes that stem cell divisions are random in respect to replacement versus commitment to differentiation (Loeffler *et al.*, 1993). If a stem cell can produce two stem cells or two cells committed to differentiate, or one of each, then there will necessarily be a progressive reduction of the number of cell lineages within the crypt, because when a stem cell produces two progeny committed to differentiate then this cell line is lost from the stem cell pool of that crypt. A 12-week renewal time for the crypt epithelium has been determined (Winton and Ponder, 1990). If a single "crypt-populating stem cell" were to provide directly the average daily output of a single crypt of approximately 250-300 cells (Potten and Loeffler, 1987) that stem cell would need to undergo about seven amplifying transit divisions, resulting in complete turnover or repopulation of the crypt epithelium (excluding any long-lived cells) by at the latest 5.5 days (Winton and Ponder, 1990). The fixation of one stem cell lineage can also be explained by crypt division (or crypt fission) (Li *et al.*, 1994; St. Clair and Osborne, 1985), a significant mechanism of crypt reproduction in which a crypt splits from the base upwards. Over the first two weeks of postnatal life, crypt number is increasing rapidly by division of pre-existing crypts (Cheng and Bjerknes, 1985). If each crypt initially contains a small number of stem cells and these are partitioned randomly between the daughter crypts, then the number of stem cells within individual crypts will progressively reduce (**Fig. 4.1. (b)**).

4.1.4. Clonal Purification in the Pancreatic Islets?

It was hypothesised that a similar process might occur in the development of the pancreatic islets. It was proposed that the neonatal islets are polyclonal, having been formed from multiple progenitor cells and subsequently undergo a process of "clonal purification" to achieve monoclonality. If shown to occur, this purification might be explained by similar mechanisms proposed to account for crypt cleansing such as the overgrowth and extrusion of existing cells at the expense of one stem cell lineage or by the division of islets and concomitant partitioning of stem cells.

Figure 4.1. Mechanisms for Clonal Purification of the Intestinal Crypts

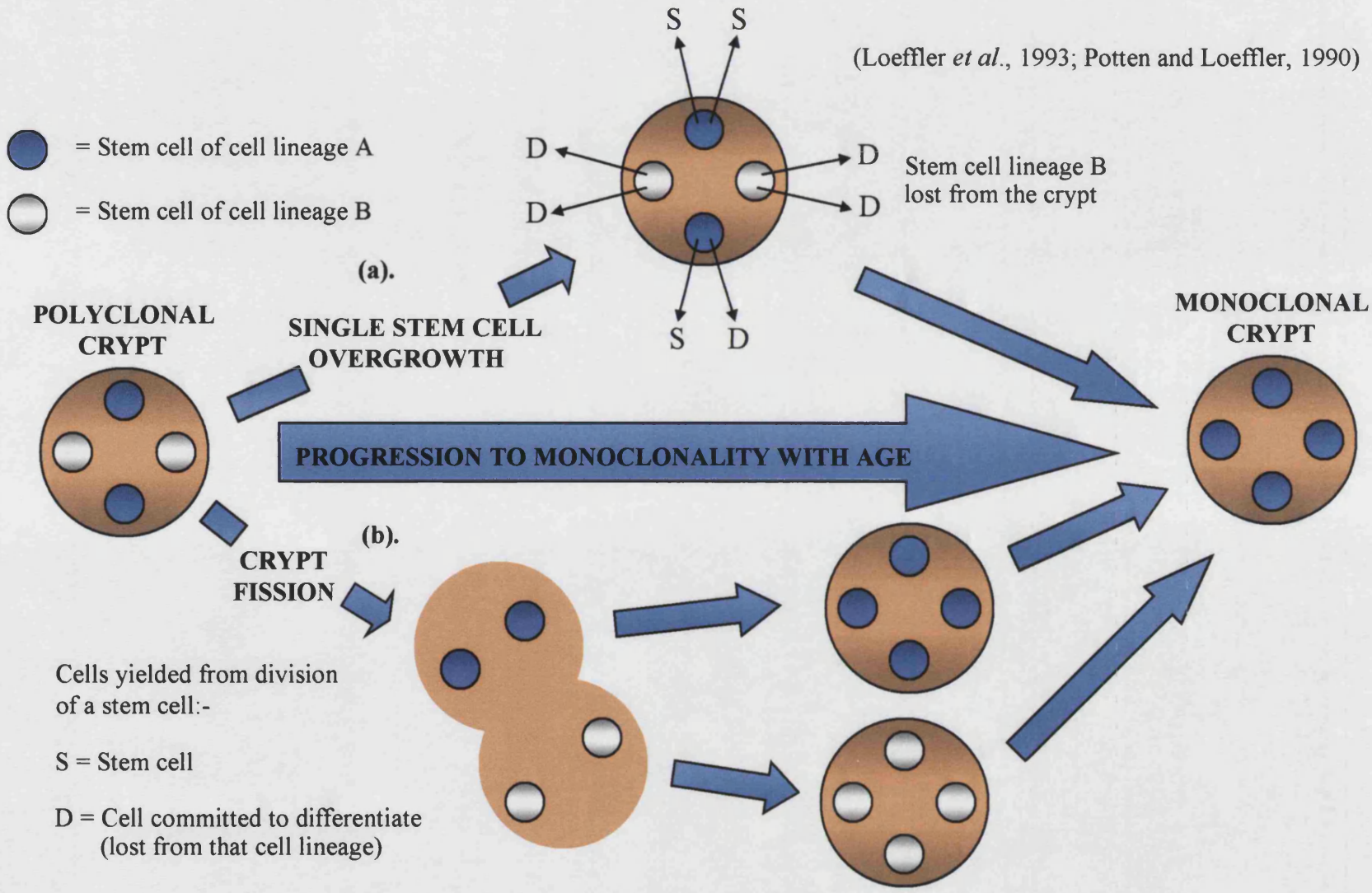

4.1.5. X-Inactivation Mosaic Mice

To follow the clonal development of the pancreatic islets, acini and ducts, X-inactivation mosaic mice were used to study the postnatal cell lineage in these structural units of the pancreas. The H253 line (Tam and Tan, 1992) of transgenic mice was exploited as a source of lineage-labelled tissue. It has 14 copies of the *E. coli lacZ* reporter gene insert in tandem close to the Hprt locus (Tan *et al.*, 1995). The transgene is driven by the promoter of the ubiquitously expressed 3-hydroxy-3-methylglutaryl coenzyme A reductase (HMG CoA reductase) gene. The transgene is transmitted in an X-linked pattern and, due to X-inactivation in which one of the two X-chromosomes in early embryonic cells of female mammals is randomly transcriptionally silenced (Lyon, 1961), it stably marks approximately 50 % of the cells of H253 female hemizygotes. This results in a mosaic pattern of β-gal expression in all tissues of female X-inactivation mosaic mice including the pancreas.

4.1.6. Current Study

An immunohistochemical and immunofluorescence analysis was conducted on paraffin and frozen sections of pancreas from H253 mosaic females using, respectively, X-gal histochemistry and an anti-β-gal antibody to visualise the distribution of the cell marker in the islets, acini and pancreatic ducts. Numbers of cells of each genotype in the islets were counted at a number of postnatal time-points to infer their clonal state. Returning to the three hypotheses of islet growth (Deltour *et al.*, 1991), if a single progenitor cell gives rise to *all* precursors of the islets, then *all* islets in the pancreas will be composed of β-gal$^+$ *or* β-gal$^-$ cells, but *not* both; the islets will be homogeneous. If each of a few progenitor cells is the founder of a *different* islet then *each* islet will be composed of β-gal$^+$ *or* β-gal$^-$ cells, but *not* both; again, all islets will be homogeneous. If, however, each islet is a mixture of cells originating from a pool of progenitor cells then one would expect islets to be predominantly mixed or mosaic, comprising cells of *both* genotypes (**Fig. 4.2.**). If mixed, polyclonal islets undergo a shift or clonal purification towards homogeneous islets in later animals, then mixed or heterogeneous β-gal$^+$/β-gal$^-$ islets would be expected in the immediate neonatal pancreas followed by their replacement by homogeneous islets of a single genotype in the later postnatal organ.

Figure 4.2. Three Hypotheses for Expansion of the Cells from which the Islet β-Cells Derive. (After Deltour *et al.*, 1991)

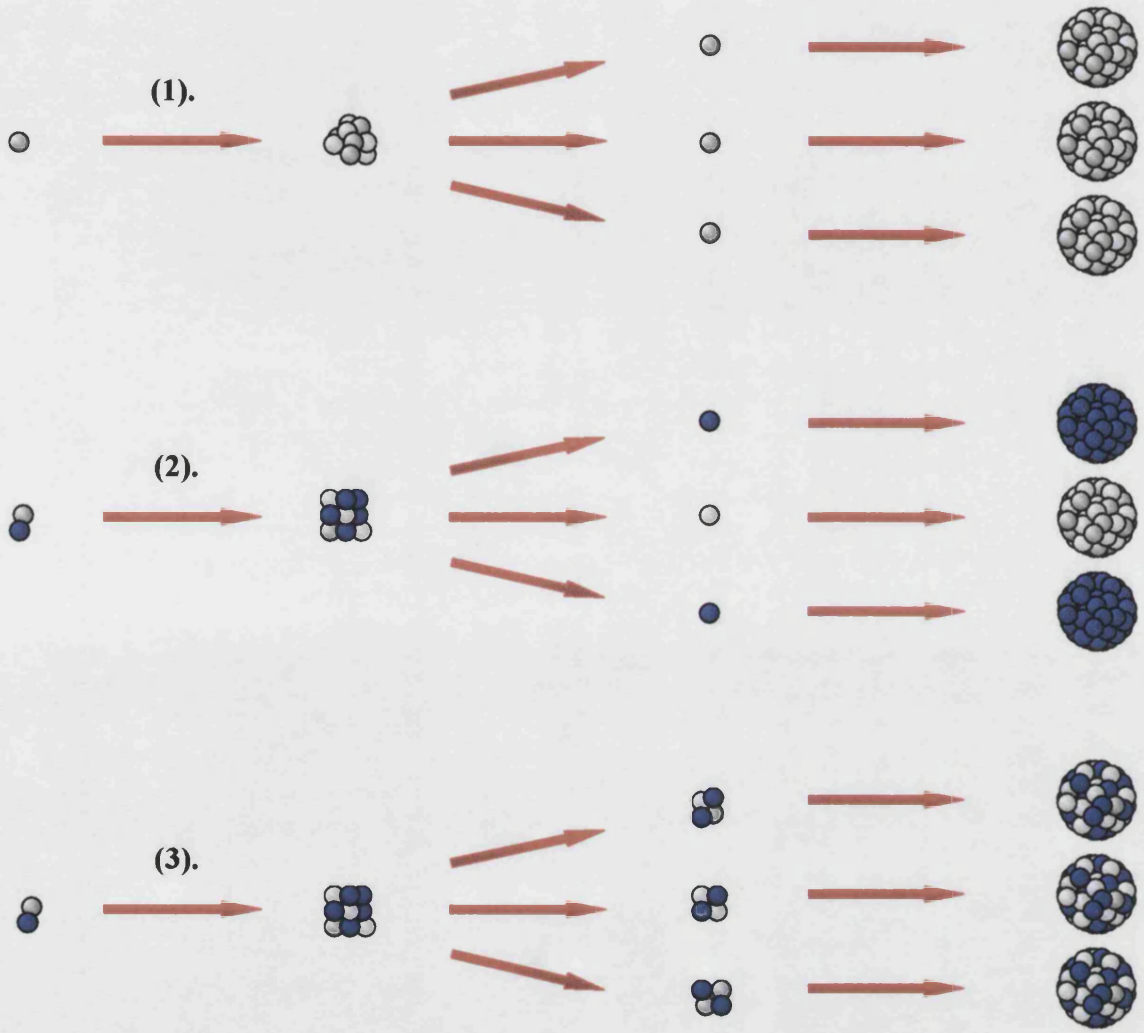

A single progenitor cell gives rise to all of the islet precursors

All islets in the pancreas will be composed of β-gal$^+$ *or* β-gal$^-$ cells but *not* both

Each of a few progenitor cells is the precursor of a different islet

Each islet will be composed of β-gal$^+$ *or* β-gal$^-$ cells but *not* both

Each islet is a mixture of cells originating from a pool of progenitor cells

All islets are mixed/ mosaic comprising β-gal$^+$ *and* β-gal$^-$ cells

4.2. Materials and Methods

4.2.1. X-Inactivation Mosaic H253 Mice

H253 mice were obtained from Harwell and housed under standard conditions on a 13 h light:11 h dark cycle (lights on 06:30-19:30, including 30 min periods of dim lighting to provide false dawn and dusk) at 21 ± 2°C and at a relative humidity of 55 ± 10 %. Food (CRM formula; Special Diets Services, Witham, Essex, UK) and water was provided *ad libitum*. The transgenic H253 mouse line was originally created by pronuclear injection of a DNA fragment containing the *lacZ* reporter gene under the control of a ubiquitously active promoter of the HMG CoA reductase gene (Tam and Tan, 1992). The line carries 14 tandem copies of an 8.9 kb fragment containing the promoter of a ubiquitously expressed mouse housekeeping gene, 3-hydroxy-3-methylglutaryl coenzyme A reductase, linked to the *E. coli lacZ* gene incorporating a SV40 T-antigen nucleus localisation signal sequence. Breeding and chromosome hybridisation experiments with the H253 line confirmed that the *lacZ* gene is integrated in the A6 region of the X-chromosome (Tan *et al.*, 1993, 1995). Male H253 animals express the X-linked *lacZ* gene in all cells of the embryo, including the developing nervous system (Tan and Breen, 1993; Tan *et al.*, 1993). Females possess two X-chromosomes per cell but to maintain dosage parity with males, one of the two X-chromosomes in each cell is randomly and irreversibly inactivated during early embryogenesis (Lyon, 1961). This phenomenon is unique to mammals and is known as X-inactivation. The initial process of random inactivation is virtually completed before E9.5, and provides an ideal method of generating mosaicism amongst embryonic cells. In hemizygous females, only one of the two X-chromosomes will bear the *lacZ* transgene and this chromosome will be randomly turned off in approximately 50 % of cells (Tan *et al.*, 1993). The cell-marking process is therefore indelible and heritable, and with each division of a cell, the *lacZ* gene and its active or inactive status is transmitted to the progeny of that cell. This process results in a marked clone in the absence of extensive cell mixing.

4.2.1.1. Generation and Genotyping of H253 Animals: Time-Series One

Transgenic H253 male mice were mated to F_1 (C57BL/6×CBA) females (**Fig. 4.3.**). All female offspring from this mating scheme were hemizygous for the X-linked

Figure 4.3. Two Common H253 Mouse Crosses

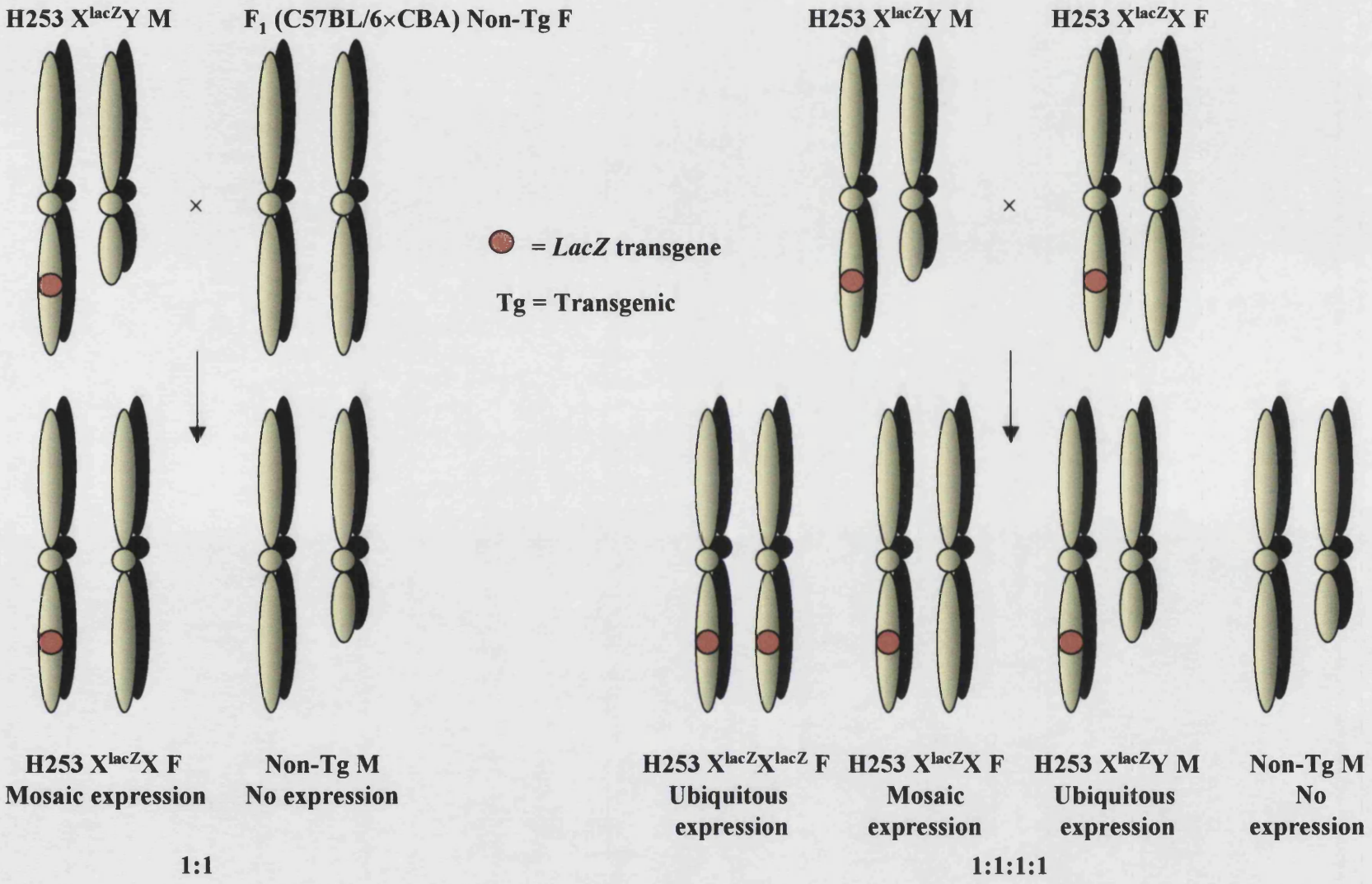

lacZ transgene. A developmental series of animals was analysed at postnatal days (PN)3 (*n* or number of animals examined = 2), PN7 (*n* = 2), PN14 (*n* = 2), PN21 (*n* = 2), PN28 (*n* = 1), PN12weeks (*n* = 2), PN26wk (*n* = 3) and PN52wk (*n* = 2) ("Time-Series One"). Animals were sacrificed by cervical dislocation, their pancreata rapidly excised and the tissue analysed immunocytochemically. In the second mating scheme (**Fig. 4.3.**), male H253 stud mice were mated to female H253 hemizygotes. Conforming to Mendelian laws, 25 % of offspring were females homozygous for the *lacZ* transgene, 25 % were hemizygous females, 25 % were hemizygous males (effectively homozygous) and the remaining 25 % of the offspring were non-transgenic males. Offspring from crosses were genotyped on the basis of β-gal expression pattern in the crypts of the small intestine or gastric glands of the stomach; both the crypts (Ponder *et al.*, 1985) and gastric glands (Canfield *et al.*, 1996; Nomura *et al.*, 1998) have previously been shown to be monoclonal. Following X-gal staining, homozygous females and hemizygous males bear ubiquitously-stained organs whilst hemizygous females exhibit a striking mosaic of homogeneous β-gal$^+$ and homogeneous β-gal$^-$ crypts (**Fig. 4.4.**) and gastric glands. However, with wholemount staining, X-gal penetrates the intestinal tissue to a depth of 3-4 crypt layers, resulting in only partial staining of (ubiquitously *lacZ*-expressing) deeper tissues. Genotyping must therefore be conducted by examining only the β-gal expression pattern of the most superficial 3-4 crypt layers at the surface of the wholemount specimen. X-Gal staining must be performed prior to paraffin-embedding as very little β-gal activity persists after processing and paraffin-embedding procedures.

Pancreatic tissue from non-transgenic male and homozygous female (or hemizygous male) littermates at each time-point was analysed to act as a negative control in the former case and as a positive control in the latter to ensure that the promoter drives transgene expression ubiquitously throughout the pancreas.

4.2.2. Time-Series One: Immunoperoxidase Immunocytochemistry of X-Gal-Stained Paraffin Sections

Fixed pancreata from Time-Series One were stained for β-gal activity as in **Chapter 2, Section 2.3.2.** then processed, paraffin-embedded and 7 μm sections cut from the tissue blocks as in **Section 2.4.1.** The paraffin sections were processed for immunoperoxidase demonstration of either insulin or glucagon then counterstained in nuclear Fast Red and mounted in DPX as in **Section 2.5.3.1.**

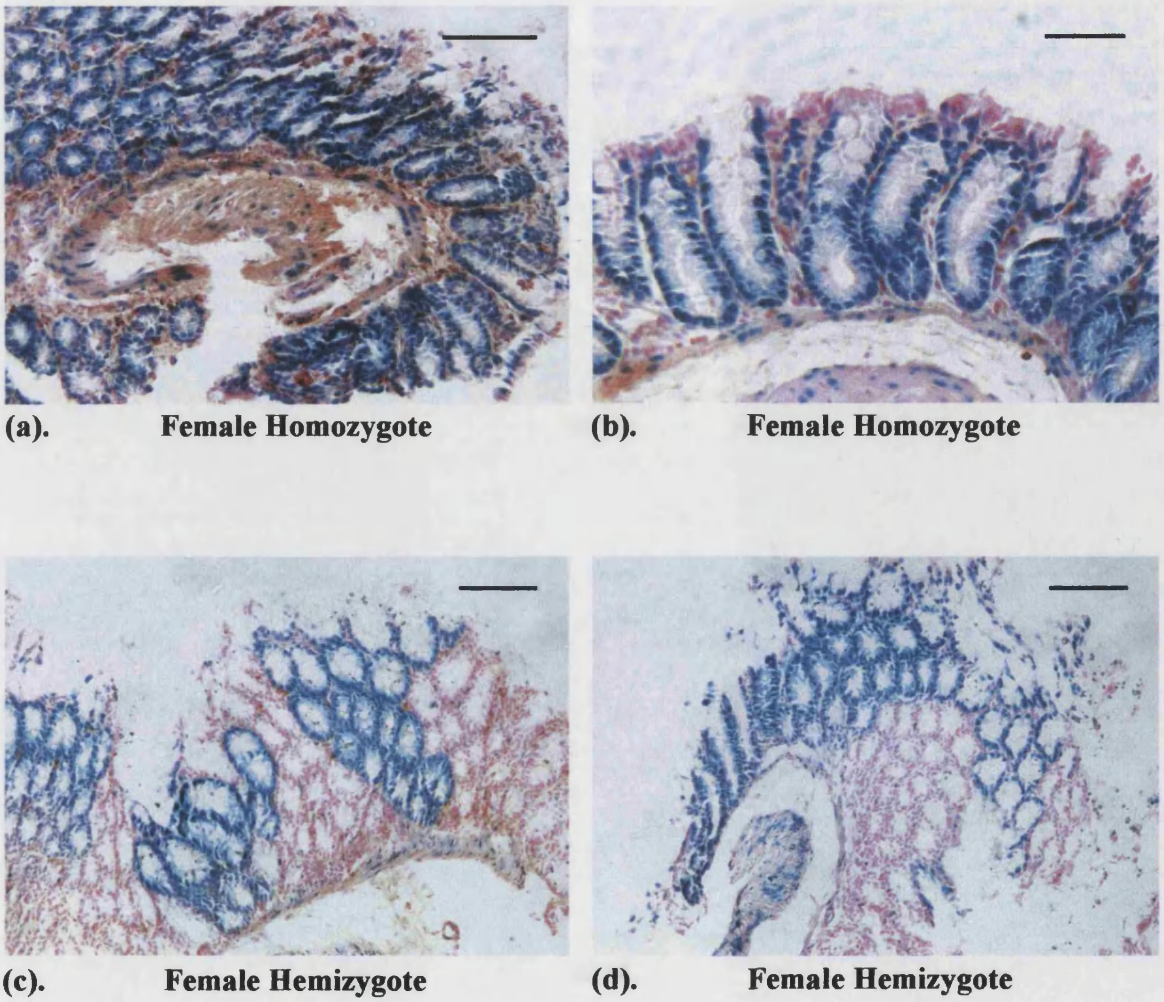

(a). Female Homozygote **(b). Female Homozygote**

(c). Female Hemizygote **(d). Female Hemizygote**

Figure 4.4. Characteristic Pattern of X-Gal Staining for β-Gal Activity in the Intestinal Crypts of H253 Homozygous (a and b) and Hemizygous (c and d) Females

(a), (c) and (d) Bar = 200 μm; (b) Bar = 50 μm

4.2.3. Time-Series Two: Immunofluorescence Cytochemistry of Frozen Sections

Superposed X-gal and electron-dense DAB stains can be difficult to resolve. To determine labelling of distinct islet cell types in H253 mosaic mice with greater resolution, immunofluorescence cytochemistry for β-galactosidase in conjunction with glucagon or insulin was performed. This was necessarily conducted on frozen tissue sections (see **Section 4.3.2.**). As Time-Series One had indicated a significant clonal purification by PN30, pancreata from a second developmental series of animals were analysed at PN5, PN10, PN15, PN20, PN25 and PN30 (*n* or number of animals examined = 5 per time-point) ("Time-Series Two"). Mice were sacrificed by cervical dislocation and their pancreata rapidly excised.

Pancreata were divided into two equal-sized portions, one of which was subjected to paraffin histology as described above. The portion destined for the preparation of frozen sections (cryosections) was fixed, cryoprotected, embedded in O.C.T. and 10-15 μm frozen sections cut as in **Section 2.4.2.** Cryosections were then processed for immunofluorescence demonstration of β-gal and glucagon or β-gal and insulin, counterstained in DAPI and mounted in Gelvatol as described in **Section 2.5.2.**

4.2.4. Time-Series Three: Analysis of Simvastatin-Treated PN30 Animals

4.2.4.1. Simvastatin Treatment

Results from Time-Series One and Two indicated some variability in the expression of β-galactosidase in islet cells, agreeing with previous observations (Stone *et al.*, 2002). To decrease this variability and to elevate the overall production of β-galactosidase in cells retaining the active marker, simvastatin (Calbiochem 567020) was administered orally (1 mg/100 ml drinking water for 10 days between PN20 and PN30 when the animals were sacrificed) to two litters of H253 mice examined at PN30. Simvastatin lowers cholesterol, a negative inhibitor of HMG CoA reductase (Goldstein and Brown, 1990). Lower cholesterol results in an increase in the transcription of HMG CoA reductase mRNA and in H253 mice, an increase in expression of the *lacZ* gene driven by the HMG CoA reductase promoter (Stone *et al.*, 2002).

4.2.4.2. X-Gal Staining and Immunofluorescence Cytochemistry of Frozen Sections

To assess the effectiveness of simvastatin treatment in ensuring ubiquitous constitutive β-gal expression in islets, and to compare the sensitivity of β-gal detection between X-gal staining and immunofluorescence cytochemistry, pancreata from two simvastatin-treated litters of two transgenic males and three hemizygous females were analysed at PN30. Mice were sacrificed by cervical dislocation and their pancreata rapidly excised. As for the animals of Time-Series Two, pancreata were divided into two equal-sized portions, one of which was subjected to paraffin histology as described. The remaining portion was fixed, cryoprotected, embedded in O.C.T. and 15 μm frozen sections cut. One of each pair of adjacent serial cryosections was processed for immunofluorescence demonstration of β-gal and glucagon, counterstained in DAPI and mounted in Gelvatol. The adjacent section was X-gal-stained as described in **Section 2.3.1.**, counterstained in nuclear Fast Red and DAPI and mounted in Gelvatol.

4.2.5. Scoring Islet β-Gal$^+$/β-Gal$^-$ Cell Composition

Sections selected for analysis were spaced throughout each pancreas such that no islet was examined more than once. Specimens were examined and scored using a Leica DMRB fluorescent microscope. Histochemically-stained islets from Time-Series One were scored directly from the paraffin sections. Under × 400 magnification islets were identified using DAB staining for glucagon to highlight the islet periphery. An islet was defined as five or more contiguous glucagon-immunopositive cells. The number of β-gal$^+$ versus β-gal$^-$ cells within each islet in each section was determined. It is unknown to what extent the mixing of β-gal$^+$ and β-gal$^-$ cells in heterogeneous islets is consistent throughout their volume from a single two-dimensional (2D) section through an islet. The larger the size of the islet, the less representative will be a single 2D section of the three-dimensional (3D) volume. However, examination of a large number of sections of different islets would suggest that the cell mixing *is* consistent throughout the volume.

Images of specimens were taken with a Spot RT Color digital camera (National Diagnostics Inc.) and stored as uncompressed 24-bit TIFF images. Immunofluorescence-stained islets from Time-Series Two and the simvastatin-treated PN30 animals of Time-Series Three were scored from hard copies of merged images

following adjustment of the three colour channels using the Adobe Photoshop 6.0 package. The total number of β-gal$^+$ and β-gal$^-$ cells in each islet in each of the analysed sections was scored. Cell composition of all of the islets within the examined sections was therefore determined from a single cross-section through each islet. For Time-Series Two, the number of glucagon- and insulin-immunopositive cells colocalising with the β-gal label was also determined. X-Gal-stained islets in frozen sections from the simvastatin-treated Time-Series Three animals were identified from glucagon immunofluorescence staining in the adjacent section and images were taken under Nomarski optics. The numbers of β-gal$^+$ and β-gal$^-$ cells within each islet were scored from hard copies of images.

4.3. Results

4.3.1. Time-Series One

Cell lineage relationships in the structural units of the pancreas were first investigated by examining paraffin sections of wholemount X-gal-stained organs from PN3-365 (PN52wk) H253 animals.

4.3.1.1. Constitutive LacZ Expression in Intestinal Crypts

Wholemount X-gal staining demonstrated uniform β-gal activity in the crypts of transgenic (hemizygous) males and homozygous females and an X-inactivation mosaic of staining in the hemizygous female crypts (**Fig. 4.4.**) as was expected. This allowed female offspring from crosses between a male transgenic and female hemizygote (**Fig. 4.3.**) to be genotyped from the characteristic staining patterns.

4.3.1.2. Constitutive LacZ Expression in Islets and Ducts

Non-transgenic animals did not show any X-gal staining activity in the pancreas. We were satisfied on this basis that the staining observed in transgenic animals was attributable to β-gal expression from the *lacZ* transgene and was not a consequence of endogenous β-gal activity.

To ensure that pancreas cells constitutively expressed HMG CoA reductase-driven *lacZ*, pancreata were examined from male transgenic and female homozygous animals as a positive control for ubiquitous staining activity. Uniform X-gal staining of islets in the centre of wholemount-stained pancreata indicated a satisfactory, high penetration of the stain throughout the pancreatic tissue.

Almost uniform β-gal activity was observed in the pancreatic acini of E15.5 embryos although from PN3 onwards, β-gal activity decreased in the acinar cells (**Fig. 4.5.**). Some variability was seen in timing of the onset of this reduction such that some individuals still displayed acinar β-gal activity at PN14. However, all acinar cells in all animals examined were β-gal$^-$ from PN21. It was considered that this postnatal loss of β-gal activity in the acini was probably due to a reduced activity of the HMG CoA reductase promoter. Cell lineage analysis of the acini was therefore discontinued.

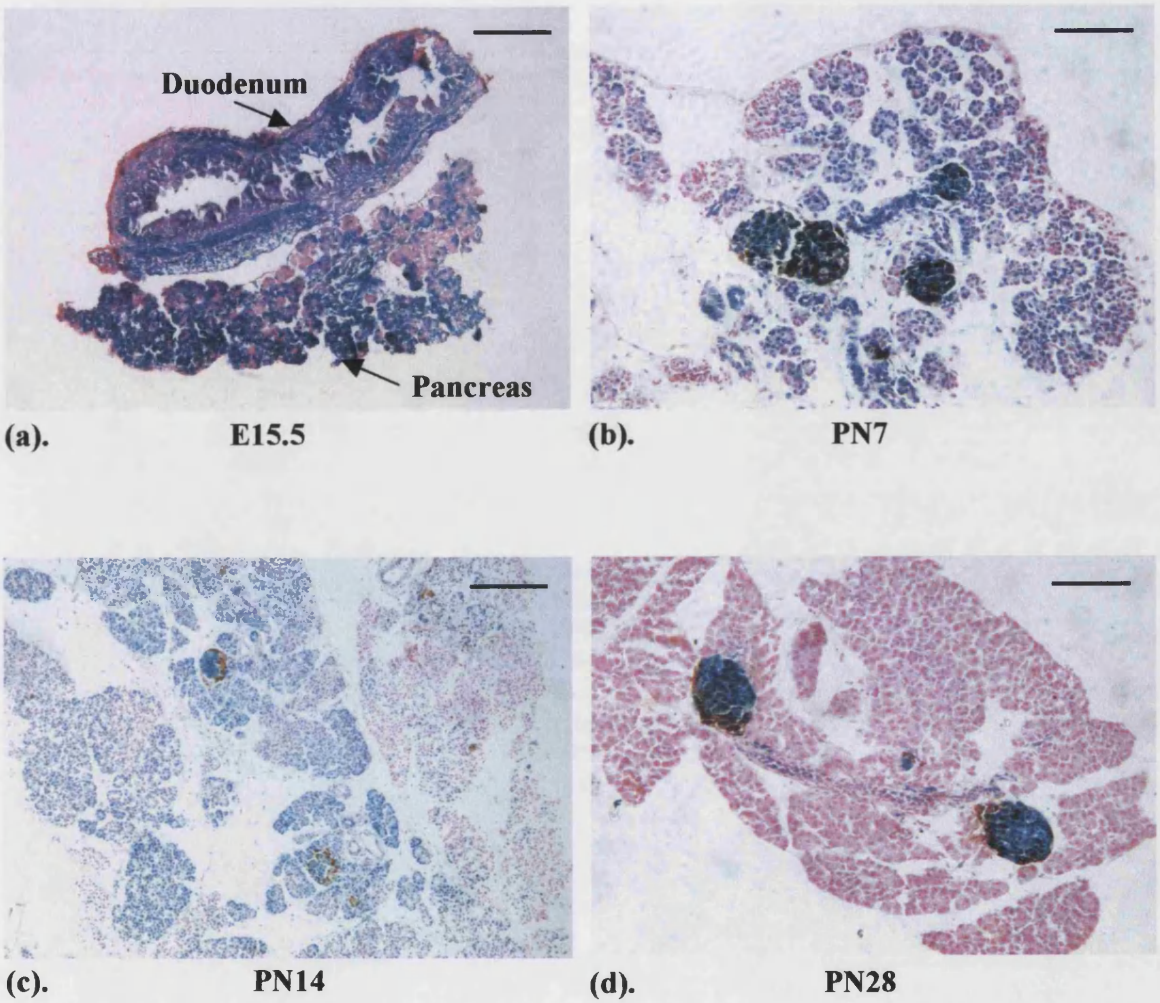

Figure 4.5. Decline in β-Gal Activity in Acinar Cells from PN3 Onwards

(a) Acini in the E15.5 embryonic pancreas showing X-gal staining for β-gal activity. (b) X-Gal staining absent in some acini in a PN7 transgenic male. (c) PN14 homozygous female showing absence of β-gal activity in some acini. (d) Complete loss of β-gal activity in the acini of a PN28 homozygous female. (b)-(d) are immunoperoxidase-stained for glucagon

(a) and (c) Bar = 200 μm; (b) and (d) Bar = 100 μm

Uniform β-gal activity was observed in all pancreatic islets and ducts of all animals under PN18wk (**Fig. 4.6.**). Low intensity X-gal staining and a complete absence of staining were seen in a number of cells in some islets of a small number of PN18wk individuals (**Fig. 4.6.**). This may also be due to promoter shutdown. Loss of endocrine cell β-gal activity in adult mice was not considered detrimental to the study however since it occurred at such a late stage in postnatal life. Testing of the hypotheses could most probably be accomplished by examining animals up to PN30, well outside the time-frame of diminishing islet β-gal activity.

4.3.1.3. Ducts Consistently Heterogeneous

At all time-points and in all female hemizygous animals examined, pancreatic ducts were consistently seen to be of a heterogeneous $\beta\text{-gal}^+/\beta\text{-gal}^-$ cell composition (**Fig. 4.7.**). No homogeneous ducts composed only of $\beta\text{-gal}^+$ cells or entirely of $\beta\text{-gal}^-$ cells were ever observed, implying that pancreatic ducts arise from multiple progenitor cells and maintain this polyclonal state throughout postnatal life.

4.3.1.4. Islet Identification

For cell lineage analysis, islets were identified by immunoperoxidase staining for glucagon or insulin, the hormone products of α- and β-cells respectively. Glucagon staining was preferred as it stains only the peripheral cells of the islet, resulting in minimal superimposition with X-gal staining. To distinguish them from isolated endocrine cells, islets were defined as *five or more contiguous glucagon-immunopositive cells.*

4.3.1.5. Neonatal Heterogeneous Islets Become Homogeneous

In the PN3-365 female hemizygous animals examined in Time-Series One, islets of all three possible conformations were observed: mixed $\beta\text{-gal}^+/\beta\text{-gal}^-$, homogeneous $\beta\text{-gal}^+$ or homogeneous $\beta\text{-gal}^-$. At the earliest neonatal time-points studied, islets were predominantly seen to be of a heterogeneous $\beta\text{-gal}^+/\beta\text{-gal}^-$ cell composition (**Fig. 4.8.**). A fine-grained mosaicism of neonatal islets was evident with widespread intermingling of unlabelled endocrine cells and labelled cells expressing the active marker. After four

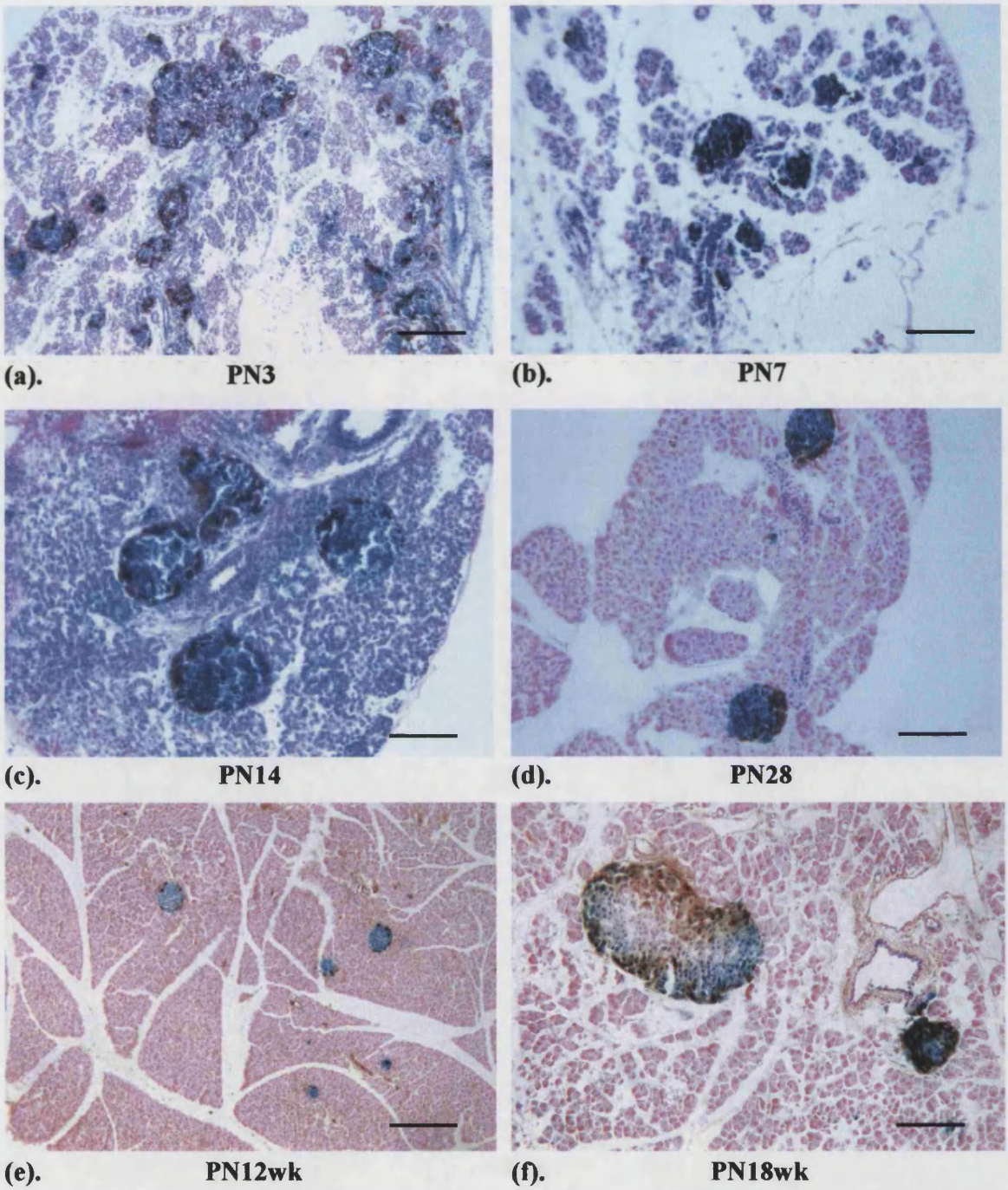

Figure 4.6. X-Gal Staining Shows β-Gal Activity is Retained in *All* Islet Cells Until PN18 Weeks

(a)-(c) and (f) Transgenic males. (d) and (e) Homozygous females. (f) Loss of β-gal activity can be seen in the islet on the left at the PN18wk time-point

All immunoperoxidase-stained for glucagon

(a) and (e) Bar = 200 μm; (b)-(d) and (f) Bar = 100 μm

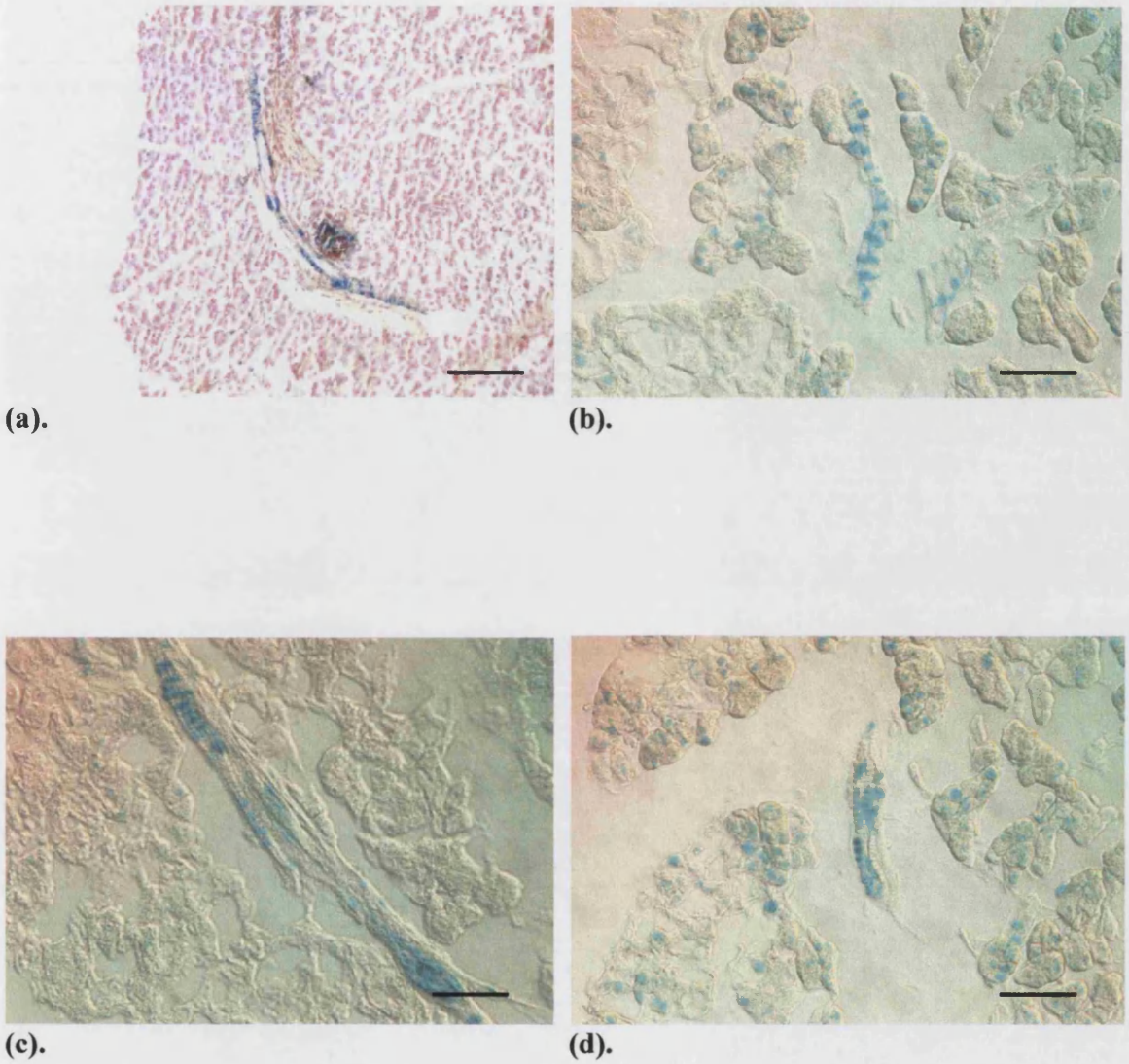

(a). **(b).**

(c). **(d).**

Figure 4.7. Pancreatic Ducts were Consistently of a Heterogeneous β-Gal$^+$/β-Gal$^-$ Cell Composition

(a) PN28 female hemizygote (Time-Series One). (b)-(d) X-Gal staining in frozen sections from simvastatin-treated PN30 female hemizygote (Time-Series Three); images collected under Nomarski optics

(a) Bar = 100 μm; (b)-(d) Bar = 50 μm

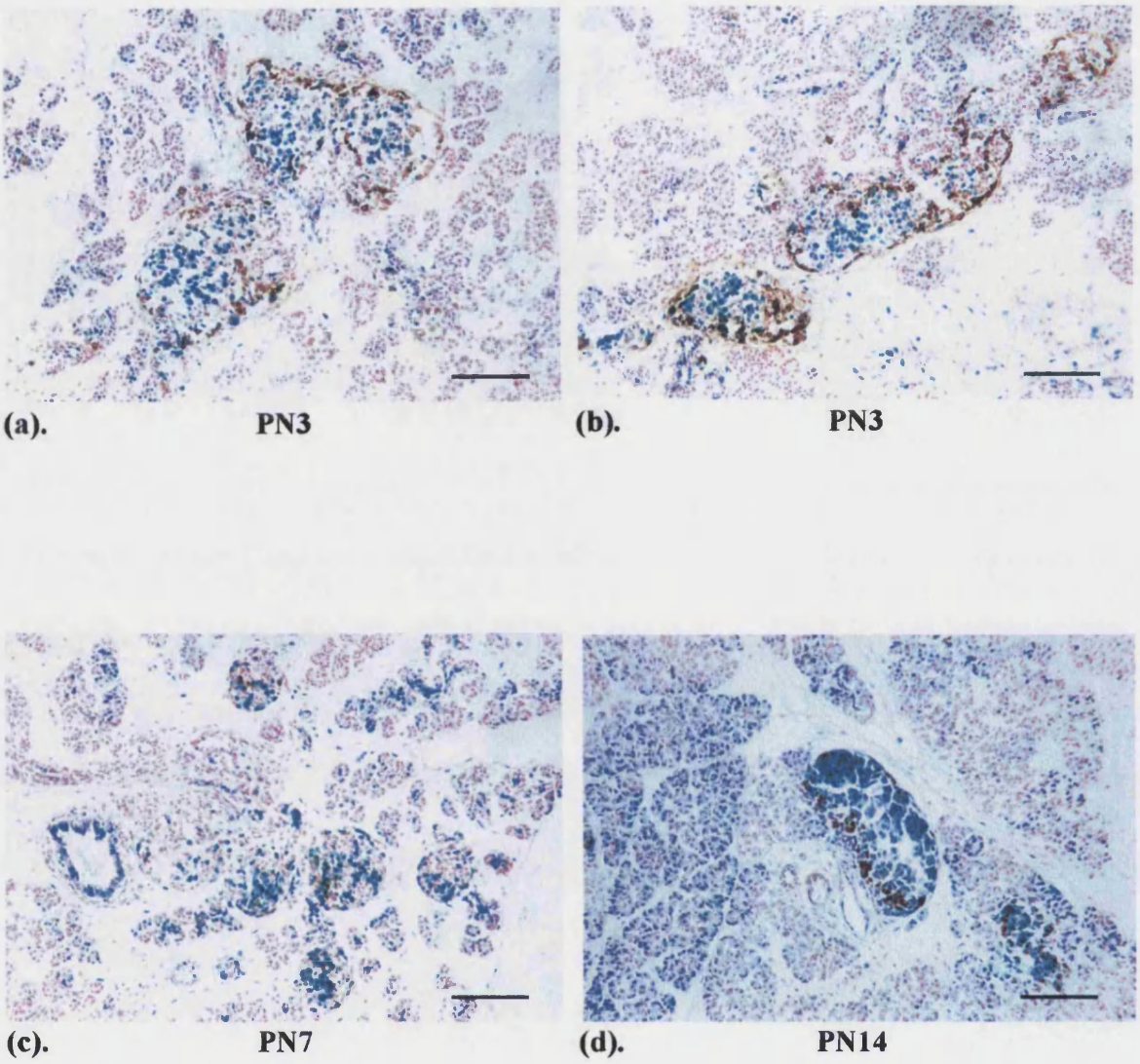

Figure 4.8. In Hemizygous Mosaic Females, Neonatal Islets are of a Heterogeneous β-Gal$^+$/β-Gal$^-$ Cell Composition but Undergo a Conversion to a Homogeneous State Comprising Cells of a Single Genotype by One Month After Birth

Heterogeneous islets in PN3 (a and b) and PN7 (c) neonates. Note fine-grained mosaicism and widespread intermingling of β-gal$^+$ and β-gal$^-$ cells. (d) Homogeneous β-gal$^+$ islets in a PN14 pancreas; note high β-gal activity in the acini in this individual All immunoperoxidase-stained for glucagon. Bar = 100 μm

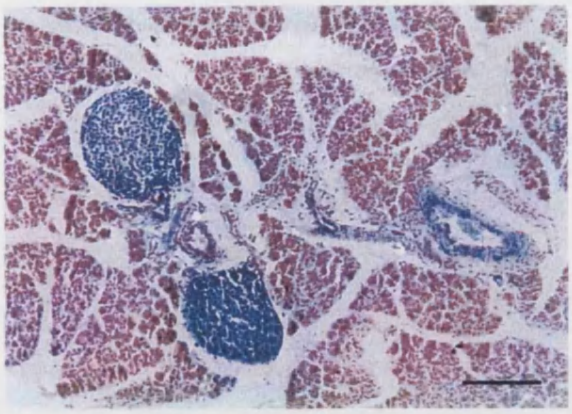

(e). PN21

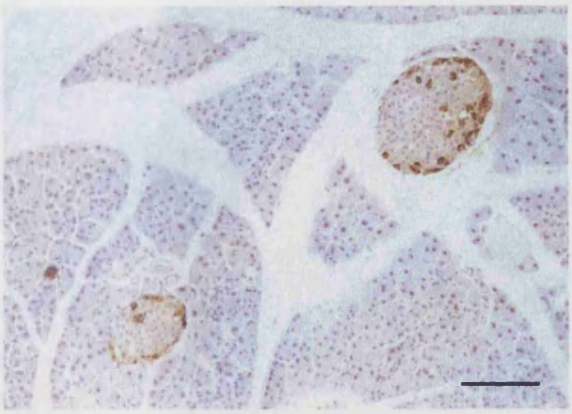

(f). PN26wk

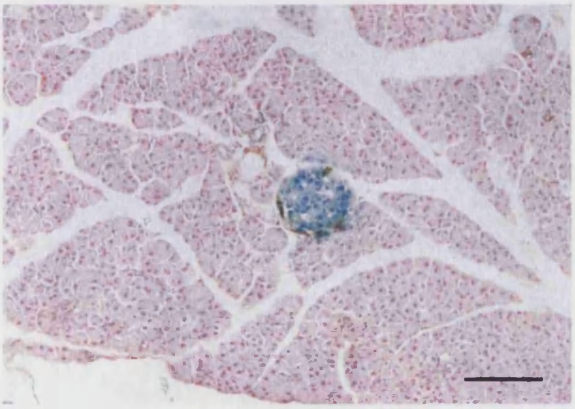

(g). PN52wk

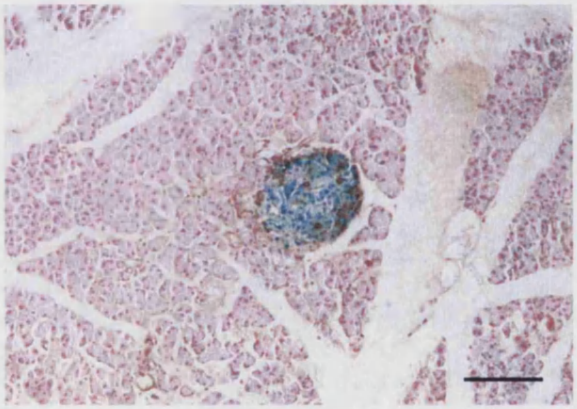

(h). PN52wk

(e) Homogeneous β-gal^{+} islets in a PN21 animal. (f) Homogeneous β-gal^{-} islets in a PN26wk animal and homogeneous β-gal^{+} islets in two PN52wk females (g and h)

(f)-(h) immunoperoxidase-stained for glucagon. Bar = 100 μm

weeks of age however, the great majority of islets were composed of cells of a single genotype. Islets were seen to be either of a homogeneous β-gal$^+$ cell composition or were composed entirely of cells not expressing the *lacZ* marker (**Fig. 4.8.**). This conversion of heterogeneous islets to a homogeneous state with age was then quantified. The final time-point examined was PN84 or PN12wk since the study of homozygous controls had indicated some loss of expression of the active marker from PN18wk onwards.

4.3.1.6. Increasing Frequency of Incidence of Homogeneous Islets with Age

The incidence of homogeneous islets amongst a sample of the total islet population was found to increase rapidly in the neonatal period (**Table 4.1.** and **Graph 4.1.**). Islets were predominantly mixed at PN3, with fewer than 2 % of the islet sample being homogeneous. Between one and three weeks, the greatest rate of conversion to homogeneity was occurring so that at PN14, 42.6 % of islets were of a single genotype and by PN21, almost 95 % were homogeneous. The same Time-Series One islet sample was then subjected to further analysis as described in this chapter and in **Chapter 5**.

Table 4.1. Increasing Frequency of Homogeneous Islets with Age

Age (Days PN)	Homogeneous Islet Frequency (% of Total Sample)	Islet Sample Size, *n*
3	1.79 ± 1.43	55
7	0.96 ± 0.961	95
14	42.6 ± 14.5	57
21	93.4 ± 6.67	26
28	92.9 ± 7.14	58
84	95.9 ± 4.17	26

4.3.1.6.1. Prevalence of Homogeneous β-Gal$^+$ Islets Over Unlabelled Islets

Overall examination revealed homogeneous islets to more frequently be composed of cells of the labelled genotype than to be homogeneously β-gal$^-$ (**Table 4.2.** and **Graph 4.2.**). This selective effect was evident at all time-points studied. The direction of selection varied between individual animals however. In a minority of

Graph 4.1. Increase in Frequency of Homogeneous Islets with Age

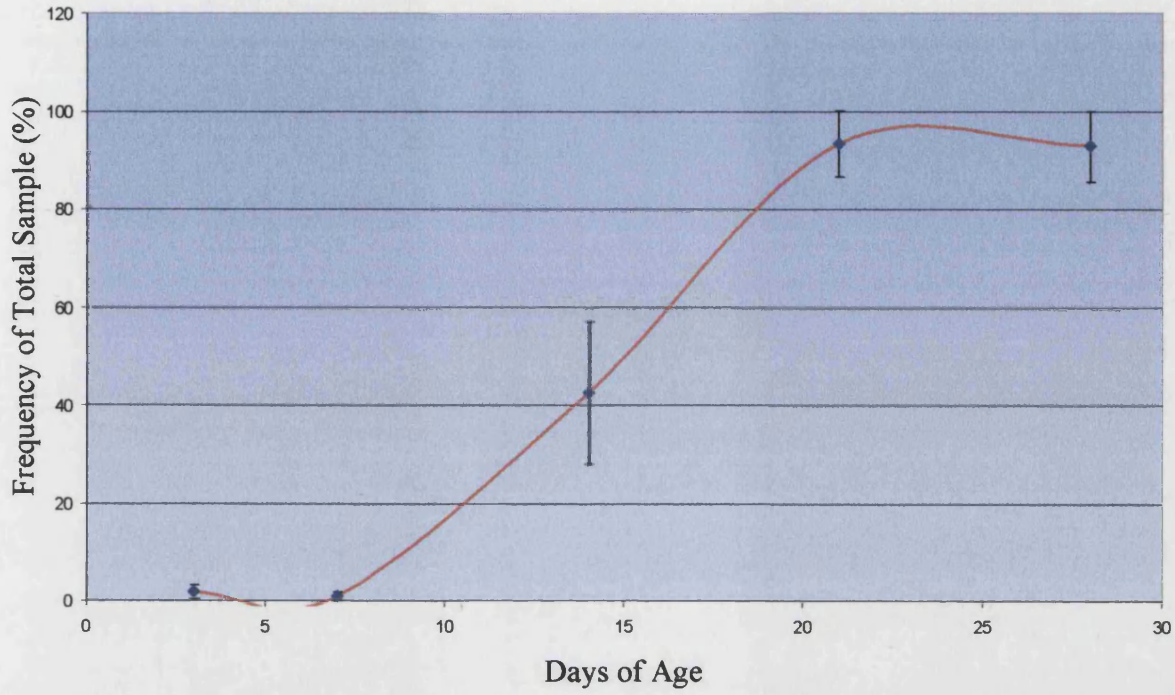

Graph 4.2. Homogeneous Islets Exhibit a Tendency to be β-Gal$^+$

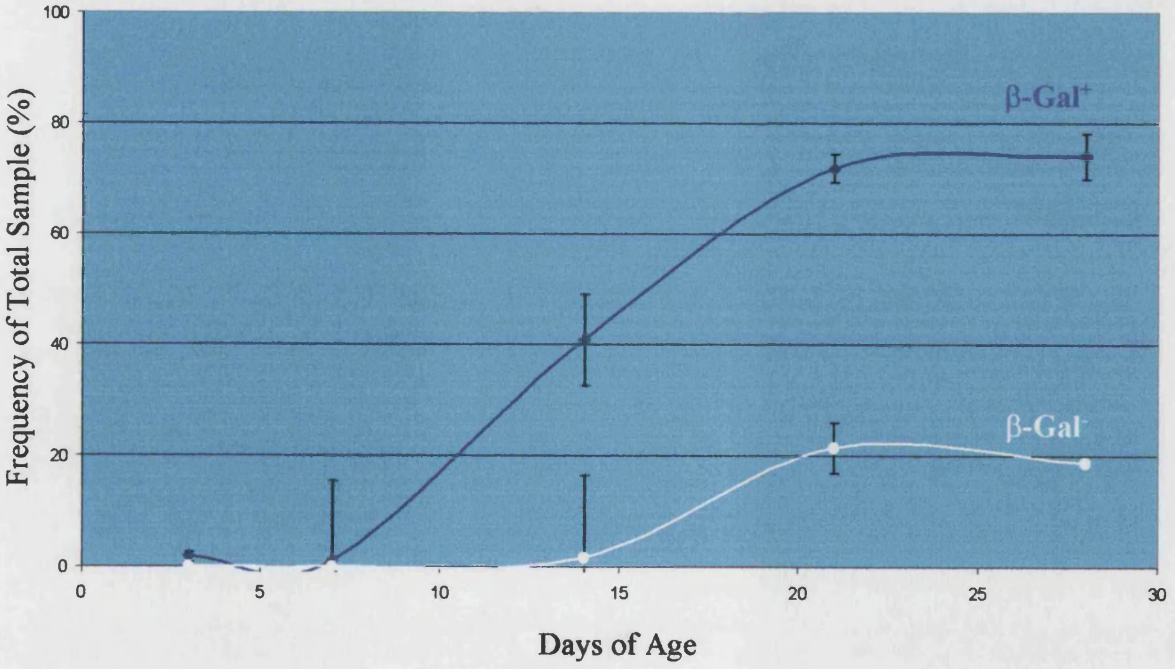

pancreata examined, homogeneous islets exhibited a tendency to be composed of unlabelled cells.

Table 4.2. Selective Effect Towards β-Gal$^+$ Over β-Gal$^-$ Homogeneous Islets

Age (Days PN)	Homogeneous Islet Frequency (% of Total Sample)		Islet Sample Size, *n*
	β-Gal$^+$	β-Gal$^-$	
3	1.79 ± 0.961	0 ± 0	55
7	0.96 ± 14.5	0 ± 1.11	95
14	40.8 ± 8.18	1.67 ± 14.8	57
21	71.8 ± 2.62	21.5 ± 14.8	26
28	74.0 ± 4.17	18.8 ± 0	58
84	95.8 ± 19.1	0 ± 18.0	26

To verify the divergence in the observed ratios of the homogeneous β-gal$^+$ to homogeneous unlabelled islets from the expected 1:1 distribution, a chi-square (χ^2) test was conducted. The proportion of homogeneous islets of each genotype as a percentage of the total sample was calculated for each time-point (**Table 4.3.**). On account of the formula:

$$\chi^2 = \sum \frac{(\text{Observed} - \text{Expected})^2}{\text{Expected}} \qquad \text{with } df = c \text{ (number of categories)} - 1$$

for the situation here in which there are only two categories, the expression

$$\frac{(\text{Observed} - \text{Expected})^2}{\text{Expected}}$$

is the same value for each category as each of the two observed percentages deviate from the expected 50 % frequency by the same value. χ^2 was therefore calculated simply by determining the square of the deviation divided by the expected 50 (%) and then multiplying this figure by two. In this manner, χ^2 was calculated for each islet sample at each time-point (**Table 4.3.**).

Table 4.3. Calculating χ^2 to Test Whether the Observed Ratio of Homogeneous β-Gal$^+$ to β-Gal$^-$ Islets Deviates Significantly from the Expected 1:1 Distribution

Age (Days PN)	Observed Distribution of Homogeneous Islets by Genotype (% of Total)		Observed (O) - Expected (E; 50 %) (Disregarding Sign)	$2\ \frac{(O-E)^2}{E} = \chi^2$
	β-Gal$^+$	β-Gal$^-$		
3	100	0	50	100
7	100	0	50	100
14	96.1	3.93	46.1	84.9
21	77.0	23.0	27.0	29.1
28	79.7	20.3	29.7	35.4
84	100	0	50	100

$\chi^2 = 6.64$, $df = 1$, $p = 0.01$. As all of the calculated values of χ^2 are greater, the null hypothesis can be rejected. The observed frequency distribution of homogeneous β-gal$^+$ to β-gal$^-$ islets therefore deviates significantly from the expected 1:1 distribution, indicating a significant bias towards homogeneous labelled islets over unlabelled ones. The existence of this effect means that the expression of the β-gal enzyme itself may exert an effect on the relative survival of stem cells, and so not be a truly neutral marker. Alternatively, the observed bias towards homogeneous β-gal$^+$ islets may be a consequence of the genetic background of the animals examined.

4.3.1.7. Increasing Homogeneity of Islets with Age

The disadvantage of expressing the conversion from heterogeneous to homogeneous islets in terms of the frequency of homogeneous islets is that no distinction is made between heterogeneous islets that are mixed to different extents. At the extreme of its definition a heterogeneous islet can contain a single cell of the less predominant genotype. For example, an islet that is composed of 90 β-gal$^+$ cells and 10 β-gal$^-$ cells is less heterogeneous than an islet composed equally of β-gal$^+$ and β-gal$^-$ cells. So, an index of the extent of homogeneity was devised. By definition, the "percentage homogeneity" of an islet is a measure of the extent of clonal purification of the islet and is calculated as: (number of cells of the prevailing genotype/total number of cells) × 100 (**Fig. 4.9.**). This figure therefore ranges between 50 % and 100 %. The mean index of homogeneity for all islets at a given time-point calculated in this manner

Figure 4.9. Calculating Islet-Weighted and Cell-Weighted Percentage Islet Homogeneity of β-Gal$^+$/β-Gal$^-$ Cell Composition

(a).

$$\text{Mean islet-weighted \% islet homogeneity} = \frac{(78.9 + 59.5 + 100 + 57.1 + 73.7)}{5}$$

$$= 73.8\,\%$$

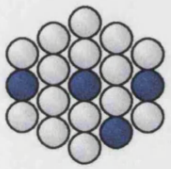

$$\frac{15\ \beta\text{-gal}^-\ \text{cells}}{19\ \text{cells total}} \times 100$$

$$= 78.9\,\%\ \text{homogeneity}$$

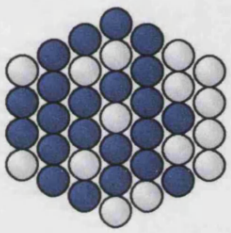

$$\frac{22\ \beta\text{-gal}^+\ \text{cells}}{37\ \text{cells total}} \times 100$$

$$= 59.5\,\%\ \text{homogeneity}$$

$$\frac{7\ \beta\text{-gal}^+\ \text{cells}}{7\ \text{cells total}} \times 100$$

$$= 100\,\%\ \text{homogeneity}$$

$$\frac{4\ \beta\text{-gal}^+\ \text{cells}}{7\ \text{cells total}} \times 100$$

$$= 57.1\,\%\ \text{homogeneity}$$

$$\frac{14\ \beta\text{-gal}^-\ \text{cells}}{19\ \text{cells total}} \times 100$$

$$= 73.7\,\%\ \text{homogeneity}$$

(b).

$$\text{Mean cell-weighted \% islet homogeneity} = \frac{15 + 22 + 7 + 4 + 14}{19 + 37 + 7 + 7 + 19} \frac{(\Sigma\ \text{of cells of predominant genotype})}{(\Sigma\ \text{of total cells in all islets})} \times 100$$

$$= 69.7\,\%$$

is independent of islet size. Equal weighting is given to islets of different sizes. Hence, this figure was termed the "Islet-weighted percentage homogeneity"

The islet-weighted percentage homogeneity of islets was seen to increase with age from 69.3 % at PN3 to in excess of 98 % by PN21 (**Table 4.4.** and **Graph 4.3.**). Again, the maximum rate of conversion to the homogeneous state occurred between one and three weeks after birth.

Table 4.4. Increasing Islet-Weighted Homogeneity of Islets with Age

Age (Days PN)	Islet-Weighted Percentage Islet Homogeneity (%)	Islet Sample Size, *n*
3	69.3 ± 2.76	55
7	61.5 ± 2.20	95
14	82.4 ± 5.34	57
21	98.9 ± 1.11	26
28	98.2 ± 1.83	58
184	99.4 ± 0.650	26

4.3.1.8. Rate of Heterogeneous-Homogeneous Conversion is Independent of Islet Size

It might be expected that the smaller the size of the islet and the fewer the number of cells, the greater the rate with which homogeneity is attained. However, islet-weighted percentage homogeneity as mentioned above, assigns equal weighting to islets of different sizes and so cannot be used to test this hypothesis. Instead, any effect of islet size on the rate of conversion to homogeneity can be inferred by comparing islet-weighted homogeneity with a similar, cell-weighted index of homogeneity. "Cell-weighted percentage homogeneity" *is* dependent on islet size and is calculated as: (sum of the number of cells of the prevailing genotype in each islet for *all* islets of sample/total number of cells of all islets in sample) × 100 (**Fig. 4.9.**).

The cell-weighted percentage homogeneity of islets at each time-point was very similar to the islet-weighted homogeneity figure (**Table 4.5.** and **Graph 4.4.**), increasing with age from 68.4 % at PN3 to 98.6 % by PN28, with the greatest rate of conversion being between one and three weeks of postnatal life. This close similarity between the islet-weighted and cell-weighted data implied that islet size exerted a limited effect on the rate with which cell homogeneity was achieved.

Graph 4.3. Increase in Islet-Weighted Percentage Islet Homogeneity with Age

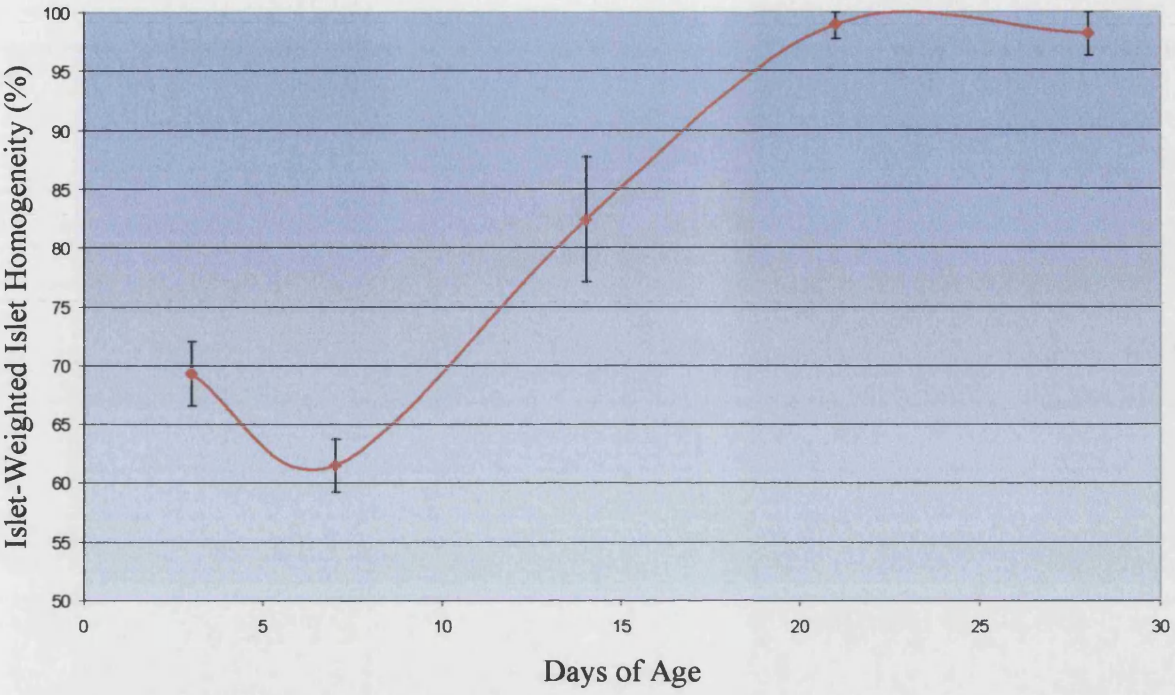

Graph 4.4. Islet-Weighted and Cell-Weighted Islet Homogeneity with Age are Very Similar

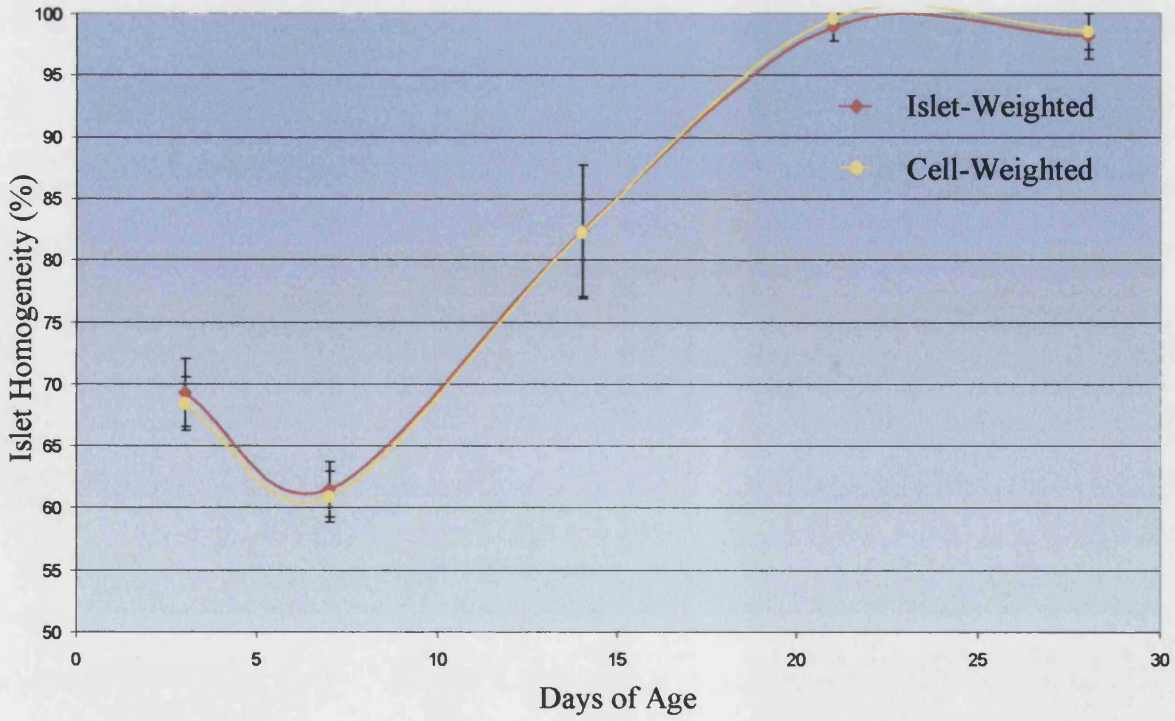

Table 4.5. Increasing Cell-Weighted Homogeneity of Islets with Age

Age (Days PN)	Cell-Weighted Percentage Islet Homogeneity (%)	Islet Sample Size, *n*
3	68.4 ± 2.13	55
7	60.9 ± 2.07	95
14	82.3 ± 5.38	57
21	96.8 ± 0.386	26
28	98.6 ± 1.44	58
184	99.4 ± 0.600	26

To confirm this finding, the islet-weighted percentage homogeneity data was segregated according to islet size (**Table 4.6.**). No significant effect of islet size class on rate of conversion to homogeneity was seen.

Table 4.6. Islet-Weighted Homogeneity of Islets Segregated by Size with Age

Islet Size (Cell No.)	Islet-Weighted Percentage Islet Homogeneity (%)				
	PN3	PN7	PN14	PN21	PN28
0-50	67.6	63.2	82.0	99.5	99.6
51-100	69.2	59.5	80.5	89.2	89.1
101-150	74.0	60.0	83.0	100	100
151-200	64.1	62.1	78.2	100	100
201-250	68.8	61.8	73.5	100	--
251-300	62.8	57.5	--	100	100
301-350	66.8	55.5	90.5	--	--
351-400	--	67.7	--	--	100
401-450	--	--	--	100	100
451-500	--	--	--	100	--

4.3.1.9. Islet Size Does Not Increase Neonatally

Islet size was investigated to determine whether the islets are increasing in cell number as they are undergoing the heterogeneous-homogeneous conversion. No significant increase in mean islet cross-sectional area was seen during the first four weeks of postnatal life when the conversion is occurring (**Table 4.7.**).

Table 4.7. Islet Size Does Not Increase Significantly Over PN3-28

Age (Days PN)	Islet Size (Cell Number)	Islet Sample Size, *n*
3	92 ± 3.45	55
7	85 ± 14.4	95
14	81 ± 19.8	57
21	103 ± 17.7	26
28	69 ± 0	58

4.3.2. Time-Series Two

Having obtained preliminary evidence for a conversion to homogeneity of heterogeneous islets, the decision was made to investigate the cell lineage of the different endocrine cell types using immunofluorescence cytochemistry in conjunction with an anti-β-gal antibody (rabbit polyclonal; Molecular Probes A-11132). This would permit colocalisation of β-gal with the endocrine markers glucagon and insulin with a high degree of resolution. Immunofluorescence does not suffer from the same problem as immunohistochemistry where one chromogen can mask another when stain superposition occurs.

Immunofluorescence staining of paraffin sections for β-gal proved to be unsuccessful despite successful demonstration of the endocrine markers. Frozen sections were instead prepared and proved highly amenable to β-gal staining using an appropriate fluorescein-conjugated secondary antibody (**Fig. 4.10.**); the fluorescence signal was clearly nuclear-localised within the H253 islet cells as expected. Once single immunofluorescence staining for β-gal was successfully accomplished, double-staining with either the anti-glucagon or anti-insulin antibodies (demonstrated with Texas Red and TRITC respectively) was conducted. The numbers of β-gal-labelled and unlabelled glucagon- or insulin-immunopositive islet cells were then determined from a second time-series of H253 female hemizygote animals at PN5, PN10, PN15, PN20, PN25 and PN30 (*n* or number of animals examined = 5 per time-point).

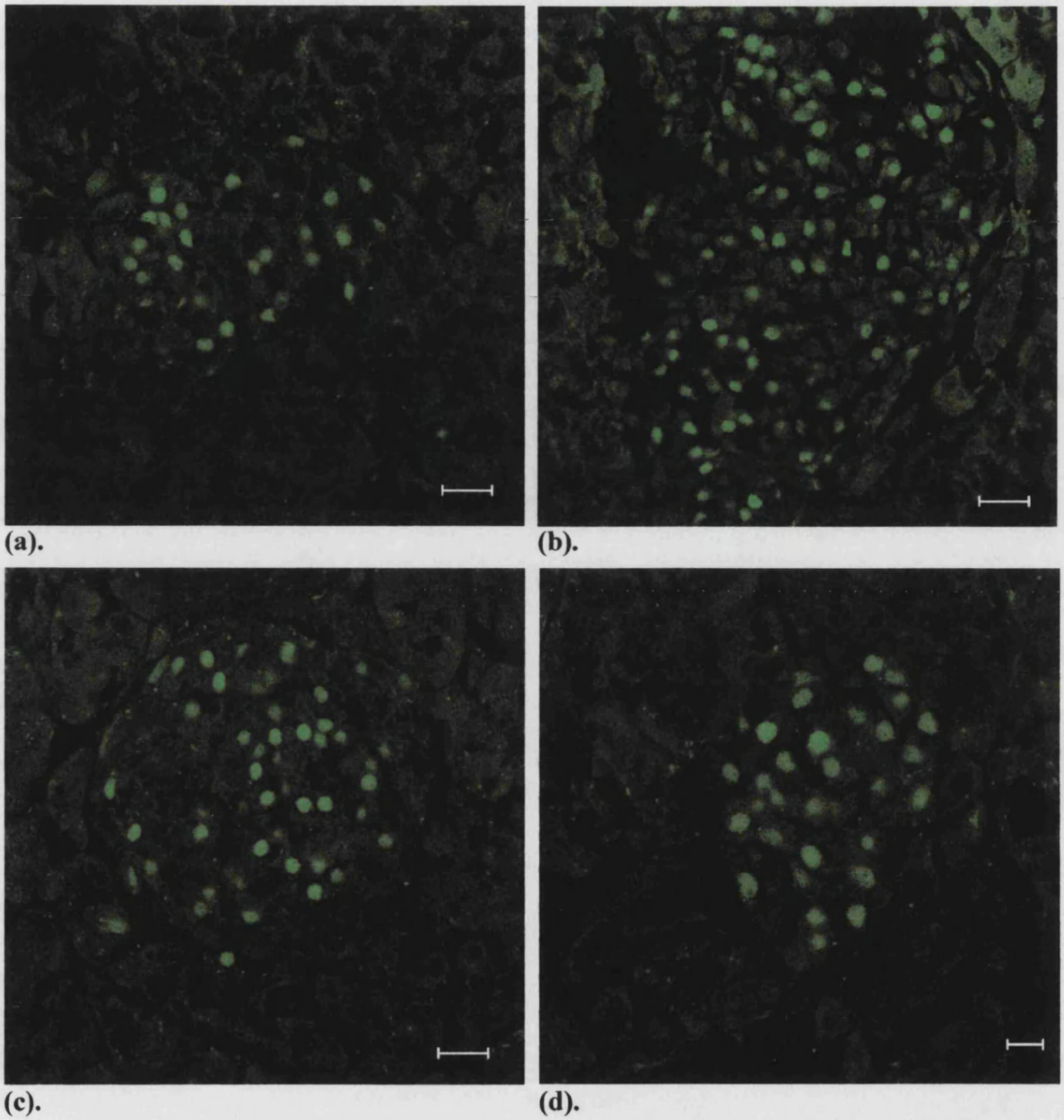

Figure 4.10. Immunofluorescence Demonstration of β-Gal in Islets of a PN10 Month H253 Female in 15 μm Frozen Sections

Images collected on a Zeiss LSM510 confocal microscope

(a)-(c) Bar = 20 μm; (d) Bar = 10 μm

4.3.2.1. High Resolution Detection of Colocalisation

Using immunofluorescence analysis, colocalisation of the β-gal label with the endocrine markers could be detected with a high degree of resolution. Furthermore, because the β-gal label is nuclear while the hormones exhibit a cytoplasmic distribution, it was possible to prepare two-colour superposed images in which there is virtually no overlap of the two signals (**Fig. 4.11.**).

4.3.2.2. No Evidence for Heterogeneous-Homogeneous Conversion from Immunofluorescence Analysis: Reduced Endocrine β-Gal Production?

In the PN5, PN10, PN25 and PN30 female hemizygous animals examined, the samples of α- and β-cell populations in individual islets appearing in section were predominantly recorded as being of a heterogeneous β-gal$^+$/β-gal$^-$ cell composition (**Table 4.8.**). PN15 and PN20 islets were therefore not examined. Islets as a whole appeared to be heterogeneously composed of cells of both genotypes. Homogeneous unlabelled α- and β-cell populations were seen with varying frequency (5.71 % to 42.8 % of the total islet cell population sample) at each time-point, some of these populations comprising almost 100 cells (98, 95 and 90 cells). In contrast, only one of the 394 α-cell populations and two of the 395 β-cell populations analysed were β-gal$^+$ homogeneous, these being three of the smallest cell populations assessed (8 cells and 5 and 6 cells in size respectively).

To verify the divergence in the observed ratios of the homogeneous β-gal$^-$ to homogeneous β-gal-labelled islet cell populations from the expected 1:1 distribution, a chi-square (χ^2) test was conducted as described in **Section 4.3.1.6.1.** above. The proportion of homogeneous α- or β-cell populations of each genotype as a percentage of the total number of homogeneous cell populations was calculated and χ^2 calculated for each time-point (**Table 4.9.**).

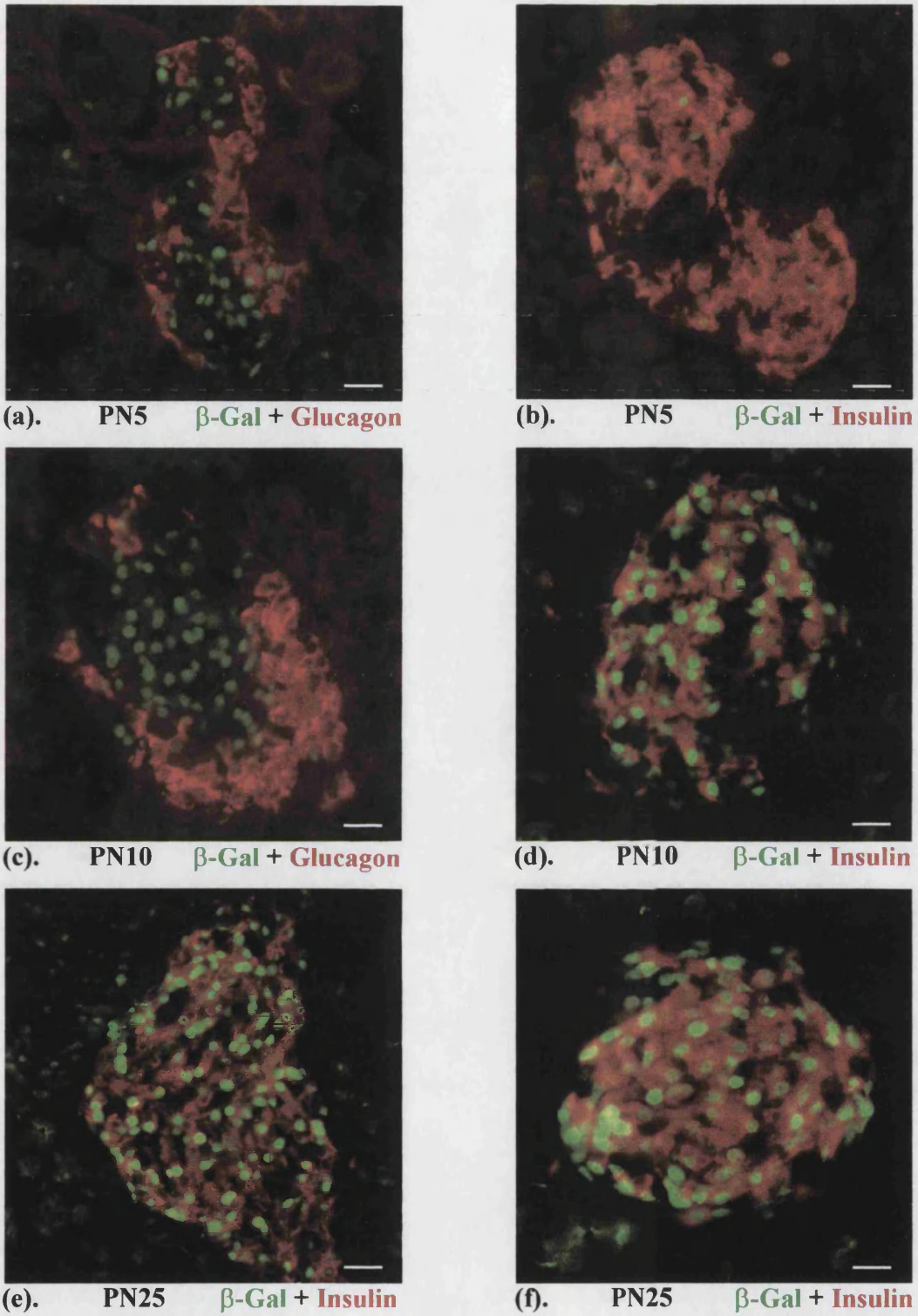

Figure 4.11. *No* Obvious Conversion from Heterogeneity to Homogeneity was Observed in Mosaic Females of Time-Series Two for which β-Gal was Detected by Immunofluorescence Cytochemistry

Double-labelling for β-gal (fluorescein) and glucagon (Texas Red) (a and c) *or* β-gal (fluorescein) and insulin (TRITC) (b and d-f). Bar = 20 μm

Table 4.8. Immunofluorescence Analysis Showed No Obvious Increase in the Homogeneity of Glucagon- or Insulin-Producing α- and β-Cell Populations Respectively Over the Neonatal Period

Hormone-Producing Islet Cell Population	Age (Days PN)	Homogeneous Cell Population Frequency (% of Total Sample)		Percentage Cell Population Homogeneity (%)		Predominant Genotype (% of Total Islet Cell Population Sample)			Islet Cell Population Sample Size, *n*
		β-Gal$^+$	β-Gal$^-$	Islet-Weighted	Cell-Weighted	β-Gal$^+$	β-Gal$^-$	1:1 β-Gal$^{+:-}$	
Glucagon	5	0	23.1	86.0 ± 4.46	87.4 ± 4.38	7.69	91.0	1.28	78
Insulin		0	22.2	84.4 ± 2.66	86.8 ± 1.80	8.89	91.1	0	45
Glucagon	10	0.690	42.8	92.6 ± 1.63	93.1 ± 1.34	2.07	97.9	0	145
Insulin		1.16	14.5	77.0 ± 2.22	72.4 ± 2.52	15.1	82.0	2.91	172
Glucagon	25	0	15.2	81.7 ± 2.38	79.9 ± 2.73	10.6	89.4	0	66
Insulin		0	15.9	74.2 ± 3.80	71.7 ± 4.19	24.6	75.4	0	69
Glucagon	30	0	5.71	68.7 ± 1.31	65.1 ± 2.91	14.3	80.0	5.71	105
Insulin		0	23.9	82.0 ± 3.41	73.0 ± 0.559	1.83	98.2	0	109

Table 4.9. Calculating χ^2 to Test Whether the Observed Ratio of Homogeneous β-Gal$^-$ to β-Gal$^+$ α- and β-Cell Populations Deviates Significantly from the Expected 1:1 Distribution

Hormone-Producing Islet Cell Population	Age (Days PN)	Observed Distribution of Homogeneous Cell Populations by Genotype (% of Total)		Observed (O) - Expected (E; 50 %) (disregarding sign)	$2\ \frac{(O-E)^2}{E} = \chi^2$
		β-Gal$^+$	β-Gal$^-$		
Glucagon	5	0	100	50	100
Insulin		0	100	50	100
Glucagon	10	1.59	98.4	48.4	93.8
Insulin		7.41	92.6	42.6	72.6
Glucagon	25	0	100	50	100
Insulin		0	100	50	100
Glucagon	30	0	100	50	100
Insulin		0	100	50	100

$\chi^2 = 6.64$, $df = 1$, $p = 0.01$. As all of the calculated values of χ^2 are greater, the null hypothesis can be rejected. The observed frequency distribution of the homogeneous β-gal$^-$ to β-gal$^+$ islet cell populations therefore deviates significantly from the expected 1:1 distribution, indicating a significant bias towards unlabelled α- and β-cell populations over β-gal$^+$ ones.

Similarly to the above, the frequency of predominantly β-gal$^-$ islet cell populations was consistently greater than the frequency of predominantly β-gal-labelled populations at all time-points (**Table 4.8.**). Predominantly β-gal$^-$ α- or β-cell populations outnumbered those cell populations composed mostly of β-gal-labelled cells by a factor of between 3.07 and 53.7 depending upon the sample. Although great variation in the degree of homogeneity was seen amongst the mixed β-gal$^+$/β-gal$^-$ populations, no trend towards homogeneity with age was evident. Furthermore, a great variability was observed in the level of β-gal fluorescence signal in cells within the same islet expressing the active marker. The data was consequently not at all consistent with that obtained from the first time-series assessed by X-gal staining (**Graph 4.5.**). One feature of this data was a considerable variability in the intensity of β-gal staining between cells. Another was the preponderance of unlabelled cells. It was considered that the deviation from the findings of Time-Series One might be due to the fact that β-gal

Graph 4.5. Percentage Islet Homogeneity with Age: Data from Immunofluorescence Cytochemistry (IF) is Inconsistent with Results from X-Gal Histochemistry (X-Gal)

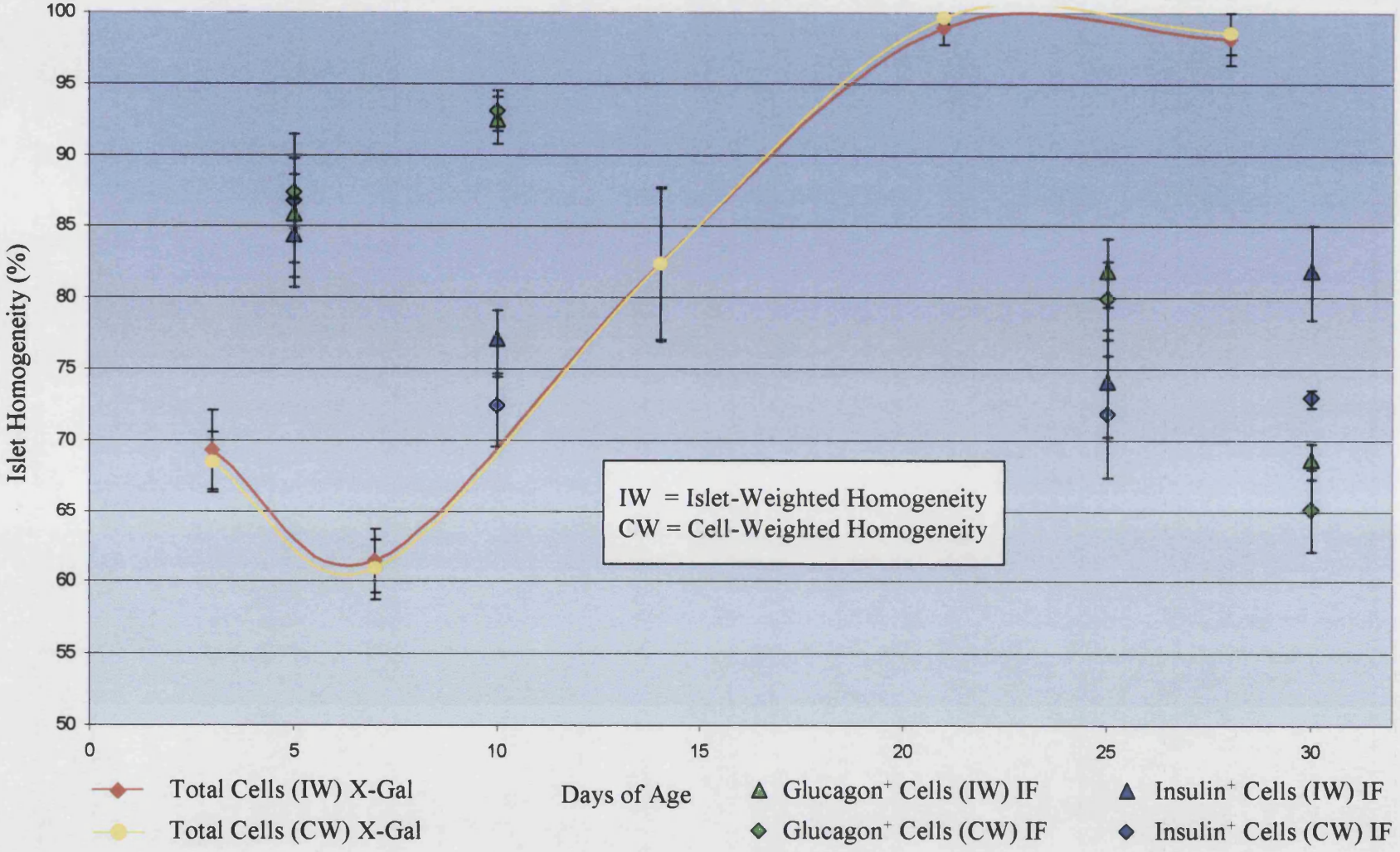

immunostaining is less sensitive than histochemical X-gal staining and does not detect *all* positive cells.

4.3.3. Simvastatin-Treated PN30 Animals

In an attempt to decrease the variability of β-gal expression in islet cells and to elevate the overall production of β-galactosidase in cells retaining the active marker, simvastatin was administered to a third and final group of animals. Simvastatin lowers cholesterol, a negative inhibitor of HMG CoA reductase (Goldstein and Brown, 1990), resulting in increased transcription of HMG CoA reductase mRNA. During the course of this work it was shown that in H253 mice this leads to an increase in expression of the *lacZ* gene driven by the HMG CoA reductase promoter (Stone *et al.*, 2002).

As in Time-Series One, *overall* islet clonality was assessed in sections. Adjacent serial 15 μm frozen sections were stained independently for β-gal activity either histochemically with X-gal or by immunofluorescence cytochemistry so that detection sensitivity could be compared. In the latter case, sections were double-stained as in Time-Series Two for β-gal and glucagon. Islets were identified by fluorescence labelling of glucagon-immunopositive cells and numbers of β-gal$^+$ and β-gal$^-$ islet cells determined. The same islet was identified in the adjacent frozen section and the numbers of labelled and unlabelled cells as revealed by X-gal staining were counted. Owing to time constraints, islets were examined from just three H253 female hemizygotes at a single PN30 time-point. The ubiquity of constitutive expression of the HMG CoA reductase-driven *lacZ* in the islet cells of simvastatin-treated animals was assessed in two H253 male transgenic pancreata.

4.3.3.1. Constitutive LacZ Expression in Islets Revealed by Histochemical Detection but Not by Immunofluorescence Analysis

Uniform β-gal activity as assayed by X-gal staining was observed in islets of the two H253 transgenic males (**Fig. 4.12.**). Of the 2803 islet cells of the 28 islets counted in the two animals, X-gal staining was not evident in only 11 cells restricted to just two of these islets; 99.6 % of the islet cells were determined to be β-gal$^+$ by histochemical detection of β-gal activity. By comparison, of the 1853 cells of the same 28 islets double-stained for β-gal and glucagon, only 1516 cells (81.8 %) were revealed to be β-

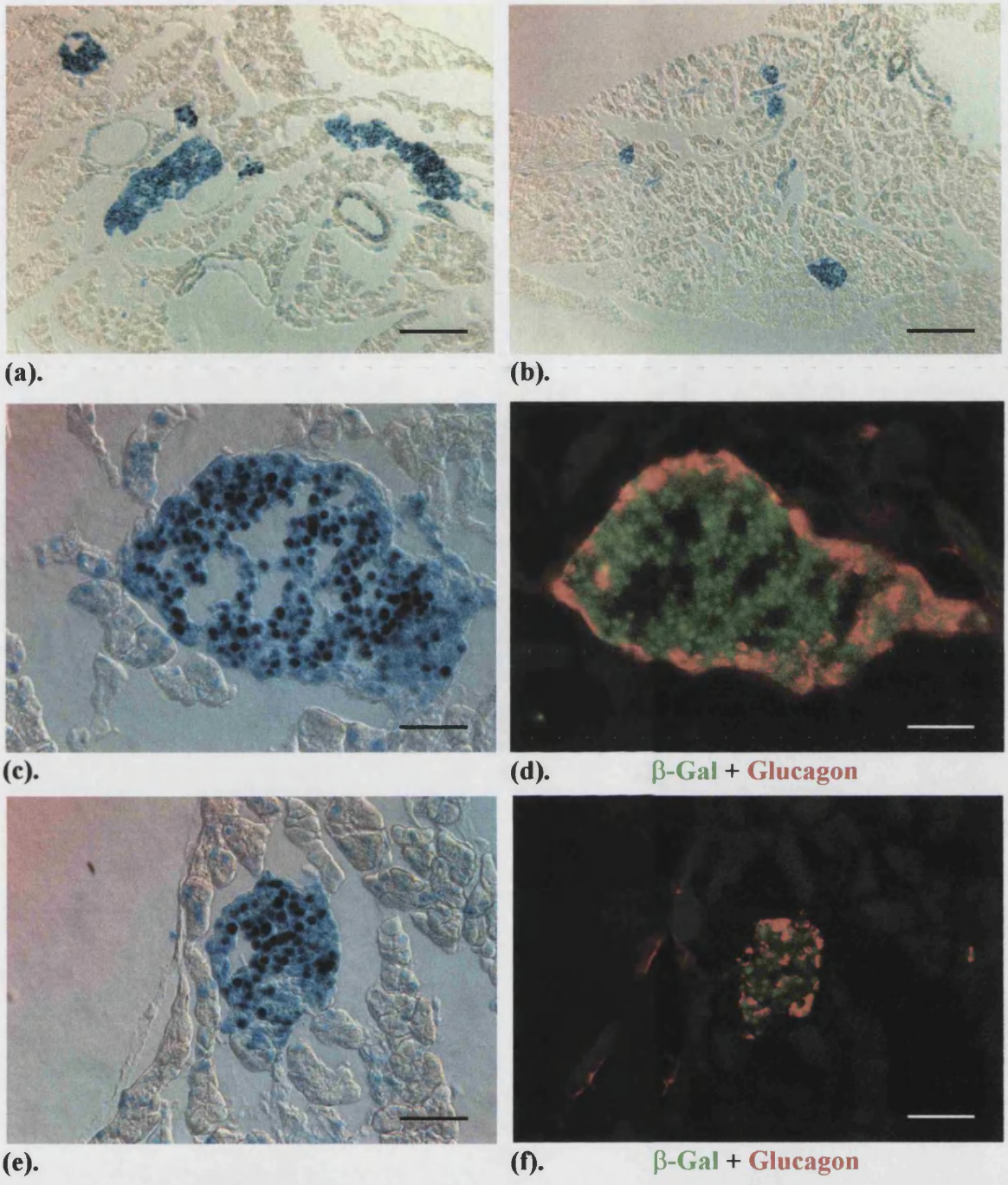

Figure 4.12. X-Gal Staining Shows β-Gal Activity is Effectively Uniform Across All Islets in PN30 Simvastatin-Treated Transgenic Males but Immunofluorescence Analysis Reveals that Islet-Weighted Islet Homogeneity in the Same Islets is Only 80.5 %

(a)-(b) Uniform X-gal staining in all islets (× 100). (c)-(f) X-Gal staining and double-labelling for β-gal (fluorescein) and glucagon (Texas Red) in adjacent frozen sections through the same islet. (a)-(c) and (e) Images collected under Nomarski optics

(a)-(b) Bar = 200 μm; (c)-(f) Bar = 50 μm

gal-immunopositive by immunofluorescence detection (**Fig. 4.12.**). Three of the 28 islets were recorded as being of a homogeneous β-gal$^+$ cell composition by immunofluorescence detection. Mean islet-weighted and cell-weighted islet homogeneity were determined to be 99.5 % and 99.6 % respectively as determined by X-gal histochemistry but 80.5 % and 80.6 % respectively as revealed by immunofluorescence analysis (**Table 4.10.**). So, the mean difference in islet-weighted islet homogeneity recorded from the same islets using the two methods was 20.8 %. This apparent difference in sensitivity of β-gal detection between histochemical X-gal staining and immunofluorescence analysis therefore caused differences in the values for cell-weighted and islet-weighted homogeneity calculated for the same set of islets but derived from the two different staining techniques.

Table 4.10. Disparity in Detection of β-Gal in Islets of H253 Transgenic Males by Histochemical Staining *vs.* Immunofluorescence Analysis

METHOD OF β-GAL DETECTION	ISLET HOMOGENEITY (%)	
	Islet-Weighted	Cell-Weighted
X-Gal	99.5 ± 0.071	99.6 ± 0.255
Immunofluorescence	80.5 ± 3.94	80.6 ± 6.16

As the greater values for islet homogeneity given by the two detection methods (namely those obtained from X-gal staining) were so near to 100 %, it was decided that simvastatin-enhanced islet β-gal expression could be considered uniformly constitutive to all intents and purposes. Isolated groups of acinar cells were also seen to stain for β-gal activity with X-gal (**Fig. 4.13.**) though were never detected by immunofluorescence analysis.

4.3.3.2. Homogeneity of Islets in Mosaic Females is Approximately 75 %

The majority of the 37 islets analysed in the three PN30 H253 female hemizygotes appeared to be of a heterogeneous β-gal$^+$/β-gal$^-$ cell composition although three small (< 40 cells) homogeneous β-gal$^+$ islets were observed (**Fig. 4.14.**). There appeared to be some individual variation in the extent of islet homogeneity amongst the three experimental animals. Mean islet-weighted and cell-weighted islet homogeneity were determined to be 76.0 % and 74.9 % respectively as determined by X-gal

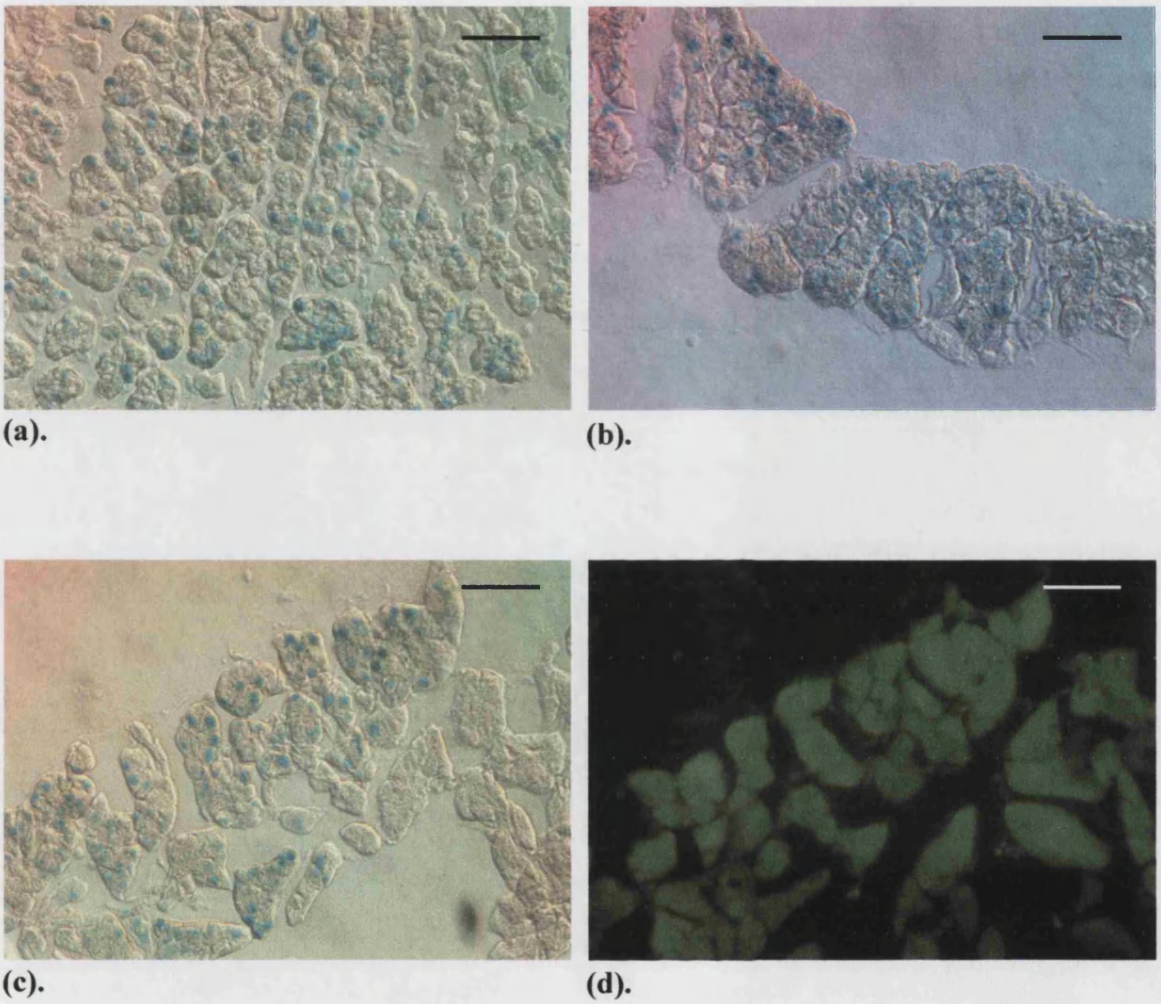

Figure 4.13. Simvastatin-Induced β-Gal Activity in PN30 Pancreatic Acini is Detected by X-Gal Staining but *Not* by Immunofluorescence Cytochemistry

(a)-(b) X-Gal staining in isolated groups of acinar cells in two PN30 transgenic males. (c)-(d) β-Gal activity in the acini of a PN30 hemizygous female is detected by X-gal staining (c) but *not* by immunofluorescence staining for β-gal with fluorescein in an adjacent frozen section (d)

(a)-(c) Images collected under Nomarski optics. Bar = 50 μm

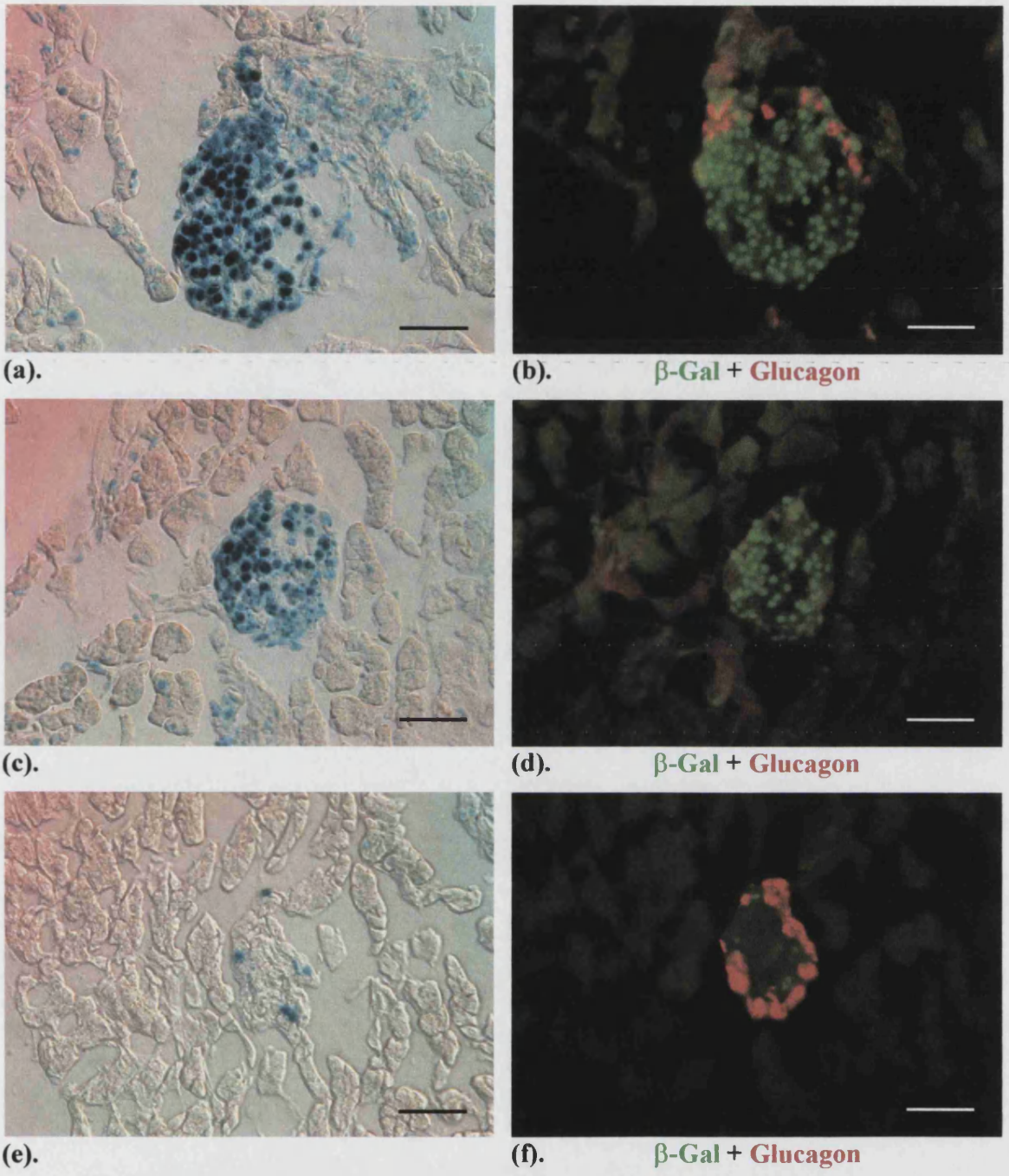

Figure 4.14. Islet-Weighted Islet Homogeneity in PN30 Simvastatin-Treated Mosaic Females Determined to be 76.0 % by X-Gal Staining but Only 68.8 % by Immunofluorescence Cytochemistry

X-Gal staining (a, c and e) and immunofluorescence double-labelling (b, d and f) for β-gal (fluorescein) and glucagon (Texas Red) in adjacent frozen sections through the same islet. (a)-(d) Predominantly β-gal$^+$ islets; (e)-(f) predominantly β-gal$^-$ islet (a), (c) and (e) Images collected under Nomarski optics. Bar = 50 μm

histochemistry and 68.8 % and 68.9 % respectively as revealed by immunofluorescence analysis (**Table 4.11.**). On account of the apparently lower resolution of detection of β-galactosidase protein by immunofluorescence staining, results generated from this technique were not subjected to further analysis.

Table 4.11. Homogeneity of Islets in H253 Female Hemizygotes as Revealed by X-Gal Staining and Immunofluorescence Analysis

METHOD OF β-GAL DETECTION	ISLET HOMOGENEITY (%)	
	Islet-Weighted	**Cell-Weighted**
X-Gal Histochemistry	57.4	56.7
	94.7	94.5
	75.7	73.4
	76.0 ± 10.8	**74.9 ± 10.9**
Immunofluorescence Analysis	65.9	65.8
	67.7	68.4
	72.8	72.5
	68.8 ± 2.07	**68.9 ± 1.94**

It was expected that in the absence of extensive cell mixing, islets (and other tissues) in the H253 hemizygote mosaic females would be composed of β-gal$^+$ and β-gal$^-$ cells in approximately equal numbers. However, this group of PN30 animals revealed quite clearly that this was not the case in the islets. So, the same data set was subjected to further analysis.

4.3.3.3. Prevalence of Predominantly β-Gal$^+$ Islets

Of the 37 islets examined, 27 were predominantly (> 50 %) composed of β-gal$^+$ cells, the remaining 10 being composed mainly of unlabelled cells. χ^2 was calculated as described in **Section 4.3.1.6.1.** above to verify this divergence in the observed ratios of the predominant genotypes of the islets from the expected 1:1 distribution. Of the 37 islets, 50 % or 18.5 would be expected to be composed primarily of β-gal$^+$ cells whilst the remaining 18.5 would be expected to contain predominantly unlabelled cells (excluding the existence of any islets containing equal numbers of cells of each genotype). As explained, in this situation with only two categories across which the distribution is expected to be symmetrical:

$$\chi^2 = 2 \frac{(\text{Observed} - \text{Expected})^2}{\text{Expected}}$$

$$\therefore \chi^2 = 2 \frac{(72.25)}{18.5} = 7.81$$

$\chi^2 = 6.64$, $df = 1$, $p = 0.01$. As the calculated value of χ^2 is greater, the null hypothesis can be rejected. The observed frequency distribution of the predominantly β-gal$^+$ to predominantly unlabelled islets therefore deviates significantly from the expected 1:1 distribution, indicating a significant bias towards β-gal-labelled islets over unlabelled ones. This selective effect was also evident in the animals from Time-Series One, when at all time-points studied, homogeneous β-gal$^+$ islets outnumbered homogeneous β-gal-negative islets. This finding confirms the suggestion that the expression of the β-gal enzyme itself may exert an effect on the relative survival of stem cells, and not be a truly neutral marker.

4.3.3.4. Rate of Heterogeneous-Homogeneous Conversion is Dependent on Islet Size

To test the hypothesis that the smaller the size of the islet, the greater the rate with which cell homogeneity is attained, the islet-weighted percentage homogeneity data was segregated according to islet size (**Table 4.12.** and **Graph 4.6.**). In contrast to the results from Time-Series One, there was an inverse relationship between islet size and islet homogeneity such that smaller islets exhibited greater percentage homogeneity than did islets of larger cell number, supporting the hypothesis.

Table 4.12. Islet-Weighted Homogeneity of Islets Segregated by Size

Islet Area (Cell Number)	Islet-Weighted Percentage Homogeneity (%)	Islet Sample Size, *n*
0-99	74.5 ± 3.61	27
100-199	71.9 ± 8.13	5
200-299	64.6 ± 9.38	4
300-399	52.6 ± 0	1

Note that the frequency of islets decreases as islet area increases. Very few islets in the PN30 pancreas are greater than 300 cells in cross-sectional area so sample size was forcibly reduced.

Graph 4.6. Islet-Weighted Homogeneity of Islets is Inversely Related to their Size

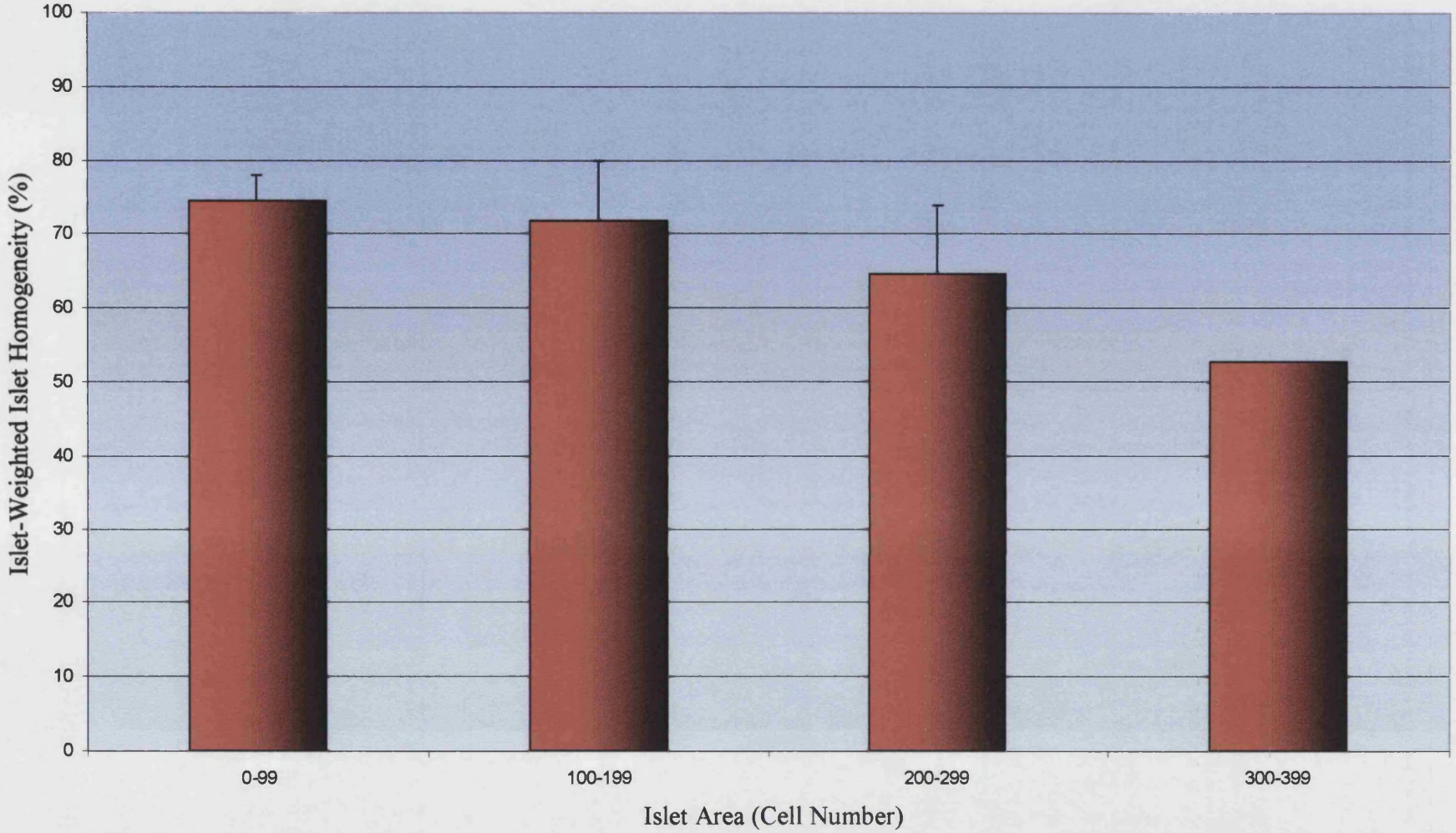

4.4. Discussion

4.4.1. Loss of HMG CoA Reductase Promoter Activity

4.4.1.1. Loss of Acinar Expression from PN3 Onwards

Analysis of pancreata from male transgenic and female homozygous animals of Time-Series One revealed there to be almost uniform β-gal activity in the acini of E15.5 embryos as assayed by histochemical X-gal staining. However, in the immediate neonatal period, between PN3 and PN21, β-gal activity was lost from the acinar cells. This phenomenon was also observed in female hemizygotes, in which little acinar β-gal activity was detected through X-gal staining (Time-Series One) or immunofluorescence analysis (Time-Series Two). In this neonatal stage, the loss of enzymic activity was restricted to only the acinar compartment. The uniform X-gal staining of islets in the centre of < PN18wk wholemount-stained control pancreata (surrounded by non-staining acini) was indicative of a satisfactory, high penetration of the stain throughout the pancreatic tissue. Although there are other possible explanations, the decline in β-galactosidase activity after birth was attributed to a loss of activity of the HMG CoA reductase promoter driving the *lacZ* transgene. The evidence in favour of this is that there is some recovery of acinar β-gal in the simvastatin-treated animals of Time-Series Three. The loss of activity of the promoter of this ubiquitously expressed gene in pancreatic acini has not been reported previously. As a result of the dramatic loss of acinar β-gal activity, cell lineage analysis of the acini was forcibly abandoned.

4.4.1.2. Loss of Islet Expression in Older Animals (> PN18wk)

In contrast to the acini, uniform β-gal activity was observed in all pancreatic islets and ducts of all male transgenic and female homozygous animals under PN18wk. Low intensity X-gal staining of some endocrine cells and a small number of completely unstained cells was however seen in some islets of a small number of PN18wk individuals. From this it was inferred that activity of the HMG CoA reductase promoter might be diminishing in a fraction of islet cells of some older animals. Due to the possible loss of β-gal for this reason, analysis of the experimental cases was confined to the first 84 days (12 weeks) of postnatal life, during which the controls all showed uniform, persistent β-gal expression in the islets and ducts.

4.4.1.3. HMG CoA Reductase: A Closely Regulated Enzyme

The housekeeping gene 3-hydroxy-3-methylglutaryl coenzyme A (HMG CoA) reductase is the rate-limiting enzyme in the synthesis of mevalonate, a crucial intermediate in the formation of sterols and non-sterol isoprenoid compounds (Goldstein and Brown, 1990; Qureschi and Porter, 1981) (**Fig. 4.15.**). Cholesterol is synthesised in virtually all tissues from acetyl CoA. Cytosolic acetyl CoA is initially condensed to acetoacetyl CoA in a reaction catalysed by a cytosolic thiolase enzyme. Acetoacetyl CoA then condenses with a further molecule of acetyl CoA catalysed by HMG CoA synthase to form 3-hydroxy-3-methylglutaryl coenzyme A (HMG CoA) as an intermediate leading to the six-carbon compound mevalonate. HMG CoA is then converted to mevalonate in a two-stage reduction by NADPH catalysed by HMG CoA reductase, a cytosolic isozyme of the mitochondrial enzymes.

HMG CoA reductase is an interconvertible enzyme that is inactivated by phosphorylation. It is subjected to control at the levels of transcription, translation, protein stability, and activity modulation (Goldstein and Brown, 1990). Both steroid and non-steroid products of mevalonate are required for total suppression of HMG CoA reductase activity in an example of multivalent regulation (Brown and Goldstein, 1980). Via a feedback mechanism, HMG CoA reductase is inhibited by mevalonate and cholesterol. Increased cholesterol concentrations lead to formation of cholesterol derivatives, which allosterically inhibit the enzyme. As a more long-term form of control, high levels of cholesterol derivatives lead to increased degradation and decreased synthesis of the enzyme. Steroids are assumed to suppress transcription of the HMG CoA reductase gene via an octanucleotide sequence in the promoter region (Osborne, 1991). HMG CoA reductase is known to be regulated by hormones, including those of the pancreas. Insulin and thyroid hormone both increase HMG CoA reductase activity, whereas glucagon and glucocorticoids decrease it.

4.4.1.4. Speculation on Causes of Loss of Acinar β-Gal

The loss of acinar activity of this ubiquitously expressed promoter has not been previously reported. Causes of this acinar-specific decline in expression in the neonatal period can be speculated upon. As an adaptation for their secretory role, the pyramidal cells of the acini contain very prominent regular arrays of rough endoplasmic reticulum, an extensive basal Golgi complex and numerous secretory zymogen granules containing

Figure 4.15. HMG CoA Reductase Plays an Integral Role in the Synthesis of Mevalonate, a Crucial Intermediate in the Formation of Cholesterol

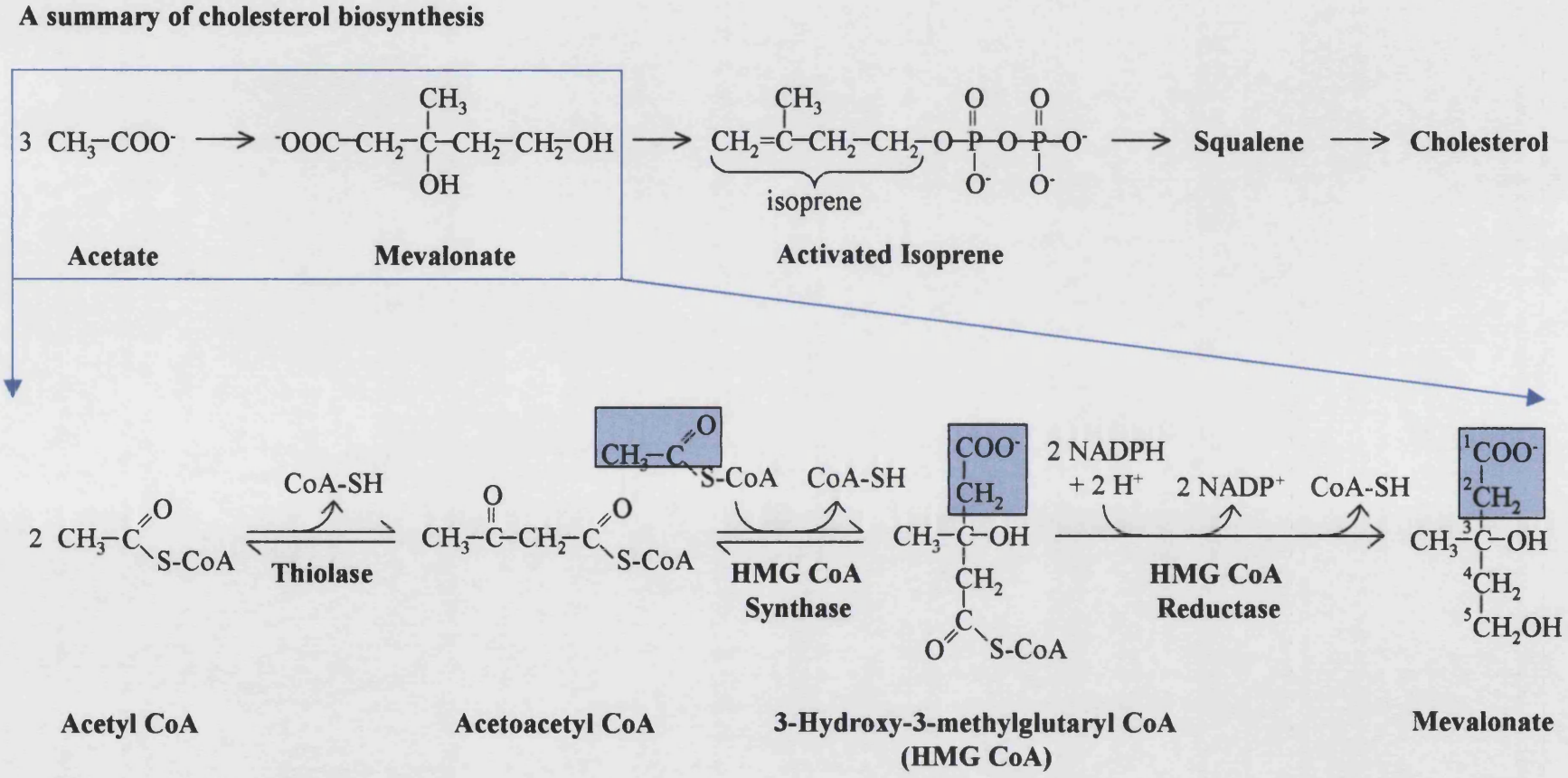

Formation of mevalonate from acetyl CoA. The origin of C-1 and C-2 of mevalonate from acetyl CoA is highlighted

digestive enzymes. It follows from this high density of membranes that the cholesterol content of such cells will be high. Furthermore, the endoplasmic reticulum of the cell is principally responsible for cholesterol synthesis. High steroid levels might directly suppress the HMG CoA reductase promoter to inhibit transcription of the endogenous gene and also the HMG CoA reductase-driven *lacZ* transgene in the pancreatic acini (Osborne, 1991). It is also a possibility that maternally-derived compounds during embryonic development *in utero* and during the early phase of weaning delivered in the colostrum, act to maintain high promoter activity by lowering cholesterol. This would account for the observed acinar β-gal activity at E15.5 and subsequent inactivity with neonatal growth. It is similarly likely that as the animals age, tissue cholesterol deposition occurs on a widespread scale, particularly given their sedentary lifestyle. Such a rise in plasma cholesterol would have the effect of suppressing HMG CoA reductase transcription throughout many tissues and organs of the adult's body, including, eventually, the pancreatic islets.

4.4.1.5. Loss of HMG CoA Reductase Promoter Activity in Neonatal Islets in Animals of Time-Series Two - Transgene Hyper-Methylation?

It was suggested (Patrick Tam, personal communication) that loss of transgene expression could be attributable to hyper-methylation of the HMG CoA reductase-driven transgene in the germline. This can result in widespread variations in transgene expression. H253 transgenic males have been observed (Patrick Tam, personal communication) to transmit the transgene to their first litters efficiently and then to subsequently sire progeny exhibiting marked variations in β-gal expression throughout their tissues. The first animals examined in Time-Series Two were born more than eight months after the last of the animals of Time-Series One. It would, in principle, be possible to investigate this by examining the methylation state of the transgene with methylation-sensitive and insensitive restriction enzymes. However, there was insufficient time for this in the current study.

4.4.1.6. Drug-Enhanced Increase in HMG CoA Reductase Promoter Activity

According to Patrick Tam (personal communication), variation in β-gal expression amongst H253 litters can be resolved by re-screening the H253 colony for strong expressers of the *lacZ* transgene by assaying the intensity of X-gal staining of

earclips. High or strong expressers can then be bred from to reconstitute the line. However, again, time constraints dictated that this was impracticable. Instead, drug treatment was employed in an attempt to upregulate transgene expression.

Its role as the rate-determining enzyme for the overall pathway of cholesterol synthesis has resulted in HMG CoA reductase being the site of action of the most effective class of cholesterol-lowering drugs, the statins. These fungal metabolites act as inhibitors of synthesis of the enzyme and include mevastatin (compactin), lovastatin (mevinolin), provastatin, and simvastatin. The negative feedback that exists between HMG CoA reductase expression and cholesterol can be manipulated to our advantage by administering statins to enhance activity of the HMG CoA reductase promoter. Through the *ad libitum* oral administration of simvastatin, the level of plasma cholesterol which negatively inhibits expression (Goldstein and Brown, 1990), is lowered, and synthesis of HMG CoA reductase is increased (**Fig. 4.16.**). Treatment of LDL receptor-deficient mice for two weeks with simvastatin has been shown to induce a 4.1-fold increase in hepatic HMG CoA reductase mRNA levels (Bisgaier *et al.*, 1997). In H253 mice, elevation of HMG CoA reductase production results in a concomitant increase in expression of the *lacZ* transgene driven by the HMG CoA reductase promoter (Stone *et al.*, 2002).

Analysis of X-gal staining in two PN30 male transgenic animals treated for 10 days with simvastatin prior to sacrifice showed β-gal expression to be effectively ubiquitous in the islets and ducts. Within these two control pancreata, 99.6 % of islet cells examined exhibited β-gal activity. Furthermore, groups of acinar cells in the PN30 pancreata were also seen to stain for β-gal activity with X-gal, a phenomenon not seen in untreated PN28 animals. Simvastatin treatment was therefore considered to be effective in enhancing activity of the HMG CoA reductase promoter. It ensured that transgene expression was effectively ubiquitous in islet cells and also partially restored the β-gal expression in the acinar cells. H253 X-inactivation mosaic females could not however be used to examine acinar cell lineage even whilst undergoing a programme of simvastatin treatment since β-gal activity was not completely restored to all acinar cells. It is possible that ubiquitous β-gal activity in the acini of H253 transgenic males or homozygous females could be demonstrated by subjecting animals to a longer time-course of simvastatin treatment or by raising the dosage. In the current experiments, the duration of the weaning period restricted the length of statin treatment of the PN30 animals. It is difficult to know with accuracy the dose of simvastatin received by pre-weaning offspring in the milk if the mother is provided with the drug *ad libitum*; risks to

Figure 4.16. Statin-Induced Upregulation of HMG CoA Reductase Transcriptional Activity

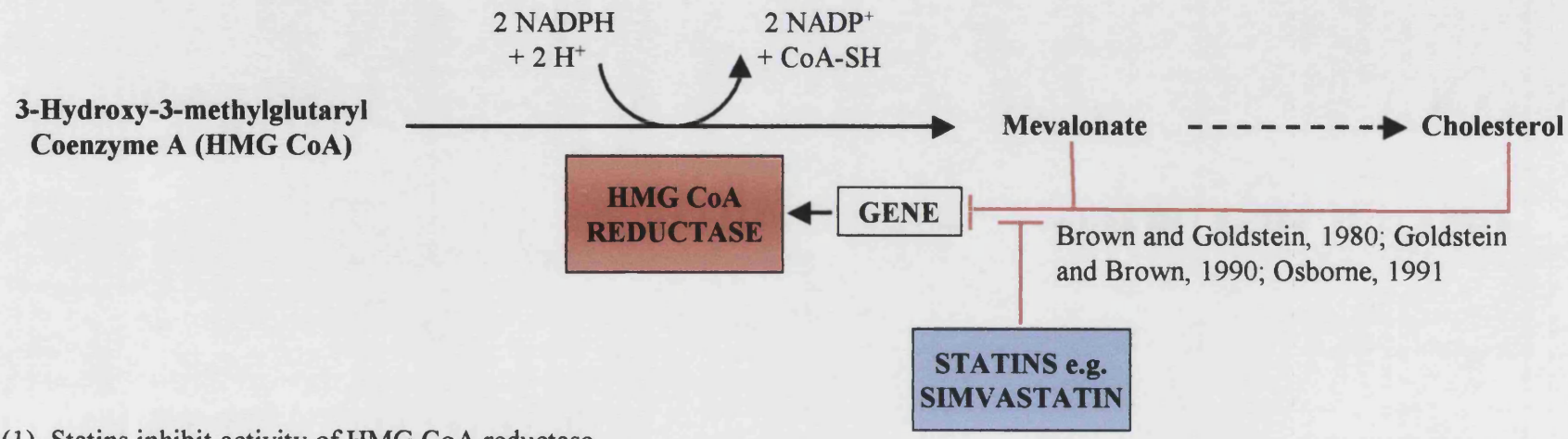

(1). Statins inhibit activity of HMG CoA reductase

(2). Mevalonate and so, cholesterol levels are reduced

(3). Feedback inhibition of mevalonate and cholesterol on HMG CoA reductase activity is diminished and steroid suppression of reductase transcription is reduced

(4). Transcriptional activity of HMG CoA reductase is increased

In H253 mice, elevation of HMG CoA reductase production results in a concomitant increase in expression of the HMG CoA reductase-driven *lacZ* transgene (Stone *et al.*, 2002)

< PN20 animals from treatment are also possible because simvastatin treatment may interrupt fetal steroid synthesis. However, there have been few reports of congenital birth abnormalities associated with the statins (Manson *et al.*, 1996). Treatment with more potent statins might also effect a complete restoration of acinar transgene expression. Treatment of LDL receptor-deficient mice for two weeks with atorvastatin and lovastatin has been shown to induce 17.2- and 10.7-fold increases in hepatic HMG CoA reductase mRNA levels respectively, in comparison to the 4.1-fold increase observed following treatment with simvastatin (Bisgaier *et al.*, 1997).

4.4.2. Differences in Sensitivity Between Methods of β-Gal Detection

The variability in the level of β-gal fluorescence signal amongst immunopositive cells in pancreas sections from the mosaic females of Time-Series Two also raised the possibility of there being a marked distinction between the thresholds of β-gal detection between histochemical X-gal staining and immunofluorescence analysis in conjunction with an anti-β-gal antibody. It might be envisaged that the former method, which relies on the catalysis of a chemical reaction by the β-galactosidase enzyme, is more sensitive than is localisation of the protein using an antibody. However, the extent of this difference in practical terms was unknown. So, to test this hypothesis, a direct comparison between the two detection methods was made by determining the proportion of β-gal$^+$ cells in the same islets of H253 transgenic males. Adjacent cryosections through the same islets were each stained by a different technique and the cell composition data compared. The difference was found to be quite striking and much greater than expected. Approximately one fifth of the β-gal$^+$ islet cells detected by X-gal staining in the male transgenic animals were *not* detected as being β-gal$^+$ by immunofluorescence analysis. It would appear that the threshold for β-gal detection by X-gal staining is significantly lower than for detection by immunofluorescence analysis. The observation that isolated groups of acinar cells in the PN30 pancreata were seen to stain for β-gal activity with X-gal but not by immunofluorescence, is also consistent with this.

4.4.3. Credibility of Data

In light of these findings, the data from Time-Series One and the results from the X-gal staining of simvastatin-treated Time-Series Three animals appeared to be most credible since:-

(1). β-gal expression was known to be effectively ubiquitous in the islets of these animals from X-gal staining of pancreata from positive control transgenic male and homozygous female animals,

(2). islet β-gal$^+$/β-gal$^-$ cell composition data in female hemizygotes was obtained from histochemical X-gal staining which is believed to reveal *all* β-gal$^+$ cells.

4.4.4. Pancreatic Ducts Arise from Multiple Progenitors and Remain Polyclonal

At all time-points and in all female hemizygous animals examined, pancreatic ducts were consistently seen to be of a heterogeneous β-gal$^+$/β-gal$^-$ cell composition. Variation was observed in the extent of homogeneity with there being a great range in the ratio of numbers of cells of the two genotypes. No homogeneous ducts composed only of β-gal$^+$ cells or entirely of β-gal$^-$ cells were ever observed. This mixed state implies that pancreatic ducts are polyclonal and arise from the association of multiple progenitor cells. This polyclonal state is then maintained throughout pancreas development and postnatal life with a number of self-renewing stem cells feeding relatively slow turnover of the duct cell compartment.

4.4.5. Homogeneous Islets Tend to be β-Gal$^+$: A Selective Advantage of β-Galactosidase?

An unexpected finding was that in the mosaic females of Time-Series One and the three PN30 animals, homogeneous islets were found to be more frequently composed of β-gal$^+$ cells than unlabelled cells. This selective effect was apparent at all time-points studied. The direction of selection varied between individual animals however; in a minority of animals, homogeneous islets tended to be composed of unlabelled cells. No asymmetry in the numbers of homogeneous β-gal$^+$ *vs.* homogeneous β-gal$^-$ gastric glands was reported by Nomura and colleagues (Nomura *et*

al., 1998) when they used H253 animals for gastric gland lineage analysis. They describe X-chromosome inactivation as a "physiological and neutral cell marking technique". Also, β-galactosidase has been reported to be biologically neutral in the mouse (Beddington *et al.*, 1989). One explanation for this asymmetry is that expression of the β-gal protein provides a selective advantage over cells not expressing the transgene, perhaps by aiding cell attachments or by enhancing the proliferative capacity of a *lacZ*$^+$ cell. Although predominantly nuclear, small amounts of enzyme might leak out of expressing cells and degrade β-galactoside linkages in extracellular carbohydrates. A counter-argument to this is that in a minority of animals, homogeneous islets tended to be β-gal$^-$, although homogeneous β-gal$^+$ islets were observed in these animals at a low frequency. One further possibility is that of reactivation of the previously silent X-chromosome carrying the transgene in certain islet cells. Nomura *et al.* (1998) considered this phenomenon when analysing gastric gland cell lineage by examining mice doubly heterozygous for the H253 *lacZ* transgene and Searle's translocation (*lacZ* +/+ *T16H*). Most, if not all, cells in adult females heterozygous for the translocation inactivate the normal X-chromosome (Lyon *et al.*, 1964; McMahon and Monk, 1983). Hence, the transgene carried on the normal silent X-chromosome in these mice would not be expressed unless a cell reactivates the silent X-chromosome, resulting in two active Xs per cell (Wareham *et al.*, 1987). At PN10, no reactivation was observed in the glands of Searle's mice, though in PN6wk stomachs, reactivation was detected in 0.04 % of fundic and 0.14 % of pyloric glands. In PN15wk stomachs, 0 % reactivation was detected in fundic glands and 0.19 % in pyloric glands. This data suggests insignificant rates of reporter gene reactivation so it seems improbable that it could account for the observed predominance of homogeneous β-gal$^+$ islets.

4.4.6. Islets Arise from Multiple Progenitor Cells

The collated data suggest that pancreatic islets, like the ducts, are initially formed from multiple progenitor cells. The mixed β-gal$^+$/β-gal$^-$ cell composition of more than 98.2 % of PN3 neonatal islets supports one of the hypotheses of islet growth proposed by Deltour *et al.* (1991), namely that "each islet is a mixture of cells originating from a pool of progenitor cells". This evidence contradicts hypotheses (1) "a single progenitor cell gives rise to all the precursors of the islets" and (2) "each of a few

progenitor cells is the founder of a different islet", both of which involve clonal growth from a single cell. Hence, nascent islets are polyclonal, being formed from the aggregation of multiple precursor cells. This finding is consistent with the mixed cellular composition of individual islets in combination cultures of a *lacZ*-expressing and an unlabelled pancreatic epithelium with an unlabelled mesenchyme (Percival and Slack, 1999). Isolated patches of cells of a single genotype were never seen in neonatal islets. PN3 islets instead displayed a fine-grained mosaicism of intermingled labelled and unlabelled cells although typically cells of one genotype predominated by an excess of approximately 40 %. This "salt and pepper" phenotype suggests widespread mixing between daughter cells of different progenitors within the forming islets.

4.4.7. Neonatal Heterogeneous Islets Rapidly Become Homogeneous

However, the islets do not maintain their nascent heterogeneous state throughout postnatal life in the same manner as the pancreatic ducts. The heterogeneous islets rapidly became replaced by homogeneous islets in the first month. This conversion occurred at its greatest rate between one and three weeks after birth. In animals of Time-Series One, the frequency of homogeneous islets increased from 1.79 % at PN3 to 42.6 % at the two-week time-point; by three weeks, almost 95 % of islets were homogeneous. The index of homogeneity, calculated to track the changes in cell composition with greater resolution, showed a similar pattern. The size-independent islet-weighted percentage homogeneity of islets increased with age from 69.3 % at PN3 to in excess of 98 % by PN21 with the maximum rate of conversion to the homogeneous state occurring between one and three weeks after birth. The mean islet-weighted and cell-weighted islet homogeneity (76.0 % and 74.9 % respectively) as calculated from X-gal staining of pancreata from the three simvastatin-treated PN30 female hemizygotes agree with this progression to islet homogeneity. These figures depart markedly from the 50 % homogeneity values expected in the absence of a heterogeneous to homogeneous shift. In Time-Series Two, no homogeneous islets were seen but this is probably because of the insufficient sensitivity of the immunofluorescence detection of β-gal. In Time-Series Three there were some homogeneous islets at PN30, although not as many as seen in Time-Series One. The conclusion is that homogeneous islets are a reality, but the timescale may not always be as rapid as shown in Time-Series One.

4.4.7.1. Inconsistent with Previous Data?

The observation of homogeneous islets in adult mice appears at first to be inconsistent with the results of a previous study on pancreatic islet chimaerism by Deltour and coworkers (Deltour *et al.*, 1991). Using the human C-peptide/proinsulin product as a cell marker in aggregation mouse chimaeras, they demonstrated that in two of four animals examined at 1.5 months or 4.5 months of age, all islets contained cells from both aggregated embryos. This finding was taken to suggest that islets originate by cell aggregation as was found in the current study. The aggregation chimaera study is not necessarily incompatible with the present investigation because, firstly only four animals were examined of which two exhibited homogeneous islets, and secondly no time-series was conducted. The data of the current study suggest that there is a trend to homogenisation of islets although the time-course may vary somewhat.

4.4.7.2. Polyclonal Neonatal Islets Become More Monoclonal

The most obvious explanation for a homogeneous islet is that it is monoclonal, i.e. that all cells are derived from a single progenitor. The shift in the cell composition of islets that was observed in the present study suggests that neonatal islets become progressively less polyclonal with age in the initial month after birth. That mixed islets are polyclonal is self-evident, but the possibility remains that a proportion of the homogeneous islets are polyclonal even though all the cells within a homogeneous islet have the same staining phenotype. For example, if adult islets are renewed by two progenitor or stem cells, then the likelihood of that islet appearing as homogeneous is 0.5 - the probability that both stem cells are of the same genotype - either β-gal$^+$ and β-gal$^+$ *or* β-gal$^-$ and β-gal$^-$. Of course as the number of stem cells supplying the islet increases, then the probability that they are all of the same genotype giving a homogeneous islet, declines exponentially. It cannot, therefore be stated emphatically that a homogeneous islet is monoclonal but one can infer from the above data that a shift *towards* monoclonality is occurring in the islets. The data indicate a rapid decline in the number of progenitors in each islet so that the number of cell lineages within each islet is reduced or "stream-lined" presumably by endocrine cell turnover in the neonatal period. Eventually, the number of stem cells is reduced to a very small number, probably just one. No islets were ever observed in which the cells of the peripheral mantle of the islet, primarily composed of α-cells were of a different genotype to the β-

cells of the central islet core. This implies that there must be a common endocrine progenitor or stem cell that continues in postnatal life to give rise to all four endocrine cell types within the islet.

4.4.7.3. A Similar Process to Clonal Purification of the Crypts and Gastric Glands?

A conversion or "clonal purification" from a neonatal polyclonal state to one of monoclonality has been well documented in the crypts of the small intestine (Schmidt *et al.*, 1988). After a 14-day purification period, intestinal crypts are, with little exception, found as monoclonal units (Ponder *et al.*, 1985; Schmidt *et al.*, 1988). A similar process has been recorded more recently in the gastric glands of the stomach by conducting lineage analysis with H253 mosaic mice as here (Nomura *et al.*, 1998). Neonatal glands are predominantly polyclonal, each requiring a minimum of three progenitor cells for their formation. Subsequently, the majority become monoclonal from PN6wk although around 10 % persist as a sub-population of polyclonal glands in the adult stomach (Canfield *et al.*, 1996; Nomura *et al.*, 1998). This residue of persistent polyclonal gastric glands has been suggested to contain larger numbers of stem cells than the general gland population and so function as a reservoir for replenishing damaged glands.

4.4.7.4. Mechanisms for Clonal Purification

A number of possible mechanisms have been put forward to account for the observed "clonal purification" from polyclonal to monoclonal composition (**Fig. 4.1.**). If there are a small number of stem cells within the gland, some of these could perhaps divide symmetrically while others divide asymmetrically (Potten and Loeffler, 1990). A stem cell can produce two stem cells or two cells committed to differentiate, or one of each. When a stem cell produces two progeny committed to differentiate then this cell lineage is lost from the stem cell pool. With time, the symmetrically dividing stem cells will "outlive" the asymmetric ones (Potten and Loeffler, 1990). In this scenario, all stem cell lineages would eventually be extruded from the islet at the expense of one stem cell, which gains the ascendancy. An alternative candidate mechanism could be gland fissioning. Crypt fission is a relatively well-documented phenomenon (Li *et al.*, 1994; St. Clair and Osborne, 1985). Gastric glands have also been reported to undergo fission by splitting across the longitudinal extent of the parental gland (Nomura *et al.*, 1998). Extremely active replication of intestinal crypts by fission during the period that they

undergo clonal purification has lead to the hypothesis of segregation of cell lineages by this process. If again, an islet is considered to be fed by a small number of stem cells, perhaps four, then fission of that islet will partition the stem cells at random between the daughter islets, reducing the number of cell lineages within the newly-formed islets. This spatial restriction of progenitor cells will lead eventually to monoclonality. Nomura and colleagues (Nomura *et al.*, 1998) found that heterogeneous β-gal^{+}/β-gal^{-} gastric glands appeared to give rise to mixed daughter glands, indicating that monoclonal glands do not necessarily arise immediately following fission of a polyclonal gland, but perhaps due to subsequent renewal by descendants of the resulting stem cell pool (Nomura *et al.*, 1998).

4.4.7.4.1. Overgrowth by the Progeny of a Single Cell

It is quite feasible that one stem cell might gain the ascendancy and populate the islet at the expense of other stem cells, which are extruded and undergo apoptosis or programmed cell death. In this manner, a relatively rapid conversion from a heterogeneous to a homogeneous islet is achieved. If one islet cell were to divide to give two daughter cells, which in turn, each divided to give two daughters, then a single cell would need only to undergo 10 divisions to populate a 1000-cell islet with its progeny (2^{10} = 1024) provided that all daughter cells are retained. It is not easily possible to extend such a simple calculation to construct a mathematical model of such islet cell overgrowth. This is due to the great variability in the indices of both cell division and cell death of islet cells as determined from many cell kinetic studies. Most notably, by extrapolating data from the work of others (Kaung, 1994; Montana *et al.*, 1994; Swenne and Eriksson, 1982), Finegood and colleagues (Finegood *et al.*, 1995) estimated the replication rate of β-cells in the neonatal rat pancreas (**Graph 4.7.**). Although approximately 20 % of β-cells in the pancreas are in a state of active proliferation at PN1, this figure declines progressively in the weeks following birth to 14 % at PN5 and 9 % at PN15. By 30 days after birth, 5 % of the β-cells are replicating. The replication rate does not stabilise at the adult level of 3 % β-cell turnover per day until approximately PN40. Finegood and coworkers (Finegood *et al.*, 1995) showed that despite the initial high rate of β-cell proliferation, β-cell mass remains stable in the neonatal rat between PN7 and PN21. This was proposed to be due to a postnatal wave of β-cell death in the developing rat pancreas peaking at 9 % of β-cells/day at PN12. This wave of islet cell death has subsequently been validated by direct histochemical

Graph 4.7. β-Cell Replication Rate with Age in Normal Rats (Finegood *et al.*, 1995) Extrapolated from Data from the Work of Others (Kaung, 1994; Montana *et al.*, 1994; Swenne and Eriksson, 1982). Reproduced with Permission

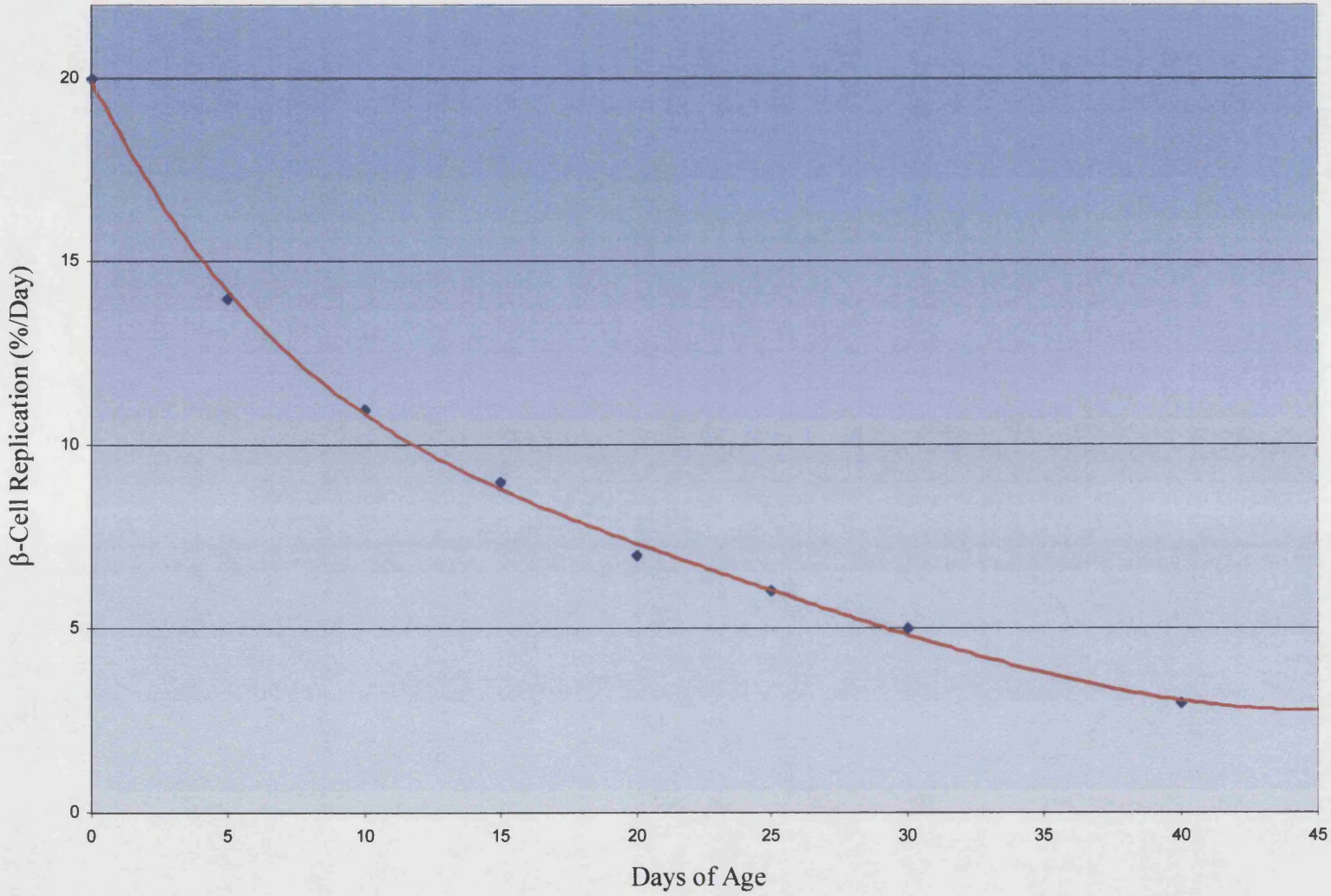

detection of apoptotic cells. Using the fluorescent dye propidium iodide to morphologically identify apoptotic cells, Scaglia *et al.* (1997) demonstrated a peak of 3.5 % in the apoptotic index of β-cells occurring at PN13 in the neonatal Sprague-Dawley rat. A separate study of Wistar rats using TUNEL revealed a similar neonatal wave of islet cell apoptosis peaking at PN14 with a value of 13.2 % cell death/day (Petrik *et al.*, 1998). More recently, this phenomenon has also been shown to occur in the mouse pancreas. Using the TUNEL method, a neonatal wave of islet cell apoptosis commencing at PN5 and peaking at PN12 (9.4 % apoptosis/day) was demonstrated in BALB/c mice (Trudeau *et al.*, 2000) (**Graph 4.8. (b)**). These studies together demonstrate the great variability in the rate of islet cell proliferation and cell death occurring in the neonatal islet, which makes it very difficult to present a model of islet cell overgrowth. It is also difficult to relate indices of either cell division or cell death to actual cell turnover. The cell kinetic studies show that β-cell replication in the neonatal rodent pancreas is sufficiently high and sustained to permit a single cell to populate a 1000-cell islet by undergoing 10 cycles of division. It is therefore credible that clonal purification might be achieved in one month if all of the progeny of the progenitor cell are retained. Even levels of β-cell replication in the adult rodent are sufficient to bring about dramatic changes in β-cell mass. Hellerström *et al.* (1988) pointed out that with a β-cell birthrate of just under the adult level of 3 % new cells per day, the β-cell mass would double in one month if there were negligible cell death or apoptosis. Alternatively, if the rate of β-cell death approaches the replication rate of 3 %, then complete replacement of the β-cell population could occur in that one-month period. Indeed, cells can only be observed as TUNEL-positive for a short period of a few hours (Petrik *et al.*, 1998), revealing estimates of apoptotic rate derived from TUNEL staining to be very conservative. This widens the possibility that levels of endocrine cell turnover in the neonatal rodent pancreas are sufficient to allow for islet clonal purification in one month via population by the progeny of a single proliferating cell. The maximum level of islet cell apoptosis coincides with the greatest rate of islet conversion from heterogeneity to homogeneity between one and three weeks after birth (**Graph 4.8.**).

The functional significance of the neonatal remodelling of the islet cell mass is unknown. However, in other systems such as in male germ cells (Wang *et al.*, 1998) and cardiac myocytes (Kajstura *et al.*, 1995), similar waves of neonatal apoptosis contribute to tissue remodelling coincident with changing function or cellular demand. The wave of β-cell apoptosis in the pancreas occurs just prior to weaning and it seems

Graph 4.8. Peak of Apoptotic Wave in the Neonatal Rodent Pancreas is Coincident with the Greatest Rate of Conversion of Heterogeneous Islets to Homogeneity

(a). Islet-Weighted and Cell-Weighted Islet Homogeneity with Age are Very Similar

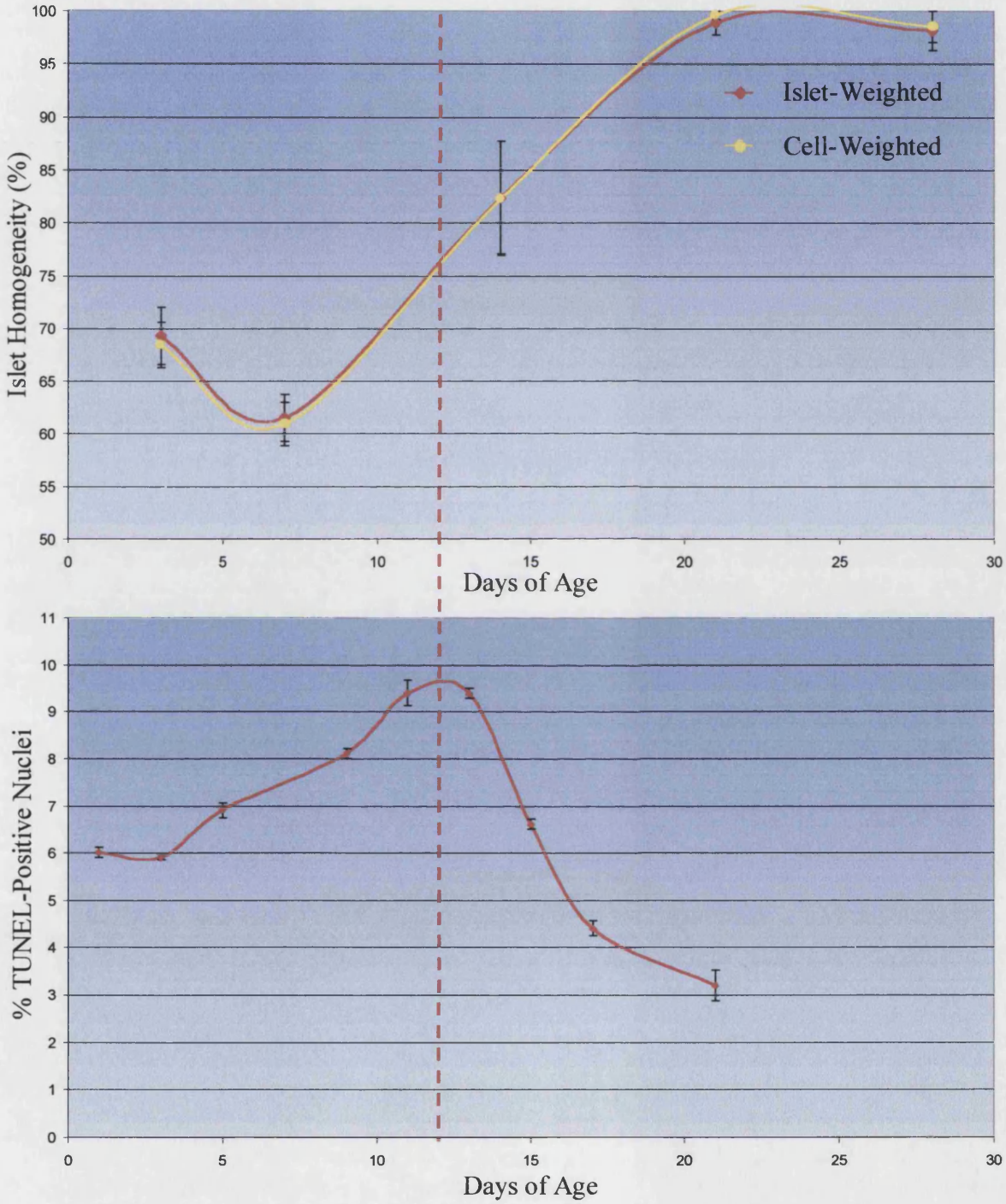

(b). Islet Cell Apoptosis (% TUNEL-Positive Nuclei) as a Function of Age in Female BALB/c Mice (Trudeau *et al.*, 2000). Reproduced with Permission

probable therefore that this remodelling may prepare the β-cell mass for changing functional demands (Trudeau *et al.*, 2000). Neonatal remodelling of the endocrine pancreas marks a change from a fetal phenotype of the β-cell, which is proliferative, has poor glucose sensitivity, and lacks acute phase insulin release, to an adult phenotype, which has a low replicative capacity but high sensitivity to glucose and an ability to rapidly release insulin (Hellerström and Swenne, 1991). Clonal purification perhaps plays a role in producing the adult islet by "synchronising" the functions of newly-generated adult phenotype β-cells formed within a short time-frame from a single stem cell. Clonal purification might alternatively simply be a by-product of the endogenous cell turnover that occurs during neonatal remodelling of the islets.

In the study of Petrik *et al.* (1998) mentioned above, the neonatal wave of islet cell apoptosis that peaks at PN14 in the rat pancreas was shown to be temporally associated with a fall in the islet cell expression of IGF-II. This growth factor was shown to function as an islet survival factor *in vitro* by suppressing cytokine-mediated islet cell death in isolated neonatal rat islets. A subsequent study (Hill *et al.*, 2000) by the same group using an IGF-II-overexpressing transgenic mouse showed that the retention of circulating IGF-II postnatally largely prevents the wave of developmental apoptosis of the islets. Consequently, islets from IGF-II transgenic mice exhibited a significantly greater mean area from PN11-16 than those of non-transgenic littermates. It would be interesting to determine whether the hyperplastic islets in such transgenic animals retain their polyclonality beyond the neonatal period. This question could be assessed by crossing the IGF-II transgenic strain with the H253 line and performing cell lineage analysis on mosaic females by staining for β-gal activity as in the current study. If clonal purification results from the progeny of a single cell populating the islet then it would be expected that if neonatal islet apoptosis is suppressed, the islet would continue to grow as islet cell replication is unabated. (Some evidence suggests that islet cell replication is actually increased in IGF-II transgenic mice on PN13 and PN16; Hill *et al.*, 2000). The islet cannot be "purged" of the cells usually extruded in the absence of the growth factor. Islet clonal purification can therefore not proceed resulting in hyperplastic polyclonal islets. It remains to be seen whether this hypothesis is validated.

4.4.7.4.2. Islet Fission

Strong histological and islet cell composition evidence have been collected in support of the "Islet Fission" model of islet clonal purification (**Chapter 5**). In this

model, as an islet grows by cell proliferation, fission is initiated, producing two daughter islets when a threshold size is attained, perhaps involving a doubling of stem cell number (Loeffler *et al.*, 1993, 1997). If islet growth and fission occur simultaneously or partially so, then little overall increase in mean islet size would result, agreeing with data obtained to this effect. The random segregation of a small number of stem cells between the daughter islets would reduce the number of cell lineages within the newly-formed islets. This compartmentalisation of progenitor cells will lead eventually to monoclonality. Division of a polyclonal islet into two daughters has the same effect on reducing stem cell lineages within an islet as apoptosis of 50 % of islet cells, on average halving progenitor cell number within the islet(s). The Islet Fission model though, is disadvantaged by the slower rate of progression to monoclonality than would be achieved by the population of an islet by the progeny of a single cell. This handicap is, however, lessened if the number of stem cells is small (four or less). There is no reason to suggest that the two mechanisms are mutually exclusive. It is also possible that following islet fission, one of the remaining, reduced number of stem cells proliferates at the expense of the other islet cells, hastening the conversion to islet homogeneity initiated by islet fission. It is equally plausible that during islet population by the progeny of a single stem cell, the islet undergoes fission, partitioning the remaining stem cells, again reducing the time taken to attain homogeneity (**Fig. 4.17.**). Nomura *et al.* (1998) found that fission of heterogeneous β-gal$^+$/β-gal$^-$ gastric glands appeared to give rise to mixed daughter glands, indicating that monoclonal glands do not arise immediately following fission of a polyclonal gland, but perhaps due to subsequent renewal by descendants of the resulting stem cell pool (Nomura *et al.*, 1998). Interestingly, they also found that in adult mice, mixed glands appeared in a state of fission much more frequently than would be expected, suggesting a greater fission capacity than homogeneous glands, possibly related to their increased stem cell number.

Figure 4.17. Clonal Purification of Islets by a Combination of Cell Overgrowth and Islet Fission

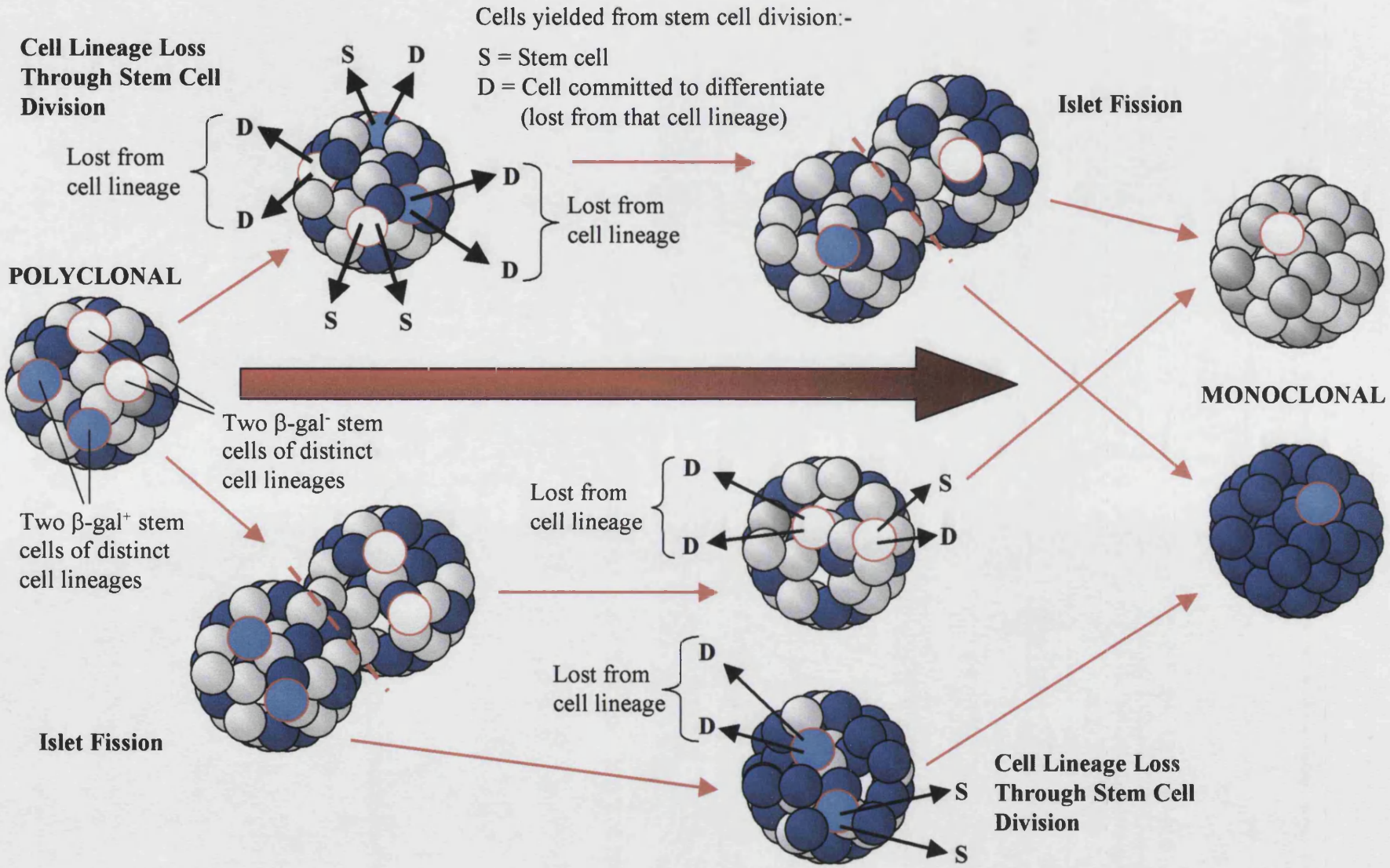

4.4.8. Summary

Clonal development of the pancreatic islets, acini and ducts was followed in X-inactivation mosaic mice with the specific aim of testing the hypothesis that neonatal polyclonal islets undergo a process of "clonal purification" to achieve monoclonality. An unreported neonatal loss of activity of the β-gal cell lineage marker in the acinar cells was attributed to downregulation of the transgene HMG CoA reductase promoter, possibly by steroids within the pancreatic acini. In support of this, some recovery of acinar β-gal was observed upon treatment with the cholesterol-lowering drug simvastatin. Clonal analysis of the acini was therefore abandoned. However, β-gal expression was retained in *all* cells of islets and ducts in animals < PN18wk to which analysis of the experimental cases was confined. At all time-points examined pancreatic ducts were consistently seen to be heterogeneously composed of β-gal-labelled and unlabelled cells implying that ducts in the pancreas arise from the association of multiple progenitor cells. This polyclonal state is retained throughout postnatal life presumably by a number of self-renewing stem cells feeding relatively slow turnover of the duct cell compartment. Immediately after birth, the pancreatic islets were also of a mixed β-gal$^+$ and β-gal$^-$ cell composition, suggesting that the islets, like the ducts, are initially formed from multiple progenitor cells, consistent with previous studies (Deltour *et al.*, 1991; Percival and Slack, 1999). However, the nascent heterogeneous islets rapidly became replaced by homogeneous islets in the first month so that by three weeks after birth, almost 95 % of islets were homogeneous. The shift in islet cell composition observed in this study suggests that neonatal islets become progressively less polyclonal with age in the initial month after birth and progress towards monoclonality via a process of clonal purification similar to that described in the intestinal crypts and gastric glands of the stomach. This is presumed to be brought about by a rapid decline in the number of progenitors in each islet to probably just one, presumably by endocrine cell turnover in the neonatal period. As no islets were observed in which cells in the mantle were of a different genotype to those in the islet core there must be a common endocrine stem cell that continues in postnatal life to give rise to all four endocrine cell types within the islet. Clonal purification can be explained by a number of mechanisms which reduce the number of stem cells in the islet such as the overgrowth and extrusion of islet cells at the expense of one stem cell lineage which gains the ascendancy. A single cell would need only to undergo 10 divisions to populate a 1000-cell islet with its progeny. Islet stem cell number could also be reduced by the partitioning of stem cells into

daughter islets by the division or fission of an islet, a phenomenon for which strong evidence is presented (**Chapter 5**). It appears most probable that a combination of the two mechanisms is responsible for the observed clonal purification of initially polyclonal islets towards a monoclonal state.

5. Dumbbell Islets and Islet Fission

5.1. Introduction

5.1.1. Fission of Intestinal Crypts

As mentioned in **Chapter 4**, it was hypothesised that islets, if initially polyclonal, undergo a conversion to monoclonality in a similar process to the intestinal crypts of Lieberkühn (Li *et al.*, 1994; Winton *et al.*, 1988; Winton and Ponder, 1990). The crypts are initially polyclonal, with multiple stem cells forming individual crypts, but become converted to a monoclonal state by "crypt cleansing". Mechanisms proposed to account for this "clonal purification" include the overgrowth and extrusion of one stem cell lineage by other lineages in the crypt. An alternative mechanism however, is that of *crypt fission* (Li *et al.*, 1994; St. Clair and Osborne, 1985). Crypt fission is an important mechanism of crypt reproduction thought to involve stem cells in which a crypt splits from the base upwards. In some instances, fission occurs asymmetrically with respect to the crypt axis, and in this case the process is termed "budding". Crypt fission of pre-existing crypts is known to be responsible for the rapid increase in crypt number which occurs over the first two weeks of postnatal life (Cheng and Bjerknes, 1985). The initially polyclonal crypt contains a small number of stem cells, most probably four although this number is assumed to vary slowly with time (Loeffler *et al.*, 1986; Loeffler and Grossman, 1991). Upon fission of the crypt, these stem cells are partitioned randomly between the daughter crypts, so the number of stem cell lineages within the crypt will progressively reduce. Over time and with successive crypt divisions, monoclonal crypts will result.

5.1.2. Fission of Gastric Glands

More recently, clonal purification of gastric glands has been shown to occur in the stomach of the mouse (Nomura *et al.*, 1998). Between 75 % and 85 % of glands are clonally mixed immediately after birth but by three months, only 5-15 % remain mixed. Fission of gastric glands has been suggested to be responsible for this conversion. Invariably, fissioning glands were found with a cleft at the base from which daughter glands appeared to unzip along the longitudinal axis of the parent gland. Two rounds of fissioning with spatial restructuring of descendant glands were demonstrated to be

sufficient to explain the observed clonal dynamics on the assumption that the stem cell number is small.

5.1.3. Islet Fission?

So, when testing the hypothesis of clonal purification of the pancreatic islets, similar mechanisms were considered. Observations of an analogous process to crypt fission in the form of any morphologically aberrant islets were to be noted.

5.2. Materials and Methods

5.2.1. Examination of Histological Sections

A morphological examination of islets was made from the 7 μm paraffin sections of wholemount X-gal-stained pancreas tissue from the X-inactivation mosaic H253 hemizygous female mice of Time-Series One which were subjected to cell lineage analysis in **Chapter 4**. A preliminary examination of general islet shape was made from the same 7 μm paraffin sections already prepared from the Time-Series One developmental series of animals analysed at PN3 (*n* or number of animals examined = 2), PN7 (*n* = 2), PN14 (*n* = 2), PN21 (*n* = 2), PN28 (*n* = 1), PN12wk (*n* = 2), PN26wk (*n* = 3) and PN52wk (*n* = 2). Similarly-prepared 7 μm paraffin sections of wholemount X-gal-stained pancreas tissue from PN3-PN52wk homozygous female and transgenic (hemizygous) male H253 animals (Time-Series One control animals for ubiquitous constitutive *lacZ* transgene expression in the pancreas) were also subjected to a rapid examination of islet morphology. This examination of islet shape was conducted on these particular sections, from mice of the H253 strain purely for convenience. There was no underlying reason to examine islet morphology in this particular strain expressing the β-gal label. Histological sections were cut, processed for immunoperoxidase demonstration of either glucagon or insulin then counterstained in nuclear Fast Red and mounted in DPX as described in **Chapter 4, Section 4.2.2.** Specimens were examined using a Leica DMRB fluorescent microscope; islets were identified using DAB staining for glucagon to highlight the islet periphery. As in **Chapter 4**, an islet was defined as five or more contiguous glucagon-immunopositive cells. Images of specimens were taken with a Spot RT Color digital camera (National Diagnostics Inc.) and stored as uncompressed 24-bit TIFF images.

5.2.2. Computer-Aided Dumbbell Islet 3D Reconstruction

This work was carried out in conjunction with Dr. Richard Adams.
Three-dimensional (3D) reconstructions of a representative "dumbbell" islet (explained in **Section 5.3.1.**) and islet distribution in a typical PN3 pancreas were generated from images of histochemically-stained sections. Images were captured from serial paraffin sections of X-gal- and glucagon-immunoperoxidase-stained H253 pancreata using the

Spot RT Color camera (National Diagnostics Inc.) in conjunction with the Leica DMRB compound microscope. These were stored as 24-bit uncompressed TIFF files.

Following spatial calibration of the images, a Macro running in NIH Image 1.6 was employed to spatially align serial images to create a *z*-stack. A straight line was positioned between two reference points on consecutive images. The orientation and centre-point of each line was calculated and used to rotate and shift the second image relative to the target image. The discrete X-gal staining of the islets permitted the blue channel from these image stacks to be extracted to provide black and white images giving high contrast between islets and surrounding non-stained acini **(Chapter 4, Section 4.3.1.2.)**. Then, using the IDL 5.5 (Research Systems, Inc.) program in conjunction with a stylus and touch-sensitive flat-panel monitor, the outlines of islets were manually traced from the stacks of aligned sections. A single object identity was assigned to each islet appearing in consecutive sections and in this manner a tessellated surface mesh was generated. This was then exported to the POV-Ray ("Persistence Of Vision") program which projected views of these outlines defining the surface of the mesh. A similar mesh was generated for the entire pancreas volume and this was rendered as a transparent object to aid the visualisation of the islets *in situ*. QuickTime™ movie files representing 360° or 720° rotations around the modelled objects were generated and four still frames extracted from each movie, each separated by a 90° rotation.

5.3. Results

5.3.1. Observations of "Dumbbell" Islets

Analysis of paraffin sections of pancreas from both sexes and all genotypes of H253 mice revealed the presence of irregularly-shaped pancreatic islets. Such islets were also observed in immunofluorescence-stained frozen pancreas sections (**Fig. 5.1.**). In contrast to the characteristic ovoid appearance of typical islets, these aberrantly-formed variants appeared to be composed of two or, rarely more, conjoined ovoid parts, each of which was similar to a more typically-formed islet. The point of contact of the parts was marked by a "neck" or "waist" of glucagon-immunopositive cells (**Fig. 5.1.**), delineating the two bodies of β-cells on either side. These uncharacteristic islets were coined "dumbbell" islets on account of their morphology and for subsequent unequivocal identification, were defined as:

> *islets composed of two (or rarely, more) conjoined parts meeting in a visible "neck" of glucagon-immunopositive cells*

In this chapter is presented data on the frequency, the 3D structure and the clonal composition of the dumbbell islets. All this work was conducted with H253 mice, although the β-gal label is only necessary for the cell composition study.

5.3.2. Declining Frequency of Incidence of Dumbbell Islets with Age

The incidence of dumbbell islets in the 7 μm paraffin sections of X-gal-stained pancreas tissue from the H253 hemizygous female mice of Time-Series One (**Chapter 4**) of age range PN3 to PN84/12wk was ascertained. As mentioned above, *n*, the number of animals examined at each time-point, was PN3, $n = 2$; PN7, $n = 2$; PN14, $n = 2$; PN21, $n = 2$; PN28, $n = 1$ and PN12wk, $n = 2$. A subset of these same pancreas sections was subjected to all further analysis described in this chapter. Islets were identified by immunoperoxidase staining for glucagon. The incidence of dumbbell islets amongst a sample of the total islet population was found to decline quite sharply in the neonatal period (**Table 5.1.** and **Graph 5.1.**).

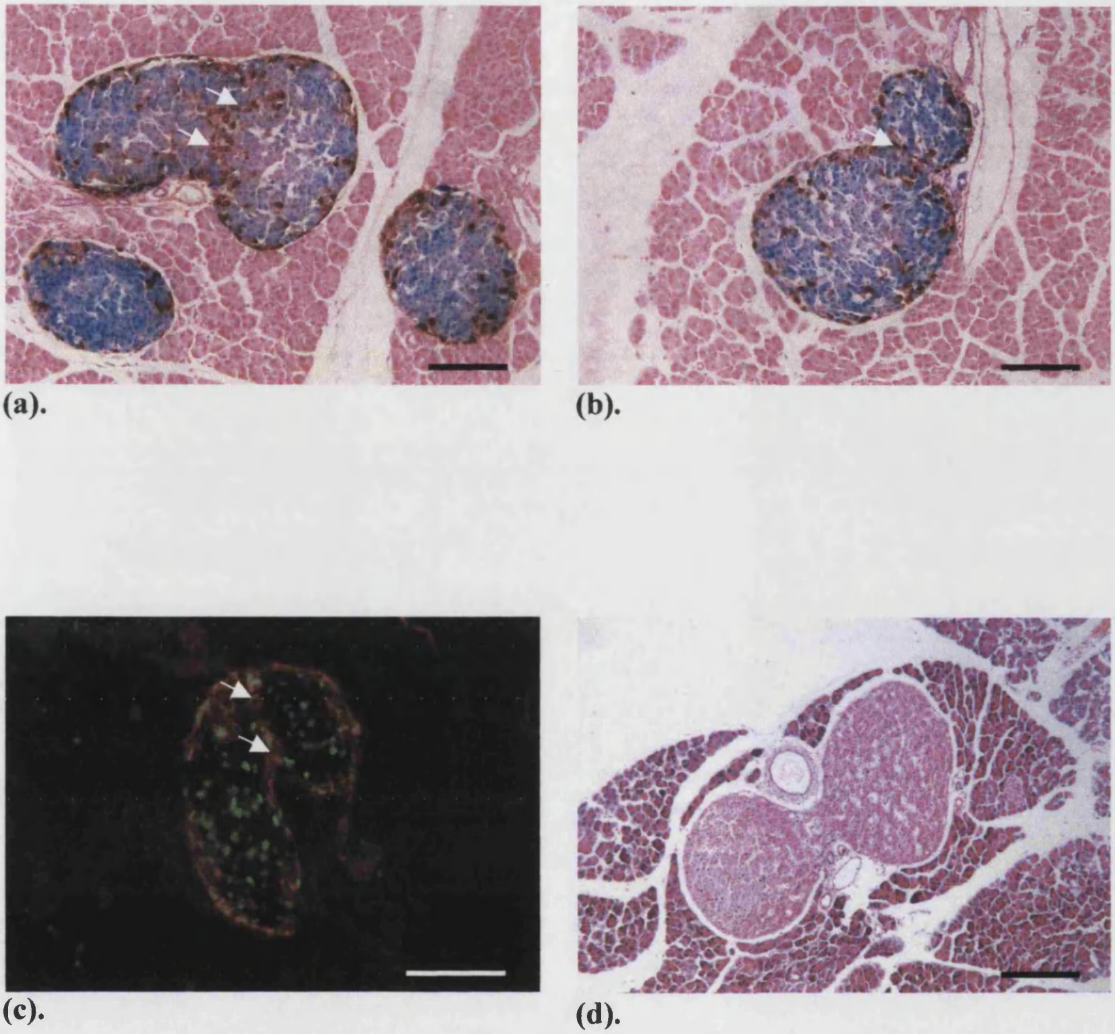

(a). (b).

(c). (d).

Figure 5.1. Dumbbell Islets in Histological Sections

(a) and (b) Paraffin sections of wholemount X-gal-stained PN52wk H253 female hemizygote pancreas immunoperoxidase-stained for glucagon and counterstained with nuclear Fast Red. (c) Frozen section of PN5 H253 female hemizygote pancreas immunofluorescence-stained for glucagon (Texas Red) and β-gal (fluorescein). (d) H & E-stained paraffin section of PN43wk Ripley non-transgenic pancreas (Chapter 6). Non-dumbbell islets also visible in (a). Note neck of glucagon-immunopositive cells in (a), (b) and (c) (arrows)

(a), (b) and (c) Bar = 100 μm; (d) Bar = 200 μm

Graph 5.1. Frequency of Dumbbell Islets with Age

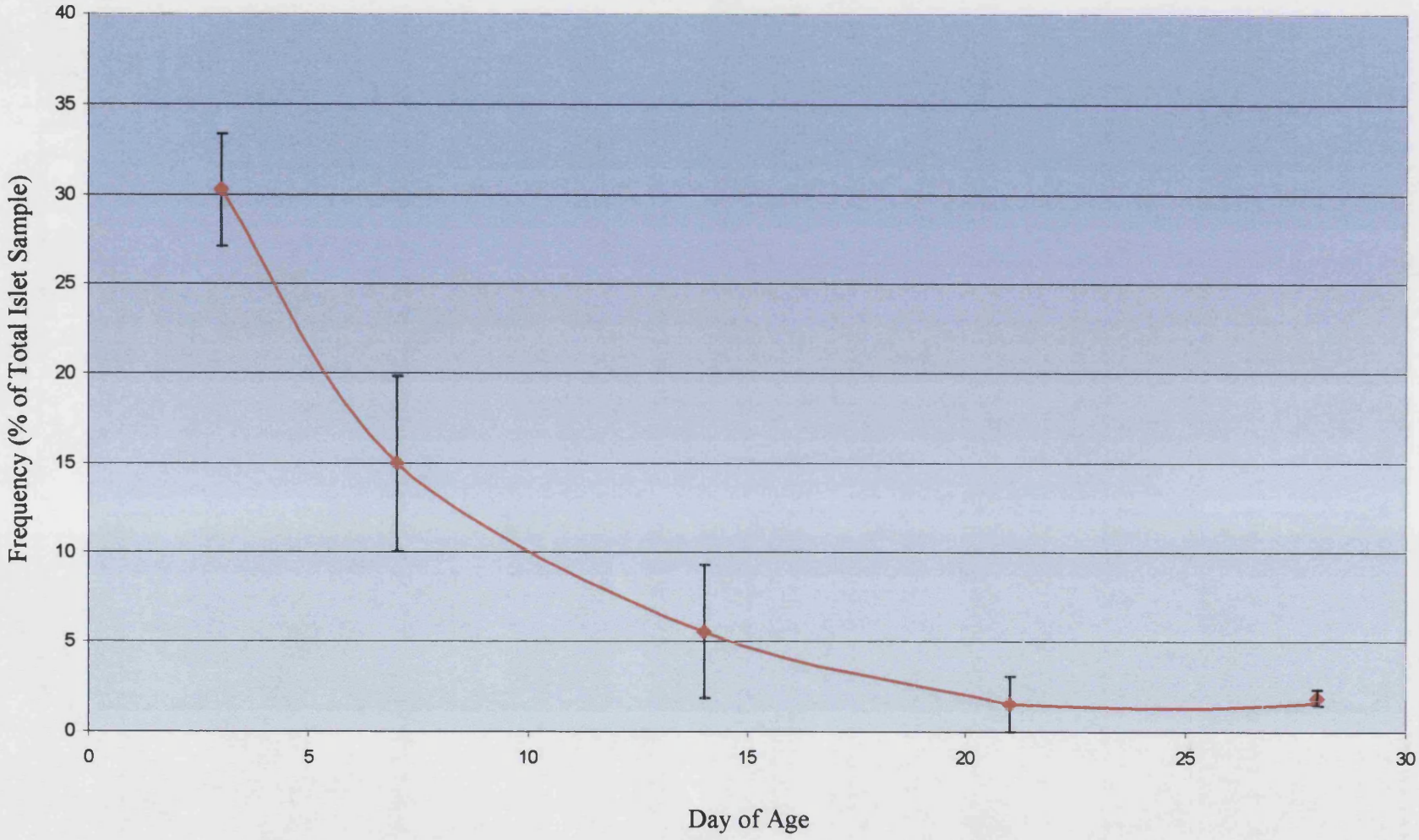

Table 5.1. Frequency of Dumbbell Islets with Age

Age (Days PN)	Dumbbell Islet Frequency (% of Total Sample)	Islet Sample Size, *n*
3	30.2 ± 3.10	55
7	15.0 ± 4.89	95
14	5.56 ± 3.70	58
21	1.54 ± 1.54	80
28	1.87 ± 0.47	783
84	4.17 ± 4.17	41

5.3.3. Computer-Aided 3D Reconstruction from Histological Sections

5.3.3.1. 3D Dumbbell Islet Reconstruction Reveals Dumbbell's Conjoined State

In order to determine the three-dimensional form of such dumbbell islets, the decision was made to conduct a 3D reconstruction of a typical example by computer-driven analysis of images of 2D histological sections. Once a suitable dumbbell islet had been located by examining random histologically-stained paraffin sections, adjacent serial sections through the islet were similarly immunoperoxidase-stained for glucagon. A *z*-stack of serial images of these slices was captured (**Fig. 5.2. (a)-(h)**) and using multiple computer programs, was used to generate a three-dimensional reconstruction. A QuickTime™ movie comprising a 360° rotation around the reconstructed islet was produced (see *Dumbbell* on enclosed **Movies** CD-Rom) and four still images separated by 90° rotations were extracted (**Fig. 5.2. (i)-(iv)**).

The typical dumbbell islet was elongated along one axis in comparison to more characteristic spheroidal islets, representing two ovoid islets in apposition at the "neck" of the dumbbell. The narrowing at the neck also occurred in the third dimension.

5.3.3.2. 3D Reconstruction of PN3 Endocrine Tissue Organisation Reveals Islet Aggregation

The relatively high incidence of dumbbell islets in the immediate neonatal period (**Table 5.1.**) led to the computer-generation of a similar 3D reconstruction of the islet arrangement in the intact pancreas of a PN3 H253 female hemizygous animal. This was achieved in a similar manner to the above. A typical PN3 whole pancreas was identified by analysing paraffin sections of whole X-gal-stained neonate pancreata.

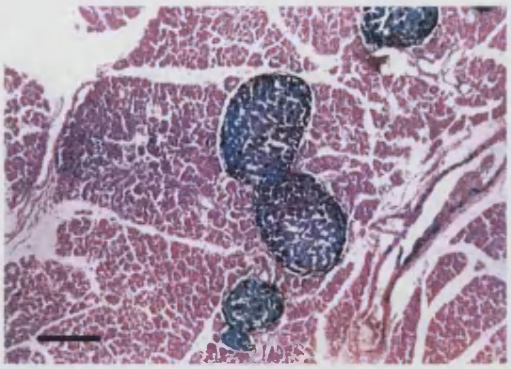

(a).

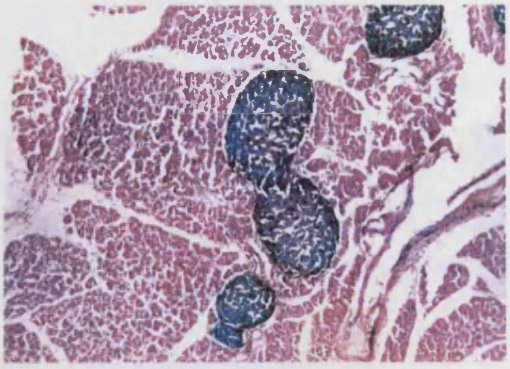

(b).

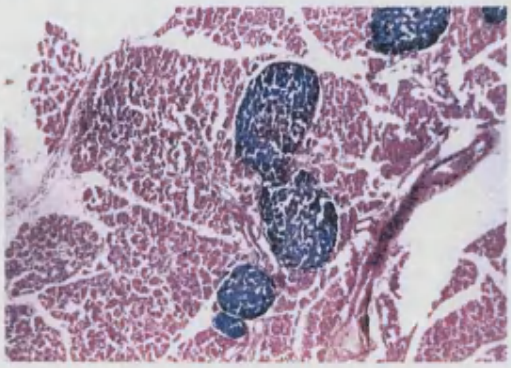

(c).

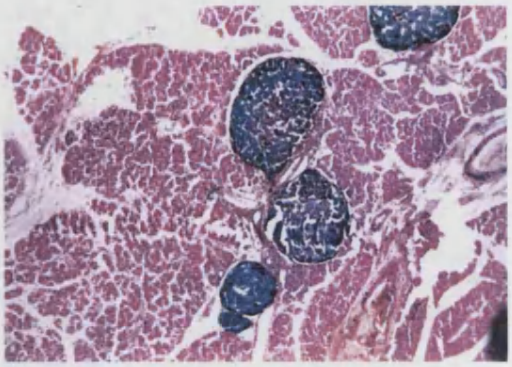

(d).

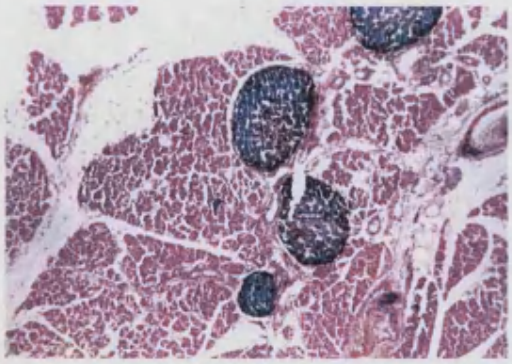

(e).

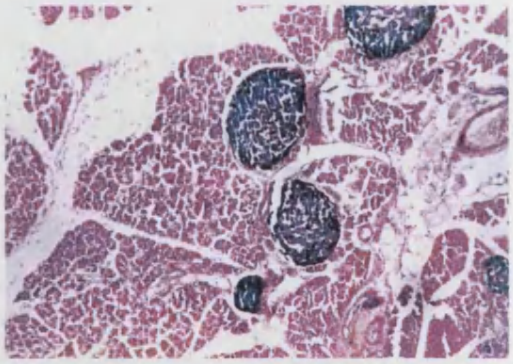

(f).

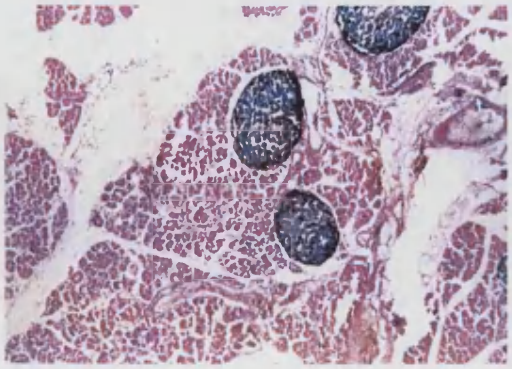

(g).

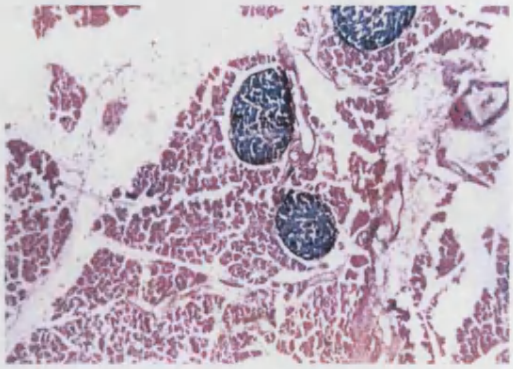

(h).

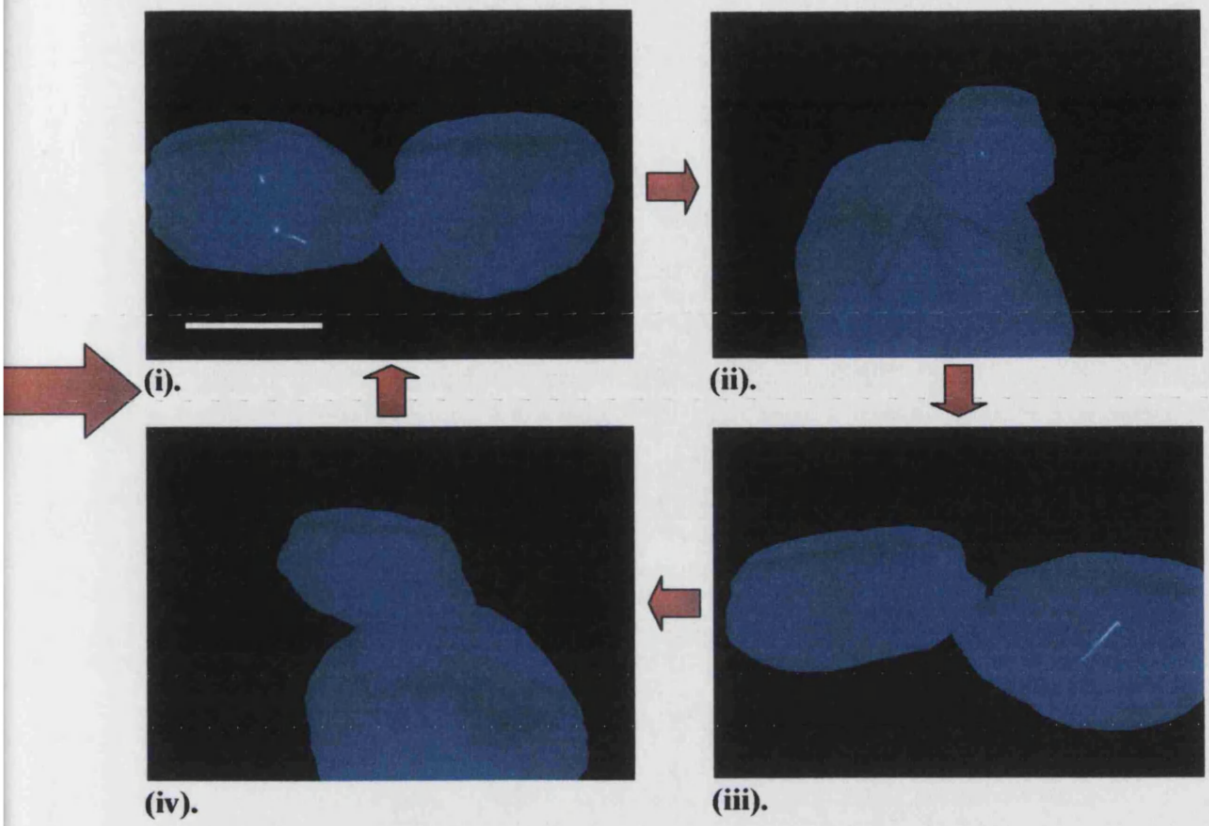

Figure 5.2. Histological Appearance and 3D Computer-Aided Reconstruction of a Typical Dumbbell Islet

Facing page: (a)-(h) Dumbbell islet in serial 7 μm paraffin sections of (wholemount) X-gal-stained pancreas from a PN52wk H253 female hemizygote. Sections immunoperoxidase-stained for glucagon

This page: (i)-(iv) Computer-aided 3D reconstruction of pictured dumbbell islet shown in four aspects separated by a 90° clockwise rotation. See enclosed CD-Rom for full QuickTime™ movie

Bar = 200 μm in both cases

Adjacent serial sections through the entire pancreas were then immunoperoxidase-stained for glucagon and from a *z*-stack of consecutive images (**Fig. 5.3. (a)-(d)**), two 3D reconstructions were generated (see *Exposed PN3 Islets* and *Shrouded PN3 Islets* on **Movies** CD-Rom and stills in **Fig. 5.3. (i)-(iv)**). The first of these shows the exposed islet arrangement whilst in the second reconstruction this islet arrangement is shrouded by the surrounding acinar tissue of the pancreas. The opacity of the representation of the surrounding tissue was necessarily reduced to permit islet visibility to be retained.

The neonatal islets were aggregated in almost a single mass of endocrine tissue confined to one extremity of the pancreas tissue with approximately five dissociated islet groups located in close proximity. Islets in the main mass appeared to be arranged in a bifurcating pattern; three "branches" of islet tissue diverged from a single "trunk".

5.3.4. Analysis of β-Gal-Labelled and Unlabelled Cell Composition of Dumbbell and Non-Dumbbell Islets

To test the hypotheses that (1) dumbbell islets represented a parent islet in a state of division or fission and (2) such islet fission is a mode of islet production in the murine pancreas, islet β-gal$^+$ and β-gal$^-$ cell composition was next analysed in the paraffin sections of X-gal-stained pancreas tissue from the PN3-PN84/12wk H253 hemizygous female mice of Time-Series One (**Chapter 4**). *n*, the number of animals examined at each time-point, was PN3, $n = 2$; PN7, $n = 2$; PN14, $n = 1$; PN21, $n = 1$; PN28, $n = 1$ and PN12wk, $n = 1$. Over this age-range, the islets are undergoing the putative shift from a heterogeneous to a homogeneous cell composition (**Chapter 4**). The rationale for the cell composition analysis is that in any given H253 female hemizygous animal, there will be some variability in the cell composition of the islets. If the two parts or "sides" of a dumbbell are very similar in composition this suggests fission of one large islet, while if the two sides are as different as random islet pairs, it suggests the amalgamation or fusion of two islets.

The number of labelled and unlabelled cells was determined for the two sides of each dumbbell islet identified in each of between one and four histochemically-stained paraffin sections from each PN3-PN84 H253 hemizygous female pancreas. Cell composition was generally determined from sections under the microscope although larger specimens were scored from hard copies of images. Each islet subjected to analysis in this way was scored from only a single cross-section through its volume. The percentage of β-gal$^+$ cells was then calculated separately for both sides of each

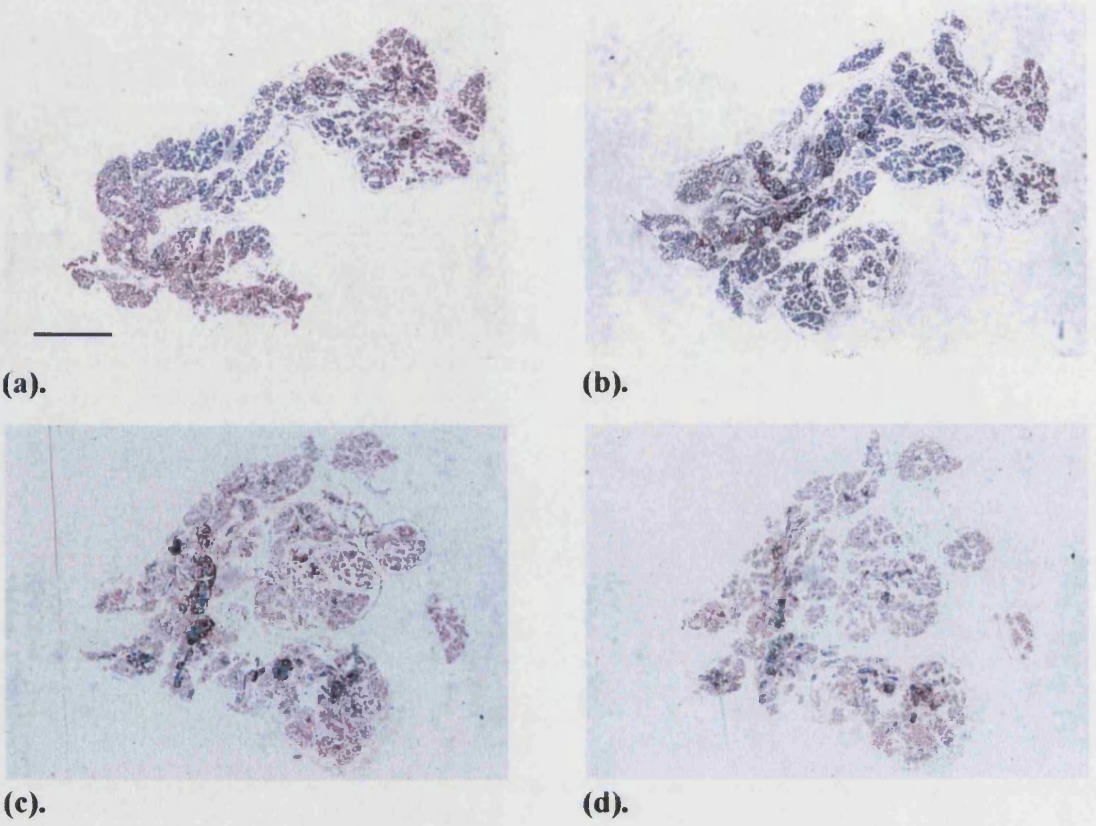

Figure 5.3. Histological Appearance and 3D Computer-Aided Reconstruction of Neonatal (PN3) Endocrine Tissue Organisation

This page: (a)-(d) Islet arrangement in four sample 7 μm paraffin sections of (wholemount) X-gal-stained pancreas from a PN3 H253 female hemizygote Sections immunoperoxidase-stained for glucagon. Bar = 500 μm

Facing page: Top panel: (i)-(iv) Computer-aided 3D reconstruction of pictured islet organisation shown in four aspects separated by a 90° clockwise rotation. Bar = 250 μm
Lower panel: (i)-(iv) Above reconstructed endocrine arrangement shrouded by surrounding acinar tissue (navy blue). Bar = 500 μm
See enclosed CD-Rom for full QuickTime™ movies

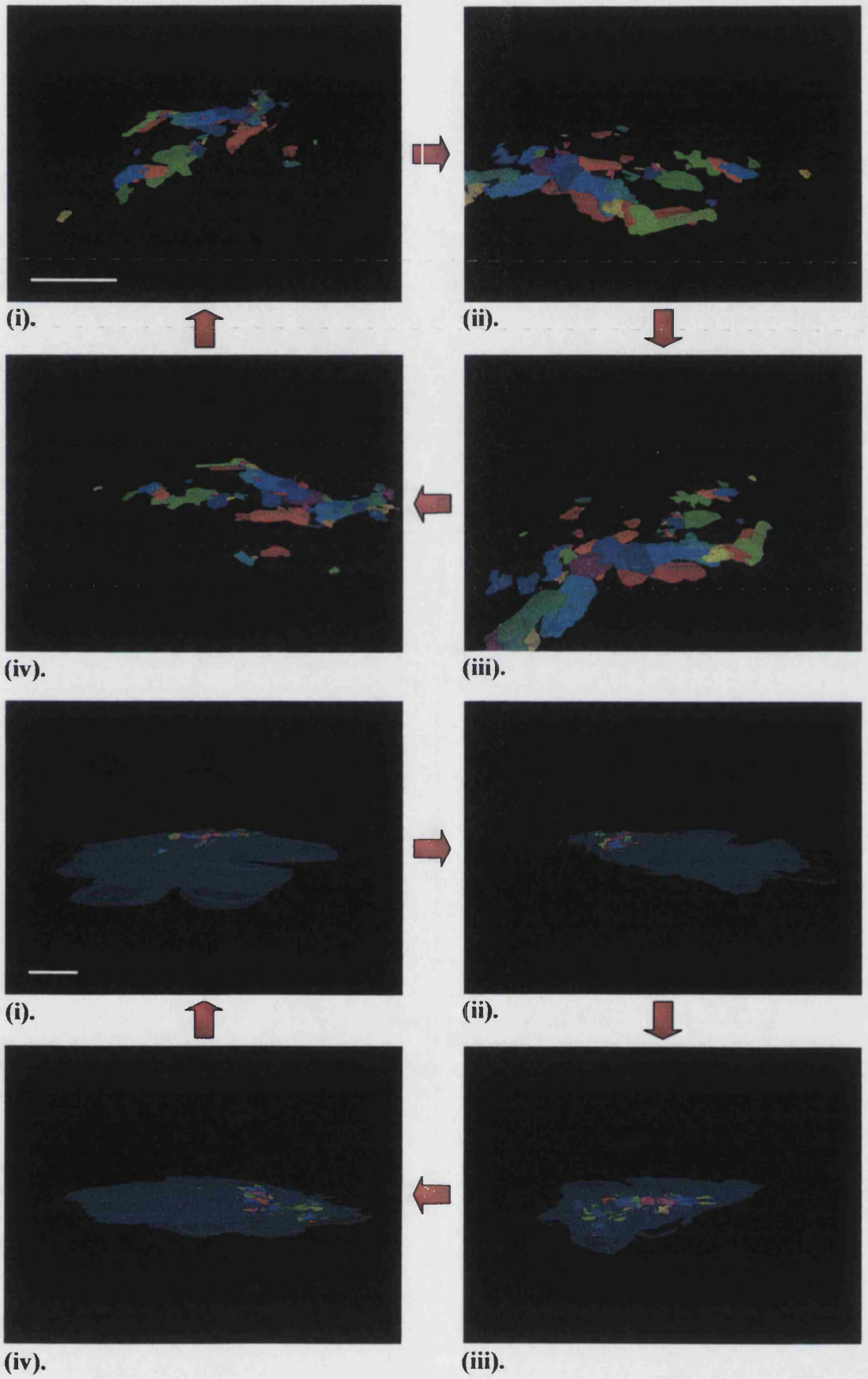
(i).
(ii).
(iv).
(iii).
(i).
(ii).
(iv).
(iii).

dumbbell as: (number of β-gal$^+$ cells/total number of β-gal$^+$ + β-gal$^-$ cells) × 100. Percentage similarity in β-gal$^+$/β-gal$^-$ cell composition between the two sides of each of the 23 identified dumbbells was then calculated as: 100 - difference in percentage β-gal$^+$ cells (**Fig. 5.4.** and **Table 5.2.**). It should be noted that this value is the same regardless of whether it is calculated by subtracting from 100 the difference in percentage of β-gal$^+$ cells or the difference in percentage of β-gal$^-$ cells. In each of the dumbbell-containing sections, cell composition and percentage of β-gal$^+$ cells was similarly scored in a random sample of non-dumbbell pairs and the "edge-to-edge" and "centre-to-centre" inter-islet distances between each of the two islets in the pair determined (**Fig. 5.4.**). Again, cell composition analysis was restricted to only a single cross-section through each of the selected islets. Percentage similarity in β-gal$^+$/β-gal$^-$ cell composition between the two non-dumbbell islets of each of 65 islet pairs was calculated as for the two sides of each dumbbell islet (**Fig. 5.4.** and **Table 5.3.**).

5.3.4.1. High Similarity in Cell Composition Between the Two Sides of a Dumbbell

Similarity in labelled/unlabelled cell composition between the two parts of each dumbbell islet was first analysed. Each of the two parts of each dumbbell islet was assigned either "side 1" or "side 2" arbitrarily. Linear regression of percentage β-gal$^+$ cell composition of side 1 against percentage β-gal$^+$ cell composition of side 2 (Minitab™ v. 13 statistical software package) yielded a significant positive correlation (**Graph 5.2.**); R^2 = 76.3 %, R^2_a = 75.2 %. R^2 is the *coefficient of determination* for a multiple regression or correlation and is considered to be a measure of "goodness of fit" of a given regression model although R^2_a, the *adjusted coefficient of determination*, gives a more accurate measure of this. The Spearman rank correlation coefficient r_s (Spearman, 1904) for non-normal data was calculated to test for a correlation (**Table 5.4.**). There was found to be a significant positive correlation between the percentage β-gal$^+$ cell composition of side 1 and the percentage β-gal$^+$ cell composition of side 2 for the 23 dumbbell islets; calculated $r_s = 0.742$; $(r_s)_{0.05(2),\,23} = 0.415$, so H_0 was rejected.

5.3.4.2. Cell Composition Similarity of Two Islets is Inversely Related to their Separation

Next, similarity in cell composition between the 65 non-dumbbell islet pairs

Figure 5.4. Calculating Percentage Similarity of β-Gal$^+$/β-Gal$^-$ Cell Composition Between the Two Sides of a Dumbbell Islet and Between Two Random Non-Dumbbell Islets

Dumbbell Islet

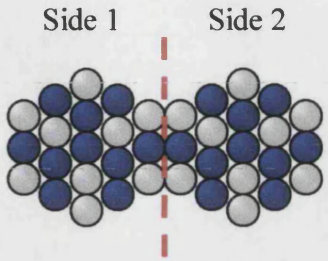

% β-gal$^+$ cells = $\frac{10}{9+10} \times 100$ = 52.6 %

% β-gal$^+$ cells = $\frac{10}{9+10} \times 100$ = 52.6 %

So, % similarity in β-gal$^+$/β-gal$^-$ cell composition = 100 - (52.6-52.6) = 100 %

Non-Dumbbell Islet Pair

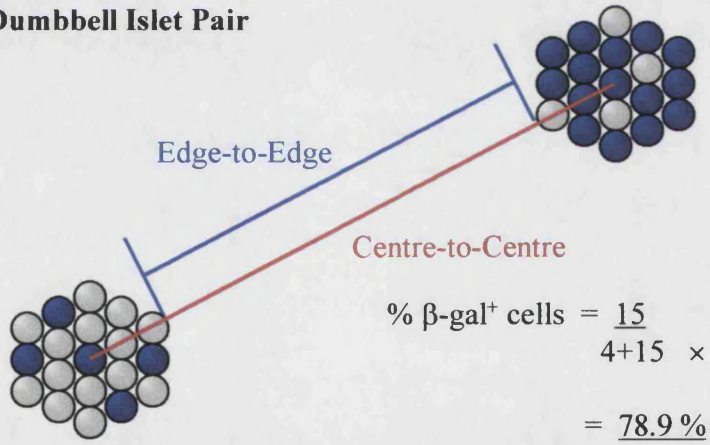

% β-gal$^+$ cells = $\frac{15}{4+15} \times 100$ = 78.9 %

% β-gal$^+$ cells = $\frac{5}{14+5} \times 100$ = 26.3 %

So, % similarity in β-gal$^+$/β-gal$^-$ cell composition = 100 - (78.9-26.3) = 47.4 %

Table 5.2. β-Gal$^+$ and β-Gal$^-$ Cell Composition of the Two Sides of Dumbbell Islets and Percentage Similarity Between the Two (n = 23)

DUMBBELL ISLET SIDE 1			DUMBBELL ISLET SIDE 2			% Cell Composition Similarity
β-Gal$^+$	β-Gal$^-$	% β-Gal$^+$	β-Gal$^+$	β-Gal$^-$	% β-Gal$^+$	
109	104	51.17	70	106	39.77	88.6
23	36	38.98	14	17	45.16	93.82
30	154	16.3	64	164	28.07	88.23
114	148	43.51	76	95	44.44	99.07
76	108	41.3	76	53	58.91	82.39
124	82	60.19	30	39	43.48	83.29
95	22	81.2	68	23	74.73	93.53
35	19	64.81	35	21	62.5	97.69
127	91	58.26	129	81	61.43	96.83
34	16	68	61	31	66.3	98.3
42	28	60	45	18	71.43	88.57
56	70	44.44	79	72	52.32	92.12
35	34	50.72	81	38	68.07	82.65
73	71	50.69	63	62	50.4	99.71
71	28	71.72	84	66	56	84.28
49	46	51.58	23	23	50	98.42
46	104	30.67	16	71	18.39	87.72
46	38	54.76	61	40	60.4	94.36
13	7	65	12	15	44.44	79.44
29	54	34.94	20	45	30.77	95.83
230	11	95.44	238	3	98.76	96.68
188	14	93.07	437	9	97.98	95.09
147	4	97.35	762	68	91.81	94.46

Table 5.3. β-Gal$^+$ and β-Gal$^-$ Cell Composition of Two Non-Dumbbell Islets, Percentage Similarity Between them and Inter-Islet Distance (Edge-to-Edge) Between the Two (n = 65)

Interislet Distance (μm)	ISLET 1			ISLET 2			% Cell Composition Similarity
	β-Gal$^+$	β-Gal$^-$	% β-Gal$^+$	β-Gal$^+$	β-Gal$^-$	% β-Gal$^+$	
654.7	46	15	75.41	16	38	29.63	54.22
107.1	35	47	42.68	18	0	100	42.68
1086.2	20	33	37.74	55	42	56.7	81.04
54.8	5	81	5.814	17	109	13.49	92.32
31.1	22	17	56.41	21	7	75	81.41
1011.8	17	18	48.57	9	21	30	81.43
425	31	49	38.75	44	35	55.7	83.05
95.9	49	56	46.67	43	49	46.74	99.93
530	52	33	61.18	56	30	65.12	96.06
114.5	75	45	62.5	38	5	88.37	74.13
224.1	32	13	71.11	138	95	59.23	88.12
982.1	27	30	47.37	135	78	63.38	83.99
714.2	36	17	67.92	36	44	45	77.08
39.8	30	38	44.12	30	30	50	94.12
24.9	24	58	29.27	24	82	22.64	93.37
1259.8	34	69	33.01	13	52	20	86.99
7.47	34	50	40.48	49	57	46.23	94.25
649.8	47	37	55.95	49	37	56.98	98.97
320	98	56	63.64	36	85	29.75	66.11
19.9	27	12	69.23	22	11	66.67	97.44
734.1	19	6	76	81	49	62.31	86.31
89.6	58	84	40.85	58	86	40.28	99.43
64.7	247	7	97.24	61	0	100	97.24
139.4	112	0	100	76	0	100	100
79.7	328	16	95.35	74	4	94.87	99.52
174.3	43	5	89.58	38	0	100	89.58
430	148	6	96.1	33	2	94.29	98.19
5420	632	0	100	0	80	0	0
2420	69	2	97.18	0	348	0	2.82
1071.4	123	8	93.89	14	11	56	62.11
154.4	22	54	28.95	424	26	94.22	65.27
907.7	28	123	18.54	358	69	83.84	34.7
1408.6	4	13	23.53	12	37	24.49	99.04
42.3	0	18	0	3	12	20	80
29.9	22	32	40.74	17	49	25.76	85.02
744	21	4	84	13	57	18.57	34.57
390	39	27	59.09	92	155	37.25	78.16
234.1	39	67	36.79	64	159	28.7	91.91
14.9	33	11	75	45	25	64.29	89.29
808.5	19	80	19.19	20	20	50	69.19
75.9	10	19	34.48	10	24	29.41	94.93
1011.8	14	14	50	7	16	30.43	80.43
4.98	37	45	45.12	44	45	49.44	95.68
615	5	5	50	36	23	61.02	88.98

67.2	27	22	55.1	78	167	31.84	76.74
892.8	73	48	60.33	17	20	45.95	85.62
714.2	36	42	76.31	44	19	69.84	76.31
26.1	47	47	50	10	6	62.5	87.5
78.4	14	9	60.87	16	7	69.57	91.3
405	29	26	52.73	35	66	34.65	81.92
902.7	11	47	18.97	17	15	53.13	65.84
1121	14	58	19.44	98	94	51.04	68.4
52.3	32	90	26.23	64	203	23.97	97.74
525	84	74	53.16	30	28	51.72	98.56
395	8	1	88.89	24	45	34.78	45.89
244	73	45	92.63	9	4	69.23	92.63
27.4	6	13	31.58	29	47	38.16	93.42
725	46	75	38.02	33	22	60	78.02
1720	27	38	41.54	37	37	50	91.54
140	102	95	51.78	303	169	64.19	87.59
672.5	4	49	7.547	5	74	6.329	98.78
273.9	115	23	83.33	132	162	44.9	61.57
1061.4	15	234	6.02	91	178	33.83	72.19
143.2	4	5	44.44	7	12	36.84	92.4
694.4	0	18	0	43	50	46.24	53.76

NB: Centre-to-centre inter-islet distances were not recorded as the data was not subjected to any analysis

Graph 5.2. Relationship Between the Percentages of β-Gal$^+$ Cells in the Two Sides of Each of 23 Dumbbell Islets

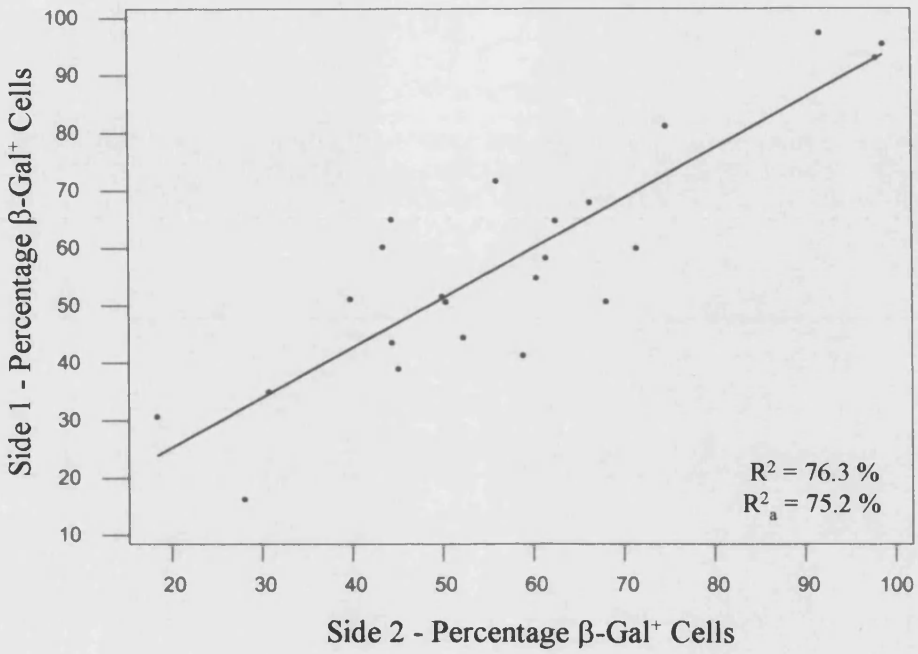

Table 5.4. Calculation of the Spearman Rank Correlation Coefficient r_s to Test for a Correlation Between the Percentage β-Gal$^+$ Cell Composition of Side 1 Against Percentage β-Gal$^+$ Cell Composition of Side 2 of Dumbbell Islets (n = 23)

DUMBBELL ISLET SIDE 1		DUMBBELL ISLET SIDE 2		d_i (X_i - Y_i)	d_i^2
% β-Gal$^+$ (X_i)	Rank of X_i	% β-Gal$^+$ (Y_i)	Rank of Y_i		
51.17	10	39.77	4	6	36
38.98	4	45.16	8	-4	16
16.3	1	28.07	2	-1	1
43.51	6	44.44	6.5	-0.5	0.25
41.3	5	58.91	13	-8	64
60.19	15	43.48	5	10	100
81.2	20	74.73	20	0	0
64.81	16	62.5	16	0	0
58.26	13	61.43	15	-2	4
68	18	66.3	17	1	1
60	14	71.43	19	-5	25
44.44	7	52.32	11	-4	16
50.72	9	68.07	18	-9	81
50.69	8	50.4	10	-2	4
71.72	19	56	12	7	49
51.58	11	50	9	2	4
30.67	2	18.39	1	1	1
54.76	12	60.4	14	-2	4
65	17	44.44	6.5	10.5	110.25
34.94	3	30.77	3	0	0
95.44	22	98.76	23	-1	1
93.07	21	97.98	22	-1	1
97.35	23	91.81	21	2	4
				$\sum d_i^2$	**522.5**

Spearman rank correlation coefficient, $r_s = 1 - \frac{6 \times (\sum d_i^2)}{n^3 - n}$

$$\therefore r_s = 1 - \frac{6 \times 522.5}{23^3 - 23} = 1 - \frac{3135}{12167 - 23}$$

$$\therefore r_s = 1 - \frac{3135}{12144} = 1 - 0.258 = \underline{0.742}$$

$(r_s)_{0.05(2),\,23} = 0.415$, so H_0 is rejected. There is a significant positive correlation between the percentage β-gal$^+$ cell composition of side 1 and the percentage β-gal$^+$ cell composition of side 2 for the identified dumbbell islets.

with inter-islet (edge-to-edge) distance between each pair was investigated. A linear regression plot was generated (Minitab™ v. 13) for similarity of cell composition against inter-islet distance (**Graph 5.3.**); R^2 = 38.6 %, R^2_a = 37.7 %. r_s was again calculated (**Table 5.5.**). There was found to be a significant negative correlation between the similarity in cell composition between two non-dumbbell islets and the distance between them; calculated r_s = -0.441; $(r_s)_{0.05(2),\ 65}$ = 0.244, so H_0 was rejected. As the plot (**Graph 5.3.**) revealed the existence of two outlying data points (outlier A = 5420 μm inter-islet distance/0 % cell composition similarity and outlier B = 2420 μm inter-islet distance/2.82 % cell composition similarity) outside the main body of data, a second regression plot was produced excluding both of these two outliers (**Graph 5.4.**); R^2 = 7.3 %, R^2_a = 5.7 %. r_s was then calculated for this smaller data set (**Table 5.6.**). There was found to be a slightly weaker although still significant negative correlation between the similarity in cell composition between two non-dumbbells and their distance of separation; calculated r_s = -0.387; $(r_s)_{0.05(2),\ 63}$ = 0.248, so H_0 was rejected. Two further regression plots were then generated excluding *either* outlier A alone (**Graph 5.5.**; R^2 = 21.3 %, R^2_a = 20.0 %) *or* outlier B alone (**Graph 5.6.**; R^2 = 32.6 %, R^2_a = 31.5 %). r_s was then calculated for the data set excluding outlier A (**Table 5.7.**) and for the data set excluding outlier B (**Table 5.8.**). The removal of either outlier alone gave the same value for r_s of -0.415, and since $(r_s)_{0.05(2),\ 64}$ = 0.246 then this gave a significant negative correlation of intermediate strength between that calculated for the complete data set and that determined for the same data set excluding *both* outliers. Clearly, even in the absence of the two outliers which strengthen the correlation, there is a significant negative correlation between the similarity in cell composition between two non-dumbbell islets and the distance between them.

5.3.4.3. Mean Cell Composition Similarity of the Two Sides of a Dumbbell Islet Agrees with that for Two Non-Dumbbells at Zero Separation

The *y*-intercepts of 89.3 % (whole data set), 87.0 % (data set excluding *both* outliers), 89.7 % (data set excluding outlier A) and 88.7 % (data set excluding outlier B) on the linear regression plots (**Graphs 5.3.** to **5.6.**) represent the percentage similarity of cell composition between islets whose edges are separated by zero distance. Dumbbell islets comply with such a criterion; mean percentage similarity of cell composition between the two sides of the 23 dumbbell islets at 91.8 %, is in very close accordance with these values.

Graph 5.3. Relationship Between Percentage Similarity of β-Gal$^+$/ β-Gal$^-$ Cell Composition of Two Non-Dumbbell Islets with Edge-to-Edge Inter-Islet Distance (*n* = 65 Pairs)

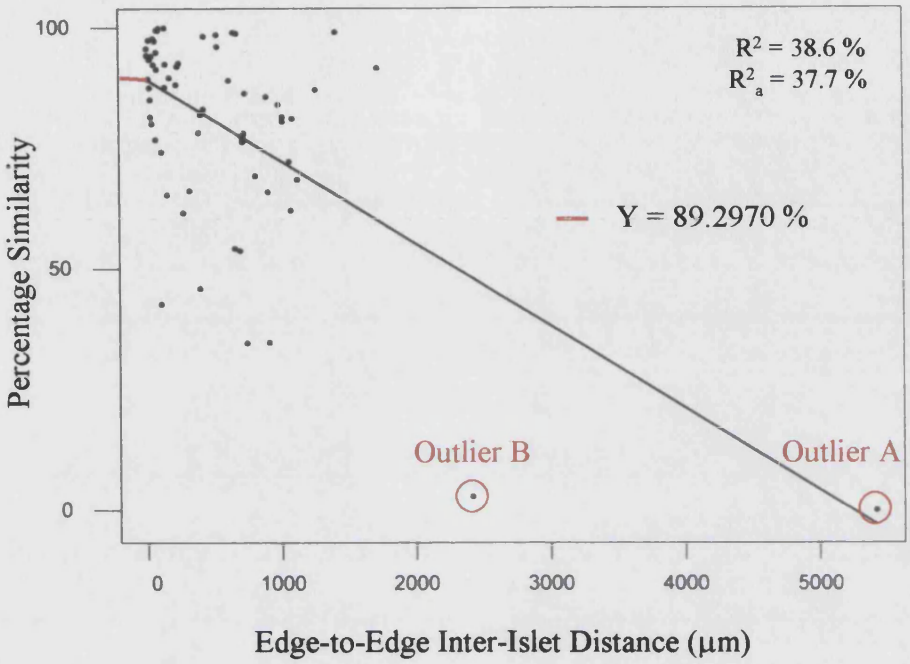

Graph 5.4. Relationship Between Percentage Similarity of β-Gal$^+$/ β-Gal$^-$ Cell Composition of Two Non-Dumbbell Islets with Edge-to-Edge Inter-Islet Distance (*Both* Outliers A *and* B Excluded; *n* = 63 Pairs)

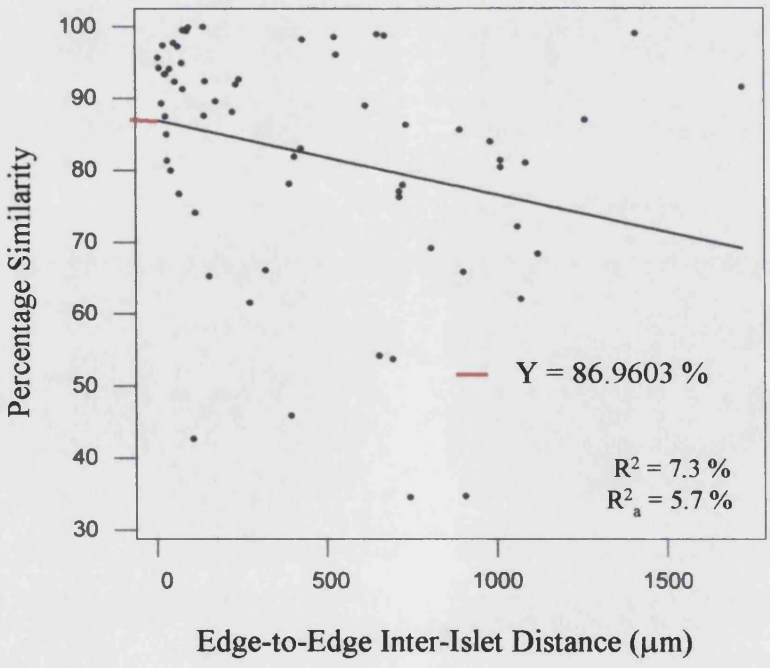

Table 5.5. Calculation of the Spearman Rank Correlation Coefficient r_s to Test for a Correlation Between the Similarity in Cell Composition Between Non-Dumbbell Islet Pairs with Inter-Islet (Edge-to-Edge) Distance Between Each Pair (n = 65)

Distance (μm) (X_i)	Rank of X_i	% Cell Composition Similarity (Y_i)	Rank of Y_i	d_i (X_i - Y_i)	d_i^2
654.7	42	54.22	8	34	1156
107.1	21	42.68	5	16	256
1086.2	59	81.04	25	34	1156
54.8	13	92.32	44	-31	961
31.1	9	81.41	26	-17	289
1011.8	55.5	81.43	27	28.5	812.25
425	36	83.05	29	7	49
95.9	20	99.93	64	-44	1936
530	39	96.06	53	-14	196
114.5	22	74.13	17	5	25
224.1	28	88.12	37	-9	81
982.1	54	83.99	30	24	576
714.2	45.5	77.08	20	25.5	650.25
39.8	10	94.12	49	-39	1521
24.9	5	93.37	47	-42	1764
1259.8	61	86.99	34	27	729
7.47	2	94.25	50	-48	2304
649.8	41	98.97	60	-19	361
320	32	66.11	13	19	361
19.9	4	97.44	55	-51	2601
734.1	48	86.31	33	15	225
89.6	19	99.43	62	-43	1849
64.7	14	97.24	54	-40	1600
139.4	23	100	65	-42	1764
79.7	18	99.52	63	-45	2025
174.3	27	89.58	40	-13	169
430	37	98.19	57	-20	400
5420	65	0	1	64	4096
2420	64	2.82	2	62	3844
1071.4	58	62.11	10	48	2304
154.4	26	65.27	11	15	225
907.7	53	34.7	4	49	2401
1408.6	62	99.04	61	1	1
42.3	11	80	23	-12	144
29.9	8	85.02	31	-23	529
744	49	34.57	3	46	2116
390	33	78.16	22	11	121
234.1	29	91.91	43	-14	196
14.9	3	89.29	39	-36	1296
808.5	50	69.19	15	35	1225
75.9	16	94.93	51	-35	1225
1011.8	55.5	80.43	24	31.5	992.25
4.98	1	95.68	52	-51	2601

615	40	88.98	38	2	4
67.2	15	76.74	19	-4	16
892.8	51	85.62	32	19	361
714.2	45.5	76.31	18	27.5	756.25
26.1	6	87.5	35	-29	841
78.4	17	91.3	41	-24	576
405	35	81.92	28	7	49
902.7	52	65.84	12	40	1600
1121	60	68.4	14	46	2116
52.3	12	97.74	56	-44	1936
525	38	98.56	58	-20	400
395	34	45.89	6	28	784
244	30	92.63	46	-16	256
27.4	7	93.42	48	-41	1681
725	47	78.02	21	26	676
1720	63	91.54	42	21	441
140	24	87.59	36	-12	144
672.5	43	98.78	59	-16	256
273.9	31	61.57	9	22	484
1061.4	57	72.19	16	41	1681
143.2	25	92.4	45	-20	400
694.4	44	53.76	7	37	1369
				$\sum d_i^2$	**65960**

Spearman rank correlation coefficient, $r_s = 1 - \frac{6 \times (\sum d_i^2)}{n^3 - n}$

$$\therefore r_s = 1 - \frac{6 \times 65960}{65^3 - 65}$$

$$\therefore r_s = 1 - \frac{395760}{274625 - 65}$$

$$\therefore r_s = 1 - \frac{395760}{274560}$$

$$\therefore r_s = 1 - 1.441$$

$$\therefore r_s = \underline{-0.441}$$

$(r_s)_{0.05(2),\,65} = 0.244$, so H_0 is rejected. There is a significant negative correlation between the similarity in cell composition between two non-dumbbell islets and the distance between them; calculated $r_s = -0.441$.

Table 5.6. Calculation of the Spearman Rank Correlation Coefficient r_s to Test for a Correlation Between the Similarity in Cell Composition Between Non-Dumbbell Islet Pairs with Inter-Islet (Edge-to-Edge) Distance Between Each Pair (Excluding *Both* of the Two Outliers from the Data Set Used in Table 5.5.; $n = 63$)

Distance (μm) (X_i)	Rank of X_i	% Cell Composition Similarity (Y_i)	Rank of Y_i	d_i ($X_i - Y_i$)	d_i^2
654.7	42	54.22	6	36	1296
107.1	21	42.68	3	18	324
1086.2	59	81.04	23	36	1296
54.8	13	92.32	42	-29	841
31.1	9	81.41	24	-15	225
1011.8	55.5	81.43	25	30.5	930.25
425	36	83.05	27	9	81
95.9	20	99.93	62	-42	1764
530	39	96.06	51	-12	144
114.5	22	74.13	15	7	49
224.1	28	88.12	35	-7	49
982.1	54	83.99	28	26	676
714.2	45.5	77.08	18	27.5	756.25
39.8	10	94.12	47	-37	1369
24.9	5	93.37	45	-40	1600
1259.8	61	86.99	32	29	841
7.47	2	94.25	48	-46	2116
649.8	41	98.97	58	-17	289
320	32	66.11	11	21	441
19.9	4	97.44	53	-49	2401
734.1	48	86.31	31	17	289
89.6	19	99.43	60	-41	1681
64.7	14	97.24	52	-38	1444
139.4	23	100	63	-40	1600
79.7	18	99.52	61	-43	1849
174.3	27	89.58	38	-11	121
430	37	98.19	55	-18	324
1071.4	58	62.11	8	50	2500
154.4	26	65.27	9	17	289
907.7	53	34.7	2	51	2601
1408.6	62	99.04	59	3	9
42.3	11	80	21	-10	100
29.9	8	85.02	29	-21	441
744	49	34.57	1	48	2304
390	33	78.16	20	13	169
234.1	29	91.91	41	-12	144
14.9	3	89.29	37	-34	1156
808.5	50	69.19	13	37	1369
75.9	16	94.93	49	-33	1089
1011.8	55.5	80.43	22	33.5	1122.25
4.98	1	95.68	50	-49	2401
615	40	88.98	36	4	16

67.2	15	76.74	17	-2	4
892.8	51	85.62	30	21	441
714.2	45.5	76.31	16	29.5	870.25
26.1	6	87.5	33	-27	729
78.4	17	91.3	39	-22	484
405	35	81.92	26	9	81
902.7	52	65.84	10	42	1764
1121	60	68.4	12	48	2304
52.3	12	97.74	54	-42	1764
525	38	98.56	56	-18	324
395	34	45.89	4	30	900
244	30	92.63	44	-14	196
27.4	7	93.42	46	-39	1521
725	47	78.02	19	28	784
1720	63	91.54	40	23	529
140	24	87.59	34	-10	100
672.5	43	98.78	57	-14	196
273.9	31	61.57	7	24	576
1061.4	57	72.19	14	43	1849
143.2	25	92.4	43	-18	324
694.4	44	53.76	5	39	1521
				Σd_i^2	**57768**

Spearman rank correlation coefficient, $r_s = 1 - \frac{6 \times (\Sigma d_i^2)}{n^3 - n}$

$$\therefore r_s = 1 - \frac{6 \times 57768}{63^3 - 63}$$

$$\therefore r_s = 1 - \frac{346608}{250047 - 63}$$

$$\therefore r_s = 1 - \frac{346608}{249984}$$

$$\therefore r_s = 1 - 1.387$$

$$\therefore r_s = \underline{-0.387}$$

$(r_s)_{0.05(2),\,63} = 0.248$, so H_0 is rejected. There is a significant negative correlation between the similarity in cell composition between two non-dumbbell islets and the distance between them; calculated $r_s = -0.387$.

Graph 5.5. Relationship Between Percentage Similarity of β-Gal$^+$/ β-Gal$^-$ Cell Composition of Two Non-Dumbbell Islets with Edge-to-Edge Inter-Islet Distance (Outlier A - 5420 μm/0 % - Excluded; *n* = 64 Pairs)

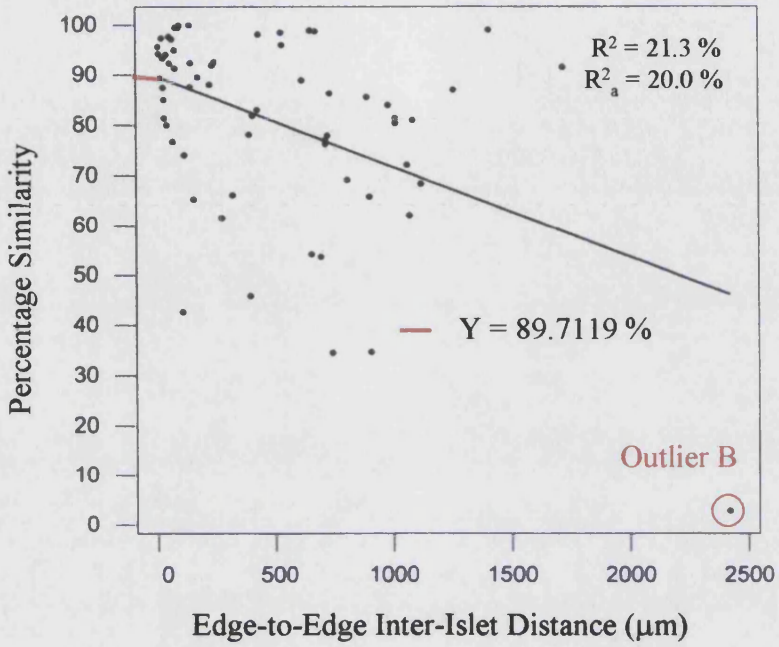

Graph 5.6. Relationship Between Percentage Similarity of β-Gal$^+$/ β-Gal$^-$ Cell Composition of Two Non-Dumbbell Islets with Edge-to-Edge Inter-Islet Distance (Outlier B - 2420 μm/2.82 % - Excluded; *n* = 64 Pairs)

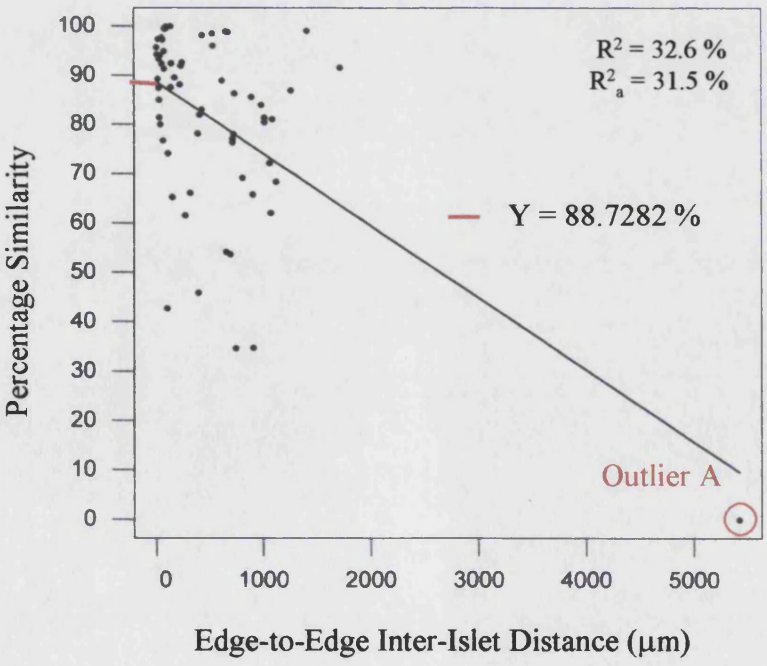

Table 5.7. Calculation of the Spearman Rank Correlation Coefficient r_s to Test for a Correlation Between the Similarity in Cell Composition Between Non-Dumbbell Islet Pairs with Inter-Islet (Edge-to-Edge) Distance Between Each Pair (Excluding *Only* Outlier A - 5420 μm/0 % - from the Data Set Used in Table 5.5.; $n = 64$)

Distance (μm) (X_i)	Rank of X_i	% Cell Composition Similarity (Y_i)	Rank of Y_i	d_i ($X_i - Y_i$)	d_i^2
654.7	42	54.22	7	35	1225
107.1	21	42.68	4	17	289
1086.2	59	81.04	24	35	1225
54.8	13	92.32	43	-30	900
31.1	9	81.41	25	-16	256
1011.8	55.5	81.43	26	29.5	870.25
425	36	83.05	28	8	64
95.9	20	99.93	63	-43	1849
530	39	96.06	52	-13	169
114.5	22	74.13	16	6	36
224.1	28	88.12	36	-8	64
982.1	54	83.99	29	25	625
714.2	45.5	77.08	19	26.5	702.25
39.8	10	94.12	48	-38	1444
24.9	5	93.37	46	-41	1681
1259.8	61	86.99	33	28	784
7.47	2	94.25	49	-47	2209
649.8	41	98.97	59	-18	324
320	32	66.11	12	20	400
19.9	4	97.44	54	-50	2500
734.1	48	86.31	32	16	256
89.6	19	99.43	61	-42	1764
64.7	14	97.24	53	-39	1521
139.4	23	100	64	-41	1681
79.7	18	99.52	62	-44	1936
174.3	27	89.58	39	-12	144
430	37	98.19	56	-19	361
2420	64	2.82	1	63	3969
1071.4	58	62.11	9	49	2401
154.4	26	65.27	10	16	256
907.7	53	34.7	3	50	2500
1408.6	62	99.04	60	2	4
42.3	11	80	22	-11	121
29.9	8	85.02	30	-22	484
744	49	34.57	2	47	2209
390	33	78.16	21	12	144
234.1	29	91.91	42	-13	169
14.9	3	89.29	38	-35	1225
808.5	50	69.19	14	36	1296
75.9	16	94.93	50	-34	1156
1011.8	55.5	80.43	23	32.5	1056.25
4.98	1	95.68	51	-50	2500

615	40	88.98	37	3	9
67.2	15	76.74	18	-3	9
892.8	51	85.62	31	20	400
714.2	45.5	76.31	17	28.5	812.25
26.1	6	87.5	34	-28	784
78.4	17	91.3	40	-23	529
405	35	81.92	27	8	64
902.7	52	65.84	11	41	1681
1121	60	68.4	13	47	2209
52.3	12	97.74	55	-43	1849
525	38	98.56	57	-19	361
395	34	45.89	5	29	841
244	30	92.63	45	-15	225
27.4	7	93.42	47	-40	1600
725	47	78.02	20	27	729
1720	63	91.54	41	22	484
140	24	87.59	35	-11	121
672.5	43	98.78	58	-15	225
273.9	31	61.57	8	23	529
1061.4	57	72.19	15	42	1764
143.2	25	92.4	44	-19	361
694.4	44	53.76	6	38	1444
				Σd_i^2	**61800**

Spearman rank correlation coefficient, $r_s = 1 - \frac{6 \times (\Sigma d_i^2)}{n^3 - n}$

$$\therefore r_s = 1 - \frac{6 \times 61800}{64^3 - 64}$$

$$\therefore r_s = 1 - \frac{370800}{262144 - 64}$$

$$\therefore r_s = 1 - \frac{370800}{262080}$$

$$\therefore r_s = 1 - 1.415$$

$$\therefore r_s = \underline{-0.415}$$

$(r_s)_{0.05(2),\,64} = 0.246$, so H_0 is rejected. There is a significant negative correlation between the similarity in cell composition between two non-dumbbell islets and the distance between them; calculated $r_s = -0.415$.

Table 5.8. Calculation of the Spearman Rank Correlation Coefficient r_s to Test for a Correlation Between the Similarity in Cell Composition Between Non-Dumbbell Islet Pairs with Inter-Islet (Edge-to-Edge) Distance Between Each Pair (Excluding *Only* Outlier B - 2420 μm/2.82 % - from the Data Set Used in Table 5.5.; $n = 64$)

Distance (μm) (X_i)	Rank of X_i	% Cell Composition Similarity (Y_i)	Rank of Y_i	d_i ($X_i - Y_i$)	d_i^2
654.7	42	54.22	7	35	1225
107.1	21	42.68	4	17	289
1086.2	59	81.04	24	35	1225
54.8	13	92.32	43	-30	900
31.1	9	81.41	25	-16	256
1011.8	55.5	81.43	26	29.5	870.25
425	36	83.05	28	8	64
95.9	20	99.93	63	-43	1849
530	39	96.06	52	-13	169
114.5	22	74.13	16	6	36
224.1	28	88.12	36	-8	64
982.1	54	83.99	29	25	625
714.2	45.5	77.08	19	26.5	702.25
39.8	10	94.12	48	-38	1444
24.9	5	93.37	46	-41	1681
1259.8	61	86.99	33	28	784
7.47	2	94.25	49	-47	2209
649.8	41	98.97	59	-18	324
320	32	66.11	12	20	400
19.9	4	97.44	54	-50	2500
734.1	48	86.31	32	16	256
89.6	19	99.43	61	-42	1764
64.7	14	97.24	53	-39	1521
139.4	23	100	64	-41	1681
79.7	18	99.52	62	-44	1936
174.3	27	89.58	39	-12	144
430	37	98.19	56	-19	361
5420	64	0	1	63	3969
1071.4	58	62.11	9	49	2401
154.4	26	65.27	10	16	256
907.7	53	34.7	3	50	2500
1408.6	62	99.04	60	2	4
42.3	11	80	22	-11	121
29.9	8	85.02	30	-22	484
744	49	34.57	2	47	2209
390	33	78.16	21	12	144
234.1	29	91.91	42	-13	169
14.9	3	89.29	38	-35	1225
808.5	50	69.19	14	36	1296
75.9	16	94.93	50	-34	1156
1011.8	55.5	80.43	23	32.5	1056.25
4.98	1	95.68	51	-50	2500

615	40	88.98	37	3	9
67.2	15	76.74	18	-3	9
892.8	51	85.62	31	20	400
714.2	45.5	76.31	17	28.5	812.25
26.1	6	87.5	34	-28	784
78.4	17	91.3	40	-23	529
405	35	81.92	27	8	64
902.7	52	65.84	11	41	1681
1121	60	68.4	13	47	2209
52.3	12	97.74	55	-43	1849
525	38	98.56	57	-19	361
395	34	45.89	5	29	841
244	30	92.63	45	-15	225
27.4	7	93.42	47	-40	1600
725	47	78.02	20	27	729
1720	63	91.54	41	22	484
140	24	87.59	35	-11	121
672.5	43	98.78	58	-15	225
273.9	31	61.57	8	23	529
1061.4	57	72.19	15	42	1764
143.2	25	92.4	44	-19	361
694.4	44	53.76	6	38	1444
				$\sum d_i^2$	**61800**

Since for the two outliers A and B, X_A (5420 μm) is ranked 65 of 65 and X_B (2420 μm) is ranked 64 of 65 and their corresponding figures for percentage cell composition similarity are ranked 1 of 65 (Y_A = 0 %) and 2 of 65 (Y_B = 2.82 %) then removal of either outlier from the data set gives the same value for r_s. As $\sum d_i^2$ = 61800 as was calculated for **Table 5.7.** and n = 64 as before, then the calculated r_s = -0.415. As $(r_s)_{0.05(2),\ 64}$ = 0.246, then H_0 is rejected. There is a significant negative correlation between the similarity in cell composition between two non-dumbbell islets and the distance between them.

5.3.5. Islets of Similar Cell Composition Occur in Discrete Groups

Analysis of the histochemically-stained pancreas sections from the developmental series of H253 hemizygous females revealed that islets of a certain β-gal$^+$ or β-gal$^-$ cell composition showed a tendency to occur together. Discrete groups of homogeneous β-gal$^+$ islets and heterogeneous β-gal$^+$/β-gal$^-$ islets were seen within the same tissue section; patches of homogeneous unlabelled islets were also observed (**Fig. 5.5.**).

5.3.6. No Marked Distinction Between Ranges of Dumbbell and Non-Dumbbell Islet Areas

It would be expected that if dumbbells are islets undergoing fission, they would be larger than non-dumbbell islets. This hypothesis was tested by comparing the cross-sectional areas (cell number) of the 23 dumbbell and 130 (65 pairs of) non-dumbbell islets (**Graph 5.7.**), calculated from **Tables 5.2.** and **5.3.** The data ranges for the two islet classes were seen to superpose to quite some extent. However, minimum and maximum dumbbell islet areas were 5.2- and 2.9-fold greater than those for non-dumbbells and the mean islet areas were 295 ± 43.6 cells and 102 ± 8.76 cells for dumbbell and non-dumbbell islets respectively (**Table 5.9.**). Using the two-sample *t*-test (Minitab™ v. 13), there was found to be a significant difference between cross-sectional area of dumbbell and non-dumbbell islets (at $\alpha(2) = 0.05$, $t = 4.35$; $P = 0$). Dumbbell islets exhibit a significantly greater cross-sectional area than that of non-dumbbell islets.

Table 5.9. Islet Cross-Sectional Area Descriptive Statistics

Statistic	Sectional Area (Cell Number)	
	Dumbbells	Non-Dumbbells
Mean ± S.E.	295 ± 43.6	102 ± 8.76
Minimum	47	9
Maximum	981	632

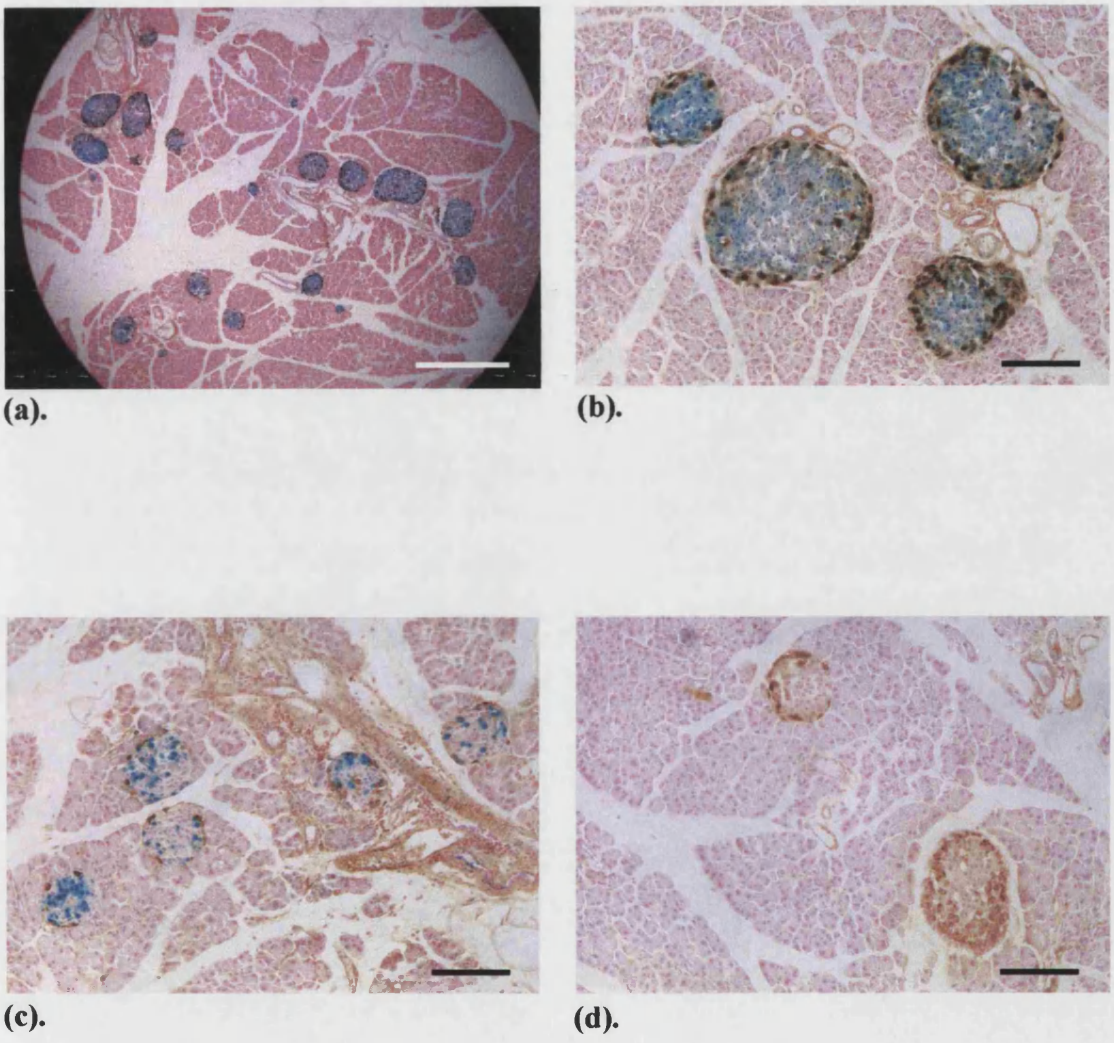

Figure 5.5. Islets of Similar Cell Composition Occur in Groups

(a) and (b) Patches of homogeneous β-gal$^+$ islets. (c) Group of heterogeneous β-gal$^+$/β-gal$^-$ islets and (d) homogeneous β-gal$^-$ islets

(a) Bar = 0.5 mm; (b), (c) and (d) Bar = 100 μm

Graph 5.7. Frequency Histogram of Cross-Sectional Areas of Dumbbell and Non-Dumbbell Islets

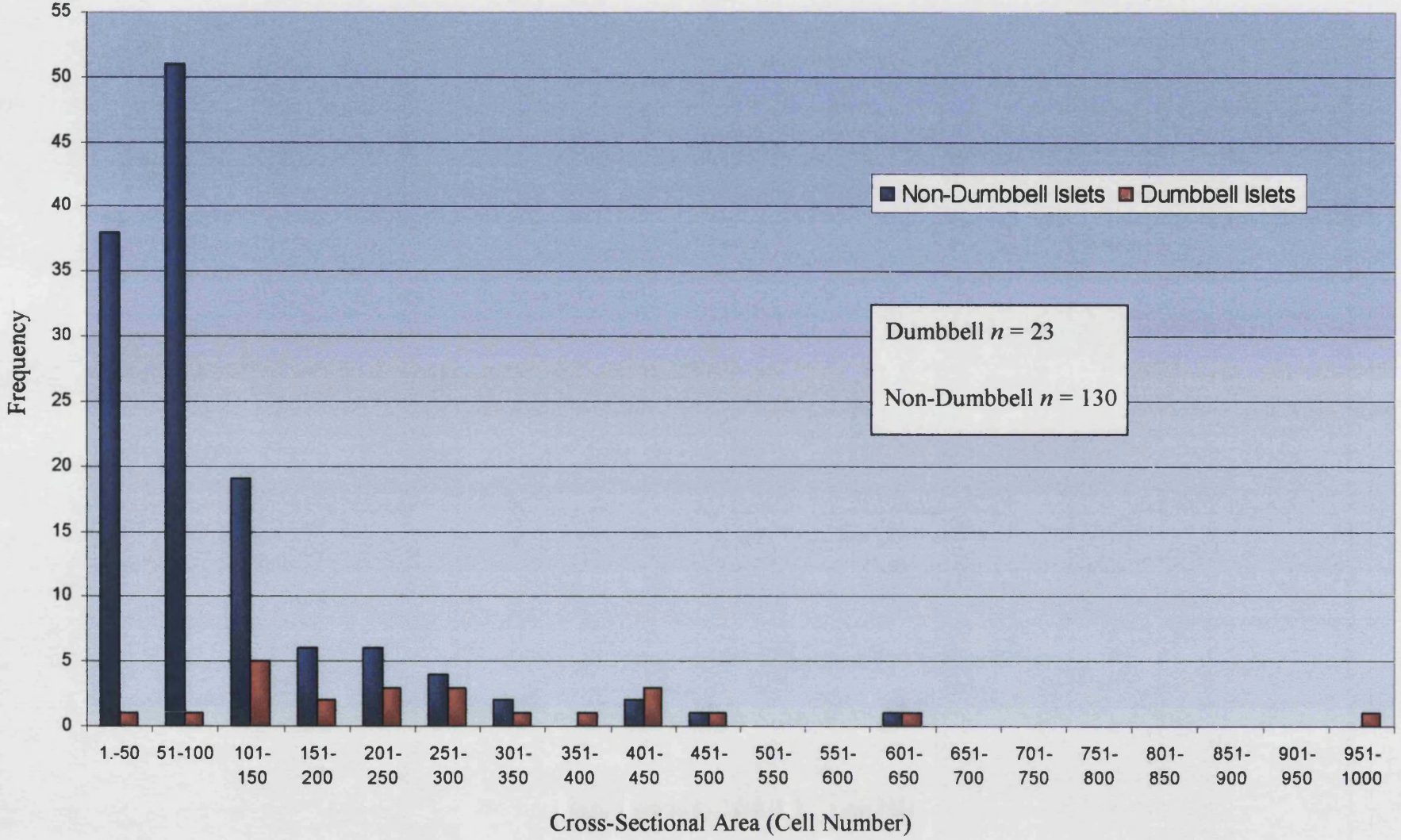

5.3.7. Areas on Both Sides of Dumbbell Islets are Generally Equal

Finally, an examination was made into whether the dumbbells of fissioning islets divide symmetrically. Linear regression plots were generated (Minitab™ v. 13) for area (total number of cells) on side 1 against the area (total number of cells) on side 2 for the identified dumbbell islets (**Graph 5.8.**). r_s was again calculated (**Table 5.10.**). There was found to be a significant positive correlation between the number of cells on each side of the dumbbells; calculated $r_s = 0.736$; $(r_s)_{0.05(2),\ 23} = 0.415$, so H_0 was rejected. As the plot (**Graph 5.8.**) revealed the existence of two outlying data points outside the main body of data, a second regression plot was produced excluding both of these two outliers (**Graph 5.9.**); $R^2 = 56.4$ %, $R^2_a = 54.1$ %. r_s was then calculated for this smaller data set (**Table 5.11.**). Excluding these two outlying data points there was found to be an even stronger significant positive correlation between the number of cells on each dumbbell side; calculated $r_s = 0.750$; $(r_s)_{0.05(2),\ 21} = 0.435$, so H_0 was rejected.

5.3.7.1. Observations of Dumbbell Islets with Asymmetrical and/or Multiple "Sides"

On rare occasions when examining the X-gal-stained paraffin sections from the PN3-PN52wk H253 female hemizygote pancreata (Time-Series One), dumbbell islets were observed displaying highly asymmetrical sides in 2D sections (**Fig. 5.6.**). Such dumbbell islets therefore reflect the existence of the outlying data points mentioned above when plotting the area (total number of cells) on side 1 against the area (total number of cells) on side 2 for the 23 identified dumbbell islets. Also and again very infrequently, morphologically aberrant islets complying with the dumbbell islet criterion (*islets composed of two or rarely, more conjoined parts meeting in a visible "neck" of glucagon-immunopositive cells*) were observed in histochemically-stained paraffin sections from PN52wk H253 female hemizygote pancreata (**Fig 5.7.**). Such dumbbell islets exhibited more than two "sides". Both forms of morphologically atypical dumbbell islets occurred at a markedly lower frequency than the typical dumbbell islets with two sides of equal area and the atypical dumbbell islets also tended to occur in older (PN52wk) animals.

Graph 5.8. Relationship Between the Areas (Total Numbers of Cells) of the Two Sides of Each of 23 Dumbbell Islets

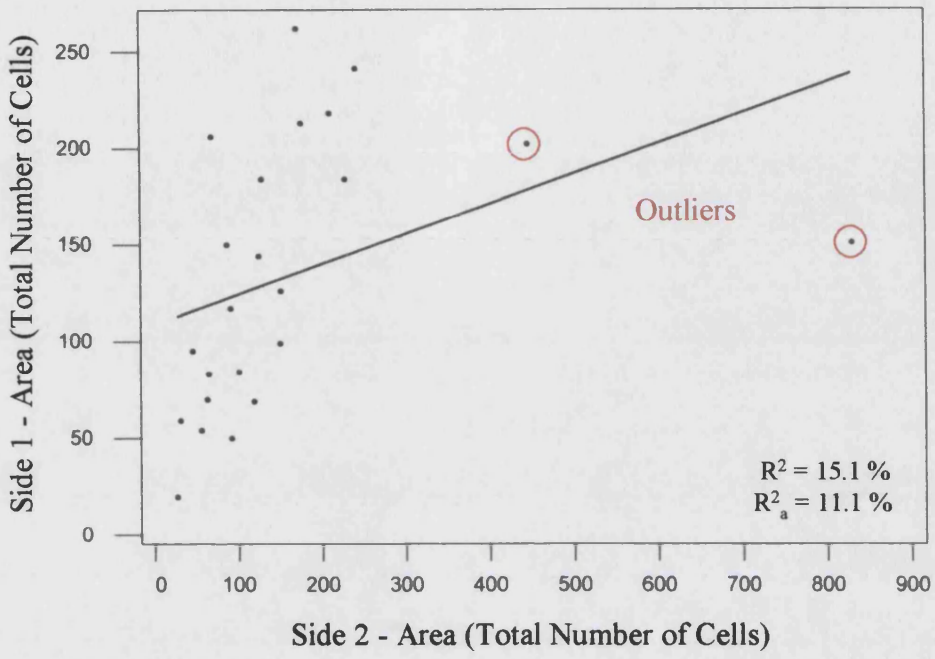

Graph 5.9. Relationship Between the Areas (Total Numbers of Cells) of the Two Sides of Each of 21 Dumbbell Islets (*Both* Outliers Excluded)

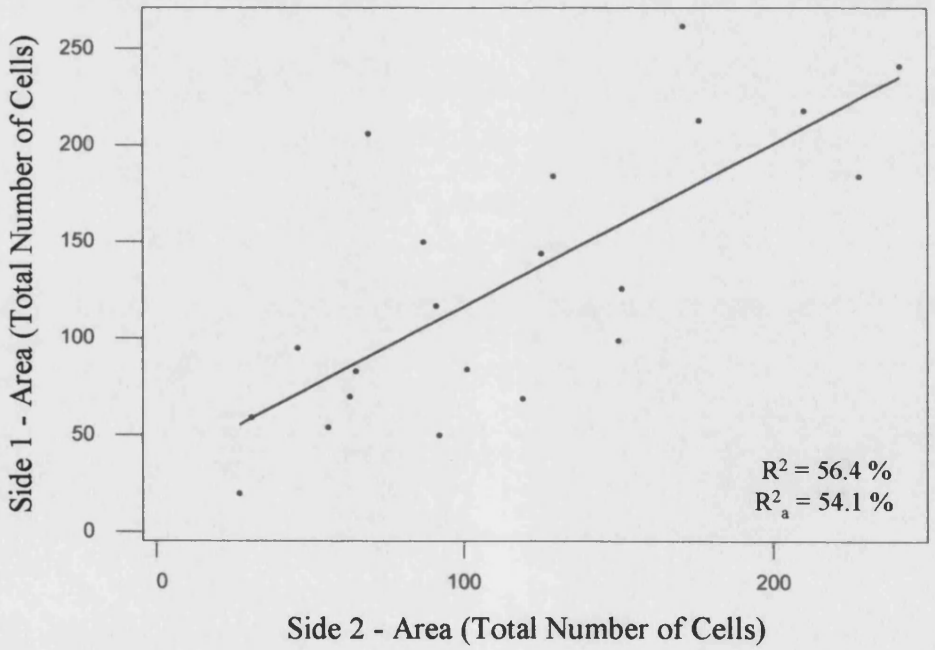

Table 5.10. Calculation of the Spearman Rank Correlation Coefficient r_s to Test for a Correlation Between the Area (Total Number of Cells) on Side 1 and the Area (Total Number of Cells) on Side 2 for Dumbbell Islets (n = 23)

DUMBBELL ISLET SIDE 1		DUMBBELL ISLET SIDE 2		d_i (X_i - Y_i)	d_i^2
Cell Number (X_i)	Rank of X_i	Cell Number (Y_i)	Rank of Y_i		
213	4	176	6	-2	4
59	20	31	22	-2	4
184	7.5	228	4	3.5	12.25
262	1	171	7	-6	36
184	7.5	129	10	-2.5	6.25
206	5	69	17	-12	144
117	13	91	15	-2	4
54	21	56	20	1	1
218	3	210	5	-2	4
50	22	92	14	8	64
70	18	63	19	-1	1
126	12	151	8	4	16
69	19	119	12	7	49
144	11	125	11	0	0
99	14	150	9	5	25
95	15	46	21	-6	36
150	10	87	16	-6	36
84	16	101	13	3	9
20	23	27	23	0	0
83	17	65	18	-1	1
241	2	241	3	-1	1
202	6	446	2	4	16
151	9	830	1	8	64
				Σd_i^2	**533.5**

Spearman rank correlation coefficient, $r_s = 1 - \frac{6 \times (\Sigma d_i^2)}{n^3 - n}$

$$\therefore r_s = 1 - \frac{6 \times 533.5}{23^3 - 23} = 1 - \frac{3201}{12167 - 23}$$

$$\therefore r_s = 1 - \frac{3201}{12144} = 1 - 0.264 = \underline{0.736}$$

$(r_s)_{0.05(2),\,23} = 0.415$, so H_0 is rejected. There is a significant positive correlation between the number of cells on each side of the identified dumbbell islets.

Table 5.11. Calculation of the Spearman Rank Correlation Coefficient r_s to Test for a Correlation Between the Area (Total Number of Cells) on Side 1 and the Area (Total Number of Cells) on Side 2 for Dumbbell Islets (Excluding *Both* of the Two Outliers from the Data Set Used in Table 5.10.; $n = 21$)

DUMBBELL ISLET SIDE 1		DUMBBELL ISLET SIDE 2		d_i $(X_i - Y_i)$	d_i^2
Cell Number (X_i)	Rank of X_i	Cell Number (Y_i)	Rank of Y_i		
213	4	176	4	0	0
59	18	31	20	-2	4
184	6.5	228	2	4.5	20.25
262	1	171	5	-4	16
184	6.5	129	8	-1.5	2.25
206	5	69	15	-10	100
117	11	91	13	-2	4
54	19	56	18	1	1
218	3	210	3	0	0
50	20	92	12	8	64
70	16	63	17	-1	1
126	10	151	6	4	16
69	17	119	10	7	49
144	9	125	9	0	0
99	12	150	7	5	25
95	13	46	19	-6	36
150	8	87	14	-6	36
84	14	101	11	3	9
20	21	27	21	0	0
83	15	65	16	-1	1
241	2	241	1	1	1
				$\sum d_i^2$	**385.5**

Spearman rank correlation coefficient, $r_s = 1 - \dfrac{6 \times (\sum d_i^2)}{n^3 - n}$

$$\therefore r_s = 1 - \frac{6 \times 385.5}{21^3 - 21} = 1 - \frac{2313}{9261 - 21}$$

$$\therefore r_s = 1 - \frac{2313}{9240} = 1 - 0.250 = \underline{0.750}$$

$(r_s)_{0.05(2),\,21} = 0.435$, so H_0 is rejected. There is a significant positive correlation between the number of cells on each side of the identified dumbbell islets.

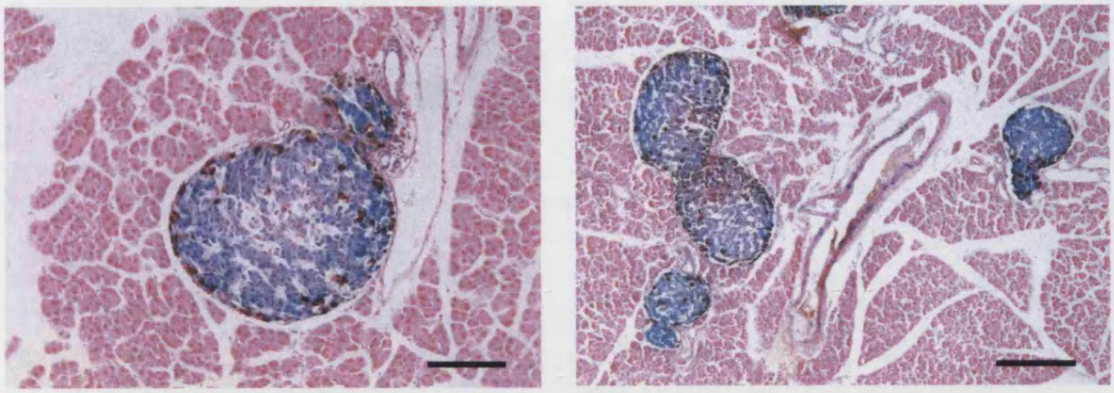

(a). (b).

Figure 5.6. Infrequent Dumbbell Islets with Asymmetrical Sides

Paraffin sections of wholemount X-gal-stained PN52wk H253 female hemizygote pancreas immunoperoxidase-stained for glucagon and counterstained with nuclear Fast Red. (b) Asymmetrically dividing dumbbells are visible on the lower left and upper right; a larger, more typical symmetrically dividing dumbbell is shown on the upper left. (a) Bar = 100 μm; (b) Bar = 200 μm

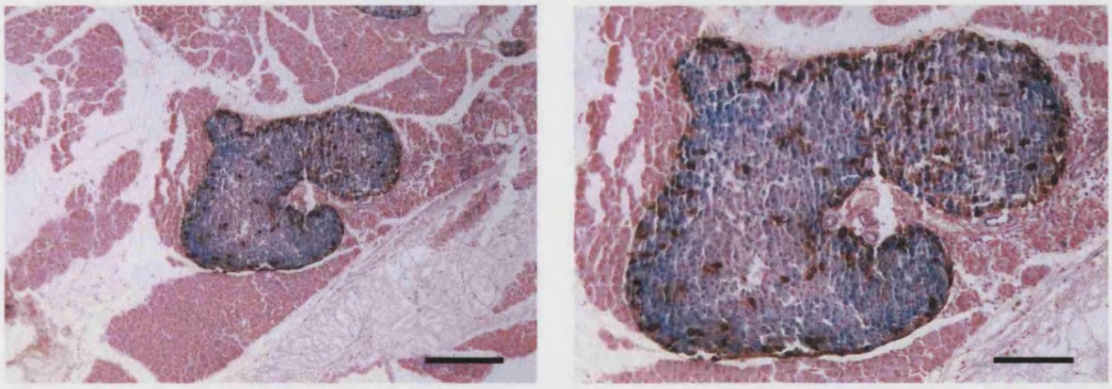

(a). (b).

Figure 5.7. Infrequent Dumbbell Islets with Multiple "Sides"

Paraffin section of wholemount X-gal-stained PN52wk H253 female hemizygote pancreas immunoperoxidase-stained for glucagon and counterstained with nuclear Fast Red. (a) Bar = 200 μm; (b) Bar = 100 μm

5.4. Discussion

5.4.1. Observations of "Dumbbell" Islets and their Frequency with Age

Uncharacteristically-shaped islets were observed in paraffin and frozen sections of pancreas from both sexes and all genotypes of H253 animals although presumably occur in all strains of mice. They were coined dumbbell islets on account of their (generally) hourglass form in 2D sections, comprising, in the vast majority of cases, two conjoined ovoid parts. In all dumbbell islets, an obvious neck or waist of glucagon-immunopositive α-cells delineated the two (or more) sides of the islet and this waist sets such islets apart from more typically-formed islets. Computer-aided 3D reconstruction of a typical dumbbell showed these islets to comprise two ovoids conjoined to form a neck, resembling a pair of rugby balls fused together at their pointed ends. This narrowing at the neck was seen to occur in the third dimension so that the dumbbell islet truly possesses this hourglass waist as seen from all aspects.

Dumbbell islets were found to occur most frequently in the pancreas of neonates immediately after birth, comprising almost one-third of the islets in three-day old mice. Their incidence then declined sharply to 15.0 % by one week of age and by 28 days after birth, dumbbell islets comprised less than 2 % of all islets.

5.4.2. Islet Fission or Fusion?

It was a point of interest whether these morphologically atypical dumbbell islets are islets in a state of fission or division, analogous to that described in the intestinal crypts of Lieberkühn (Li *et al.*, 1994; St. Clair and Osborne, 1985). As with the intestinal crypts in the gut, fission of islets in the mouse might be a mechanism for expanding the number of islets. The initially high dumbbell incidence during the neonatal period suggested that this mode of new islet production is prevalent immediately following birth and contributes to expansion of islet number especially during the first few weeks of postnatal life.

Of course, the equally valid hypothesis that such dumbbell islets instead represent smaller aggregating islets in a state of fusion could not be discounted. The obvious neck of α-cells in the centre of the β-cell mass of the elongated islet counters arguments that such dumbbells are malformed or aberrantly-shaped islets. The α-cells, usually localised to the peripheral islet mantle, are clearly "sandwiched" between two

bodies of β-cells and so internalised within the dumbbell. It is suggested that the α-cell layer is delaminating from the islet mantle to separate the two bodies of β-cells before generating the two daughter islets. The presence of the α-cell neck though, can be equally well incorporated into the islet fusion hypothesis as representing the residual α-cell mantle of the nearest points of the two recently fused islets.

5.4.3. Cell Composition Analysis Supports Islet Fission

So, to test the hypotheses that (1) dumbbell islets represented a parent islet in a state of division or fission and (2) such islet fission is a mode of islet production in the murine pancreas, an examination was made of the β-gal-labelled and unlabelled cell composition of both dumbbell and non-dumbbell islets in paraffin sections of X-gal-stained pancreata from PN3-PN84/12wk H253 female hemizygous mice. Over this age-range, the islets are undergoing the putative shift from a heterogeneous to a homogeneous cell composition (**Chapter 4**). With endogenous cell turnover within the endocrine compartment, if islets are generated by fission at least to a measurable extent then as daughter islets are produced and separate within the pancreatic tissue, the similarity of the β-gal$^+$/β-gal$^-$ cell composition of two islets (their "relatedness") would be expected to decrease the greater the distance between the two. By this hypothesis, the labelled/unlabelled cell composition of the two sides of a dumbbell or putative fissioning islet would be identical (or almost so), and certainly greater than the relatedness of pairs of non-dumbbell islets. However, if the two sides of dumbbells show similar variation to random pairs, this would support the islet fusion hypothesis **(Fig. 5.8.)**.

Linear regression of percentage β-gal$^+$ cell composition between the two sides of each dumbbell islet and subsequent calculation of r_s gave a significant strong positive correlation (r_s = 0.742). So, the relatedness of the two sides of a dumbbell islet is significantly higher than between two non-dumbbell islets. Moreover, there was found to be a significant negative correlation (absence of the two outliers withstanding: r_s = -0.441 for the intact data set, -0.387 excluding *both* outliers and -0.415 excluding *one* outlier *or the other*) between the similarity in cell composition between two non-dumbbell islets and the inter-islet distance. So, the relatedness of two randomly selected islets decreases as the distance between them increases. Using the non-dumbbell data, the extrapolated values (87.0-89.7 %) for the percentage similarity of cell composition

Figure 5.8. Predicted Outcomes of Cell Composition Analysis in the Event of Islet Fission (a) or Islet Fusion (b)

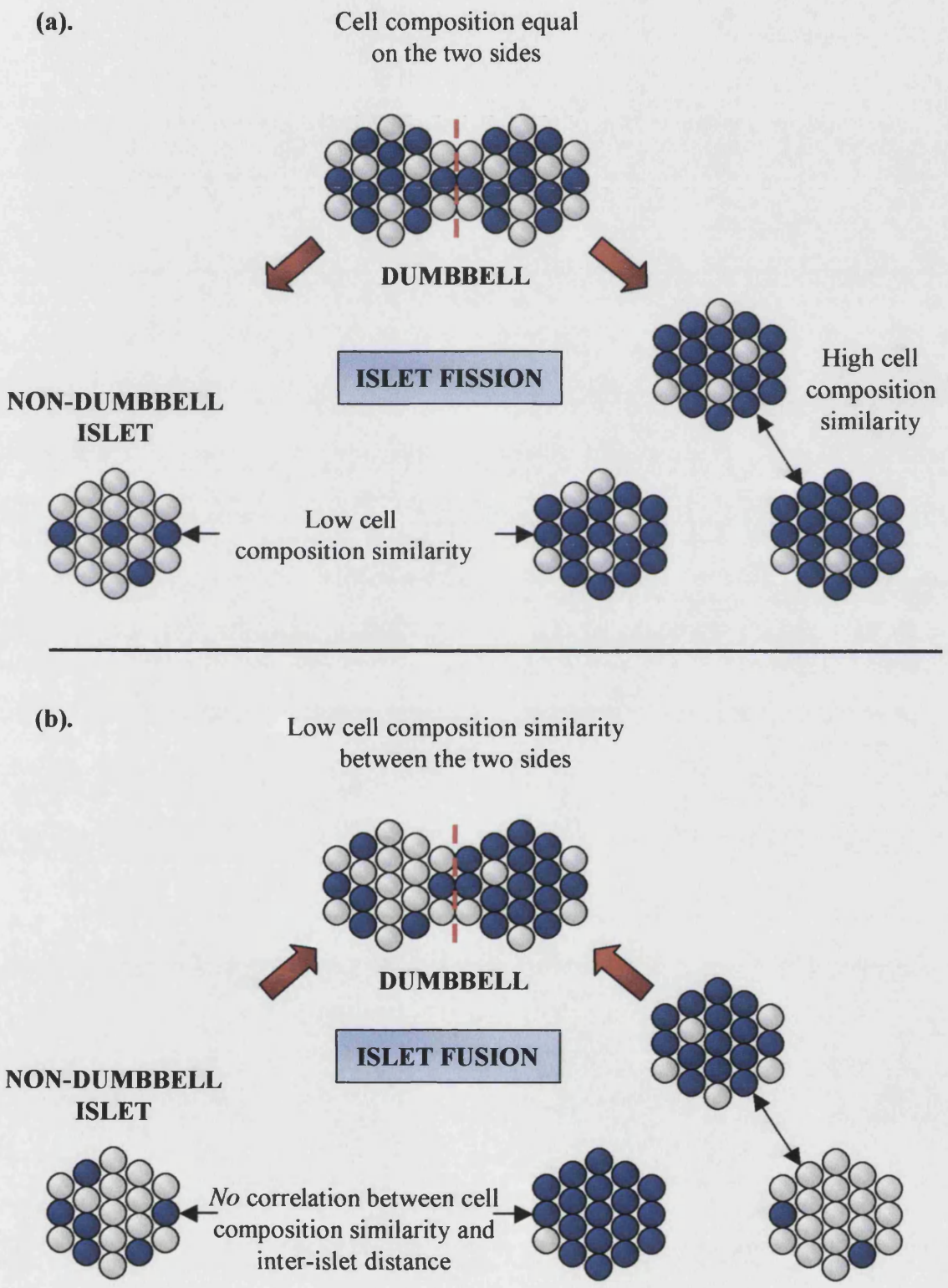

between the two sides of a dumbbell islet are in strong agreement with the actual mean value measured from the dumbbells themselves (91.8 %).

All of the results of the cell composition analysis strongly support the argument for islet fission. The results support both hypotheses that (1) dumbbell islets represent a parent islet in a state of division or fission and (2) such islet fission is a mode of islet production in the pancreas of the mouse. In light of the above, it is highly improbable that dumbbell islets are formed from the amalgamation of smaller islets. Islet fission as a mode of expansion of islet number is also favoured by related though more circumstantial evidence: that of similar islets occurring in clusters. Islets of a certain β-gal$^+$ or β-gal$^-$ cell composition showed a tendency to occur together in the H253 female hemizygote pancreas. This suggests that islets occurring in a patch are formed by the fission of one or a small number of parent islets. Pancreatic islets in a wide range of mammalian species have been shown to cluster together within the exocrine tissue, resulting in a spatial distribution pattern that suggests that mammalian islet formation follows an iterative or fractal growth law used to describe branching structures (Hastings *et al.*, 1992; Schneider *et al.*, 1996). The authors suggested that islet patterns can be explained by a fractal branching structure for exocrine ductules and random islet formation at their tips, concordant with the belief that islets bud from tips of ductules during embryogenesis (Falkmer, 1985). This finding does not exclude the possibility that an islet derived from the ductule epithelium subsequently undergoes fission to produce daughter islets retaining a close affinity with the duct system.

5.4.4. Comparison with Crypt Fission: Stimuli for Fission

Studies of the dynamics of fission of the intestinal crypts (Bjerknes, 1995, 1996; Totafurno *et al.*, 1987) have led to the concept of the crypt cycle. Crypts in the mouse small intestine, generated by fission, gradually increase in size and undergo fission after about 108 days. This process of division takes approximately 12 h to complete. Crypts at the upper end of the size distribution were found to initiate fission. These studies suggest that crypts must attain a given size before fission commences. It has been proposed (Loeffler *et al.*, 1993, 1997) that the threshold for initiation of fission is a doubling of the stem cell number. A further proposal is that there exists a given threshold value for the number of stem cells per crypt which, when reached, triggers fission.

5.4.5. No Threshold Islet Size for Triggering Fission

An analysis was then made of the sectional areas in terms of cell number of both dumbbell and non-dumbbell islets to test the hypothesis that islet size is bivariate; that islets fall within two size categories (**Fig. 5.9.**).

Figure 5.9. Bivariate Distribution of Islet Areas if a Threshold Size for Islet Fission Exists

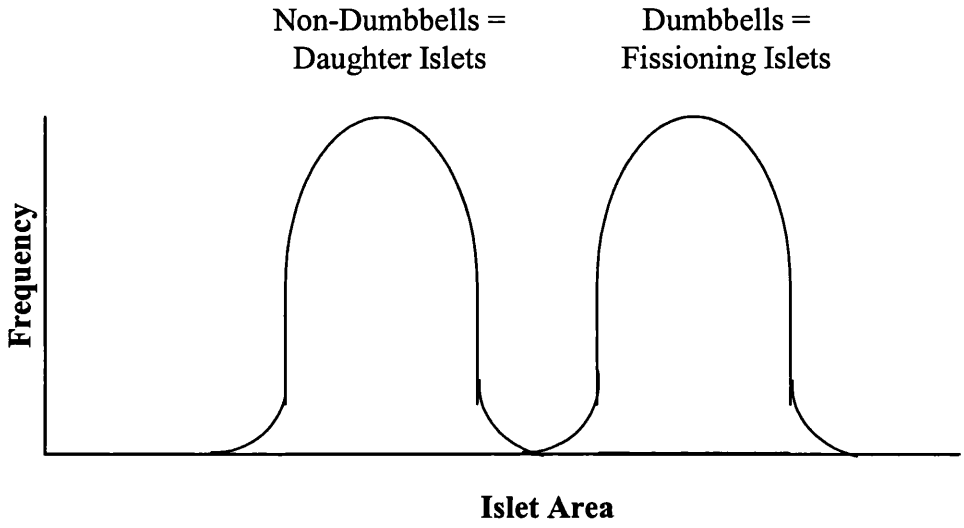

Dumbbell islet areas would be expected to be two-fold greater than the non-dumbbell daughter islets that they generate upon division, suggesting there to be a threshold islet size at which islet fission is initiated. Dumbbell islets were found to be significantly larger than non-dumbbell islets; mean dumbbell islet area (295 ± 43.6 cells) was almost three-fold greater than non-dumbbell islet area (102 ± 8.76 cells). This translates to dumbbell islets being 3.48-fold greater in volume and hence, mass, than the non-dumbbells if the assumptions are made that non-dumbbell islets are perfect spheres, that dumbbell islets represent two spheres conjoined at their very periphery with no overlap and that the sectional areas are "equatorial". However, the ranges in islet area for the dumbbell and non-dumbbell population samples superposed to some extent, meaning that no clear size/area threshold for triggering fission could be discerned.

5.4.5.1. Could a Change in α-Cell:β-Cell Ratio Trigger Fission?

The islet is a microorgan whose functionality is dependent on the relationships between the four different endocrine cell types of which it is composed. The islet

comprises a heterocellular peripheral mantle composed mainly of α-cells and a small number of somatostatin-secreting δ-cells and a homocellular core of β-cells. The thin mantle of α-cells is therefore more a function of surface area than the β-cell core. Neighbouring cells are able to communicate via junctional complexes (Orci *et al.*, 1975). Somatostatin is able to powerfully inhibit insulin and glucagon secretion from neighbouring β- and α-cells respectively. Owing to their arrangement within the islet, the percentage of the total α-cell mass in contact with δ-cells must be greater than the percentage of the β-cell mass, the majority of which has no δ-cell contacts. It has been speculated (Orci and Unger, 1975) that if somatostatin functions as a local inhibitor of neighbouring α- and β-cells, it would have a greater influence upon pancreatic glucagon secretion than on insulin secretion. In addition, insulin is known to inhibit glucagon secretion (Marks, 1971; Samols *et al.*, 1969). If the islet diameter doubles, surface area of the islet will increase four-fold but volume will increase by a factor of eight. So, as the islet grows in size, the relative surface areas of the α-, β- and δ-cells exposed to one another will change and so too will the paracrine effects of somatostatin and insulin. It is conceivable that there will exist a maximum islet size at which any further increase in islet volume leads to declines in efficiency of function of the microorgan as a whole. It is speculated that the ratio between different endocrine cell types, especially the α- and β-cells and their inter-relationships play a role in initiating islet fission, perhaps when the islet has attained a certain size at which efficiency of function is declining. If endocrine cells similarly require trophic signals from different endocrine cell types for maintaining their survival then this might also limit the maximum islet volume. If so, endocrine cell expansion and increase in islet diameter would be halted when the diffusible distance between different cell types is in excess of that required for satisfactory trophic support, resulting in cell death of some islet cells. Elevated levels of endocrine cell apoptosis within the islet might then trigger fission.

5.4.6. Mechanism of Islet Fission: Significance of Aberrant α-Cell Localisation in Dumbbells

As mentioned, a definite neck of α-cells was observed in the centre of the β-cell mass of the dumbbell islets. α-Cells, usually restricted to the peripheral islet mantle, are internalised within the two bodies of β-cells of the dumbbell. It can be speculated that the α-cell layer delaminates from the islet mantle and drives the division of the two

bodies of β-cells to generate the daughter islets. Migration of α-cells from the mantle would result from changes in cell adhesion properties of different endocrine cell types, most notably the α- and β-cells. The mechanisms for cell rearrangement during development including segregation of unlike cells were explained by Holfreter as differences in tissue affinities (Townes and Holfreter, 1955). Steinberg and Takeichi (1994) showed that two motile cell types differing only in the levels of expression of a single adhesion system, will segregate from one another but moreover arrange themselves in the form of an envelope of less cohesive cells surrounding a core of more cohesive cells. According to the differential adhesion hypothesis, β-cells, forming the islet core, should be more cohesive than peripheral α-cells. Through the overexpression of dominant negative E-cadherin, members of the cadherin family were shown to be required for the aggregation of endocrine cells into islets and the typical cell organization of islets *in vivo* (Dahl *et al.*, 1996). N-CAM (neural cell adhesion molecule) was shown to be expressed more strongly on peripheral (α-) cells of the islet than central β-cells and so to play a role in islet cell segregation *in vitro* (Cirulli *et al.*, 1994). By knocking out N-CAM, Esni *et al.* (1999) showed that cadherin-mediated adhesion in islets is increased. As a result of this, they suggested that N-CAM negatively influences the cadherin-mediated basic adhesion machinery in islets. Differential expression of N-CAM in α-cells would render them less cohesive than β-cells, resulting in their typical peripheral islet distribution. In more than two-thirds of the islets of N-CAM knockout mice, α-cells were found centrally within the β-cell core. This can be attributed to increased cadherin-mediated adhesion between α-cells in the absence of N-CAM. Similarly, an increased cadherin-mediated adhesion between dumbbell islet α-cells in the neck region might be responsible for their migration into the β-cell mass, driving division of the islet.

5.4.7. Islet Fission is Generally Symmetrical

The aforementioned theoretical bivariate distribution of islet areas in the event of there being a threshold size for islet fission, will only hold true if a dumbbell islet divides symmetrically. Determining whether this is so is very challenging. The β-gal$^+$/β-gal$^-$ cell composition of the two spheroidal (and so 3D) sides of a dumbbell islet (as with a non-dumbbell islet) can be compared fairly robustly from 2D sections if it is assumed that the cell composition throughout each islet is homogeneous and so

equivalent to the analysed section. Volume of a sphere or spheroid cannot, however be extrapolated from a 2D section with quite the same robustness. The equations defining the relationship between the apparent size distribution - that observed in a section - and the actual size distribution of spherical and ellipsoidal bodies were derived by Wicksell (1925, 1926). With the assumption that these bodies are evenly distributed, the relationship can be expressed in the form of Abelian integrals. As mentioned, however, islets in a wide range of mammalian species are not distributed randomly in the exocrine tissue but instead cluster together (Hastings *et al.*, 1992; Schneider *et al.*, 1996).

If a comparison is made between the area of side 1 with that of side 2 for each of the 23 dumbbell islets, the ratio of the two areas is highly susceptible to effects from the plane of section through the dumbbell. Thus, even if the areas of the two sides of a dumbbell are exactly equal, the plane of section must pass through the "equator" of each side of the dumbbell for the two areas to be measured as being equal from that 2D section (**Fig. 5.10.**). Considering the multitudes of possible combinations between orientation of the dumbbell and plane of section, it is highly improbable that this will occur. The plane of section through the islet was not problematic for the comparison of dumbbell *vs.* non-dumbbell islet area above since the outcome of the analysis is less affected by plane of section. Bearing this limitation in mind, r_s was still calculated to test for a correlation between the area (total number of cells) on side 1 and the area (total number of cells) on side 2 for the identified dumbbell islets. There was found to be a significant positive correlation (r_s = 0.736 and 0.750 including and excluding the two outliers respectively) between the numbers of cells on each side of the dumbbells. So, especially in light of the above critique, it can be assumed that dumbbells *generally* divide symmetrically and the two daughter islets generated are of equal size.

5.4.8. Asymmetrical Islet "Budding" and "Multiple" Islet Fission

There were notable exceptions to the symmetrical division of dumbbell islets, as demonstrated by the two pairs of outlying data points in the data set for examining this question (**Graph 5.8.**). Observations were made of dumbbells exhibiting highly asymmetrical sides in 2D sections (**Fig. 5.6.**) when plane of section effects were considered i.e. it was considered highly improbable that these images simply represent oblique sections of symmetrically-dividing dumbbells. For example, if the section depicted in **Fig. 5.6. (a)** represented an oblique section through a symmetrical dumbbell

Figure 5.10. Susceptibility of the Ratio of the Areas of the Two Dumbbell Sides to Effects from the Plane of Section Through the Dumbbell

Even if the areas of the two sides of a dumbbell are exactly equal, the plane of section must pass through the "equator" of each side of the dumbbell (**a**) for the two areas to be measured as being equal. Deviation from this plane (**b**) will result in an asymmetry of the two sides being extrapolated from that 2D section

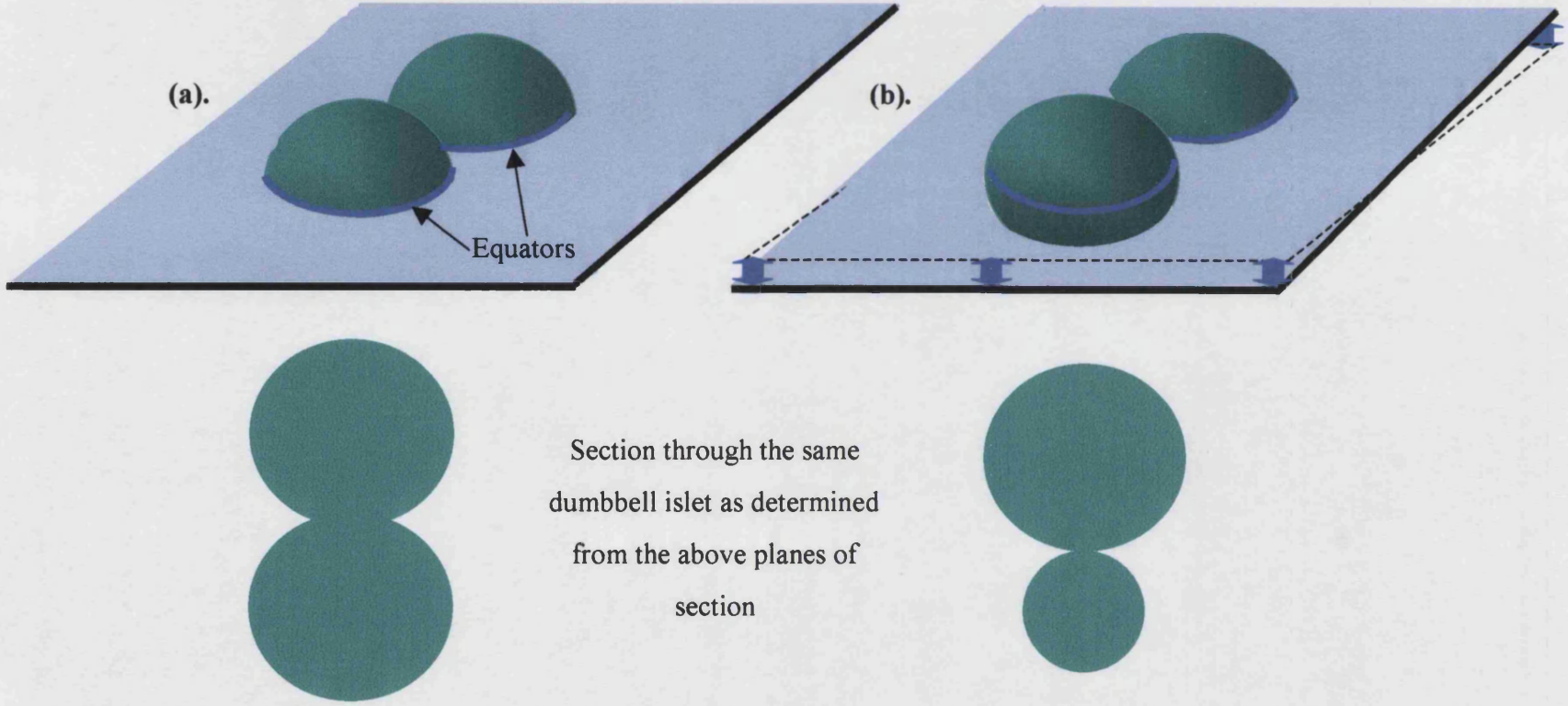

islet, then one would expect that the section "glancing" one of the dumbbell sides would be separated from the more equatorial section through the other dumbbell side by intervening acinar tissue. This of course excludes the possibility that the side appearing smaller in the section exhibits a highly aberrant shape. The similar appearance of apparently non-symmetrical dumbbells in adjacent serial sections (not shown) supports to some extent the notion that highly asymmetrical dumbbells are a reality. Of the 23 dumbbells examined, two (**Table 5.2.**; final two rows), exhibited particularly asymmetrical cell distributions between the two sides of the dumbbell; 202 cells *vs.* 446 cells and 151 cells *vs.* 830 cells. These figures translate to total dumbbell cell distributions between the two sides of 31.2 % to 68.8 % and 15.4 % to 84.6 % respectively.

In some instances, fission of intestinal crypts into two daughters occurs asymmetrically with respect to the crypt axis, and in this case the process is termed "budding". This lead to speculation that such budding might apply to islets also. In more infrequent cases than the above, islets might also divide asymmetrically into one smaller and one larger daughter islet.

There are two types of crypt fission. That described here so far is the typical binary fission and involves a crypt dividing into two daughters. A much more infrequent event is multiple fission which involves the crypt splitting simultaneously into many crypts, notably following radiation (Cairnie and Millen, 1975). In the immediate neonatal period, islets initially occur in multi-complex clusters (**Fig. 5.3.**) exhibiting very atypical morphology in relation to the more mature spheroidal islets. It is speculated that these complexes undergo fission, generating more than two distinct islets from a single mass of endocrine tissue. This therefore resembles multiple fission of crypts but applies only to the dispersion of the initial endocrine tissue mass formed during the embryonic period. This does not discount the possibility that "multiple fission" of a recognisably distinct islet can occur in the later pancreas. Very occasionally in adult (PN52wk) animals, aberrantly-shaped islets complying with the dumbbell islet criterion were observed that exhibited more than two parts or "sides" (**Fig. 5.7.**). It is speculated that such adult islets are undergoing multiple fission, paralleling the multiple fission of intestinal crypts. As with the crypts however, this event would appear to be much more infrequent that the more typical binary fission of a dumbbell islet into two symmetrical daughters.

5.4.9. Proposed Role of Islet Fission in the Normal and Regenerating Pancreas

It was a widespread belief that because β-cell replication after the neonatal period is low, the β-cell mass does not turn over significantly and that the number of β-cells remains virtually static from birth. However, the β-cell mass continues to grow well into adulthood. Morphometric data from wild-type mice aged from four weeks to six months and of the same mixed background (C57Bl/6J/129J) (Bruning *et al.*, 1997; Kopin *et al.*, 1999; Westphal *et al.*, 1999; Withers *et al.*, 1998) shows that β-cell mass increases at least 10-fold over this period and is linearly correlated with body weight. β-Cell production can be achieved through the replication of pre-existing β-cells (Hellerström *et al.*, 1988) or via neogenesis, the budding of endocrine cells from the ducts (Bonner-Weir, 2000). Islets formed by neogenesis are initially likely to be clustered together in close apposition to the ducts (**Fig. 5.3.**). They may migrate a small distance from the ducts (aided by expansion of the surrounding exocrine tissue) and undergo islet fission, generating "islet fields". In the study presented in **Chapter 4**, there was found to be very little increase in the size of individual islets in the H253 animals in the neonatal period (**Chapter 4, Section 4.3.1.9.**). It follows that the rapid increase in β-cell mass must be accompanied by a large increase in islet number after birth (Nielsen *et al.*, 2001). According to Hughes (1956), the number of islets increases from 664 in the neonatal rat to 4673 in the adult. It is likely that islet fission plays a large role in expanding the number of islets in the immediate neonatal period by redistributing the endocrine tissue; dumbbell islets were found to occur with greatest incidence in the early neonate. High cell proliferation in neonatal islets accompanied by rapid fission would lead to little detectable increase in islet size. In this way, total endocrine mass does not change but the number of islets increases. It can be speculated that this redistribution of endocrine tissue also optimises the association of islets with blood vessels, ensuring that islets retain optimal access to blood supply.

Cell turnover of the endocrine (and exocrine) compartment does not cease after the neonatal period however. Hellerström *et al.* (1988) demonstrated that with a β-cell birth rate of just less than 3 % new cells per day, rodent β-cell mass would double in one month if there were negligible cell death. The β-cell mass does not continue to double each month in postnatal life so the β-cell like the majority of other cell types, must have a finite life span (Finegood *et al.*, 1995). If the rate of β-cell death

approaches the replication rate, complete replacement of the β-cell population could occur within a one-month period. So, the endocrine pancreas of the adult should be considered to be a slowly renewed tissue (Finegood *et al.*, 1995). As above, cell renewal can come from the replication of pre-existing β-cells (Hellerström *et al.*, 1988) and by neogenesis from the adult ductal epithelium. Evidence for neogenesis is found in pancreata from obese humans and a number of animal models. In the partial pancreatectomized rat model of pancreatic regeneration (Bonner-Weir *et al.*, 1993, 1997; Sharma *et al.*, 1999) within four weeks of 90 % pancreas removal, the β-cell mass was 45 % and pancreatic weight (reflecting exocrine mass) was 27 % that of sham-treated animals. Rapid regeneration of both endocrine and exocrine tissues occurred in a discordant fashion, due to both enhanced replication of pre-existing differentiated cells and expansion of duct tissue and its subsequent differentiation of new acinar and islet cells. Whole new lobes of pancreas were formed in patterns seeming to recapitulate embryonic development. Islet fission might be speculated to play a role in such endocrine regeneration. The fission of existing islets or islets newly formed by neogenesis from precursors residing in the ductal epithelium would expand islet numbers post-surgery. The continued growth of the novel daughter islets would permit further cycles of fission and would account for pancreatic regeneration and the production of new lobes in the manner described. It is probable that the lack of identification of dumbbell islets until now in the normal pancreas has also meant their lack of detection in the regenerating organ. Dumbbell islets have been observed in adult animals, albeit rarely (**Figs. 5.1., 5.6.** and **5.7.**). It therefore seems reasonable to suggest that islet fission, like neogenesis, might play a small role in the normal, slow turnover of the endocrine compartment in postnatal life by redistributing endocrine tissue, maintaining optimal access to the blood supply. It is also reasonable to suggest that dumbbell islets might feature in certain pathophysiological conditions. Neogenesis appears to occur in certain pathological processes, particularly those causing chronic trauma or inflammation of the pancreas (Gu and Sarvetnick, 1993; Gu *et al.*, 1994; Rosenberg *et al.*, 1983). Novel islets appear to be formed continuously in the rare human condition of nesidioblastosis (Goossens *et al.*, 1989). So, might islet production by fission also be stimulated in this disease? This proposal could be investigated by scoring the incidence of dumbbell islets in histopathological specimens against sections from control pancreas. Although there was insufficient time to pursue this avenue in the current study, this might form the basis of future work.

5.4.10. Summary

Morphologically atypical islets with two or rarely, more "sides" and a characteristic "neck" of α-cells were observed in histological pancreas sections from male and female mice, appearing with decreasing frequency with age from neonates to mature animals. Computer-aided 3D reconstruction confirmed the three-dimensional morphology of such "dumbbell" islets which emulated conjoined spheroidal islets. Analysis of the β-gal-labelled and unlabelled cell composition of dumbbell and non-dumbbell islets in PN3-PN84/12wk X-inactivation mosaic mice showed that (1) the relatedness of the two sides of a dumbbell islet is significantly higher than between two non-dumbbell islets and (2) the relatedness of two randomly selected islets decreases as the distance between them increases. Cell composition evidence therefore supports the hypotheses that (1) dumbbell islets represent a parent islet in a state of fission and (2) islet fission is a mode of islet production in the murine pancreas, consistent with the observation that islets of a similar β-gal^{+}/β-gal^{-} cell composition tend to occur in clusters. Like fission of the intestinal crypts, islet fission might be initiated by an islet doubling its number of stem cells or attaining a threshold stem cell number. The process might be driven by delamination of the α-cell layer from the islet mantle to segregate the two bodies of β-cells. A significant positive correlation between the numbers of cells on each side of the dumbbells shows that dumbbells *generally* divide symmetrically although some histological evidence provides support for asymmetrical islet "budding" and the "multiple fission" of islets into more than two daughters. It is likely that islet fission contributes quite markedly to the dramatic expansion of islet numbers that occurs in the immediate neonatal period and continues to act as a source of novel islets in later life, playing a role in the normal, slow turnover of the endocrine compartment. Redistribution of endocrine tissue in this way would help to optimise the association of islets with blood vessels.

5.4.10.1. Therapeutic Applications and Further Work

The morphological and cell composition evidence presented above provides clear evidence for islet fission. This is the first discovery of the phenomenon. It would appear probable that this process contributes quite markedly to expansion of islet numbers in the normal pancreas. It is of interest to determine what role islet fission plays in the redistribution of islet cells generated by neogenesis of ductal tissue. The

involvement of this putative process in regeneration models and pathophysiological states affecting the pancreas is also worthy of examination.

The discovery also opens the possibility of new therapeutic applications in the treatment of diabetes. A major obstacle to successful islet transplantation for both type 1 and type 2 diabetes is an adequate supply of insulin-producing tissue. This requirement for transplantable human islets has intensified efforts to expand existing pancreatic islets and/or grow new ones. If the trigger for islet fission were to be elucidated, then this would raise the possibility of harvesting limited numbers of islets and expanding them *in vitro* before re-implanting them into diabetic recipients. This approach may provide a potential new source of pancreatic islets for transplantation.

Further work is needed to characterise the frequency of fission in varying regeneration and disease states of the pancreas. The stimulus for initiation of fission and its mechanism will be challenging to elucidate.

6. Characterisation of IGF-II Transgenic Lines

6.1. Introduction

6.1.1. The Extended Insulin Family

The phenomenon of growth is one of the least well understood aspects of development. Growth is achieved largely by cell division supplemented by secretion of extracellular matrix and by some increase in cell size (hypertrophy). The coordination of growth between different regions and organs of the body remains an obscure process. Gene targeting studies have demonstrated that peptides in the extended insulin family, insulin, and insulin-like growth factors (IGFs)-I and -II are important trophic hormones during embryonic and fetal development whose absence results in profound fetal growth retardation (DeChiara *et al.*, 1990; Duvillié *et al.*, 1997; Liu *et al.*, 1993). IGF-II is synthesised primarily by the liver, but is also produced locally by many tissues, where it acts in an autocrine or paracrine manner (LeRoith, 1991, 1997; Schofield, 1992). Although it is expressed at high levels during embryonic development, its expression is progressively extinguished in most tissues after birth (LeRoith, 1991, 1997; Schofield, 1992).

6.1.2. IGFs and Pancreas Development

There is substantial evidence that continuous β-cell proliferation in early life is dependent on the IGFs. Exogenous IGF-I and IGF-II can promote DNA synthesis in β-cells *in vitro* through the type 1 IGF receptor (Asfari *et al.*, 1995; Hogg *et al.*, 1993; Sieradzki *et al.*, 1988; Swenne *et al.*, 1987; Van Schravendijk *et al.*, 1987). A role for IGFs in islet cell development is further supported by the complex pattern of pancreatic expression. IGF-I expression is low during fetal life and does not attain adult levels until after weaning. IGF-I mRNA is barely detectable in the islets but its expression in the pancreatic acini increases with age (Hogg *et al.*, 1994). Conversely, IGF-II is expressed most abundantly in the fetal rat pancreas in the islets and ductal epithelium, and then declines neonatally, immediately preceding the developmental wave of neonatal islet cell apoptosis (Hill *et al.*, 1999; Hogg *et al.*, 1994; Petrik *et al.*, 1998). IGF-I and IGF-II have both been shown to function as islet survival factors *in vitro* by suppressing cytokine-mediated islet cell death in isolated neonatal rat islets (Petrik *et al.*, 1998).

6.1.3. Pancreas Development in IGF-II Overexpression Mouse Models

Until recently, few studies had yielded evidence for a trophic action of IGF-I or IGF-II on islet development *in vivo*. In 1999, Petrik and coworkers (Petrik *et al.*, 1999) examined IGF-II transgenic animals for possible changes in pancreatic islet morphology that might result from altered pancreatic expression of IGF-II or from an increase in its circulating levels. In these mice the endogenous mouse IGF-II gene becomes widely overexpressed during the second half of gestation (Sun *et al.*, 1997). E19.5-20 transgenic fetuses were found to exhibit significantly elevated circulating levels of IGF-II, compared with control mice. Islets in transgenic animals were of irregular shape and mean islet area was five-fold greater than in controls as a result of islet cell hyperplasia (increase in cell number). The mean number of islets per tissue section was found to be unaltered however. Transgenic islets were shown to be composed of proportionately fewer β-cells but a greater proportion of α-cells than islets in control mice and normal islet morphology was disrupted with the appearance of α-cells in the islet centre. Whilst cell proliferation in transgenic islets was twice that in non-transgenic siblings, the apoptotic index was significantly reduced. These findings show that IGF-II overexpression in fetal life has a profound effect on islet morphology, causing islet hyperplasia with an increased population of all three major endocrine cell types. It is however, unclear whether islet cell hyperplasia in the transgenic animals is primarily caused by increased local pancreatic IGF-II expression or from exposure to the increased circulating levels.

The same group (Hill *et al.*, 2000) subsequently investigated whether IGF-II regulates β-cell apoptosis *in vivo* using the Blast line of IGF-II transgenic mouse. In this line, mouse IGF-II is selectively overexpressed in skin, gut, and uterus driven by the keratin 10 promoter. Circulating IGF-II is retained postnatally instead of declining after birth to disappear by weaning as occurs in normal animals (Brown *et al.*, 1986) resulting in local overgrowth of tissues at sites of targeted overexpression (Ward *et al.*, 1994). The two- to three-fold rise in islet cell apoptosis observed in control animals between PN11 and PN16 was substantially decreased in IGF-II transgenic mice. Islets from transgenic pancreas consequently exhibited a significantly greater mean area from PN11 to PN16 although proportions of β- and α-cells were unaltered. The persistent presence of circulating IGF-II postnatally largely prevents the neonatal wave of islet cell apoptosis, resulting in an increased mean islet size with increases in both α- and β-cell populations.

Most recently, Devedjian *et al.* (2000) demonstrated that a local increase in IGF-II in the pancreas leads to islet hyperplasia by overexpressing IGF-II specifically in the pancreatic β-cells under the control of the rat insulin I (RIP) promoter. Islets from transgenic animals displayed high levels of IGF-II mRNA and protein and their pancreata as a whole exhibited a three-fold increase in β-cell mass and a consequent increase in insulin mRNA levels relative to controls. The islets in transgenic mice were enlarged compared with controls and displayed a more elongated, irregular shape. As in the previous two mouse models of IGF-II overexpression (Hill *et al.*, 2000; Petrik *et al.*, 1999), transgenic islets exhibited altered architecture with α-cells randomly distributed throughout the islet core. The transgenic mice exhibited hyperinsulinaemia and mild hyperglycaemia with about 30 % of these animals subsequently developing overt diabetes when fed a high-fat diet.

6.1.4. Current Study

The aim of the present study was to investigate the effects of specifically targeted and hence, local overexpression of IGF-II within the main tissue compartments of the pancreas: the pancreatic acini and the islets and to compare the effects of expression in distinct tissue compartments. Little is known about growth factors that mediate exocrine pancreatic proliferation (Kim and Hebrok, 2001). However, several studies have shown that development of the exocrine pancreas is critically dependent upon mesenchymal-epithelial interactions, suggesting that locally produced growth factors play a significant role in this process (Ahlgren *et al.*, 1996; Gittes *et al.*, 1996; Rose *et al.*, 1999; Sanvito *et al.*, 1994). While most growth factors are able to promote growth of pancreatic explant cultures *in vitro* (Vila *et al.*, 1995), the factors acting physiologically *in vivo* are unknown. Hence, it is particularly interesting to investigate the morphological effects of targeted expression of IGF-II within the pancreatic acini.

Unlike in the IGF-II overexpression models of the first two studies above (Hill *et al.*, 2000; Petrik *et al.*, 1999) in which additional IGF-II is made available to the pancreas by the circulation, the intention was to create a local and well-defined source of IGF-II. Two IGF-II-overexpressing transgenic mouse lines were generated. In the first line, expression of an IGF-II transgene was driven by the rat elastase I promoter within the acini. In the second line, the rat insulin I promoter (RIP) was used to drive expression of the IGF-II transgene specifically within the pancreatic islets as in the study of Devedjian *et al.* (2000). These two lines were named Elijah and Ripley

respectively after the transgene constructs used to generate them. IGF-II transgenic animals were examined for possible changes in pancreatic morphology of the acini and/or islets that might result from altered pancreatic expression of IGF-II. Animals were examined at mature adult stages well after endogenous gene expression had ceased to ensure that the only source of IGF-II in the pancreas was that expressed from the transgene. A specific aim of the study was to investigate whether the exogenous IGF-II protein can traverse different tissue compartments within the pancreas to impact on growth of another tissue (e.g. the islets) to that in which it is expressed (e.g. the acini).

6.2. Materials and Methods

6.2.1. Generation of Transgenic Animals

Transgenic lines were constructed by Dr. Bill Bennett as described fully in **Appendices, Section 8.1.** Briefly, two transgene constructs were generated: the ~3.5 kb coding region of the mouse Igf2 gene (exons 4 to 6 of the Igf2 gene, including introns) was either coupled with a 213 bp promoter region of the rat elastase I gene (EIP-Igf2 construct) or a 720 bp rat insulin I gene promoter (RIP) fragment (RIP-Igf2 construct). Fertilised eggs were harvested from PN4wk-6wk super-ovulated F_1 (C57BL/6×CBA) females mated with stud F_1 (C57BL/6×CBA) males and the transgene DNA constructs were inserted into the single cell embryos with visible pro-nuclei by pronuclear injection. Successfully injected embryos were then implanted into pseudopregnant MF1 female mice. Potential founders were tested by PCR of earclip biopsies for the presence of the transgene at around PN3wk. Positive potential founders were crossed to non-transgenic F_1 (C57BL/6×CBA) animals and two or three litters of offspring were tested for transmission. Only one founder for each construct was found to transmit consistently. The line carrying the EIP-Igf2 construct was designated *Elijah*, and the line carrying the RIP-Igf2 construct was designated *Ripley*.

6.2.2. Serum Collection and Histology

Transgenic and non-transgenic littermate control animals were identified on the basis of earclip markings before weighing. After being sacrificed by cervical dislocation, blood samples were rapidly collected by cardiac puncture and tail tips and liver lobes taken for DNA analysis. Blood samples were centrifuged at 15000 rpm for 10 min and the supernatant serum drawn off for measurement of glucose, insulin, and IGF-II. The complete gut was removed to facilitate careful dissection of the whole pancreas. Pancreatic wet weight was recorded before the organ was divided into two equal portions for regular paraffin histology and the preparation of frozen sections as described in **Chapter 2, Sections 2.2.3.** and **2.4.**

Representative paraffin sections separated by a distance of not less than 150 μm were counterstained in Ehrlich's haematoxylin and eosin (H & E) or subjected to immunoperoxidase staining for glucagon or insulin by the avidin-biotin peroxidase (ABC) method (**Section 2.5.3.1.**). Further Elijah and Ripley, as well as non-transgenic

control pancreas sections were also immunoperoxidase-stained to localise IGF-II (work performed by Dr. Janet Smith, University of Birmingham).

6.2.3. Morphometric and Statistical Analysis

Histological sections from five transgenic Elijah and five transgenic Ripley pancreata were subjected to morphometric analysis. For each study, five pancreata from non-transgenic littermates of the same sex were similarly examined as controls. Analysis of H & E-stained paraffin sections was performed using the Leica DMRB compound microscope at a magnification of × 50 (Elijah line) or × 200 (Ripley line). Images of one randomised field (representing only a *partial* section) from each section examined (Elijah) or each islet in all analysed sections (Ripley) were captured with a Spot RT Color digital camera (National Diagnostics Inc.). Also, using a binocular dissecting microscope, images of whole pancreas sections were captured for the Ripley characterisation study. Analyses of the uncompressed 24-bit TIFF images were performed with the Image-Pro Plus™ version 3.0.1 morphometric analysis software (Media Cybernetics, Maryland, USA). The stylus of a wireless graphics tablet (Trust Wireless Design and Work Tablet 200) was used to manually trace around acini or islets in images and in conjunction with the area measurement tool was used to determine acini or islet area. The relative area of each random field occupied by pancreatic acini and islets (**Fig. 6.1.**) was calculated from five sections of each Elijah pancreas. The number and area of islets (**Fig. 6.2.**) was calculated from five sections of each Ripley pancreas, representing the head region. Islets were defined on the criterion that they were composed of five or more contiguous endocrine cells (as for determination of cell lineage in **Chapter 4**) as identified by H & E histochemistry. Finally, total section area was determined for each section of Ripley pancreas examined (**Fig. 6.3.**). Manual grey scale thresholding ("gating") was performed on grey scale images to distinguish the object area (pancreas section) from the background and when the section image was correctly highlighted, the section area was obtained. In all cases sections selected for analysis contained a minimum of five islets. Differences between mean values for each variable were compared for statistical difference by the student's paired *t*-test using the Minitab™ Version 13 statistical software package (and for the Elijah study, were further compared by the Wilcoxon paired-sample test). Finally, the number of islets within each immunoperoxidase-stained section of transgenic pancreas displaying aberrant glucagon-immunopositive cell localisation was ascertained.

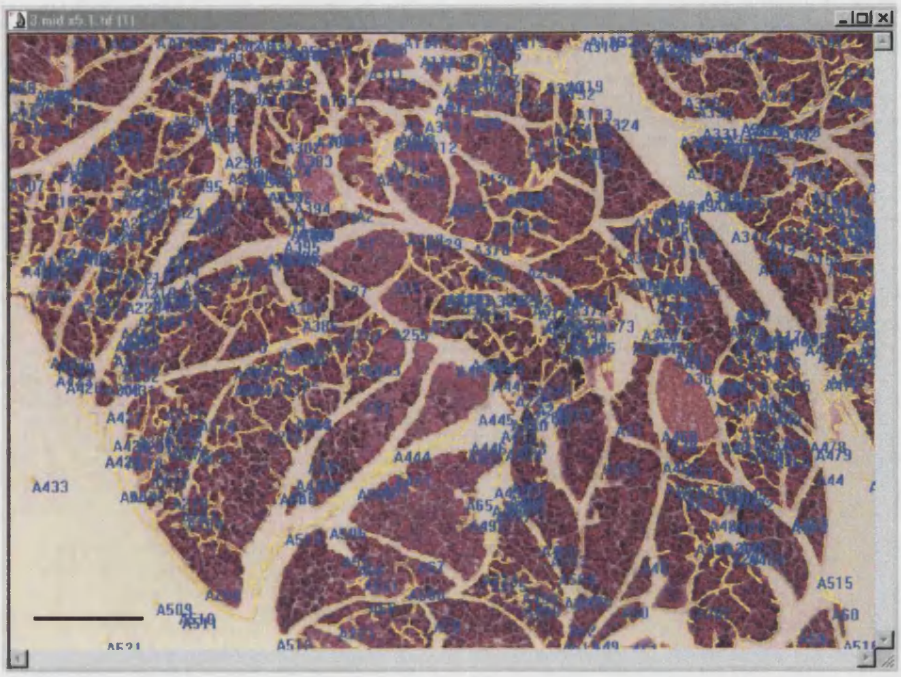

Figure 6.1. Example of Morphometric Analysis with Image ProPlus™ for a Random Field of a Transgenic Elijah Pancreas Section (Above; Bar = 400 μm) with Calculated Measurements of the First Ten Highlighted Areas (Below)

Tool	Length	Area (μm²)	Angle
A1		15062.29	
A2		4362.303	
A3		9903.102	
A4		3026.675	
A5		4006.884	
A6		6116.952	
A7		41071.5	
A8		6745.482	
A9		33993.04	
A10		42807.44	

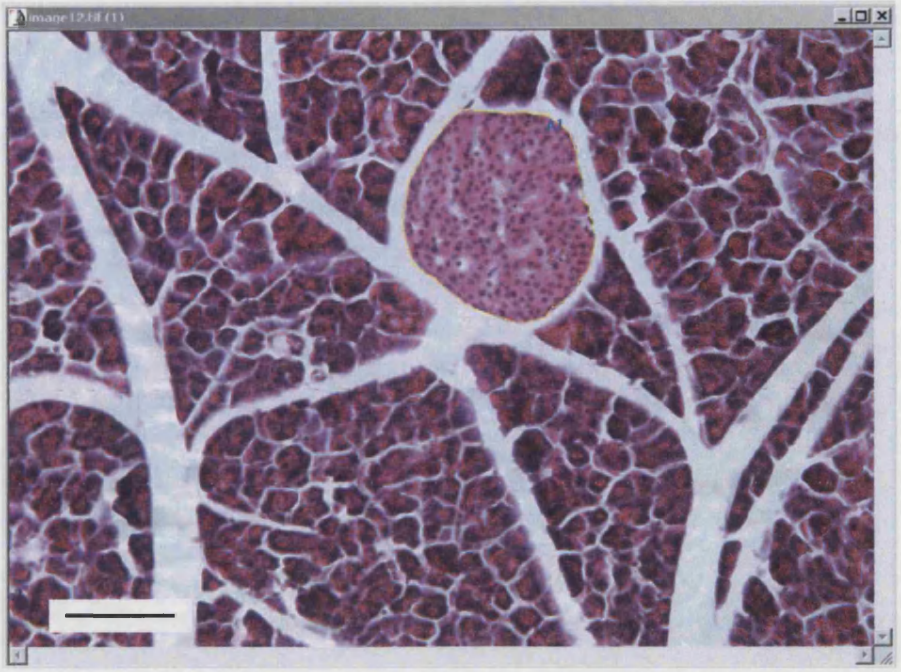

Figure 6.2. Example of Morphometric Analysis with Image ProPlus™ for an Islet in a Transgenic Ripley Pancreas Section. Bar = 100 μm

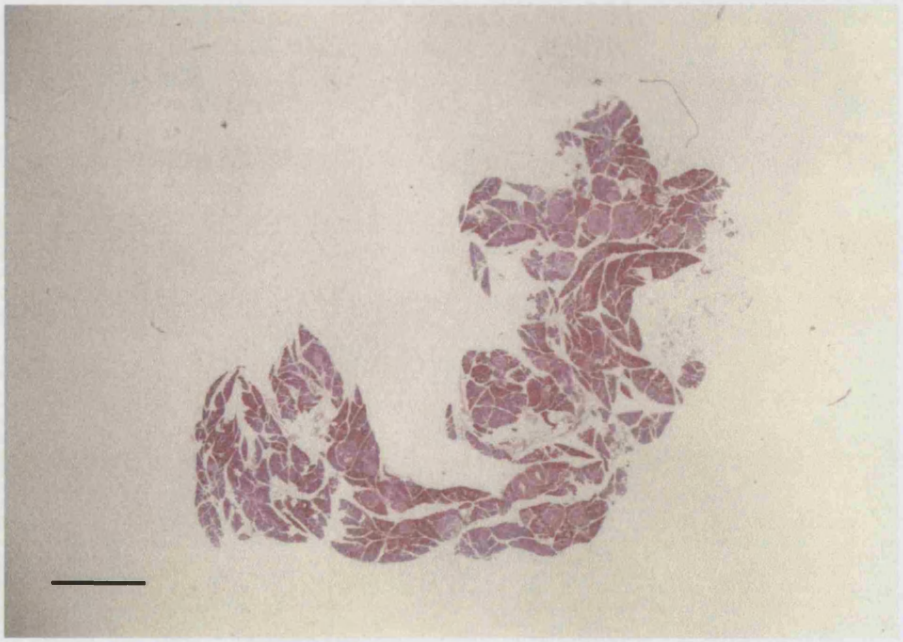

Figure 6.3. Image of a Whole Transgenic Ripley Pancreas Section Captured for Total Sectional Area Measurement with Image ProPlus™. Bar = 2 mm

6.3. Results

6.3.1. Statistical Considerations

Differences between mean values for each variable examined were compared for statistical difference initially by the student's paired *t*-test. Mean values for transgenic and control animals were only compared directly between animals of the same sex from the same litter and sacrificed at the same time (and so of the same age when examined). Hence, the data could be considered as being paired. Of the five Elijah transgenic and five control animals examined, four of each were from a different litter. Similarly, the five Ripley transgenic (and five non-transgenic) mice were obtained from three different litters. When more than one transgenic animal of a given sex and age was obtained from the same litter, mean values were calculated and compared between the transgenic and control littermates and in this way, the mean figures could be considered as being paired. Four pairs of mean values were therefore compared in a pair-wise manner in the Elijah study and three pairs of means were similarly compared in the Ripley work.

Similar studies (Devedjian *et al.*, 2000; Hill *et al.*, 2000; Petrik *et al.*, 1999) in which equivalent numbers of animals have been examined have compared mean values for statistical difference by parametric tests such as ANOVA, Scheffe's test or the Student-Newman-Keuls test (multiple comparison procedures). In such cases as here, the sample size is so reduced that one cannot assume a Gaussian or normal distribution of data to be compared (although there is no reason to suggest that this is not the situation). Hence, the decision was made to compare mean values for each variable by the student's paired *t*-test (using MiniTab™ v.13) *and* the Wilcoxon paired-sample test as a confirmation of the outcome from the former. The Wilcoxon test is a nonparametric analogue to the paired-sample *t*-test. The testing procedure involves the calculation of differences, as does the paired-sample *t*-test. The absolute values of the differences are then ranked, from low to high and the sign of each difference is affixed to the corresponding rank. The ranks of each sign are then each summed separately and for a two-tailed test if either summed value (T_+ and T_-) is less than or equal to the critical value $T_{\alpha(2),n}$, then the null hypothesis H_0 is rejected. Whenever the paired-sample *t*-test is applicable, the Wilcoxon paired-sample test is also applicable. However, if the data being compared *are* from a normal distribution, then the Wilcoxon test has only $3/\pi$ (i.e. 95 %) of the power in detecting differences as the former (Conover, 1980; Mood, 1954). Both statistical tests were used to compare the four paired mean values for each variable

from the Elijah study. The small size of the data sets for comparison meant that null hypotheses could only be tested at $\alpha(2) = 0.20$, so that even comparably (to $\alpha(2) = 0.05$) very small differences in a variable were deemed as being of statistical significance. However, the three pairs of mean values in the case of the Ripley animals were too few for analysis by the Wilcoxon test and only the paired-sample *t*-test was conducted.

6.3.2. Elijah Line

6.3.2.1. IGF-II Expressed by Both Acinar and Islet Cells in Adult Elijah Transgenic Animals

Immunoperoxidase staining (Dr. Janet Smith) demonstrated that IGF-II is expressed exogenously in adult Elijah transgenic pancreas in scattered cells throughout the pancreatic acini and in a small number of cells within the islets (**Fig. 6.4.**). Some staining was also observed in pancreatic ducts of both transgenic and control pancreata which was also attributed to endogenous expression by connective tissue. This result shows that the transgene expression is mostly in exocrine tissue. When the line was generated, the elastase element used was believed to be exocrine-specific. However, we now know that expression can occur also in some endocrine cells (Kruse *et al.*, 1993). It cannot be known for sure whether the immunopositive islet cells in Dr. Smith's images are endocrine or some other cell type such as ductule or capillary. Scattered islet cell expression might be attributable to the transgene integrating into a random position within the genome. However, despite there being only one line carrying the EIP-Igf2 transgene, the study by Kruse and coworkers (Kruse *et al.*, 1993) using the same rat elastase I promoter element suggests that the transgene behaved as expected.

6.3.2.2. No Significant Difference in Pancreatic Weight

To determine whether rat elastase I promoter-driven expression of IGF-II in the pancreatic acini resulted in an increase in pancreas mass, pancreatic wet weight was compared between ten intact pancreata from transgenic animals and ten organs from control non-transgenic littermates of the same sex. Wet weight of transgenic pancreata was found to be 497 ± 30 mg, (mean ± S.E.) compared with 496 ± 31 mg for control pancreata (**Table 6.1.**). For the five transgenic pancreata subjected to morphometric analysis, mean wet weight was 533 ± 50 mg, in comparison to 525 ± 54 mg for the five non-transgenic organs (**Graph 6.1.**). No significant difference in pancreatic weight

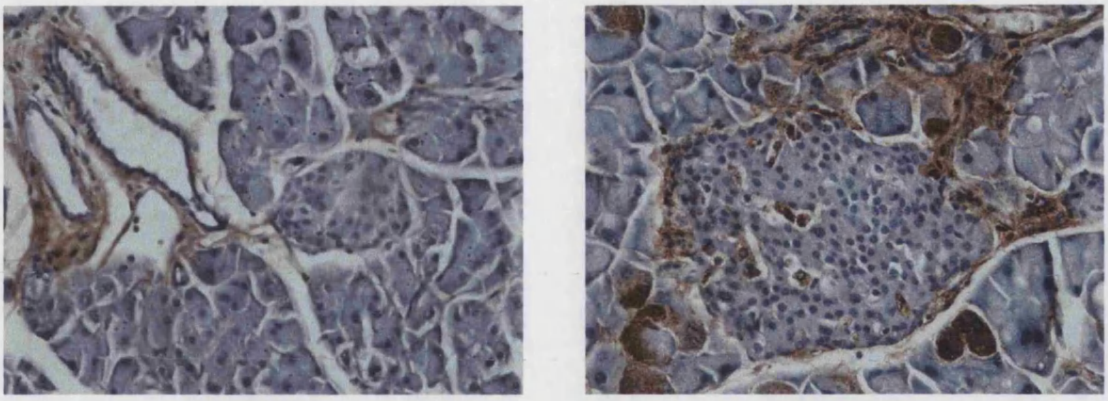

(a). Control × 40 **(b). Transgenic × 40**

Figure 6.4. Immunoperoxidase Staining for IGF-II in Pancreas Sections from PN35wk Elijah Transgenic and Control Animals (Dr. Janet Smith)

Graph 6.1. Mean Pancreatic Wet Weight for Elijah Transgenic Animals and Non-Transgenic Sibling Controls

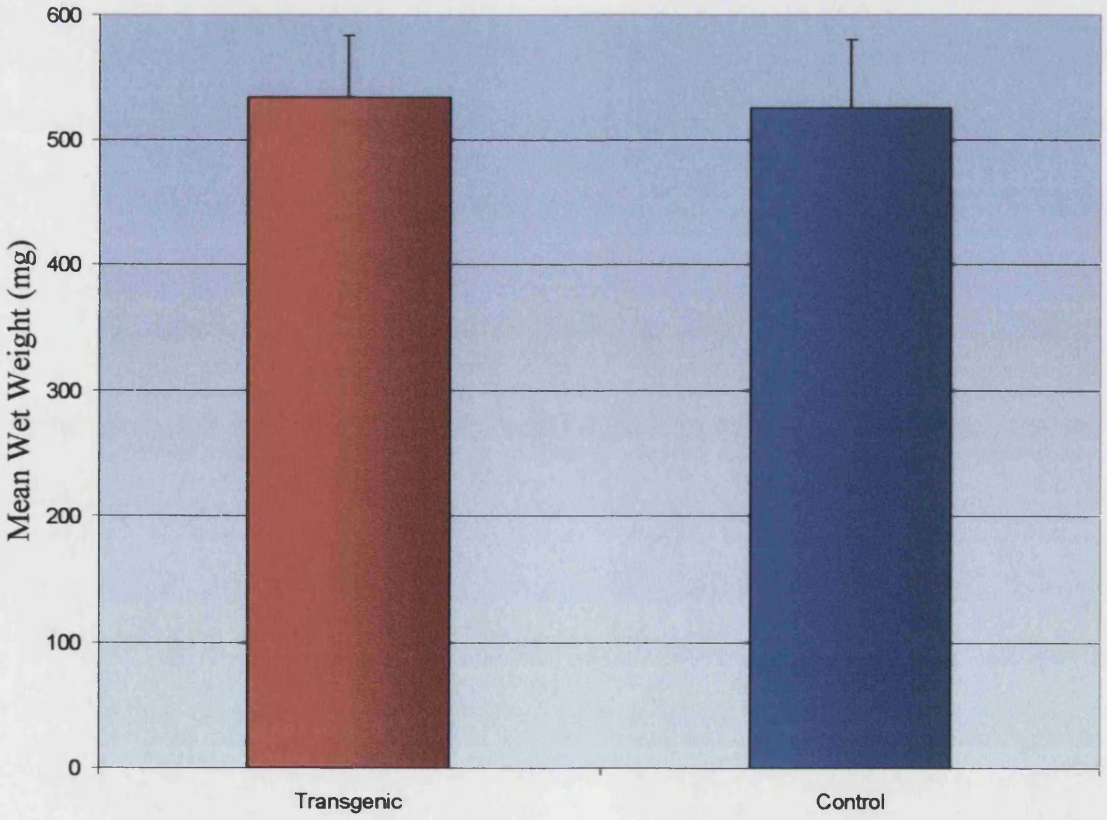

between control animals and those carrying the IGF-II transgene was evident (for all data in **Table 6.1.**, $t = 0.24$; $P = 0.818$; $T_+ = 12$, $T_- = 9$; $T_{0.20(2),4} = 0$; for the animals subjected to morphometric analysis, $t = 0.32$; $P = 0.770$; $T_+ = 5$, $T_- = 5$; $T_{0.20(2),4} = 0$).

Table 6.1. Wet Weight of Elijah Transgenic and Control Intact Pancreata

LITTER/SEX	AGE (Wks)	PANCREATIC WET WEIGHT (mg)	
		Transgenic	Control
Litter 1 Male	35	651*	409*
		470	505
Litter 2 Female	33	379*	511*
		417	469
Litter 3 Male	31	670*	593*
		513*	721*
Litter 3 Female	31	473	451
	32	454*	393*
Litter 2 Male	35	513	441
		427	469
Mean ± S.E.	**N/A**	**497 ± 30**	**496 ± 31**

* Pancreata subjected to morphometric analysis.

6.3.2.3. Area of Pancreas Tissue Within Each Field is Significantly Greater in Elijah Transgenic Animals

For subsequent direct comparisons between total islet and acini area in randomly selected fields in transgenic and control pancreas sections, it was necessary to show that total pancreas area per field was *not* significantly different between transgenic and control subjects. However, total mean area of pancreas per field *did* tend to be greater in transgenic than control animals (3.35 ± 0.169 mm^2 and 2.89 ± 0.163 mm^2 respectively; **Table 6.2.**, **Graph 6.2.** and **Tables 8.1. (a).** and **(b).**, **Appendices**), and this difference *did* reach statistical significance ($t = 3.75$; $P = 0.033$; $T_+ = 10$, $T_- = 0$; $T_{0.20(2),4} = 0$). Hence, endocrine and acinar contribution to pancreas area were necessarily calculated as percentage of total pancreas area before being compared. This had the disadvantage of reducing the power to detect differences in the variables since statistical tests were to be performed on data subjected to manipulation.

Table 6.2. Summary of Individual Animal Mean Values from Statistical Morphometry Study of Pancreas Sections from Elijah Transgenic (TG) and Age- and Sex-Matched Non-Transgenic Littermate Control (CTL) Animals

LITTER / SEX	AGE (Wks)	VARIABLE (MEAN)													
		Total Pancreas Tissue Area/ Field (mm^2)		Total Acini Area/Field (mm^2)		Percentage Acini Area/ Field (%)		Total Islet Area/ Field (μm^2)		Percentage Islet Area/ Field (%)		Mean Islet Number/Field		Mean Islet Area (μm^2)	
		TG	CTL	TG	CTL	TG	CTL	TG	CTL	TG	CTL	TG	CTL	TG	CTL
1/Male	35	3.409	3.269	3.222	3.184	95.37	97.41	83187	26073	2.010	0.8010	5.6	1.8	9233	13376
2/Female	33	3.775	3.053	3.655	2.976	96.86	97.59	33995	37422	0.8878	1.084	6	4.4	3813	6074
3/ Male	31	3.327	2.840	3.184	2.756	96.45	97.15	79955	45661	1.828	1.510	3.4	4.2	11818	9804
		3.559	3.072	3.458	2.950	97.05	95.05	56812	63042	1.640	1.857	2.2	4.4	17953	14806
3/Female	32	2.654	2.213	2.590	2.076	97.56	93.89	5749	52835	0.2216	2.305	1.6	3.8	4535	13234
Mean ± S.E.	**N/A**	**3.35 ± 0.169**	**2.89 ± 0.163**	**3.22 ± 0.161**	**2.79 ± 0.170**	**96.7 ± 0.329**	**96.2 ± 0.663**	**51939 ±13024**	**45007 ± 5667**	**1.32 ± 0.299**	**1.51 ± 0.240**	**3.76 ± 0.791**	**3.72 ± 0.44**	**9470 ± 2314**	**11459 ± 1411**

Graph 6.2. Mean Area of Pancreas Tissue Per Field for Elijah Transgenic Animals and Non-Transgenic Sibling Controls

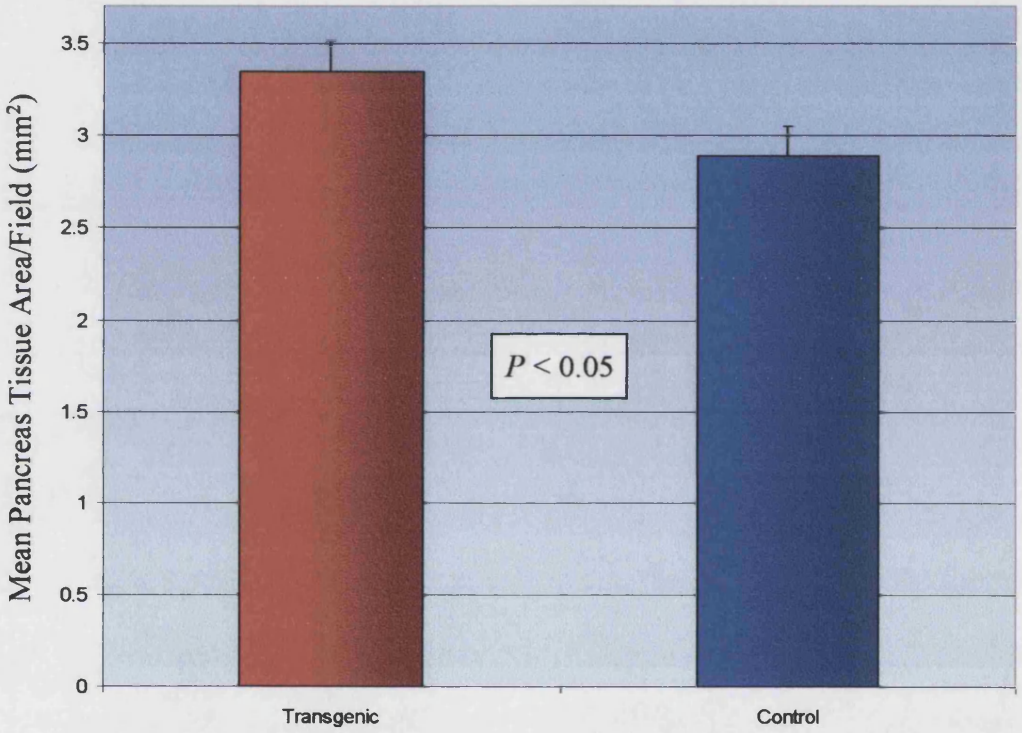

6.3.2.4. No Significant Difference in Percentage Acini Area Per Field

Mean percentage acini area per field for transgenic animals at 96.7 ± 0.329 % was not significantly different from the control value of 96.2 ± 0.663 % (**Table 6.2.** and **Graph 6.3.**) (t = 0.32; P = 0.770; T_+ = 5, T_- = 5; $T_{0.20(2),4}$ = 0). As a consequence of the greater total area of pancreas tissue per field in transgenic animals, the absolute area of acinar tissue per field in transgenic animals at 3.22 ± 0.161 mm^2, was greater than that in non-transgenic siblings (2.79 ± 0.170 mm^2). This difference still failed to reach statistical significance at $\alpha(2)$ = 0.05 according to the outcome of the paired-sample t-test (t = 3.10; P = 0.053) although it was proved significant by the Wilcoxon paired-sample test at $\alpha(2)$ = 0.20 (T_+ = 10, T_- = 0; $T_{0.20(2),4}$ = 0).

6.3.2.5. No Significant Difference in Percentage Endocrine Contribution to Pancreas Area

Endocrine tissue represented a 1.32 ± 0.299 % contribution to total pancreas area per field in animals carrying the IGF-II transgene compared with a 1.51 ± 0.240 % contribution in non-transgenic siblings (**Table 6.2.** and **Graph 6.4.**). This difference was not statistically significant (t = -0.37; P = 0.733; T_+ = 4, T_- = 6; $T_{0.20(2),4}$ = 0). As with the absolute acini area per field, the absolute area of islet tissue per field was greater in transgenic animals than control (51939 ± 13024 μm^2 and 45007 ± 5667 μm^2 respectively) as a result of the greater total area of pancreas tissue per field in transgenic animals. This difference however, failed to reach statistical significance (t = 0.24; P = 0.826; T_+ = 6, T_- = 4; $T_{0.20(2),4}$ = 0).

6.3.2.6. No Significant Difference in Islet Number Per Field

The number of islets was counted in the random fields from sections of transgenic and control pancreas to determine whether the IGF-II transgene affects islet number. Islets within the field and those contacting its upper and right boundaries were counted whilst those touching the bottom and left edges were excluded from the count as per typical quadrat sampling protocol. Islet number was found to be very similar between transgenic and control animals: 3.76 ± 0.791 and 3.72 ± 0.440 islets/field

Graph 6.3. Mean Percentage Acini Area Per Field for Elijah Transgenic Animals and Non-Transgenic Sibling Controls

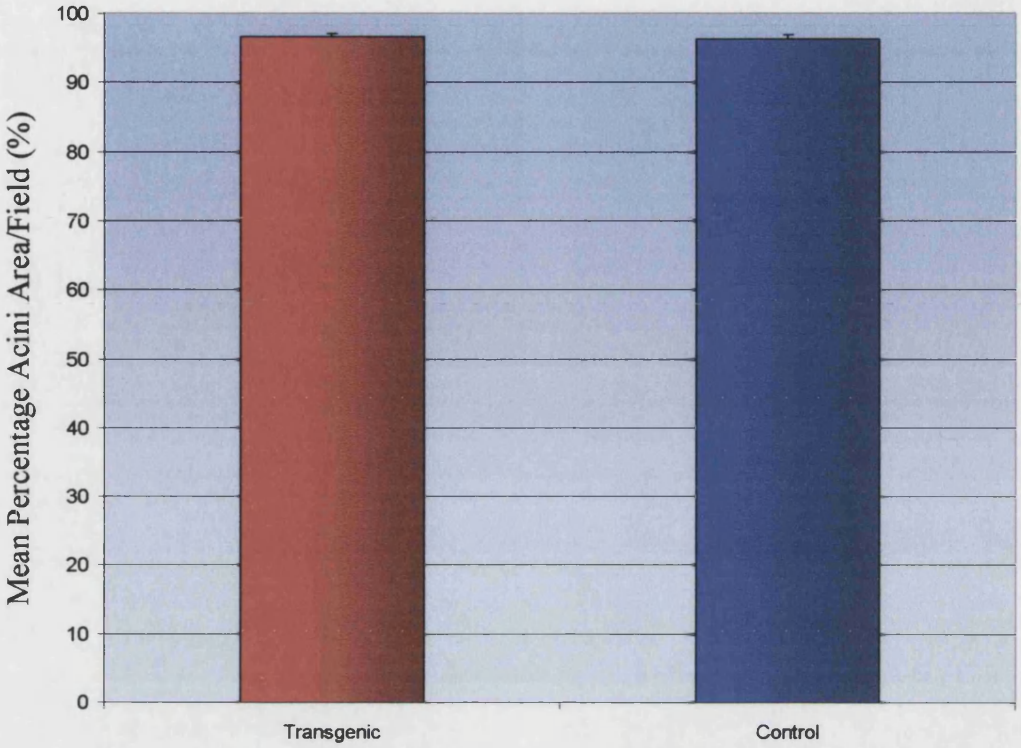

Graph 6.4. Mean Percentage Islet Area Per Field for Elijah Transgenic Animals and Non-Transgenic Sibling Controls

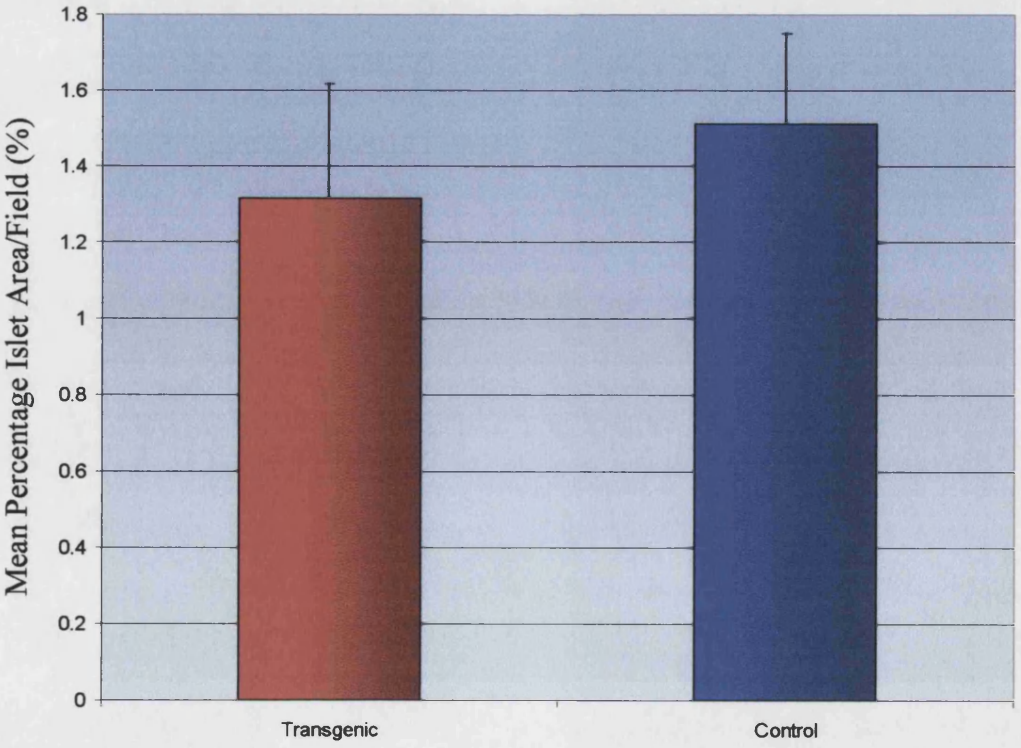

respectively (**Table 6.2.** and **Graph 6.5.**) with no significant difference being evident (t = 0.30; P = 0.781; T_+ = 6, T_- = 4; $T_{0.20(2),4}$ = 0).

6.3.2.7. No Significant Difference in Mean Islet Area

As a preliminary assessment of whether rat elastase I promoter-driven IGF-II exerts any effect on islet size, mean islet area was determined from those islets present within the random fields examined. Areas were not obtained for islets falling only partially within the field so as not to artificially reduce the calculated sample mean. The mean islet area for transgenic animals at 9470 ± 2314 μm^2 was not significantly different (t = -1.34; P = 0.272; T_+ = 2, T_- = 8; $T_{0.20(2),4}$ = 0) from the control figure of 11459 ± 1411 μm^2 (**Table 6.2.** and **Graph 6.6.**).

6.3.2.8. Oversized Islets (> 0.1 mm^2) in Elijah Transgenic Animals

The frequency of islets of distinct size (area) classes was compared between transgenic and control animals to ascertain whether there was any difference in islet size distribution as a result of the IGF-II transgene (**Graphs 6.7.** and **6.8.**). The normal range of islet areas as inferred from non-transgenic animals could be segregated into "small" (0-19999 μm^2), "intermediate" (20000-39999 μm^2) and "large" islets (40000-59999 μm^2). When this was done, the size distribution of smaller-sized islets in transgenic and control animals was very similar (**Table 6.3.** and **Graph 6.7.**); 83.7 % of the 92-islet sample in transgenic pancreata fell within the "small" category compared with 83.9 % of the 87 control islets. Of the transgenic islets, 7.61 % were categorised as intermediate-sized with 9.2 % of the non-transgenic islets being categorised as such. The remaining 6.9 % of the control islet sample were classified as large islets in the normal islet size spectrum. In the transgenic animals however, only 2.17 % of islets exhibited a cross-sectional area of 40000-59999 μm^2. The remaining six islets (or 6.52 %) of the 92-islet sample exceeded the normal islet size range seen in the control animals. These "mega-islets", from three different transgenic pancreata, possessed areas of 60466, 67395, 79255, 104905, 176359 and 180194 μm^2. The largest two islets were more than three-fold the largest control islets measured. Such mega-islets were typically of a very irregular shape in cross-section, compared with the more characteristic spherical islet profile; furthermore, fibrous inclusions were often visible within these islets (**Fig. 6.5.**).

Graph 6.5. Mean Number of Islets Per Field for Elijah Transgenic Animals and Non-Transgenic Sibling Controls

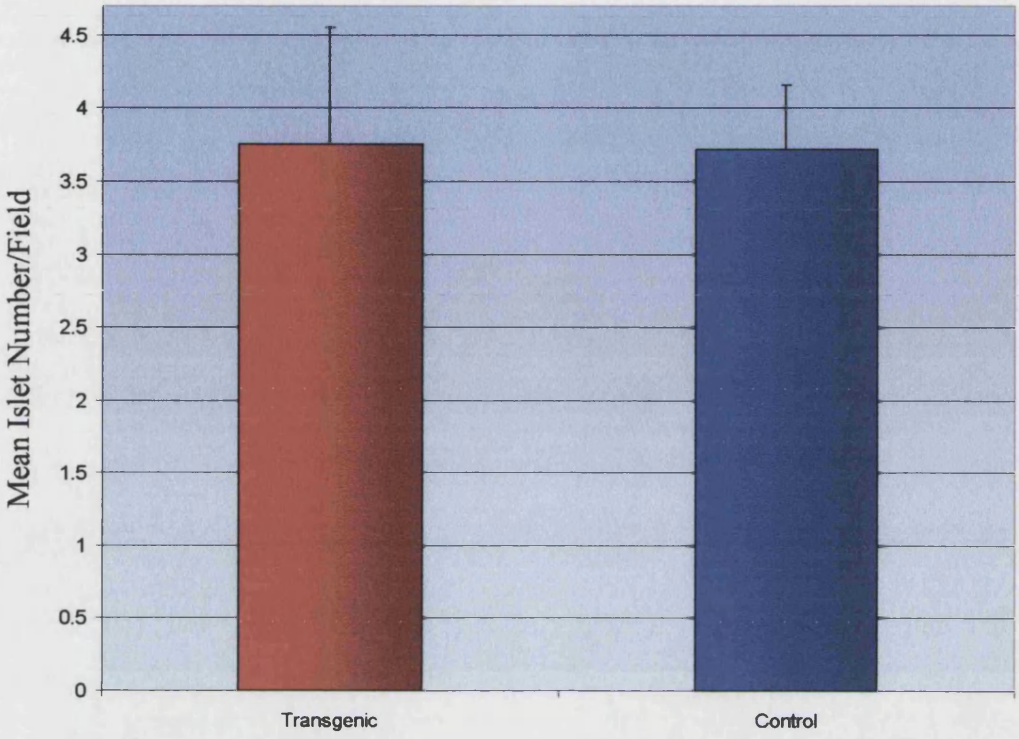

Graph 6.6. Mean Islet Area in Elijah Transgenic Animals and Non-Transgenic Sibling Controls

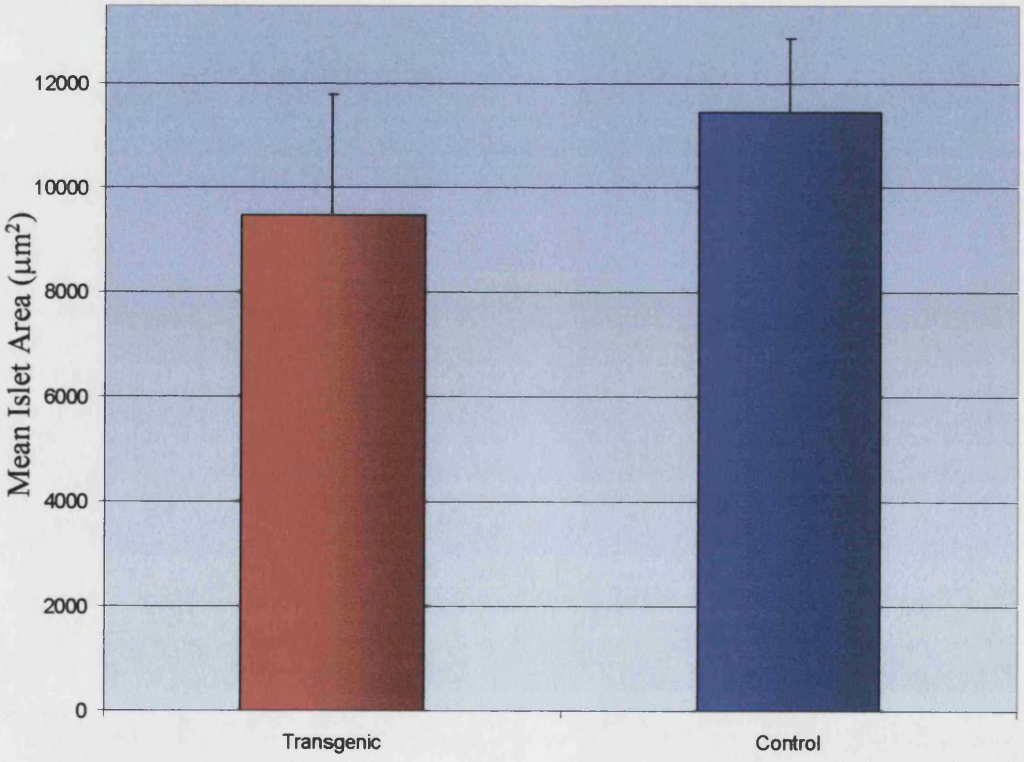

Graph 6.7. Frequency Histogram Comparing Islet Area in Elijah Transgenic Animals and Non-Transgenic Sibling Controls

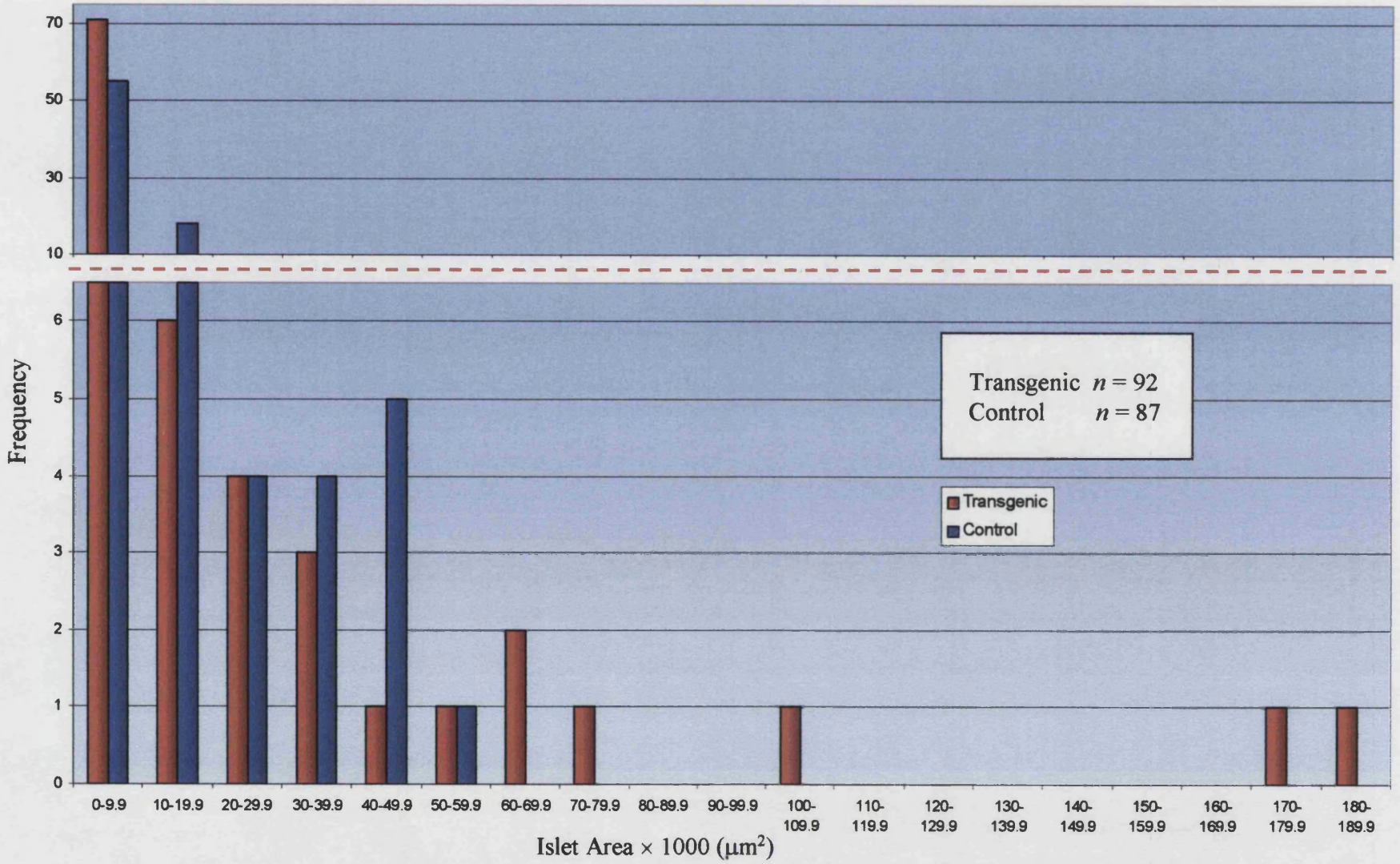

Graph 6.8. Frequency Histogram Comparing Observed Islet Areas in Elijah Transgenic Animals with "Expected" Islet Size Distribution as Calculated from Non-Transgenic Sibling Controls

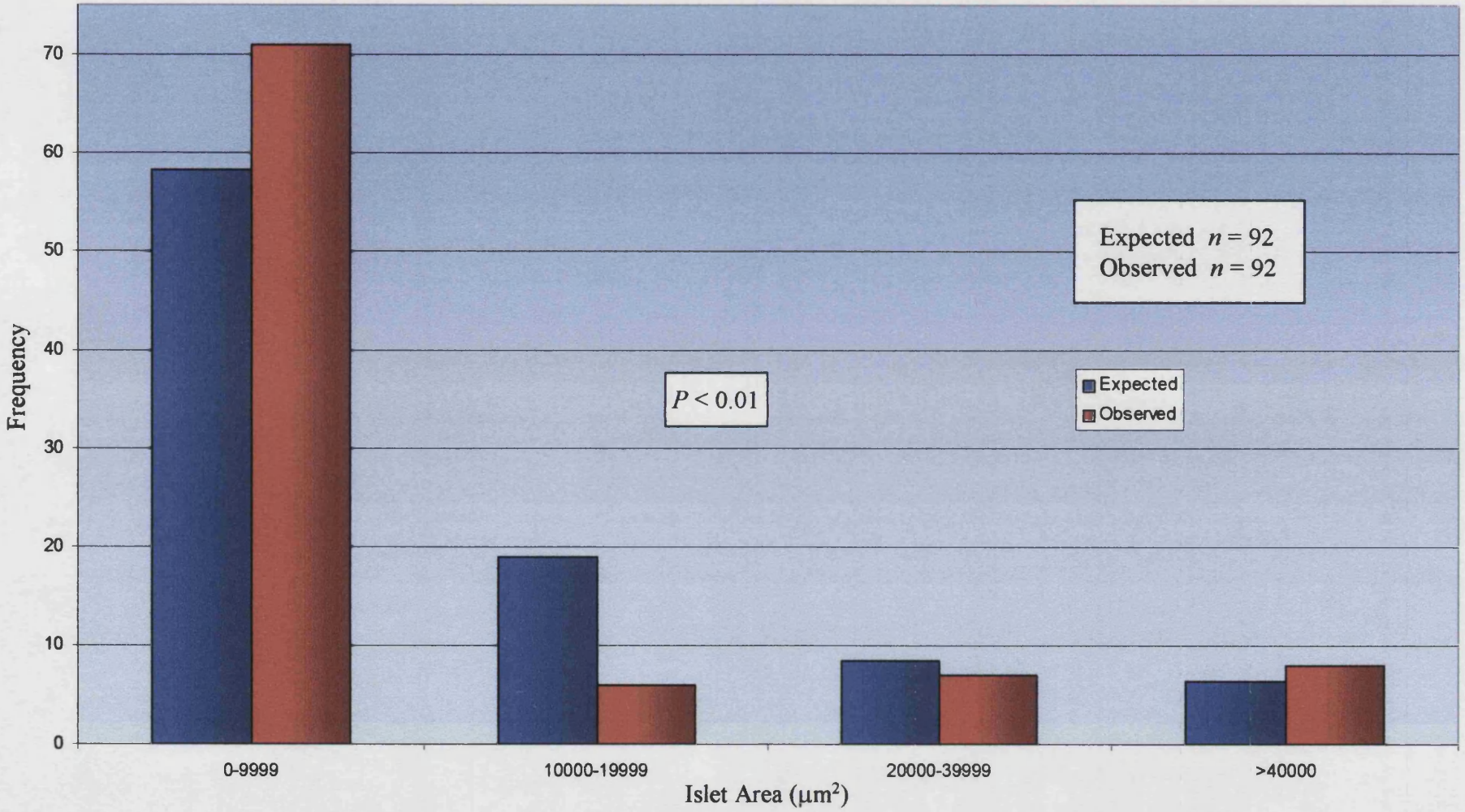

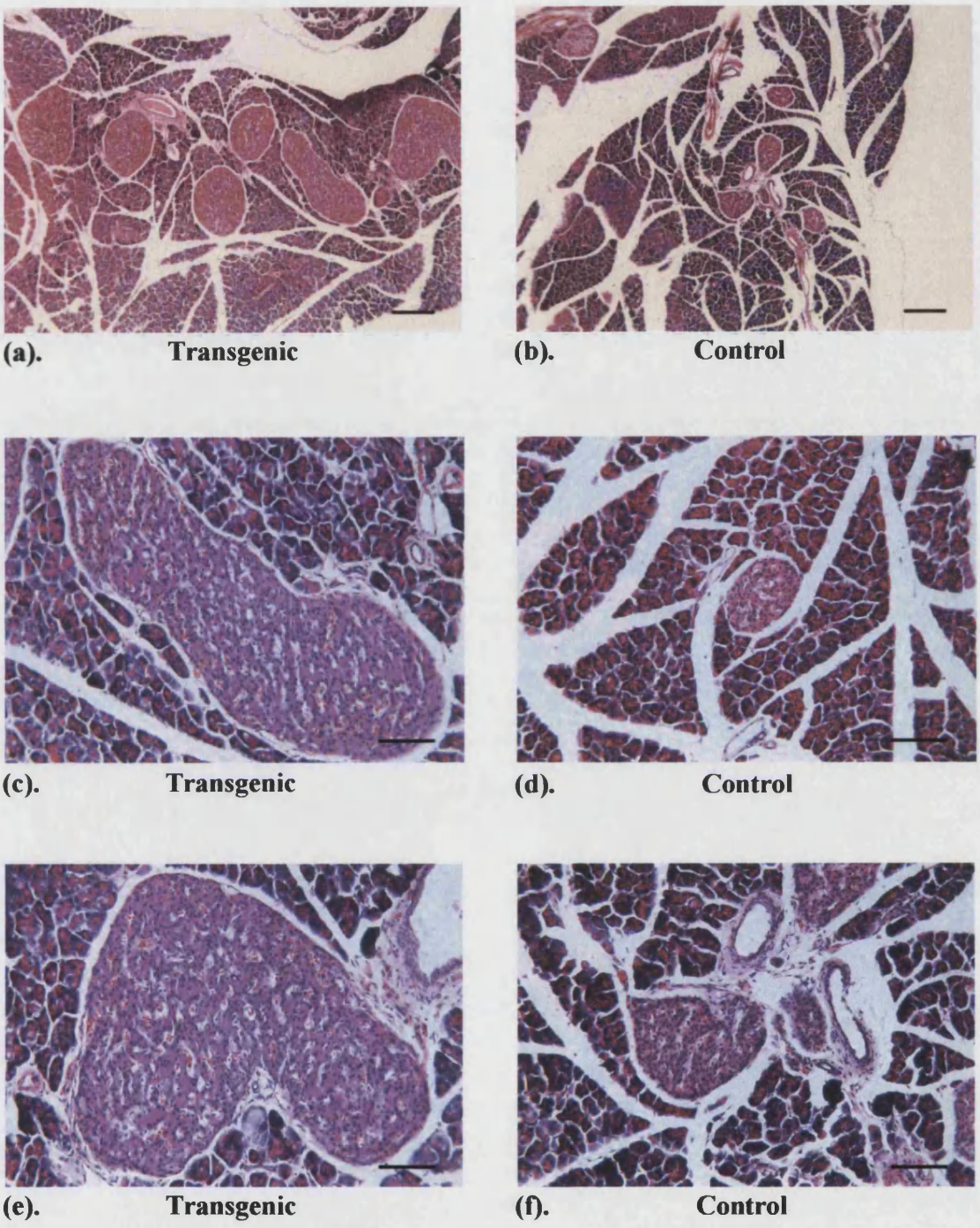

Figure 6.5. "Mega-Islets" in H & E-Stained Pancreas Sections from PN31wk Elijah Transgenic and Control Animals

(a)-(b) Bar = 250 μm; (c)-(f) Bar = 100 μm

Table 6.3. Size Distribution of Islets in Elijah Transgenic and Control Animals

ISLET AREA (μm^2)	PROPORTION OF TOTAL ISLET SAMPLE (%)	
	Transgenic (n = 92)	**Control (n = 87)**
0-19999 - "Small"	83.7	83.9
20000-39999 - "Intermediate"	7.61	9.2
40000-59999 - "Large"	2.17	6.9
> 60000	6.52	0

To verify the divergence in size distribution of the transgenic and control islet population samples, a chi-square (χ^2) test was conducted to compare "expected" size distribution, based on data from control animals, with the "observed" distribution of islets in transgenic pancreata (**Table 6.4.** and **Graph 6.8.**). There was found to be a highly significant difference ($P < 0.01$) between observed and expected (control) islet size distributions.

$$\chi^2 = \Sigma \frac{(\text{Observed} - \text{Expected})^2}{\text{Expected}} \qquad \text{with } df = c \text{ (number of categories)} - 1$$

Table 6.4. Calculating χ^2 to Test Whether the Observed Islet Size Distribution in Elijah Transgenic Animals Differs from that Expected (from Control Data)

ISLET AREA (μm^2)	NUMBER OF ISLETS			Observed - Expected	$O - E^2$	$\frac{O - E^2}{E}$
	Control	Transgenic (Observed)	Transgenic (Expected)			
0-9999	55	71	58.2	12.8	165	2.83
10000-19999	18	6	19.0	-13.0	170	8.93
20000-39999	8	7	8.50	-1.46	2.13	0.252
> 40000	6	8	6.34	1.66	2.74	0.432
Σ	**87**	**92**	**92**	**0**	**340**	**12.4 (χ^2)**

NB: Data was segregated into the above categories of islet area by considering that:-

(1). in the χ^2 test, the expected frequency of each category under the null hypothesis must be at least *five*,

(2). the higher the number of categories, the greater the sensitivity of the test.

$\chi^2 = 11.34$, $df = 3$, $p = 0.01$. As the calculated value of χ^2 is greater, the null hypothesis can be rejected.

6.3.2.9. Mega-Islets Formed by Hyperplasia, Not Hypertrophy

In order to ascertain whether over-sized mega-islets in transgenic animals were a result of hyperplasia of endocrine tissue, or hypertrophy (increase in cell size) of existing islet cells, the area of individual islet cells was determined in transgenic mega-islets and control islets in both transgenic and non-transgenic animals. The area of control islets selected for comparison was less than 60000 μm^2, within the normal range of islet size in control animals. The mean area of individual islet cells in mega-islets was found to be 76.6 ± 9.28 μm^2, in comparison with mean cell areas of 71.7 ± 5.71 μm^2 and 77.2 ± 5.14 μm^2 for endocrine cells within control islets in transgenic and non-transgenic animals, respectively (**Table 6.5.** and **Graph 6.9.**). No significant difference was found between these values (for comparison between mega-islets and transgenic control islets $t = 1.05$; $P = 0.403$; between mega-islets and non-transgenic control islets $t = -0.37$; $P = 0.774$; insufficient paired data for Wilcoxon paired-sample test). Mega-islets were therefore a product of islet hyperplasia.

Table 6.5. Mean Area of Individual Islet Cells in Mega-Islets from Elijah Transgenic Animals and Control Islets (< 60000 μm^2) in Transgenic Animals and Non-Transgenic Littermates

LITTER / SEX	AGE (Wks)	INDIVIDUAL ISLET CELL AREA (μm^2)		
		Transgenic Mega-Islets	Transgenic Control Islets	Non-Transgenic Control Islets
Litter 1 Male	35	55.06	57.88	78.44
Litter 3 Male	31	80.99	76.72	65.75
		93.67	80.50	87.44
Mean ± S.E.	**N/A**	**76.57 ± 9.278**	**71.70 ± 5.710**	**77.21 ± 5.137**

Graph 6.9. Mean Individual Islet Cell Area in Mega-Islets *vs.* Control Islets in Elijah Transgenic Animals and in Control Islets in Non-Transgenic Siblings

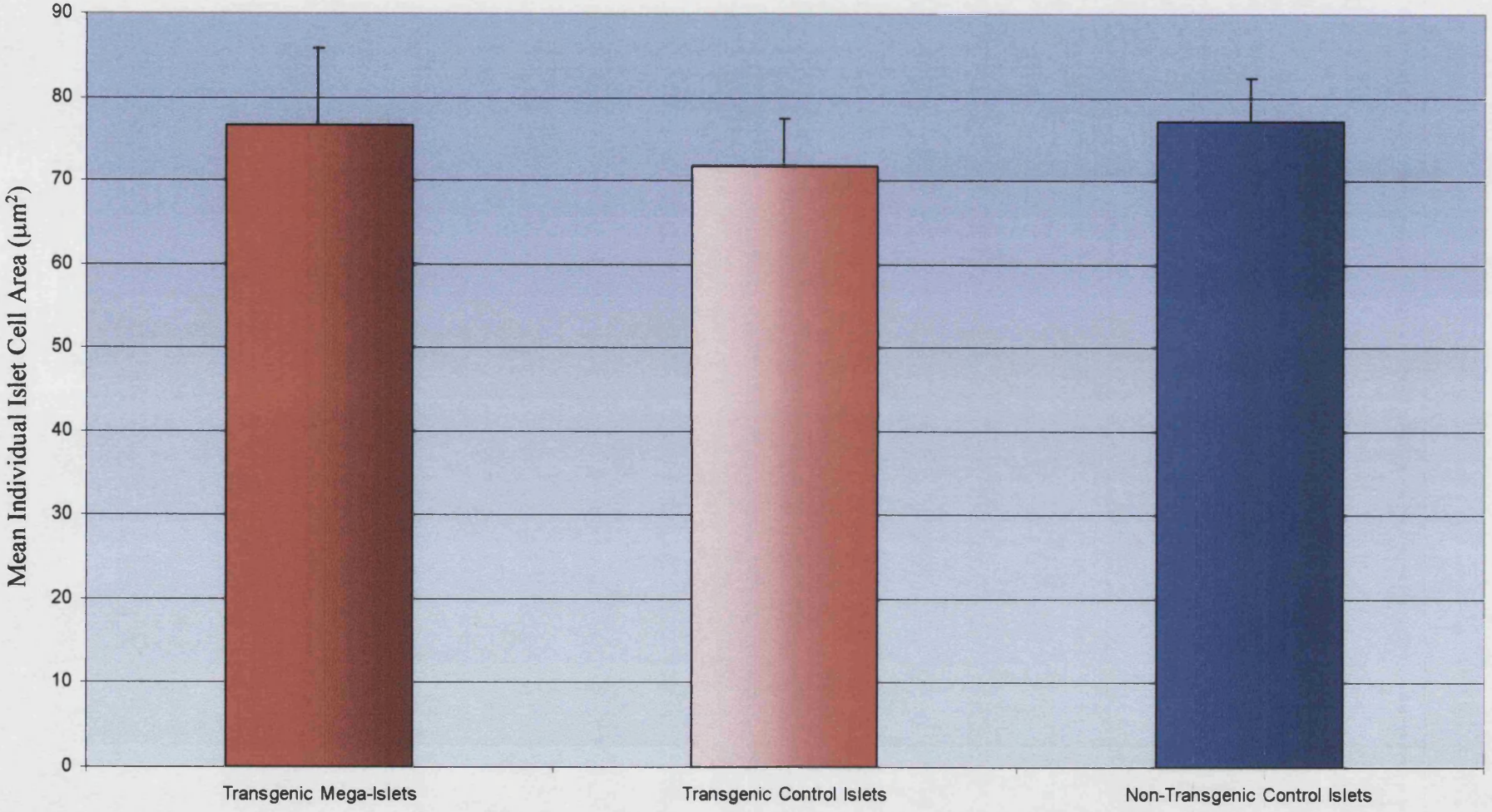

6.3.2.10. "Hepatocyte-Like" Cells in an Elijah Transgenic Islet

In one of the transgenic pancreata, H & E histochemistry revealed the presence of large cells which morphologically resembled hepatocytes (**Fig. 6.6.**). These cells were clearly distinguishable from adjacent endocrine cells by their abundant eosinophilic cytoplasm and were located at the islet periphery.

6.3.2.11. Aberrant α-Cell Localisation in Elijah Transgenic Islets

Immunoperoxidase staining for glucagon revealed a disruption in the distribution of α-cells in many islets of transgenic animals. In control animals, α-cells were restricted to the peripheral mantle of the islet but in 44.6 % (n = 74) of islets in transgenic animals, a large number of centrally-located α-cells were visible in addition to those at the islet periphery (**Fig. 6.7.**). Immunoperoxidase staining for insulin showed no apparent difference in β-cell distribution between islets in transgenic or control animals (**Fig. 6.7.**). Furthermore, no difference was seen in the intensity of immunohistochemical staining for either glucagon or insulin between transgenic or control islets.

6.3.2.12. Glucagon-Immunopositive Acinar Cells in an Elijah Transgenic Pancreas

In one of the transgenic pancreata, immunoperoxidase staining revealed a marked proportion of acinar cells to be immunopositive for glucagon (**Fig. 6.8.**). These isolated acinar cells were widely scattered throughout the exocrine tissue of a few pancreatic lobes where they were evident both within acini and at the acinus periphery.

6.3.3. Ripley Line

6.3.3.1. IGF-II Expressed Exclusively in Islets in Adult Ripley Transgenic Animals

Immunoperoxidase analysis (Dr. Janet Smith) demonstrated high levels of IGF-II in the islets of adult Ripley transgenic animals (**Fig. 6.9.**). The IGF-II protein was localised throughout the islet cells of transgenic pancreas. Islets in control animals demonstrated a complete absence of immunoperoxidase staining for IGF-II (**Fig. 6.9.**). Despite there being only one line carrying the RIP-Igf2 transgene, results from the study by Devedjian and coworkers (Devedjian *et al.*, 2000) using the same RIP promoter to

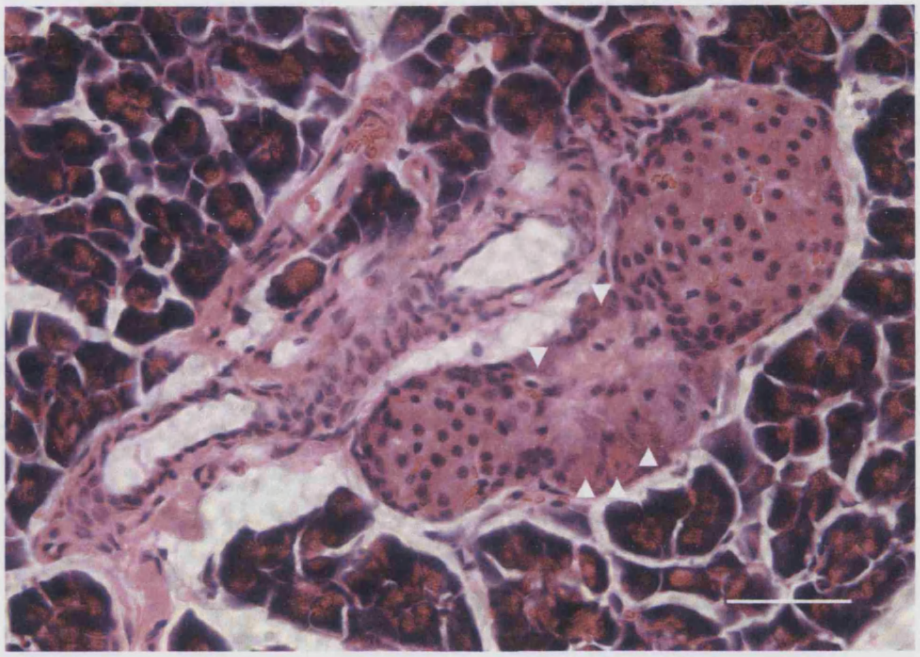

Figure 6.6. Large "Hepatocyte-Like" Cells (Arrowheads) at Islet Periphery in an H & E-Stained Elijah Transgenic Pancreas Section

Such cells exhibit abundant eosinophilic cytoplasm. Bar = 50 μm

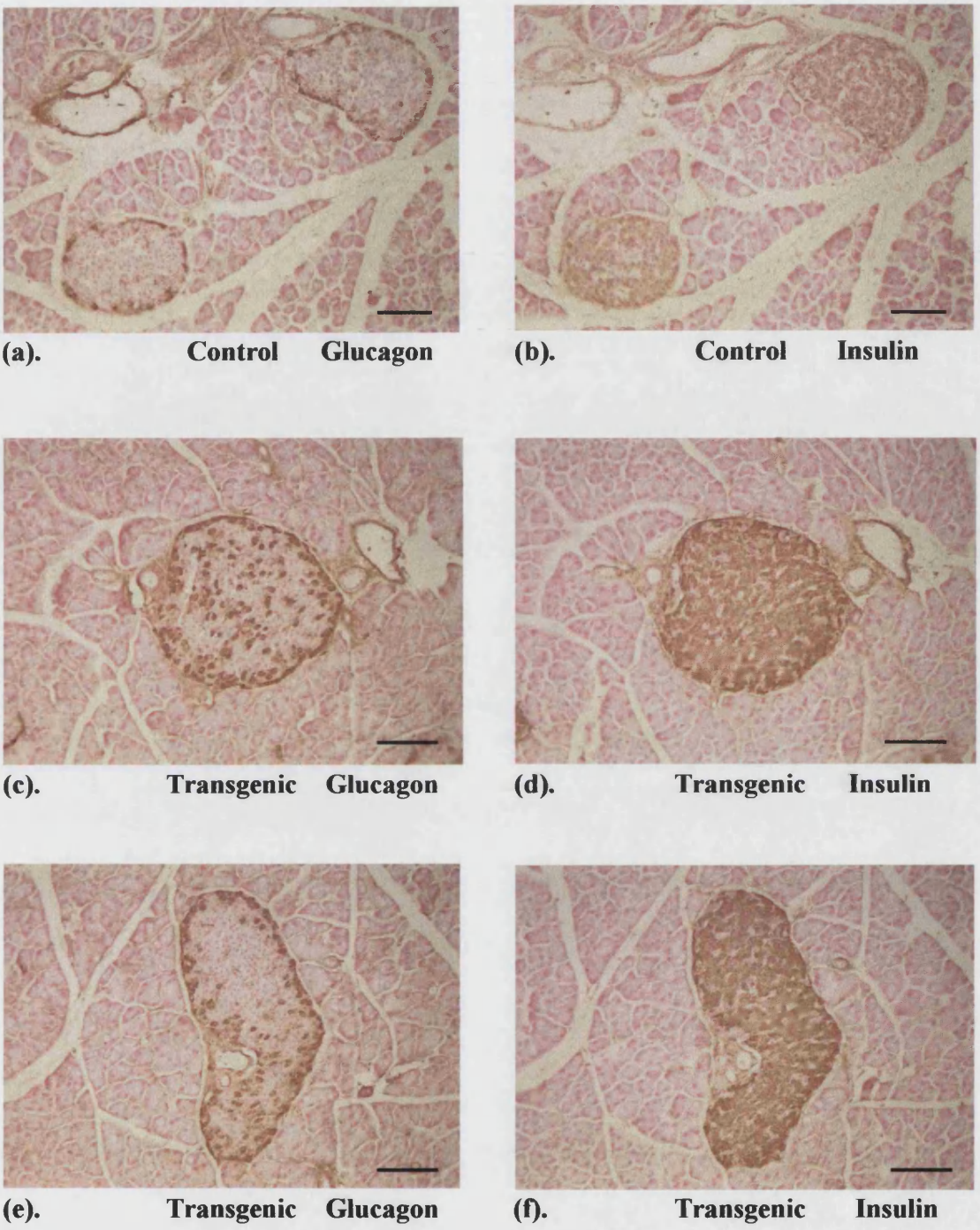

Figure 6.7. Aberrant α-Cell Localisation in Islets from Elijah Transgenic Pancreas

Immunoperoxidase staining for glucagon (α-cell marker) or insulin (β-cell marker) in adjacent pancreas sections from PN31wk Elijah transgenic (c-f) or control (a and b) animals. α-Cells seen in islet core in transgenic islets. Bar = 100 μm

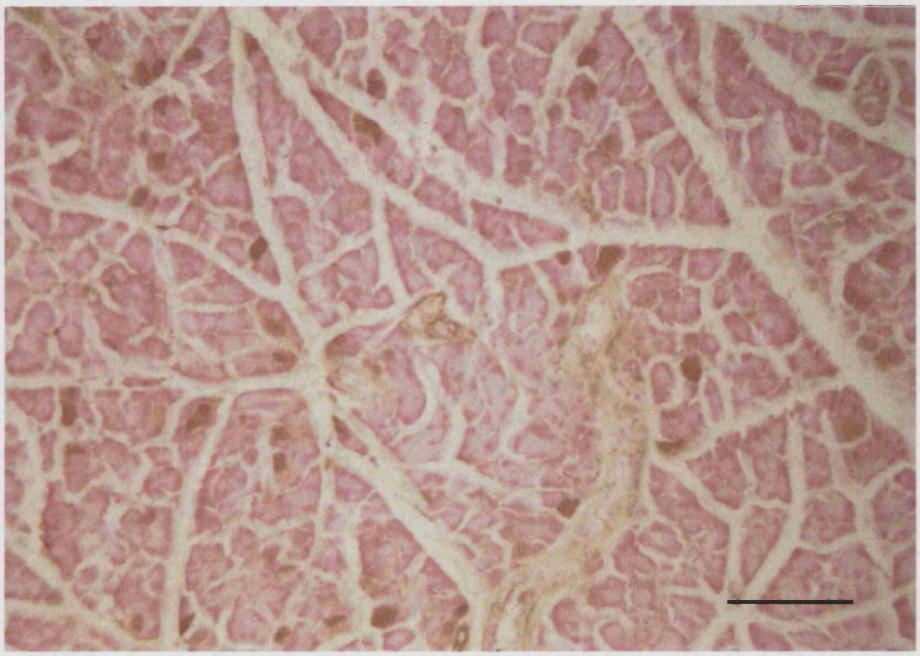

Figure 6.8. Immunoperoxidase Staining Reveals Scattered Glucagon-Immunopositive Acinar Cells Throughout the Exocrine Tissue of a Few Lobes in a PN35wk Elijah Transgenic Pancreas. Bar = 100 μm

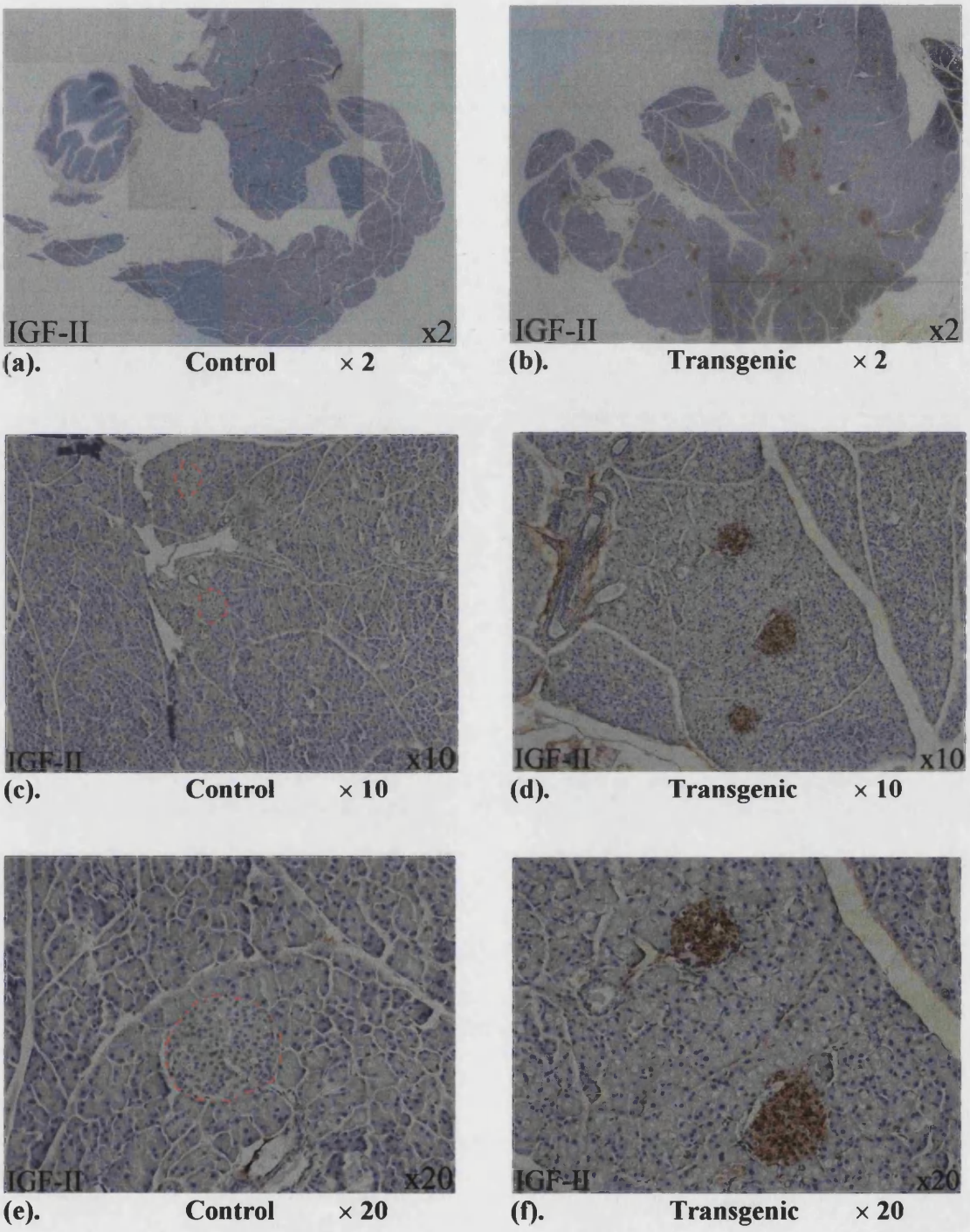

(a). Control × 2 **(b). Transgenic × 2**

(c). Control × 10 **(d). Transgenic × 10**

(e). Control × 20 **(f). Transgenic × 20**

Figure 6.9. Immunoperoxidase Staining for IGF-II in Pancreas Sections from PN43wk Ripley Transgenic and Control Animals (Dr. Janet Smith)

Islets in non-transgenic control pancreas, all of which show no immunoperoxidase staining, are highlighted (red dashed lines) in (c) and (e). Staining for IGF-II is clearly visible in the islets of Ripley transgenic pancreas in (b), (d) and (f)

drive IGF-II expression in the islet β-cells suggest that the transgene behaved as expected.

6.3.3.2. Increased Ripley Transgenic Pancreatic Weight

To determine whether rat insulin I promoter-driven expression of IGF-II in islets resulted in an increase in pancreas mass, pancreatic wet weight was compared between five intact pancreata from transgenic animals and five organs from control non-transgenic littermates of the same sex. Wet weight of transgenic pancreata was 540 ± 23 mg compared with 479 ± 25 mg for control pancreata (**Table 6.6.** and **Graph 6.10.**). Although pancreatic weight tended to be greater in transgenic animals, this just failed to reach statistical significance ($t = 3.67$; $P = 0.067$).

Table 6.6. Wet Weight of Ripley Transgenic and Control Intact Pancreata

LITTER/SEX	AGE (Wks)	PANCREATIC WET WEIGHT (mg)	
		Transgenic	Control
Litter 1 Female	43	505	455
		467	409
Litter 1 Male	46	569	538
Litter 2 Male	43	543	442
		618	551
Mean ± S.E.	**N/A**	**540 ± 23**	**479 ± 25**

6.3.3.3. No Significant Difference in Islet Number Per Section

The number of islets per pancreas section was counted for transgenic and control animals to determine whether the IGF-II transgene affects islet number. Mean islet number per section was found to be similar between transgenic and control animals: 30.6 ± 6.18 and 26.3 ± 2.81 islets/section respectively (**Table 6.7.**, **Graph 6.11.** and **Table 8.2., Appendices**) with one notable exception. The mean islet number per section of pancreas from the transgenic male from litter 1 was found to be 56.0 ± 5.18 as compared to 15.8 ± 1.66 for the non-transgenic littermate control. Overall, no significant difference was determined ($t = 0.68$; $P = 0.565$).

Graph 6.10. Mean Pancreatic Wet Weight for Ripley Transgenic Animals and Non-Transgenic Sibling Controls

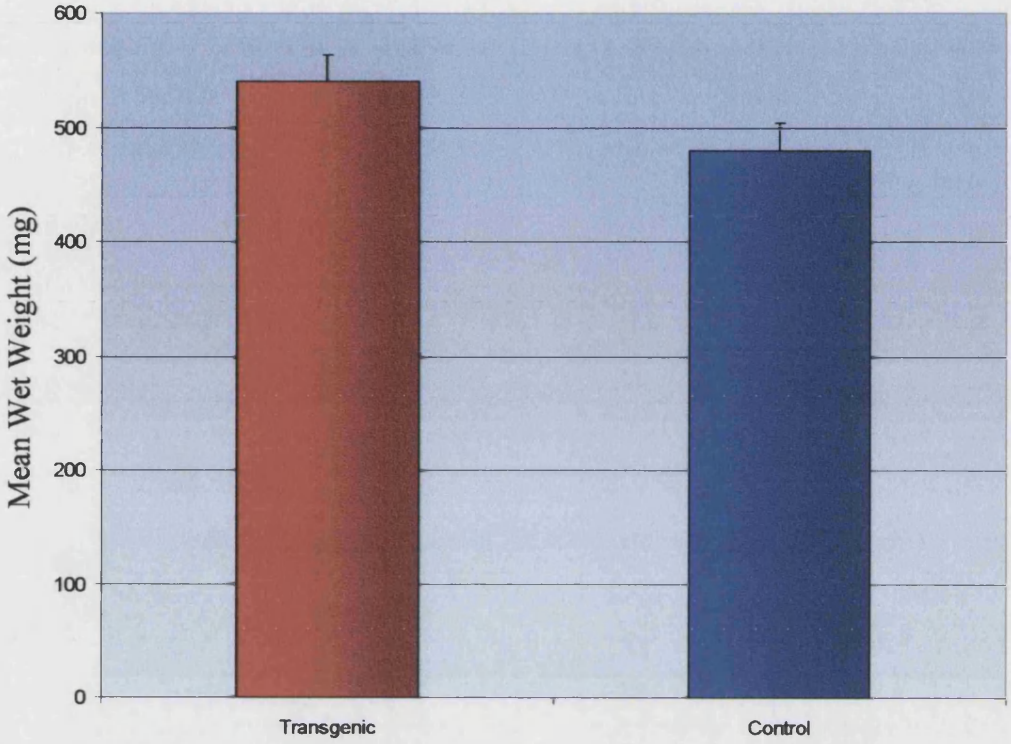

Graph 6.11. Mean Number of Islets Per Section for Ripley Transgenic Animals and Non-Transgenic Sibling Controls

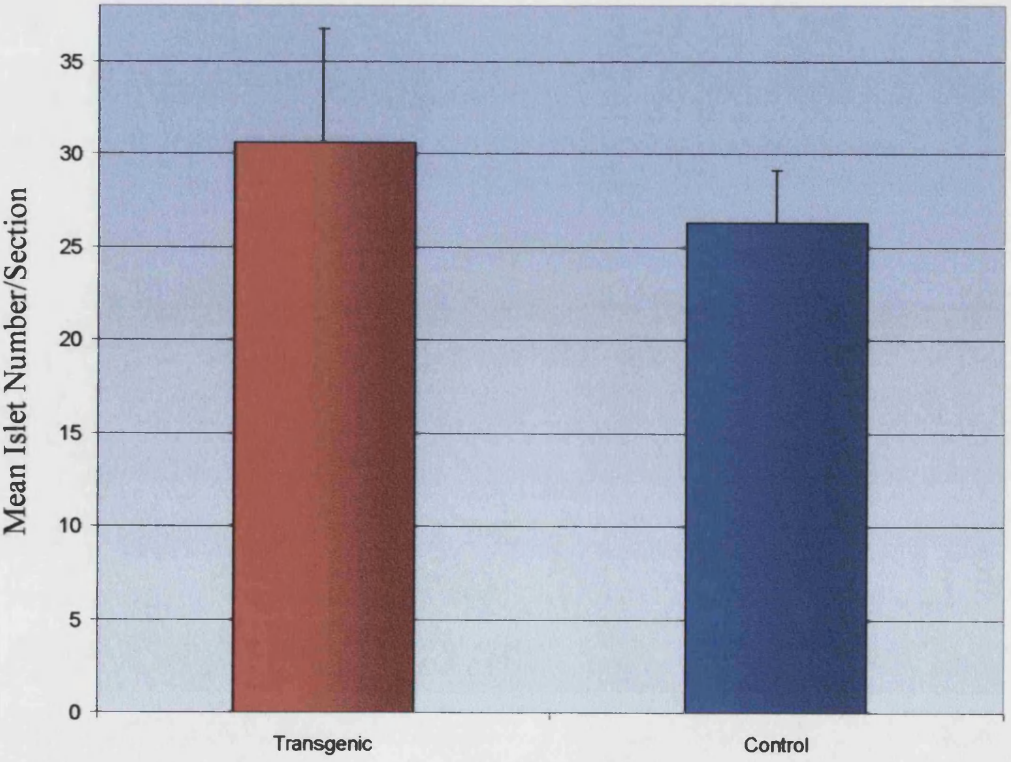

Table 6.7. Summary of Individual Animal Mean Values from Statistical Morphometry Study of Pancreas Sections from Ripley Transgenic (TG) and Age- and Sex-Matched Non-Transgenic Littermate Control (CTL) Animals

LITTER / SEX	AGE (Wks)	VARIABLE (MEAN)					
		Number of Islets/ Section		Total Section Area (mm^2)		Mean Islet Area (μm^2)	
		TG	CTL	TG	CTL	TG	CTL
1 / Female	43	21.6	28.2	25.21	30.10	7944	14920
		22.8	23.4	28.58	35.03	8322	11131
1 / Male	46	56	15.8	26.83	20.93	25737	34020
2 / Male	43	34.2	34	36.94	29.46	12098	8627
		18.2	30.2	27.97	21.17	38904	18039
Mean ± S.E.	**N/A**	**30.56 ± 6.176**	**26.32 ± 2.805**	**29.10 ± 1.825**	**27.34 ± 2.452**	**18601 ± 5384**	**17347 ± 3995**

6.3.3.4. No Significant Difference in Total Section Area

To ensure that a direct comparison could be made between mean number of islets per pancreas section in transgenic and control animals, total section area was compared. Total mean section area was very similar between transgenic and control animals: 29.1 ± 1.83 mm^2 and 27.3 ± 2.45 mm^2 respectively (**Table 6.7.** and **Graph 6.12.**); no significant difference was found (t = 0.60; P = 0.609). Hence, absolute islet number per section could be directly compared.

6.3.3.5. No Significant Difference in Mean Islet Area

As a preliminary assessment of whether the RIP-driven IGF-II exerts any effect on islet size, mean islet area was determined. The mean islet area for transgenic animals at 18601 ± 5384 μm^2 was not significantly different (t = -0.05; P = 0.963) from the control figure of 17347 ± 3995 μm^2 (**Table 6.7.** and **Graph 6.13.**)

6.3.3.6. Greater Proportion of Large Islets in Ripley Transgenic vs. Control Animals

The frequency of islets of distinct size (area) classes was compared between transgenic and control animals to determine any difference in islet size distribution as a result of the IGF-II transgene (**Graphs 6.14.** and **6.15.**). The size distribution of islets in

Graph 6.12. Mean Section Area for Ripley Transgenic Animals and Non-Transgenic Sibling Controls

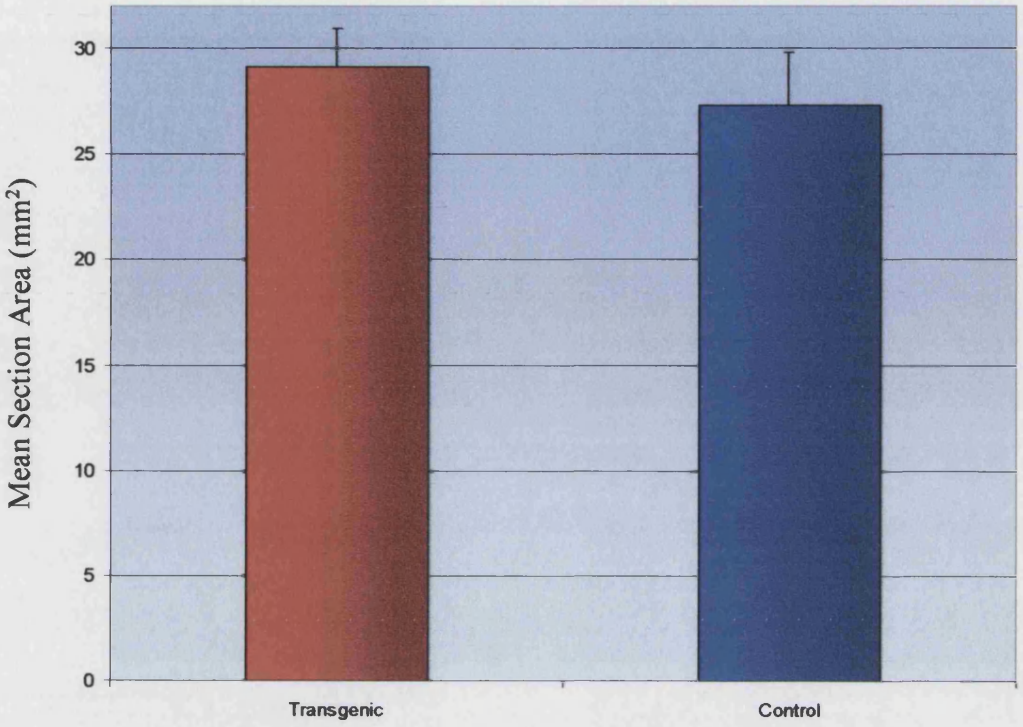

Graph 6.13. Mean Islet Area in Ripley Transgenic Animals and Non-Transgenic Sibling Controls

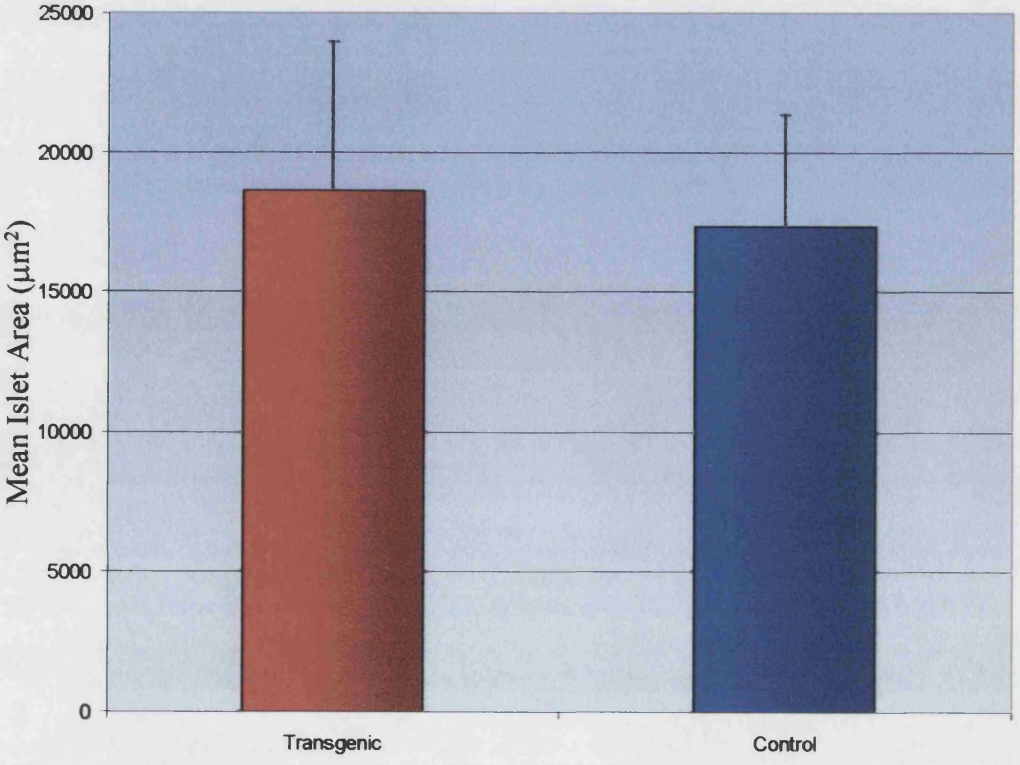

Graph 6.14. Frequency Histogram Comparing Islet Area in Ripley Transgenic Animals and Non-Transgenic Sibling Controls

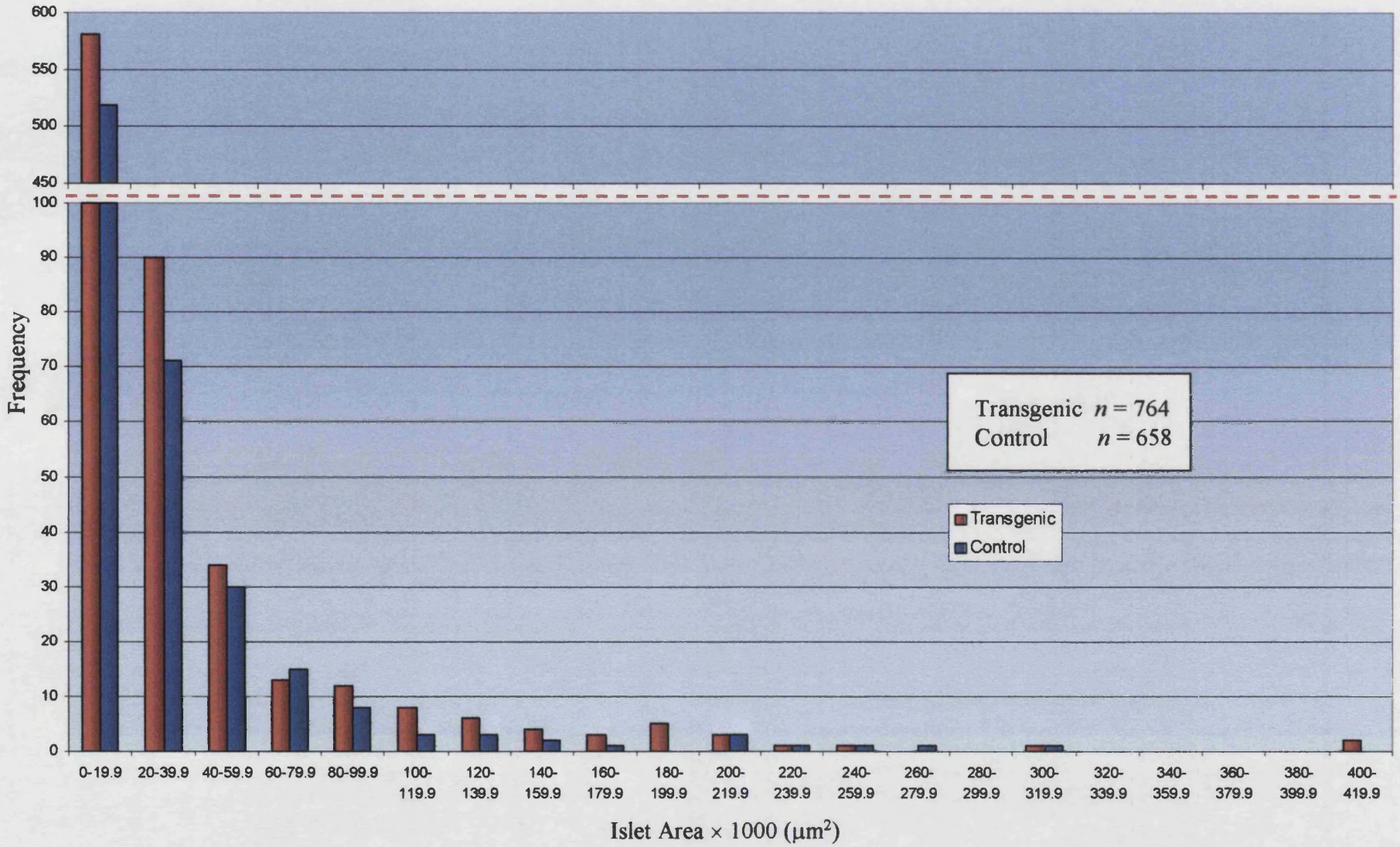

Graph 6.15. Frequency Histogram Comparing Observed Islet Areas in Ripley Transgenic Animals with "Expected" Islet Size Distribution as Calculated from Non-Transgenic Sibling Controls

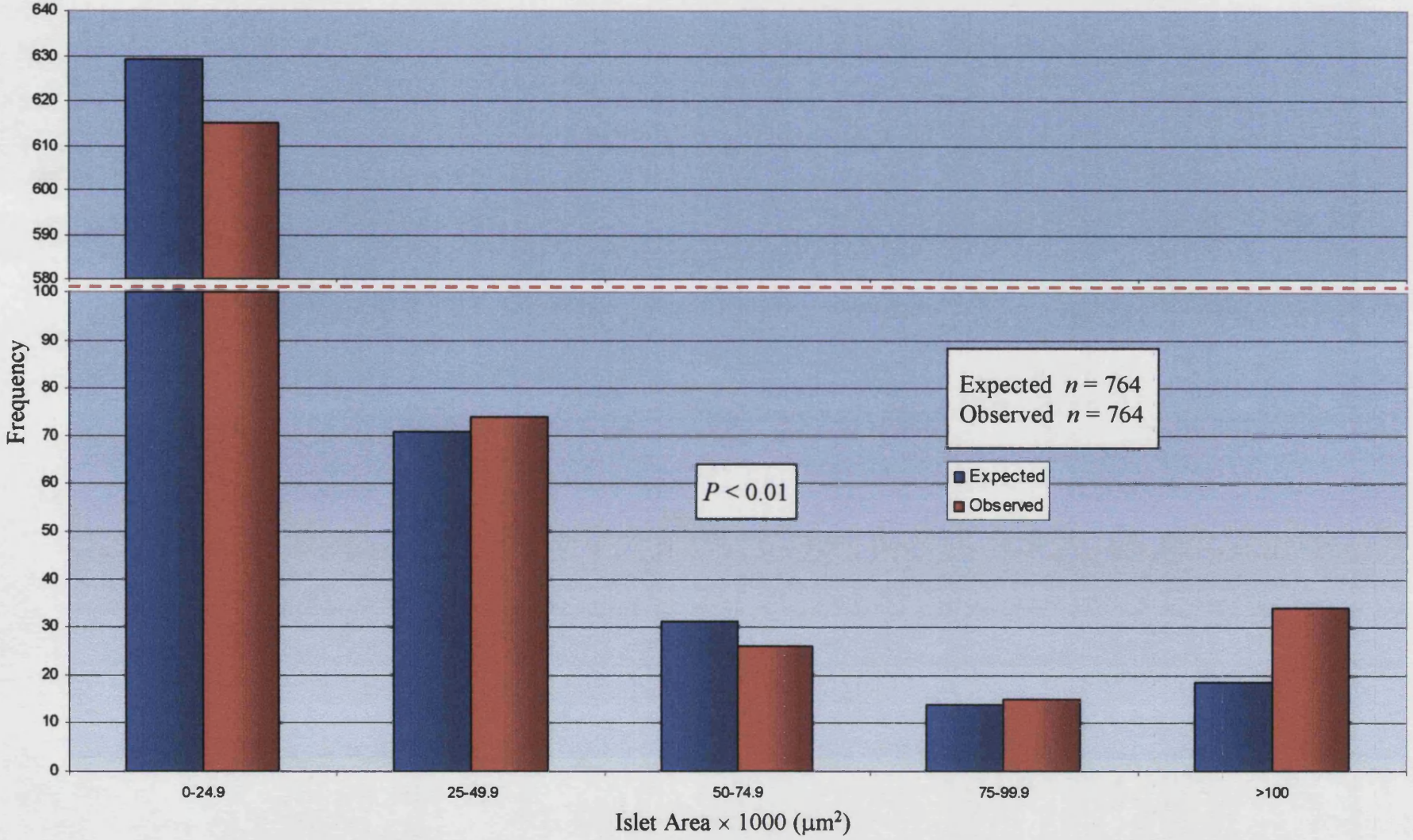

transgenic and control animals appeared to be generally very similar (**Table 6.8.** and **Graph 6.14.**). However when compared with control values, a smaller proportion of the islets in transgenic pancreata fell within the lower end of the normal islet size spectrum whereas a greater proportion (compared with control) tended to lie at the upper end of the islet size range. 730 or 95.5 % of the 764-islet sample in transgenic pancreata were below 100000 μm^2 (0.1 mm^2) in cross-sectional area compared to 642 or 97.6 % of the 658 control islets. Of these islets, 76.0 % (transgenic) and 78.7 % (control) fell below 20000 μm^2. In transgenic animals, 32 islets (4.19 %) possessed an area of 100000-399999 μm^2 compared with 16 islets (2.43 %) in control mice. The largest control islet observed in the "normal" islet size spectrum was 313362 μm^2 in cross-sectional area. However, two "mega-islets" of 414088 and 417005 μm^2 in area, well exceeding the size of the largest control islet, were observed in two of the transgenic pancreata. As with those mega-islets observed in transgenic pancreas sections from animals of the Elijah line, the largest islets present in Ripley transgenic pancreata displayed a very irregular shape (**Fig. 6.10.**).

Table 6.8. Size Distribution of Islets in Ripley Transgenic and Control Animals

ISLET AREA (μm^2)	PROPORTION OF TOTAL ISLET SAMPLE (%)	
	Transgenic (n = 764)	Control (n = 658)
0-99999	95.5	97.6
100000-199999	3.40	1.37
200000-299999	0.654	0.912
300000-399999	0.131	0.152
> 400000	0.262	0

As with the Elijah study, to verify the divergence in size distribution of the Ripley transgenic and control islet population samples, a chi-square (χ^2) test was conducted to compare expected size distribution, based on control data, with the observed distribution of transgenic islets (**Table 6.9.** and **Graph 6.15.**). There was found to be a highly significant difference ($P < 0.01$) between observed and expected (control) islet size distributions.

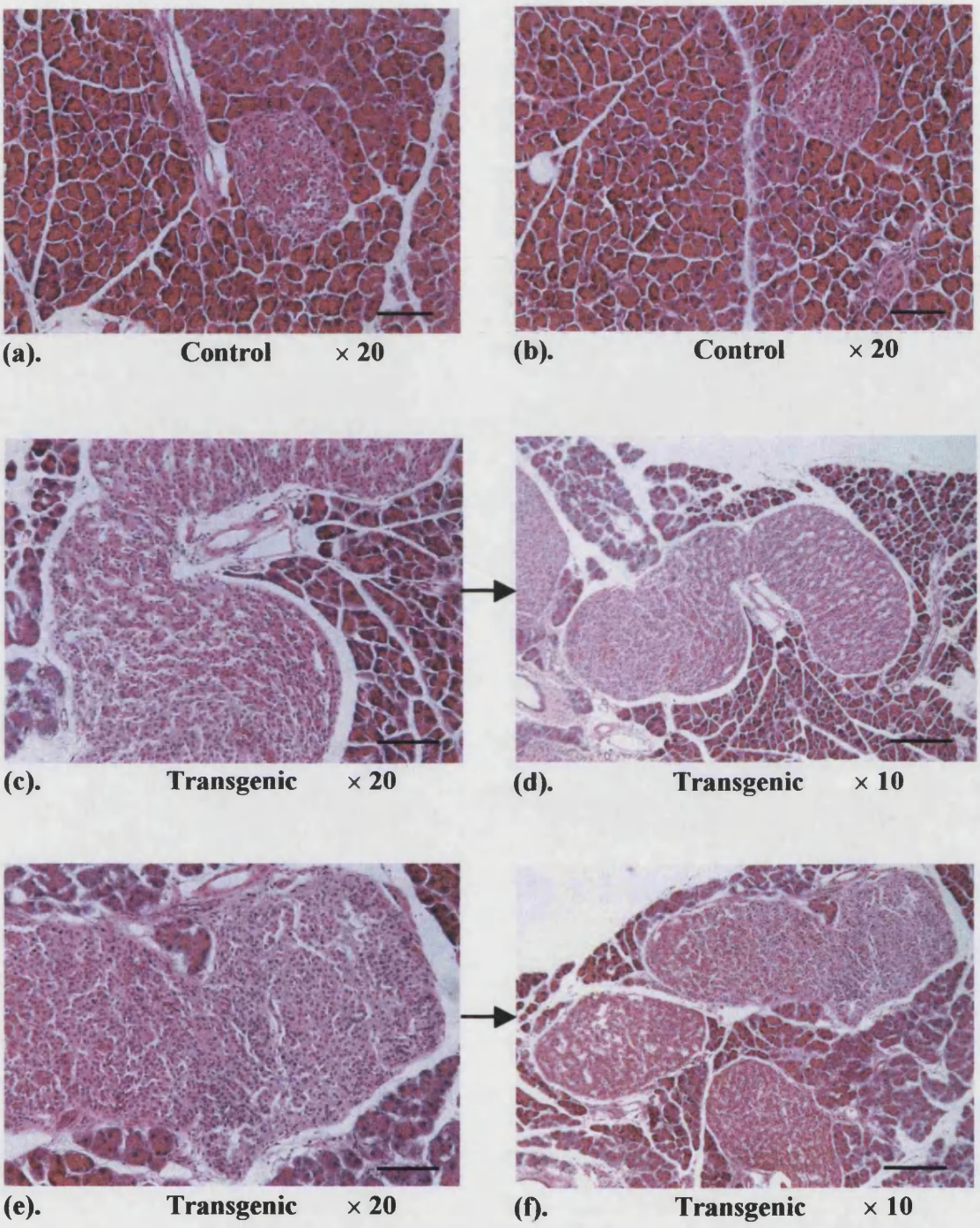

Figure 6.10. "Mega-Islets" in H & E-Stained Pancreas Sections from PN43wk Ripley Transgenic and Control Animals

Islets in (c) and (e) pictured at lower magnification in (d) and (f) respectively. (a)-(c) and (e) Bar = 100 μm; (d) and (f) Bar = 200 μm

Table 6.9. Calculating χ^2 to Test Whether the Observed Islet Size Distribution in Ripley Transgenic Animals Differs from that Expected (from Control Data)

ISLET AREA (μm^2)	NUMBER OF ISLETS			Observed - Expected	$O - E^2$	$\frac{O - E^2}{E}$
	Control	Transgenic (Observed)	Transgenic (Expected)			
0-24999	542	615	629.3	-14.3	205	0.326
25000-49999	61	74	70.8	3.17	10.1	0.142
50000-74999	27	26	31.3	-5.35	28.6	0.913
75000-99999	12	15	13.9	1.07	1.14	0.0817
> 100000	16	34	18.6	15.4	238	12.8
Σ	**658**	**764**	**764**	**0**	**483**	**14.3 (χ^2)**

$\chi^2 = 13.28$, $df = 4$, $p = 0.01$. As the calculated value of χ^2 is greater, the null hypothesis can be rejected.

6.3.3.7. "Hepatocyte-Like" Cells in a Ripley Transgenic Islet

As in one of the Elijah transgenic pancreata, H & E histochemistry revealed the presence of large cells which morphologically resembled hepatocytes within a Ripley transgenic islet (**Fig. 6.11.**). Such cells could be clearly distinguished from adjacent endocrine cells by their abundant eosinophilic cytoplasm and were located at the islet periphery.

6.3.3.8. Aberrant α-Cell Localisation in Ripley Transgenic Islets

Immunoperoxidase staining for glucagon revealed a disruption in the distribution of α-cells in many islets of transgenic animals. In control animals, α-cells were restricted to the peripheral mantle of the islet but in 41.7 % (n = 72) of islets in transgenic animals, α-cells were seen to be much reduced in number in the mantle and/or were centrally-located (**Fig. 6.12.**). In some transgenic islets, isolated α-cells

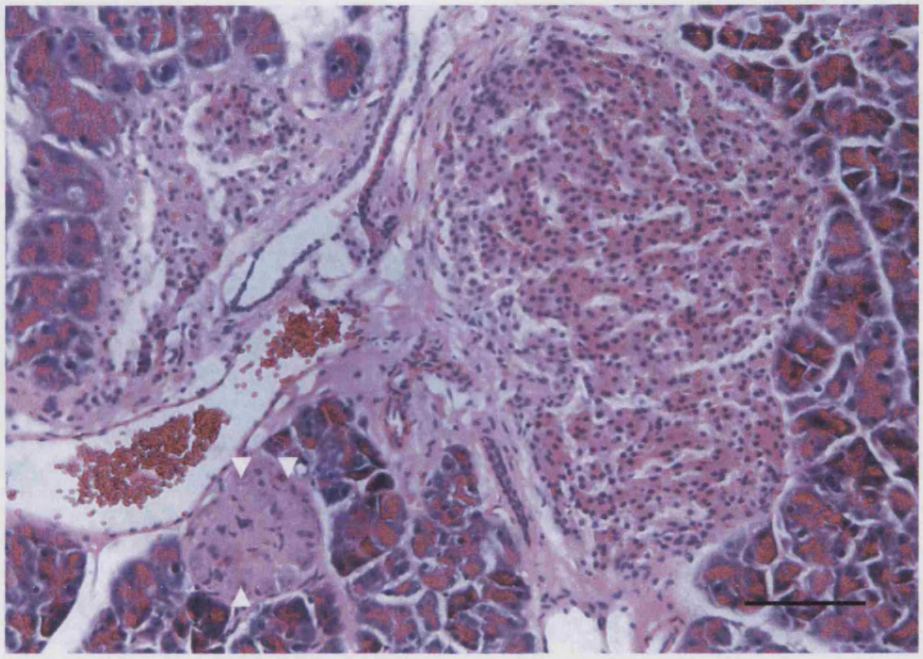

Figure 6.11. Large "Hepatocyte-Like" Cells (Arrowheads) at the Periphery of an Islet (Lower Left) in an H & E-Stained PN43wk Ripley Transgenic Pancreas Section

Such cells exhibit abundant eosinophilic cytoplasm. Bar = 100 μm

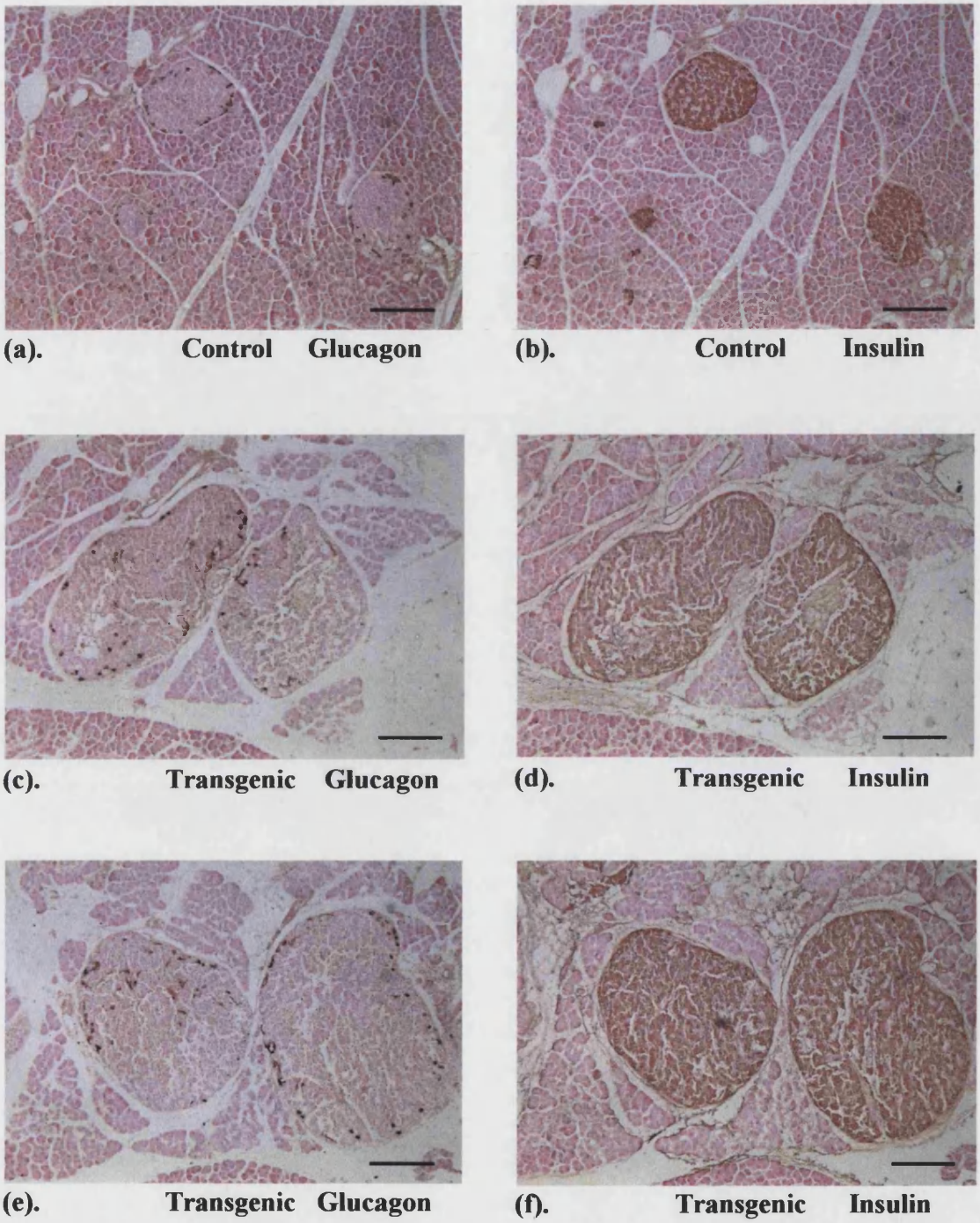

Figure 6.12. Aberrant α-Cell Localisation in Islets from Ripley Transgenic Pancreas

Immunoperoxidase staining for glucagon (α-cell marker) or insulin (β-cell marker) in adjacent pancreas sections from Ripley transgenic (c-f) or control (a and b) animals. α-Cells in mantle depleted and also seen in islet core in transgenic islets Bar = 100 μm

were scattered no more than one cell layer deep around the islet periphery and in extreme cases, no glucagon-immunopositive cells were evident within the entire islet cross-section. Immunoperoxidase staining for insulin showed no apparent difference in β-cell distribution between islets in transgenic or control animals (**Fig. 6.12.**). No obvious difference was seen in the intensity of immunohistochemical staining for either glucagon or insulin between transgenic or control islets.

6.4. Discussion

6.4.1. IGF-II Transgene Expression

6.4.1.1. IGF-II Expressed by Both Acinar and Islet Cells in Adult Elijah Transgenic Animals

Immunoperoxidase staining (Dr. Janet Smith) demonstrated that IGF-II was expressed ectopically in adult Elijah transgenic pancreas in scattered cells throughout the pancreatic acini and in a small number of cells within the transgenic islets. Some staining was evident in ducts of control animals which was attributed to endogenous expression in the mesenchyme. Scattered islet cell expression might be attributable to inappropriate random integration of the transgene within the genome. However, the limited islet cell expression in transgenic animals was attributed to the non-specificity of the IGF-II transgene promoter. Between the construction and phenotypic characterisation of the Elijah line, it was noted that the rat elastase I promoter fragment used is not entirely specific to the pancreatic acini (Kruse *et al.*, 1993). Therefore, despite there being only one line carrying the EIP-Igf2 transgene, the study by Kruse *et al.* (1993) using the same rat elastase I promoter element suggests that the transgene behaved as expected in the current study. The rat elastase I promoter fragment used here was selected to drive transgene expression in the acini owing to initial reports of specificity of its activity within this tissue compartment. However, some transgene expression within the islets was not considered particularly detrimental to the study since transgene expression was mostly confined to exocrine tissue and IGF-II expression was still confined to within the pancreas. However, the specific aim of investigating the ability of the IGF-II protein to act across tissue compartments within the pancreas could not be achieved with the anticipated level of integrity.

6.4.1.2. IGF-II Expressed Exclusively in Islets in Adult Ripley Transgenic Animals

Immunoperoxidase staining (Dr. Janet Smith) demonstrated that IGF-II is exclusively expressed throughout the endocrine tissue in the pancreas of adult Ripley transgenic animals. The IGF-II protein was seen to be localised throughout the islet cells of transgenic pancreas. Islets in control animals demonstrated a complete absence of staining, showing that endocrine IGF-II expression in transgenic animals is exogenous and that the RIP-driven transgene is expressed exclusively throughout the transgenic islets. Devedjian and coworkers (Devedjian *et al.*, 2000) similarly

demonstrated high levels of immunoreactive IGF-II restricted to the islets of PN4month transgenic mice in which the RIP promoter was used to drive β-cell-specific expression of IGF-II. Islets from PN4month non-transgenic animals displayed an absence of IGF-II immunoreactivity (Devedjian *et al.*, 2000). So, despite there being only one line carrying the RIP-Igf2 transgene in the current study, the transgene behaved as expected. The absence of IGF-II immunostaining in islets from control mice in the present study is consistent with the findings of Devedjian *et al.* (2000). IGF-II immunoreactivity has, however, been detected in β-cells of healthy rats and humans (Hoog *et al.*, 1996; Maake and Reinecke, 1993). Devedjian and colleagues (Devedjian *et al.*, 2000) attributed the lack of immunodetection to a high threshold of detection by the IGF-II antibody (rabbit anti-human; GroPep Pty. Ltd., North Adelaide, Australia) used in the study, which probably detects only high levels of the IGF-II protein.

6.4.2. Pancreatic Weight

6.4.2.1. No Difference in Pancreatic Weight Between Elijah Transgenic and Control Animals

There was no significant difference in pancreatic wet weight between Elijah transgenic animals and control (497 ± 30 mg *vs.* 496 ± 31 mg respectively; $t = 0.24$; $P = 0.818$). This finding was not consistent with a significant increase in the volume and mass of exocrine tissue but it was not unexpected in the light of the observed islet hyperplasia. The relatively small (1-2 %) contribution of endocrine tissue to the total pancreas mass means that quite substantial changes in islet morphology and size can occur with no noticeable increase in overall weight of the organ.

6.4.2.2. No Significant Increase in Ripley Transgenic Pancreatic Weight

Pancreatic wet weight tended to be greater amongst transgenic animals of the Ripley line than controls (540 ± 23 mg *vs.* 479 ± 25 mg respectively). This increase just failed to reach statistical significance however ($t = 3.67$; $P = 0.067$). Mean pancreas weight for RIP-IGF-II transgenic animals was also found to be greater than for control animals by Devedjian *et al.* (2000). Transgenic pancreas mean weight at 157.0 ± 4 mg was 29.3 % greater than control at 121.4 ± 12 mg. This compares to an increase of 12.7 % over control pancreatic weight in the present study. It might be expected that with

increasing age, the effects of the RIP-Igf2 transgene diminish and that the extent of the IGF-II-induced islet overgrowth decreases. This might perhaps be as a result of a decrease in endocrine tissue growth as a compensatory response to maintain normoglycaemia. Hence, the IGF-II-induced increase in overall pancreatic weight in RIP-Igf2 transgenic animals relative to non-transgenic sibling controls might be expected to decline with age.

6.4.3. Area of Pancreas Tissue Within Each Field is Significantly Greater in Elijah Transgenic Animals

The total mean area of pancreas tissue per field was found to be significantly greater in animals carrying the IGF-II transgene than in control animals, meaning that it was necessary to express the acinar and endocrine contribution to pancreas area as a proportion of total area. This was unfortunate as it removed some of the statistical power of subsequent comparisons although this was not felt to be a significant disadvantage. In the absence of alternative explanations, the increased area of pancreas tissue per field in transgenic animals would imply that the lobes of transgenic pancreas are more closely arranged than in control animals, such that the pancreas is more "dense". A more close-packed arrangement of tissue in the organ would result in a greater area of pancreatic tissue coverage within the same area of field. Spaces are commonly observed between adjacent pancreatic lobules in tissue sections as a fixation artefact. Hence, different durations of fixation might be expected to cause differing extents of separation between pancreatic lobules and so different spatial densities of tissue within two-dimensional sections. However, excised pancreas tissue from animals carrying the IGF-II transgene and non-transgenic siblings was subjected to the same program of fixation and processing for paraffin wax embedding. The reason for this finding therefore remains obscure.

6.4.4. No Increase in Percentage Acini or Islet Contribution to Pancreas Area in Elijah Transgenic Animals

Mean percentage acini area per field for transgenic animals at 96.7 ± 0.329 % was not significantly different from the control value of 96.2 ± 0.663 % ($t = 0.32$; $P = 0.770$). Neither was there found to be any difference between the percentage

contribution of endocrine tissue in transgenic animals (1.32 ± 0.299 %) *vs.* controls (1.51 ± 0.240 %; t = -0.37; P = 0.733). It was assumed from this result that IGF-II expression in the pancreatic acini (and islets to some extent) does not selectively influence the postnatal growth of the acinar tissue (or islets). In the transgenic mouse IGF-II overexpression model of Petrik *et al.* (1999), in which widely-overexpressed IGF-II was made available to the pancreas in the circulation, no increase in exocrine tissue was apparent. No such change was investigated however and the difficulty in evaluating the wet weight of the fetal (E19.5-20) pancreas accurately meant that this parameter was not measured. The total mean area of pancreas per section did tend to be greater in transgenic than in control animals however, implying a greater organ volume and mass (Petrik *et al.*, 1999). In transgenic mice in which the keratin 10 promoter was used to drive IGF-II overexpression producing high circulating levels of IGF-II postnatally, pancreatic weight did not differ from control animals (Hill *et al.*, 2000). This would imply no significant increase in exocrine tissue mass in transgenic mice although again, morphological changes in acinar tissue were not analysed. The apparent lack of a significant overgrowth effect of rat elastase I promoter-driven IGF-II overexpression on the pancreatic acini was unexpected. Using 125I-labelled IGFs and insulin, distinct receptors for IGF-I, IGF-II, and insulin have been demonstrated on isolated mouse pancreatic acini (Williams *et al.*, 1984). mRNA for IGFBP2, one of the IGFBPs which modulate the biological availability to tissues and mitogenic effects of IGFs (Hogg *et al.*, 1993; McCusker and Clemmons, 1992) has been shown to be localised in postnatal rat acinar tissue (Hill *et al.*, 1999). Therefore, the pancreatic acinar cells appear competent to respond to an increased local availability of IGF-II. The apparent absence of significant IGF-II-induced acinar hyperplasia in the current study is also inconsistent with the results from a recent study demonstrating that combined inactivation of the *Insulin receptor* (*Insr*) and the *Igf1 receptor* (*Igf1r*) result in a reduced size of the exocrine pancreas due to reduced cellular proliferation whilst islet development is unaffected (Kido *et al.*, 2002). Compared to wild-type mice, mean acinar diameter was reduced by approximately 40 % in $Insr^{-/-}Igf1r^{-/-}$ embryos whilst islet diameter and architecture was unchanged. Inactivation of either receptor alone however, produced no effect. Furthermore, combined ablation of the two ligands *Igf1* and *Igf2* resulted in an identical phenotype (Kido *et al.*, 2002). Some data suggest that there is functional overlap between the growth-promoting functions of the two receptors (Efstratiadis, 1998); IGF-II stimulates embryonic growth in mice not only through its cognate receptor IGF1R, but also in part through INSR (Louvi *et al.*, 1997). Mice

lacking both IGF receptors, IGF1R and IGF2R, are rescued from perinatal lethality by IGF-II acting through INSR to promote growth (Ludwig *et al.*, 1996). Since exocrine tissue reduction is not observed in single *Insr*$^{-/-}$ or *Igf1r*$^{-/-}$ mutant embryos, it is unlikely to be a consequence of impaired insulin or IGF-I signalling, which activate only the cognate receptor. IGF-II is known to bind to both the IGF1R and INSR receptors with a high affinity (Frasca *et al.*, 1999). On the basis of the known interaction of IGF-II with both IGF1R and INSR, the decrease of exocrine tissue in double *Insr*$^{-/-}$*Igf1r*$^{-/-}$ mutants but not in single *Insr*$^{-/-}$ or *Igf1r*$^{-/-}$ mutant embryos is consistent with the hypothesis that acinar tissue growth is mediated by the IGF-II ligand (Louvi *et al.*, 1997). This was further supported by the finding that at E12.5 when the mutational consequences of the lack of IGF-II alone begin manifesting (preceding those from IGF-I ablation by one day), exocrine pancreas reduction was already apparent. The findings from the 2002 study (Kido *et al.*, 2002) are consistent with the observation that IGF signalling promotes growth of cultured acinar cells and amylase gene expression (Ludwig *et al.*, 1999; O'Brien and Granner, 1996; Williams *et al.*, 1984).

It was considered that the method used to compare exocrine and endocrine contribution to total pancreas area was not sufficiently accurate to detect small differences in exocrine area and so exocrine tissue mass within the pancreas. As mentioned, the preferred method of comparing absolute areas of exocrine tissue and islet tissue per field between Elijah transgenic and control animals could not be conducted due to the increased total pancreas area per field in animals carrying the IGF-II transgene. The necessity of expressing the area of exocrine (and endocrine) tissue as a proportion of total pancreas area removed some of the statistical power with which transgenic and control data sets could be compared. The very large (96-97 %) exocrine contribution and very small (1-2 %) endocrine contribution to pancreas area mean that the percentage exocrine tissue area is highly robust and very resistant to change. Conversely, the exocrine:endocrine tissue area ratio is highly susceptible to variation resulting from the number of islets within an area field. Islets do not occur in a random arrangement within the surrounding acinar tissue; they instead cluster together in a pattern of spatial distribution that can be explained by a fractal branching structure for ductules and random islet formation at their tips (Hastings *et al.*, 1992; Schneider *et al.*, 1996). Hence, random sampling of fields for area measurement within a pancreas tissue section produces great variation in the number of islets per field, vastly affecting the exocrine:endocrine tissue area ratio measured for each field. Nevertheless, this sample variation should be comparable for data obtained from Elijah transgenic and control

animals. An alternative of measuring the separation distance between islet centres as an index of acinar tissue area is also impeded by the same considerations. To obtain an absolute measure of exocrine pancreatic size, mean acinar diameter might have been measured as in the study of Kido *et al.* (2002). However, no noticeable difference was evident between the size of individual acini in Elijah transgenic and control pancreata.

6.4.5. Similar Islet Morphology in Transgenic Animals of Elijah and Ripley Lines

6.4.5.1. No Difference Between Islet Number in Elijah and Ripley Transgenic Animals and Respective Controls

Neither Elijah nor Ripley transgenic animals exhibited any difference in islet number from control animals. In transgenic Elijah mice, a mean of 3.76 ± 0.791 islets were counted in each field *vs.* 3.72 ± 0.440 islets/field in control animals ($t = 0.30$; $P = 0.781$). Transgenic Ripley mice exhibited a mean of 30.6 ± 6.18 islets per tissue section whilst this was not significantly different ($t = 0.68$; $P = 0.565$) from the 26.3 ± 2.81 islets counted per pancreas section in non-transgenic littermates. This direct comparison was justified by the lack of difference in total sectional area between transgenic (29.1 ± 1.83 mm^2) and control (27.3 ± 2.45 mm^2) animals ($t = 0.60$; $P = 0.609$).

6.4.5.2. Mean Islet Area Unaltered in Animals Carrying the IGF-II Transgene

Islets from both Elijah and Ripley transgenic animals showed no difference in mean area in section to those from control mice. The mean islet area for Elijah transgenic animals at 9470 ± 2314 μm^2 was not significantly different ($t = -1.34$; $P = 0.272$) from the control figure of 11459 ± 1411 μm^2. Ripley mice overexpressing IGF-II bore islets with a mean area of 18601 ± 5384 μm^2 *vs.* 17347 ± 3995 μm^2 in control siblings ($t = -0.05$; $P = 0.963$).

6.4.5.3. "Mega-Islets" Exceeding the Normal Islet Size Range Seen in Elijah and Ripley Transgenic Animals

In both Elijah and Ripley transgenic mice, the samples of the islet population showed a broadly similar size (area) distribution to those in control animals, with a

significant shift towards larger islets. In both cases, a significant number of strikingly large "mega-islets" were seen which far exceeded the normal islet size range evident in control animals. Of the 92-islet sample measured in Elijah mice bearing the transgene, 83.7 % of islets were categorised as small (below 20000 μm^2 in area) compared with 83.9 % of control islets. 7.61 % of islets in transgenic animals were 20000-39999 μm^2 in area *vs.* 9.2 % of islets in non-transgenic siblings. The remaining 6.9 % of the control islet sample were classified as large (40000-59999 μm^2) in the normal islet size spectrum but only 2.17 % of islets in the transgenic animals fell into this category. Instead, 6.52 % or six "mega-islets" from three of the five pancreata from transgenic animals exhibited areas of 60466-180194 μm^2, up to three-fold the largest control islets measured. Similarly, of the much larger islet population sample (764 islets) in transgenic animals of the Ripley line, 95.5 % were below 100000 μm^2 in area compared to 97.6 % of the 658 control islets, of which 76.0 % (transgenic) and 78.7 % (control) fell below 20000 μm^2. In Ripley animals overexpressing IGF-II, 4.19 % of the islet sample exhibited an area of 100000-399999 μm^2 *vs.* 2.43 % of the control sample. Two mega-islets of 414088 and 417005 μm^2 in area, well exceeding the size of the largest control islet, were observed in two of the transgenic pancreata.

In both the Elijah and Ripley studies, the observed size distribution of islets in the transgenic animals diverged highly significantly ($P < 0.01$) from the expected size distribution extrapolated from the respective control animals (Elijah: calculated χ^2 = 12.4; $\chi^2 = 11.34$, $df = 3$, $p = 0.01$; Ripley: calculated $\chi^2 = 14.3$; $\chi^2 = 13.28$, $df = 4$, p = 0.01). The discrepancy in size distribution was greatest at the upper end of the size spectrum, reflecting a shift amongst the islet population in transgenic animals towards larger islets. In both Elijah and Ripley mice expressing the IGF-II transgene, the mega-islets displayed a very irregular shape and fibrous inclusions were often visible within them.

6.4.5.3.1. Mega-Islets Result from Hyperplasia

The frequent incidence of unusually large and irregularly-shaped mega-islets in both Elijah and Ripley transgenic mice suggested that local IGF-II overexpression led to islet cell hyperplasia. To ensure that increased islet size was not a consequence of hypertrophy, the area of individual endocrine cells within islets was measured. The lack of difference in mean islet cell areas between cells in Elijah mega-islets (76.6 ± 9.28

μm^2) and smaller, control islets (transgenic; 71.7 ± 5.71 μm^2 and non-transgenic; 77.2 ± 5.14 μm^2; t = 1.05; P = 0.403 and t = -0.37; P = 0.774 respectively) was taken to support the hypothesis that mega-islets are hyperplastic, resulting from islet overgrowth. Considering the similarity of islet morphology between animals of the Elijah and Ripley lines carrying the transgene, it would appear valid to assume that mega-islets in Ripley transgenic animals are similarly a product of hyperplasia.

6.4.5.3.2. Aberrant Islet Architecture

Immunoperoxidase staining for glucagon revealed a disruption in the distribution of α-cells in many islets of Elijah and Ripley transgenic animals. In animals overexpressing IGF-II, 44.6 % of islets in Elijah transgenic animals demonstrated a large number of centrally-located α-cells. Amongst the islet sample from Ripley mice carrying the transgene, 41.7 % of islets exhibited altered architecture including aberrant presence of α-cells in the islet core but also markedly reduced α-cell number in the islet mantle; in extreme cases α-cells were completely absent. In neither of the two lines were any differences in islet β-cell distribution seen between transgenic and control animals.

6.4.5.3.3. IGF-II-Induced Islet Hyperplasia

It has been postulated that the mitogenic signalling of IGF-II is mediated by the type 1 IGF receptor (De Meyts *et al.*, 1994; LeRoith *et al.*, 1995). As α-, β- and δ-cells all express type 1 IGF receptors (Fehmann *et al.*, 1996; Van Schravendijk *et al.*, 1987; Withers *et al.*, 1999), the presence of islet overgrowth in the Ripley transgenic animals suggests that the IGF-II produced by the β-cells probably interacted in a paracrine or autocrine manner with IGF-1 receptors on the islet cells. Studies in fibroblasts from mouse embryos homozygous for null alleles of *Igfr1* have shown that IGF-II can also stimulate cell proliferation through the insulin receptor (Morrione *et al.*, 1997). β-Cells also express insulin receptors, and mice lacking insulin receptor specifically in β-cells show reduced islet size and insulin content (Kulkarni *et al.*, 1999). Therefore, IGF-II produced by β-cells of transgenic mice might also induce β-cell proliferation through the insulin receptor. Devedjian *et al.* (2000) found that the hyperplastic islets of their RIP-IGF-II transgenic mice were composed of similar percentages of α-, β- and δ-cells

as in controls. It was inferred from this result that overexpression of IGF-II in β-cells led to induction of *islet* hyperplasia, providing a mitogenic stimulus to *all* endocrine cell types. Consistent with this, Hill and coworkers (Hill *et al.*, 2000) found that in neonatal transgenic mice overexpressing IGF-II, hyperplastic islets exhibited the same proportions of α- and β-cells as control siblings. In their transgenic mouse IGF-II overexpression model, Petrik *et al.* (1999) discovered that the proportions of α- and β-cells in hyperplastic islets were increased and decreased respectively relative to controls although absolute numbers of α- and β-cells were still increased over control islets (Petrik *et al.*, 1999). Owing to time constraints, proportions of α- and β-cells within the mega-islets of Ripley transgenic animals were not determined in the current study. However, it was evident from immunoperoxidase staining for glucagon that in a marked proportion of total islets in transgenic animals, the proportion of α-cells was reduced compared with control islets even considering centrally-located α-cells in transgenic islets. Satisfactory immunostaining within other islets in the same tissue section and within different sections on the same slide implied that absence of glucagon staining in such islets was a genuine phenomenon. It might be speculated from this result that IGF-II production by the β-cells in some transgenic islets causes β-cell hyperplasia at the expense of α-cell growth. In such cases, α-cells might be extruded from the islet by β-cell overgrowth. No noticeable difference in immunoperoxidase staining for insulin was seen between Ripley transgenic and control animals, though β-cell proportion in islets was not determined so a small (< 5 %) but significant increase in β-cell proportion at the expense of α-cells cannot be excluded. Further work to determine α-, β- and δ-cell proportions within islets of Ripley transgenic and control mice is therefore necessary.

In the Elijah transgenic animals, islet overgrowth was also suggestive of IGF-II-induced islet hyperplasia. However, owing to the uncertainty regarding the precise expression domain of the rat elastase I promoter, the source of IGF-II responsible for the overgrowth effect could be defined with less precision. The islet cells in which the IGF-II transgene is expressed in Elijah transgenic animals were not determined. There appeared to be no obvious difference in the proportion of α-cells between Elijah transgenic and control islets unlike the observations made in the Ripley study. The β-cell proportion also appeared to be unchanged between Elijah transgenic and control islets. In the absence of quantitative data, it would appear probable that IGF-II induces hyperplasia of the whole islet in Elijah animals carrying the transgene. Ascertaining α-, β- and δ-cell proportions within such islets should prove whether this is the case.

Petrik *et al.* (1999) found that islet hyperplasia in E19.5-20 transgenic mice widely overexpressing IGF-II was caused by an increased rate of islet cell proliferation. They showed immunoreactivity for PCNA in α- and β-cells from hyperplastic islets to be twice that in controls (transgenic, 33.4 ± 0.7 % *vs.* control, 20.2 ± 5.8 %; $P < 0.05$ and transgenic, 24.4 ± 0.9 % *vs.* control, 10.1 ± 0.5 %; $P < 0.01$ respectively). Petrik *et al.* (1998) had earlier demonstrated a transient increase in the number of islet cells expressing inducible nitric oxide synthase (iNOS) in the neonatal rat just preceding an increase in apoptosis. It is also known that the apoptosis characterising β-cell destruction in response to cytokines in type 1 diabetes involves increased intracellular concentration of nitric oxide and increased expression of iNOS (Corbett and McDaniel, 1995). Petrik and colleagues (Petrik *et al.*, 1999) found the number of islet cells in IGF-II-overexpressing mice containing immunoreactive iNOS to be significantly less than in controls. The proportion of islet cells undergoing apoptosis was also significantly less in transgenic animals than non-transgenic siblings. From these results, Petrik *et al.* (1999) proposed that the mechanisms underlying the observed islet hyperplasia evident in IGF-II transgenic animals are most probably a combination of increased cell proliferation coupled with enhanced survival. The percentages of α- and β-cells undergoing cell replication was greater in islets from transgenic animals than controls. Again, this is consistent with IGF-II providing a mitogenic stimulus to each of the endocrine cell populations. The number of islet cells undergoing apoptosis was reduced in islets from transgenic mice compared with controls. Although apoptotic cells proved difficult to identify, apoptosis during rat development has been shown to predominantly occur within the β-cells (Petrik *et al.*, 1998). The IGFs are known to prevent apoptosis in a variety of cell types (Geier *et al.*, 1992; Stewart and Rotwein, 1996), including isolated rat islets (Petrik *et al.*, 1998), by mechanisms that include an inhibition of caspases (Jung *et al.*, 1996). Although islets from IGF-II transgenic mice showed a decrease in the percentage of iNOS-immunoreactive cells, it could not be ascertained whether cells that expressed iNOS later progressed to apoptosis. Hill and colleagues (Hill *et al.*, 2000) showed that in their IGF-II-overexpressing mice in which circulating IGF-II is retained postnatally, the wave of developmental islet cell apoptosis seen in control animals between PN11-16 was substantially reduced in the IGF-II transgenic animals (PN11; transgenic, 6 ± 1 % TUNEL-positive nuclei; control, 12 ± 1 %; $P < 0.01$). Both α- and β-cell DNA synthesis in the resulting hyperplastic islets of transgenic animals was greater at PN13 and PN16 than in controls (Hill *et al.*, 2000). Also, the proportion of α-

to β-cells in the hyperplastic islets did not change over the course of the study. Both observations suggest that the additional IGF-II availability provided a mitogenic stimulus to both islet cell types consistent with previous results (Petrik *et al.*, 1999).

Presented with data from these two studies (Hill *et al.*, 2000; Petrik *et al.*, 1999), it appears likely that islet hyperplasia in the Elijah and Ripley transgenic animals also resulted from a combination of an IGF-II-induced increase in cell proliferation coupled with enhanced survival. However, further work will be necessary to determine the exact mechanisms of the islet overgrowth. Indices of islet cell replication and apoptosis can be obtained from measures of PCNA immunoreactivity and TUNEL respectively. By examining transgenic and control animals at a range of postnatal time-points, the progression of islet hyperplasia can be determined with greater precision. Potentially, examination of pancreata from PN2wk-PN3wk animals when the developmental wave of islet cell apoptosis is occurring will give most insight into the mechanisms of endocrine overgrowth. Whether IGF-II overexpression in Elijah and Ripley transgenic animals suppresses this neonatal apoptotic wave and whether this contributes to islet hyperplasia remain to be determined.

The extent of islet hyperplasia in both the Elijah and Ripley transgenic animals appeared to be appreciably less than that observed in the transgenic mouse model of widespread IGF-II overexpression in which mean islet area in E19.5-20 fetal pancreas was five-fold higher than in controls (Petrik *et al.*, 1999). It was not clear from the outcome of this study whether the generation of islet hyperplasia was primarily caused by an increased local expression of IGF-II within the pancreas of transgenic animals or resulted from exposure to the increased (65 % over control) circulating levels. IGF-II mRNA and peptide were abundant in the islets of transgenic mouse pancreata, although this could be an effect of increased mean islet size, as well as a cause (Petrik *et al.*, 1999). Considering the results of the current study, it appears prudent to speculate that the more acute phenotype shown by the transgenic animals of Petrik and coworkers (Petrik *et al.*, 1999) is primarily a product of the increased serum levels of IGF-II relative to their non-transgenic siblings. This hypothesis is supported in the Ripley transgenic animals by the finding that RIP-IGF-II transgenic mice exhibit only low levels of circulating IGF-II (Devedjian *et al.*, 2000).

Comparing the extent of islet hyperplasia between the Elijah and Ripley transgenic mice raises issues regarding differences in sampling used in the two studies. Owing to the different nature of the Elijah study, a much smaller number of islets (n = 92) were sampled than in the Ripley study (n = 764). Also, because of the different

hypotheses being tested, magnification of images for morphometric analysis was much greater (× 200) in the Ripley study than the Elijah analysis (× 50), so that error (in real terms) associated with islet area measurement data from the latter analysis was greater than in the former study. Considering these factors, islet hyperplasia in Elijah transgenic animals would appear to be more extensive, both in terms of the extent of overgrowth of each mega-islet and also the incidence of hyperplasia within the respective islet samples. IGF-II expression within islets in Ripley animals bearing the transgene was clearly greater than in transgenic Elijah mice. If the assumption is made that islet overgrowth effects are relative to the amount of exogenous IGF-II, then it is impossible to explain the greater effects in the Elijah mice without invoking acinar-expressed IGF-II in these animals. This is taking the low circulating level of IGF-II (relative to controls) in the RIP-IGF-II transgenic mice of Devedjian *et al.* (2000) into consideration. The more acute phenotype of Elijah transgenic animals indicates that the IGF-II protein is able to traverse the boundary between acini and islets to exert its mitogenic effects on the endocrine compartment. IGF-II availability to the islet by acinar tissue surrounding it on all aspects is likely to result in islet hyperplasia with overgrowth of different endocrine cell types, particularly if IGF-II is also expressed to some extent within the islet.

6.4.5.3.4. Interaction Between Hyperplasia and Disrupted Architecture of Islets

In all three IGF-II overexpression mouse models mentioned above (Devedjian *et al.*, 2000; Hill *et al.*, 2000; Petrik *et al.*, 1999), disrupted islet architecture was seen to accompany islet hyperplasia as in the current study. Centrally-localised clusters of α-cells were seen within the β-cell mass of the islet core in contrast to their characteristic peripheral arrangement within the islet mantle. Similar changes in islet morphology are observed in animal models of type 2 diabetes and obesity, such as prediabetic Zucker Diabetic Fatty (ZDF) rats (Larsson *et al.*, 1977; Polonsky, 1995; Tokuyama *et al.*, 1995) and *ob/ob* (Shino *et al.*, 1973) and *db/db* mice (Like and Chick, 1970), which present enlarged islets with disorganised intra-islet cell distribution. Devedjian *et al.* (2000) argued that the alteration in α-cell distribution evident in islets of transgenic IGF-II-overexpressing mice may not be a general occurrence with β-cell hyperplasia, since transgenic mice overexpressing growth hormone are highly hyperinsulinaemic and normoglycaemic (Valera *et al.*, 1993), and show high hyperplasia of islets but normal α-cell distribution (J. Visa and F. Bosch, unpublished observations). Similarly,

overexpression of IGF-I in β-cells of transgenic mice resulted in islet hyperplasia but normal distribution of α-cells (C. Costa and F. Bosch, unpublished observations). Devedjian *et al.* (2000) suggested from the disrupted islet architecture in their RIP-IGF-II transgenic mice that overexpression of IGF-II might alter the location of islet cells and lead to islet disorganisation. This is consistent with the finding that "starfish-shaped" islets of Goto-Kakizaki (GK) rats show increased IGF-II expression (Hoog *et al.*, 1996). The GK rat is a model of mild type 2 diabetes without obesity. Greater amounts of a high-molecular-weight form of IGF-II were found in pancreatic extracts from PN2month and PN6month GK rats than in extracts from PN1month GK and control rats (Hoog *et al.*, 1996, 1997). More IGF-II mRNA was detected in starfish-shaped islets of GK rats than in either GK rat islets with normal structure or islets of control rats (Hoog *et al.*, 1996).

One explanation for the disorganised islet architecture in islets of IGF-II-overexpressing mice is that islet IGF-II expression causes changes in cell adhesion properties of the different endocrine cells. α-Cells were also seen to be ingressing into the islet body from the mantle in dumbbell islets (**Chapter 5**). It was speculated that migration of α-cells from the mantle drives islet fission and results from changes in cell adhesion properties of different endocrine cell types, most notably the α- and β-cells. By generating N-CAM knockout mice, Esni *et al.* (1999) showed that cadherin-mediated adhesion in islets is increased, resulting in aberrant α-cell localisation in the islet core. This disruption of normal islet architecture was attributed to increased cadherin-mediated adhesion between α-cells in the absence of N-CAM (Esni *et al.*, 1999). Hence, IGF-II expression in endocrine cells might cause differential expression of N-CAM and/or cadherin within the islet cells. This might possibly be in the form of a recapitulation of islet ontogeny preceding the loss of endogenous IGF-II at PN2wk-3wk. An alternative and attractive hypothesis is that IGF-II-expressing islets exhibit defective putative islet fission and as a result, α-cells ingressing from the islet mantle become isolated within the islet core and the hyperplastic islet remains as one "mega-islet", unable to divide into daughters. Incomplete or partial islet fission could explain the unusual shapes typically exhibited by hyperplastic islets (Devedjian *et al.*, 2000; Hill *et al.*, 2000; Petrik *et al.*, 1999) and similarly account for the "starfish-shaped" islets in GK rats (Hoog *et al.*, 1996).

6.4.5.3.5. IGF-II Primarily a Mitogenic Stimulus for Existing Islets

It was found in the current study that the number of islets per pancreas section was not different between IGF-II transgenic animals and controls. This finding is concordant with results from the earlier studies (Hill *et al.*, 2000; Petrik *et al.*, 1999) of pancreatic morphology in IGF-II-overexpressing mouse models. This suggests that although IGF-II is likely to function as an islet cell mitogen, it may not be a significant factor in the generation of novel islets from the pancreatic ductal epithelium by neogenesis. This hypothesis is supported by the pattern of immunostaining for the immature endocrine cell marker Pdx1, in the pancreata of IGF-II transgenic animals (Petrik *et al.*, 1999). Pdx1 immunoreactivity was seen predominantly within the differentiated β-cell population of existing islets, with little presence in isolated clusters of endocrine cells indicative of neogenesis. However, Petrik and colleagues (Petrik *et al.*, 1999) found an increase in the number of isolated cells immunopositive for insulin per tissue section over control animals. This was taken to suggest that a limited degree of neogenesis was occurring. This result is consistent with a finding from the current study. In one pancreas from an Elijah transgenic mouse, immunoperoxidase staining revealed scattered glucagon-immunopositive acinar cells throughout the exocrine tissue of a few pancreatic lobes where they were evident both within acini and at the acinus periphery. Since glucagon is held to be a marker of primitive endocrine cells, it is speculated that these infrequent glucagon$^+$ cells in the exocrine pancreas represent cases of neogenesis. Demonstrating such cells to be Pdx1-immunopositive would support this hypothesis. Considering the low incidence of such cells however, it would appear that IGF-II primarily functions as a mitogenic factor for existing endocrine cells, activating hyperplasia of existent islets. This is consistent with its ability to increase DNA synthesis within isolated islet-like cell clusters containing β-cells, from human fetal pancreas, but its relatively poor ability to increase the numbers of such structures compared with hepatocyte growth factor or FGF7 (Otonkoski *et al.*, 1988b, 1994).

6.4.5.4. Predisposition to Type 2 Diabetes in Elijah and Ripley Transgenic Animals?

As mentioned above, islet hyperplasia and/or aberrant α-cell localisation within the islet core as seen in Elijah and Ripley transgenic mice is also observed in animal models of type 2 diabetes and obesity, such as prediabetic Zucker Diabetic Fatty (ZDF) rats (Larsson *et al.*, 1977; Polonsky, 1995; Tokuyama *et al.*, 1995) and *ob/ob* (Shino *et*

al., 1973) and *db/db* mice (Like and Chick, 1970), which exhibit enlarged islets with disorganised islet cell distribution. Islets from RIP-IGF-II transgenic mice have been shown to display enhanced glucose-stimulated insulin secretion and glucose utilisation (Devedjian *et al.*, 2000). Such mice exhibited hyperinsulinaemia, mild hyperglycaemia, and altered glucose and insulin tolerance tests consistent with insulin resistance as in the prediabetic state. Approximately 30 % of animals showed increased insulin resistance and developed overt diabetes with severe hyperglycaemia when fed a high-fat diet (Devedjian *et al.*, 2000). It was inferred that an increase in circulating lipids may exacerbate the prediabetic phenotype in these mice. The authors proposed that islet hyperplasia was an early event in the RIP-IGF-II transgenic animals overexpressing IGF-II that led to hyperinsulinaemia as a result of which insulin resistance developed. The results were taken to support the hypothesis that hyperinsulinaemia may be an initial event in type 2 diabetes and that insulin resistance may be a consequence of the increased insulinaemia (Devedjian *et al.*, 2000). Interestingly, in E19.5-20 transgenic mice widely overexpressing IGF-II, despite the presence of islet cell hyperplasia, circulating insulin concentrations and plasma glucose levels were found to be no different from controls (Petrik *et al.*, 1999). This was suggested to be due to a downregulation of insulin secretion by IGF-II, as for islet-like cell clusters from human fetuses (Otonkoski *et al.*, 1988b) and for perifused adult rat islets (Hill *et al.*, 1997). Alternatively, if glucagon release was increased in transgenic animals as a result of the increased α-cell proportion in their hyperplastic islets, this might also suppress insulin release (Petrik *et al.*, 1999).

Further work remains to be performed to determine whether the Elijah and/or Ripley transgenic mice display insulinaemia and insulin resistance as do the RIP-IGF-II mice of Devedjian *et al.* (2000). If so, these transgenic mice may be a suitable model in which to study the processes that lead to type 2 diabetes.

6.4.5.5. Presence of "Hepatocyte-Like" Cells in Islets from Transgenic Animals

In two pancreata from Elijah and Ripley transgenic mice, H & E histochemistry revealed the presence of large cells which morphologically resembled hepatocytes and so these cells were referred to as "hepatocyte-like" cells. These cells were clearly distinguishable from adjacent endocrine cells by their abundant eosinophilic cytoplasm and were located at the islet periphery. This phenomenon was not observed frequently, occurring with an incidence of 0.13 % in islets of Ripley transgenic animals. However,

the occurrence of such cells in transgenic animals of both lines at an estimated similar frequency would suggest that it is a real phenomenon. Similar "hepatocyte-like" cells within islets have been reported in a transgenic mouse model of FGF8 overexpression in which the mouse FGF8 transgene was driven by the rat glucagon promoter (Yamaoka *et al.*, 2002). In this mouse model, the hepatocyte-like cells were localised to the periphery of islets as was seen in the present study, and displayed large clear nuclei with several small nucleoli and abundant eosinophilic cytoplasm. They were described as being morphologically indistinguishable from hepatocytes (Yamaoka *et al.*, 2002). These cells were found to produce neither insulin nor glucagon on the immunohistochemical basis. It was inferred that FGF8 had stimulated the transdifferentiation (the direct transformation of one differentiated cell type to another) of a proportion of endocrine cells into hepatocyte-like cells (Yamaoka *et al.*, 2002). This hypothesis was supported by the expression of the mature hepatocyte marker albumin in the FGF8 transgenic islets. The lack of expression of the immature hepatocyte marker α-fetoprotein by these islets was taken to imply that highly differentiated hepatocytes were generated in the islets of FGF8-overexpressing animals. An alternative explanation is that FGF8 may induce only albumin expression, but not α-fetoprotein expression, regardless of hepatocyte maturity. Parallels can be drawn between the current study and that of Yamaoka *et al.* (2002): both transgenic models involve a highly local overexpression of a growth factor within and/or adjacent to the pancreatic islets. However, FGF8 might also be made available to the pancreatic islets via the bloodstream. It was speculated that the level of FGF8 protein in the circulation of FGF8-overexpressing animals would be considerably higher than in controls although blood concentration was not measured (Yamaoka *et al.*, 2002). Transgenic mice expressing interferon-γ under the control of the same glucagon promoter exhibit a mean serum interferon-γ concentration 50-fold greater than in control animals (Yamaoka *et al.*, 1999). It remains to be seen whether the "hepatocyte-like" cells observed in the Elijah and Ripley IGF-II overexpression mouse models do indeed express transcription products characteristic of hepatocytes and resemble hepatocytes not just morphologically but also functionally. If so, it also remains to be proven whether such cells are actually generated by the transdifferentiation of endocrine cells. If so, then the observation of these cells in the islets of IGF-II-overexpressing animals might prove to be a very interesting finding. If an hepatocyte identity of such cells can be confirmed then it could be speculated that a high local concentration of IGF-II induces hepatocytes within the pancreas, perhaps by transdifferentiation of islet endocrine cells. So, one avenue of future work might involve

the characterisation of these "hepatocyte-like" cells in islets from Elijah and Ripley transgenic mice. A lack of expression of endocrine markers such as insulin and glucagon and the exocrine marker amylase and positive immunostaining for the liver-specific proteins albumin, α-fetoprotein, transferrin, and/or transthyretin (prealbumin) would lend support to the ability of IGF-II to stimulate the induction of hepatocytes in the pancreatic islets.

On the basis that hepatocyte-like cells are found within the pancreatic islets, Yamaoka and colleagues (Yamaoka *et al.*, 2002) suggested that such cells are most probably derived from endocrine precursor cells. They went on to argue that although hepatocyte-like cells are localised to the islet mantle where non-β-cells such as α-cells are usually located, this finding does not necessarily imply that such cells originated from non-β-cells. As mentioned above, the arrangement of islet cells has been considered to be dependent on adhesion molecules of each islet cell. If adhesion molecules such as cadherin, which has been shown to be essential for β-cell aggregation (Dahl *et al.*, 1996), are not expressed in hepatocyte-like cells, they will lose contact with β-cells and become relegated to the islet mantle, outside the β-cell aggregate.

6.4.6. Summary

In conclusion, dramatically similar phenotypes affecting islet morphology were seen in two lines of transgenic mice overexpressing IGF-II in different compartments of the pancreas: the acini or islets. Transgenic animals displayed islet hyperplasia in conjunction with disorganised islet architecture as a result of IGF-II overexpression. Circumstantial evidence suggests that IGF-II produced in the acinar compartment is able to exert its mitogenic effects on the adjacent endocrine compartment and so the effects of IGF-II are not cell-autonomous but can be exerted over a distance. Furthermore, the appearance of "hepatocyte-like" cells morphologically resembling hepatocytes in the islets of transgenic animals of both lines permits speculation on possible IGF-II induction of hepatocytes, perhaps by the transdifferentiation of endocrine cells. Further work is needed to determine whether all endocrine populations are affected by the hyperplasia in both lines and to elucidate mechanisms of islet overgrowth. An immunocytochemical characterisation of the "hepatocyte-like" cells to confirm an hepatocyte identity is also an avenue of future study. Finally, investigation is required to determine whether transgenic animals display insulinaemia and insulin resistance as a result of islet hyperplasia, predisposing to type 2 diabetes.

7. Induction of Hepatocytes in Dexamethasone-Treated Embryonic Pancreas In Vitro

7.1. Introduction

7.1.1. Hepatic Transdifferentiation of the Pancreas

It is widely believed that the differentiated state is permanent and irreversible. However, in some cases, terminally differentiated cells can interconvert (Slack, 1986, 1992), undergoing phenotypic alterations after an appropriate stimulus and in a permissive environment. Such alterations are associated with distinct morphological changes and are accompanied by the elaboration of new gene products, indicating activation of genes that are normally repressed in that cell type (DiBerardino *et al.*, 1984; Okada, 1986). The phenotypic interconversion of one differentiated cell to another usually arises in situations of chronic tissue damage and associated regeneration. Some changes may be indirect, occurring via an intervening stem cell, whereas others may be direct transformations, sometimes called *transdifferentiations* (Eguchi and Kodama, 1993; Okada, 1991). Many examples have been reported, some of which are known to predispose to cancer (Slack, 1986, 1992). However, the molecular and cellular mechanisms involved remain largely uncharacterised.

The appearance of hepatocytes in the pancreas has been described both in animal experiments and in human pathology. Hepatic foci have been reported to occur in the pancreas of rats or hamsters in response to various experimental treatments including treatment with the protein synthesis inhibitor ethionine (Scarpelli and Rao, 1981), copper depletion of the diet (Rao *et al.*, 1986b; Rao and Reddy, 1995), after transplantation (Dabeva *et al.*, 1997), or in transgenic mice overexpressing keratinocyte growth factor (KGF, also known as FGF7) in the pancreas (Krakowski *et al.*, 1999). The phenomenon has also been observed spontaneously in the vervet monkey (Wolfe-Coote *et al.*, 1996), and the reverse transformation has been observed in the liver of a human cancer patient (Wolf *et al.*, 1990), and has recently been experimentally induced in *Xenopus laevis* tadpoles by overexpressing an activated form of the *Xenopus* homolog of *Pdx1*, *Xlhbox8-VP16*, in the liver (Horb *et al.*, 2003). It has been pointed out that although such whole-organism observations cannot prove that the hepatocytes derive from pancreatic cells, they suggest a relatively high-frequency conversion

between pancreatic cells and hepatocytes (Shen *et al.*, 2000). These observations may reflect the intimate developmental relationship between the two tissues; the liver and pancreas originate from adjacent regions of the foregut endoderm (Slack, 1995; Zaret, 2000).

7.1.2. Induction of Hepatocytes in Pancreatic Buds In Vitro

Using an *in vitro* system to study the transdifferentiation of pancreas to liver, Shen *et al.* (2000) showed that the pancreatic cell line AR42J-B13, yields foci of hepatocytes on treatment with the synthetic glucocorticoid dexamethasone. Immunofluorescence analysis showed that treatment with 10 nM dexamethasone for five days increased amylase expression in a proportion of cells. Another sub-population of cells progressively flattened onto the substratum and amylase expression was reduced in these cells after five days of treatment. After two weeks of treatment, expression of amylase was almost non-existent. After three weeks these cells showed strong expression of the liver-specific protein albumin. Such cells were shown by electron microscopy to exhibit typical features of hepatocytes such as extensive endoplasmic reticulum and structures resembling bile canaliculi. Testing the dexamethasone-treated cultures for the induction of eight liver-specific markers showed the markers to appear in sequence according to hepatocyte maturation. When more than one was stained simultaneously all cells expressing a later marker were also found to express the earlier marker. The consistent coexpression of liver proteins in the cultured cells strongly suggested that dexamethasone provokes the formation of hepatocytes and not just the ectopic expression of a few liver proteins. The changes induced by dexamethasone represented a coordinated program of hepatocyte differentiation rather than the activation of one or a few individual genes. Shen *et al.* (2000) demonstrated that indeed a proportion of the hepatocytes arose directly from differentiated exocrine-like cells, with no intervening cell division. Initially the cells lost the pancreatic phenotype and lost their expression of amylase. They then started to express hepatic genes that are produced in fetal liver and later they expressed larger amounts of albumin and other gene products characteristic of adult liver. Based on immunofluorescence detection, these hepatocytes were subsequently shown to demonstrate mature liver characteristics such as the expression of liver genes involved in phase I and II detoxification pathways, ammonia detoxification, and the metabolism of glucose (Tosh *et al.*, 2002). The conversion of differentiated exocrine-like cells into hepatocytes was shown by Shen *et*

al. (2000) to be associated with induction of the transcription factor C/EBP (CCAAT enhancer binding protein)β. Furthermore, Shen *et al.* (2000) went on to demonstrate dexamethasone induction of hepatocytes concomitant with C/EBPβ activation in cultures of mouse embryonic pancreatic buds established using the system of Percival and Slack (1999) as described in **Chapter 3**. This result demonstrated that dexamethasone-induced conversion is not restricted to the AR42J-B13 cells, but that it also occurs in the normal developing pancreas (Shen *et al.*, 2000). Moreover, it also demonstrates the eminent suitability of the embryonic pancreatic bud culture system for studying the phenomenon of dexamethasone-induced hepatic conversion of pancreas to liver.

7.1.3. Current Study

It has been observed (Dr. D. Tosh, unpublished observations) that following dexamethasone treatment of intact pancreatic bud cultures, induced hepatocytes express, amongst a number of liver-specific markers, one of two ammonia-detoxifying enzymes: glutamine synthetase (GS) or carbamoylphosphate synthetase I (ammonia; CPS I). In the mammalian liver the distribution of these two enzymes is mutually exclusive in that they are expressed in two distinct populations of hepatocytes that are zonally demarcated in the liver acinus/lobule. In each acinus hepatocytes extend from the upstream portal to the downstream central venules (Lamers *et al.*, 1989; Rappaport, 1973). In the adult rat, CPS I protein and mRNA is exclusively expressed in a contiguous large compartment (**Fig. 7.1.**) including the periportal (afferent) zone, intermediate zone and early perivenous zone with expression decreasing in a porto-central direction (Bartels *et al.*, 1989; Moorman *et al.*, 1988, 1990). Expression of GS protein and mRNA is also exclusive and restricted to the late perivenous (efferent) zone, a small compartment comprising the last downstream pericentral hepatocytes lining the central vein in each acinus (Bartels *et al.*, 1989; Moorman *et al.*, 1988, 1990). Therefore, expression of these enzymes exhibits a strict reciprocal relationship (Gebhardt, 1992). The enzyme heterogeneity in the liver has been attributed largely to gradients of metabolites and regulatory factors along the liver acinus (Gumucio, 1989). Kuo *et al.* (1988) attributed the highly restricted pattern of GS expression to specific geographically located signals such as possible variations in the composition of extracellular matrix between the pericentral and periportal regions of the acinus. It has

Figure 7.1. Complementary Expression Pattern of Carbamoylphosphate Synthetase I and Glutamine Synthetase in an Acinus/Lobule of the Mammalian Liver

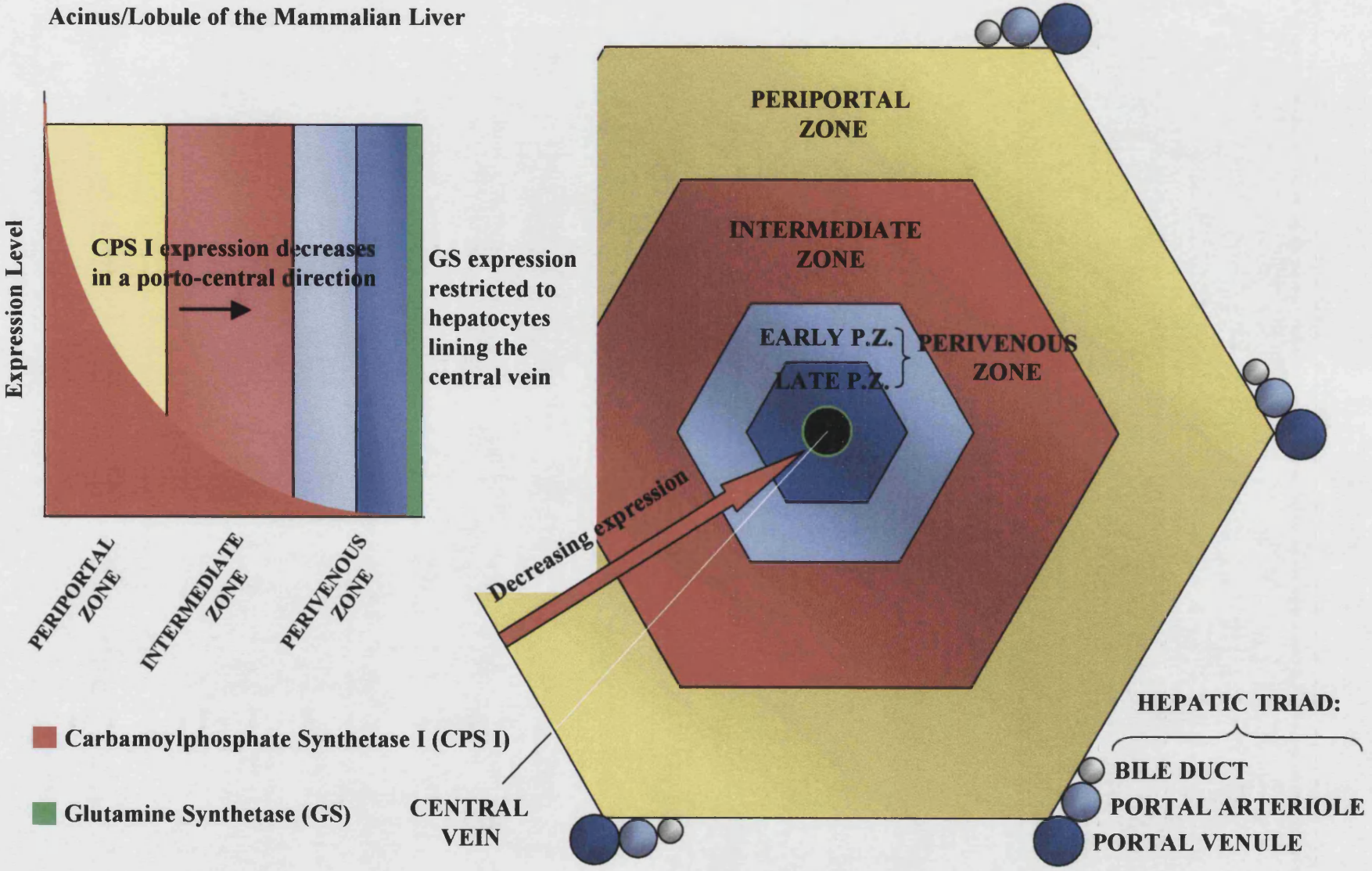

been proposed (Shiojiri *et al.*, 1997) that factors associated with central veins direct the hepatocytes lining the central vein to express GS and to suppress CPS I expression. Blood-borne modulatory factors such as hormones, substrates and oxygen, are supposed to be the major determinants for the establishment and the dynamics of a gradient type of protein zonation (Jungermann, 1988; Jungermann and Katz, 1989). Such blood-borne factors are assumed to constitute the primary determinants for CPS I expression within the hepatic acinus (Moorman *et al.*, 1990).

Mirroring observations *in vivo*, GS and CPS I expression have also been shown to be complementary in dexamethasone-treated AR42J-B13 cells (Tosh *et al.*, 2002) and in pancreatic bud cultures *in vitro*. By conducting immunofluorescence analysis on dexamethasone-treated intact pancreatic bud cultures, CPS I expression was demonstrated in cells throughout the majority of the epithelium whilst GS expression was restricted to cells in a much smaller compartment at the periphery of the epithelium, adjacent to the surrounding mesenchyme (Dr. D. Tosh, unpublished observations). This latter finding raised the possibility that epithelium-mesenchyme interactions might play a role in the induction of at least one population of hepatocytes formed during dexamethasone-induced hepatic transdifferentiation. Consequently, two interesting questions arose: (1) Does hepatic transdifferentiation of dexamethasone-treated pancreatic buds still occur in the absence of mesenchyme? (2) If transdifferentiation *does* occur, is the GS^+ hepatocyte population induced, and if not, does induction of CPS I-expressing hepatocytes still occur in their absence? In order to address these questions, E11.5 pancreatic epithelium was carefully dissected free of its surrounding mesenchyme and cultured in isolation. As a positive control, E11.5 intact pancreatic buds were established and maintained *in vitro* in parallel with the isolated epithelial cultures. After inducing hepatic conversion in half of the cultures with dexamethasone treatment, cultures were fixed and immunofluorescence analysis performed for liver- or pancreas-specific protein markers to determine whether or not hepatic conversion had occurred and if so, which (periportal or perivenous) hepatocyte population(s) had been induced.

7.2. Materials and Methods

The protocol employed for establishing pancreatic bud cultures and subsequent immunofluorescence analysis was essentially that developed by Percival and Slack (1999) with some minor procedural modifications.

7.2.1. Pancreatic Bud Dissection and Establishing Cultures

Pancreatic buds were obtained from either MF1 albino mice or embryos of the ROSA-26 gene trap mouse strain (Zambrowicz *et al.*, 1997) following their outbreeding since recombinant pancreatic bud cultures (**Chapter 3**) were established in parallel. In this chapter the *lacZ* status of cultures is not relevant. Dorsal pancreatic buds were dissected and intact pancreatic bud cultures, isolated epithelial cultures, and in later experiments, segregated epithelium/mesenchyme co-cultures were established as in **Chapter 2, Section 2.1.**

7.2.2. Treatment of Cultures

From either day (d) 2 or 3 of the culture period, the synthetic glucocorticoid dexamethasone or "Dex" (Sigma D-1756) was added daily to the newly replenished 2 ml culture medium to a final concentration of 1 μM. As a control, Dex was withheld from the medium. In later experiments, 100 ng/ml of recombinant Fibroblast Growth Factor (FGF)1/acidic (a)FGF, FGF7/KGF, FGF8b (the latter was also added at 1 μg/ml) or FGF10 (all R & D Systems: 232-FA, 251-KG, 423-F8 and 345-FG respectively) were added to isolated epithelial cultures from d2. FGF was added directly onto the culture prior to addition of fresh medium. Dex treatment was either concurrent with FGF incubation or was commenced 1-2 days after FGF treatment was begun.

7.2.3. Immunofluorescence Cytochemistry

Cultures were fixed as described in **Section 2.2.1.** Then, immediately thereafter or following storage (in PBSA with 0.02 % NaN_3 at 4°C), cultures were subjected to immunofluorescence cytochemistry as in **Section 2.5.2.** The primary and secondary antisera used together with their source and working concentrations are summarised in

Tables 2.1. and **2.2.** respectively (**Section 2.5.1.**). The first staining cycle was typically completed before the second was commenced except when double-staining for CPS I and GS: only one incubation was conducted with both primary antibodies, each used at a working dilution of 1/500. One 2.5 h incubation (at room temperature) was then performed with the two secondary antisera. In some experiments when staining for neurogenin3, antigen retrieval was performed with citrate buffer or ammonium chloride following the permeabilisation stage and occasionally, staining intensity was enhanced by avidin-biotin signal amplification as in **Section 2.5.2.2.**

7.2.4. Scoring Immunopositive Cells and Image Capture

During their treatment *in vitro*, live cultures were periodically observed using a Leica DMIRB inverted compound microscope; images of live specimens were collected from a Zeiss LSM510 confocal microscope. Immunofluorescence-stained pancreatic bud cultures were examined using a Leica DMRB fluorescent microscope. Images of stained specimens were taken with a Spot RT Color digital camera (National Diagnostics Inc.) and stored as uncompressed 24-bit TIFF images. Immunopositive cells were scored as absolute numbers or as an approximate percentage of total cells either directly or from merged images following adjustment of colour channels using the Adobe Photoshop 6.0 package.

7.3. Results

7.3.1. Growth and Morphology of Cultures In Vitro

Once placed on to the fibronectin substrate, intact pancreatic buds adhered within a few hours and gradually flattened out over the first one-two days as described by Percival and Slack (1999) and in **Chapter 3**. Mesenchymal cells spread rapidly out of the explant to form a monolayer of cells around the epithelium and on the second or third day of culture, the epithelium began to branch. Over the subsequent six days *in vitro*, the epithelium became an extended branched structure radiating from the original centre (**Fig. 7.2. (a)**). The mesenchyme resolved into a periphery mainly composed of smooth muscle cells and an inner region dominated by fibroblastic cells with occasional patches of lymphoid tissue. The presence of 1 μM dexamethasone (Dex) in the culture medium for 6 days from 2d of culture produced a change in pancreatic bud morphology (**Fig. 7.2. (b)**). The number of epithelial branches was reduced and large, flattened cells became evident from day 4 of Dex exposure. Cultures also appeared very dense, presumably due to increased deposition of zymogen granules. These observations were consistent with the previously described induction of hepatic conversion (Shen *et al.*, 2000).

Isolated epithelia rapidly adhered to the fibronectin substrate within a few hours and survived in the culture system, forming an epithelial monolayer. However, epithelia deprived of their mesenchyme did not undergo the typical morphogenetic behaviour of the intact cultures, showing no branching morphogenesis even after 8 days' maintenance *in vitro* (**Fig. 7.2. (c)**). Following exposure to 1 μM Dex from 2d, cultured epithelia showed changes in morphology. Cell aggregates or "islands" of cells began to appear after 4 days of Dex treatment (**Fig. 7.2. (d)**). By 7 days of Dex exposure, some cell detachment from the substrate was evident as the free ends of chains of cells tethered to the fibronectin substrate floated in the culture medium. Large, flattened cells were not visible in the Dex-treated epithelia as they had been in the Dex-treated intact buds, implying that hepatic conversion had not been induced in the absence of mesenchyme. An analysis of pancreatic and liver marker expression would confirm this suggestion and determine the identity of the cell islands.

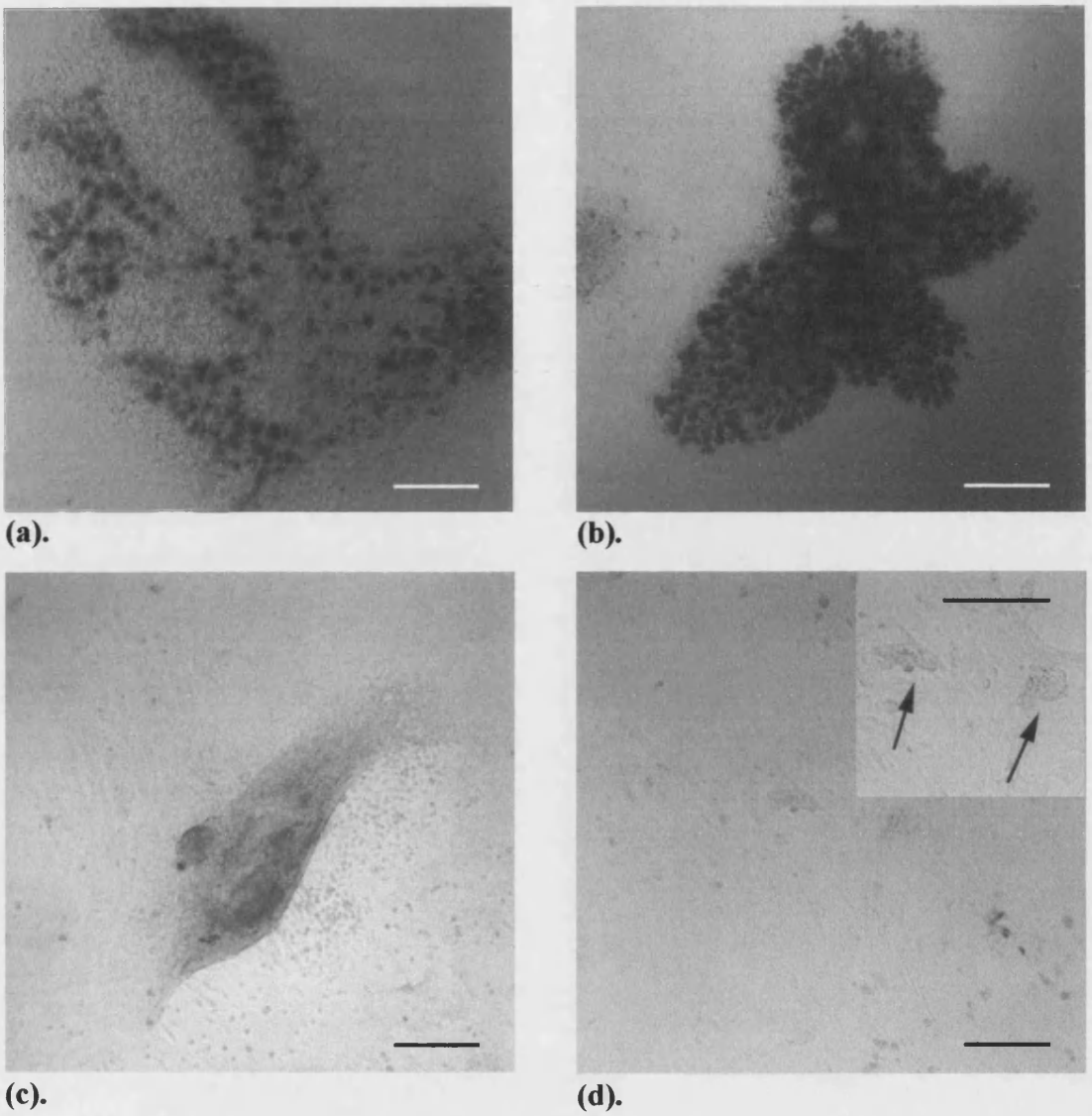

Figure 7.2. Cell Aggregates are Generated by Dexamethasone Treatment of Isolated Pancreatic Epithelium

(a) Intact 8d pancreatic bud culture. (b) Intact 8d pancreatic bud following treatment with dexamethasone for 6d. (c) Isolated 8d pancreatic epithelium. (d) Isolated 8d pancreatic epithelium after 6d of dexamethasone treatment; cell "islands" are shown at greater magnification in inset

Images collected on Zeiss LSM510 confocal microscope. Bar = 200 μm

7.3.2. Immunofluorescence Analysis

7.3.2.1. Hepatic Conversion of Intact Pancreatic Buds

Control intact pancreatic buds cultured for 9d without Dex exhibited the characteristic appearance of exocrine and endocrine markers: approximately 80 % of the epithelial cells were associated into acinus-like structures and expressed amylase, but insulin- and glucagon-immunopositive cells were also evident in islet-like structures (**Fig. 7.3. (a)**). Intact buds cultured without Dex failed to show expression of the liver-specific proteins CPS I and GS (**Fig. 7.3. (b)**). Whole pancreatic buds exposed to 1 μM Dex for 7 days from 2d of culture retained expression of amylase throughout the explant (**Fig. 7.3. (c)**). The monoclonal mouse anti-glucagon antibody (Sigma G-2654) used in the current study was that employed by Shen *et al.* (2000). Although (α-) amylase is commonly accepted as a marker of pancreatic acinar cells, it is also expressed in immature hepatocytes and in the epithelia of intrahepatic bile ducts in fetal and adult human liver (Terada and Nakanuma, 1991, 1995; Terada *et al.*, 1998). No signal has, however, been reported (Professor J. M. W. Slack, personal communication) from immunofluorescence analysis with this anti-glucagon antibody, in cultured cells from the human hepatoma cell line, HepG2, or in *Xenopus laevis* liver. Therefore in practice, the anti-glucagon antibody used in the present study was capable of distinguishing between pancreatic exocrine cells and hepatocytes.

Whilst whole pancreatic buds exposed to 1 μM Dex for 7 days retained their expression of amylase throughout the culture, no insulin-immunopositive cells were evident and the number of glucagon$^+$ cells was negligible compared with control untreated buds. Liver proteins were induced by treatment with dexamethasone, as judged from high expression of the liver-specific protein transferrin or TFN (**Fig. 7.3. (e)**), indicating hepatocyte induction. Expression of both CPS I and GS was also seen in Dex-treated whole cultures (**Fig. 7.3. (d)**). Between 60 % and 70 % of epithelial cells were CPS I-immunopositive whilst 10-20 % of epithelial cells stained for GS. No colocalisation of the two liver markers was observed, consistent with previous observations (Dr. D. Tosh, unpublished observations). This suggested the induction of distinct CPS I$^+$ periportal-like and GS$^+$ perivenous-like hepatocyte populations.

The patterns of differentiation resulting from the pancreatic epithelium being subjected to a particular environment and/or treatment such as Dex exposure are summarised in **Table 7.1.** The data were derived from an average of four replicates for each experiment. The proportions of cells immunopositive for each cell marker stained

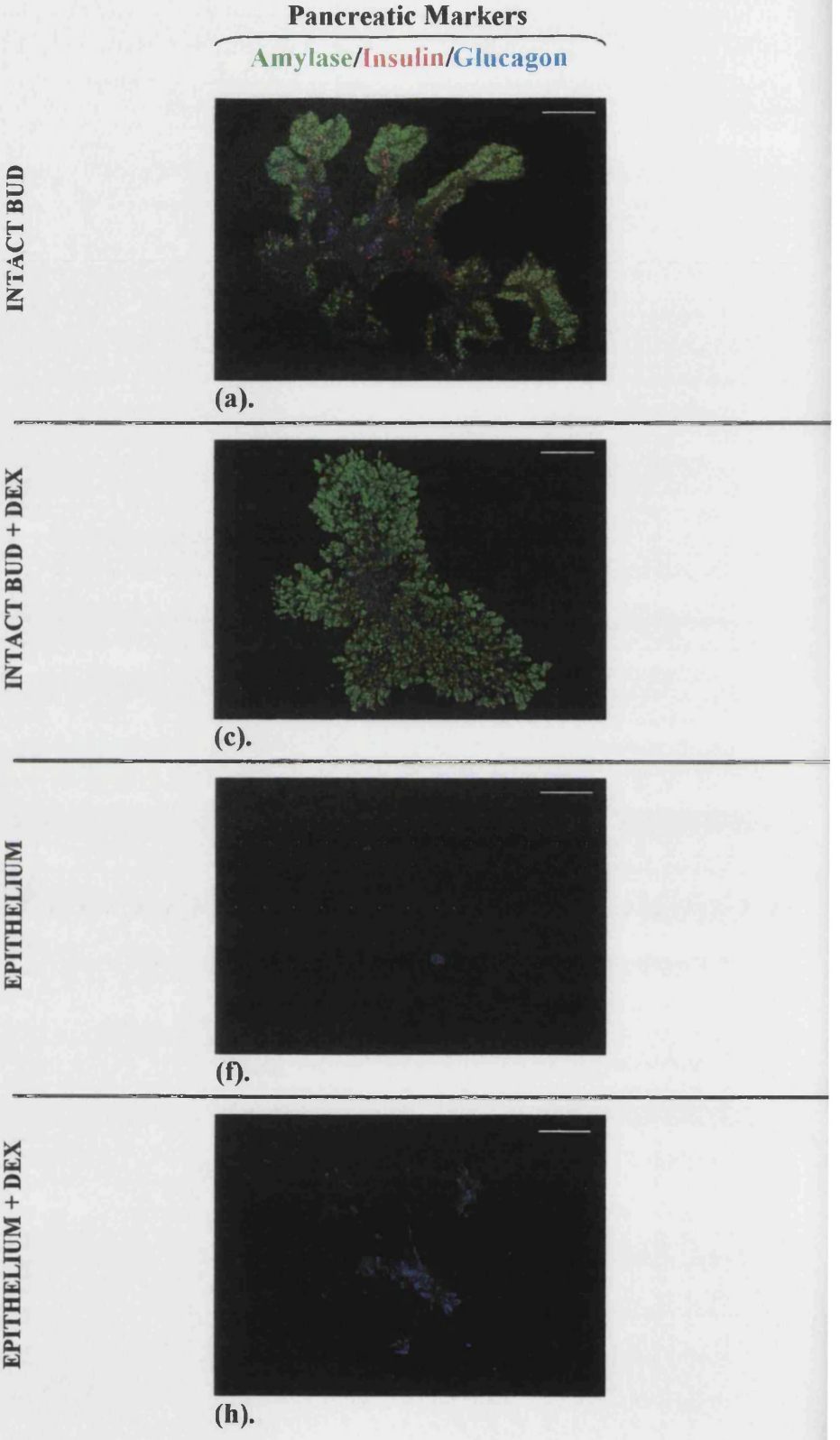

Figure 7.3. Hepatic Conversion of Pancreatic Buds by Dexamethasone Does Not Occur in the Absence of Mesenchyme

Hepatic Markers

CPS I/GS

Transferrin (TFN)

(b).

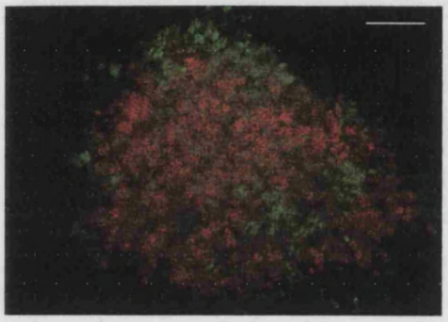

(d).

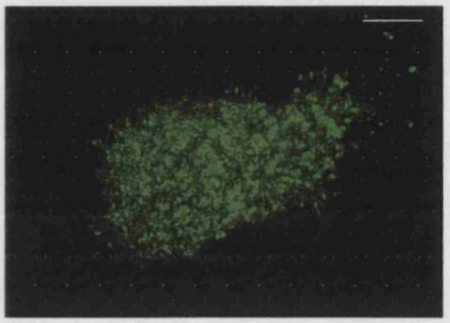

(e).

(g).

(i).

(j).

Immunofluorescence analysis of pancreatic and hepatic markers in 9d intact buds and isolated epithelium cultured without (a-b and f-g) or with (c-e and h-j) 1 μM dexamethasone for 7d

(a), (c) and (e) Bar = 200 μm; (b), (d) and (f)-(i) Bar = 100 μm; (j) Bar = 50 μm

for are represented as -, +, ++ or +++. On this qualitative scale as used by Horb and Slack (2000), ++ denotes the proportion of amylase$^+$ cells and insulin$^+$ cells in untreated intact pancreatic buds; + represents the smaller proportion of glucagon-immunopositive cells in the control intact buds. Since no CPS I or GS staining was detected in intact cultures, - is used to denote an absence of CPS I$^+$ cells and GS$^+$ cells in the control buds. According to this scale, a higher or lower number of +'s than the control value indicates a greater or lesser number of immunopositive cells relative to the control, respectively, whilst a - denotes the absence of cells staining for the marker concerned.

Table 7.1. Cell Differentiation Patterns of Pancreatic Epithelium Subjected to Different Environments and Culture Conditions

CULTURE TYPE & TREATMENT	RELATIVE ABUNDANCE OF CELL MARKER					
	Amylase	Insulin	Glucagon	CPS I	GS	TFN
Intact Bud (Control)	++	++	+	-	-	
Intact Bud + Dex	+++	-	+	++	+	++
Isolated Epithelium	-	+	+	-	-	
Isolated Epithelium + Dex	-	+	+++	-	- *	-
Isolated Epithelium + FGF1	-	+	+++	-	-	
Isolated Epithelium + FGF1 + Dex	+	+	+++	-	+	
Isolated Epithelium + FGF10 + Dex	+	++	+++			
Co-Culture Epithelium + Mesenchyme	+	+++	++			
Co-Culture Epithelium + Mesenchyme + Dex	+	++	+++	+	+	

* Refer to **Section 7.3.2.9.**

7.3.2.2. Absence of Hepatocytes in Dex-Treated Isolated Epithelia

Isolated pancreatic epithelia cultured for 9d in Dex-free medium showed small numbers (< 5) of scattered glucagon- or insulin-immunopositive cells although no amylase expression was seen (**Fig. 7.3. (f)**), indicating an absence of exocrine differentiation. No CPS I$^+$ cells or GS-expressing cells were observed in these cultures

(**Fig. 7.3. (g)**). Isolated epithelia subjected to 1 μM Dex over 2-9d of culture also showed no staining for the liver markers CPS I, GS (**Fig. 7.3. (i)**) or transferrin (**Fig. 7.3. (j)**), suggesting that dexamethasone-induced conversion cannot occur in the absence of pancreatic mesenchyme. In the Dex-exposed epithelia as in control untreated epithelia, small numbers of insulin-immunopositive cells were observed and amylase expression was absent (**Fig. 7.3. (h)**). However, isolated epithelia exposed to Dex for 7 days showed markedly greater numbers of glucagon-expressing cells than epithelia cultured in Dex-free media. The glucagon-immunopositive cells in the Dex-treated epithelia were associated together in small aggregates or clusters (**Fig. 7.4.**), presumed to correspond to the cell "islands" identified initially (**Fig. 7.2. (d)**). The earliest differentiated cells to emerge during normal pancreas development are glucagon-expressing cells (Pictet and Rutter, 1972) and increased early differentiation of precursor epithelial cells would result in an excessive number of glucagon-positive cells (Apelqvist *et al.*, 1999; Jensen *et al.*, 2000b). Hence, a specific increase in the numbers of glucagon-expressing cells might suggest that dexamethasone promotes the expansion of a primitive endocrine precursor cell population. This Dex-driven increase in the numbers of glucagon$^+$ cells in isolated epithelial cultures was then partially quantified by further immunofluorescence analysis.

7.3.2.3. Dexamethasone-Stimulated Increase in the Number of Glucagon$^+$ Cells in Isolated Epithelia

Whilst the number of insulin-immunopositive cells was not appreciably increased in Dex-treated isolated epithelial cultures compared to untreated control epithelia (mean ± S.E. was 1.6 ± 1.04 cells and 0.5 ± 0.354 cells per culture respectively), the 10.2 ± 2.83 glucagon-immunopositive cells counted in each Dex-treated isolated epithelial culture was markedly higher than the 1.0 ± 0.707 cells control value (**Fig. 7.4.** and **Graph 7.1.**). The small numbers of cells were attributed in part to some detachment from the substrate with prolonged culture duration. Although the Dex-induced increase in the number of glucagon$^+$ cells was obvious, it could be argued that this figure is dependent upon the original volume of explanted epithelial tissue. Hence, the number of glucagon-immunopositive cells could be expressed as a proportion of the total number of epithelial cells. Expressing glucagon-labelling index as a proportion of DAPI-labelled cells fails to account for the presence of any mesenchyme that might conceivably contaminate the "isolated" epithelium. It was decided to determine the total

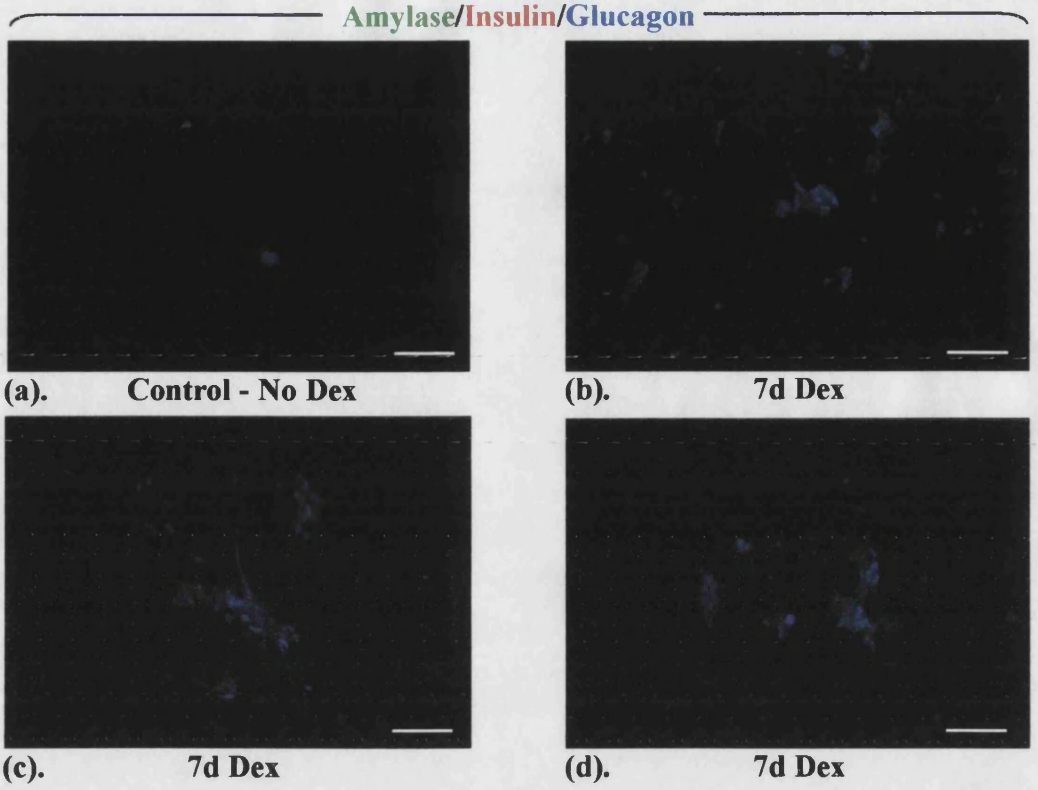

Immunofluorescence analysis for amylase, insulin and glucagon in 9d isolated epithelia cultured without (a) or with (b-d) 1 μM dexamethasone for 7d. Bar = 100 μm

Figure 7.4. and Graph 7.1. Dexamethasone Increases the Number of Glucagon$^+$ Cells in Isolated Epithelium

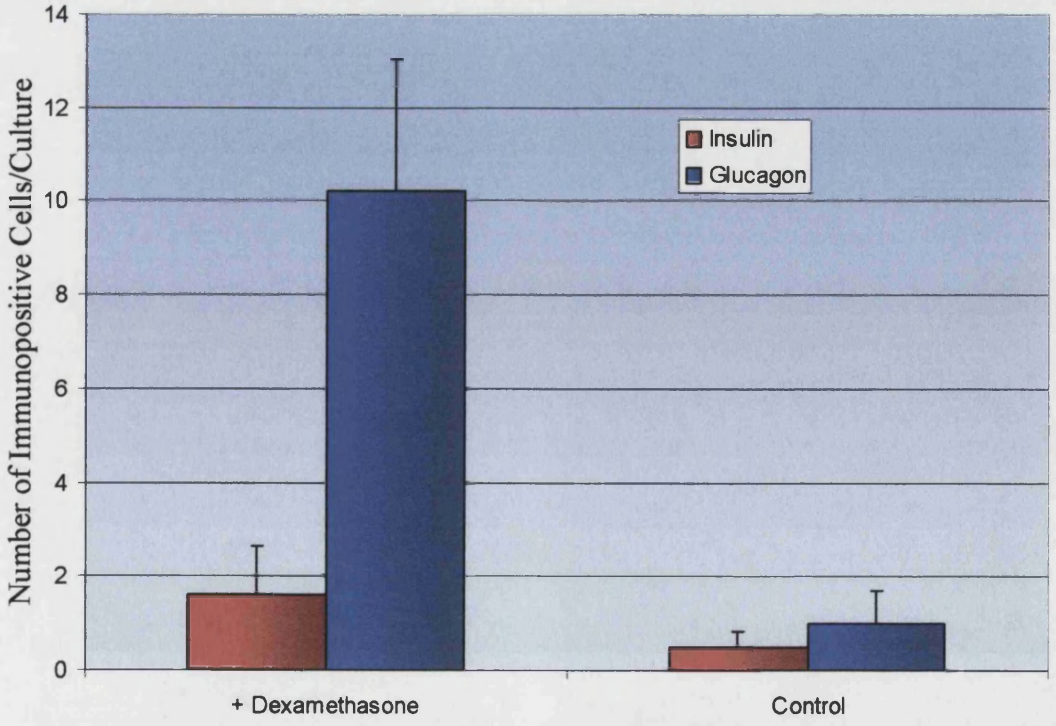

number of epithelial cells by staining for the epithelial marker pan-cytokeratin. Since the anti-pan-cytokeratin antibody used (Sigma C-2931) was raised in mouse as was the anti-glucagon antibody (Sigma G-2654) employed until this point, double immunofluorescence analysis for pan-cytokeratin and glucagon was attempted using one of two polyclonal antibodies raised in rabbit (DAKO A0565 and Abcam ab9379). However, the 1:1 acetone:methanol fixation of the cultured epithelium required for staining with the pan-cytokeratin antibody was not conducive to successful staining with either of the two anti-glucagon antisera. Due to time constraints, further staining attempts were deemed unnecessary.

Efforts were also made to characterise the glucagon$^+$ cell population expanded by dexamethasone treatment by staining for neurogenin3 (ngn3) as a marker of endocrine cell progenitors (Apelqvist *et al.*, 1999; Jensen *et al.*, 2000a; Schwitzgebel *et al.*, 2000). However, as reported in **Chapter 3**, despite repeated attempts, immunofluorescence cytochemistry using either of the two anti-ngn3 antibodies (mouse monoclonal, Transduction Laboratories N63520 and rabbit polyclonal, Abcam ab7560) proved to be unsuccessful, irrespective of fixation conditions, and inclusion of citrate buffer or ammonium chloride antigen retrieval and/or avidin-biotin signal amplification steps in the staining protocol.

7.3.2.4. Time-Course of Dexamethasone-Induced CPS I$^+$ Periportal-Like and GS$^+$ Perivenous-Like Hepatocytes

To determine the time-course and zonation of dexamethasone-induced CPS I$^+$ hepatocytes and GS$^+$ hepatocytes in intact pancreatic buds, expression of the two markers was examined in intact buds exposed to 1 μM dexamethasone for 3-9 days from 2d of culture onwards (**Fig. 7.5.**). The numbers of both CPS I$^+$ cells and GS$^+$ cells increased over 3-7 days of Dex treatment whereupon the abundance of cells expressing either of the two proteins appeared to plateau. At no time-point examined, did GS$^+$ cells outnumber cells expressing CPS I. CPS I and GS expression were seen to be clearly distinct in all cultures examined at all time-points. Colocalisation of the two proteins was never encountered in any of the cells in the cultures.

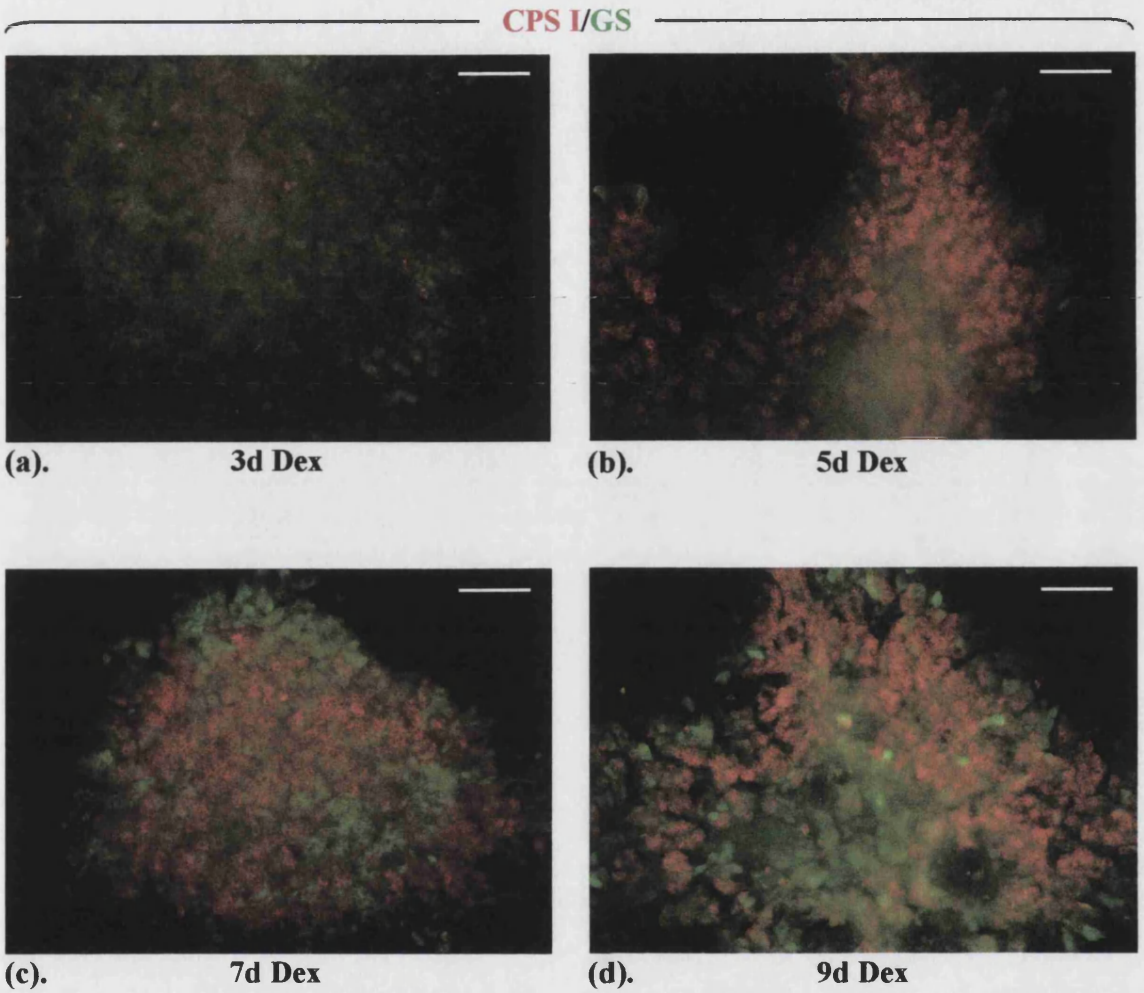

Figure 7.5. Numbers of CPS I$^+$ Hepatocytes and GS$^+$ Hepatocytes in Intact Pancreatic Buds Increase with Duration of Dexamethasone Exposure

Immunofluorescence analysis for CPS I and GS in 5-11d intact buds cultured with 1 μM dexamethasone from 2d of culture for 3 (a), 5 (b), 7 (c) or 9 (d) days

Bar = 100 μm

7.3.2.5. Can Either the CPS I$^+$ Hepatocyte or the GS$^+$ Hepatocyte Population be Induced in the Absence of the Other?

As dexamethasone-induced conversion had been shown not to occur with a *total* depletion of mesenchyme, attempts were made to examine induction of hepatocytes by staining for liver-specific proteins in an environment only *partially* deprived of mesenchyme or factors from it. It was proposed that in the absence of exocrine differentiation, Dex-induced conversion cannot proceed if hepatocytes arise directly from exocrine cells (Shen *et al.*, 2000). Therefore, an environment must be engineered in which only a limited amount of exocrine differentiation occurs to address the original aim of the study. To this end, epithelium and mesenchyme from the same dorsal pancreatic bud were segregated and co-cultured in the same dish at a separation of approximately 5 mm from one another. It has been shown that FGF can promote exocrine differentiation from isolated pancreatic epithelium (Horb and Slack, 2000; Miralles *et al.*, 1999). On the basis of this finding, isolated epithelium was cultured in the presence of FGF then exposed to Dex in an attempt to yield some exocrine cells which might then be induced to form hepatocytes. Such an outcome would also indirectly support the role of FGF10 in the development of the pancreas as Bhushan and coworkers (Bhushan *et al.*, 2001) suggest. In preliminary experiments, isolated epithelium was cultured with FGF1 also known as acidic (a)FGF as in the study by Horb and Slack (2000) in which 22 h exposure to 100 ng/ml FGF1 was shown to promote exocrine differentiation. FGF1 is capable of stimulating all known FGF receptors (Ornitz *et al.*, 1996) and should therefore be able to replicate the effect of any of the 22 known FGFs.

7.3.2.6. Mesenchyme Stimulates Epithelial Expression of Endocrine and Exocrine Markers

The co-cultures of segregated epithelium and mesenchyme displayed expression of amylase, insulin and glucagon when subjected to immunofluorescence analysis (**Fig. 7.6. (c)-(e)**). Approximately 40 % of cells expressed amylase whilst about 50 % and 10 % of cells were immunopositive for insulin and glucagon respectively. Consequently, the numbers of cells expressing each of the three proteins was substantially elevated compared with isolated epithelium (**Fig. 7.6. (b)**). In comparison with intact buds (**Fig. 7.6. (a)**), the proportion of cells staining for amylase was reduced although the

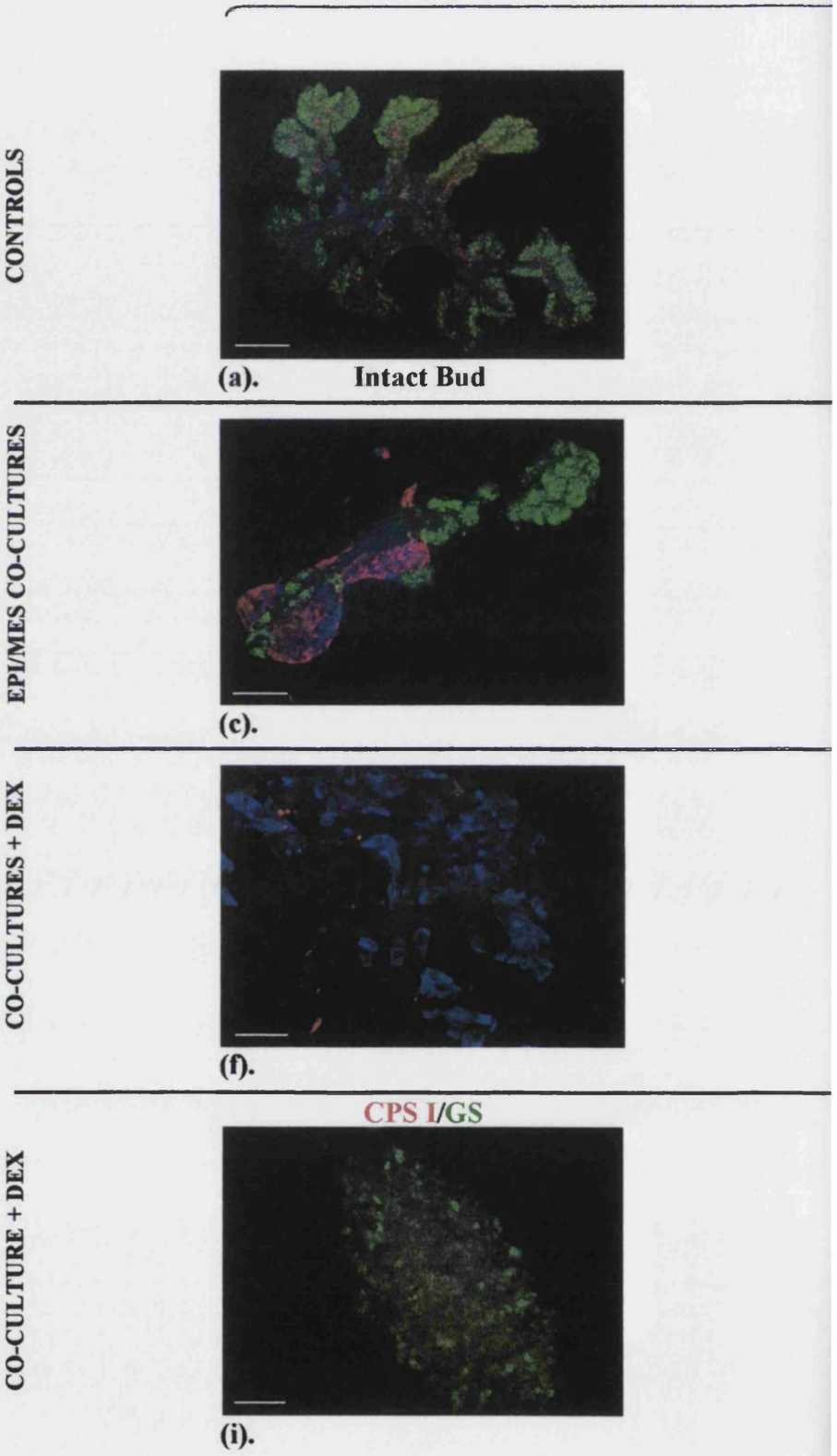

Figure 7.6. Mesenchyme Increases Exocrine but Suppresses Endocrine Differentiation

Amylase/Insulin/Glucagon

(b). Isolated Epithelium

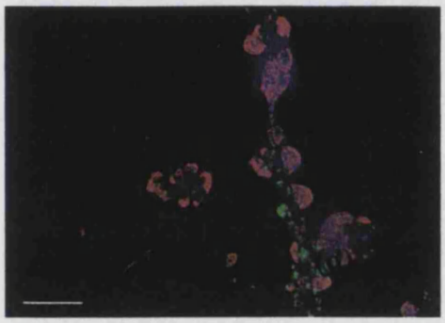

(d).

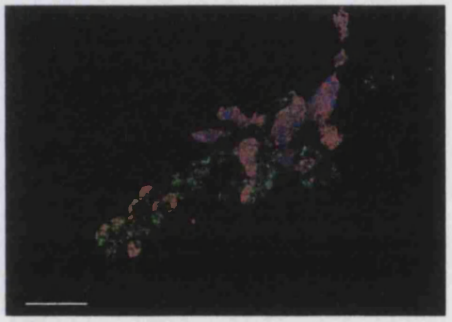

(e).

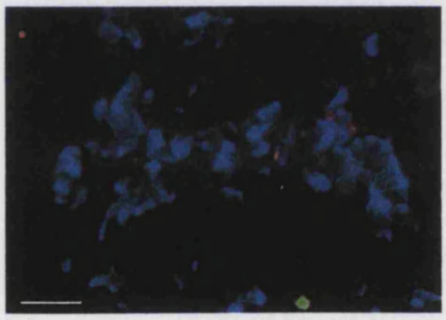

(g).

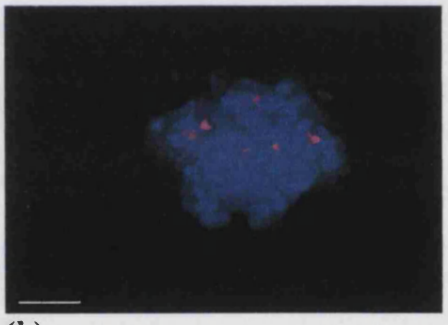

(h).

In the Presence of Mesenchyme, Dexamethasone Increases the Number of Glucagon$^+$ Cells at the Expense of Insulin$^+$ Cells and Induces Hepatic Conversion

Immunofluorescence analysis for amylase, insulin and glucagon in control intact bud (a) and isolated epithelium (b) and in co-cultured segregated epithelium and mesenchyme cultured without (c-e) or with (f-h) 1 μM dexamethasone. Immunofluorescence staining shows CPS I$^+$ hepatocytes and GS$^+$ hepatocytes in co-cultured epithelium and mesenchyme cultured for 3d with 1 μM dexamethasone (i). (a) and (d)-(e) Bar = 200 μm; (b)-(c) and (i) Bar = 100 μm; (f)-(h) Bar = 50 μm

percentages of both insulin$^+$ cells and glucagon$^+$ cells were notably higher. Furthermore, in three of four epithelium and mesenchyme co-cultures, islet-like clusters of insulin- and glucagon-immunopositive cells were much larger in size than those seen in intact bud cultures, and were also frequently interconnected. These observations suggest that low levels of mesenchyme promote both exocrine and endocrine differentiation of the pancreatic epithelium. Moreover, the apparent decrease in exocrine expression and elevation in endocrine expression in the co-cultures compared with intact buds indicates that abundant mesenchyme stimulates exocrine expression whilst suppressing endocrine differentiation to some extent.

7.3.2.7. Dexamethasone Increases the Number of Glucagon$^+$ Cells at the Expense of Insulin$^+$ Cells in Co-Cultures

Co-cultures of segregated epithelium and mesenchyme exposed to 1 μM Dex for 3-9d showed expression of amylase, insulin and glucagon (**Fig. 7.6. (f)-(h)**). Approximately 25 % of cells stained for amylase whilst about 15 % and 60 % of cells proved to be immunopositive for insulin and glucagon respectively. Interestingly, in the co-cultures dexamethasone exposure increased the number of glucagon-immunopositive cells as in isolated epithelial cultures, but at the expense of the insulin-immunopositive cell population. When co-cultures were subjected to immunofluorescence analysis for the hepatic enzymes CPS I and GS, six of seven cultures showed no cells immunopositive for either marker. However, in one co-culture treated for 3d with Dex, 19 cells stained for CPS I whilst a further 24 cells demonstrated GS expression (**Fig. 7.6. (i)**). As in Dex-treated intact cultures, no coexpression of the two enzymes was observed and the complementary CPS I and GS expression pattern was retained. Some exocrine cells were present in the co-cultures of segregated epithelium and mesenchyme and hepatic conversion *did* occur albeit infrequently in these co-cultures. To date though, no evidence had been generated to support the dissociation of induction of either the CPS I$^+$ periportal-like or GS$^+$ perivenous-like hepatocyte population from the other.

7.3.2.8. FGF1-Treated Isolated Epithelia

Isolated epithelium cultured for 3d in the presence of 100 ng/ml FGF1 showed no staining for amylase though demonstrated both insulin$^+$ cells and glucagon-

immunopositive cells (**Fig. 7.7. (b)**). The proportion of insulin$^+$ cells was comparable to that in control untreated isolated epithelial cultures (**Fig. 7.7. (a)**), although numbers of glucagon-immunopositive cells were greater than those in control epithelia. Neither CPS I$^+$ cells nor GS-immunopositive cells were seen in FGF1-exposed epithelia.

7.3.2.9. Dexamethasone Can Induce GS$^+$ Hepatocytes in the Absence of the CPS I$^+$ Hepatocyte Population

Isolated epithelium cultured for 2-6d in the presence of 100 ng/ml FGF1 or FGF10 and exposed to Dex for 3-7d showed similar patterns of staining for amylase, insulin and glucagon irrespective of the FGF employed (**Fig. 7.7. (c)-(f)**). Isolated epithelia exposed to both FGF and Dex showed similar proportions of insulin$^+$ cells and cells immunopositive for glucagon as isolated epithelia exposed to FGF1 (**Fig. 7.7. (b)**). Those epithelia subjected to Dex in addition to FGF however, showed expression of amylase (notably **Fig. 7.7. (e)**) which was absent from FGF1-treated epithelia not exposed to the dexamethasone. This implied the presence of exocrine cells in the Dex- and FGF-treated epithelia. Three of seven isolated epithelia cultured with Dex and FGF1 also contained cells expressing GS (**Fig. 7.7. (g)-(h)**) although in none of these cultures were CPS I$^+$ hepatocytes also induced. Staining for GS showed that hepatic conversion can be induced in FGF-treated isolated epithelia but moreover demonstrated conclusively that CPS I$^+$ hepatocytes need not be induced to initiate induction of the GS-expressing population and that induction of the two hepatocyte populations occurs independently of one another. In two of the eight negative controls for FGF treatment in which isolated epithelia were exposed to Dex only for 3d, some GS$^+$ cells were also observed (**Fig. 7.7. (i)-(j)**) although again, CPS I-immunopositive cells were absent. This again demonstrated the dissociation of the induction of GS$^+$ hepatocytes from that of the CPS I$^+$ population. The reason for such hepatic conversion being observed was however, unclear since no liver markers were detected in previous experiments.

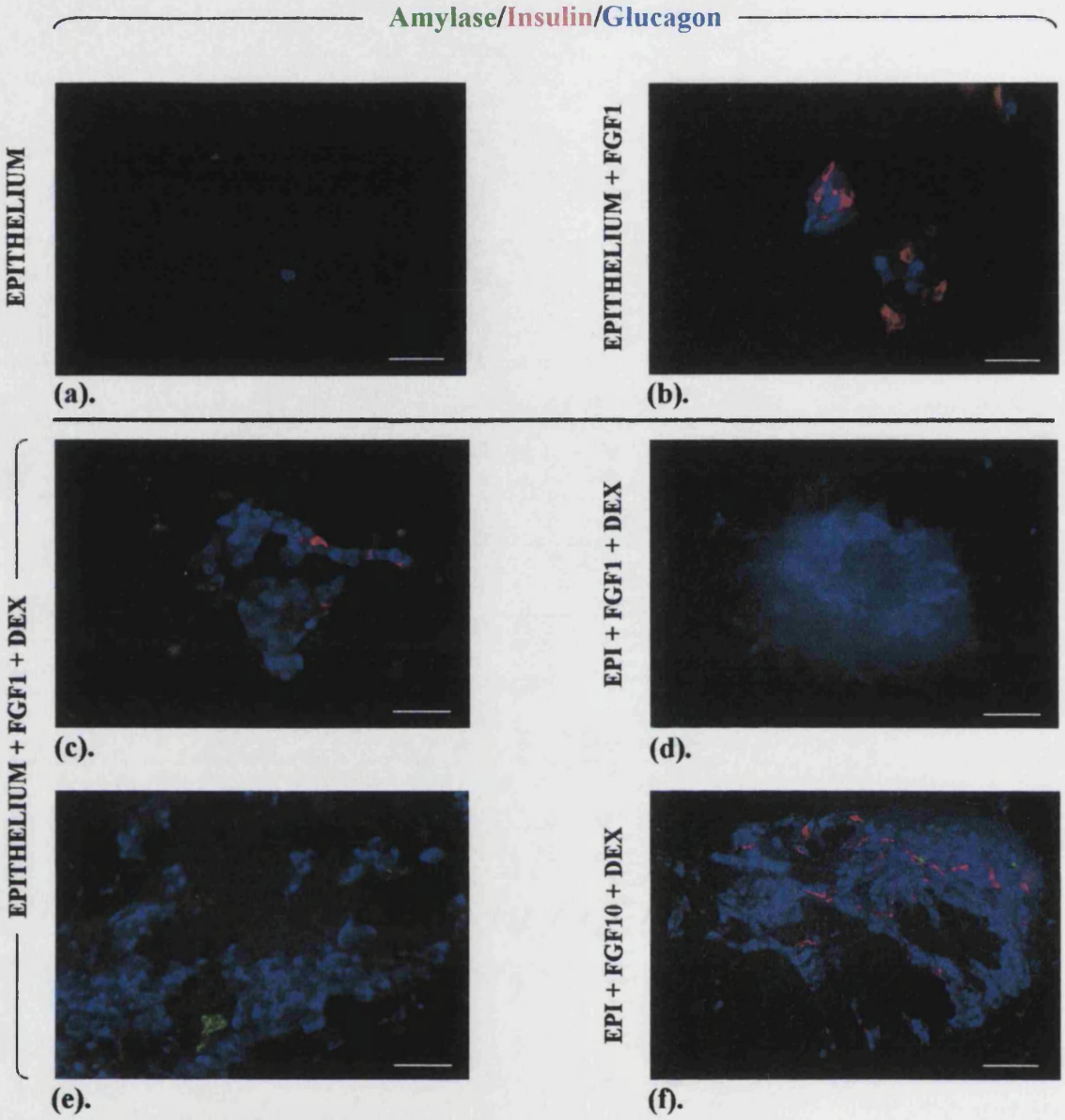

Figure 7.7. FGF1 Increases the Number of Glucagon$^+$ Cells in Isolated Epithelium

The Proportion of Amylase-Staining Cells in Dexamethasone- and FGF-Treated Isolated Epithelia is Greater than that in Epithelia Exposed Only to FGF (This Page). Dexamethasone Induces Hepatic Conversion in FGF1- or FGF10-Treated Isolated Epithelia in which GS$^+$ Hepatocytes are Induced in the Absence of CPS I$^+$ Hepatocytes (Facing Page). Hepatic Conversion in Dexamethasone-Treated Isolated Epithelia Controls is Believed to be a Consequence of Mesenchymal Contamination

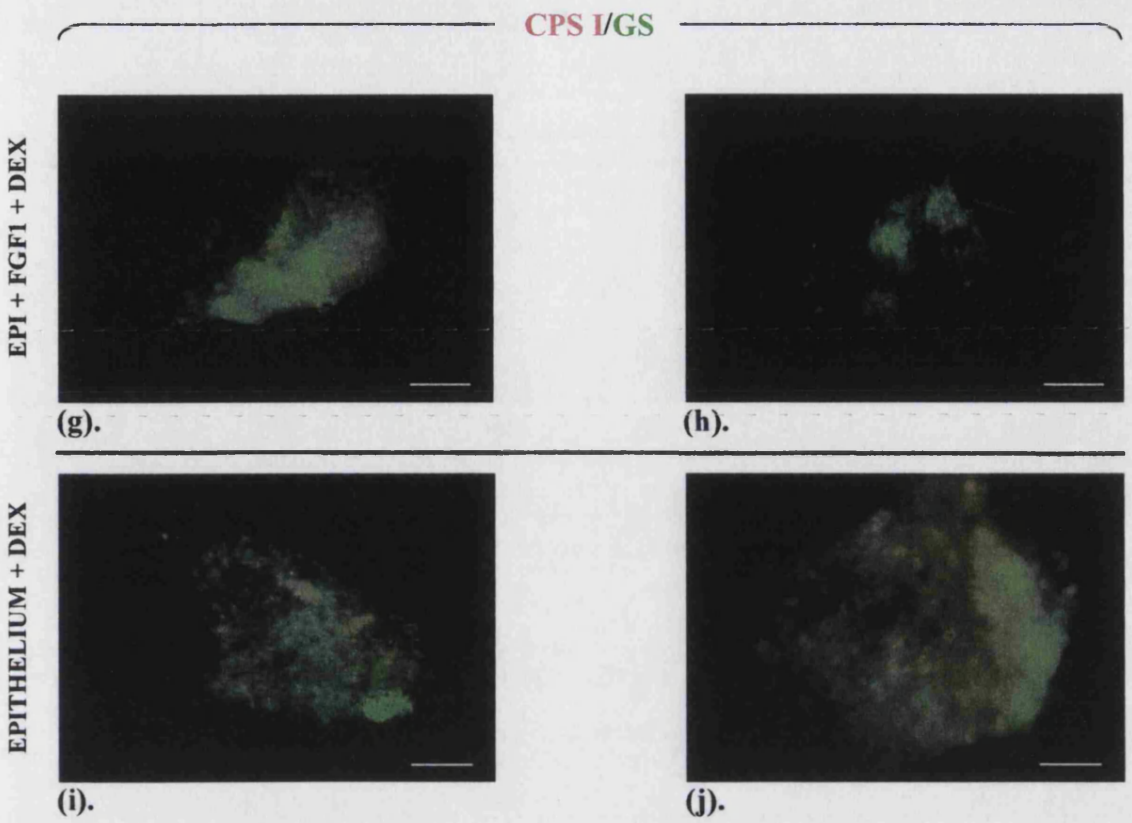

Immunofluorescence analysis for amylase, insulin and glucagon in control epithelia cultured without (a) or with (b) 100 ng/ml FGF1 for 3d and in epithelia cultured with 1 μM dexamethasone and either 100 ng/ml FGF1 (c-e) or 100 ng/ml FGF10 (f) (facing page)

Immunofluorescence analysis shows staining for GS but not CPS I in epithelia cultured with 1 μM dexamethasone and 100 ng/ml FGF1 for 3d (g-h) or control epithelia cultured with only 1 μM dexamethasone for 3d (i-j) (this page)

(a) and (f)-(i) Bar = 100 μm; (b)-(e) and (j) Bar = 50 μm

7.4. Discussion

7.4.1. Independence of GS^+ Hepatocyte and CPS I^+ Hepatocyte Induction in Dexamethasone-Induced Hepatic Conversion

The original aim of this study was to address the questions: (1) Does hepatic transdifferentiation of dexamethasone-treated pancreatic buds still occur in the absence of mesenchyme? (2) If transdifferentiation *does* occur, is the GS^+ hepatocyte population induced, and if not, does induction of CPS I-expressing hepatocytes still occur in their absence? In investigating the role of epithelial-mesenchymal interactions in dexamethasone-induction of CPS I^+ hepatocyte and GS^+ hepatocyte populations, a number of interesting findings were made regarding the influence of the mesenchyme and the effects of dexamethasone in exocrine and endocrine differentiation.

In intact pancreatic buds, the numbers of both CPS I^+ hepatocytes and GS^+ hepatocytes induced by exposure to 1 μM dexamethasone increased over 3-7 days of Dex treatment whereupon the abundance of the cells expressing either protein attained a plateau. CPS I and GS expression was always clearly distinct in all cultures examined at all time-points. Colocalisation of the two proteins was never encountered *in vitro*. Hence, the complementary fashion of CPS I and GS expression *in vitro* mirrors the mutually exclusive complementary expression pattern of CPS I and GS within the mammalian liver *in situ* (Bartels *et al.*, 1989; Moorman *et al.*, 1988, 1990). The finding from the current study is also consistent with the complementary GS and CPS I expression observed *in vitro* in hepatocytes induced from pancreatic AR42J-B13 cells by treatment with dexamethasone (Tosh *et al.*, 2002). GS was found to be expressed first after 3d of Dex treatment and then CPS I appeared after around 5d of dexamethasone exposure (Tosh *et al.*, 2002). However, the mutual exclusivity of CPS I and GS expression observed in the pancreatic hepatocytes induced *in vitro* in this study (Tosh *et al.*, 2002) and the current study is inconsistent with the coexpression of the two enzymes in hepatocytes in the pancreata of rats fed a copper-depleted diet (Yeldandi *et al.*, 1990). The concomitant expression of GS and CPS I genes in pancreatic hepatocytes *in vivo* was attributed in part to the absence of a portal blood supply to the pancreas (the portal vein does not drain into the pancreas) resulting in a lack of hormonal or metabolic gradients and also to the possible cell matrix homogeneity in the pancreas (Yeldandi *et al.*, 1990). It is clear from the present study however that such factors cannot solely be responsible for GS and CPS I coexpression in pancreatic

hepatocytes *in situ*. In the *in vitro* cultures of AR42J-B13 cells and pancreatic buds it is unlikely that there are any local gradients existing across the cultures to mimic a portal blood supply. The observations from the present study and those of Tosh *et al.* (2002) that the complementary pattern of GS and CPS I expression is retained in cultured pancreatic hepatocytes, suggest that the normal liver zonation need not be maintained by continued environmental variations such as differences in the composition of extracellular matrix within the acinus (Kuo *et al.*, 1988) and the presence of factors associated with central veins (Shiojiri *et al.*, 1997). Instead, once established, the periportal and perivenous hepatocytes represent two relatively stable subtypes of hepatocyte (Tosh *et al.*, 2002).

In order to answer the questions posed at the outset, isolated epithelia were exposed to dexamethasone but as a consequence of the lack of hepatic conversion in a totally mesenchyme-deficient environment, Dex-treated epithelia could not be employed to address these questions. In order to provoke some exocrine differentiation, isolated epithelia were exposed to FGF or co-cultured with mesenchyme. Co-cultures subjected to dexamethasone treatment however, were found to contain both CPS I^+ hepatocytes and GS-expressing hepatocytes. Three of seven isolated epithelia cultured with Dex and FGF1 displayed GS-immunopositive cells although in none of these cultures were CPS I^+ hepatocytes induced. Furthermore, in two of the eight negative controls for FGF treatment in which isolated epithelia were exposed only to Dex, GS-expressing cells were again observed in the absence of CPS I-immunopositive hepatocytes. The hepatic conversion in these control cultures was assumed to be a consequence of the presence of some contaminating mesenchyme. The five cultures showing only GS^+ cells demonstrated quite strikingly that in dexamethasone-induced hepatic conversion of pancreas *in vitro*, CPS I^+ hepatocytes need not be induced for the GS^+ hepatocyte population to be induced and that induction of the two populations occurs independently of one another. In none of the cultures examined were CPS I^+ hepatocytes ever induced in the absence of GS-expressing hepatocytes.

The results from the current study show that a model in which the induction of either GS^+ perivenous hepatocytes or CPS I^+ periportal hepatocytes induces the formation of the other hepatocyte population cannot be supported. It might be assumed from the evidence presented here that the inductive signal is mesenchymal in origin and can be mimicked by FGF. Furthermore, the induction of GS^+ hepatocytes would appear to be initiated at a lower threshold of the inducing signal than CPS I^+ cell induction since the CPS I^+ hepatocytes were never found in isolation from GS^+ cells. Dissociation

of induction of the two hepatocyte populations was only observed when the presumptive inductive signal was suppressed to a low level.

7.4.2. Hepatic Conversion Cannot Occur in the Absence of Exocrine Cells

Whole pancreatic buds exposed to 1 μM Dex for 7 days from 2d of culture retained a high proportion of amylase-staining cells throughout the explant. Hepatocytes were induced by treatment with dexamethasone, as judged from expression of the liver-specific proteins transferrin, CPS I and GS. In the present study cultures were not simultaneously stained for amylase and either transferrin, CPS I or GS so it could not be ascertained whether cells expressing a liver marker also expressed the exocrine product amylase. Shen *et al.* (2000) found that in dexamethasone-treated intact pancreatic bud cultures, albumin expression was often found in cells negative for amylase, or the two proteins were often coexpressed. This was in contrast to their finding that in AR42J-B13 cells, amylase was lost from all cells that had reached the stage of albumin expression. It is known that glucocorticoids can increase the expression of amylase in pancreatic (AR42J) cells (Logsdon *et al.*, 1985). The persistence of amylase expression in cells expressing liver markers may represent a partial hepatic conversion. It is possible that cells coexpressing amylase and a liver protein(s) lose their amylase expression with prolonged culture in the presence of dexamethasone as do the AR42J-B13 cells.

Unlike Dex-treated intact pancreatic buds, epithelia denuded of their mesenchyme and similarly subjected to 1 μM Dex over 2-9d of culture showed no cells expressing any of the three liver markers stained for. When denuded epithelium was co-cultured with pancreatic mesenchyme however, both CPS I^+ hepatocytes and GS^+ hepatocytes were observed. These findings suggest that dexamethasone-induced hepatic conversion cannot occur in the absence of pancreatic mesenchyme. Isolated epithelial cultures failed to stain for the exocrine marker amylase. This is consistent with the suggestion that mesenchyme promotes exocrine differentiation (Gittes *et al.*, 1996; Miralles *et al.*, 1998b). Shen *et al.* (2000) showed that in the hepatic conversion of the AR42J-B13 cell line, some hepatocytes arose directly from the differentiated exocrine-like cells, with no intervening cell division. Although this does not exclude the generation of hepatocytes from stem cells or other types of progenitor cell, exocrine cells are the precursor cells for hepatocyte production for a proportion of hepatocytes.

Whilst isolated epithelia did not express amylase, culturing the denuded epithelium with mesenchyme yielded amylase expression in approximately 40 % of the cultured cells. As mentioned above, in three of seven isolated epithelia cultured with Dex and FGF1, cells immunopositive for the liver marker GS were induced, suggesting that hepatic conversion had occurred. In such cultures, amylase$^+$ cells were frequently detected, consistent with FGF-driven promotion of exocrine differentiation from isolated pancreatic epithelium (Horb and Slack, 2000; Miralles *et al.*, 1999). It is also possible however that in the cultures exposed to both FGF1 and Dex, dexamethasone induced an increase in amylase expression. The findings from the experiments are consistent with the induction of hepatocytes only in the presence of exocrine cells.

7.4.3. Requirement of Mesenchyme for Differentiation of the Pancreatic Epithelium

7.4.3.1. Mesenchymal Factor(s) Promote Pancreatic Differentiation

In the present study, it was demonstrated that pancreatic epithelia deprived of their mesenchyme fail to undergo the typical morphogenetic behaviours of developing intact pancreatic buds *in vitro*. Isolated epithelia showed no branching morphogenesis throughout an 8-day culture period. For 40 years it has been known that inductive signals originating in the mesenchyme play an essential role in the development of the pancreatic epithelium. Classic studies by Golosow and Grobstein (1962) and Wessels and Cohen (1967) used recombined embryonic tissues to show that pancreatic buds could develop *in vitro*, but that isolated epithelium would not undergo any growth or morphogenesis in the absence of mesenchyme. In the study by Golosow and Grobstein (1962), salivary mesenchyme was shown to be even more effective than pancreatic mesenchyme in promoting growth and differentiation of the mouse pancreatic epithelium *in vitro*. As the effects of mesenchyme could be exerted across a Millipore filter, it was suggested that the mesenchyme secreted a soluble growth factor required by the epithelium (Golosow and Grobstein, 1962). In some circumstances, the mesenchyme could be substituted by a chick embryo extract, the necessary factor being trypsin-sensitive (Rutter *et al.*, 1964). Although the mitogen from chick embryos was partially purified (Ronzio and Rutter, 1973), the identity of the "mesenchymal factor" remains elusive, partly because it may in fact comprise multiple substances.

In the present study, isolated pancreatic epithelia cultured for 9d in Dex-free medium showed small numbers of glucagon$^+$ cells and insulin-immunopositive cells

although no amylase-expressing cells were seen, indicating an absence of exocrine differentiation. However, culturing denuded epithelium in the presence of mesenchyme rescued exocrine development: in co-cultures of epithelium and mesenchyme approximately 40 % of cells expressed amylase. The proportion of amylase$^+$ cells in denuded epithelium cultured with mesenchyme was however, lower than that seen in intact pancreatic buds which are supported by a greater amount of mesenchyme. It is envisaged that the epithelium in such co-cultures receives markedly fewer inductive signals than does that in intact buds owing to the massively greater distance of separation between epithelium and mesenchyme in co-cultures. In the current study it was also found that proportions of insulin$^+$ cells and glucagon$^+$ cells in co-cultures of epithelium and mesenchyme were much higher than in intact pancreatic buds: in co-cultures approximately 50 % and 10 % of cells were insulin- and glucagon-immunopositive respectively. Furthermore, islet-like clusters of insulin$^+$ cells and glucagon$^+$ cells in denuded epithelium cultured with mesenchyme were much larger in size than those seen in intact bud cultures. Taken together, these results are consistent with work suggesting that the default state of the pancreatic epithelium is to form islets, and mesenchyme provides an instructive signal for differentiation of exocrine cells (Gittes *et al.*, 1996; Miralles *et al.*, 1998b). Mesenchyme acts quantitatively as a repressor of endocrine tissue development (Miralles *et al.*, 1998b). It had been hypothesised that the pancreatic epithelium produces factors such as activins or bone morphogenetic proteins (BMPs) which act on epithelial cells in an autocrine manner to promote endocrine differentiation (Furukawa *et al.*, 1995; Lyons *et al.*, 1995; Ritvos *et al.*, 1995). This was subsequently confirmed when exogenous application of the activin inhibitor follistatin (Nakamura *et al.*, 1990) was shown to promote amylase expression whilst repressing insulin expression and thus mimics the effects of the mesenchyme (Miralles *et al.*, 1998b).

7.4.3.2. Promotion of Exocrine Differentiation by FGF?

One candidate for the "mesenchymal factor" mentioned above is FGF. FGF1, FGF7 and FGF10 are all expressed in the pancreas during development and have been shown to be capable of activating epithelial cell proliferation in isolated pancreatic epithelium *in vitro* (Bhushan *et al.*, 2001; Mason *et al.*, 1994; Miralles *et al.*, 1999). These three FGFs bind to a specific receptor, FGFR2IIIb which is known to be expressed in the fetal pancreatic epithelium (Finch *et al.*, 1995; Orr-Urtreger *et al.*,

1993). Culturing intact pancreatic buds in the presence of a dominant negative form of the FGFR2b receptor has the effect of reducing cell proliferation (Miralles *et al.*, 1999). It has been shown that FGF can promote exocrine differentiation from isolated pancreatic epithelium (Horb and Slack, 2000; Miralles *et al.*, 1999). On account of these findings, isolated epithelium was cultured with FGF in an attempt to promote differentiation of exocrine cells which might then be induced to form hepatocytes by dexamethasone. It was envisaged that hepatocyte production in such circumstances would indirectly support the exocrine promoting effects of FGF (Horb and Slack, 2000; Miralles *et al.*, 1999). However, the results of the immunofluorescence analysis were somewhat inconclusive. Isolated epithelia were cultured in the presence of 100 ng/ml FGF1 which is capable of stimulating all known FGF receptors (Ornitz *et al.*, 1996) and should therefore be able to replicate the effect of any of the 22 known FGFs. Denuded epithelia cultured for 3d under such conditions showed no cells staining for amylase though demonstrated both insulin$^+$ cells and glucagon$^+$ cells. No effect of FGF on exocrine differentiation was therefore observed in these cultures. Neither CPS I$^+$ hepatocytes nor GS$^+$ hepatocytes were seen in FGF1-exposed epithelia, demonstrating that the FGF1 alone was not capable of inducing hepatic conversion. Consistent with the ability of FGF1 to mimic the effects of FGF10, isolated epithelia cultured for 2-6d with 100 ng/ml FGF1 or FGF10 and exposed to Dex for 3-7d showed similar patterns of staining for amylase, insulin and glucagon. Denuded epithelia subjected to Dex in addition to FGF showed expression of the exocrine pancreatic marker amylase which was absent from the FGF1-treated epithelia cultured in Dex-free medium. Three of the seven Dex- and FGF1-treated epithelia also displayed staining for GS indicating the induction of hepatic conversion. These findings would suggest that exocrine cells *are* present within the FGF- and Dex-treated isolated epithelia. However, it could not be determined with certainty whether amylase expression in these cultures was a consequence of exposure to FGF or Dex. Although the observations are consistent with FGF-driven promotion of exocrine differentiation it is equally if not more plausible that the Dex stimulated an increase in amylase expression, especially since the isolated epithelial cultures exposed only to FGF1 showed no amylase expression. The latter hypothesis is consistent with the observation that glucocorticoids can increase the expression of amylase in pancreatic (AR42J) cells (Logsdon *et al.*, 1985).

7.4.4. FGF1-Induced Expansion of Glucagon$^+$ Cells

It was shown in the current study that in isolated epithelia subjected to FGF1 for 3d, whilst the proportion of insulin$^+$ cells was comparable to that in control untreated epithelia, numbers of glucagon$^+$ cells were substantially greater in the FGF1-treated epithelia. This finding suggests that FGF1 stimulates some endocrine differentiation. Although the study of Horb and Slack (2000) found no evidence for an effect of FGF1 treatment on insulin expression in isolated epithelia, glucagon expression was not examined. The earliest differentiated cells to emerge during normal pancreas development are glucagon-expressing cells (Pictet and Rutter, 1972) and increased early differentiation of precursor epithelial cells would result in an excessive number of glucagon-positive cells (Apelqvist *et al.*, 1999; Jensen *et al.*, 2000b). Hence the FGF1-stimulated increase in the number of glucagon-expressing cells is concordant with FGF1 promoting the expansion of a primitive pancreatic precursor cell population. It has been demonstrated that FGF10 signalling regulates the size of the Pdx1-expressing epithelial progenitor cell population during early pancreatic organogenesis (Bhushan *et al.*, 2001). Mutant mice in which *Fgf10* had been inactivated showed significantly fewer Pdx1$^+$ pancreatic cells compared to wild-type littermates. This was taken to show that although the specification of Pdx1$^+$ cells occurs in the absence of *Fgf10*, the maintenance and expansion of the Pdx1$^+$ progenitor cell population is dependent upon FGF10 signalling from the mesenchyme (Bhushan *et al.*, 2001). More recently, it has been shown that culturing the pancreatic epithelium for 7d in the presence of FGF7 represses endocrine differentiation whilst an undifferentiated endocrine progenitor cell population is expanded (Cras-Méneur *et al.*, 2001; Elghazi *et al.*, 2002). Interestingly, FGFR1-IIIb transcripts have been shown to be enriched in pancreatic epithelia cultured with FGF7 or epidermal growth factor (EGF) when compared with untreated epithelia, suggesting that FGFR1-IIIb represents a marker for pancreatic progenitor cells (Cras-Méneur and Scharfmann, 2002). The fact that FGF1 is able to stimulate all known FGF receptors (Ornitz *et al.*, 1996) and therefore mimic the effects of all known 22 FGFs permits speculation that the FGF1 used in the current study similarly promoted the expansion of a pancreatic precursor cell population. Further work is needed to characterise these glucagon-expressing cells by immunostaining for markers of endocrine progenitor cells, notably Isl1 and ngn3 (Apelqvist *et al.*, 1999; Jensen *et al.*, 2000a; Schwitzgebel *et al.*, 2000).

7.4.5. Dexamethasone-Induced Expansion of Glucagon$^+$ Cells

Similarly to the above, isolated epithelia exposed to dexamethasone for 7d showed substantially greater numbers of glucagon$^+$ cells than control epithelia cultured in Dex-free media. Whilst the number of insulin-immunopositive cells was not appreciably increased by Dex exposure, the 10.2 ± 2.83 glucagon-immunopositive cells counted in each Dex-treated epithelial culture was markedly higher than the 1.0 ± 0.707 cells control value. One of the reasons for these cell numbers being quite low was the detachment of epithelial cells from the fibronectin substrate. Isolated epithelia initially attached to the substrate rapidly and formed a monolayer showing that cell adhesion of epithelial cells was not detrimentally affected by the absence of mesenchyme. However, with prolonged culture periods (> 7d), cell detachment occurred increasingly so that culture duration and treatment times were reduced in subsequent experiments to minimise cell loss from coverslips.

In addition to the increased number of glucagon$^+$ cells, such cells in the Dex-treated epithelia were aggregated together into islet-like cell clusters which most probably corresponded to the cell "islands" observed under brightfield magnification. Additionally, dexamethasone exposure was also seen to selectively increase the number of glucagon-immunopositive cells in co-cultures of epithelium and mesenchyme, but at the expense of the insulin-immunopositive cell population. The observed increase in the numbers of glucagon-expressing cells suggests that dexamethasone, like FGF1, promotes expansion of a primitive endocrine precursor cell population. Efforts were made to characterise the glucagon-expressing cells by staining for ngn3 as a marker of endocrine cell progenitors (Apelqvist *et al.*, 1999; Jensen *et al.*, 2000a; Schwitzgebel *et al.*, 2000). However, despite repeated attempts, immunofluorescence cytochemistry for ngn3 proved to be unsuccessful. Therefore, the precise identity of this epithelial cell population expanded by dexamethasone treatment proves elusive until further attempts to characterise these cells prove fruitful. Another unresolved question is whether the expanded glucagon$^+$ cell population and the few insulin-immunopositive cells account for *all* of the cells within the isolated epithelia exposed to Dex treatment. It is for example, conceivable that pancreatic duct cells might occur within such cultures. The current results also do not exclude any effects of Dex on the δ- and PP-cell populations.

7.4.6. Summary

In the current study, the relationship between the induction of two hepatocyte populations expressing either of two hepatic enzymes during dexamethasone-induced hepatic conversion of the pancreas was investigated by subjecting the pancreatic epithelium to a mesenchyme-deficient environment *in vitro*. Using this approach it was demonstrated quite conclusively that Dex-induction of the glutamine synthetase$^+$ hepatocyte and carbamoylphosphate synthetase I$^+$ hepatocyte populations is independent of the other by showing that the GS$^+$ perivenous-like hepatocytes can be induced in the absence of the CPS I$^+$ periportal-like hepatocyte population. Moreover, it was demonstrated that hepatic conversion cannot occur in the absence of exocrine cells, consistent with the finding that some hepatocytes arise from differentiated exocrine cells without cell division (Shen *et al.*, 2000). By manipulating the ratio of mesenchyme to epithelium it was shown that pancreatic epithelium denuded of its mesenchyme will form endocrine tissue whilst the mesenchyme provides an instructive signal for differentiation of exocrine cells as previously reported (Gittes *et al.*, 1996; Miralles *et al.*, 1998b). Furthermore, it was discovered that dexamethasone enhances the number of glucagon$^+$ cells in pancreatic epithelium deprived either completely or partially of mesenchyme, consistent with dexamethasone-induced expansion of a primitive endocrine precursor cell population. Further work is needed to characterise this population of cells to prove an endocrine progenitor role. This finding might be employed to amplify pancreatic cells *in vivo* or *in vitro* to develop therapeutic approaches to manage type 1 and type 2 diabetes.

8. Appendices

8.1. Generation of IGF-II Transgenic Lines by Dr. Bill Bennett (Chapter 6): Methodology Written by Dr. Bill Bennett

8.1.1. Elijah: Rat Elastase I Promoter-Igf2 Construct

Plasmid pEGH3 (Ornitz *et al.*, 1985) was a kind gift of Dr. G. H. Swift and contains a 213 bp promoter region (spanning positions -205 to +8 relative to start of transcription) of the rat elastase I gene coupled with human growth hormone (hGH). This promoter fragment is flanked by unique SalI and BamHI sites at the 5' and 3' ends respectively. A XhoI site was added to the 3' end by digestion of pEGH3 with BamHI and ligation of a linker containing the XhoI site which also reconstituted the BamHI site. The resulting plasmid was digested with SalI and XhoI to release a 223 bp fragment containing the elastase promoter.

p99a:5 consists of a pUC19 plasmid backbone with an insert comprising the coding region of the mouse Igf2 gene, corresponding to the last three exons of the gene: exons 4, 5 and 6, the latter including transcription termination and polyA signals endogenous to *Igf2*, as described previously (Ward *et al.*, 1994). The Igf2 coding region was a ~3.5 kb KpnI (partial digest) fragment from a cosmid containing Igf2 genomic sequence. There is a unique SalI site immediately upstream of the Igf2 coding region, and p99a:5 was digested with SalI and the elastase promoter Sal-Xho fragment inserted. The resultant construct, designated pEIP-IGF2, was checked for correct orientation by restriction mapping and partial sequencing at each end. Bulk DNA was prepared using the Endofree Maxiprep kit (Qiagen) according to the manufacturer's instructions. The final pellet was redissolved in endotoxin-free TE and checked for purity by A280/260 spectrophotometry and gel electrophoresis.

Construct DNA was prepared for injection by digesting 150 μg pEIP-IGF2 with 20 U SalI and 30 U EcoRI overnight and then running the digest out on a preparative agarose gel. The 5.4 kb construct band was excised from the gel and purified using a QiaEx gel extraction kit (Qiagen) according to the manufacturer's instructions. The extracted construct DNA was dialysed for 3 days at 4°C into injection buffer (10 mM Tris.HCl, 0.1 mM EDTA, pH 7.4) with several changes of buffer. The DNA was quantified by spectrophotometry and gel electrophoresis and diluted to a final

concentration of 1-2 ng/μl in injection buffer, then particles removed by passing through endotoxin-free 0.2 μm spin filters (Costar).

8.1.2. Ripley: Rat Insulin I Promoter-Igf2 Construct

The Rip1-DipA plasmid (Palmiter *et al.*, 1987) was obtained from Dr. D. Tosh and consisted of the rat insulin I gene promoter region (spanning positions -205 to +8 relative to start of transcription) coupled with the diphtheria A toxin coding region.

The rat insulin I (RIP) promoter region was subcloned into BlueScript KS+ by cutting Rip1-DipA with XbaI and BamHI to release a 700 bp fragment containing the promoter. This was gel purified and ligated into BlueScript KS+ previously digested with XbaI and BamHI, to give plasmid RIP-BSKS+. In order to add a unique XhoI site to the 5' end of the subcloned promoter fragment, a PCR primer was designed with 17 bp homology to the Bluescript polylinker region immediately upstream of the insert, but with an additional non-homologous 9nt added on 5' to this containing a XhoI site and 3 flanking nucleotides (to give efficient restriction). This XHOI-127 primer (5'-GCGCCTCGAGTGGCGGCCGCTCTAGA-3') was used in combination with a standard Bluescript KS sequencing primer to amplify a 735 bp fragment from plasmid RIP-BSKS+ containing the promoter fragment flanked by unique XhoI and SalI sites at the 5' and 3' ends respectively.

100 ng of plasmid RIP-BSKS+ was added to a 50 μl PCR reaction containing 75 mM Tris.HCl, pH 9.0, 20 mM $(NH_4)SO_4$, 0.01 % Tween-20, 3 mM $MgCl_2$, 250 μM dNTPs, 2 U *Taq* polymerase and 150 nM of each primer. 36 reaction cycles were carried out, each consisting of 60 sec denaturation at 95°C, 60 sec annealing at 60°C and 60 sec extension at 72°C. After final extension for 10 min at 72°C, the PCR product was purified away from the reaction mixture and unincorporated nucleotide using a QiaEx spin column (Qiagen) according to the manufacturer's instructions. The PCR product was then subcloned into pGEM-T to give plasmid pGEM-RIP.

An NheI site was added to the 3' end of the Igf2 coding region by cutting the plasmid p99a:5 at the unique EcoRI site and ligating in a linker containing the NheI site which also reconstituted the EcoRI site. This gave plasmid p99-Nhe. This plasmid was then linearised by digestion with SalI, which cuts directly upstream of the Igf2 coding region, and the ends phosphatased to prevent re-ligation. pGEM-RIP was digested with XhoI and SalI to release the 720 bp RIP fragment. This was gel purified and ligated into

linearised p99-Nhe to give the final construct plasmid pRIP-IGF2. With the promoter inserted in the correct orientation, this contains the transgene construct flanked by unique SalI and NheI sites.

pRIP-IGF2 was checked by restriction mapping and partial sequencing, then a bulk prep was prepared as described above using the Endofree Maxiprep kit. Approximately 50 μg plasmid was digested overnight with 20 U SalI and 15 U NheI then the 5.9 kb transgene construct fragment was gel purified, dialysed and diluted into injection buffer as before.

8.1.3. Construct Microinjection

F_1 (C57BL/6×CBA) females were super-ovulated at PN4-6wk by intra-peritoneal (i.p.) administration of 5 IU Folligon (PMSG or pregnant mare serum gonadotrophin; Intervet Ltd.) mid-afternoon followed by 5 IU Chorulon i.p. (hCG or human chorionic gonadotrophin; Intervet Ltd.) 48 h later. Females were then immediately paired with stud F_1 (C57BL/6×CBA) males, then on the following morning were checked for plugs to ensure that mating had occurred and if so, were sacrificed by cervical dislocation, and fertilised eggs harvested from the dissected ampullae into M2 medium. The egg clutch was treated with hyaluronidase to remove the cumulus cells, and embryos transferred into KSOM medium in a 37°C, 5 % CO_2 incubator.

Single cell embryos with visible pro-nuclei were injected with transgene construct DNA using standard methods (Hogan *et al.*, 1994). Briefly, approximately 20-40 picolitres of injection buffer (containing about 1000-4000 copies of the transgene construct) were injected directly into one of the pro-nuclei using a micro-injection needle drawn on a Sutter P97 needle puller and using a shaped holding pipette and gentle suction to hold the embryo in position in a drop of M2 medium during injection.

Successfully injected embryos were transferred back into KSOM medium and placed in the incubator during preparations for oviduct transfer, or in some cases cultured overnight to the 2-cell stage prior to surgery. Pseudopregnant MF1 female mice, prepared by mating 12 h previously with a vasectomised male were weighed and anaesthetised by i.p. administration of 0.009 ml/g bodyweight Hypnorm/Hypnovel mixture, comprising 0.079 mg/ml fentanyl citrate, 2.5 mg/ml fluanisone and 1.25 mg/ml midazolam. Following laparotomy, the oviduct was exposed, and a polished transfer pipette loaded with approximately 20 injected embryos in a minimal volume of M2

medium was used to transfer embryos into the infundibulum of the pseudopregnant recipient.

8.1.4. Transgenic Line Derivation

Potential founders born to the pseudopregnant host mothers were tested by PCR for the presence of the transgene at around PN3wk. Earclips from animals to be tested were boiled for 10 min in 1 ml freshly prepared 50 mM NaOH, then neutralised by the addition of 50 µl 1M Tris.HCl, pH 8.0. 1 µl of this was added to 24 µl reaction mix to give a 25 µl reaction containing 75 mM Tris.HCl, pH 9.0, 20 mM $(NH_4)SO_4$, 0.01 % Tween-20, 3 mM $MgCl_2$, 250 µM dNTPs, 1 U *Taq* polymerase and 150 nM of each primer. 36 reaction cycles were carried out, each consisting of 60 sec denaturation at 95°C, 60 sec annealing at 60°C and 60 sec extension at 72°C. Primers were designed to span the junction between promoter and Igf2, so as to be unique to the transgene.

For mice injected with the EIP-Igf2 construct, forward primer ELAS-141 (5'-TAACTGAGTGCCGGCCTTGTTCTG-3') and the reverse primer IGF2R142 (5'-TGAGAAGCACCAACATCGACTTCC-3') amplify a 279 bp product.

For mice injected with the RIP-Igf2 construct, forward primer RIP-153 (5'-CTGAGGTGAGGACACAGCTATCAG-3') and reverse primer IGF2R142 amplify a 655 bp product.

Positive potential founders were crossed to non-transgenic F_1 (C57BL/6×CBA) animals and two or three litters of offspring tested for transmission. Only one founder for each construct was found to transmit consistently. The line carrying the EIP-Igf2 construct was designated *Elijah*, and the line carrying the RIP-Igf2 construct was designated *Ripley*.

Table 8.1. (a). Measurements for Each Field (Partial Section) Analysed for Statistical Morphometry Study of Pancreas Sections from Elijah Transgenic Animals

Litter / Sex	Age Wks	Field	Total Pancreas Area (mm^2)	Absolute Acini Area (mm^2)	Percent. Acini Area (%)	Absolute Islet Area (μm^2)	Percent. Islet Area (%)	Islet No.	Mean Islet Area (μm^2)
1 /	35	1	3.678140	3.620442	98.43133	21429.90747	0.58263	6	1863.14488
Male		2	4.367803	3.638905	83.31202	342672.75652	7.84543	10	34316.86810
		3	2.894609	2.868588	99.10105	2929.40255	0.10120	3	976.46752
		4	3.263429	3.167421	97.05806	43746.4925	1.34051	6	7291.08208
		5	2.842980	2.813476	98.96222	5155.44915	0.18134	3	1718.48305
		Mean	**3.4093922**	**3.2217664**	**95.37294**	**83186.80164**	**2.01022**	**5.6**	**9233.20913**
2 /	33	1	3.902151	3.681844	94.35422	22353.9975	0.57286	7	3193.42821
Female		2	4.064567	3.853347	94.80338	94810.8793	2.33262	11	8346.73947
		3	3.780493	3.758012	99.40534	998.91503	0.02642	2	499.45752
		4	3.699910	3.659789	98.91562	1466.57189	0.03964	2	733.28595
		5	3.430177	3.321815	96.84092	50342.32447	1.46763	8	6292.79056
		Mean	**3.7754596**	**3.6549614**	**96.86390**	**33994.53764**	**0.88783**	**6**	**3813.14034**
3 /	31	1	4.385866	3.821666	87.13595	388663.9973	8.86174	13	29897.23056
Male		2	3.979068	3.923895	98.61342	6173.0704	0.15514	2	3086.5352
		3	3.973527	3.926802	98.82409	4938.45633	0.12428	2	2469.22817
		4	1.918774	1.909364	99.50958	0	0	0	-
		5	2.380220	2.336960	98.18252	0	0	0	-
		Mean	**3.327491**	**3.1837374**	**96.45311**	**79955.10481**	**1.82823**	**3.4**	**11817.66464**
3 /	31	1	3.779808	3.759104	99.45225	0	0	0	-
Male		2	3.836032	3.760197	98.02309	73171.4616	1.90748	5	14634.29232
		3	3.736200	3.684855	98.62574	2435.5569	0.06519	1	2435.5569
		4	3.353148	3.056654	91.15774	204945.942	6.11205	4	51236.4855
		5	3.090613	3.028576	97.99273	3505.5558	0.11343	1	3505.5558
		Mean	**3.5591602**	**3.4578772**	**97.05031**	**56811.70326**	**1.63963**	**2.2**	**17952.97263**
3 /	32	1	2.526211	2.508575	99.30188	6992.4052	0.27679	3	2330.80173
Female		2	2.963545	2.911373	98.23954	2300.8717	0.07764	1	2300.8717
		3	2.522893	2.399461	95.10752	2813. 4237	0.11152	2	1406.71185
		4	2.686221	2.619144	97.50292	3296.0455	0.12270	1	3296.0455
		5	2.569980	2.509226	97.63601	13341.315	0.51912	1	13341.315
		Mean	**2.653770**	**2.5895558**	**97.55757**	**5748.81222**	**0.22155**	**1.6**	**4535.14916**

Table 8.1. (b). Measurements for Each Field (Partial Section) Analysed for Statistical Morphometry Study of Pancreas Sections from Age- and Sex-Matched Non-Transgenic Littermate Control Animals

Litter / Sex	Age Wks	Field	Total Pancreas Area (mm^2)	Absolute Acini Area (mm^2)	Percent. Acini Area (%)	Absolute Islet Area (μm^2)	Percent. Islet Area (%)	Islet No.	Mean Islet Area (μm^2)
1 /	35	1	2.935007	2.884485	98.27864	18081.485	0.61606	1	18081.485
Male		2	3.253608	3.214370	98.79402	7995.0615	0.24573	4	1998.76538
		3	3.500546	3.413349	97.50905	45265.4416	1.29310	2	22632.7208
		4	3.190314	2.983606	93.52076	59022.0358	1.85004	2	10791.6494
		5	3.463268	3.426013	98.92428	0	0	0	-
		Mean	**3.2685486**	**3.1843646**	**97.40535**	**26072.80478**	**0.800986**	**1.8**	**13376.15515**
2 /	33	1	1.638737	1.619309	98.81445	796.88728	0.04863	1	796.88728
Female		2	3.316559	3.277440	98.82049	3135.1715	0.09453	2	1795.8023
		3	3.603008	3.575278	99.23037	21875.1169	0.60713	3	7291.70563
		4	4.006719	3.836765	95.75828	107931.46014	2.69376	11	9811.95092
		5	2.697980	2.572550	95.35097	53372.7422	1.97825	5	10674.54844
		Mean	**3.0526006**	**2.9762684**	**97.59491**	**37422.27560**	**1.08446**	**4.4**	**6074.17891**
3 /	31	1	2.953204	2.928097	99.14984	4455.8345	0.15088	0	-
Male		2	2.643451	2.582599	97.69801	41262.2994	1.56093	5	8252.45988
		3	3.349646	3.232826	96.51247	71828.3516	2.14436	5	14365.67032
		4	2.144876	2.096622	97.75027	8739.5713	0.40746	4	2024.01887
		5	3.106341	2.939425	94.62660	102020.2782	3.28426	7	14574.32546
		Mean	**2.8395036**	**2.7559138**	**97.14744**	**45661.267**	**1.50958**	**4.2**	**9804.11863**
3 /	31	1	1.371308	1.194848	87.13199	13004.60178	0.94834	3	4334.86726
Male		2	3.857204	3.666650	95.05979	145179.3935	3.76385	8	16485.21582
		3	2.814067	2.753014	97.83044	54446.481	1.93480	2	27223.2405
		4	3.885761	3.720940	95.75833	102577.7238	2.63984	9	11182.14285
		5	3.431711	3.413079	99.45706	0	0	0	-
		Mean	**3.0720102**	**2.9497062**	**95.04752**	**63041.64002**	**1.85737**	**4.4**	**14806.36661**
3 /	32	1	1.879079	1.780037	94.72923	10662.5762	0.56744	2	5331.2881
Female		2	2.198481	2.071323	94.21610	79946.874	3.63646	5	10902.95183
		3	2.272752	2.228261	98.04242	26899.6225	1.18357	5	5379.9245
		4	2.211194	2.001280	90.50676	52007.1828	2.35200	4	13001.7957
		5	2.501223	2.299517	91.93571	94661.229	3.78460	3	31553.743
		Mean	**2.2125458**	**2.0760836**	**93.88604**	**52835.4969**	**2.30481**	**3.8**	**13233.94063**

Table 8.2. Measurements for Each Section Analysed for Statistical Morphometry Study of Pancreas Sections from Ripley Transgenic and Age- and Sex-Matched Non-Transgenic Littermate Control Animals

Litter / Sex	Age Wks	Section	Number of Islets/Section		Total Section Area (mm^2)		Mean Islet Area (μm^2)	
			TG	CTL	Transgenic	Control	Transgenic	Control
1 /	43	1	19	12	20.93247	24.01568	4772.524	11576.04
Female		2	19	26	20.4464	31.18273	7567.221	11311.78
		3	22	38	25.29856	31.76815	5386.319	18976.35
		4	15	34	28.06826	33.00867	10345.22	13786
		5	33	31	31.28911	30.53618	11646.43	18949.95
		Mean	**21.6**	**28.2**	**25.20696**	**30.10228**	**7943.542**	**14920.02**
1 /	43	1	13	14	23.06994	35.75626	6606.624	9554.675
Female		2	28	29	28.34825	43.37217	6811.023	13294.45
		3	28	35	27.00852	37.94556	9977.058	15365.33
		4	19	21	33.112	32.74346	12105.03	6215.452
		5	26	18	31.35083	25.32661	6112.7	11227.14
		Mean	**22.8**	**23.4**	**28.57791**	**35.02881**	**8322.487**	**11131.41**
1 /	46	1	62	12	22.78584	15.39916	16543.73	9062.731
Male		2	75	14	26.9128	19.78081	44551.4	30618.13
		3	43	18	23.66573	22.99312	25370.39	34247.78
		4	46	22	29.29795	24.01552	18497.74	48172.05
		5	54	13	31.47079	22.47093	23719.75	47998.05
		Mean	**56**	**15.8**	**26.82662**	**20.93191**	**25736.6**	**34019.75**
2 /	43	1	34	36	32.5697	31.4275	9068.161	9363.398
Male		2	49	32	43.73049	29.40998	14516.35	9990.518
		3	52	58	43.31973	34.14004	15229.79	12565.62
		4	28	22	37.31668	28.23698	10681.13	5202.081
		5	8	22	27.74574	24.10819	10994.75	6013.707
		Mean	**34.2**	**34**	**36.93647**	**29.46454**	**12098.04**	**8627.065**
2 /	43	1	13	25	20.53161	18.31792	16600.57	13431.27
Male		2	17	31	30.19614	19.09829	49520.66	16375.09
		3	18	28	31.0707	20.68021	60153.31	16134.86
		4	16	32	31.03061	23.29445	44575.04	29116.31
		5	27	35	27.00943	24.47704	23671.98	15135.39
		Mean	**18.2**	**30.2**	**27.9677**	**21.17358**	**38904.31**	**18038.58**

TG = Transgenic

CTL = Control

9. References

Ahlgren, U., Jonsson, J. and Edlund, H. (1996) The morphogenesis of the pancreatic mesenchyme is uncoupled from that of the pancreatic epithelium in IPF1/PDX1-deficient mice. *Development* **122**, 1409-1416.

Ahlgren, U., Pfaff, S. L., Jessell, T. M., Edlund, T. and Edlund, H. (1997) Independent requirement for ISL1 in formation of pancreatic mesenchyme and islet cells. *Nature* **385**, 257-260.

Ahlgren, U., Jonsson, J., Jonsson, L., Simu, K. and Edlund, H. (1998) Beta-cell-specific inactivation of the mouse Ipf1/Pdx1 gene results in loss of the beta-cell phenotype and maturity onset diabetes. *Genes Dev.* **12**, 1763-1768.

Ali-Rachedi, A., Varndell, I. M., Adrian, T. E., Gapp, D. A., Van Noorden, S., Bloom, S. R. and Polak, J. M. (1984) Peptide YY (PYY) immunoreactivity is co-stored with glucagon-related immunoreactants in endocrine cells of the gut and pancreas. *Histochemistry* **80**, 487-491.

Alpert, S., Hanahan, D. and Teitelman, G. (1988) Hybrid insulin genes reveal a developmental lineage for pancreatic endocrine cells and imply a relationship with neurons. *Cell* **53**, 295-308.

Andrew, A. (1976) An experimental investigation into the possible neural crest origin of pancreatic APUD (islet) cells. *J. Embryol. Exp. Morph.* **35**, 577-593.

Ang, S. L., Wierda, A., Wong, D., Stevens, K. A., Cascio, S., Rossant, J. and Zaret, K. S. (1993) The formation and maintenance of the definitive endoderm lineage in the mouse: involvement of HNF3/forkhead proteins. *Development* **119**, 1301-1315.

Ang, S. L. and Rossant, J. (1994) HNF-3 beta is essential for node and notochord formation in mouse development. *Cell* **78**, 561-574.

Apelqvist, Å., Ahlgren, U. and Edlund, H. (1997) Sonic hedgehog directs specialised mesoderm differentiation in the intestine and pancreas. *Curr. Biol.* **7**, 801-804.

Apelqvist, Å., Li, H., Sommer, L., Beatus, P., Anderson, D. J., Honjo, T., Hrabe de Angelis, M., Lendahl, U. and Edlund, H. (1999) Notch signalling controls pancreatic cell differentiation. *Nature* **400**, 877-881.

Araki, E., Lipes, M. A., Patti, M. E., Bruning, J. C., Haag, B. III., Johnson, R. S. and Kahn, C. R. (1994) Alternative pathway of insulin signalling in mice with targeted disruption of the IRS-1 gene. *Nature* **372**, 186-190.

Arany, E. and Hill, D. J. (2000) Ontogeny of fibroblast growth factors in the early development of the rat endocrine pancreas. *Pediatr. Res.* **48**, 389-403.

Asfari, M., Wei, D., Noel, M., Holthuizen, P. E. and Czernichow, P. (1995) IGF-II gene expression in a rat insulin-producing β-cell line (INS-1) is regulated by glucose. *Diabetologia* **38**, 927-935.

Asplund, K. (1973) Dynamics of insulin release from the foetal and neonatal rat pancreas. *Eur. J. Clin. Invest.* **3**, 338-344.

Bartels, H., Linnemann, H. and Jungermann, K. (1989) Predominant localization of phosphoenolpyruvate carboxykinase mRNA in the periportal zone of rat liver parenchyma demonstrated by *in situ* hybridization. *FEBS Lett.* **248**, 188-194.

Beattie, G. M., Rubin, J. S., Mally, M. I., Otonkoski, T. and Hayek, A. (1996) Regulation of proliferation and differentiation of human fetal pancreatic islet cells by extracellular matrix, hepatocyte growth factor, and cell-cell contact. *Diabetes* **45**, 1223-1228.

Beatus, P. and Lendahl, U. (1998) Notch and neurogenesis. *J. Neurosci. Res.* **54**, 125-136.

Beatus, P., Lundkvist, J., Oberg, C. and Lendahl, U. (1999) The Notch 3 intracellular domain represses Notch 1-mediated activation through Hairy/Enhancer of split (HES) promoters. *Development* **26**, 3925-3935.

Beddington, R. S. P., Morgernstern, J., Land, H. and Hogan, A. (1989) An *in situ* transgenic enzyme marker for the midgestation mouse embryo and the visualization of inner cell mass clones during early organogenesis. *Development* **106**, 37-46.

Bhushan, A., Itoh, N., Kato, S., Thiery, J. P., Czernichow, P., Bellusci, S. and Scharfmann, R. (2001) *Fgf10* is essential for maintaining the proliferative capacity of epithelial progenitor cells during early pancreatic organogenesis. *Development* **128**, 5109-5117.

Bisgaier, C. L., Essenburg, A. D., Auerbach, B. J., Pape, M. E., Sekerke, C. S., Gee, A., Wolle, S. and Newton, R. S. (1997) Attenuation of plasma low density lipoprotein

cholesterol by select 3-hydroxy-3-methylglutaryl coenzyme A reductase inhibitors in mice devoid of low density lipoprotein receptors. *J. Lipid Res.* **38**, 2502-2515.

Bitgood, M. J. and McMahon, A. P. (1995) Hedgehog and Bmp genes are coexpressed at many diverse sites of cell-cell interaction in the mouse embryo. *Dev. Biol.* **172**, 126-138.

Bjerknes, M. (1995) The crypt cycle and the asymptotic dynamics of the proportion of differently sized mutant crypt clones in the mouse intestine. *Proc. Roy. Soc. Lond. B* **260**, 1-6.

Bjerknes, M. (1996) Expansion of mutant stem cell populations in the human colon. *J. Theor. Biol.* **178**, 381-385.

Blackburn, A., Schmitt, A., Schmidt, P., Wanke, R., Hermanns, W., Brem, G. and Wolf, E. (1997) Actions and interactions of growth hormone and insulin-like growth factor-II: body and organ growth of transgenic mice. *Transgenic Res.* **6**, 213-222.

Bonner-Weir, S., Trent, D. F., Honey, R. N. and Weir, G. C. (1981) Responses of neonatal rat islets to streptozotocin. *Diabetes* **30**, 64-69.

Bonner-Weir, S., Deery, D., Leahy, J. L. and Weir, G. C. (1989) Compensatory growth of pancreatic B-cells in adult rats after short-term glucose infusion. *Diabetes* **38**, 49-53.

Bonner-Weir, S., Baxter, L. A., Schuppin, G. T. and Smith, F. E. (1993) A second pathway for regeneration of the adult exocrine and endocrine pancreas: a possible recapitulation of embryonic development. *Diabetes* **42**, 1715-1720.

Bonner-Weir, S. and Smith, F. E. (1994) Islet cell growth and the growth factors involved. *Trends Endocrinol. Metab.* **5**, 60-64.

Bonner-Weir, S., Stubbs, M., Reitz, P., Taneja, M. and Smith, F. E. (1997) Partial pancreatectomy as a model of pancreatic regeneration. In *Pancreatic Growth and Regeneration* (ed. N. Sarvetnick), pp. 138-153. Karger Landes Systems.

Bonner-Weir, S. (2000) Islet growth and development in the adult. *J. Mol. Endocrinol.* **24**, 297-302.

Boschero, A. C., Crepaldi, S. C., Carneiro, E. M., Delattre, E. and Atwater, I. (1993) Prolactin induces maturation of glucose sensing mechanisms in cultured neonatal rat islets. *Endocrinology* **133**, 515-520.

Branch, C. D. and Gross, R. E. (1935) Aberrant pancreatic tissue in the gastrointestinal tract. *Arch. Surg.* **31**, 200-224.

Brelje, T. C., Scharp, D. W., Lacy, P. E., Ogren, L., Talamantes, F., Robertson, M., Friesen, H. G. and Sorenson, R. L. (1993) Effect of homologous placental lactogens, prolactins, and growth hormones on islet B-cell division and insulin secretion in rat, mouse, and human islets: implication for placental lactogen regulation of islet function during pregnancy. *Endocrinology* **132**, 879-887.

Briscoe, J., Sussel, L., Serup, P., Hartigan-O'Connor, D., Jessell, T. M., Rubenstein, J. L. and Ericson, J. (1999) Homeobox gene Nkx2.2 and specification of neuronal identity by graded Sonic hedgehog signalling. *Nature* **398**, 622-627.

Brockenbrough, J., Weir, G. C. and Bonner-Weir, S. (1988) Discordance of exocrine and endocrine growth after 90 % pancreatectomy in rats. *Diabetes* **37**, 232-236.

Brosky, G. and Logothetopoulos, J. (1969) Streptozotocin diabetes in the mouse and the guinea pig. *Diabetes* **18**, 606-611.

Brown, A. L., Graham, D. E., Nissley, S. P., Hill, D. J., Strain, A. J. and Rechler, M. M. (1986) Developmental regulation of insulin-like growth factor II mRNA in different rat tissues. *J. Biol. Chem.* **261**, 13144-13150.

Brown, M. S. and Goldstein, J. L. (1980) Multivalent feedback regulation of HMG CoA reductase, a control mechanism coordinating isoprenoid synthesis and cell growth. *J. Lipid Res.* **21**, 505-517.

Bruning, J. C., Winnay, J., Bonner-Weir, S., Taylor, S. I., Accili, D. and Kahn, C. R. (1997) Development of a novel polygenic model of NIDDM in mice heterozygous for IR and IRS-1 null alleles. *Cell* **88**, 561-572.

Cairnie, A. B. and Millen, B. H. (1975) Fission of crypts in the small intestine of the irradiated mouse. *Cell Tissue Kinet.* **8**, 189-196.

http://www.cancerhelp.org.uk/help/default.asp?page=352

Canfield, V., West, A. B., Goldenring, J. R. and Levenson, R. (1996) Genetic ablation of parietal cells in transgenic mice: a new model for analyzing cell lineage relationships in the gastric mucosa. *Proc. Natl. Acad. Sci. USA* **93**, 2431-2435.

Carty, M. D., Lillquist, J. S., Peshavaria, M., Stein, R. and Soeller, W. C. (1997) Identification of cis- and trans-active factors regulating human islet amyloid polypeptide gene expression in pancreatic β-cells. *J. Biol. Chem.* **272**, 11986-11993.

Celli, G., LaRochelle, W. J., Mackem, S., Sharp, R. and Merlino, G. (1998) Soluble dominant-negative receptor uncovers essential roles for fibroblast growth factors in multi-organ induction and patterning. *EMBO J.* **17**, 1642-1655.

Chang, A. Y. and Diani, A. R. (1985) Chemically and hormonally induced diabetes mellitus. In *The Diabetic Pancreas*, 2nd edition (ed. B. W. Volk and E. R. Arquilla), pp. 415-438. New York: Plenum Press.

Chen, L., Komiya, I., Inman, L., McCorkle, K., Alam, T. and Unger, R. H. (1989) Molecular and cellular responses of islets during perturbations of glucose homeostasis determined by *in situ* hybridization histochemistry. *Proc. Natl. Acad. Sci. USA* **86**, 1367-1371.

Cheng, H. and Bjerknes, M. (1985) Whole population cell kinetics and postnatal development of the mouse intestinal epithelium. *Anat. Rec.* **211**, 420-426.

Cheon, H. G., LaRochelle, W. J., Bottaro, D. P., Burgess, W. H. and Aaronson, S. A. (1994) High-affinity binding sites for related fibroblast growth factor ligands reside within different receptor immunoglobulin-like domains. *Proc. Natl. Acad. Sci. USA* **91**, 989-993.

Christofori, G., Naik, P. and Hanahan, D. (1994) A second signal supplied by insulin-like growth factor II in oncogene-induced tumorigenesis. *Nature* **369**, 414-418.

Christofori, G., Naik, P. and Hanahan, D. (1995) Deregulation of both imprinted and expressed alleles of the insulin-like growth factor 2 gene during β-cell tumorigenesis. *Nat. Genet.* **10**, 196-201.

Cirulli, V., Baetens, D., Rutishauser, U., Halban, P. A., Orci, L. and Rouiller, D. G. (1994) Expression of neural cell adhesion molecule (N-CAM) in rat islets and its role in islet cell type segregation. *J. Cell. Sci.* **107**, 1429-1436.

Cockell, M., Stevenson, B. J., Strubin, M., Hagenbüchle, O. and Wellauer, P. K. (1989) Identification of a cell-specific DNA-binding activity that interacts with a transcriptional activator of genes expressed in the acinar pancreas. *Mol. Cell. Biol.* **9**, 2464-2476.

Conover, W. J. (1980) *Practical Nonparametric Statistics*, 2nd edition, pp. 494. New York: John Wiley.

Corbett, J. A. and McDaniel, M. L. (1995) Intraislet release of interleukin-1 inhibits β-cell function by inducing β-cell expression of inducible nitric oxide synthase. *J. Exp. Med.* **181**, 559-568.

Cras-Méneur, C., Elghazi, L., Czernichow, P. and Scharfmann, R. (2001) Epidermal growth factor increases undifferentiated pancreatic embryonic cells *in vitro*: a balance between proliferation and differentiation. *Diabetes* **50**, 1571-1579.

Cras-Méneur, C. and Scharfmann, R. (2002) FGFR1-IIIb is a putative marker of pancreatic progenitor cells. *Mech. Dev.* **116**, 205-208.

Dabeva, M. D., Hwang, S. G., Vasa, S. R., Hurston, E., Novikoff, P. M., Hixson, D. C., Gupta, S. and Shafritz, D. A. (1997) Differentiation of pancreatic epithelial progenitor cells into hepatocytes following transplantation into rat liver. *Proc. Natl. Acad. Sci. USA* **94**, 7356-7361.

Da Costa, T. H. M., Williamson, D. H., Ward, A., Bates, P., Fisher, R., Richardson, L., Hill, D. J., Robinson, I. C. A. F. and Graham, C. F. (1994) High plasma insulin-like growth factor-II and low lipid content in transgenic mice: measurements of lipid metabolism. *J. Endocrinol.* **143**, 433-439.

Dahl, U., Sjödin, A. and Semb, H. (1996) Cadherins regulate aggregation of pancreatic β-cells *in vivo*. *Development* **122**, 2895-2902.

Danielian, P. S., Muccino, D., Rowitch, D. H., Michael, S. K. and McMahon, A. P. (1998) Modification of gene activity in mouse embryos *in utero* by a tamoxifen-inducible form of Cre recombinase. *Curr. Biol.* **8**, 1323-1326.

De Castro Barbosa, J. J., Dockerty, M. B. and Waugh, J. M. (1946) Pancreatic heterotopia. *Surg. Gyn. Obs.* **82**, 527-542.

DeChiara, T. M., Efstratiadis, A. and Robertson, E. J. (1990) A growth-deficiency phenotype in heterozygous mice carrying an insulin-like growth factor II gene disrupted by targeting. *Nature* **345**, 78-80.

DeChiara, T. M., Robertson, E. J. and Efstratiadis, A. (1991) Parental imprinting of the mouse insulin-like growth factor II gene. *Cell* **64**, 849-859.

Delehaye-Zervas, M. C., Mertani, H., Martini, J. F., Nihoul-Fekete, C., Morel, G. and Postel-Vinay, M. C. (1994) Expression of the growth hormone receptor gene in human digestive tissue. *J. Clin. Edocrinol. Metab.* **78**, 1473-1480.

Deltour, L., Leduque, P., Paldi, A., Ripoche, M. A., Dubois, P. and Jami, J. (1991) Polyclonal origin of pancreatic islets in aggregation mouse chimaeras. *Development* **112**, 1115-1121.

De Mazancourt, P., Carneiro, E. M., Atwater, I. and Boschero, A. C. (1994) Prolactin treatment increases GLUT2 but not the G protein subunit content in cell membranes from cultured neonatal rat islets. *FEBS Lett.* **343**, 137-140.

De Meyts, P., Wallach, B., Christofferson, C. T., Urso, B., Gronskov, K., Latus, L. J., Yakushiji, F., Ilondo, M. M. and Shymko, R. M. (1994) The insulin-like growth factor-I receptor. Structure, ligand-binding mechanism and signal transduction. *Horm. Res.* **42**, 152-169.

Deutsch, G., Jung, J., Zheng, M., Lóra, J. and Zaret, K. S. (2001) A bipotential precursor population for pancreas and liver within the embryonic endoderm. *Development* **128**, 871-881.

Devedjian, J.-C., George, M., Casellas, A., Pujol, A., Visa, J., Pelegrín, M., Gros, L. and Bosch, F. (2000) Transgenic mice overexpressing insulin-like growth factor-II in β cells develop type 2 diabetes. *J. Clin. Invest.* **105**, 731-740.

DiBerardino, M. A., Hoffner, N. J. and Etkin, L. D. (1984) Activation of dormant genes in specialized cells. *Science* **224**, 946-952.

Dolva, L. O., Nielsen, J. H., Welinder, B. S. and Hanssen, K. F. (1983) Biosynthesis and release of thyrotropin-releasing hormone immunoreactivity in rat pancreatic islets in organ culture. Effects of age, glucose, and streptozotocin. *J. Clin. Invest.* **72**, 1867-1873.

Dong, J., Asa, S. L. and Drucker, D. J. (1991) Islet cell and extrapancreatic expression of the LIM domain homeobox gene *isl-1*. *Mol. Endocrinol.* **5**, 1633-1641.

Dubois, P. M. (1989) Ontogeny of the endocrine pancreas. *Horm. Res.* **32**, 53-60.

Dudek, R. W., Lawrence, I. E. Jr., Hill, R. S. and Johnson, R. C. (1991) Induction of islet cytodifferentiation by fetal mesenchyme in adult pancreatic ductal epithelium. *Diabetes* **40**, 1041-1048.

Dumonteil, E., Laser, B., Constant, I. and Philippe, J. (1998) Differential regulation of the glucagon and insulin I gene promoters by the basic helix-loop-helix transcription factors E47 and BETA2. *J. Biol. Chem.* **273**, 19945-19954.

Duncan, S. A., Navas, M. A., Dufort, D., Rossant, J. and Stoffel, M. (1998) Regulation of a transcription factor network required for differentiation and metabolism. *Science* **281**, 692-695.

Duvillié, B., Cordonnier, N., Deltour, L., Dandoy-Dron, F., Itier, J.-M., Monthioux, E., Jami, J., Joshi, R. L. and Bucchini, D. (1997) Phenotypic alterations in insulin-deficient mutant mice. *Proc. Natl. Acad. Sci. USA* **94**, 5137-5140.

Ebert, M., Friess, H., Buchler, M. W. and Korc, M. (1995) Differential distribution of human epidermal growth factor receptor family in acute pancreatitis. *Dig. Dis. Sci.* **40**, 2134-2142.

Edlund, H. (2001) Developmental biology of the pancreas. *Diabetes* **50**, Suppl. 1, S5-9.

Efstratiadis, A. (1998) Genetics of mouse growth. *Int. J. Dev. Biol.* **42**, 955-976.

Eguchi, G. and Kodama, R. (1993) Transdifferentiation. *Curr. Opin. Cell Biol.* **5**, 1023-1028.

Elghazi, L., Cras-Méneur, C., Czernichow, P. and Scharfmann, R. (2002) Role for FGFR2IIIb-mediated signals in controlling pancreatic endocrine progenitor cell proliferation. *Proc Natl. Acad. Sci. USA* **99**, 3884-3889.

Elliott, W. M. and Youson, J. H. (1993) Development of the adult endocrine pancreas during metamorphosis in the sea lamprey, *Petromyzon marinus* L. II. Electron microscopy and immunocytochemistry. *Anat. Rec.* **237**, 271-290.

Emens, L. A., Landers, D. W. and Moss, L. G. (1992) Hepatocyte nuclear factor 1 alpha is expressed in a hamster insulinoma line and transactivates the rat insulin I gene. *Proc. Natl. Acad. Sci. USA* **89**, 7300-7304.

Ericson, J., Rashbass, P., Schedl, A., Brenner-Morton, S., Kawakami, A., van Heyningen, V., Jessell, T. M. and Briscoe, J. (1997) Pax6 controls progenitor cell identity and neuronal fate in response to graded Shh signaling. *Cell* **90**, 169-180.

Esni, F., Täljedal, I.-B., Perl, A.-K., Cremer, H., Christofori, G. and Semb, H. (1999) Neural cell adhesion molecule (N-CAM) is required for cell type segregation and normal ultrastructure in pancreatic islets. *J. Cell Biol.* **144**, 325-337.

Evans, G. A. (1989) Dissecting mouse development with toxigenics. *Genes Dev.* **3**, 259-263.

Fajans, S. S. (1990) Scope and heterogeneous nature of MODY. *Diabetes Care* **13**, 49-64.

Falkmer, S. (1985) Comparative morphology of pancreatic islets in animals. In *The Diabetic Pancreas* (ed. B. W. Volk and E. R. Arquilla), pp. 17-52. New York: Plenum Press.

Fehmann, H. C., Jehle, P., Markus, U. and Goke, B. (1996) Functional receptors for insulin-like growth factors-I (IGF-I) and IGF-II on insulin-, glucagon-, and somatostatin-producing cells. *Metabolism* **45**, 759-766.

Feil, R., Walter, J., Allen, N. D. and Reik, W. (1994) Developmental control of allelic methylation in the imprinted mouse IGF2 and H19 genes. *Development* **120**, 2933-2943.

Finch, P., Cunha, G., Rubin, J., Wong, J. and Ron, D. (1995) Pattern of keratinocyte growth factor and keratinocyte growth factor receptor expression during mouse fetal development suggests a role in mediating morphogenetic mesenchymal-epithelial interactions. *Dev. Dyn.* **203**, 223-240.

Finegood, D. T., Scaglia, L. and Bonner-Weir, S. (1995) Dynamics of β-cell mass in the growing rat pancreas: estimation with a simple mathematical model. *Diabetes* **44**, 249-256.

Fitzgerald, P. J., Carol, B. M. and Rosenstock, L. (1966) Pancreatic acinar cell regeneration. *Nature* **212**, 594-596.

Fode, C., Gradwohl, G., Morin, X., Dierich, A., LeMeur, M., Goridis, C. and Guillemot, F. (1998) The bHLH protein NEUROGENIN 2 is a determination factor for epibranchial placode-derived sensory neurons. *Neuron* **20**, 483-494.

Francis, P. J., Southgate, J. L., Wilkin, T. J. and Bone, A. J. (1992) Expression of an islet regenerating (reg) gene in isolated rat islets: effects of nutrient and non-nutrient growth factors. *Diabetologia* **35**, 238-242.

Frasca, F., Pandini, G., Scalia, P., Sciacca, L., Mineo, R., Costantino, A., Goldfine, I. D., Belfiore, A. and Vigneri, R. (1999) Insulin receptor isoform A, a newly recognized,

high-affinity insulin-like growth factor II receptor in fetal and cancer cells. *Mol. Cell. Biol.* **19**, 3278-3288.

Freemark, M., Driscoll, P., Maaskant, R., Petryk, A. and Kelly, P. A. (1997) Ontogenesis of prolactin receptors in the human fetus in early gestation. Implications for tissue differentiation and development. *J. Clin. Invest.* **99**, 1107-1117.

Friedmann, N. B. and Marble, A. (1941) Island hyperplasia in the partially depancreatized rat. *Endocrinology* **29**, 577-582.

Furukawa, M., Eto, Y. and Kojima, I. (1995) Expression of immunoreactive activin A in fetal rat pancreas. *Endocr. J.* **42**, 63-68.

Gaich, G., Orloff, J. J., Atillasoy, E. J., Burtis, W. J., Ganz, M. B. and Stewart, A. F. (1993) Amino-terminal parathyroid hormone-related protein: specific binding and cytosolic calcium responses in rat insulinoma cells. *Endocrinology* **132**, 1402-1409.

Gannon, M., Ray, M. K., Van Zee, K., Rausa, F., Costa, R. H. and Wright, C. V. E. (2000) Persistent expression of HNF6 in islet endocrine cells causes disrupted islet architecture and loss of beta cell function. *Development* **127**, 2883-2895.

Garcia-Caballero, T., Morel, G., Gallego, R., Fraga, M., Pintos, E., Gago, D., Vonderhaar, B. K. and Beiras, A. (1996) Cellular distribution of prolactin receptors in human digestive tissues. *J. Clin. Endocrinol. Metab.* **81**, 1861-1866.

Gartner, L. P. and Hiatt, J. L. (1997) *Color Textbook of Histology*. Philadelphia: W. B. Saunders Publishing Co.

Gebhardt, R. (1992) Metabolic zonation of the liver: regulation and implications for liver function. *Pharmacol. Ther.* **53**, 275-354.

Geier, A., Haimshon, M., Beery, R. and Lunenfeld, B. (1992) Insulin-like growth factor-I inhibits cell death induced by cycloheximide in MCF-7 cells - a model system for analyzing control of cell death. *In Vitro Cell. Dev. Biol.* **28A**, 725-729.

Githens, S. (1988) The pancreatic duct cell: proliferative capabilities, specific characteristics, metaplasia, isolation and culture. *J. Pediatr. Gastroenterol. Nutrition* **7**, 486-506.

Gittes, G. K. and Rutter, W. J. (1992) Onset of cell-specific gene expression in the developing mouse pancreas. *Proc. Natl. Acad. Sci. USA* **89**, 1128-1132.

Gittes, G. K., Galante, P. E., Hanahan, D., Rutter, W. J. and Debase, H. T. (1996) Lineage-specific morphogenesis in the developing pancreas: role of mesenchymal factors. *Development* **122**, 439-447.

Goldstein, J. L. and Brown, M. S. (1990) Regulation of the mevalonate pathway. *Nature* **343**, 425-430.

Golosow, N. and Grobstein, C. (1962) Epitheliomesenchymal interaction in pancreatic morphogenesis. *Dev. Biol.* **4**, 242-255.

Goossens, A., Gepts, W., Saudubray, J. M., Bonnefont, J. P., Nihoul-Fekete, Heitz, P. U. and Klöppel, G. (1989) Diffuse and focal nesidioblastosis. A clinicopathological study of 24 patients with persistent neonatal hyperinsulinemic hypoglycemia. *Am. J. Surg. Pathol.* **13**, 766-775.

Gorden, D. L., Mandriota, S. J., Montesano, R., Orci, L. and Pepper, M. S. (1997) Vascular endothelial growth factor is increased in devascularized rat islets of Langerhans *in vitro*. *Transplantation* **63**, 436-443.

Goss, R. J. (1978) *The Physiology of Growth*. Chapters 13 and 19. New York: Academic Press.

Gradwohl, G., Dierich, A., LeMeur, M. and Guillemot, F. (2000) *neurogenin3* is required for the development of the four endocrine cell lineages of the pancreas. *Proc. Natl. Acad. Sci. USA* **97**, 1607-1611.

Gu, D. and Sarvetnick, N. (1993) Epithelial cell proliferation and islet neogenesis in IFNγ transgenic mice. *Development* **118**, 33-46.

Gu, D., Lee, M. S., Krahl, T. and Sarvetnick, N. (1994) Transitional cells in the regenerating pancreas. *Development* **120**, 1873-1881.

Gu, G., Dubauskaite, J. and Melton, D. A. (2002) Direct evidence for the pancreatic lineage: NGN3+ cells are islet progenitors and are distinct from duct progenitors. *Development* **129**, 2447-2457.

Gualdi, R., Bossard, P., Zheng, M., Hamada, Y., Coleman, J. R. and Zaret, K. S. (1996) Hepatic specification of the gut endoderm *in vitro*: cell signalling and transcriptional control. *Genes Dev.* **10**, 1670-1682.

Guiot, Y., Sempoux, C., Moulin, P. and Rahier, J. (2001) No decrease of the beta-cell mass in type 2 diabetic patients. *Diabetes* **50**, Suppl. 1, S188.

Gumucio, J. J. (1989) Hepatocyte heterogeneity: the coming of age from the description of a biological curiosity to a partial understanding of its physiological meaning and regulation. *Hepatology* **9**, 154-160.

Guz, Y., Montminy, M. R., Stein, R., Leonard, J., Gamer, L. W., Wright, C. V. E. and Teitelman, G. (1995) Expression of murine STF-1, a putative insulin gene transcription factor, in β cells of the pancreas, duodenal epithelium and pancreatic exocrine and endocrine progenitors during ontogeny. *Development* **121**, 11-18.

Hagemann, R. F., Sigdestad, C. P. and Lesher, S. (1970) A quantitative description of the intestinal epithelium of the mouse. *Am. J. Anat.* **129**, 41-52.

Hamming, N. A. and Reynolds, W. A. (1977) DNA synthesis in pancreatic islet and acinar cells in rats with streptozotocin induced diabetes. *Horm. Metab. Res.* **9**, 114-116.

Hani, E. H., Suaud, L., Boutin, P., Chevre, J. C., Durand, E., Philippi, A., Demenais, F., Vionnet, N., Furuta, H., Velho, G., Bell, G. I., Laine, B. and Froguel, P. (1998) A missense mutation in hepatocyte nuclear factor-4 alpha, resulting in a reduced transactivation activity, in human late-onset non-insulin-dependent diabetes mellitus. *J. Clin. Invest.* **101**, 521-526.

Hani, E. H., Stoffers, D. A., Chevre, J. C., Durand, E., Stanojevic, V., Dina, C., Habener, J. F. and Froguel, P. (1999) Defective mutations in the insulin promoter factor-1 (IPF-1) gene in late-onset type 2 diabetes mellitus. *J. Clin. Invest.* **104**, R41-R48.

Harbeck, M. C., Louie, D. C., Howland, J., Wolf, B. A. and Rothenberg, P. L. (1996) Expression of insulin receptor mRNA and insulin receptor substrate 1 in pancreatic islet β-cells. *Diabetes* **45**, 711-717.

Harrison, K. A., Druey, K. M., Deguchi, Y., Tuscano, J. M. and Kerhl, J. H. (1994) A novel human homeobox gene distantly related to proboscipedia is expressed in lymphoid and pancreatic tissues. *J. Biol. Chem.* **269**, 19968-19975.

Harrison, K. A., Thaler, I., Pfaff, S. L., Gu, H. and Kehrl, J. H. (1999) Pancreas dorsal lobe agenesis and abnormal islets of Langerhans in Hlxb9-deficient mice. *Nat. Genet.* **23**, 71-75.

Hart, A., Baeza, N., Apelqvist, Å. and Edlund, H. (2000) Attenuation of FGF-signalling in mouse β-cells leads to diabetes. *Nature* **408**, 864-868.

Hastings, H. M., Schneider, B. S., Schreiber, M. A., Gorray, K., Maytal, G. and Maimon, J. (1992) Statistical geometry of pancreatic islets. *Proc. Roy. Soc. Lond. B* **250**, 257-261.

Hayek, A., Beattie, G. M., Cirulli, V., Lopez, A. D., Ricordi, C. and Rubin, J. S. (1995) Growth factor/matrix-induced proliferation of human adult β-cells. *Diabetes* **44**, 1458-1460.

Hebrok, M., Kim, S. K. and Melton, D. A. (1998) Notochord repression of endodermal Sonic hedgehog permits pancreas development. *Genes Dev.* **12**, 1705-1713.

Hebrok, M., Kim, S. K., St. Jacques, B., McMahon, A. P. and Melton, D. A. (2000) Regulation of pancreas development by hedgehog signaling. *Development* **127**, 4905-4913.

Hellerström, C. and Swenne, I. (1985) Growth pattern of pancreatic islets in animals. In *The Diabetic Pancreas*, 2nd edition (ed. B. W. Volk and E. R. Arquilla), pp. 53-79. New York: Plenum Press.

Hellerström, C., Swenne, I. and Andersson, A. (1988) Islet cell replication and diabetes. In *The Pathology of the Endocrine Pancreas in Diabetes* (ed. P. J. Lefebvre and D. G. Pipeleers), pp. 141-170. Heidelberg, Germany: Springer-Verlag.

Hellerström, C., Andersson, A., Korsgren, O., Jansson, L. and Sandler, S. (1989) Aspects of pancreatic islet transplantation in diabetes mellitus. *Baillière's Clin. Gastroenterol.* **3**, 851-863.

Hellerström, C. and Swenne, I. (1991) Functional maturation and proliferation of fetal pancreatic beta-cells. *Diabetes* **40** Suppl. 2, 89-93.

Herrera, P. L., Huarte, J., Sanvito, F., Meda, P., Orci, L. and Vassalli, J. D. (1991) Embryogenesis of the murine endocrine pancreas; early expression of pancreatic polypeptide gene. *Development* **113**, 1257-1265.

Herrera, P. L., Huarte, J., Zuffery, R., Nichols, A., Mermillod, B., Philippe, J., Muniesa, P., Sanvito, F., Orci, L. and Vassalli, J. D. (1994) Ablation of islet endocrine cells by targeted expression of hormone promoter-driven toxigenes. *Proc. Natl. Acad. Sci. USA* **91**, 12999-13003.

Herrera, P. L. (2000) Adult insulin- and glucagon-producing cells differentiate from two independent cell lineages. *Development* **127**, 2317-2322.

Hill, D. J. and Hogg, J. (1991) Growth factor control of pancreatic B cell hyperplasia. *Baillieres Clin. Endocrinol. Metab.* **5**, 689-698.

Hill, D. J., Sedran, R. J., Brenner, S. L. and McDonald, T. J. (1997) Insulin-like growth factor-I (IGF-I) has a dual effect on insulin release from isolated, perifused adult rat islets of Langerhans. *J. Endocrinol.* **153**, 15-25.

Hill, D. J., Hogg, J., Petrik, J., Arany, E. and Han, V. K. M. (1999) Cellular distribution and ontogeny of insulin-like growth factors (IGFs) and IGF binding protein messenger RNAs and peptides in developing rat pancreas. *J. Endocrinol.* **160**, 305-317.

Hill, D. J., Strutt, B., Arany, E., Zaina, S., Coukell, S. and Graham, C. F. (2000) Increased and persistent circulating insulin-like growth factor II in neonatal transgenic mice suppresses developmental apoptosis in the pancreatic islets. *Endocrinology* **141**, 1151-1157.

Hinton, P. R. (1995) *Statistics Explained. A Guide for Social Science Students*. New York: Routledge.

Hoar, W. S. (1975) *General and Comparative Physiology*. Englewood Cliffs, New Jersey: Prentice-Hall, Inc.

Hogan, B., Beddington, R., Costantini, F. and Lacy, E. (1994) *Manipulating the Mouse Embryo: A Laboratory Manual*, 2nd edition. Cold Spring Harbour Laboratory Press.

Hogg, J., Han, V. K. M., Clemmons, D. R. and Hill, D. J. (1993) Interactions of glucose, insulin-like growth factors (IGFs) and IGF binding proteins in the regulation of DNA synthesis by isolated fetal rat islets of Langerhans. *J. Endocrinol.* **138**, 401-412.

Hogg, J., Hill, D. J. and Han, V. K. M. (1994) The ontogeny of insulin-like growth factor (IGF) and IGF binding protein gene expression in the rat pancreas. *J. Mol. Endocrinol.* **13**, 49-58.

Hole, R. L., Pian-Smith, M. C. and Sharp, G. W. (1988) Development of the biphasic response to glucose in fetal and neonatal rat pancreas. *Am. J. Physiol.* **254**, E167-174.

Hoog, A., Sandberg-Nordqvist, A. C., Abdel-Halim, S. M., Carlsson-Skwirut, C., Guenifi, A., Tally, M., Ostenson, C. G., Falkmer, S., Sara, V. R., Efendic, S., Schalling, M. and Grimelius, L. (1996) Increased amounts of a high molecular weight insulin-like growth factor II (IGF-II) peptide and IGF-II messenger ribonucleic acid in pancreatic islets of diabetic Goto-Kakizaki rats. *Endocrinology* **137**, 2415-2423.

Hoog, A., Hu, W., Abdel-Halim, S. M., Falkmer, S., Qing, L. and Grimelius, L. (1997) Ultrastructural localization of insulin-like growth factor-2 (IGF-2) to the secretory granules of insulin cells: a study in normal and diabetic (GK) rats. *Ultrastruct. Pathol.* **21**, 457-466.

Horb, L. D. and Slack, J. M. W. (2000) Role of cell division in branching morphogenesis and differentiation of the embryonic pancreas. *Int. J. Dev. Biol.* **44**, 791-796.

Horb, M. E., Shen, C.-N., Tosh, D. and Slack, J. M. W. (2003) Experimental conversion of liver to pancreas. *Curr. Biol.* **13**, 105-115.

Horikawa, Y., Iwasaki, N., Hara, M., Furuta, H., Hinokio, Y., Cockburn, B. N., Lindner, T., Yamagata, K., Ogata, M., Tomonaga, O., Kuroki, H., Kasahara, T., Iwamoto, Y. and Bell, G. I. (1997) Mutation in hepatocyte nuclear factor-1 beta gene (TCF2) associated with MODY [letter]. *Nat. Genet.* **17**, 384-385.

Huang, H. P., Liu, M., El-Hodiri, H. M., Chu, K., Jamrich, M. and Tsai, M.-J. (2000) Regulation of the pancreatic islet-specific gene BETA2 (neuroD) by neurogenin 3. *Mol. Cell. Biol.* **20**, 3292-3307.

Hughes, H. (1956) An experimental study of regeneration in the islets of Langerhans with reference to the theory of balance. *Acta Anatomica.* **27**, 1-61.

Hugl, S. R., White, M. F. and Rhodes, C. J. (1998) Insulin-like growth factor I (IGF-I)-stimulated pancreatic β-cell growth is glucose-dependent. Synergistic activation of insulin receptor substrate-mediated signal transduction pathways by glucose and IGF-I in INS-1 cells. *J. Biol. Chem.* **273**, 17771-17779.

Hunziker, E. and Stein, M. (2000) Nestin-expressing cells in the pancreatic islets of Langerhans. *Biochem. Biophys. Res. Comm.* **271**, 116-119.

Hutton, J. C., Christofori, G., Chi, W. Y., Edman, U., Guest, P. C., Hanahan, D. and Kelly, R. B. (1993) Molecular cloning of mouse pancreatic islet R-cadherin: differential expression in endocrine and exocrine tissue. *Mol. Endocrinol.* **7**, 1151-1160.

Igarashi, M., Finch, P. W. and Aaronson, S. A. (1998) Characterization of recombinant human fibroblast growth factor (FGF)-10 reveals functional similarities with keratinocyte growth factor (FGF-7). *J. Biol. Chem.* **273**, 13230-13235.

Iwasaki, N., Ogata, M., Tomonaga, O., Kuroki, H., Kasahara, T., Yano, N. and Iwamoto, Y. (1998) Liver and kidney function in Japanese patients with maturity-onset diabetes of the young. *Diabetes Care* **21**, 2144-2148.

Jacquemin, P., Durviaux, S. M., Jensen, J., Godfraind, C., Gradwohl, O., Guillemot, F., Madsen, O. D., Carmeliet, P., Dewerchin, M., Collen, D., Rousseau, O. O. and Lemaigre, F. P. (2000) Transcription factor hepatocyte nuclear factor 6 regulates pancreatic endocrine cell differentiation and controls expression of the proendocrine gene ngn3. *Mol. Cell. Biol.* **20**, 4445-4454.

Jensen, J., Serup, P., Karlsen, C., Nielsen, T. F. and Madsen, O. D. (1996) mRNA profiling of rat islet tumors reveals nkx 6.1 as a β-cell-specific homeodomain transcription factor. *J. Biol. Chem.* **271**, 18749-18758.

Jensen, J., Heller, R. S., Funder-Nielsen, T., Pedersen, E. E., Lindsell, C., Weinmaster, G., Madsen, O. D. and Serup, P. (2000a) Independent development of pancreatic alpha- and beta-cells from neurogenin3-expressing precursors: a role for the notch pathway in repression of premature differentiation. *Diabetes* **49**, 163-176.

Jensen, J., Pedersen, E. E., Galante, P., Hald, J., Heller, R. S., Ishibashi, M., Kageyama, R., Guillemot, F., Serup, P. and Madsen, O. D. (2000b) Control of endodermal endocrine development by Hes-1. *Nat. Genet.* **24**, 36-44.

Jhappan, C., Stahle, C., Harkins, R. N., Fausto, N., Smith, G. H. and Merlino, G. T. (1990) TGFα overexpression in transgenic mice induces liver neoplasia and abnormal development of the mammary gland and pancreas. *Cell* **61**, 1137-1146.

Jonsson, J., Carlsson, L., Edlund, T. and Edlund, H. (1994) Insulin-promoter-factor 1 is required for pancreas development in mice. *Nature* **371**, 606-609.

Jung, J., Zheng, M., Goldfarb, M. and Zaret, K. S. (1999) Initiation of mammalian liver development from endoderm by fibroblasts growth factors. *Science* **284**, 1998-2003.

Jung, Y., Miura, M. and Yuan, J. (1996) Suppression of IL-1 beta converting enzyme-mediated cell death by insulin-like growth factor. *J. Biol. Chem.* **271**, 5112-5117.

Jungermann, K. (1988) Metabolic zonation of liver parenchyma. *Semin. Liver Dis.* **8**, 329-341.

Jungermann, K. and Katz, N. (1989) Functional specialization of different hepatocyte populations. *Physiol. Rev.* **69**, 708-764.

Kaestner, K. H., Katz, J., Liu, Y., Drucker, D. J. and Schutz, G. (1999) Inactivation of the winged helix transcription factor HNF3alpha affects glucose homeostasis and islet glucagon gene expression *in vivo*. *Genes Dev.* **13**, 495-504.

Kajstura, J., Mansukhani, M., Cheng, W., Reiss, K., Krajewski, S., Reed, J. C., Quaini, F., Sonnenblick, E. H. and Anversa, P. (1995) Programmed cell death and expression of the protooncogene bcl-2 in myocytes during postnatal maturation of the heart. *Exp. Cell Res.* **219**, 110-121.

Kanaka-Gantenbein, C., Tazi, A., Czernichow, P. and Scharfmann, R. (1995) *In vivo* presence of the high affinity nerve growth factor receptor Trk-A in the rat pancreas: differential localization during pancreatic development. *Endocrinology* **136**, 761-769.

Kaneto, H., Miyagawa, J., Kajimoto, Y., Yamamoto, K., Watada, H., Umayahara, Y., Hanafusa, T., Matsuzawa, Y., Yamasaki, Y., Higashiyama, S. and Taniguchi, N. (1997) Expression of heparin-binding epidermal growth factor-like growth factor during pancreas development. *J. Biol. Chem.* **272**, 29137-29143.

Karlsson, O., Thor, S., Norberg, T., Ohlsson, H. and Edlund, T. (1990) Insulin gene enhancer binding protein Isl-1 is a member of a novel class of proteins containing both a homeo- and a Cys-His domain. *Nature* **344**, 879-882.

Kasselberg, A. G., Orth, D. N., Gray, M. E. and Stahlman, M. T. (1985) Immunocytochemical localization of human epidermal growth factor/urogastrone in several human tissues. *J. Histochem. Cytochem.* **33**, 315-322.

Kato, S. and Sekine, K. (1999) FGF-FGFR signaling in vertebrate organogenesis. *Cell. Mol. Biol.* **45**, 631-638.

Kaung, H.-L. C. (1994) Growth dynamics of pancreatic islet cell populations during fetal and neonatal development of the rat. *Dev. Dyn.* **200**, 163-175.

Kawaguchi, Y., Cooper, B., Gannon, M., Ray, M., MacDonald, R. J. and Wright, C. V. (2002) The role of the transcriptional regulator Ptf1a in converting intestinal to pancreatic progenitors. *Nat. Genet.* **32**, 128-134.

Kawano, H., Daikoku, S. and Saito, S. (1983) Location of thyrotropin-releasing hormone-like immunoreactivity in rat pancreas. *Endocrinology* **112**, 951-955.

Kellett, M., Potten, C. S. and Rew, D. A. (1992) A comparison of *in vivo* cell proliferation measurement in the intestine of mouse and man. *Epith. Cell Biol.* **1**, 147-155.

Kido, Y., Nakae, J., Hribal, M. L., Xuan, S., Efstratiadis, A. and Accili, D. (2002) Effects of mutations in the insulin-like growth factor signaling system on embryonic pancreas development and β-cell compensation to insulin resistance. *J. Biol. Chem.* **277**, 36740-36747.

Kim, S. K., Hebrok, M. and Melton, D. A. (1997) Notochord to endoderm signaling is required for pancreas development. *Development* **124**, 4243-4252.

Kim, S. K. and Melton, D. A. (1998) Pancreas development is promoted by cyclopamine, a hedgehog signaling inhibitor. *Proc. Natl. Acad. Sci. USA* **95**, 13036-13041.

Kim, S. K., Hebrok, M., Li, E., Oh, S. P., Schrewe, H., Harmon, E. B., Lee, J. S. and Melton, D. A. (2000) Activin receptor patterning of foregut organogenesis. *Genes Dev.* **14**, 1866-1871.

Kim, S. K. and Hebrok, M. (2001) Intercellular signals regulating pancreas development and function. *Genes Dev.* **15**, 111-127.

Kopin, A. S., Mathes, W. F., Nguyen, M., Kethir, W., Schmitz, F., Bonner-Weir, S., Kanarek, R. and Beinborn, M. (1999) The cholecystokinin-A receptor mediates inhibition of food intake yet is not essential for the maintenance of body weight. *J. Clin. Invest.* **103**, 383-391.

Krakowski, M. L., Kritzik, M. R., Jones, E. M., Krahl, T., Lee, J., Arnush, M., Gu, D. and Sarvetnick, N. (1999) Pancreatic expression of keratinocyte growth factor leads to differentiation of islet hepatocytes and proliferation of duct cells. *Am. J. Pathol.* **154**, 683-691.

Krapp, A., Knöfler, M., Frutiger, S., Hughes, G. J., Hagenbüchle, O. and Wellauer, P. K. (1996) The p48 DNA-binding subunit of transcription factor PTF1 is a new exocrine pancreas-specific basic helix-loop-helix protein. *EMBO J.* **15**, 4317-4329.

Krapp, A., Knöfler, M., Ledermann, B., Bürki, K., Berney, C., Zoerkler, N., Hagenbüchle, O. and Wellauer, P. K. (1998) The bHLH protein PTF1-p48 is essential

for the formation of the exocrine and the correct spatial organization of the endocrine pancreas. *Genes. Dev.* **12**, 3752-3763.

Kruse, F., Rose, S. D., Swift, G. H., Hammer, R. E. and MacDonald, R. J. (1993) An endocrine-specific element is an integral component of an exocrine-specific pancreatic enhancer. *Genes Dev.* **7**, 774-786.

Kulkarni, R. N., Bruning, J. C., Winnay, J. N., Magnuson, M. and Kahn, C. R. (1998) Tissue-specific disruption of the insulin receptor in the pancreatic β-cell results in impaired glucose tolerance. *Diabetes* **47** Suppl. 1, abs. A57.

Kulkarni, R. N., Bruning, J. C., Winnay, J. N., Postic, C., Magnuson, M. A. and Kahn, C. R. (1999) Tissue-specific knockout of the insulin receptor in pancreatic β cells creates an insulin secretory defect similar to that in type 2 diabetes. *Cell* **96**, 329-339.

Kuo, C. F., Paulson, K. E. and Darnell, J. E. Jr. (1988) Positional and developmental regulation of glutamine synthetase expression in mouse liver. *Mol. Cell. Biol.* **8**, 4966-4971.

Kuo, C. J., Conley, P. B., Chen, L., Sladek, F. M., Darnell, J. E. Jr. and Crabtree, G. R. (1992) A transcriptional hierarchy involved in mammalian cell-type specification. *Nature* **355**, 457-461.

Lai, E., Prezioso, V. R., Tao, W. F., Chen, W. S. and Darnell, J. E. Jr. (1991) Hepatocyte nuclear factor 3 alpha belongs to a gene family in mammals that is homologous to the *Drosophila* homeotic gene fork head. *Genes Dev.* **5**, 416-427.

Lamers, W. H., Hilberts, A., Furt, E., Smith, J., Jonges, G. N., van Noorden, C. J., Janzen, J. W., Charles, R. and Moorman, A. F. (1989) Hepatic enzyme zonation: a reevaluation of the concept of the liver acinus. *Hepatology* **10**, 72-76.

Landry, C., Clotman, F., Hioki, T., Oda, H., Picard, J. J., Lemaigre, F. P. and Rousseau, G. G. (1997) HNF-6 is expressed in endoderm derivatives and nervous system of the mouse embryo and participates to the cross-regulatory network of liver-enriched transcription factors. *Dev. Biol.* **192**, 247-257.

Lannoy, V. J., Burglim, T. R., Rousseau, G. G. and Lemaigre, F. P. (1998) Isoforms of hepatocyte nuclear factor-6 differ in DNA-binding properties, contain a bifunctional homeodomain, and define the new ONECUT class of homeodomain proteins. *J. Biol. Chem.* **273**, 13552-13562.

Larsson, L. I., Boder, G. B. and Shaw, W. N. (1977) Changes in the islets of Langerhans in the obese Zucker rat. *Lab. Invest.* **36**, 593-598.

Larsson, L. I. (1998) On the development of the islets of Langerhans. *Microsc. Res. Tech.* **43**, 284-291.

Le Douarin, N. M. (1982) In *The Neural Crest* (ed. P. W. Barlow, P. B. Green and C. C. Wylie). London: Cambridge University Press.

Le Douarin, N. M. (1988) On the origin of pancreatic endocrine cells. *Cell* **53**, 169-171.

Leduque, P., Aratan-Spire, S., Czernichow, P. and Dubois, P. M. (1986) Ontogenesis of thyrotropin-releasing hormone in the human fetal pancreas. A combined radioimmunological and immunocytochemical study. *J. Clin. Invest.* **78**, 1028-1034.

Leduque, P., Aratan-Spire, S., Wolf, B., Dubois, P. M. and Czernichow, P. (1987) Localization of thyrotropin-releasing hormone- and insulin-immunoreactivity in the pancreas of neonatal rats after injection of streptozotocin at birth. *Cell Tissue Res.* **248**, 89-94.

Lee, B. C., Hendricks, J. D. and Bailey, G. S. (1989) Metaplastic pancreatic cells in liver tumors induced by diethylnitrosamine. *Exp. Mol. Pathol.* **50**, 104-113.

Lee, C. S., Sund, N. J., Vatamaniuk, M. Z., Matschinsky, F. M., Stoffers, D. A. and Kaestner, K. H. (2002) Foxa2 controls Pdx1 gene expression in pancreatic β-cells *in vivo*. *Diabetes* **51**, 2546-2551.

Lee, J. E., Hollenberg, S. M., Snider, L., Turner, D. L., Lipnick, N. and Weintraub, H. (1995) Conversion of *Xenopus* ectoderm into neurons by NeuroD, a basic helix-loop-helix protein. *Science* **268**, 836-844.

Lee, Y. H., Sauer, B. and Gonzalez, F. J. (1998) Laron dwarfism and non-insulin-dependent diabetes mellitus in the hnf-1α knockout mouse. *Mol. Cell. Biol.* **18**, 3059-3068.

Lehninger, A. L., Nelson, D. L. and Cox, M. M. (1993) *Principles of Biochemistry*, 2nd edition. New York: Worth Publishers, Inc.

Lehv, M. and Fitzgerald, P. J. (1968) Pancreatic acinar cell regeneration IV. Regeneration after surgical resection. *Am. J. Pathol.* **53**, 513-535.

Leibiger, I. B., Leibiger, B., Moede, T. and Berggren, P. O. (1998) Exocytosis of insulin promotes insulin gene transcription via the insulin receptor/PI-3 kinase/p70 s6 kinase and CaM kinase pathways. *Mol. Cell* **1**, 933-938.

Lemaigre, F. P., Durviaux, S. M., Truong, O., Lannoy, V. J., Hsuan, J. J. and Rousseau, G. G. (1996) Hepatocyte nuclear factor 6, a transcription factor that contains a novel type of homeodomain and a single cut domain. *Proc. Natl. Acad. Sci. USA* **93**, 9460-9464.

Lendahl, U., Zimmerman, L. B. and McKay, R. D. (1990) CNS stem cells express a new class of intermediate filament protein. *Cell* **60**, 585-595.

Leonard, J., Serup, P., Gonzalez, G., Edlund, T. and Montminy, M. (1992) The LIM family transcription factor Isl-1 requires cAMP response element binding protein to promote somatostatin expression in pancreatic islet cells. *Proc. Natl. Acad. Sci. USA* **89**, 6247-6251.

Leonard, J., Peers, B., Johnson, T., Ferreri, K., Lee, S. and Montminy, M. R. (1993) Characterization of somatostatin transactivating factor-1, a novel homeobox factor that stimulates somatostatin expression in pancreatic islet cells. *Mol. Endocrinol.* **7**, 1275-1283.

LeRoith, D. (1991) *Insulin-Like Growth Factors: Molecular and Cellular Aspects*, pp. 88-110. Boca Raton, FL.: CRC Press.

LeRoith, D., Werner, H., Beitner-Johnson, D. and Roberts, C. T. (1995) Molecular and cellular aspects of the insulin-like growth factor 1 receptor. *Endocr. Rev.* **16**, 143-163.

LeRoith, D. (1997) Insulin-like growth factors. *N. Engl. J. Med.* **336**, 633-640.

Lewis, J. (1996) Neurogenic genes and vertebrate neurogenesis. *Curr. Opin. Neurobiol.* **6**, 3-10.

Li, H., Arber, S., Jessell, T. M. and Edlund, H. (1999) Selective agenesis of the dorsal pancreas in mice lacking homeobox gene Hlxb9. *Nat. Genet.* **23**, 67-70.

Li, Y. Q., Roberts, S. A., Paulus, U., Loeffler, M. and Potten, C. S. (1994) The crypt cycle in mouse small intestinal epithelium. *J. Cell Sci.* **107**, 3271-3279.

Like, A. A. and Chick, W. L. (1970) Studies in the diabetic mutant mouse: electron microscopy of pancreatic islets. *Diabetologia* **6**, 216-242.

Lindner, T. H., Njolstad, P. R., Horikawa, Y., Bostad, L., Bell, G. I. and Sovik, O. (1999) A novel syndrome of diabetes mellitus, renal dysfunction and genital malformation associated with a partial deletion of the pseudo-POU domain of hepatocyte nuclear factor-1 beta. *Hum. Mol. Genet.* **8**, 2001-2008.

Liu, J.-K., DiPersio, C. M. and Zaret, K. S. (1991) Extracellular signals that regulate liver transcription factors during hepatic differentiation *in vitro*. *Mol. Cell. Biol.* **11**, 773-784.

Liu, J.-P., Baker, J., Perkins, A. S., Robertson, E. J. and Efstratiadis, A. (1993) Mice carrying null mutations of the genes encoding insulin-like growth factor I (Igf-1) and type 1 IGF receptor (Igf1r). *Cell* **75**, 59-72.

Lobe, C. G., Koop, K. E., Kreppner, W., Lomeli, H., Gertsenstein, M. and Nagy, A. (1999) Z/AP, a double reporter for cre-mediated recombination. *Dev. Biol.* **208**, 281-292.

Lobie, P. E., Breipohl, W. and Waters, M. J. (1990) Growth hormone receptor expression in the rat gastrointestinal tract. *Endocrinology* **126**, 299-306.

Loeffler, M., Stein, R., Wichmann, H. E., Potten, C. S., Kaur, P. and Chwalinski, S. (1986) Intestinal cell proliferation. I. A comprehensive model of steady-state proliferation in the crypt. *Cell Tissue Kinet.* **19**, 627-645.

Loeffler, M. and Grossmann, B. (1991) A stochastic branching model with formation of subunits applied to the growth of intestinal crypts. *J. Theor. Biol.* **150**, 175-191.

Loeffler, M., Birke, A., Winton, D. J. and Potten, C. S. (1993) Somatic mutation, monoclonality and stochastic models of stem cell organisation in the intestinal crypt. *J. Theor. Biol.* **160**, 471-491.

Loeffler, M., Bratke, T., Paulus, U., Li, Y. Q. and Potten, C. S. (1997) Clonality and life cycles of intestinal crypts explained by a state-dependent stochastic model of epithelial stem cell organisation. *J. Theor. Biol.* **186**, 41-54.

Logsdon, C. D., Moessner, J., William, J. A. and Goldfine, I. D. (1985) Glucocorticoids increase amylase mRNA levels, secretory organelles, and secretion in pancreatic acinar AR42J cells. *J. Cell. Biol.* **100**, 1200-1208.

Louvi, A., Accili, D. and Efstratiadis, A. (1997) Growth-promoting interaction of IGF-II with the insulin receptor during mouse embryonic development. *Dev. Biol.* **189**, 33-48.

Ludwig, C. U., Menke, A., Adler, G. and Lutz, M. P. (1999) Fibroblasts stimulate acinar cell proliferation through IGF-I during regeneration from acute pancreatitis. *Am. J. Physiol.* **276**, G193-198.

Ludwig, T., Eggenschwiler, J., Fisher, P., D'Ercole, A. J., Davenport, M. L. and Efstratiadis, A. (1996) Mouse mutants lacking the type 2 IGF receptor (IGF2R) are rescued from perinatal lethality in Igf2 and Igf1r null backgrounds. *Dev. Biol.* **177**, 517-535.

Lyon, M. F. (1961) Gene action in the X-chromosome of the mouse (*Mus. musculus* L.). *Nature* **190**, 372-373.

Lyon, M. F., Searle, A. G., Ford, C. E. and Ohno, S. (1964) A mouse translocation suppressing sex-linked variegation. *Cytogenetics* **3**, 306-323.

Lyons, K., Hogan, B. and Robertson, E. (1995) Colocalization of BMP 7 and BMP 2 RNAs suggests that these factors cooperatively mediate tissue interactions during mouse development. *Mech. Dev.* **50**, 71-83.

Ma, Q., Chen, Z., del Barco Barrantes, I., de la Pompa, J. L. and Anderson, D. J. (1998) *neurogenin1* is essential for the determination of neuronal precursors for proximal cranial sensory ganglia. *Neuron* **20**, 469-482.

Maake, C. and Reinecke, M. (1993) Immunohistochemical localization of insulin-like growth factor 1 and 2 in the endocrine pancreas of rat, dog, and man, and their coexistence with classical islet hormones. *Cell Tissue Res.* **273**, 249-259.

Madsen, O. D., Jensen, J., Blume, N., Petersen, H. V., Lund, K., Karlsen, C., Andersen, F. G., Jensen, P. B., Larsson, L.-I. and Serup, P. (1996) Pancreatic development and maturation of the islet B cell - studies of pluripotent islet cultures. *Eur. J. Biochem.* **242**, 435-445.

Malecki, M. T., Jhala, U. S., Antonellis, A., Fields, L., Doria, A., Orban, T., Saad, M., Warram, J. H., Montminy, M. and Krolewski, A. S. (1999) Mutations in NEUROD1 are associated with the development of type 2 diabetes mellitus. *Nat. Genet.* **23**, 323-328.

Manson, J. M., Freyssinges, C., Ducrocq, M. B. and Stephenson, W. P. (1996) Postmarketing surveillance of lovastatin and simvastatin exposure during pregnancy. *Reprod. Toxicol.* **10**, 439-446.

Marks, V. (1971) In *Current Topics on Glucagon, Proceedings of the European Day on Glucagon* (ed. M. Austoni, C. Scandellari, C. Federspil and A. Trisotto), p. 63. Padua.

Martino, E., Lernmark, A., Seo, H., Steiner, D. F. and Refetoff, S. (1978) High concentration of thyrotropin-releasing hormone in pancreatic islets. *Proc. Natl. Acad. Sci. USA* **75**, 4265-4267.

Marynissen, G., Aerts, L. and Van Assche, F. A. (1983) The endocrine pancreas during pregnancy and lactation in the rat. *J. Dev. Physiol.* **5**, 373-381.

Mashima, H., Ohnishi, H., Wakabayashi, K., Mine, T., Miyagawa, J., Hanafusa, T., Seno, M., Yamada, H. and Kojima, I. (1996a) Betacellulin and activin A coordinately convert amylase-secreting pancreatic AR42J cells into insulin-secreting cells. *J. Clin. Invest.* **97**, 1647-1654.

Mashima, H., Shibata, H., Mine, T. and Kojima, I. (1996b) Formation of insulin-producing cells from pancreatic acinar AR42J cells by hepatocyte growth factor. *Endocrinology* **137**, 3969-3976.

Mason, I., Fuller-Pace, F., Smith, R. and Dickson, C. (1994) FGF-7 (keratinocyte growth factor) expression during mouse development suggests roles in myogenesis, forebrain regionalization and epithelial-mesenchymal interactions. *Mech. Dev.* **45**, 15-30.

McCusker, R. H. and Clemmons, D. R. (1992) The insulin-like growth factor binding proteins: structure and biological functions. In *The Insulin-Like Growth Factors, Structure and Biological Functions* (ed. P. N. Schofield), pp.110-150. Oxford: Oxford University Press.

McGinnis, W. and Krumlauf, R. (1992) Homeobox genes and axial patterning. *Cell* **68**, 283-302.

McMahon, A. and Monk, M. (1983) X-chromosome activity in female mouse embryos heterozygous for *Pgk-1* and Searle's translocation, T(X; 16) 16H. *Genet. Res.* **41**, 69-83.

Metzger, D., Clifford, J., Chiba, H. and Chambon, P. (1995) Conditional site-specific recombination in mammalian cells using a ligand-dependent chimeric Cre recombinase. *Proc. Natl. Acad. Sci. USA* **92**, 6991-6995.

Miettinen, P. J. and Heikinheimo, K. (1992) Transforming growth factor-α (TGF-α) and insulin gene expression in human fetal pancreas. *Development* **114**, 833-840.

Miettinen, P. J., Otonkoski, T. and Voutilainen, R. (1993) Insulin-like growth factor-II and transforming growth factor-α in developing human fetal pancreatic islets. *J. Endocrinol.* **138**, 127-136.

Miller, C. P., McGehee, R. E. Jr. and Habener, J. F. (1994) IDX-1: a new homeodomain transcription factor expressed in rat pancreatic islets and duodenum that transactivates the somatostatin gene. *EMBO J.* **13**, 1145-1156.

Miralles, F., Battelino, T., Czernichow, P. and Scharfmann, R. (1998a) TGF-beta plays a key role in morphogenesis of the pancreatic islets of Langerhans by controlling the activity of the matrix metalloproteinase MMP-2. *J. Cell Biol.* **143**, 827-836.

Miralles, F., Czernichow, P. and Scharfmann, R. (1998b) Follistatin regulates the relative proportions of endocrine versus exocrine tissue during pancreatic development. *Development* **125**, 1017-1024.

Miralles, F., Philippe, P., Czernichow, P. and Scharfmann, R. (1998c) Expression of nerve growth factor and its high-affinity receptor Trk-A in the rat pancreas during embryonic and fetal life. *J. Endocrinol.* **156**, 431-439.

Miralles, F., Czernichow, P., Ozaki, K., Itoh, N. and Scharfmann, R. (1999) Signaling through fibroblast growth factor receptor 2b plays a key role in the development of the exocrine pancreas. *Proc. Natl. Acad. Sci. USA* **96**, 6267-6272.

Miyata, T., Maeda, T. and Lee, J. E. (1999) NeuroD is required for differentiation of the granule cells in the cerebellum and hippocampus. *Genes Dev.* **13**, 1647-1652.

Monaghan, A. P., Kaestner, K. H., Grau, E. and Schutz, G. (1993) Postimplantation expression patterns indicate a role for the mouse forkhead/HNF-3 alpha, beta and gamma genes in determination of the definitive endoderm, chordamesoderm and neuroectoderm. *Development* **119**, 567-578.

Montana, E., Bonner-Weir, S. and Weir, G. C. (1994) Transplanted beta cell response to increased metabolic demand. *J. Clin. Invest.* **93**, 1577-1582.

Montanya, E., Nacher, V., Biarnés, M. and Soler, J. (2000) Linear correlation between β-cell mass and body weight throughout the lifespan in Lewis rats: role of β-cell hyperplasia and hypertrophy. *Diabetes* **49**, 1341-1346.

Mood, A. M. (1954) On the asymptotic efficiency of certain non-parametric two-sample tests. *Ann Math. Statist.* **25**, 514-522.

Moorman, A. F., de Boer, P. A., Geerts, W. J., van den Zande, L., Lamers, W. H. and Charles, R. (1988) Complementary distribution of carbamoylphosphate synthetase (ammonia) and glutamine synthetase in rat liver acinus is regulated at a pretranslational level. *J. Histochem. Cytochem.* **36**, 751-755.

Moorman, A. F. M., de Boer, P. A. J., Charles, R. and Lamers, W. H. (1990) Diet- and hormone-induced reversal of the carbamoylphosphate synthetase mRNA gradient in the rat liver lobulus. *FEBS Lett.* **276**, 9-13.

Morrione, A., Valentinis, B., Xu, S. Q., Yumet, G., Louvi, A., Efstratiadis, A. and Baserga, R. (1997) Insulin-like growth factor II stimulates cell proliferation though the insulin receptor. *Proc. Natl. Acad. Sci. USA* **94**, 3777-3782.

Mutoh, H., Naya, F. J., Tsai, M. J. and Leiter, A. B. (1998) The basic helix-loop-helix protein BETA2 interacts with p300 to coordinate differentiation of secretin-expressing enteroendocrine cells. *Genes Dev.* **12**, 820-830.

Nagy, A. and Mar, L. (2001) Creation and use of a Cre recombinase transgenic database. *Methods Mol. Biol.* **158**, 95-106.

Nakamura, T., Takio, K., Eto, Y., Shibai, H., Titani, K. and Sugino, H. (1990) Activin-binding protein from rat ovary is follistatin. *Science* **247**, 836-838.

Narushima, Y., Unno, M., Nakagawara, K., Mori, M., Miyashita, H., Suzuki, Y., Noguchi, N., Takasawa, S., Kumagai, T., Yonekura, H. and Okamoto, H. (1997) Structure, chromosomal localization and expression of mouse genes encoding type III reg, regIIIα, regIIIβ, regIIIγ. *Gene* **185**, 159-168.

Naya, F. J., Stellrecht, C. M. M. and Tsai, M.-J. (1995) Tissue-specific regulation of the insulin gene by a novel basic helix-loop-helix transcription factor. *Genes Dev.* **9**, 1009-1019.

Naya, F. J., Huang, H.-P., Qiu, Y., Mutoh, H., DeMayo, F. J., Leiter, A. B. and Tsai, M.-J. (1997) Diabetes, defective pancreatic morphogenesis, and abnormal

enteroendocrine differentiation in BETA2/neuroD-deficient mice. *Genes Dev.* **11**, 2323-2334.

Nguyen, H. Q., Danilenko, D. M., Bucay, N., DeRose, M. L., Van, G. Y., Thomason, A. and Simonet, W. S. (1996) Expression of keratinocyte growth factor in embryonic liver of transgenic mice causes changes in epithelial growth and differentiation resulting in polycystic kidneys and other organ malformations. *Oncogene* **12**, 2109-2119.

Nielsen, J. H. (1982) Effects of growth hormone, prolactin, and placental lactogen on insulin content and release, and deoxyribonucleic acid synthesis in cultured pancreatic islets. *Endocrinology* **110**, 600-606.

Nielsen, J. H., Galsgaard, E. D., Møldrup, A., Friedrichsen, B. N., Billestrup, N., Hansen, J. A., Lee, Y. C. and Carlsson, C. (2001) Regulation of β-cell mass by hormones and growth factors. *Diabetes* **50** Suppl. 1, S25-29.

Nishigori, H., Yamada, S., Kohama, T., Tomura, H., Sho, K., Horikawa, Y., Bell, G. I., Takeuchi, T. and Takeda, J. (1998) Frameshift mutation, A263fsinsGG, in the hepatocyte nuclear factor-1beta gene associated with diabetes and renal dysfunction. *Diabetes* **47**, 1354-1355.

Nomura, S., Esumi, H., Job, C. and Tan, S.-S. (1998) Lineage and clonal development of gastric glands. *Dev. Biol.* **204**, 124-135.

Oberg-Welsh, C., Sandler, S., Andersson, A. and Welsh, M. (1997) Effects of vascular endothelial growth factor on pancreatic duct cell replication and the insulin production of fetal islet-like cell clusters *in vitro*. *Mol. Cell. Endocrinol.* **126**, 125-132.

O'Brien, R. M. and Granner, D. K. (1996) Regulation of gene expression by insulin. *Physiol. Rev.* **76**, 1109-1161.

Offield, M. F., Jetton, T. L., Labosky, P. A., Ray, M., Stein, R. W., Magnuson, M. A., Hogan, B. L. M. and Wright, C. V. E. (1996) PDX-1 is required for pancreatic outgrowth and differentiation of the rostral duodenum. *Development* **122**, 983-995.

Ogawa, K., Abe, K., Kurosawa, N., Kurohmaru, M., Sugino, H., Takahashi, M. and Hayashi, Y. (1993) Expression of α, βA and βB subunits of inhibin or activin and follistatin in rat pancreatic islets. *FEBS Lett.* **319**, 217-220.

Ohlsson, H., Karlsson, K. and Edlund, T. (1993). IPF-1, a homeodomain-containing transactivator of the insulin gene. *EMBO J.* **12**, 4251-4259.

Okada, T. S. (1986) Transdifferentiation in animal cells: fact or artifact. *Dev. Growth Diff.* **28**, 213-221.

Okada, T. S. (1991) *Transdifferentiation. Flexibility in Cell Differentiation.* Oxford: Clarendon.

Orci, L., Malaisse-Lagae, F., Ravazzola, M., Rouiller, D., Renold, A. E., Perrelet, A. and Unger, R. J. (1975) A morphological basis for intercellular communication between alpha- and beta-cells in the endocrine pancreas. *J. Clin. Invest.* **56**, 1066-1070.

Orci, L. and Unger, R. H. (1975) Functional subdivision of islets of Langerhans and possible role of D cells. *Lancet* **2**, 1243-1244.

Ornitz, D. M., Palmiter, R. D., Hammer, R. E., Brinster, R. L., Swift, G. H. and MacDonald, R. J. (1985) Specific expression of an elastase-human growth hormone fusion gene in pancreatic acinar cells of transgenic mice. *Nature* **313**, 600-602.

Ornitz, D. M., Xu, J., Colvin, J. S., McEwen, D. G., MacArthur, C. A., Coulier, F., Gao, G. and Goldfarb, M. (1996) Receptor specificity of the fibroblast growth factor family. *J. Biol. Chem.* **271**, 15292-15297.

Orr-Urtreger, A., Bedford, M. T., Burakova, T., Arman, E., Zimmer, Y., Yayon, A., Givol, D. and Lonai, P. (1993) Developmental localization of the splicing alternatives of fibroblast growth factor receptor-2 (FGFR2). *Dev. Biol.* **158**, 475-486.

Osborne, T. F. (1991) Single nucleotide resolution of sterol regulatory region in promoter for 3-hydroxy-3-methylglutaryl coenzyme A reductase. *J. Biol. Chem.* **266**, 13947-13951.

Oster, A., Jensen, J., Serup, P., Galante, P., Madsen, O. D. and Larsson, L. I. (1998) Rat endocrine pancreatic development in relation to two homeobox gene products (Pdx-1 and Nkx 6.1). *J. Histochem. Cytochem.* **46**, 707-715.

Otonkoski, T., Andersson, S., Knip, M. and Simell, O. (1988a) Maturation of insulin response to glucose during human fetal and neonatal development. *Diabetes* **37**, 286-291.

Otonkoski, T., Knip, M., Wong, I. and Simell, O. (1988b) Effects of growth hormone and insulin-like growth factor I on endocrine function of human fetal islet-like cell clusters during long-term tissue culture. *Diabetes* **37**, 1678-1683.

Otonkoski, T., Beattie, G. M., Rubin, J. S., Lopez, A. D., Baird, A. and Hayek, A. (1994a) Hepatocyte growth factor/scatter factor has insulinotropic activity in human fetal pancreatic cells. *Diabetes* **43**, 947-953.

Otonkoski, T., Mally, M. I. and Hayek, A. (1994b) Opposite effects of β-cell differentiation and growth on reg expression in human fetal pancreatic cells. *Diabetes* **43**, 1164-1166.

Otonkoski, T., Cirulli, V., Beattie, G. M., Mally, M. I., Soto, G., Rubin, J. S. and Hayek, A. (1996) A role for hepatocyte growth factor/scatter factor in fetal mesenchyme-induced pancreatic β-cell growth. *Endocrinology* **137**, 3131-3139.

Ouafik, L., Giraud, P., Salers, P., Dutour, A., Castanas, E., Boudouresque, F. and Oliver, C. (1987) Evidence for high peptide α-amidating activity in the pancreas from neonatal rats. *Proc. Natl. Acad. Sci. USA* **84**, 261-264.

Palmiter, R. D., Behringer, R. R., Quaife, C. J., Maxwell, F., Maxwell, I. H. and Brinster, R. L. (1987) Cell lineage ablation in transgenic mice by cell-specific expression of a toxin gene. *Cell* **50**, 435-443.

Parsons, J. A., Hartfel, M. A., Hegre, O. D. and McEvoy, R. C. (1983) Effect of MtTW15 mammosomatotropic tumors on pancreatic islet hormones. *Diabetes* **32**, 67-74.

Parsons, J. A., Brelje, T. C. and Sorenson, R. L. (1992) Adaptation of islets of Langerhans to pregnancy: increased islet cell proliferation and insulin secretion correlates with the onset of placental lactogen secretion. *Endocrinology* **130**, 1459-1466.

Parsons, J. A., Bartke, A. and Sorenson, R. L. (1995) Number and size of islets of Langerhans in pregnant, human growth hormone-expressing transgenic, and pituitary dwarf mice: effect of lactogenic hormones. *Endocrinology* **136**, 2013-2021.

Pearse, A. G. E. (1984) Islet development and the APUD concept. In *Pancreatic Pathology* (ed. G. Klippel and P. U. Heitz), pp. 125-132. Edinburgh: Churchill Livingstone, Inc.

Peers, B., Sharma, S., Johnson, T., Kamps, M. and Montminy, M. (1995) The pancreatic islet factor STF-1 binds cooperatively with Pbx to a regulatory element in the

somatostatin promoter: importance of the FPWMK motif and of the homeodomain. *Mol. Cell. Biol.* **15**, 7091-7097.

Percival, A. C. and Slack, J. M. W. (1999) Analysis of pancreatic development using a cell lineage label. *Exp. Cell Res.* **247**, 123-132.

Peshavaria, M., Gamer, L., Henderson, E., Teitelman, G., Wright, C. V. E. and Stein, R. (1994) XlHbox 8, an endoderm-specific *Xenopus* homeodomain protein, is closely related to a mammalian insulin gene transcription factor. *Mol. Endocrinol.* **8**, 806-816.

Petersen, H. V., Serup, P., Leonard, J., Michelsen, B. K. and Madsen, O. D. (1994) Transcriptional regulation of the human insulin gene is dependent on the homeodomain protein STF1/IPF1 acting through the CT boxes. *Proc. Natl. Acad. Sci. USA* **91**, 10465-10469.

Petrik, J., Arany, E., McDonald, T. J. and Hill, D. J. (1998) Apoptosis in the pancreatic islet cells of the neonatal rat is associated with a reduced expression of insulin-like growth factor II that may act as a survival factor. *Endocrinology* **139**, 2994-3004.

Petrik, J., Pell, M., Arany, E., McDonald, T. J., Dean, W. L., Reik, W. and Hill, D. J. (1999) Overexpression of insulin-like growth factor-II in transgenic mice is associated with pancreatic islet cell hyperplasia. *Endocrinology* **140**, 2353-2363.

Petrucco, S., Wellauer, P. K. and Hagenbüchle, O. (1990) The DNA-binding activity of transcription factor PTF1 parallels the synthesis of pancreas-specific mRNAs during mouse development. *Mol. Cell. Biol.* **10**, 254-264.

Pfaff, S. L., Mendelsohn, M., Stewart, C. L., Edlund, T. and Jessell, T. M. (1996) Requirement for LIM homeobox gene Isl1 in motor neuron generation reveals a motor neuron-dependent step in interneuron differentiation. *Cell* **84**, 309-320.

Pictet, R. L., Clarke, W. R., Williams, R. H. and Rutter, W. J. (1972) An ultrastructural analysis of the developing embryonic pancreas. *Dev. Biol.* **29**, 436-467.

Pictet, R. and Rutter, W. J. (1972) Development of the embryonic endocrine pancreas. In *Handbook of Physiology*, section 7, vol. 1, American Physiological Society (ed. D. F. Steiner and N. Frenkel), pp. 25-66. Washington DC: The Williams and Wilkins Co.

Polonsky, K. S. (1995) Lilly Lecture 1994. The β-cell in diabetes: from molecular genetics to clinical research. *Diabetes* **44**, 705-717.

Ponder, B. A. J., Schmidt, G. H., Wilkinson, M. M., Wood, J., Monk, M. and Reid, A. (1985) Derivation of mouse intestinal crypts from a single progenitor cell. *Nature* **313**, 689-691.

Pontoglio, M., Sreenan, S., Roe, M., Pugh, W., Ostrega, D., Doyen, A., Pick, A. J., Baldwin, A., Velho, G., Froguel, P., Levisetti, M., Bonner-Weir, S., Bell, G. I., Yaniv, M. and Polonsky, K. S. (1998) Defective insulin secretion in hepatocyte nuclear factor 1α-deficient mice. *J. Clin. Invest.* **101**, 2215-2222.

Porter, S. E., Sorenson, R. L., Dann, P., Garcia-Ocana, A., Stewart, A. F. and Vasavada, R. C. (1998) Progressive pancreatic islet hyperplasia in the islet-targeted, parathyroid hormone-related protein-overexpressing mouse. *Endocrinology* **139**, 3743-3751.

Potten, C. S. and Hendry, J. H. (1983) Stem cells in murine small intestine. In *Stem Cells* (ed. C. S. Potten), pp. 159-199. New York: Churchill Livingstone, Inc.

Potten, C. S. and Loeffler, M. (1987) A comprehensive model of the crypts of the small intestine of the mouse provides insight into the mechanisms of cell migration and the proliferation hierarchy. *J. Theor. Biol.* **127**, 381-391.

Potten, C. S. and Loeffler, M. (1990) Stem cells: attributes, cycles, spirals, pitfalls and uncertainties. Lessons for and from the crypt. *Development* **110**, 1001-1020.

Prasadan, K., Daume, E., Preuett, B., Spilde, T., Bhatia, A., Kobayashi, H., Hembree, M., Manna, P. and Gittes, G. K. (2002) Glucagon is required for early insulin-positive differentiation in the developing mouse pancreas. *Diabetes* **51**, 3229-3236.

Quaife, C. J., Mathews, L. S., Pinkert, C. A., Hammer, R. E., Brinster, R. L. and Palmiter, R. D. (1989) Histopathology associated with elevated levels of growth hormone and insulin-like growth factor-I in transgenic mice. *Endocrinology* **124**, 40-48.

Qureschi, N. and Porter, J. W. (1981) *Biosynthesis of Isoprenoid Compounds* (ed. J. W. Porter and S. L. Spurgeon). New York: Wiley.

Rafaeloff, R., Barlow, S. W., Rosenberg, L. and Vinik, A. I. (1995) Expression of reg gene in the Syrian golden hamster pancreatic islet regeneration model. *Diabetologia* **38**, 906-913.

Rafaeloff, R., Pittenger, G. L., Barlow, S. W., Qin, X. F., Yan, B., Rosenberg, L., Duguid, W. P. and Vinik, A. I. (1997) Cloning and sequencing of the pancreatic islet

neogenesis associated protein (INGAP) gene and its expression in islet neogenesis in hamsters. *J. Clin. Invest.* **99**, 2100-2109.

Rao, M. S., Bendayan, M., Kimbrough, R. D. and Reddy, J. K. (1986a) Characterization of pancreatic-type tissue in the liver of rat induced by polychlorinated biphenyls. *J. Histochem. Cytochem.* **34**, 197-201.

Rao, M. S., Subbarao, V. and Reddy, J. K. (1986b) Induction of hepatocytes in the pancreas of copper-depleted rats following copper repletion. *Cell Differentiation* **18**, 109-117.

Rao, M. S., Dwivedi, R. S., Yeldandi, A. V., Subbarao, V., Tan, X., Usman, M. I., Thangada, S., Nemali, M. R., Kumar, S., Scarpelli, D. G. and Reddy, J. K. (1989) Role of periductal and ductular epithelial cells of the adult rat pancreas in pancreatic hepatocyte lineage. *Am. J. Pathol.* **134**, 1069-1086.

Rao, M. S., Yeldandi, A. V. and Reddy, J. K. (1990) Stem cell potential of ductular and periductular cells in the adult rat pancreas. *Cell Diff. Dev.* **29**, 155-163.

Rao, M. S. and Reddy, J. K. (1995) Hepatic transdifferentiation in the pancreas. *Semin. Cell Biol.* **6**, 151-156.

Rappaport, A. M. (1973) The microcirculatory hepatic unit. *Microvasc. Res.* **6**, 212-228.

Rausa, F., Samadani, U., Ye, H., Lim, L., Fletcher, C. F., Jenkins, N. A., Copeland, N. G. and Costa, R. H. (1997) The cut-homeodomain transcriptional activator HNF-6 is coexpressed with its target gene HNF-3β in the developing murine liver and pancreas. *Dev. Biol.* **192**, 228-246.

Ritvos, O., Tuuri, T., Eramaa, M., Sainio, K., Hilden, K., Saxen, L. and Gilbert, S. F. (1995) Activin disrupts epithelial branching morphogenesis in developing glandular organs of the mouse. *Mech. Dev.* **50**, 229-245.

Roberts, D. J., Johnson, R. L., Burke, A. C., Nelson, C. E. and Morgan, B. A. (1995) Sonic hedgehog is an endodermal signal inducing BMP-4 and Hox genes during induction and regionalization of the chick hindgut. *Development* **121**, 3163-3174.

Roberts, D. J., Smith, D. M., Goff, D. J. and Tabin, C. J. (1998) Epithelial-mesenchymal signaling during the regionalization of the chick gut. *Development* **125**, 2791-2801.

Ronzio, R. A. and Rutter, W. J. (1973) Effects of a partially purified factor from chick embryos on macromolecular synthesis of embryonic pancreatic epithelia. *Dev. Biol.* **30**, 307-320.

Rooman, I., Schuit, F. and Bouwens, L. (1997) Effect of vascular endothelial growth factor on growth and differentiation of pancreatic ductal epithelium. *Lab. Invest.* **76**, 225-232.

Rose, M. I., Crisera, C. A., Colen, K. L., Connelly, P. R., Longaker, M. T. and Gittes, G. K. (1999) Epithelio-mesenchymal interactions in the developing mouse pancreas: morphogenesis of the adult architecture. *J. Pediatr. Surg.* **34**, 774-779.

Rosenbaum, T., Vidaltamayo, R., Sanchez-Soto, M. C., Zentella, A. and Hiriart, M. (1998) Pancreatic β cells synthesize and secrete nerve growth factor. *Proc. Natl. Acad. Sci. USA* **95**, 7784-7788.

Rosenberg, L., Brown, R. A. and Duguid, W. P. (1983) A new approach to the induction of duct epithelial hyperplasia and nesidioblastosis by cellophane wrapping of the hamster pancreas. *J. Surg. Res.* **35**, 63-72.

Rosenberg, L. (1995) *In vivo* cell transformation: neogenesis of beta cells from pancreatic ductal cells. *Cell Transplant.* **4**, 371-383.

Rossant, J. and McMahon, A. (1999) "Cre"-ating mouse mutants - a meeting review on conditional mouse genetics. *Genes Dev.* **13**, 142-145.

Rouiller, D. G., Cirulli, V. and Halban, P. A. (1990) Differences in aggregation properties and levels of neural cell adhesion molecule (NCAM) between islet cell types. *Exp. Cell Res.* **191**, 305-312.

Royster, M., Driscoll, P., Kelly, P. A. and Freemark, M. (1995) The prolactin receptor in the fetal rat: cellular localization of messenger ribonucleic acid, immunoreactive protein, and ligand-binding activity and induction of expression in late gestation. *Endocrinology* **136**, 3892-3900.

Rudnick, A., Ling, T. Y., Odagiri, H., Rutter, W. J. and German, M. S. (1994) Pancreatic beta cells express a diverse set of homeobox genes. *Proc. Natl. Acad. Sci. USA* **91**, 12203-12207.

Ruiz i Altaba, A., Prezioso, V. R., Darnell, J. E. and Jessell, T. M. (1993) Sequential expression of HNF-3 beta and HNF-3 alpha by embryonic organizing centers: the dorsal lip/node, notochord and floor plate. *Mech. Dev.* **44**, 91-108.

Rutter, W. J., Wessells, N. K. and Grobstein, C. (1964) Control of specific synthesis in the developing pancreas. *Natl. Cancer Inst. Monographs* **13**, 51-65.

St. Clair, W. H. and Osborne, J. W. (1985) Crypt fission and crypt number in the small and large bowel of adult rats. *Cell Tissue Kinet.* **14**, 467-477.

St.-Onge, L., Sosa-Pineda, B., Chowdhury, K., Mansouri, A. and Gruss, P. (1997) Pax6 is required for differentiation of glucagon-producing alpha-cells in mouse pancreas. *Nature* **387**, 406-409.

St.-Onge, L., Wehr, R. and Gruss, P. (1999) Pancreas development and diabetes. *Curr. Opin. Genet. Dev.* **9**, 295-300.

Samols, E., Tyler, J. M. and Mialhe, P. (1969) Suppression of pancreatic glucagon release by the hypoglycaemic sulphonylureas. *Lancet* **1**, 174-176.

Sander, M. and German, M. S. (1997) The β cell transcription factors and development of the pancreas. *J. Mol. Med.* **75**, 327-340.

Sander, M., Neubüser, A., Kalamaras, J., Ee, H. C., Martin, G. R. and German, M. S. (1997) Genetic analysis reveals that PAX6 is required for normal transcription of pancreatic hormone genes and islet development. *Genes Dev.* **11**, 1662-1673.

Sander, M., Sussel, L., Conners, J., Scheel, D. W., Kalamaras, J., Dela Cruz, F., Schwitzgebel, V. M., Hays-Jordan, A. and German, M. S. (2000) Homeobox gene Nkx6.1 lies downstream of Nkx2.2 in the major pathway of β-cell formation in the pancreas. *Development* **127**, 5533-5540.

Sandgren, E. P., Luetteke, N. C., Palmiter, R. D., Brinster, R. L. and Lee, D. C. (1990) Overexpression of TGFα in transgenic mice: induction of epithelial hyperplasia, pancreatic metaplasia, and carcinoma of the breast. *Cell* **61**, 1121-1135.

Sanvito, F., Herrera, P. L., Huarte, J., Nichols, A., Montesano, R., Orci, L. and Vassalli, J. D. (1994) TGFβ-1 influences the relative development of the exocrine and endocrine pancreas *in vitro*. *Development* **120**, 3451-3462.

Sasai, Y., Kageyama, R., Tagawa, Y., Shigemoto, R. and Nakanishi, S. (1992) Two mammalian helix-loop-helix factors structurally related to *Drosophila hairy* and *Enhancer of split*. *Genes Dev.* **6**, 2620-2634.

Sasaki, H. and Hogan, B. L. (1993) Differential expression of multiple fork head related genes during gastrulation and axial pattern formation in the mouse embryo. *Development* **118**, 47-59.

Satomura, Y., Sawabu, N., Ohta, H., Watanabe, H., Yamakawa, O., Motoo, Y., Okai, T., Toya, D., Makino, H. and Okamoto, H. (1993) The immunohistochemical evaluation of PSP/reg-protein in normal and diseased human pancreatic tissues. *Int. J. Pancreatol.* **13**, 59-67.

Sauer, B. (1993) Manipulation of transgenes by site-specific recombination: use of Cre recombinase. *Methods Enzymol.* **225**, 890-900.

Sauer, B. (1994) Site-specific recombination: developments and applications. *Curr. Opin. Biotechnol.* **5**, 521-527.

Sauer, B. (1998) Inducible gene targeting in mice using the Cre/lox system. *Methods* **14**, 381-392.

Scaglia, L., Cahill, C. J., Finegood, D. T. and Bonner-Weir, S. (1997) Apoptosis participates in the remodeling of the endocrine pancreas in the neonatal rat. *Endocrinology* **138**, 1736-1741.

Scarpelli, D. G. and Rao, M. S. (1981) Differentiation of regenerating pancreatic cells into hepatocyte-like cells. *Proc. Natl. Acad. Sci. USA* **78**, 2577-2581.

Scharfmann, R., Tazi, A., Polak, M., Kanaka, C. and Czernichow, P. (1993) Expression of functional nerve growth factor receptors in pancreatic β-cell line and fetal rat islets in primary culture. *Diabetes* **42**, 1829-1836.

Schmidt, G., Winton, D. J. and Ponder, B. A. J. (1988) Development of the pattern of cell renewal in the crypt-villus unit of the chimaeric mouse small intestine. *Development* **103**, 785-790.

Schneider, B. S., Hastings, H. M. and Maytal, G. (1996) The spatial distribution of pancreatic islets follows a universal power law. *Proc. Roy. Soc. Lond. B* **263**, 129-131.

Schofield, P. N. (1992) *The Insulin-Like Growth Factors: Structure and Biological Function*, pp. 12-44. Oxford: Oxford University Press.

Schuppin, G. T., Bonner-Weir, S., Montana, E., Kaiser, N. and Weir, G. C. (1992) Replication of adult pancreatic beta-cells cultured on bovine corneal endothelial cell extracellular matrix. *In Vitro Cell Dev. Biol.* **29A**, 339-344.

Schuppin, G. T., Pons, S., Hugl, S., Aiello, L. P., King, G. L., White, M. and Rhodes, C. J. (1998) A specific increased expression of insulin receptor substrate 2 in pancreatic β-cell lines is involved in mediating serum-stimulated β-cell growth. *Diabetes* **47**, 1074-1085.

Schwitzgebel, V. M., Scheel, D. W., Conners, J. R., Kalamaras, J., Lee, J. E., Anderson, D. J., Sussel, L., Johnson, J. D. and German, M. S. (2000) Expression of neurogenin3 reveals an islet cell precursor population in the pancreas. *Development* **127**, 3533-3542.

Selander, L. and Edlund, H. (2002) Nestin is expressed in mesenchymal and not epithelial cells of the developing mouse pancreas. *Mech. Dev.* **113**, 189-192.

Sharma, A., Zangen, D. H., Reitz, P., Taneja, M., Lissauer, M. E., Miller, C. P., Weir, G. C., Habener, J. F. and Bonner-Weir, S. (1999) The homeodomain protein IDX-1 increases after an early burst of proliferation during pancreatic regeneration. *Diabetes* **48**, 507-513.

Sharma, S., Leonard, J., Lee, S., Chapman, H. D., Leiter, E. H. and Montminy, M. R. (1996) Pancreatic islet expression of the homeobox factor STF-1 relies on an E-box motif that binds USF. *J. Biol. Chem.* **271**, 2294-2299.

Sharma, S., Jhala, U. S., Johnson, T., Ferreri, K., Leonard, J. and Montminy, M. (1997) Hormonal regulation of an islet-specific enhancer in the pancreatic homeobox gene *STF-1. Mol. Cell. Biol.* **17**, 2598-2604.

Shen, C.-N., Slack, J. M. W. and Tosh, D. (2000) Molecular basis of transdifferentiation of pancreas to liver. *Nat. Cell Biol.* **2**, 879-887.

Shibata, H., Yasuda, H., Sekine, N., Mine, T., Totsuka, Y. and Kojima, I. (1993) Activin A increases intracellular free calcium concentrations in rat pancreatic islets. *FEBS Lett.* **329**, 194-198.

Shing, Y., Christofori, G., Hanahan, D., Ono, Y., Sasada, R., Igarashi, K. and Folkman, J. (1993) Betacellulin: a mitogen from pancreatic β cell tumors. *Science* **259**, 1604-1607.

Shino, A., Matsueo, T., Iwatsuka, H. and Zuzuki, Z. (1973) Structural changes of pancreatic islets in genetically obese rats. *Diabetologia* **9**, 413-421.

Shiojiri, N., Ohta, T., Ogawa, K. and Gebhardt, R. (1997) Complementary expression of glutamine synthetase and carbamoylphosphate synthetase I in ornithine carbamoyltransferase-deficient mouse liver (spf-ash mouse). *Histochem. Cell Biol.* **108**, 489-494.

Siddle, K. (1992) The insulin receptor and type I IGF receptor: comparison of structure and function. *Prog. Growth Factor Res.* **4**, 301-320.

Sidorova, V. F. (1978) *The Postnatal Growth and Restoration of Internal Organs in Vertebrates*. Calcutta: PSG Publishing Co., Inc.

Sieradzki, J., Fleck, H., Chatterjee, A. K. and Schatz, H. (1988) Stimulatory effect of insulin-like growth factor-I on [3H]thymidine incorporation, DNA content and insulin biosynthesis and secretion of isolated pancreatic rat islets. *J. Endocrinol.* **117**, 59-62.

Sjödin, A., Dahl, U. and Semb, H. (1995) Mouse R-cadherin: expression during the organogenesis of pancreas and gastrointestinal tract. *Exp. Cell. Res.* **221**, 413-425.

Slack, J. M. W. (1986) Epithelial metaplasia and the second anatomy. *Lancet* **2**, 268-271.

Slack, J. M. W. (1992) In *Oxford Textbook of Pathology* (ed. J. O'D. McGee, P. G. Isaacson and N. A. Wright), pp. 565-568. Oxford: Oxford University Press.

Slack, J. M. W., Holland, P. W. H. and Graham, C. F. (1993) The zootype and the phylotypic stage. *Nature* **361**, 490-492.

Slack, J. M. W. (1995) Developmental biology of the pancreas. *Development* **121**, 1569-1580.

Slack, J. M. W. (1999) Developmental biology of the β-cell. In *The Biology of the Pancreatic β-Cell* vol. 29 (ed. S. L. Howell), pp. 3-19. Stamford, Connecticut: Jai Press, Inc.

Sommer, L., Hagenbüchle, O., Wellauer, P. K. and Strubin, M. (1991) Nuclear targeting of the transcription factor PTF1 is mediated by a protein subunit that does not bind to the PTF1 cognate sequence. *Cell* **67**, 987-994.

Sommer, L., Ma, Q. and Anderson, D. J. (1996) Neurogenins, a novel family of atonal-related bHLH transcription factors, are putative mammalian neuronal determination genes that reveal progenitor cell heterogeneity in the developing CNS and PNS. *Mol. Cell. Neurosci.* **8**, 221-241.

Sorenson, R. L. and Parsons, J. A. (1985) Insulin secretion in mammosomatotropic tumor-bearing and pregnant rats. A role for lactogens. *Diabetes* **34**, 337-341.

Sorenson, R. L. and Brelje, T. C. (1997) Adaptation of islets of Langerhans to pregnancy: beta-cell growth, enhanced insulin secretion and the role of lactogenic hormones. *Horm. Metab. Res.* **29**, 301-307.

Sosa-Pineda, B., Chowdhury, K., Torres, M., Oliver, G. and Gruss, P. (1997) The Pax4 gene is essential for differentiation of insulin-producing beta cells in the mammalian pancreas. *Nature* **386**, 399-402.

Spearman, C. (1904) The proof and measurement of association between two things. *Am. J. Psychol.* **15**, 72-101.

Spooner, B. S., Walther, B. T. and Rutter, W. J. (1970) The development of the dorsal and ventral mammalian pancreas in vivo and in vitro. *J. Cell Biol.* **47**, 235-246.

Steinberg, M. S. and Takeichi, M. (1994) Experimental specification of cell sorting, tissue spreading, and specific spatial patterning by quantitative differences in cadherin expression. *Proc. Natl. Acad. Sci. USA* **91**, 206-209.

Steiner, H., Oelz, O., Zahnd, G. and Froesch, E. R. (1970) Studies on islet cell regeneration, hyperplasia and intrainsular cellular interactions in long lasting streptozotocin diabetes in the rat. *Diabetologia* **6**, 558-564.

Stewart, C. E. and Rotwein, P. (1996) Insulin-like growth factor-II is an autocrine survival factor for differentiating myoblasts. *J. Biol. Chem.* **271**, 11330-11338.

Stoffel, M. and Duncan, S. A. (1997) The maturity-onset diabetes of the young (MODY1) transcription factor HNF4α regulates expression of genes required for glucose transport and metabolism. *Proc. Natl. Acad. Sci. USA* **94**, 13209-13214.

Stoffers, D. A., Zinkin, N. T., Stanojevic, V., Clarke, W. L. and Habener, J. F. (1997) Pancreatic agenesis attributable to a single nucleotide deletion in the human IPF 1 gene coding sequence. *Nat. Genet.* **15**, 106-110.

Stoffers, D. A., Stanojevic, V. and Habener, J. F. (1998) Insulin promoter factor-1 gene mutation linked to early-onset type 2 diabetes mellitus directs expression of a dominant negative isoprotein. *J. Clin. Invest.* **102**, 232-241.

Stone, L. M., Tan, S.-S., Tam, P. P. L. and Finger, T. E. (2002) Analysis of cell lineage relationships in taste buds. *J. Neurosci.* **22**, 4522-4529.

Sun, F. L., Dean, W. L., Kelsey, G., Allen, N. D. and Reik, W. (1997) Transactivation of Igf2 in a mouse model of Beckwith-Wiedemann syndrome. *Nature* **389**, 808-815.

Sussel, L., Kalamaras, J., Hartigan-O'Connor, D. J., Meneses, J. J., Pedersen, R. A., Rubenstein, J. L. and German, M. S. (1998) Mice lacking the homeodomain transcription factor Nkx2.2 have diabetes due to arrested differentiation of pancreatic beta cells. *Development* **125**, 2213-2221.

Suzuki, Y., Yonekura, H., Watanabe, T., Unno, M., Moriizumi, S., Miyashita, H. and Okamoto, H. (1994) Structure and expression of a novel rat RegIII gene. *Gene* **144**, 315-316.

Swenne, I. and Eriksson, U. (1982) Diabetes in pregnancy: islet cell proliferation in the fetal rat pancreas. *Diabetologia* **23**, 525-528.

Swenne, I., Hill, D. J., Strain, A. J. and Milner, R. D. G. (1987) Growth hormone regulation of somatomedin-C/insulin-like growth factor I production and DNA replication in fetal rat islets in tissue culture. *Diabetes* **36**, 288-294.

Swenne, I. (1992) Pancreatic beta-cell growth and diabetes mellitus. *Diabetologia* **35**, 193-201.

Szebenyi, G. and Fallon, J. F. (1999) Fibroblast growth factors as multifunctional signaling factors. *Int. Rev. Cytol.* **185**, 45-106.

Taguchi, M., Yamaguchi, T. and Otsuki, M. (2002) Induction of PDX-1-positive cells in the main duct during regeneration after acute necrotizing pancreatitis in rats. *J. Pathol.* **197**, 638-646.

Tam, P. P. L. and Tan, S.-S. (1992) The somitogenic potential of cells in the primitive streak and the tail bud of the organogenesis-stage mouse embryo. *Development* **115**, 703-715.

Tamemoto, H., Kadowaki, T., Tobe, K., Yagi, T., Sakura, H., Hayakawa, T., Terauchi, Y., Ueki, K., Kaburagi, Y., Satoh, S., Sekihara, H., Yoshioka, S., Horikoshi, H., Furuta,

Y., Ikawa, Y., Kasuga, M., Yazaki, Y. and Aizawa, S. (1994) Insulin resistance and growth retardation in mice lacking insulin receptor substrate-1. *Nature* **372**, 182-186.

Tan, S.-S. and Breen, S. (1993) Radial mosaicism and tangential cell dispersion both contribute to mouse neocortical development. *Nature* **362**, 638-639.

Tan, S.-S., Williams, E. A. and Tam, P. P. L. (1993) X-chromosome inactivation occurs at different times in different tissues of the post-implantation mouse embryo. *Nat. Genet.* **3**, 170-174.

Tan, S.-S., Faulkner-Jones, B., Breen, S. J., Walsh, M., Bertram, J. F. and Reese, B. E. (1995) Cell dispersion patterns in different cortical regions studied with an X-inactivated transgenic marker. *Development* **121**, 1029-1039.

Teitelman, G. and Lee, J. K. (1987) Cell lineage of pancreatic islet cell development: glucagon and insulin cells arise from catecholaminergic precursors present in the pancreatic ducts. *Dev. Biol.* **121**, 454-466.

Teitelman, G., Lee, J. K. and Alpert, S. (1987) Expression of cell type-specific markers during pancreatic development in the mouse: implications for pancreatic cell lineages. *Cell Tissue Res.* **250**, 435-439.

Teitelman, G. (1990) Insulin cells of the pancreas extend neurites but do not arise from the neurectoderm. *Dev. Biol.* **142**, 368-379.

Teitelman, G., Alpert, S., Polak, J. M., Martinez, A. and Hanahan, D. (1993) Precursor cells of mouse endocrine pancreas coexpress insulin, glucagon and the neuronal proteins tyrosine hydroxylase and neuropeptide Y, but not pancreatic polypeptide. *Development* **118**, 1031-1039.

Teitelman, G., Guz, Y., Ivkovic, S. and Ehrlich, M. (1998) Islet injury induces neurotrophin expression in pancreatic cells and reactive gliosis of peri-islet Schwann cells. *J. Neurobiol.* **34**, 304-318.

Terada, T. and Nakanuma, Y. (1991) Immunohistochemical demonstration of pancreatic alpha-amylase and trypsin in intrahepatic bile ducts and peribiliary glands. *Hepatology* **14**, 1129-1135.

Terada, T. and Nakanuma, Y. (1995) Expression of pancreatic enzymes (alpha-amylase, trypsinogen, and lipase) during human liver development and maturation. *Gastroenterology* **108**, 1236-1245.

Terada, T., Kato, M., Horie, S., Endo, K. and Kitamura, Y. (1998) Expression of pancreatic alpha-amylase protein and messenger RNA in hilar primitive bile ducts and hepatocytes during human fetal liver organogenesis: an immunohistochemical and *in situ* hybridization study. *Liver* **18**, 313-319.

Terazono, K., Yamamoto, H., Takasawa, S., Shiga, K., Yonemura, Y., Tochino, Y. and Okamoto, H. (1988) A novel gene activated in regenerating islets. *J. Biol. Chem.* **263**, 2111-2114.

Terazono, K., Uchiyama, Y., Ide, M., Watanabe, T., Yonekura, H., Yamamoto, H. and Okamoto, H. (1990) Expression of reg protein in rat regenerating islets and its co-localization with insulin in the β cell secretory granules. *Diabetologia* **33**, 250-252.

Thor, S., Ericson, J., Brännström, T. and Edlund, T. (1991) The homeodomain LIM protein isl-1 is expressed in subsets of neurons and endocrine cells in the adult rat. *Neuron* **7**, 881-889.

Tokuyama, Y., Sturis, J., DePaoli, A. M., Takeda, J., Stoffel, M., Tang, J., Sun, X., Polonsky, K. S. and Bell, G. I. (1995) Evolution of β-cell dysfunction in the male Zucker diabetic fatty rat. *Diabetes* **44**, 1447-1457.

Tosh, D., Shen, C.-N. and Slack, J. M. W. (2002) Differentiated properties of hepatocytes induced from pancreatic cells. *Hepatology* **36**, 534-543.

Totafurno, J., Bjerknes, M. and Cheng, H. (1987) The crypt cycle: evidence for crypt and villus production in the adult mouse small intestine. *Biophys. J.* **52**, 279-294.

Totsuka, T., Tabuchi, M., Kojima, I., Shibai, H. and Ogata, E. (1988) A novel action of activin A: stimulation of insulin secretion in rat pancreatic islets. *Biochem. Biophys. Res. Comm.* **156**, 335-359.

Townes, P. L. and Holfreter, J. (1955) Directed movements and selective adhesion of embryonic amphibian cells. *J. Exp. Zool.* **128**, 53-120.

Trudeau, J. D., Dutz, J. P., Arany, E., Hill, D. J., Fieldus, W. E. and Finegood, D. T. (2000) Neonatal β-cell apoptosis: a trigger for autoimmune diabetes? *Diabetes* **49**, 1-7.

Turque, N., Plaza, S., Radvanyi, F., Carriere, C. and Saule, S. (1994) *Pax-QNR/Pax-6*, a paired box- and homeobox-containing gene expressed in neurons, is also expressed in pancreatic endocrine cells. *Mol. Endocrinol.* **8**, 929-938.

Ueno, K., Hiramoto, Y., Hayashi, S. and Kondoh, H. (1987) Introduction and expression of recombinant β-galactosidase genes in cleavage stage mouse embryos. *Develop. Growth & Differ.* **30**, 61-73.

Unno, M., Yonekura, H., Nakagawara, K., Watanabe, T., Miyashita, H., Moriizumi, S., Okamoto, H., Itoh, T. and Teraoka, H. (1993) Structure, chromosomal localization, and expression of mouse reg genes, reg I and reg II. A novel type of reg gene, reg II, exists in the mouse genome. *J. Biol. Chem.* **268**, 15974-15982.

Unno, M., Nata, K., Noguchi, N., Narushima, Y., Akiyama, T., Ikeda, T., Nakagawa, K., Takasawa, S. and Okamoto, H. (2002) Production and characterization of Reg knockout mice: reduced proliferation of pancreatic β-cells in Reg knockout mice. *Diabetes* **51** Suppl. 3, S478-483.

Upchurch, B. H., Aponte, G. W. and Leiter, A. B. (1994) Expression of peptide YY in all four islet cell types in the developing mouse pancreas suggests a common peptide YY-producing progenitor. *Development* **120**, 245-252.

Upchurch, B. H., Fung, B. P., Rindi, G., Ronco, A. and Leiter, A. B. (1996) Peptide YY expression is an early event in colonic endocrine cell differentiation: evidence from normal and transgenic mice. *Development* **122**, 1157-1163.

Valera, A., Rodriguez-Gil, J. E., Yun, J. S., McGrane, M. M., Hanson, R. W. and Bosch, F. (1993) Glucose metabolism in transgenic mice containing a chimeric P-enolpyruvate carboxykinase/bovine growth hormone gene. *FASEB J.* **7**, 791-800.

Van Schravendijk, C. F., Foriers, A., Van Den Brande, J. L. and Pipeleers, D. G. (1987) Evidence for the presence of type I insulin-like growth factor receptors on rat pancreatic A and B cells. *Endocrinology* **121**, 1784-1788.

Van Schravendijk, C. F. H., Heylen, L., Van Den Brande, J. L. and Pipeleers, D. G. (1990) Direct effect of insulin and insulin-like growth factor-I on the secretory activity of rat pancreatic beta cells. *Diabetologia* **33**, 649-653.

Vasavada, R. C., Cavaliere, C., D'Ercole, A. J., Dann, P., Burtis, W. J., Madlener, A. L., Zawalich, K., Philbrick, W. and Stewart, A. F. (1996) Overexpression of parathyroid hormone-related protein in the pancreatic islets of transgenic mice causes islet hyperplasia, hyperinsulinemia, and hypoglycemia. *J. Biol. Chem.* **271**, 1200-1208.

Velloso, L. A., Carneiro, E. M., Crepaldi, S. C., Boschero, A. C. and Saad, M. J. (1995) Glucose- and insulin-induced phosphorylation of the insulin receptor and its primary substrates IRS-1 and IRS-2 in rat pancreatic islets. *FEBS Lett.* **377**, 353-357.

Verspohl, E. J. and Ammon, H. P. (1980) Evidence for presence of insulin receptors in rat islets of Langerhans. *J. Clin. Invest.* **65**, 1230-1237.

Vila, M. R., Nakamura, T. and Real, F. X. (1995) Hepatocyte growth factor is a potent mitogen for normal human pancreas cells *in vitro*. *Lab. Invest.* **73**, 409-418.

Vincent, M. T., Carroll, R. J., Hammer, R. E., Chan, S. J., Guz, Y., Steiner, D. F. and Teitelman, G. (1995) A transgene coding for a human insulin analog has a mitogenic effect on murine embryonic β cells. *Proc. Natl. Acad. Sci. USA* **92**, 6239-6243.

Wada, M., Shintani, Y., Kosaka, M., Sano, T., Hizawa, K. and Saito, S. (1996) Immunohistochemical localization of activin A and follistatin in human tissues. *Endocrinol. J.* **43**, 375-385.

Waeber, G., Thompson, N., Nicod, P. and Bonny, C. (1996) Transcriptional activation of the GLUT2 gene by the IPF-1/STF-1/IDX-1 homeobox factor. *Mol. Endocrinol.* **10**, 1327-1334.

Wang, M. and Drucker, D. J. (1995) The LIM domain homeobox gene *isl-1* is a positive regulator of islet cell-specific proglucagon gene transcription. *J. Biol. Chem.* **270**, 12646-12652.

Wang, M. and Drucker, D. J. (1996) Activation of amylin gene transcription by the LIM domain homeobox gene isl-1. *Mol. Endocrinol.* **10**, 243-251.

Wang, R. A., Nakane, P. K. and Koji, T. (1998) Autonomous cell death of mouse male germ cells during fetal and postnatal period. *Biol. Reprod.* **58**, 1250-1256.

Wang, R. N., Bouwens, L. and Klöppel, G. (1994) Beta-cell proliferation in normal and streptozotocin-treated newborn rats: site, dynamics and capacity. *Diabetologia* **37**, 1088-1096.

Wang, R. N., Klöppel, G. and Bouwens, L. (1995) Duct-to-islet-cell differentiation and islet growth in the pancreas of duct-ligated adult rats. *Diabetologia* **38**, 1405-1411.

Ward, A., Bates, P., Fisher, R., Richardson, L. and Graham, C. F. (1994) Disproportionate growth in mice with *Igf-2* transgenes. *Proc. Natl. Acad. Sci. USA* **91**, 10365-10369.

Wareham, K. A., Lyon, M. F., Glenister, P. H. and Williams, E. D. (1987) Age related reactivation of an X-linked gene. *Nature* **327**, 725-727.

Watada, H., Kajimoto, Y., Kaneto, H., Matsuoka, T., Fujitani, Y., Miyazaki, J. and Yamasaki, Y. (1996a) Involvement of the homeodomain-containing transcription factor PDX-1 in islet amyloid polypeptide gene transcription. *Biochem. Biophys. Res. Comm.* **229**, 746-751.

Watada, H., Kajimoto, Y., Miyagawa, J., Hanafusa, T., Hamaguchi, K., Matsuoka, T., Yamamoto, K., Matsuzawa, Y., Kawamori, R. and Yamasaki, Y. (1996b) PDX-1 induces insulin and glucokinase gene expression in αTC1 clone 6 cells in the presence of betacellulin. *Diabetes* **45**, 1826-1831.

Watada, H., Kajimoto, Y., Umayahara, Y., Matsuoka, T., Kaneto, H., Fujitani, Y., Kamada, T., Kawamori, R. and Yamasaki, Y. (1996c) The human glucokinase gene β-cell-type promoter: an essential role of insulin promoter 1/PDX-1 in its activation in HIT-T15 cells. *Diabetes* **45**, 1478-1488.

Watanabe, T., Yonekura, H., Terazono, K., Yamamoto, H. and Okamoto, H. (1990) Complete nucleotide sequence of human reg gene and its expression in normal and tumoral tissues. The reg protein, pancreatic stone protein, and pancreatic thread protein are one and the same product of the gene. *J. Biol. Chem.* **265**, 7432-7439.

Watanabe, T., Shintani, A., Nakata, M., Shing, Y., Folkman, J., Igarashi, K. and Sasada, R. (1994a) Recombinant human betacellulin. Molecular structure, biological activities, and receptor interaction. *J. Biol. Chem.* **269**, 9966-9973.

Watanabe, T., Yonemura, Y., Yonekura, H., Suzuki, Y., Miyashita, H., Sugiyama, K., Moriizumi, S., Unno, M., Tanaka, O., Kondo, H., Bone, A. J., Takasawa, S. and Okamoto, H. (1994b) Pancreatic β-cell replication and amelioration of surgical diabetes by Reg protein. *Proc. Natl. Acad. Sci. USA* **91**, 3589-3592.

Weinhaus, A. J., Poronnik, P., Cook, D. I. and Tuch, B. E. (1995) Insulin secretagogues, but not glucose, stimulate an increase in $[Ca^{++}]_i$ in the fetal rat β-cell. *Diabetes* **44**, 118-124.

Weinhaus, A. J., Stout, L. E. and Sorenson, R. L. (1996) Glucokinase, hexokinase, glucose transporter 2, and glucose metabolism in islets during pregnancy and prolactin-treated islets *in vitro*: mechanisms for long term up-regulation of islets. *Endocrinology* **137**, 1640-1649.

Weinstein, D. C., Ruiz i Altaba, A., Chen, W. S., Hoodless, P., Prezioso, V. R., Jessell, T. M. and Darnell, J. E. Jr. (1994) The winged-helix transcription factor HNF-3 beta is required for notochord development in the mouse embryo. *Cell* **78**, 575-588.

Wells, J. M. and Melton, D. A. (2000) Early mouse endoderm is patterned by soluble factors from adjacent germ layers. *Development* **127**, 1563-1572.

Weng, J. P., Lehto, M., Forsblom, C., Huang, X., Li, H. and Groop, L. C. (2000) Hepatocyte nuclear factor-1 beta (MODY5) gene mutations in Scandinavian families with early-onset diabetes or kidney disease or both. *Diabetologia* **43**, 131-132.

Wessells, N. K. and Cohen, J. H. (1967) Early pancreas organogenesis: morphogenesis, tissue interactions, and mass effects. *Dev. Biol.* **15**, 237-270.

Wessells, N. K. and Evans, J. (1968) Ultrastructural studies of early morphogenesis and cytodifferentiation in the embryonic mammalian pancreas. *Dev. Biol.* **17**, 413-446.

Wessells, N. K. (1977) *Tissue Interactions and Development*. Menlo Park, CA.: W. A. Benjamin.

Westphal, C. H., Muller, L., Zhou, A., Zhu, X., Bonner-Weir, S., Schambelan, M., Steiner, D. F., Lindberg, I. and Leder, P. (1999) The neuroendocrine protein 7B2 is required for peptide hormone processing *in vivo* and provides a novel mechanism for pituitary Cushing's disease. *Cell* **96**, 689-700.

Wicksell, S. D. (1925) The corpuscle problem. *Biometrika* **17**, 84-99.

Wicksell, S. D. (1926) The corpuscle problem II. *Biometrika* **18**, 152-172.

Williams, J. A., Bailey, A., Humbel, R. and Goldfine, I. D. (1984) Insulinlike growth factors bind to specific receptors in isolated pancreatic acini. *Am. J. Physiol.* **246**, G96-99.

Williams, P. L. (1995) *Gray's Anatomy: The Anatomical Basis of Medicine and Surgery*, 38th edition. Edinburgh: Churchill Livingstone, Inc.

Winter, W. E., Nakamura, M. and House, D. V. (1999) Monogenic diabetes mellitus in youth. The MODY syndromes. *Endocrinol. Metab. Clin. North. Am.* **28**, 765-785.

Winton, D. J., Blount, M. A. and Ponder, B. A. J. (1988) A clonal marker induced by mutation in mouse intestinal epithelium. *Nature* **333**, 463-466.

Winton, D. J. and Ponder, B. A. J. (1990) Stem cell organisation in mouse intestinal epithelium. *Proc. Roy. Soc. Lond. B* **241**, 13-18.

Withers, D. J., Gutierrez, J. S., Towery, H., Burks, D. J., Ren, J.-M., Previs, S., Zhang, Y., Bernal, D., Pons, S., Shulman, G. I., Bonner-Weir, S. and White, M. F. (1998) Disruption of IRS-2 causes type 2 diabetes in mice. *Nature* **391**, 900-904.

Withers, D. J., Burks, D. J., Towery, H. H., Altamuro, S. L., Flint, C. L. and White, M. F. (1999) Irs-2 coordinates Igf-1 receptor-mediated β-cell development and peripheral insulin signalling. *Nat. Genet.* **23**, 32-40.

Wolf, E., Kramer, R., Blum, W. F., Foll, J. and Brem, G. (1994) Consequences of postnatally elevated insulin-like growth factor-II in transgenic mice: endocrine changes and effects on body and organ growth. *Endocrinology* **135**, 1877-1886.

Wolf, H. K., Burchette, J. L., Garcia, J. A. and Michalopoulos, G. (1990) Exocrine pancreatic tissue in human liver: a metaplastic process? *Am. J. Surg. Pathol.* **14**, 590-595.

Wolfe-Coote, S., Louw, J., Woodroof, C. and DuToit, D. F. (1996) The non-human primate endocrine pancreas: development, regeneration potential and metaplasia. *Cell Biol. Intl.* **20**, 95-101.

Wright, C. V. E., Schnegelsberg, P. and De Robertis, E. M. (1988) XlHbox-8: a novel *Xenopus* homeoprotein restricted to a narrow band of endoderm. *Development* **104**, 787-794.

Wright, N. A. (2000) Epithelial stem cell repertoire in the gut: clues to the origin of cell lineages, proliferative units and cancer. *Int. J. Exp. Path.* **81**, 117-143.

Wu, K.-L., Gannon, M., Peshavaria, M., Offield, M. F., Henderson, E., Ray, M., Marks, A., Gamer, L. W., Wright, C. V. E. and Stein, R. (1997) Hepatocyte nuclear factor 3β is involved in pancreatic β-cell-specific transcription of the *pdx-1* gene. *Mol. Cell. Biol.* **17**, 6002-6013.

Wysocka-Diller, J., Aisemberg, G. O. and Macagno, E. R. (1995) A novel homeobox cluster expressed in repeated structures of the midgut. *Dev. Biol.* **171**, 439-447.

Xu, G. G. and Rothenberg, P. L. (1998) Insulin receptor signaling in the β-cell influences insulin gene expression and insulin content: evidence for autocrine β-cell regulation. *Diabetes* **47**, 1243-1252.

Yamada, M., Saga, Y., Shibusawa, N., Hirato, J., Murakami, M., Iwasaki, T., Hashimoto, K., Satoh, T., Wakabayashi, K., Taketo, M. and Mori, M. (1997) Tertiary hypothyroidism and hyperglycemia in mice with targeted disruption of the thyrotropin-releasing hormone gene. *Proc. Natl. Acad. Sci. USA* **94**, 10862-10867.

Yamagata, K., Furuta, H., Oda, N., Kaisaki, P. J., Menzel, S., Cox, N. J., Fajans, S. S., Signormi, S., Stoffel, M. and Bell, G. I. (1996a) Mutations in the hepatocyte nuclear factor-4alpha gene in maturity-onset diabetes of the young (MODY1). *Nature* **384**, 458-460.

Yamagata, K., Oda, N., Kaisaki, P. J., Menzel, S., Furuta, H., Vaxillaire, M., Southam, L., Cox, R. D., Lathrop, G. M., Boriraj, V. V., Chen, X., Cox, N. J., Oda, Y., Yano, H., Le Beau, M. M., Yamada, S., Nishigori, H., Takeda, J., Fajans, S. S., Hattersley, A. T., Iwasaki, N., Hansen, T., Pedersen, O., Polonsky, K. S., Bell, G. I. *et al.* (1996b) Mutations in the hepatocyte nuclear factor-1alpha gene in maturity-onset diabetes of the young (MODY3). *Nature* **384**, 455-458.

Yamagata, K., Yang, Q., Yamamoto, K., Iwahashi, H., Miyagawa, J., Okita, K., Yoshiuchi, I., Miyazaki, J., Noguchi, T., Nakajima, H., Namba, M., Hanafusa, T. and Matsuzawa, Y. (1998) Mutation P291fsinsC in the transcription factor hepatocyte nuclear factor-1α is dominant negative. *Diabetes* **47**, 1231-1235.

Yamaoka, T., Idehara, C., Yano, M., Matsushita, T., Yamada, T., Ii, S., Moritani, M., Hata, J., Sugino, H., Noji, S. and Itakura, M. (1998) Hypoplasia of pancreatic islets in transgenic mice expressing activin receptor mutants. *J. Clin. Invest.* **102**, 294-301.

Yamaoka, T. and Itakura, M. (1999) Development of pancreatic islets (review). *Int. J. Mol. Med.* **3**, 247-261.

Yamaoka, T., Yano, M., Idehara, C., Yamada, T., Tomonari, S., Moritani, M., Ii, S., Yoshimoto, K., Hata, J. and Itakura, M. (1999) Apoptosis and remodelling of beta cells by paracrine interferon-γ without insulitis in transgenic mice. *Diabetologia* **42**, 566-573.

Yamaoka, T., Yoshino, K., Yamada, T., Yano, M., Matsui, T., Yamaguchi, T., Moritani, M., Hata, J., Noji, S. and Itakura, M. (2002) Transgenic expression of FGF8 and FGF10 induces transdifferentiation of pancreatic islet cells into hepatocytes and exocrine cells. *Biochem. Biophys. Res. Comm.* **292**, 138-143.

Yasuda, H., Inoue, K., Shibata, H., Takeuchi, T., Eto, Y., Hasegawa, Y., Sekine, N., Totsuka, Y., Mine, T., Ogata, E. and Kojima, I. (1993) Existence of activin A in A and D cells of rat pancreatic islet. *Endocrinology* **133**, 624-630.

Yeldandi, A. V., Tan, X., Dwivedi, R. S., Subbarao, V., Smith, D. D. Jr., Scarpelli, D. G., Rao, M. S. and Reddy, J. K. (1990) Coexpression of glutamine synthetase and carbamoylphosphate synthase I genes in pancreatic hepatocytes of rat. *Proc. Natl. Acad. Sci. USA* **87**, 881-885.

Yi, E. S., Yin, S., Harclerode, D. L., Bedoya, A., Bikhazi, N. B., Housley, R. M., Aukerman, S. L., Morris, C. F., Pierce, G. F. and Ulich, T. R. (1994) Keratinocyte growth factor induces pancreatic ductal epithelial proliferation. *Am. J. Pathol.* **145**, 80-85.

Yokouchi, Y., Sakiyama, J. I. and Kuroiwa, A. (1995) Coordinated expression of AbdB subfamily genes of the HoxA cluster in the developing digestive tract of chick embryo. *Dev. Biol.* **169**, 76-89.

Yonemura, Y., Takashima, T., Miwa, K., Miyazaki, I., Yamamoto, H. and Okamoto, H. (1984) Amelioration of diabetes mellitus in partially depancreatized rats by polyADP-ribose synthetase inhibitors. *Diabetes* **33**, 401-404.

Zambrowicz, B. P., Imamoto, A., Fiering, S., Herzenberg, L. A., Kerr, W. G. and Soriano, P. (1997) Disruption of overlapping transcripts in the ROSAβgeo 26 gene trap strain leads to widespread expression of β-galactosidase in mouse embryos and hematopoietic cells. *Proc. Natl. Acad. Sci. USA* **94**, 3789-3794.

Zar, J. H. (1999) *Biostatistical Analysis*, 4th edition. London: Prentice-Hall, Inc.

Zaret, K. S. (2000) Liver specification and early morphogenesis. *Mech. Dev.* **92**, 83-88.

Zenilman, M. E., Magnuson, T. H., Swinson, K., Egan, J., Perfetti, R. and Shuldiner, A. R. (1996) Pancreatic thread protein is mitogenic to pancreatic-derived cells in culture. *Gastroenterology* **110**, 1208-1214.

Zhang, Q., Berggren, P. O., Hansson, A. and Tally, M. (1998) Insulin-like growth factor-I-induced DNA synthesis in insulin-secreting cell line RINm5F is associated with phosphorylation of the insulin-like growth factor receptor-I and the insulin receptor substrate-2. *J. Endocrinol.* **156**, 573-581.

Zhang, X., Heaney, S. and Maas, R. L. (2003) Cre-loxp fate-mapping of Pax6 enhancer active retinal and pancreatic progenitors. *Genesis* **35**, 22-30.

Zhu, Q., Yamagata, K., Yu, L., Tomura, H., Yamada, S., Yang, Q., Yoshiuchi, I., Surni, S., Miyagawa, J., Takeda, J., Hanafusa, T. and Matsuzawa, Y. (2000) Identification of missense mutations in the hepatocyte nuclear factor-3beta gene in Japanese subjects with late-onset Type II diabetes mellitus. *Diabetologia* **43**, 1197-1200.

Zimmet, P., Alberti, K. G. M. M. and Shaw, J. (2001) Global and societal implications of the diabetes epidemic. *Nature* **414**, 782-787.

Zulewski, H., Abraham, E. J., Gerlach, M. J., Daniel, P. B., Moritz, W., Muller, B., Vallejo, M., Thomas, M. K. and Habener, J. F. (2001) Multipotential nestin-positive stem cells isolated from adult pancreatic islets differentiate *ex vivo* into pancreatic endocrine, exocrine, and hepatic phenotypes. *Diabetes* **50**, 521-533.